Scientific Support Plan for a Sustainable Development Policy SPSD I

Belgian Scientific Research Programme on the Antarctic

Phase 4 (1997-2001)   Scientific results

Volume I   Marine biota and Global change

ANTARCTICA

PPS SCIENCE POLICY

BELGIAN RESEARCH PROGRAMME ON THE ANTARCTIC
SCIENTIFIC RESULTS OF PHASE IV (1997-2001)

Volume I   Marine biota

and

global change

LEGAL NOTICE

Additional information on the Belgian Research Programme on the Antarctic is available on Internet: (http://www.belspo.be/antar)

Contact person:

Mrs Maaike Vancauwenberghe (vcau@belspo.be)

Secr.: +32-2-238.36.49

FOREWORD

This Volume presents the scientific results of research projects in the area of **"Marine biota and Global change"** funded under the **Fourth Phase of the Belgian research programme on the Antarctic (1997-2001)**. The achievements of the research projects in the other areas of the Programme are represented in the second Volume *"Dynamics of the Southern Ocean and Paleoenvironmental records"*.

In 1985, the Belgian Government took the initiative of setting up a structured scientific research programme regarding Antarctica with a manifest view to maximally integrate with the activities of the Antarctic Treaty System. The research programme has continued uninterruptedly up to today, with the following broad objectives:

- Maintain and strengthen Belgium's relevant expertise;
- Increase Belgium's visibility within the Antarctic Treaty System;
- Contribute to a rational management of the Antarctic environment and its natural resources;
- Determine the global consequences of the natural processes that take place in Antarctica and its surrounding oceans.

Four major research areas can be distinguished:
- Marine biology and biological geochemistry;
- Glaciology and climatology;
- Hydrodynamics and sea ice;
- Marine geophysics.

The research takes the form of four-year projects that are entrusted to research teams of universities or (federal) scientific institutions. The emphasis is on a multidisciplinary approach of the dynamics of the major Antarctic natural systems' comprehensive functioning, development and interactions. The research themes and priorities fully tie in with other important international projects and programmes, such as ANTOSTRAT (Antarctic Offshore Stratigraphy Project), EPICA (European Project on Ice Coring in Antarctica), IGBP (International Geosphere-Biosphere Programme),…

As Belgium has no infrastructure of its own in Antarctica (base, appropriate research ships,…), the necessary fieldwork is conducted through participation in scientific expeditions set up by other countries.

All research costs are defrayed by the Federal Scientific Policy, which is also in charge of the financing, management, co-ordination and dissemination of the Programme. The scientific link with the Antarctic Treaty System also lies within the scope of the Federal Scientific Policy.

The fourth phase of the programme (1997–2000) was integrated into the 'Scientific Support Plan for a Sustainable Development Policy – PODO I'. Although sustainable development as such is not explicitly mentioned neither in the objectives nor in the strategy of the Treaty System, the underlying concept is in full keeping with the System. This can be gathered from the System's numerous measures and actions aimed at preserving the fauna and flora, establishing protected areas, preventing ocean pollution, eliminating waste or protecting

endemic animal species. As Antarctica is recognized by the Madrid Protocol as a 'natural reserve', in which all human activities are closely monitored, it can model for the broad-scale implementation of the sustainable development concept.

Apart from the budget for research projects within this phase, which amounted to about 6 MEUR, Belgium also contributed 0,5 MEUR to the cost of working of the European Project on Ice Coring in Antarctica (EPICA).

Contents
Marine biota and global change

3 AN INTEGRATED APPROACH TO ASSESS CARBON DYNAMICS IN THE SOUTHERN OCEAN

F. Dehairs et al.

4 SOUTHERN OCEAN GLOBAL ECOSYSTEM RESPONSE TO PHYSICAL AND TROPHIC CONSTRAINTS

J.-H. Hecq et al.

Contents of VOLUME II
Dynamics of the Southern Ocean and Palaeoenvironmental records

MEIOBENTHIC BIODIVERSITY AND FLUXES WITHIN THE ANTARCTIC BIOGEOCHEMICAL ENVIRONMENT

SANDRA VANHOVE[1]

HEE-JOONG LEE

JOHAN VAN DE VELDE

ANN DEWICKE

BERNARD TIMMERMAN

THIERRY JANSSENS

and

MAGDA VINCX

K.L. Ledeganckstraat 35
B-9000 Gent
Belgium

[1] Corresponding author E-mail : sandra.vanhove@rug.ac.be

TABLE OF CONTENTS

1

ABSTRACT

The aim of the program is to improve the understanding of the structure and dynamics of the Antarctic coastal and shelf marine ecosystem, the most complex and productive area in Antarctica, and likely the most sensitive to global environmental change. Central themes are the biodiversity and fluxes in the Antarctic ecosystem, with focus on the meiobenthic communities. An answer is searched on the following questions:
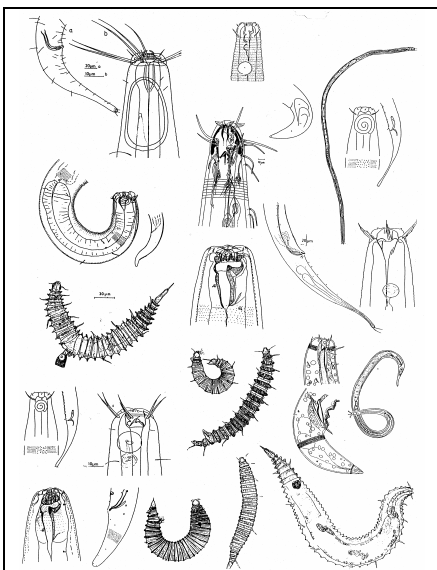
Subtheme 1: *The importance of production for meiofaunal biodiversity in the Antarctic coastal zone:* How tight is the temporal variability related to the ambient seasonal environment? Is the variability at Signy Island predictable? Are low Antarctic meiofaunal communities comparable to their high Antarctic counterparts?

Subtheme 2: *Biodiversity and recovery potential in the deep bathyal waters of the Southern Ocean:* What is the impact of ice scouring on the diversity of the meiofauna in iceberg disrupted sediments? How rapid and how does recolonisation processes start and proceed?
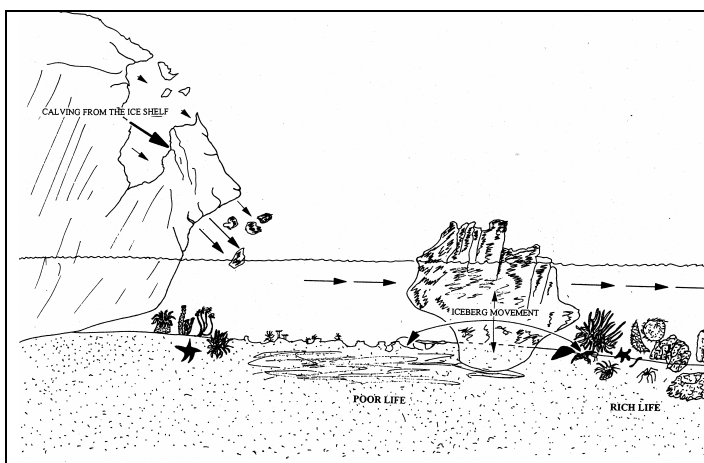
Subtheme 3: *The role of Southern Ocean meiobenthos in benthic pelagic coupling:* What is the ecological significance of free-living marine nematodes in Antarctic carbon cycling?

key words: meiofauna, nematodes, temporal changes, temperature and food, biodiversity, disturbance and recovery potential, stable isotopes.

2

<div style="border: 2px solid black; padding: 10px;">

GENERAL INTRODUCTION

</div>

The aim of the program is to improve the understanding of the structure and dynamics of the Antarctic coastal and shelf marine ecosystem, the most complex and productive area in Antarctica, and likely the most sensitive to global environmental change. The focus of the research is based upon the meiobenthic subsystem.

Meiofauna are benthic metazoans of intermediate size; these organisms are smaller than those which are traditionally called macrobenthos, but larger than the microbenthos (size boundaries based on the standardised mesh width of sieves with 1000 µm as upper and 31-42 µm as lower limits). Meiofauna occur in a wide diversity of habitats, from high on the beach to the deepest depth of the water body, from the softest mud to the coarsest shell gravel, and all those in between. They are also common as epiphytes on sea-grasses and algae, in sea ice and in various animal structures, as commensals or parasites. Meiofauna can be divided into temporary forms, which spend only their larval stages as part of meiobenthos (usually larvae of the macrofauna), and permanent forms, which throughout their life cycle have meiobenthic size. Nematodes, harpacticoid copepoda and turbellarians are the most important and common metazoan groups; they occupy more than 95% of the meiofauna in most sediment.

The interactive relations of meiofauna to other faunal elements and the contribution of meiobenthos to the energy flux through the benthic ecosystem can be assessed by measuring numerical parameters such as population abundance, biomass and production. The relevant biological parameters such as fecundity, natural and predative mortality, generation time, and other data on population dynamics are little known and highly variable. Compared to macrofauna, meiofauna usually have a low standing stock; but even in tidal flats and in the shallow subtidal, where macrofauna is relatively rich, higher turnover rates of meiobenthos generate a high production frequently exceeding that of the macrofauna. Energy flux diagrams have repeatedly been designed to quantify the energetic connections of meiofauna with other faunal compartments in the benthic system.

The close links between microorganisms, detritus and meiofauna integrate meiofauna into a detrital trophic complex. By preying on bacteria meiofauna maintains the bacterial populations in an exponential growth phase. Meiofauna bioturbation also activate geochemical fluxes. In particular the diffusion rate of oxygen becomes activated, enlarging the oxic habitats of aerobic bacteria and meiofauna. The grazing impact of meiobenthos on phytobenthos is also well documented. A high, but species-specific grazing pressure of meiofauna on for example diatoms is noted.

MARINE BENTHIC ANIMALS (ZOOBENTHOS)

MICRO   MEIO   MACRO
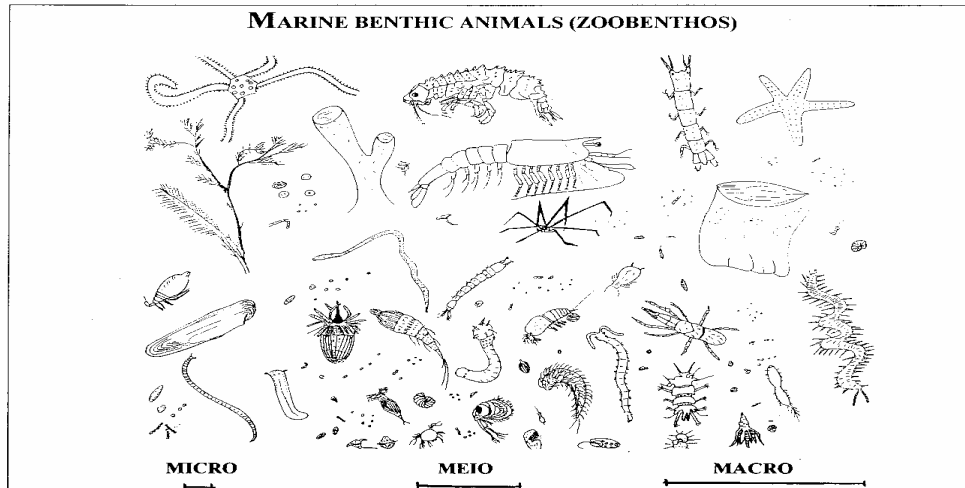
In conclusion, meiofauna are tightly linked to macro- and micro-organisms and to the biogeochemical benthic environment. The prime interest of our meiobenthic study is to substantiate –or disprove- the influence of the above described forces on meiobenthic distribution and functioning. By focusing on the extreme environment of Antarctica, several questions are tagged. The attention is put onto three subjects; e.g. 1) The importance of production for meiofaunal biodiversity in the Antarctic coastal zone, 2) Biodiversity and recovery potential in the deep bathyal waters of the Southern Ocean, and 3) The role of Southern Ocean meiobenthos in benthic pelagic coupling.

MARINE BIOTA AND GLOBAL CHANGE

MEIOBENTHIC BIODIVERSITY AND FLUXES WITHIN THE ANTARCTIC BIOGEOCHEMICAL ENVIRONMENT

ECOFUNCTIONAL BIODIVERSITY

The importance of production for meiofaunal biodiversity in the Antarctic coastal zone

Biodiversity and recovery potential in the deep bathyal waters of the Southern Ocean

The role of Southern Ocean meiobenthos in benthic pelagic coupling
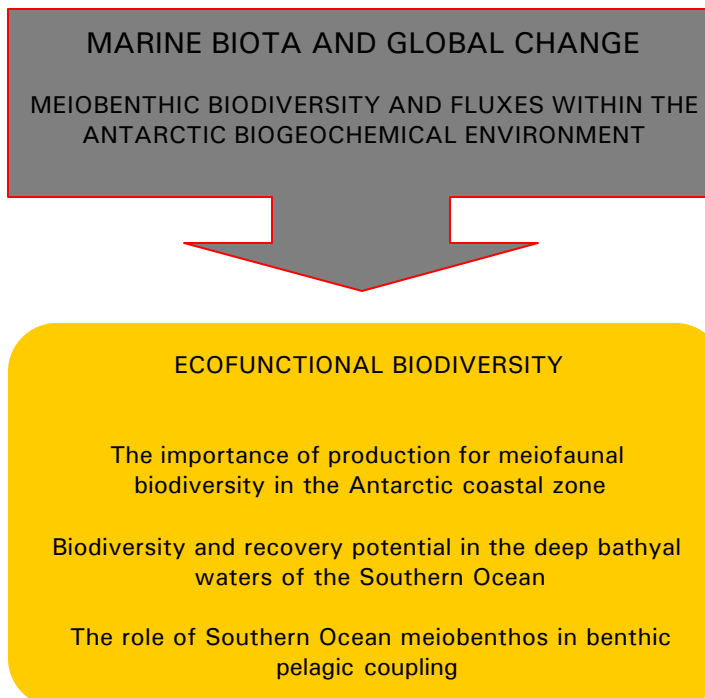
3

<div style="border:2px solid black; text-align:center;">

THE IMPORTANCE OF PRODUCTION FOR

MEIOFAUNAL BIODIVERSITY

IN THE ANTARCTIC COASTAL ZONE

</div>

3.1 INTRODUCTION

During the ANTAR III project the role of the meiobenthos was estimated by interpreting the data of production and metabolic processes in accordance with the determination of the biomass balance between the water column, sediment-water interface (nepheloid layer) and interstitial water. The resulting carbon budget proposed suggested that the meiofauna may provide an important pathway by which deposited and *in situ* organic matter is channelled through the differing benthic components and from the sediment back into the water column (e.g. about 13-42 % of the mean total benthic oxygen demand and 22% of the annual benthic organic production was channelled through the nematode community) (Vanhove et al. 1997). The results stressed the possibility of tight coupling between the benthos and the depositional pelagial.

The extremely seasonal input of food from the sea ice and the water column is considered to be of great importance (Clarke 1988, 1990). Episodic availability of food requires adaptive responses, which impose specific constraints on the types of organisms able to exploit such resources (Pearson and Rosenberg 1987). The current question arises how does the interstitial benthic fauna behave throughout the Antarctic seasons.

Over the last few years, it has become increasingly apparent that the Southern ocean zone exhibits also marked variability at interannual time scales. This variation, whether arising from external forcing or generated by intrinsic variability, manifests itself in changes in patterns of sea-ice distribution, sea-surface temperature, and atmospheric pressure. It has clear consequences for the physical system, and in this turn impinges on the marine ecosystem. (Hofmann and Priddle 2000).
Within the frame of the current ANTAR-4 project we tried to find an answer on the following questions:

1. *How tight (months, weeks, days) is the temporal variability related to the ambient seasonal environment?* Here fore the meiobenthos was monitored regularly along the Antarctic season to detect a response of the fauna to pelagic input from primary production.

2. *Is the seasonal variability at Signy Island predictable?* Two time series at the same site should enable us to detect how big interannual variation within the meiobenthos is.

3. *Are low Antarctic meiofaunal communities comparable to their high Antarctic counterparts?* Samples from Rothera (e.g. 67°S) will give information about the impact of seasonal primary production on the meiofaunal community structure at higher latitudes, south of the Antarctic Circle.

3.2 MATERIALS AND METHODS

Metazoan meiofauna and the surrounding sediments were studied as part of an integrated British research programme (e.g. Antarctica 2000, Ecological and Physiological adaptations, NERC) at Signy Island, South Orkney Islands, Antarctica (60°43' S, 45°38' W) and Adelaide Island (Rothera base; 67°34' S, 68°08' W).

Meiofaunal sampling in the low Antarctic (Signy Island) was done fortnightly in 1991-1992, covering two austral winters and the intervening summer; and even more regularly in 1994-1995, covering an entire annual cycle. In the high Antarctic (Rothera) 3 sites were sampled during the austral summer of 1998 (between 28.01 and 31.01.'98), e.g. North Cove, 31 m, North Cove, 11 m, Grifter Pipe, 5 m. The specific methods used for meiofaunal treatment were described in detail in Vanhove et al., (1997, 1998, 2000).

The pelagic environment off the Signy site has been extensively monitored revealing a long-term dataset of seawater temperature, ice cover, macronutrients and chlorophyll standing crop (Whitaker 1982; Clarke et al. 1988; Leakey et al. 1994; Clarke and Leaky 1996). The data for the first period of investigation (time series 1991/92) were available from British Antarctic Survey (pers. comm., A. Clarke). Particulate organic matter (carbon, nitrogen), pigment (chlorophyll *a*, chlorophyll *c*, fucoxanthin, β-carotene) and dissolved organic carbon (DOC) were monitored in the sediments (for methods see Vanhove et al. 2000).

Environmental impact was tested with a Spearman Rank correlation analysis (Sokal and Rohlf 1981) on meiofaunal variables and nematode parameters, sediment features and water column variables. For all statistical analyses, the .05 significance level was used as the rejection value by convention.

3.3 RESULTS AND DISCUSSION

3.3.1 The response of the meiofauna to pelagic input from primary production

3.3.1.1. Environment

In essence pelagic activity at Signy Island occurs through a summer bloom (Dec and Jan) of large diatoms and colonial forms, superimposed on a less intense but longer nanoflagellate bloom. At the heart of the winter nanoplankton chlorophyll concentrations often exceed the microplankton chlorophyll concentrations that are generally very low (0.05 mg m^{-3}) (Clarke and Leaky 1996).
However, two unusual summer seasons characterized the current sampling period (fig.1):
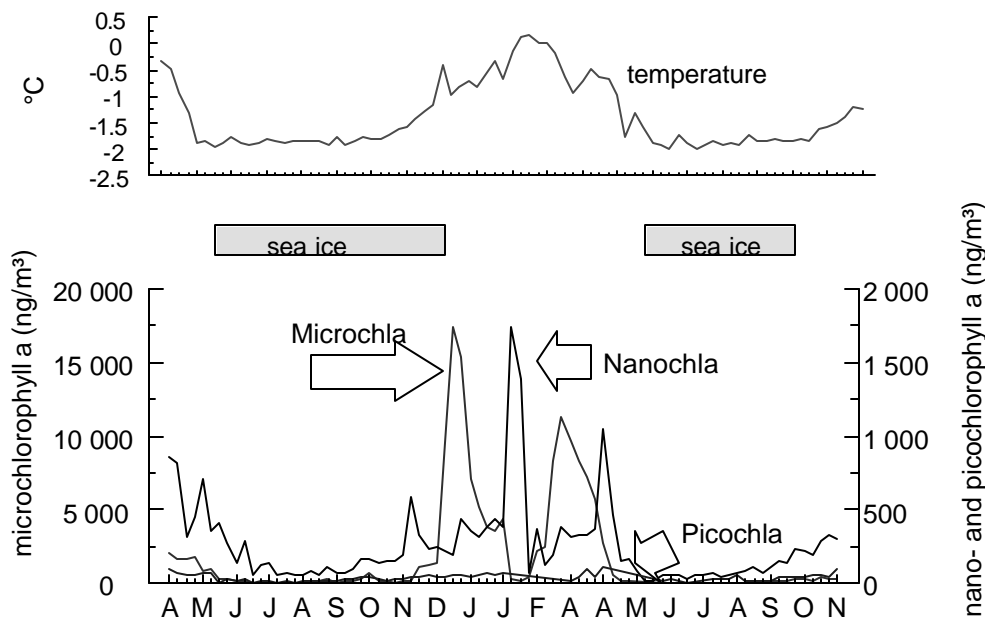
Figure 1: Variation in sea-ice cover (indicated by shaded bars), temperature and phytoplankton biomass from April 1991 to November 1992 at Signy Island (data from British Antarctic Survey)

1) Next to the normal diatom bloom in the summer season of 1990/91 (16 mg m^{-3}), a small supplement of microchlorophyll (2.1 mg m^{3}) was added to the early winter water. Having a different species composition from the spring bloom, this mini-bloom peaked in the period preceding our sampling (in March 1991). Superimposed, there was a long-lived nanoplankton production prevailing from early summer 1990 to early winter 1991;
2) The 1991/92-summer season was the only since 1972 that had two consecutive microchlorophyll blooms with peaks of 17.5 and 11.5 mg m^{-3} in, respectively, early summer (Nov/Dec) and autumn (Mar/Apr). Furthermore, two nanoplankton peaks (1.75 and 1 mg m^{-3}) before the appearance of sea-ice mirrored the two blooms in the microplankton size fraction (Clarke and Leaky 1996).

The sediments consisted of moderately sorted, very fine sands (62-125 µm), with little shifting of particle sizes (median grain size range: 73-95 µm; standard deviation: 0.71-1.00; both of total sediment) and a mean organic loading of 0.5 %C and 0.03 %N. Dissolved organic carbon (DOC) varied between 340 and 1040 mg l^{-1}.

Seasonality in the organic carbon and nitrogen readings from upper (0-2 cm), middle (2-5 cm) and deeper (5-10 cm) sediment horizons (fig. 2) showed-although not very clear, and especially in the upper layers- low carbon values during the ice-covered period (0.3-0.5 %), and apart from the late winter of 1992, peaks (0.9-1.1 %) were closely associated with the disappearance of the fast-ice.
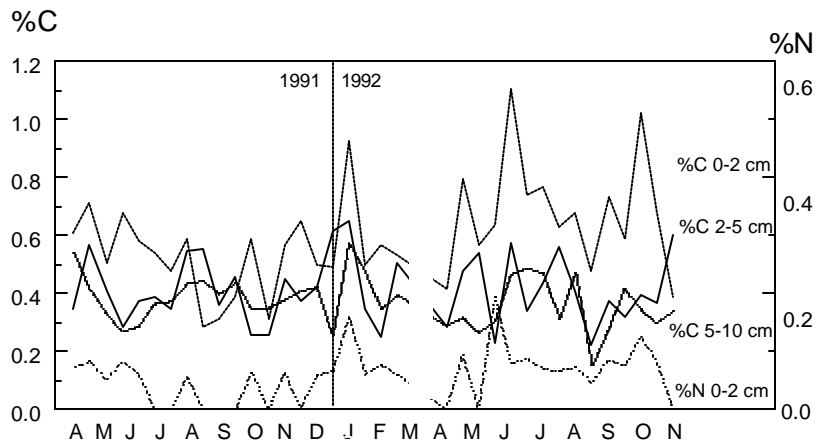
Figure 2: Variation in organic carbon (mass%) in the 0-2, 2-5, 5-10 cm core sections and organic nitrogen (mass%) in 0-2 cm horizon from April 1991 to November 1992 at Signy Island

Chloropigment variation (table I) synchronized organic matter fluxes: being fairly stable from May till August (austral winter values of about 30 µg Chl-a g[-1] sediment), the concentrations suddenly decreased with an order of magnitude at the middle of the ice-covered period (Sep 1991), and then gradually increased again to a maximum of 60 µg Chl-a in summer (Jan 1992). Albeit DOC concentrations were very variable during the entire monitored period, a very low value in Sep 1991 (342 mg l^{-1}) paralleled late winter minima of the other trophic sources.

A spearman rank analysis (table II) expressed correlations between the benthic pigments from our study, and sediment trap and water column variables from the study of Clarke and Leaky (1996). This held not for total organic matter (TC, TN), and correlations occurred mainly with the nanochlorophyll fraction ($\approx$ flagellates). Peaks of benthic food followed also maximum settlement rates of chlorophyll and phaeophytin in the sediment traps ($\approx$ diatoms) with, however, a delay of a few weeks (not depicted).

All together this indicates that production and deposition events described above can be tracked in the sediments, with some weeks of delay for diatom blooms, and no visible delay for flagellate blooms, the latter mainly due to its long production period. This confirms the findings that pelagic rapid growing cells, including diatom resting

spores and sea-ice algae, settle periodically from the water column without being grazed *in situ* (Gilbert 1991a; Nedwell et al. 1993), in contrast to the slowly, almost continuously, settling pelagic flagellates (Smetacek 1984).

Table I: Dissolved organic carbon (mg. l^{-1}) and chloropigment concentrations (µg. g^{-1}) in the sediments of Factory Cove during the 1991/1992 time series.

	DOC		Chlorophyll a		Fucoxanthins		Chorophyll c		Beta-carotenes	
	mean	SD	mean	SD	mean	SD	mean	SD	mean	SD
1991										
27/04	1037	(571)								
14/05			26	(2.6)	13	(2.6)	7	(1.1)	9	(1.7)
28/05	528	(118.2)								
11/06			31	(13.3)	14	(5.1)	10	(8.3)	10	(3.4)
26/06	630	(365.4)								
12/07			18	(4.5)	7	(1.4)	4	(4.2)	5	(1.0)
28/07	938	(1048)								
10/08			28	(2.6)	13	(1.2)	7	(0.7)	9	(0.8)
23/08	639	(248.6)								
05/09			3	(0.3)	2	(0.0)	1	(0.1)	1	(0.0)
20/09	342	(182.7)								
04/10			14	(14.1)	6	(5.8)	4	(3.5)	4	(3.9)
17/10	851	(768.5)								
14/11	594	(56.4)								
28/11			27	(6.1)	12	(2.5)	8	(2.0)	8	(1.7)
13/12	919	(591.2)								
27/12			23	(20.4)	13	(6.3)	8	(4.2)	9	(4.2)
1992										
10/01	598	(663.7)								
22/01			58	(16.2)	28	(7.8)	16	(3.4)	19	(5.2)
09/02	786	(693.3)								
26/02			49	(33.5)	26	(11.6)	13	(6.5)	18	(7.8)

Table II: Probability levels of the Spearman rank correlation between detrital sources in the sediment (Chl-a, fucoxanthin, Chl-c, ß-carotene, organic carbon and nitrogen) and respectively sediment trap (chlorophyll, phaeopigments, dry mass, ash free dry mass, carbon and nitrogen) and water column (micro Chl-a, micro phaeopigments, nano Chl-a and nano phaeopigments); N=10; sediment trap and water column data were obtained from Clarke (BAS, Cambridge)

	Sediment trap						Water column			
	Chl	Phae	Dw t	AFDM	N	C	micro Chl-a	micro phaeo	nano Chl-a	nano phae
Chl-a		+	+							+ +
Fucoxanthins			+		+			+	+	+ + +
Chl-c	+	+ +	+						+	+ +
ß-carotenes			+		+			+	+	+ + +
TOC										
TON										

p ≤ .05: +   .05 < p ≤ .01: + +   .01 < p ≤ .001: + + +

By converting Chl-a data to carbon equivalents (C: Chl-a of 40:1, de Jonge 1980), the fraction of sediment organic carbon represented by algal material was calculated (table III). Low values in Sep (4%, Sep 5) were indicative for a low nutritional status of the environment during late winter, whereas in summer (Jan 22), when algal cells were actively dividing, nearly 50 % of the organic record in the sediments was induced by chlorophyll input.

Table III: Calculation of the percentage of the POC pool attributed to pigments in the sediments of Factory Cove; values of organic carbon were only from the upper two centimetres of the sediment core.

	Chl-a mg c g^{-1}	TC Mg c g^{-1}	Chl-a : TC %
14/05/1991	1.04	7.092	14.7
11/06/1991	1.24	6.757	18.4
12/07/1991	0.72	5.404	13.3
10/08/1991	1.12	5.898	19.0
05/09/1991	0.12	3.126	3.8
04/10/1991	0.56	5.869	9.5
28/11/1991	1.08	6.513	16.6
27/12/1991	0.92	4.882	18.8
22/01/1991	2.32	4.965	46.7
26/02/1991	1.96	5.31	36.9

Despite the high contribution of algae, still a great deal of the POC pool was not covered, and C:N ratio's (19±9.4) based on weight values of TN and TC in the sediments were high compared to similar ratios in the sediment traps (7±1.1). The latter are indicative of phytoplankton derived organic matter (Tyson 1995), which in turn reflect some state of detrital decomposition in the sediment. Such processes occur very rapidly by microbial oxidative respiration and sulphate reduction, tightly following the seasonal trace of depositional fluxes (Nedwell et al. 1993). Measured by a bioassay, peak concentrations of available organic matter, occurred at roughly the same time as detrital transmission of primary production to the sediment surface, namely in Apr 1991, Dec 1991 and Mar 1992 (each 9% of total carbon, Walker 1993), and presumably in May 1992 and Oct/Nov 1992. In late winter the concentrations of available carbon were highly suppressed and remained stable at about 7% of total carbon (Walker 1993). This was the only period of the year occurring in a state of trophic resource limitation.

Another part of the organic matter recovered must have been deviated also from burial of inactive algal components and inefficient aerobic breakdown of primary food sources as a consequence of anaerobic conditions (Jφrgensen 1982). Especially in the deeper layers (from 2 cm on) detritus was refractory (Vanhove et al. 1998). In these benthic horizons background levels of organic matter were high all year round and made detection of seasonality virtually impossible. Hence temporal signals were highly damped below the surface of the sediments and essentially constant throughout the year.

3.3.1.2. Meiofaunal responses to the seasonal dynamics in the Antarctic environment

Meiofaunal density and biomass, fig.3

As to the hypothesis of Findlay that systems receiving pulses of directly available detritus should exhibit population fluctuations closely tied to the rate of food supply (1982), a strong impact on the meiofauna structure and dynamics was highly suggestive.
Early winter (May-Jun) recordings of total density and biomass in 1991 were very high and distinct from other seasons (respectively, p < .05 and < .001). This was shortly after the minibloom of nanoflagellates (see earlier) and high carbon availability in the sediments. Stock sizes declined sharply to a minimum in the middle of the ice-covered period (p < .05), coinciding with the winter stop in primary production. Depauperation occurred until only 10% of the initial peak density was reached, and slightly more than a poor 1% of the initial total biomass remained. So, it is reasonable to conclude that fresh food availability was limiting for the meiofauna population.
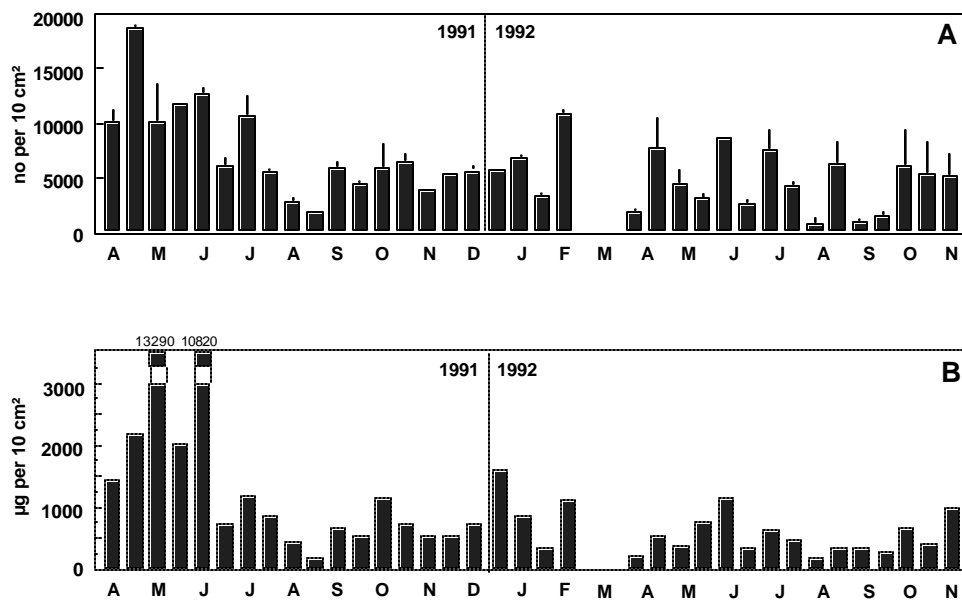
Figure 3: (A) Total density (ind. Per 10 cm² ± 1SD, n=2) and (B) total biomass (µg per 10 cm²) from April 1991 to November 1992 at Signy Island

However, two remarks need more attention: (1) even when stocks were drastically depressed, minimum figures (1.9 10^6 ind. and 0.19 g dwt m^{-2}, 5 Sep 1991) were still comparable to average values in many shallow soft bottom communities (see tables Rudnick et al. 1985), and (2) the winter, rather than being a long period of low stocks, was confined to at most two months during late winter. Both features were probably interconnected. Seemingly, population sizes during 'burst' periods were so high that reduction, although occurring at a fast rate, was not extreme enough to depauperate

the meiofauna communities before a new input of fresh food in spring made a new increase of the population size possible.

The main reason for this has to be searched in the uncommon character of the pelagic environment during that season (*e.g.* 1990/91). As earlier described the strong seasonal variation in the pelagic of Signy Island with the short bloom of large microphytoplanktonic diatoms in mid-summer was essentially prolonged by a second mini-bloom, superimposed on a long-lived nanophytoplankton production, both inducing a food input into the system to May/June in early winter.
This confirms the findings of Barnes, that despite the brevity of the summer peak in diatom cell numbers, the levels of nanoplankton occurring throughout much of the year may be sufficient for many benthic suspension feeders, leaving only a very short period of inactivity in their feeding behaviour during winter (Barnes and Clarke 1994).

A new though less obvious density/biomass increase was registered at the start of the summer (early summer records of density and biomass were not significant different from the other seasons), followed by the establishment of a 'dynamically fluctuating equilibrium' slightly above 5000 individuals and 500 µg dwt per 10 cm². By the complete disappearance of fast-ice (Dec 1991) strongly oscillating values characterized the meiofauna communities in Jan and Feb.

During the second year total density did not obscure a clear temporal pattern ($p > .05$). Seasonality in total biomass was less pronounced than in the previous year, though again higher total biomass values in late summer (Jan/Feb) in the trace of the first diatom bloom and high bio-availability of the food in the sediments (Walker 1993), followed by elevated biomass in early winter, lagging the second autumn bloom, were again confirming the response of meiofaunal standing stock to the ambient environment. However, fluctuations were much higher resulting in a less pronounced seasonal pattern, and probably were a result of two blooms, closely following one another (Clarke and Leaky 1996).

As a consequence of their high relative contribution to total numbers, nematodes strongly followed the pattern of total density (fig.4), though parallel trends between the two years were stronger. The harpacticoid copepod pattern was sinusoid. Maxima of adult copepods were situated on Apr 27 of 1991 and on Feb 26, Jun 13 of 1992. Nauplii and copepodites were present throughout the year, but occurred in highest proportions during the summer season (*e.g.* Dec 27 until Feb 26 1991/92). Harpacticoid copepods followed the patterns of water column productivity with high densities in productive periods and low numbers in late winter. They showed immediate responses to the temperature and nanochlorophyll fraction in the seawater, and were related with a time delay to all food components in the water column and to pigments in the sediments. The combination of immediate and retarded responses made the harpacticoid copepods as the meiofauna taxon the most tightly associated with temporal events of fresh food supply. The observations were more or less similar to those in literature. Generally, the periodicity of juvenile harpacticoid copepods was related to late winter/early spring events (nauplii in the current study were also highly variable in densities during late winter prior to the blooms), and adults reached their highest densities during summer (Kauffman 1977; Rudnick et al. 1985; Schizas and Shirley 1996). Consistent among these and other

studies was that this taxon was strongly associated with fresh inputs of food into the system, often with time lags of about two months.
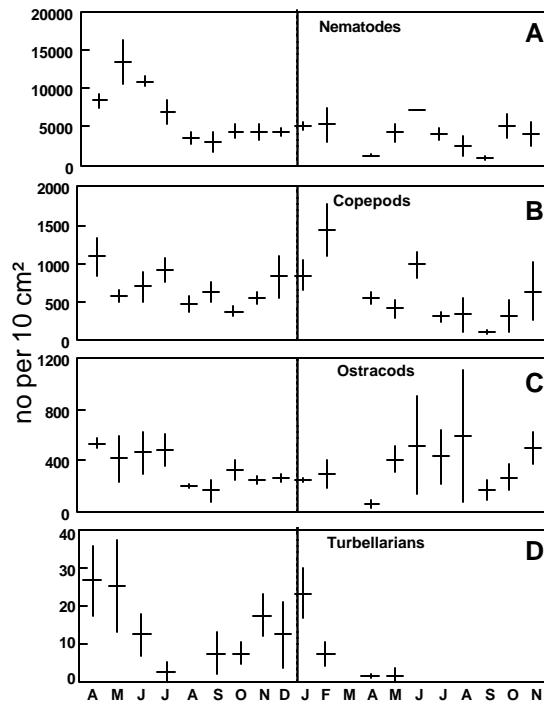
Figure 4: Abundance (ind. per 10 cm² ± 1 SD, n = pooled number of replicates per month) of the 4 major taxa from April 1991 to November 1992 at Signy Island

The ostracods exhibited no obvious temporal patterns at all, mainly as to the high variability between the replicates (*e.g.* the coefficient of variation ranged between 2 and 106%, with an average of 44%). It is, however, known that some ostracods occur year-round and others may have one or two population peaks each year, either in summer of winter. They endure the unfavourable season either in special larval stage or as eggs or as adult (Higgins and Thiel 1988).

A distinct trough in turbellarian density was indicating that they were vulnerable to the unfavourable features of the Antarctic winter. Their affinity to higher food levels in summer was confirmed by the positive correlation of their densities with water column chlorophyll.

Nematode body size spectra and genus densities

The nematode community has been assigned to a body size class distribution (fig. 5). The class divisions selected were regular between 0 and 2.5 µg dwt. An additional size class was chosen for animals larger than the highest class.

8 biomass classes:
0-0.15 0.15-0.25 0.25-0.35 0.35-0.45 0.45-0.55 0.55-1.5 1.5-2.5 >2.5 µg dwt
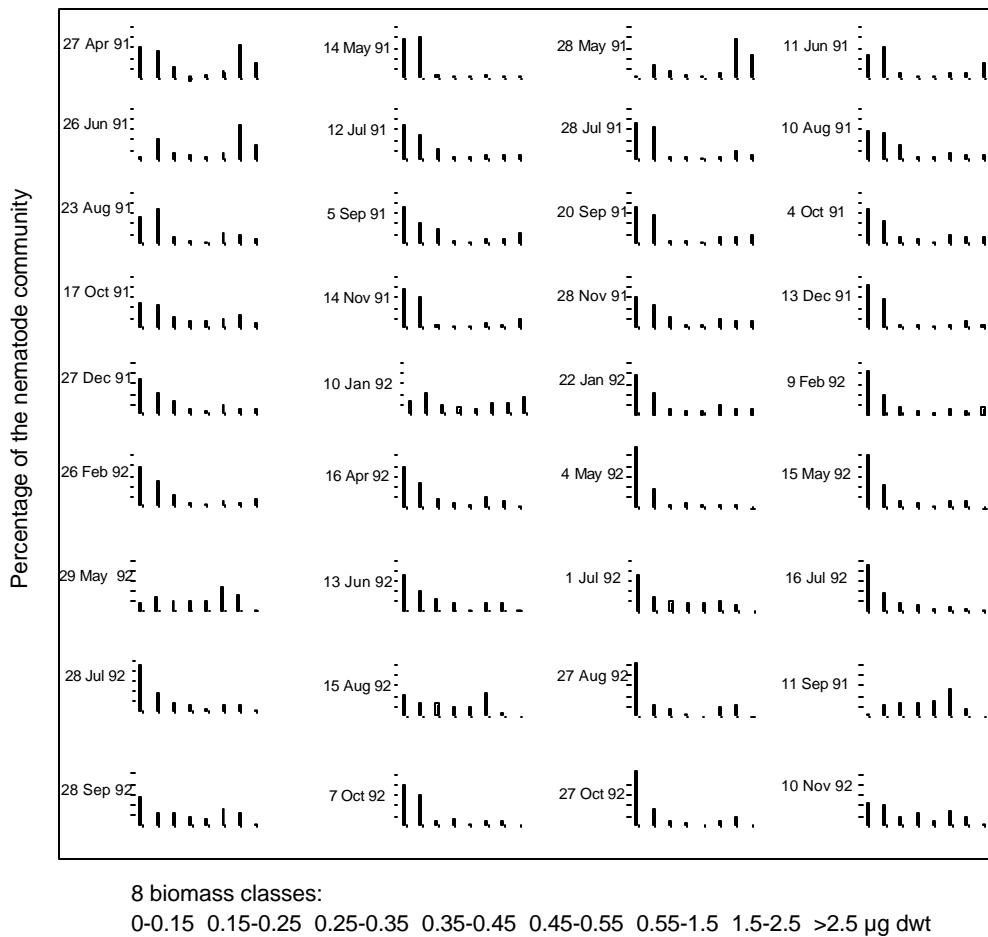
Figure 5: Individual biomass distribution all community members from April 1991 to November 1992
at Signy Island

Cohort separation has neither been achieved when looking to the individual populations of the six predominant nematode genera separately (graphs not depicted). This is an indication for the absence of a seasonal signal in life history patterns.

The numerical abundances of the predominant nematode genera expressed as a percentage of the total were also highly variable during the course of the time study (fig. 6).
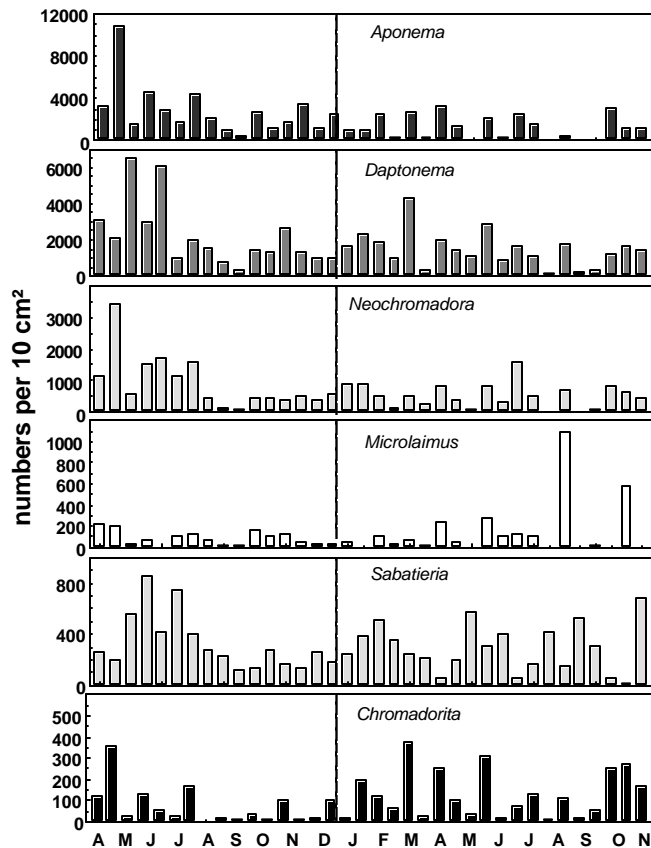
Figure 6: Abundance (ind. per 10 cm² ± 1 SD, n = pooled number of replicates per month) of the 4 major taxa from April 1991 to November 1992 at Signy Island

No clear seasonal trend was discernible, as within short periods (≈ weeks) genus densities of *Aponema*, *Daptonema*, *Microlaimus* and *Chromadorita* augmented to episodic peaks irrespective of season (ANOVA, p < .05). Only *Sabatieria,* and to a lesser degree *Neochromadora,* deviated slightly from this heterogeneous trend by revealing a sinusoid density profile during the first year (ANOVA on differences between monthly absolute and relative numbers of these two genera, p < .05).

In early winter 1991 virtually all genera, among which the predominating *Aponema*, *Daptonema*, *Sabatieria* and *Neochromadora*, showed significantly deviating peaks in absolute numbers (and hence, also the trophic groups to which they were categorized). Each of them, probably, has developed specific adaptations to exploit the short-term deposition pulse of the highly diverse plankton communities and subsequent elevations of organic matter concentrations and microbial activity in the sediments.

The combination of all trophic sources produced energy for the benthic fauna during most of the year. This lead to discontinuous nematode community changes in which, depending on the availability of each trophic source, nematode genera responded by some degree of competitive interaction (an example was *Aponema* demonstrating

highly fluctuating densities in early winter 1991, early summer 1991 and late winter 1992). Even during midwinter nematode community composition did not change. Sufficient energy probably accumulated on the bottom (food reserve?), so that most genera could accommodate the winter months by slightly alternating their trophic strategy. Such external nutritional reserve can be important for all nematodes as they lack internal reserves (Giere 1993).

Correlation analyses

Correlations with the environment mainly pointed towards nanochlorophyll production in the water column (Vanhove et al. 2000). When shifting the environmental variables one and two months later, and repeating the spearman rank analysis on the same meiofaunal parameters (table IV), several delayed responses of meiobenthos to the ambient environment appear. Within the pelagial all chlorophyll categories (micro, nano and pico) were responsible for the high number of significant correlations. The possibility of seasonal time lags in the assimilation of phytodetritus by benthic fauna is surprising because phytoplankton lack complex structural materials, such as lignin (Tenore et al. 1982). However, some mechanisms may exist that delay the mineralization of phytodetritus (e.g. depression of metabolic activity by low temperatures and/or anoxic conditions) in the current biotope.

Although correlations between the meiofauna and the benthic environment existed, they represented only a very limited proportion of all possible relations, and they were rather scarce when compared to the many correlations with water column variables. The most likely reason for the apparent lack of response to benthic organic food sources has to be searched in the quality, rather than the quantity of organic detritus. As recently produced and deposited detritus is more readily assimilated than older refractory organic carbon (Rudnick 1989), the organic matter in the sediment is a bad indicator of food input to the bottom. Because of this, it is very difficult to relate density or biomass patterns of meiofauna with organic matter concentrations in the bottom. On the other hand, correlations with pigments were more obvious. Unfortunately the data did not cover the entire study period, and intervals between subsequent monitoring were probably too long to discover all possible relationships.

Table IV: Summary of the Spearman Rank correlation analysis between meiofauna and delayed environmental variables

1 MONTH DELAYED (n=18)		WATER COLUMN						SEDIMENT							
		Micro chla	Micro phe	Nano chla	Nano phe	Pico chla	Pico phe	Chl a	Chl c	Fuco	B-car	DOC	OrgC	OrgN	C:N
MEIOFAUNA															
	Amphipods														
	Bivalves														
	Adult harpacticoids				+ +										
	Juvenile harpacticoids														
	Total harpacticoids	+		+ +				+	+ +	+ +	+ +				
	Nematodes	+ +		+		+ +									
	Ostracods												+		
	Turbellarians	+				+									
	Total meiofauna	+ +		+		+ +									
Genera															
	Daptonema	+ +		+	+	+ + +									
	Aponema														
	Neochromadora														
	Sabatieria														
	Microlaimus														
	Chromadorita	+	+ +		+ +	+ +	+								
2 MONTHS DELAYED (n=17)															
MEIOFAUNA															
	Amphipods														
	Bivalves							-							
	Adult harpacticoids	+ + +	+ +	+ +	+ +	+									
	Juvenile harpacticoids														
	Total harpacticoids		+ +	+		+ +									
	Nematodes					+									
	Ostracods														
	Turbellarians							-	-	- -	- -				
	Total meiofauna	+				+ +									
Genera															
	Daptonema														
	Aponema					+			-	-	-		-		
	Neochromadora					+ +									
	Sabatieria														
	Microlaimus														
	Chromadorita														

Nematode life history patterns

In a seasonal environment, wherein trophic resources fluctuate significantly, different possible adaptive life strategies in nematodes can predominate: seasonality

in reproduction with the number of generations restricted to particular seasons (cf. the univoltine *Enoplus communis*, the bivoltine *Viscosia viscosia*, or the polyvoltine *Theristus setosus*), or life strategies completely uncoupled from environmental events (cf the continuous reproduction of *Microlaimus turgofrons*). The latter is the most common. As the population increases, the successive generations will come to overlap and the amount of overlapping will increase progressively as times goes on (Heip et al. 1985).
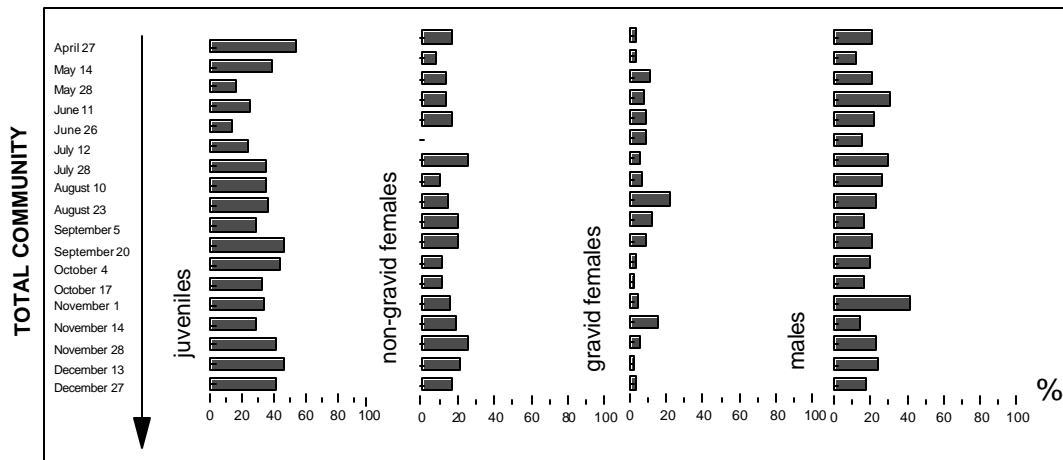
Figure 7: Relative frequency distribution (%) of four life stages within the nematode community during a nine months period in 1991. Data presented are the mean of two replicate cores

Nematode reproduction looked continuous as the four life history categories were encountered throughout the year and juveniles dominated within the range of 14-59% (mean: 42 %)(fig. 7). This confirmed with population life-history studies of nematodes in temperate regions where many nematodes reproduce continuously throughout the year (Heip et al. 1985).

Maxima in reproductive females (gravid specimens with eggs in uterus) (*e.g.* during Aug 23 and Nov 14) were weakly followed by maxima in juveniles (*e.g*. during Sep 20 and Dec 13). Assuming that reproductive activity occurred more during these relatively low nutritional periods, it could be possible that reproduction before the season of bulk supply was an advantageous life strategy to cope with periods of low energy production. Such strategy has been found in many Antarctic benthic invertebrates (Clarke 1988), and is explained by the fact that the reproduction facet of the life cycle is generally characterised by a reduced activity, stoppage of growth, and cessation of feeding. In addition, young stages develop by the end of the low food period enabling them to take advantage of the new blooms of the next productive season.

Downloading this demography study to the six numerically predominant genera (fig. 8) similarly showed rather unclear fortnightly population patterns with high heterogeneity on a small time scale. No clear cohorts could be recognised. The only

consistent observation was that the percentage juveniles were lower during winter (for *Aponema*: May, *Daptonema*: May/Jun, *Neochromadora*: May/Jun, *Sabatieria*: Jul).
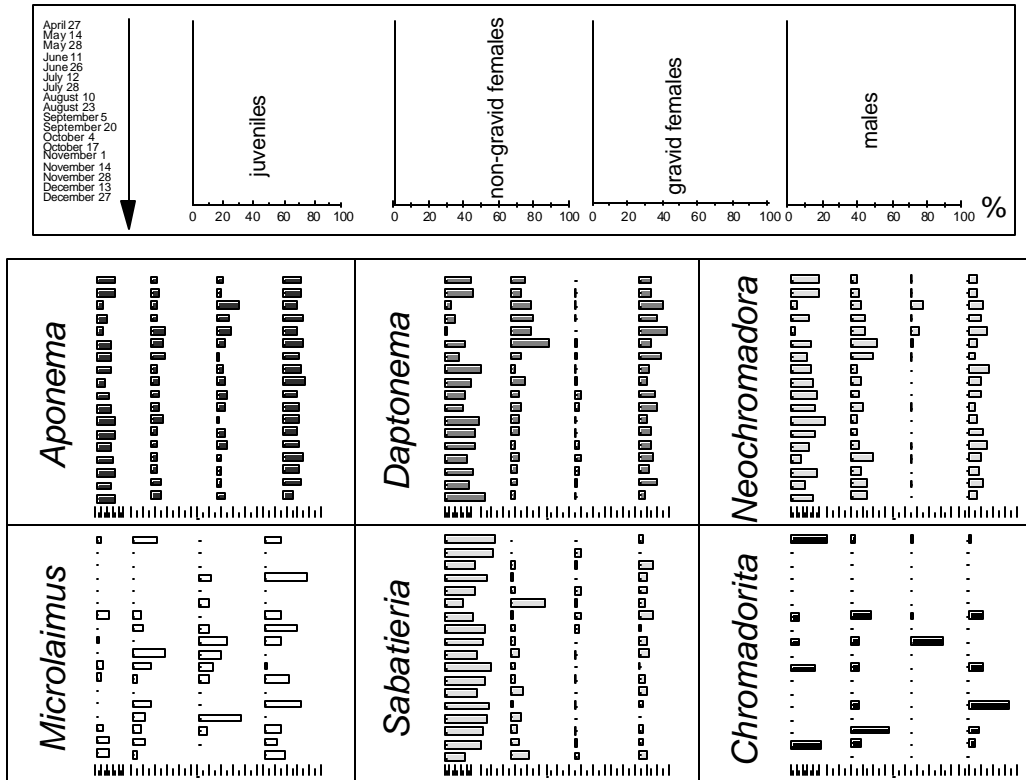
Figure 8: Relative frequency distribution (%) of four life stages (juveniles, non-gravid females, gravid females, males) within the six predominant genera (*Aponema, Daptonema, Neochromadora, Microlaimus, Sabatieria, Chromadorita*) during a nine-month period in 1991. Data presented are the mean of two replicate cores.

3.3.2 Interannual variability within the meiobenthos from Signy Island

3.3.2.1. Meiobenthos in a second time series at Signy Island (e.g. from January 1994 to January 1995)

In accordance with the first time series a very high temporal variability on a short time scale of a few days is observed (fig. 9). This occurred between the extremes of 854 (11 Jun 1994) and 21 840 (25 Jan 1994) ind. per 10 cm². The maximum coincided with the peak of summer primary production and the minimum with the annual winter stop (although a short period of elevated density was again visible between 12 May and 25 May). Strikingly the low abundances occurred when higher taxon numbers (diversity) were observed (e.g. on 22 May, 2475 ind. per 10 cm² and 14 meiofauna

taxa) and on 15 Jun 1994, 1272 ind. per 10 cm² and 11 meiofauna taxa). Among 17 taxa recovered the nematodes dominate, followed by harpacticoid copepods, ostracods and crustacean nauplii (fig. 10).
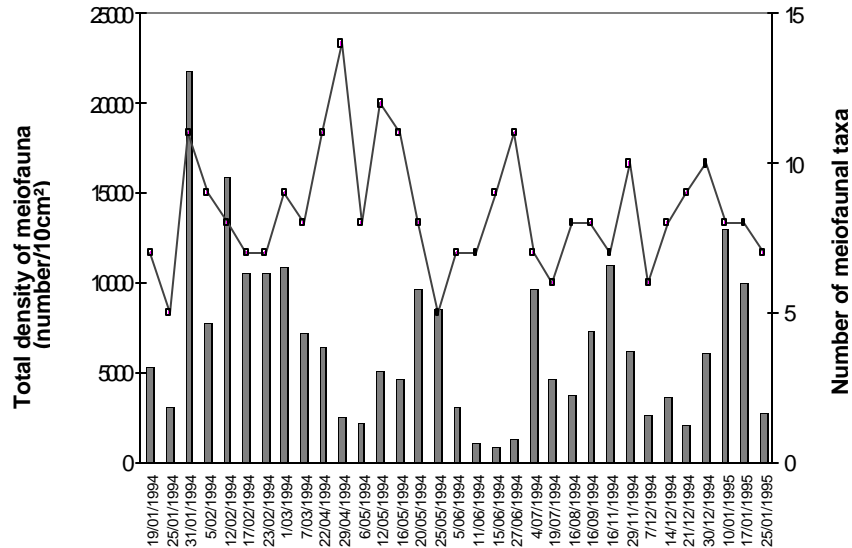
Figure 9: Fluctuations of total meiofaunal density (bars) and taxon number (line) during the period from January 1994 till January 1995 at Signy Island
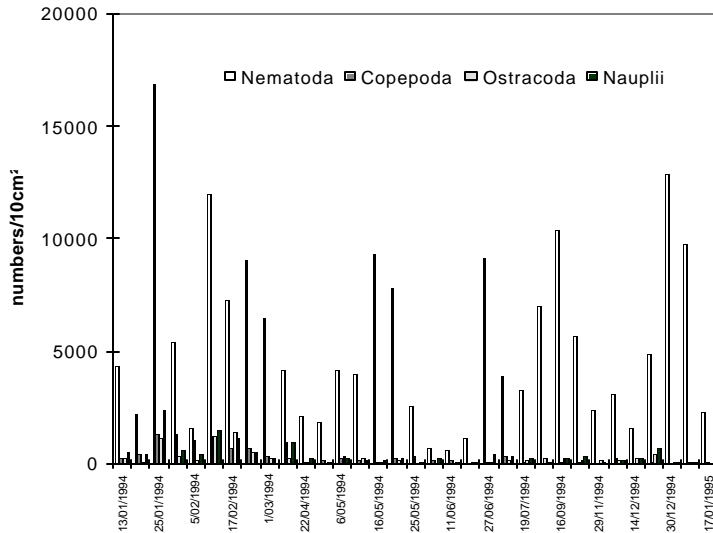
Figure 10: Appearance of the four major meiofaunal groups during the period from January 1994 till January 1995 at Signy Island

3.3.2.2. Relationships with the environment

The sediments consisted, as during the first time series, of moderately sorted, very fine sands (62-125 µm). Only very little shifting of particle sizes were found during the entire period of study. Chl-a values varied between 5 and 124 µg.g^{-1} with very high oscillations during summer and autumn 1994 and more stable values during late winter (Sep). Organic carbon varied between 0.2 and 1.1 %. Highest values were recorded during the summer. C: N ratio's varied between 5.7 and 12.1, without clear seasonal trend.

A Spearman Rank analysis between the environmental and meiofaunal variables revealed that, from the four most dominant meiofaunal taxa, only the copepods and their nauplii were significantly correlated with sediment properties (table VI). This confirms to the findings in former time series study.

Table VI: Results from the Spearman Rank correlation analysis between meiofaunal taxon densities and sediment properties during the second time series (only the significant relationships were retained).

		Valid N	Spearman R	P-level
Adult copepods	Chl-a	31	0.355	0.049
	%Carbon	33	0.482	0.004
	%Nitrogen	33	0.502	0.003
Juvenile copepods	%Nitrogen	33	0.402	0.020

3.3.2.3. Interannual variability at Signy Island

Many environmental factors at Signy Island change greatly from year-to-year and are associated with regional scale variability in the Weddell Sea basin.

Sea ice	Duration (days)	Thickness (cm)
1991	215	30
1992	115	77
1993	100	40
1994	74	55
1995	74	NA

Sea temperature and linked to it, sea-ice formation and break-up, for example, are highly variable on interannual base (Murphy et al. 1995; Clarke and Leaky 1996).

Sea-ice characteristics on their turn impact primary production. In general, the bulk of the phytoplankton production (microplankton consisting of larger diatoms, chains of globular clusters of cells) occurs over a small period of time, rather constantly around December and January (Clarke and Leaky 1996). Over 11 years peak chlorophyll standing crop varied from 2.2 to 41.6 mg.m^{-3} and integrated biomass varied by a factor of 25. The duration of the bloom varied from only 41 days in 1981/82 to 170 days in 1976/77 (Clarke and Leaky 1996). The 1991 and 1992 seasons, for example, showed also a distinct autumnal bloom (as seen earlier) (fig. 11). In 1993 peak microplankton levels of

almost 40000 ng Chl-a per day were measured and in 1994 one single, but long bloom was observed. Also nanoplankton chlorophyll concentrations, which often exceed microplankton chlorophyll concentrations, show a marked year-to-year variability. In conclusion, the size of the summer bloom varies greatly between years.
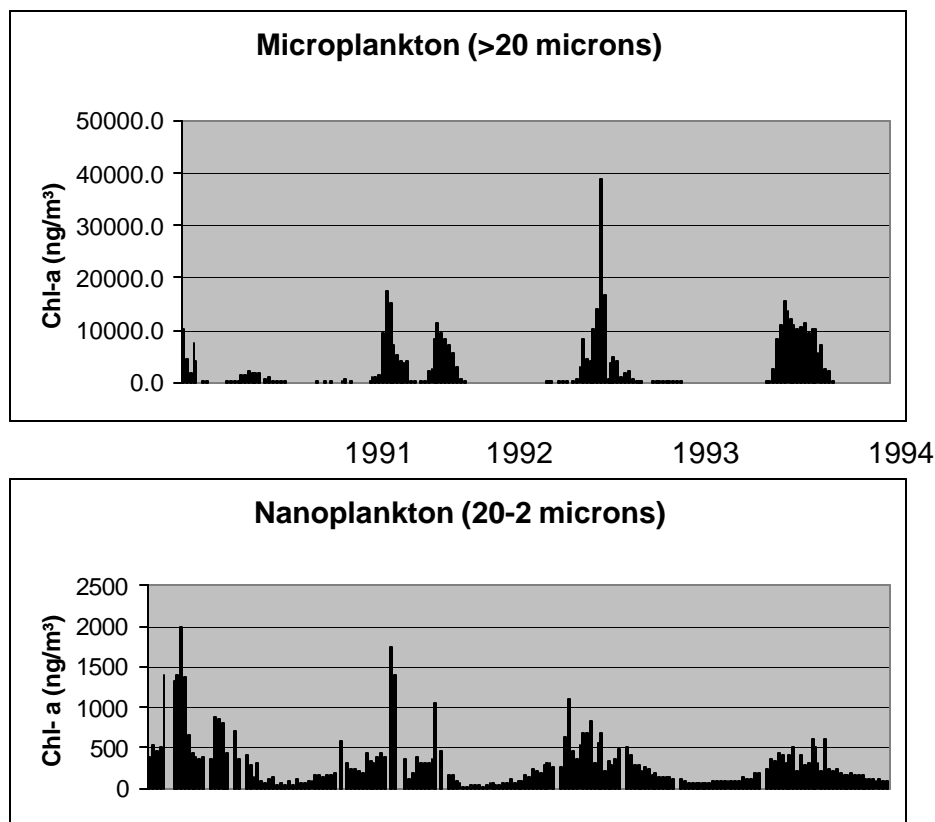
Figure 11: Interannual variation in size fractioned pigments
(Data obtained from Clarke, BAS).

	1991	1992	1994	1995
N	17	18 (2)	30	3
Organic carbon (%)				
Average	1.3	1.4	0.5	0.5
Standard deviation	0.18	0.29	0.24	0.06
Organic nitrogen (%)				
Average	0.1	0.1	0.1	0.1
Standard deviation	0.19	0.04	0.04	0.11
Chl-a (µg.g^{-1})				
Average	21	53	33	45
Standard deviation	9.1	6.4	31.9	15.4

Table VII: Interannual variability within sediment parameters at Signy Island

As a result of vertical fluxes the trophic sources in the sediment and, by inference, food for benthic detritivores obviously vary on an interannual base too (table VII).

Table VIII: Interannual variability within sediment texture at Signy Island

	1991	1992	1994	1995
N	17	19	30	3
Mean grain size (µm)				
Average	69	72	83	71
Standard deviation	5.1	5.4	12.5	5.7
Silt and clay (%)				
Average	33	30	25	33
Standard deviation	3.7	4.6	8.2	2.9
Medium sand (%)				
Average	1.5	1.4	2.7	3.2
Standard deviation	0.56	0.67	1.43	0.24
Coarse sand (%)				
Average	0.6	0.2	0.3	0.2
Standard deviation	0.29	0.12	0.41	0.09

The sediment texture also varies, although to a minor degree. This might be the result of physical forcing by hydrodynamics, ice impact, macrofaunal burrowing, etc.

All these year-to-year variations are of enormous ecological significance. For organisms dependent directly on the phytoplankton bloom, there are significant year-to-year variations in growth rate, survival and recruitment. So were benthic suspension feeding bryozoans, hydroids, polychaetes and holothurians heavily impacted by this variability (Clarke et al. 1988; Barnes and Clarke 1994).

As was expected from the pelagic-benthic coupling (earlier discussion), there is a big difference in meiofaunal properties between the years too (table IX) with average total meiofaunal density ranging between 4913 and 7547 ind. per 10 cm² per year. In particular nematodes exhibit pronounced year-to-year variation between 3980 and 6505 ind. per 10 cm². De order of magnitude is less though still prominent for the other predominant taxa (for example 202-308 ind. per 10 cm² for harpacticoids; 37-355 ind. per 10 cm² for ostracods). The high standard deviation indicates that a high variability occurs within these years (see earlier descriptions).

Table IX: Interannual variability within meiofaunal parameters at Signy Island.
Taxon densities are expressed as ind. per 10 cm $^{-2}$

	1991		1992		1994		1995	
N	17		19		31		3	
	average	stdev	average	stdev	average	stdev	average	stdev
Nematoda	6505	4065.7	3980	2350.4	5388	3976.1	4400	4660.2
%	83	8.7	80	9.4	82	9.8	72	32.2
Harpacticoida	289	176.3	302	243.2	334	406.8	202	226.8
Nauplii	371	177.3	250	289.3	452	505.3	618	790.5
Ostracoda	336	164.8	355	294.9	275	349.9	37	30.0
Turbellaria	12	10.4	4	7.8	19	20.0	30	32.5
Amphipoda	9	14.3	3	4.1	5	4.6	9	9.8
Bivalvia	10	8.1	11	11.9	24	20.2	12	2.1
# taxa	6	0.9	6	1.4	8	2.0	8	1.0
total density	7547	4269.8	4913	2789.7	6893	4971.7	5316	4030.1

3.3.3 The high and low Antarctic meiobenthos compared

The meiofaunal communities from Rothera consisted of Nematoda (94.70%), Polychaeta (2.04%), Turbellaria (0.93%), Copepoda (0.83%), Nauplii (0.65%), Ostracoda (0.26%), Oligochaeta (0.24%), Priapulida (0.11%), juvenile Bivalvia (0.09%), Tanaidacea (0.09%), juvenile Annelida (0.04%), Gastrotricha (0.03%), Kinoryncha (0.01%) and Rotifera (0.01%). Nematode densities varied between 93 and 14072 ind.10 cm^{-2} and were spread over 48 genera (see list) and 20 families.

Enoplolaimus De Man, 1893	*Paramicrolaimus* Wieser, 1954
Mesacanthion Filipjev, 1927	*Daptonema* Cobb, 1920
Oxyonchus Filipjev, 1927	*Metadesmolaimus* Stekhoven, 1935
Anoplostoma Bütschli, 1874	*Paramonohystera* Steiner, 1916
Anticoma Bastian, 1865	*Theristus* Bastian, 1865
Halalaimus De Man, 1888	*Sphaerolaimus* Bastian, 1865
Oxystomina Filipjev, 1921	*Linhomoeus* Bastian, 1865
Prooncholaimus Micoletzky, 1924	*Metalinhomoeus* De Man, 1907
Acantholaimus Allgén, 1933	*Paralinhomoeus* De Man, 1907
Actinonema Cobb, 1920	*Linhomoeidae gen.*
Chromadorina Filipjev, 1918	*Ascolaimus* Ditlevsen, 1919
Dichromadora Kreis, 1929	*Axonolaimus* De Man, 1889
Endeolophos Boucher, 1976	*Odontophora* Bütschli, 1874
Neochromadora Micoletzky, 1924	*Odontophoroides* Boucher and Helléouët, 1977
Prochromadorella Micoletzky, 1924	*Campylaimus* Cobb, 1920
Laimella Cobb, 1920	*Southerniella* Allgén, 1932
Pierrickia Vitiello, 1970	*Selachinematidae gen.*
Sabatieria Rouville, 1903	*Molgolaimus,* Ditlevsen, 1921
Ethmolaimidae gen.	*Microlaimus* De Man, 1880
Longicyatholaimus Micoletzky, 1924	*Microlaimidae gen.*
Marylynnia Hopper, 1977	*Camacolaimus* De Man, 1889
Pomponema Cobb, 1917	*Leptolaimus* De Man, 1876
Cyatholaimidae gen.	*Aegial oalaimus* De Man, 1907
Choniolaimus Ditlevsen, 1918	*Cyartonema* Cobb, 1920

Sabatieria dominated (36.15 %). Others were *Odontophoroides* (13.78 %)*, Metalinhomoeus* (8.15 %)*, Molgolaimus* (7.85 %) and *Prochromadorella* (6.07 %).

Figure 12: Feeding guild structure of the nematode communities in Rothera.

Following Wieser, (1953) the non-selective deposit-feeders (1b in fig.12), were dominant. Feeding types 1a en 2a, respectively selective deposit-feeders and epistratum feeders, followed. Predators/omnivores (2b) were low abundant.
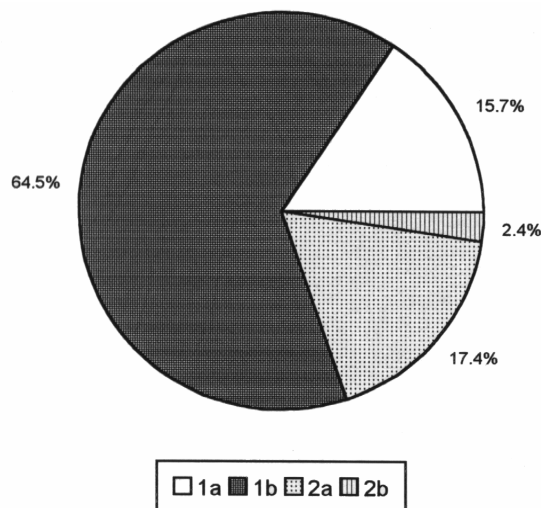
Table VIII discriminates between the three sites studied. North Cove clearly differs from Grifter Pipe, in that the communities from the latter showed extremely low meiofauna abundances and low diversity. *Sabatieria* was highly dominant. This genus is often related to suboxic pathways (Soetaert and Heip 1995). Pollution may be responsible for this phenomenon, as the sampling site was situated close to the sewage outfall of the research station. The differences between the two North Cove sediments probably originate from water depth influences.

Table VIII: Meiofaunal parameters at Rothera

	North Cove 31 m	North Cove 11m	Grifter Pipe 5m
Number of meiofauna taxa	7	12	10
Nematode dominance (%)	94	95	86
Nematodes numbers (ind.10cm^{-2})	2250	13042	68
Genus numbers	20.3	19.5	11
***Sabatieria* (%)**	25	27	63
Trophic dominance	0.4	0.5	0.6
Epistrate grazers (%)	22	23	5
Non-selective deposit feeders (%)	54	67	77

Trophic dominance (T) = S?² with ? = the proportion of each feeding type

Despite comparable high meiofaunal abundances in similar circumstances (e.g. at about 10 m depth and during austral summer, densities of 13 689 and 4950 to 13170 ind. 10cm^{-2}) fundamental differences were found between the communities from Rothera and Signy. Especially, the nematode populations from Rothera were represented by less dominant genera, whereas the nematodes retrieved from sediments of Signy belonged for 97% to 6 genera only (*Daptonema, Aponema, Neochromadora, Sabatieria, Microlaimus* and *Chromadorita*). The remaining 3% was

composed of 22 genera. Eutrophication was the possible explanation for this observation (Vanhove et al. 2000). Excess labile organic matter may have accumulated, producing a high demand for oxygen and leading locally to hyperoxic, sulphidic bottom-water. In this case, structural characteristics such as high abundance and biomass with low diversity typified the faunal communities as found in Signy. The major differences between the two nematode communities may be coupled to the latitudinal position of the sites. Signy lies pretty close to the polar front (Knox 1994). This upwelling zone may be responsible for higher primary production and hence, food transport to the benthos. However, frequently observed medium-sized icebergs, brash and ice-floes (pers. comm., Clarke) might have structured the benthic communities too (as was the case for the iceberg area near our time series sampling site at Signy Island, Peck et al. 1999). Unfortunately, these events prevented us to perform time-series analysis.

3.4 CONCLUSIONS

The long run of data available from Signy Island exhibits two key features. The first is marked <u>seasonality</u>, long known to be a characteristic of polar regions. The pattern of seasonal variation in phytoplankton standing crop and production is of fundamental significance to the marine ecosystem. The availability of phytoplankton determines the ecology of both benthic and pelagic herbivores, and this influence permeates the higher levels of the food web (Clarke 1988). Studies of the deposit feeding fauna were needed to confirm or disaffirm this.

The extent of the coupling of benthic production to the overlying water column is therefore illustrated for the meiofauna from Signy Island. The subtidal ecosystem in question is characterized by a high seasonal and interannual variation in

The major response mechanisms of meiofaunal standing stock were:
1) Distinct peak abundances, lagging with a few weeks behind peak diatom production (that lead to excess concentrations of rapidly sinking fresh bio-available food)
2) Lower, though still highly fluctuating, stocks during most of the year with immediate and lagged responses to lower quality nanophytoplankton input (*e.g.* lower sinking rates allow bacterial decomposition within the water column, Smetacek 1984)
3) Strong reduced stocks with a short duration in mid winter, when food availability was at its lowest
4) The degree of meiofaunal dependence on the primary production and sedimentation of organic matter differs with higher meiofaunal taxon, and within the nematode community
5) The nematode populations show poor or no patterns of seasonal reproduction as no clear cohorts can be recognised.

The second, less well established, is significantly <u>year-to-year variability</u>. Interannual variability has been demonstrated at Signy Island in seawater temperature and winter sea-ice. As a result there were clearly considerable year-to-year variations in the timing, intensity and duration of phytoplankton blooms. These variations are of enormous ecological significance. Our study evidence indicates that also benthic detritivores, such as the meiofauna, strongly show interannual variability in their

community properties making them less predictable, as would be expected from their seasonal variability. The observed up-side-down control suggest that meiobenthos is strongly influenced by the year-to-year variations in plankton production.

Of course response mechanisms of the meiofauna might be more complex, and food items other than those related to pelagic blooms may have contributed to the temporal variability of the meiofauna:

1. *In situ* microphytobenthic production around Signy Island can be substantial and highly seasonally variable, amounting to slightly over 100 mg C m^{-2} during the ice-free summer, with peaks of 700 mg C m^{-2} d^{-1} (Gilbert 1991a). The primary production rates by microphytobenthos compare favourably with planktonic productivity and bacterial turnover and will be an important food source to the numerous infauna.

2. Meiofauna has frequently been found under the sea-ice (Cross 1982; Carey and Montagna 1982; Grainger and Hsiao 1990). Food requirements may be met by the sedimentation of ice-algae and faecal material of herbivores grazing underneath the ice (Sasaki and Hoshiai 1986; Matsuda et al. 1987), and by microphytobenthic production under the ice (Gilbert 1991a).

3. Sedimented and *in situ* produced organic sources might be directly ingested or become part of the microbial loop. In benthic food chains, the microbial communities important, due to their fast growth and high metabolic activity in association with organic material (Meyer-Reil 1983), and, along with diatoms, bacteria may belong to the available food for the meiobenthos (Montagna et al. 1983).

4. As stated by Rudnick, (1989), the balance of benthic food input and demand may shift seasonally and deficits may be particularly acute for benthos that feed at the sediment interface and depend on fresh inputs. In contrast, the food resources for subsurface feeders are more stable because they have access to and assimilate a portion of the buried pool of older organic matter.

Physical factors such as coastal storms with associated high winds perturb the generally low-energy nearshore system of Signy Island, leading to significant resuspension of surficial sediments (White et al. 1993). This might result in a mixing and the destruction of the benthic microbial mats, but also induce deposition of ice-algae, ending in augmented benthic activity. All factors together, undoubtedly had a pronounced effect on the meiobenthos populations (Peck et al. 1999).

Finally, from a continuous spectrum of variability probably half the variability is related to the above-described features, but many fluctuations might be due to factors of unknown nature (for example macrofaunal activity, biological interactions within the meiofauna, etc.).

Despite comparable high meiofaunal abundances in similar circumstances fundamental differences were found between the communities from Rothera and Signy. Latitudinal differences, such as the Polar Front nearby the South Orkneys, were proposed, but not proved, to be at the base of the variability between high and low Antarctic nematode communities.

4

| BIODIVERSITY AND RECOVERY POTENTIAL |
| IN THE DEEP BATHYAL WATERS |
| OF THE SOUTHERN OCEAN |

4.1 INTRODUCTION

Ecological studies of high Antarctic meiobenthos in deep waters are restricted to only a few study programmes (Herman and Dahms 1992; Vanhove et al. 1995; Fabiano and Danovaro 1999). The benthic community in the deep Weddell Sea is rich in terms of abundance and biomass, and exhibits a high level of heterogeneity (Gerdes et al. 1992; Knox 1994). The species assemblages of intertidal, subtidal and deep-sea communities are generally rich and diverse, despite the harshness of the environment (Arntz and Gallardo 1994). Especially, the benthic organisms live in extreme situations induced by low temperatures, covered by ice most of the year and supplied with fresh primary production only during a short period in spring and summer. The origin of the spatial patchiness and the complexity of organization (biodiversity), however, cannot be understood with the current available knowledge. In contrast to the large-scale approach of the ANTAR III program, which gave an elaborate introduction to the meiobenthos communities and their relation with the ambient environment on a broad scale in the deep Weddell Sea, more extensive evaluations of the varying forces at a higher spatial resolution are needed.

Major changes and influences of typical polar conditions are expected to be found near the shelf-ice edge. In the EASIZ program the effect of typical polar conditions on biodiversity are investigated on specific areas of the shallower part of the Weddell Sea - shelf, in particular close to the Antarctic continent off Kapp Norvegia. One such important agent is the disturbance by ice. A prominent feature of the Antarctic Ocean is the calving of icebergs (Lien et al. 1989), especially close to the ice shelves. Icebergs, which float with about 80 % of their bulk submerged, can have a considerable impact on the benthic realm. Yet, little information is available about sediment-recolonisation in Antarctica (Peck et al. 1999) and nothing is known considering the capacity of meiobenthos in the same region.

Assessing the rates and processes involved in the recolonisation by *in situ* fauna is one of the more recent aims of biological investigations as to marine mineral exploitation and the dumping of radioactive and other chemical wastes. Moreover, with reference to the global warming, the calving of icebergs may be a frequent phenomenon in the near future. Yet, with the prospect of protecting the Antarctic environment, it is of fundamental importance having knowledge about the benthic regulation after disturbance, both by natural and human origin.

Meiofaunal organisms are advantageous for this kind of experimentation because their short generation times result in a faster potential response to disturbance incidents: thus recovery of the community structure takes place over a reasonable time-span.

Recolonisation studies of the deep water meiofauna parallels studies in the shallow, and similar work on the macrofauna is carried out by the benthos research group of the Alfred-Wegener-Institiute (AWI) and the British Antarctic Survey (BAS).

4.2 MATERIALS AND METHODS

Sampling area and methods. The continental shelf off Kapp Norvegia in the eastern Weddell Sea is selected for our study. During the second EASIZ cruise, from 13 January till 26 March 1998, sediment samples were taken by a multi-box corer (Gerdes 1990) for the study of iceberg scouring effects on meiobenthic communities. Three recognisably contrasting stations were selected for this study: Sta. 225 (water depth, 278 m), Sta. 187 (water depth, 255 m) and Sta 228 (water depth, 298 m). Those stations were regarded as a very fresh scour, a relatively old scour and an undisturbed site, respectively. This discrimination was based on the combination of *in situ* observations of the bottom scenery produced by a video camera attached to the sampling gear, sediment textual conditions and macro-epifaunal occurrence (table IX).

Table IX: Coordinates and description of the sampling stations in the Weddell Sea, Antarctica

Type	Station	Depth	Latitude	Longitude	Sediment type	Sediment condition	Epigrowth
Fresh scour	48/225	278 m	70°50.1S	10°35.2W	Silt	Very fluid	No
Old scour	48/187	255 m	71°32.3S	13°31.7W	Very fine sand	Normal	One hydrozoa
Reference	48/228	298 m	70°49.8S	10°38.0W	Silt	Sponge spicule mat	Diverse

Three standard meiofauna-hand-cores (with a diameter about 3.5 cm which corresponding a 10 cm^2 surface area) for the meiofauna and a large hand core (diameter about 6 cm) for sediment analysis were taken from one box-core of each station.

Sample treatment. The length of meiofauna sediment cores was sliced into 5 layers (0-1, 1-3, 3-5, 5-10 and the rest) immediately after the samples were recovered. Only the three first top layers, where the majority of meiofauna dwells, were used for this study. Standard procedures for meiofaunal extraction and sorting were applied (see Lee et al. *in press a* for details). Developmental stages and sex of specimens were categorised into four different groups: juvenile, non-gravid female, gravid female and male. The feeding type classification was according to Wieser, (1953): selective deposit feeder (1A), non-selective deposit feeder (1B), epistratum feeder (2A) and predators/omnivore (2B). Sediment analysis was performed with a Coulter-Counter. Prior to the operation of Coulter-Counter, the sponge spicule mats on the top of sediments from Sta. 48/228 were removed for practical reasons.

Statistical analysis. Analysis of variance (ANOVA) was used to determine significant differences (p< .05) for the parameters: diversity, feeding type, age guild, maturity index and dominance of nematode genera between stations. Subsequent post hoc comparison (Turkey HSD) was used on stations. Nematode species diversity was measured using Hill's diversity indices (Hill 1973): N_0 is the number of

genera, N_1 is the exponential of the Shannon's index, N_2 is the reciprocal of the Simpson's dominance index, $N8$ is the reciprocal of the relative abundance of the most dominant genus. The maturity index (MI; Bongers 1990; Bongers et al. 1991) is used to characterize the life style of nematode communities. A weighted mean of c-p (colonisers-persisters) values is assigned to each taxon, ranging from 1 for extreme colonisers and 5 for extreme persisters. Bongers et al., (1991), suggested that the MI may be useful to study disturbance effects on in marine communities.

4.3 RESULTS

4.3.1 Sediment composition

The sediments from the fresh scour and the undisturbed site consisted of silt (median grain size 43.4 µm and 32.4 µm, respectively) while that of the older scour was very fine sand (median grain size 101 µm) (table IX). Although the grain size distributions of the fresh scour and the undisturbed site were similar to each other, there were clear differences in sediment condition as it was observed during the sample treatment. The sediment from the fresh scour was very fluid with obviously much more interstitial water than that of the older scour or the undisturbed site. The sediment from the undisturbed site differed from the other stations in having a 1 cm thick sponge-spicule mat on the top layer, which looked like glass fibre cotton.

4.3.2 Meiofauna

In total 20 different meiofauna groups were recovered from the three stations (table X). There were big difference in density and the number of meiofauna groups between the fresh scour and the other stations whilst comparable numbers were found between older scour and undisturbed site (fresh scour: 120±15.4 ind./10 cm^2, 7 groups; older scour: 1,326±287.5 ind./10 cm^2, 16 groups; undisturbed site: 1,342±70.8 ind./10 cm^2, 13 groups). The relative abundance of nematodes, the most dominant group in all the stations, increased from fresh scour (60.6%) to older scour (77.6%) and undisturbed site (92.0%), while crustaceans (copepods, ostracods and nauplii where nauplii was treated as separated group for practical reasons), which were subdominant, showed the opposite tendency. These major groups made up more than 97% of communities in all stations.

Table X: Mean densities, with standard deviation in parentheses (n=3), of all meiofaunal groups recovered during the study.

Station	Fresh	Older	Undisturbed
Nematoda	72.7(9.3)	1028.7(217.5)	1234.3(69.3)
Copepoda	21.0(11.3)	89.7(23.1)	30.7(10.6)
Ostracoda	1.3(1.5)	12.0(10.1)	5.7(4.7)
Nauplii	22.7(8.0)	162.0(25.2)	49.7(17.1)
Priapulida	0	2.0(1.0)	0
Kinorhyncha	0	0.7(1.2)	4.3(4.9)
Tardigrada	0	0.7(0.6)	4.7(0.6)
Turbellaria	0	2.7(3.1)	0.3(0.6)
Tanaidacea	0.3(0.6)	0	0
Rotifera	1.3(1.5)	0.7(0.6)	3.0(1.0)
Isopoda	0	0.3(0.6)	0
Amphipoda	0	0.7(1.2)	0
Polychaeta	0.7(0.6)	22.0(10.8)	5.3(5.9)
Oligochaeta	0	1.0(1.0)	0
Bivalvia	0	1.0(1.0)	0
Sipuncula	0	0.3(0.6)	0
Hydrozoa	0	0	1.0(1.0)
Acari	0	1.7(2.9)	2.0(1.0)
Aplacophora	0	0	0.3(0.6)
Bryozoa	0	0	1.0(1.0)
Total	120(15.4)	1326.0(287.5)	1342.3(70.8)

4.3.3 Nematode communities

The abundance of nematodes was significantly lower (73±9.3 ind./10 cm^2) in the fresh scour compared to the older scour (1029±217.5 ind./10 cm^2) and undisturbed site (1234±69.3 ind/10 cm^2) (table X).

The average genus number expressed as N_0 of Hill's diversity numbers increased significantly with the stage of recolonisation (fresh scour, $N_0 = 17±2.0$; older scour, N0 = 36±8.0; undisturbed, $N_0 = 56±4.0$ (fig. 13). All other Hill's diversity numbers showed the same tendency with N_0, although the difference of other indices between the fresh scour and the older scour were not significant. In the case of N_8, only the difference between fresh scour and undisturbed site was significant.

There were clear differences in genus composition between all three stations (table XI, fig. 14). The genus *Monhystera* was the most dominant in all stations, but the dominance decreased towards the undisturbed site (26.1% in fresh scour, 18.8% in older scour and 16.7% in undisturbed site). Next to *Monhystera*, *Neochromadora* and *Daptonema* were the subdominant genera in fresh scour and older scour, but of less importance in undis turbed site.
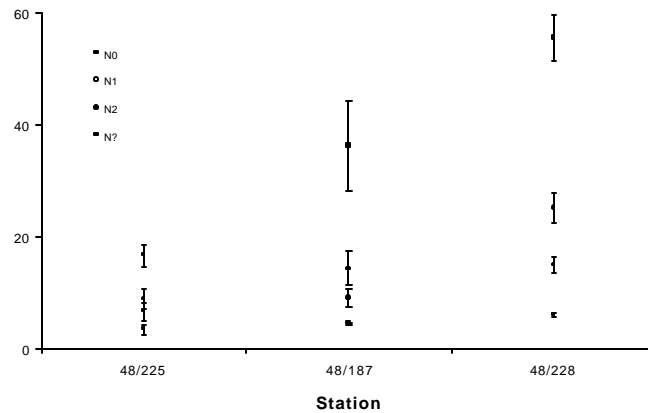
Figure 13. Hill's diversity numbers of nematode communities (error bar, standard deviation) (Sta 225, fresh; Sta 187, older; Sta 228, undisturbed).

Table XI: Mean density (ind./10 cm², n=3) of the important nematode genera
(> 1% at any station)

Genus	Fresh	Older	Undisturbed
Monhystera	19.7	192.4	206.1
Neochromadora	17.0	181.9	13.2
Daptonema	9.0	119.4	52.6
Sabatieria	1.3	90.4	85.4
Leptolaimus	-	25.1	121.6
Acantholaimus	0.3	45.7	88.0
Pareudesmoscolex	-	30.5	86.1
Halalaimus	3.0	67.5	42.4
Tricoma	-	7.6	78.4
Desmoscolex	-	9.4	59.7
Cervonema	4.3	35.0	1.9
Amphimonhystrella	2.5	3.3	33.1
Molgolaimus	-	9.4	24.9
Aegialoalaimus	1.0	14.6	15.9
Prochromadorella	0.5	19.3	6.4
Sphaerolaimus	4.0	7.0	11.7
Odontanticoma	-	18.5	1.8
Anticoma	0.3	17.0	2.5
Actinonema	-	7.3	12.6
Diplolaimella	-	18.5	-
Tylenchidae genus	1.3	6.1	10.9
Spilophorella	-	11.2	6.7
Camacolaimus	-	5.6	12.0
Microlaimus	-	0.3	15.0
Oxystomina	1.0	2.3	3.0
Pseudosteineria	1.3	3.3	-
Chromadoridae genus	1.5	-	1.9
Prism atolaimus	2.0	0.3	-
Other (No. of other genera)	2.7 (11)	78.8 (39)	240.4 (67)
Total	72.7	1028.7	1234.3

Leptolaimus and *Acantholaimus* were the second and third dominant genera in undisturbed site; however, they were less important in older scour and even absent or very rare in fresh scour. The most unexpected fact was the rareness of the suborder Leptolaimina and Desmoscolecina in the fresh scour.

The suborder Leptolaimina was represented only by *Aegialoalaimus* (1.3%), *Prismatolaimus* (2.7%) and *Teratocephalus* (0.7%), and there was no single individual of the suborder Desmoscolecina. The genus number and abundance of these suborders showed an increasing tendency with the age of scour (older scour: 9.3%, 7 genera; undisturbed site 34.2%, 15 genera); nonetheless *Prismatolaimus* and *Teratocephalus* did not occur in the undisturbed site. *Sabatieria* was one of the common genera in all stations, although this genus was less important in the fresh scour compared with the other stations. *Sphaerolaimus* was one of the subdominant genera in the fresh scour (5.3%, 5th rank), but not in the other stations (<1.0%). The dominance of *Leptolaimus*, *Acantholaimus*, *Pareudesmoscolex*, *Tricoma* and *Desmoscolex* showed an increasing tendency from fresh scour to undisturbed site (fig. 14a). *Sabatieria*, *Halalaimus*, *Amphimonhystrella* and *Sphaerolaimus* showed no constant pattern (fig. 14b). The proportion of *Monhystera*, *Neochromadora*, *Daptonema*, *Cervonema* and *Prismatolaimus* tend to increase at the more recently scoured site (fig. 14c).

A similar trend was found at a higher taxonomic level (mostly family level), except for the family Comesomatidae. Therefore pooling the genera together into family groups reduce the data with minimal lose of information. However, since both dominant genera, *Sabatieria* and *Cervonema*, of the Comesomatidae showed an opposite tendency they were not considered at the family level. Table 5 shows the dominance rank of families with a density higher than 0.5%. The family Monhysteridae, Chromadoridae and Xyalidae were commonly dominant in all stations. The family Comesomatidae and Oxystominidae were also common and subdominant in all three stations.

Among four different age and sex groups, the juveniles were predominant in all stations (average: 64.0-69.3%) followed by males (average: 13.7-17.7|), but the differences between stations were not significant. The non-gravid females, the third dominant group (average: 7.9-19.7), were significantly (p<. 05) low in the fresh scour compared with the undisturbed site, but differences between fresh and older scour and between older scour and undisturbed site were not significant. The gravid females were least abundant (average: 1.3-6.0%) and their proportion was significantly lower in the undisturbed site compared with the other stations. The proportion of the total females was significantly lower in the fresh scour compared with the other stations. The ratio of the gravid females to the non-gravid females significantly increased with the freshness of the scours.
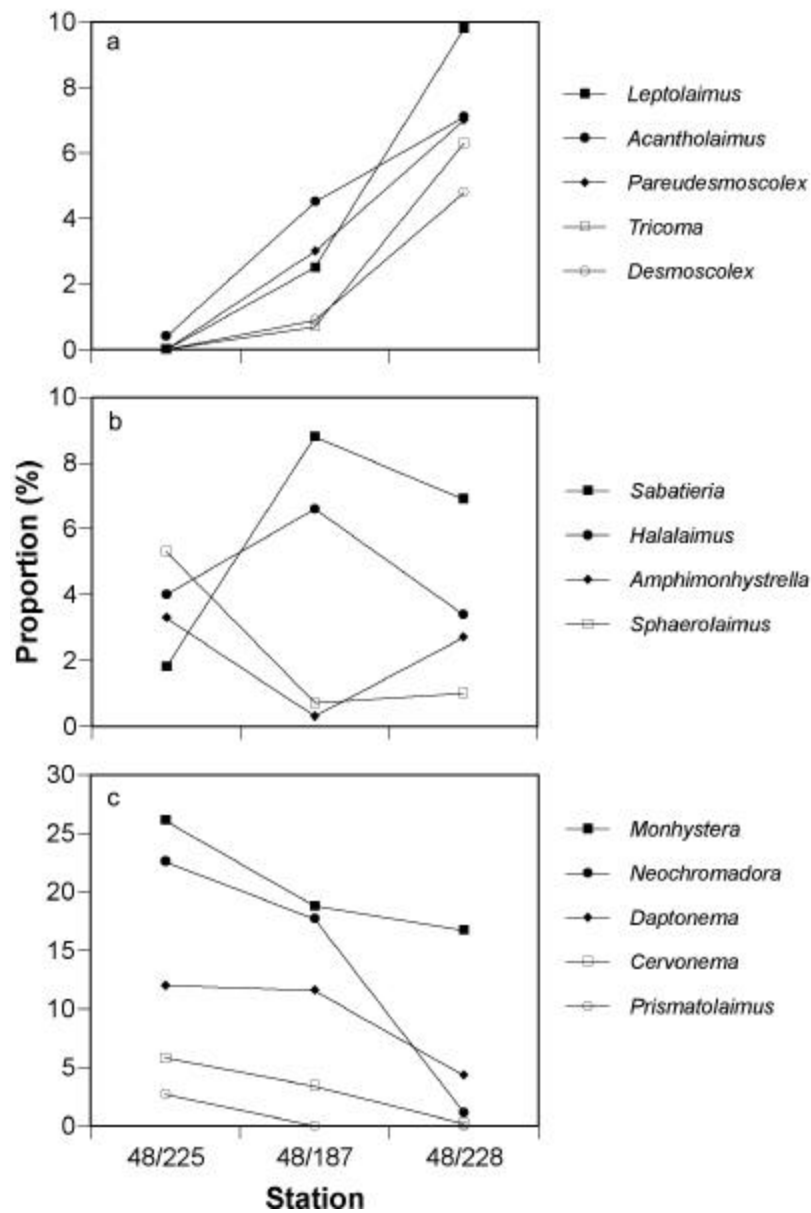
Figure 14: Different tendencies of major nematode genera expressed as a relative proportion according to different degrees of freshness of scours. The nematodes proportionally decreased due to scouring were regarded as persisters (a),) and those which increased by scouring were regarded as colonisers (c). The intermediate group (b) did not show a clear trend. (Sta 225, fresh; Sta 187, older; Sta 228, undisturbed).

Among four feeding guilds, the 1A group showed increasing tendency from fresh scour to undisturbed site (fig. 15). The proportion of this group was significantly higher in the undisturbed site compared with other stations. The proportion of the 1B group was significantly lower only in the undisturbed site compared to the fresh scour. No significant difference between the stations was observed for the 2A group.

The 2B group was the smallest with a proportion significantly higher in the fresh scour compared with the other stations.
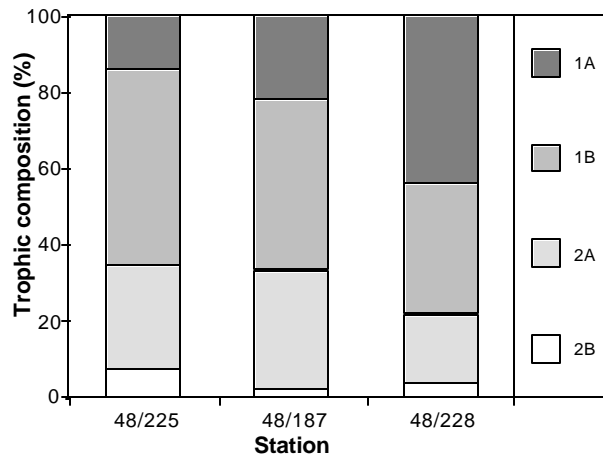
Figure 15: Trophic guild composition of the nematode community in the three stations with different stages of recovery. (Sta 225, fresh; Sta 187, older; Sta 228, undisturbed).

The maturity index showed a significantly decreasing tendency with the freshness of disturbance (table XII, fig.16).
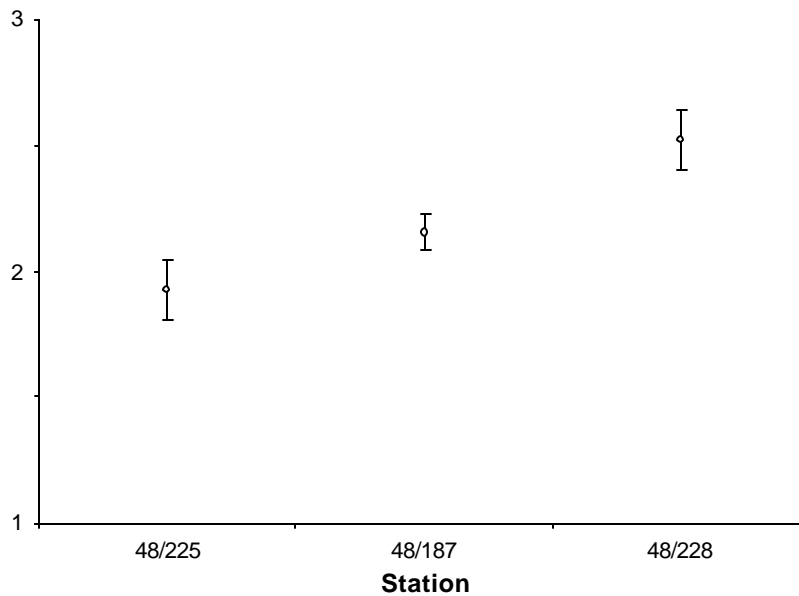
Figure 16. Maturity index (MI) of the nematode community (error bar, standard deviation). (Sta 225, fresh; Sta 187, older; Sta 228, undisturbed). Calculations were based upon table.

Table XII: Relative importance, feeding type (FT) and c-p (coloniser-persister) value of the nematodes grouped into families.

Nematode group	Fresh	Older	Undisturbed	FT	C-p value
Monhysteridae	*****	*****	****	1B	1
Chromadoridae	*****	*****	****	2A	3
Xyalidae	****	****	****	1B	2
Oxystominidae	***	***	***	1A	4
Comesomatidae *Cervonema*	***	**	*	1A	2
Sphaerolaimidae	***	*	*	2B	3
Prismatolaimidae	**			1B	?
Rhabditidae	*	*		1A	1
Teratocephalidae	*	*		1A	3
Comesomatidae *Sabatieria*	*	***	***	1B	2
Trefusiidae			*	1A	4
Epsilonematidae			*	1A	4
Microlaimidae			*	2A	3
Ceramonematidae		*	*	1A	3
Diplopeltidae		*	*	1A	3
Cyatholaimidae		*	*	2A	3
Desmodoridae		*	*	2B	3
Meyliidae		*	***	1A	4
Leptolaimidae		**	****	1A	3
Desmoscolecidae		**	****	1A	4

*: >0.5%, **: 2.5-5%, ***: 5-10%, ****: 10-20%, *****: >20%.
?: unknown.

4.4 DISCUSSION

4.4.1 Age estimation of scour marks

Age estimation is the critical point for recolonisation analysis, especially for observational study, and must be based on concrete evidence. Since there is yet no standard methods developed for the estimation of iceberg scour mark and the very fresh scour marks are not distinguishable from the video images provided by sampler the study in this field, especially on meiobenthos, which recover much faster than macrobenthos, has been hampered.

Among many samples taken for this study we selected three contrasting samples, which showed more clear evidences for the age assumptions. The age assumption of scour marks for this study was made based on the combination of *in situ* observations of the bottom scenery produced by a video camera attached to the sampling gear, sediment textual conditions and faunal occurrence (Table).

At a glance at the video images both Sta. 225 and Sta. 187 looked very fresh. However, Sta. 225 was regarded as a very fresh scour based on the lack of epifauna and especially on the very fluid sediment condition. As it was described by Lien et al., (1989), ploughing and pumping are the major destructive activities during the iceberg scouring. The ploughing and pumping activities of the iceberg resuspend the sediment. This resuspended material will settle down especially on the depression of scour marks. This sediment should be more fluid because it must contain much more

interstitial water than in normal conditions. After some time, however, water currents will probably easily blow the fluid fine sediment away, and underlying compact sediments will remain in scour marks. The fluid sediment at Sta. 225, for this reason, can be considered as an evidence of a very fresh scour mark. The under water video images for more than 10 minutes drifting time by multibox-corer occasionally showed *Mogula pepedunculata*. The sediment from this station was not fluid unlike in Sta. 225. Also the presence of a sessile hydrozoan found in one sediment sample from this station, *Symplectoscyphus plectilis*, one month old (J-M Gilli, personal communication), provides a clue that the scour mark at this station is at least older than one month. Although the possible maximum age of this scour remains uncertain, it is considered that it may not be older than one year. The undisturbed reference station, Sta. 228, showed a typical dense cover of epifauna on the seabed, which was contrasting to the barren surface at the scoured sites. The sediment samples from this station were also different from the sediments of the other stations, in that they were covered with sponge spicule mat of about 1 cm thick.

4.4.2 Influence of Iceberg scouring on meiofauna

The very low meiofaunal abundance in the fresh scour compared with that in the older scour and the undisturbed site was in accordance with the effect of the assumed recent scouring at this station, e.g. in the present study the total number of metazoan meiofauna abundance in the fresh scour was less than 10% of that in the old scour and the undisturbed site. This figure agrees with the 93% reduction of meiofauna abundance after iceberg scouring in the shallow coastal sediments of Signy Island (Lee et al. *in press b*).

Iceberg scouring also decreased the total number of meiofauna taxa. Initially it removed most of sessile and some motile animals, e.g. hydrozoans, bryozoans, kinorhynches, tardigrades, turbellarians and acaries. The first immigrants in the old scour were motile organisms such as amphipods and isopods. They can be considered as early colonisers. The absence of some lesser motile burrowers, e.g. priapulids, bivalves, sipuncules and oligochaetes, in the undisturbed site in spite of their presence in the older scour may be due to the obstacle of sponge spicule mats covering the sediment in the undisturbed site.

Many studies show various time scales of meiofaunal recovery from different disturbances (within a couple of days or shorter: Sherman and Coull 1980 – physical disturbance; some weeks: Brylinsky and Gibson 1994 – physical disturbance, Danovaro et al. 1995 – oil spill; some months: Coull 1969 – physical disturbance; more than one year: Wormald 1976 – oil spill, Bodin and Boucher 1983 – oil spill, Elmgren et al. 1983 – oil spill). A general conclusion is that the recovery of meiofauna is relatively fast although it may depend on the type, frequency and scale of disturbance. In our study the meiofaunal abundance in the older scour had already recovered to the level of the undisturbed site and the taxon number in the older scour even exceeded that of the undisturbed site (Table). Unfortunately we cannot propose a good estimation of the recovery time for the meiofauna community in the current deep-water study. Recolonisation of the shallow coast meiofauna community at Signy Island occurred between 30 and 80 days (Lee et al. *in press, b*). Because of major differences of ecological condition between shallow coastal and deep-water

habitat (e.g. hydrodynamics, primary production, vertical fluxes, physical condition) one can expect nematode community restoration in this area can take at least some years.

4.4.3 Influence of Iceberg scouring on nematode communities

Abundance. The nematode abundance coincided with total meiofauna abundance. The extremely low density in the fresh scour shows the severity of iceberg scouring impact in the initial stage. Although the nematode density in the older scour recovered to the level of the undisturbed site, their proportions among meiofauna were low in the scours implying that nematodes recolonise more slowly than other major meiofauna, e.g. copepods and ostracods. This is probably because of the slower movement of nematodes rather than their weaker resistance to the physical impact of iceberg scouring.

Diversity. The nematode diversity was greatly influenced by scouring. The relatively high diversity of nematodes in terms of genus number in the undisturbed site ($N_0=56\pm4.0$) was in accordance with the results of Vanhove et al., (1999) from Kapp Norvegia and Halley Bay ($N_0=56\pm5.0$) and $N_0=52\pm10.8$, respectively) in the Weddell Sea. However, it was very low in the fresh scour of this study ($N_0=17\pm2.0$). The diversity (N_0) of the old scour in this study was fairly comparable with the data of undisturbed control sites ($N_0=13.5\pm0.5$, even though it was based on species, it is still comparable because most genera were mono-specific) of the coast at Signy Island (Lee et al, *in press b*). The drastic decrease of diversity due to scouring implicates that nematode community structure in this area is very fragile against such a disturbance. Unlike the abundance, the genus number of the old scour site was still low compared to the undisturbed site, which suggests that the restoration of community structure is a slower process than the abundance recovery. The drastic decrease of diversity due to scouring implies that nematode community structure in this area is very fragile against such disturbances. This is contrasting to the shallow water nematode community, which diversity appeared to be influenced by a complexity of physical and biochemical properties rather than iceberg scouring alone (Lee et al. *in press b*).

Iceberg scouring also resulted in the increase of the dominance of a few nematode genera. Each of the three most abundant genera in the fresh and the older scour, *Monhystera*, *Neochromadora* and *Daptonema*, dominated for more than 10% while only *Monhystera* dominated for more than 10% in the undisturbed site. Those three dominant genera made up 60.6% in the fresh scour and 48.1% in the older scour. The three most dominant genera in the undisturbed site, *Monhystera*, *Desmoscolex* and *Leptolaimus*, comprised only 33.6% of the community.

Composition. The genus composition of the fresh scour was more similar with the community in the older scour than with the undisturbed community, despite that the fresh scour was located much closer to the undisturbed site than to the older scour. Three different trends of nematode response to scouring effects were found. The first group, which showed a higher relative abundance in the undisturbed site, was mostly represented by selective deposit feeders (1A). *Acantholaimus* (2A), an exceptional genus in this group, seems to be a typical deep-sea nematode (Soetaert and Heip 1995; Vanaverbeke et al. 1997) and prefers physically more stable environments. It is not clear which factors influence the sensitivity of *Acantholaimus* to iceberg scouring. The second group, which was composed of nematodes with various feeding types and different reproductive strategies, showed intermediate properties. The last group of nematodes showed a higher relative abundance in the fresh scour reflecting their recolonisation ability. The common feature of this nematode group was that most of them were non-selective deposit feeders (1B). Among these three groups the second group seemed to be most sensitive to iceberg scouring. The sensitivity of nematodes in this group is probably caused by their restricted food preference and/or due to their reproductive strategy, because most of them were either selective deposit feeders (1A) and/or persisters.
In general, the feeding guilds in the Antarctic deeper water are more or less evenly shared between 1A, 1B and 2A groups with a slight dominance of the 2A group while the 2B group appears to be the least abundant group (Vanhove et al. 1999). The results of the present study broadly confirmed this tendency although it was biased towards the 1A group in the undisturbed site and towards the 1B group in the other stations.

When we consider the nematodes with c-p value 3 as the intermediate group that can behave as either coloniser or persister according to the habitat and community structure, our results show that the colonisers become more dominant in the fresh scour while the dominance is shared between colonisers and persisters in undisturbed site. This result matches well with c-p classification (Bongers et al. 1991) except for Oxystominidae. Nematodes belonging to this family are considered as persisters (c-p=4) by Bongers et al., (1991), but they behaved more like coloniser in this area. According to Bongers et al., (1991) a nematode can show a conflicting character complex. Oxystominidae may be an example of such an exceptional case.

A close look at the relation between feeding types and MI reveals an interesting fact. When the MI of different feeding group was calculated based on the list presented as an appendix in Bongers et al., (1991) the results are 1A=3.6, 1B=2.0, 2A=3.0 and 2 B=3.4. This shows that the nematodes of 1A feeding type tend to be persisters while the ones of 1B feeding type tend to be colonisers. This implies in general that the disturbances that cause a low MI will result in increasing dominance of 1B group. On the contrary, a stable environment that shows higher MI may contain more 1A feeding members. A possible reason for the higher dominance of the 1B group in disturbed habitats is that, as it was mentioned by Bongers et al., (1991), this group is less specialised in its feeding behaviour and can feed on more various forms of food. Neilson et al., (1996) found a negative correlation of 1B/2A ratio with MI. However, the correlation they found was due to the positive correlation between 2A and MI rather than to a negative correlation between 1B and MI.

In addition to this there was a close relationship between the high MI, high proportion of 1A feeding group and high dominance of the suborder Leptolaimina and Desmoscolecina in the undisturbed site. Leptolaimina and Desmoscolecina, which have a strong tendency to a persister life strategy (c-p=4) and belong to 1A feeding group, were dominant nematode groups in the undisturbed site. Therefore the reduction of these nematodes by iceberg scoring naturally affected the trophic composition and MI in the undisturbed site. The interwoven features of the feeding type, MI and Leptolaimina and Desmoscolecina eventually characterised the nematode communities in this area.

Age and sex composition. It seems that the reproduction at the scoured site is higher than in the undisturbed site. Among the different age and sex guilds, the proportion of gravid females increased prominently in the scours. One of the reasons for the high proportion of the gravid females is due to the changes of nematode generic composition in the communities. The dominant genera in the undisturbed site, *Leptolaimus*, *Tricoma*, *Pareudesmoscolex* and *Desmoscolex,* showed a relatively lower fecundity. Therefore the low proportion of *Leptolaimus* and the Desmoscolecina genera in the scours must have influenced the proportion of gravid females. On the other hand, the lower density of the population and therefore the lower competition in the scours may have stimulated the reproduction of nematodes.

Shallow water community vs. continental shelf community in the Antarctic. The influence of iceberg scouring has also been investigated at a shallow coast site at Signy Island (Lee et al. *in press b*). The comparison of the results from Signy Island and the Weddell Sea, from this study, provides more insight about the featuring mechanisms of iceberg scouring on the meiofauna and nematode communities. Both areas are under the influence of catastrophic physical disturbances of iceberg scouring, however, the frequency of disturbance is different. The study site on the shelf off Kapp Norvegia is deeper and an occasional iceberg scouring happens at each square meter once every 340 years on the average (Gutt, *in press*), whereas scouring can happen much more frequently in the case of the coast at Signy Island (50-75 years, Peck and Bullough 1993). Between the catastrophes the seabed of Kapp Norvegia remains more or less constant, but the coast of Signy Island is under the continuous disturbance of wave action and frequent ice induced disturbances, e.g. iceberg scouring and anchor ice formation. Therefore the combined effect of various physical disturbances are structuring the nematode community at shallow Antarctic coasts while only iceberg disturbance primarily influences the nematode community at Kapp Norvegia shelf in a long-term aspect. The originally undisturbed nematode communities of both areas are very different. The nematode community at Signy Island is characterised by a low diversity, a high dominance, a low MI and a low proportion of the 1A feeding group. The undisturbed nematode community at Kapp Norvegia shows opposite characteristics. However, iceberg scouring leads to a higher similarity between the characteristics of both nematode communities of Kapp Norvegia and Signy Island. Similarly Conlan et al., (1998) found that the scour communities of macrofauna closely resembled inshore shallow water benthos despite remoteness of several hundred meters.

4.5 CONCLUSIONS

The greatest potential threats for the Antarctic deep-water communities are probably increased iceberg scouring due to global warming (Doake and Vaughan 1991; Gammie 1995). Gutt et al., (1996) concluded that a slight increased effect, which might be caused by increasing frequency of iceberg grounding in the Antarctic due to global warming could be buffered by the macrobenthic system due to its adaptation. This can be partly confirmed by the meiobenthos. Meiofauna has a strong natural capacity of recovery to all kinds of disturbance including disturbance by iceberg scouring, but a big contrast is observed between shallow and deep-water communities. Shallow meiofauna seems to be strongly adapted to iceberg scouring as they are frequently faced with different kinds of physical constrains characteristic for shallow water environments. However, the structural recovery of the meiofauna, and more specifically the nematodes, from the deeper continental shelf is a slower process that can take some years, in contrast to the rapid recovery of abundance. This indicates that the communities are much more fragile and that they do not show similar adaptations as shallow water communities. Probably this is mainly because of the relative constancy of the Antarctic deep-water environment. Hence, the increasing frequency of iceberg scouring due to global warming might have much stronger effects on a deep-water meiofauna community as compared with a shallow community.

5

<div style="border:1px solid">

THE ROLE OF SOUTHERN OCEAN MEIOBENTHOS

IN BENTHIC PELAGIC COUPLING

</div>

5.1 INTRODUCTION

The metazoan meiobenthic communities of the eastern Weddell Sea shelf attain high or similar densities during summer as communities from the same depths elsewhere (Herman and Dahms 1992; Vanhove et al. 1995). Food availability is one of the main structuring factors (Vanhove et al. 1995; Vanhove et al. 2000). Food arives as vertical and lateral detrital fluxes from pelagic production. It has a strong spatial variability, which is likewise the consequence of ice-related and other processes (Fukuchi et al. 1984; Sasaki and Hoshiai 1986; Matsuda et al. 1987; Fischer et al. 1988; Nöthig and von Bodungen 1989; Bathmann et al. 1991; Schlüter 1991; Gutt et al.1998).
This study focusses on the contribution of the meiobenthos community (and especially the most abundant taxon, the nematodes) in the C-flux of the Antarctic benthic ecosystem. We believe that the high meiobenthic densities and biomasses fit strongly in the framework of the episodic (seasonal ?) food supply by preferentially utilizing labile organic matter. The dimension of the carbon flux through the Antarctic meiobenthos is, however, not known yet (Jarre-Teichmann et al. 1997).
The use of stable isotopes, such as 13-C/12-C, 15-N/14-N, 34-S/32-S, may contribute to a better understanding of the trophic food chains because the diet of consumers/predators is primary determinant of animal isotopic composition (Peterson and Fry 1987). The technique is new to meiofauna ecology, but can be an interesting tool for identifying the position of the meiofauna in the trophic food web (Moens et al. subm.). Especially in the deep-sea where the origin and structure of the food items can not always be determined visually, this method can reveal promising results. In addition, it can give information about the past feeding history of meiofaunal organisms in a seasonal limiting environment (such as the Antarctic marine ecosystem).

The first aim of this survey is to study the role of the meiobenthos in a comparative way, by the use of the natural $^{14}N/^{15}N$ & $^{12}C/^{13}C$ ratios of the numerically dominant nematodes. The natural stable isotope ratios from the meiobenthos will be compared with the isotope signature from the suspended particulate matter in the near bottom water (more labile) and from the organic matter in the sediment (more degraded). Complementary comparisons can be made with Antarctic isotope values from literature (Wada et al. 1987; Rau et al. 1991a, Rau et al. 1991b).

Secondly, the role of the meiobenthos (nematodes) is studied in an experimental way, by following a ^{13}C-tracer through an intact benthos community. The ^{13}C assimilation by the meiobenthic community is investigated in an incubation experiment with a simulated plankton bloom, during a period of two weeks (by fourth-night intervals) and along a vertical sediment profile. A similar experiment has proven the ecological importance of benthic Foraminifera in the C-flux of Oosterschelde sediments (Moodley et al., in press).

5.2 MATERIALS AND METHODS

5.2.1. Sampling and initial treatments on board

Sampling for the natural isotope composition of the nematodes occurred during two campaigns with RV *Polarstern* to the Weddell Sea and along the Antarctic Peninsula.

Locality from EASIZ II-stations (KN: Kapp Norvegia; KG: King George Island, BS : Bransfield Strait; DP : Drake Passage)

During EASIZ II (ANT XV/3; 25/1 to 21/3/1998) multboxcorer (MG) samples were taken between 245 and 2009m depth at Kapp Norvegia and near King George Island (Bransfield Strait en Drake Passage).

	Locality (°S, °W)	depth
KN	70°52,1' 10°29,3'	245
KN	70°49,8' 10°38,0'	298
KG (BS)	62°20,1' 58°38,8'	606
KG (DP)	61°20,6' 58°15,1'	2009
KG (DP)	61°26,7' 58°06,6'	1028
KG (DP)	61°53,3' 59°06,9'	218

Date	Station n°	Name	Position
24.04.00	148(1)	MUC 1	62°42,80'S 56°52,50'W
	148(2)	MUC 2	62°42,80'S 56°52,60'W
	148(4)	MUC 3	62°42,80'S 56°52,80'W

Locality from the EASIZ III-station (Bransfield Strait)

During the EASIZ III campaign (ANT XVII/3; 17/03 to11/05/00), station 148 located at ± 230 m in the Bransfield Strait was sampled by means of three replicate drops with a multicorer (MUC). This station was situated in a depression between hard substrata. From this site (e.g. Sta. 148, Bransfield Strait) cores (30,2 cm²) were treated for the incubation experiment as well (table XIII).

Table XIII: Sample destany

	Purpose	MUC 1	MUC 2	MUC 3
Station		148(1)	148(2)	148(4)
#cores		6	9	5
24/04/00	Community analysis + natural ^{14}N/^{15}N ratios of SPM	1	1	1
	Environmental variables + natural ^{14}N/^{15}N & ^{12}C/^{13}C ratios of sediment + nematodes	1	1	
29/04/00	^{13}C-tracer	1	1	1
3/05/00	^{13}C-tracer	1	2	1
7/05/00	^{13}C-tracer	1	2	1
10/05/00	^{13}C-tracer	1	2	1

The sediment of two cores were divided for the analysis of granulometry, Chl-*a*, C/N and detrital $^{15}N/^{14}N$ & $^{13}C/^{12}C$ ratios. The remainder of this sediment was used for the analysis of the natural $^{15}N/^{14}N$ & $^{13}C/^{12}C$ ratios of the nematodes. The samples were stored immediately at -20°C. Three additional cores were used to study the nematode community composition. From these cores 1 liter of near bottom water was collected and filtered over a pre-glowed (2 hours at 450°C) Millipore GFF filter (pore width, 0.7 µm ; diamter 47 mm) to determine the organic and natural isotopic content of the suspended particulate matter. The sediment of these 3 cores were preserved with a buffered, hot (60°C) 4% formaline solution.
All cores were studied along a vertical profile (0-1, 1-2, 2-5 & 5-10 cm depth).

For the incubation experiment (^{13}C-tracer) fifteen replicate, 30.2 cm² sediment cores, more than 10 cm deep, were incubated in dark conditions at –1°C, approaching the habitat temperature, with 20 cm of original bottom water above the sediment. To each core, 4 mg of freeze dried ^{13}C-labelled algal cells (*Cambridge Isotope Laboratories*) were applied in a frozen sea-water icecube, for better suspension and avoiding the disturbance of the sediment surface. These algal cells were enriched in ^{13}C (δ-value) and consisted of 26 mass% carbon. The amount of carbon applied in this way, 1,04 mg C/core (34,4 mg C/m²), lies within the range of daily organic carbon fluxes (table XIV). An intermediate enrichment value was chosen to prevent anoxic conditions. Incubation was stopped after respectively 5, 9, 13 and 16 days.

Table XIV: Sedimentation of organic carbon in Antarctic waters
(The values in bold are calculated from year-round values divided by 365)

Study	Location	Depth (m)	Vertical flux		Notes
			g C m^{-2} y^{-1}	mg C m^{-2} d^{-1}	
Wefer *et al.* (1982)	Drake Passage (Dec-Jan)	0	36.5	**100**	
		965	5.41	**15**	
		2540	4.78	**13**	
Sasaki & Hoshiai (1986)	Lützow-Holm Bay (Nov-Jan)	0.3		±10-70 (Nov-Jan)	Sedimentation of phytoplankton & ice-related biota (algae)
		10		± 20-60 (Nov-Jan)	
		30		±50 (Jan)	
Matsuda *et al.* (1987)	Lützow-Holm Bay (year round)	5-25		1.5-136	Sedimentation of phytoplankton & ice-related biota (algae)
Liebezeit & von Bodungen (1987) *in:* Knox (1994)	Bransfield Strait (Nov-Dec)	18		8	
		323		131.9	
		539		120.3	
		963		80.3	
		1410		94.3	
Fischer *et al.* (1988)	Weddell Sea (Jan-Dec)	3880	20	**0.05**	Lowest flux yet observed
Wefer *et al.* (1990), Wefer & Fischer (1991)	Bransfield Strait	494	7.7	**21.09**	
		693	0.35	**0.95**	
		687	1.1	**3.01**	
	Northern WS	863	0.021	**0.06**	Extremely low value!
	Maud Rise	4556	0.17	**0.47**	
		360	2.28	**14.24**	
		352	0.16	**0.44**	
	Polar Front	700	2.86	**7.84**	
Bathman *et al.* (1991)	Weddell Sea (Jan-Feb)	250		3.3-112.2	

5.2.1. Later treatments in the laboratory

The sediment frozen for isotopic analysis of the fauna was thawed, sieved over a 1mm sieve and the sediment remaining on the 38 µm sieve, after washing thoroughly, was centrifugated three times, during ten minutes, with a Ludox HS-40 (colloidal silica) solution with a density of 1.18. The influence of the organic residue present in the Ludox colloid is known to be negligible (De Man 1998). Following extraction, the meiobenthos fraction was rinsed and stored in distilled water and stored at -20°C. Following thawing of the deep-frozen samples of extracted nematodes, 50 to 100 and 500, respectively for ^{13}C-tracer and natural $^{15}N/^{14}N$ & $^{13}C/^{12}C$ ratios, were picked out from every sediment slice and rinsed two times in distilled water. Subsequently they were brought into aluminium cups, 2,5x 6 mm, Van Loenen Instruments (pre-glowed at 450°C during three hours to remove organic particles). The filled aluminium cups were finally dried during at least half an hour at 60°C. Finally they were folded up and stored refrigerated in air-tight vials until analysis of the isotope ratios. The GF/F filters with SPM of near-bottom water were dried at 60°C prior to analysis. The meiobenthos for community analysis was extracted similarly as described above. In contrast to the method for the nematodes used for the isotope analysis, this material was stored in a 4% formaline solution and dyed with Bengal Rose.

The abundance of the meiobenthos was determined by enumerating the individuals to higher taxon level. In addition, the nematode community was studied by identifying ±100 nematodes from each sediment slice; which were studied in glycerine slides following a dehydratation treatment (Seinhorst 1959). The nematodes were examined with a Leica DMLB light microscope under a magnification of 100x (immersion oil) and identified up to genus level by using a pictorial key (Platt & Warwick 1988), and a collection of descriptive papers. Finally the genera were consigned a feeding type (Wieser 1953).

Granulometry analysis was performed with a Coulter ® LS Particle Size Analyzer. Prior to analysis the samples were dried in a stove at 60°C and subsequently they were wetted and sieved through a 1mm sieve. During the treatment the samples were always sonicated during 1 minute to prevent chunks of fine sediment to be formed which would behave like larger grains. Nevertheless only the grain sizes between 4 and 800 µm could be registered by using this technique.

Prior to C/N analysis, the sediment samples were dried at 60 °C and thereafter they were treated with 10-20 µl of 10 volume% HCl to remove $CaCO_3$ from the sediment. Addition of the HCl solution to the dried sediment was repeated until the addition did not cause any more foaming of the samples. Afterwards these samples were dried again during at 60°C. From each of these samples a subsample of several mg of sediment was weighed and transferred to pre-glowed (4 hours at 450°C) pre-weighed Sn cups (The rest of these samples was kept to analyse the isotope ratios of the sediment detritus). The analysis of the C and N content was finally achieved with a Carlo Erba elemental analyzer.

The carbon isotopic composition of the samples was determined with a Fisons CN-analyser coupled online via a con-flo 2 interface to a Finnigan Delta S mass spectrometer. Results are reported in he d notation relative to Vienna PDB and expressed in units of ‰, according to the standard formula : $dX = [R_{sample}/R_{standard}) -1] x 10^3$ ‰ where $X = {}^{13}C$ or ${}^{15}N$, and $R = {}^{13}C:{}^{12}C$ or ${}^{15}N:{}^{14}N$. Reproducibility of the d values was better than 0.2 ‰.

Statistical analysis consisted of Spearman rank correlations with incubation time for the variables considered in each sediment slice, to explore the depth penetration of the organic matter from the pelagial and its assimilation by the meiobenthos. The 0,05 significance level was used, all p-values smaller were considered significant.

5.3 RESULTS

5.3.1 Community analysis and natural nematode ${}^{15}N/{}^{14}N$ & ${}^{13}C/{}^{12}C$ ratios

$d^{13}C$ signals from nematodes during EASIZ II showed no clear water depth related trend, but lower signals in Kapp Norvegia hint to some regional variability (fig. 17). Moreover, nematodes from a sponge spicule mat were relatively more enriched in ${}^{13}C$ compared to bryozoan debris covered bottoms and silty sediments which could point to substrate variability. Communities in the sponge spicule mat consisted of a high percentage of nematode genera such as *Monhystera, Leptolaimus, Acantholaimus, Pareudesmoscolex, Tricoma* and *Desmoscolex*, mainly belonging to selective feeding groups. Nematodes in bare silty sediments were less enriched. They belong mainly to *Monhystera, Neochromadora, Daptonema* and *Sabatieria* and are relatively more composed of non-selective feeders (Lee et al. *in press*).

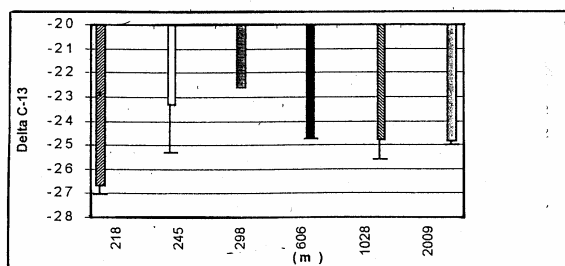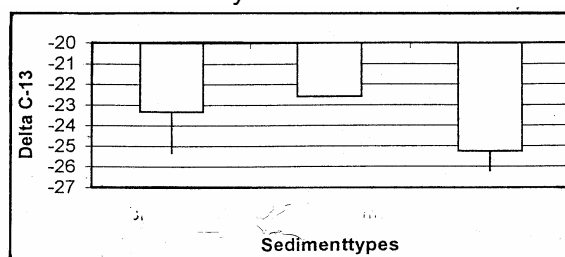No clear relationships were observed between the $d^{13}C$ data and concentrations of bulk organic food sources.

Figure 17: ${}^{13}C$ isotopic ratios from nematodes during the EASIZ II campaign (top: arranged according to sedimenttypes bryozoan mat, sponge spicule mat, silt; bottom : according to water depth).

The densities of the meiobenthos during EASIZ III ranged between 3038 and 5056 ind./10 cm² (table XV). Both in the cores from MUC 2 and MUC 3 the highest

densities were situated in the 2-5 cm horizon. Only in the core from MUC 1 there was a clear decrease in density with depth. The densities in this station are very high compared to other Antarctic deep-water studies (Vanhove *et al.* 1995, Fabiano & Danovaro 1999). Nematodes were the most abundant taxon (more than 95% of the individuals). In the sediment cores from MUC 2 and MUC 3 the diversity in taxa decreases sharply from the 5-10 cm on. This is already the case from the 1-2 cm in the MUC 1 core.

Table XV : Station 148 (EAS IZ III) : Densities of meiobenthos (ind./10 cm²).

	MUC 1	MUC 1	MUC 1	MUC 1	MUC 2	MUC 2	MUC 2	MUC 2	MUC 3	MUC 3	MUC 3	MUC 3	Total	%
	0-1 cm	1-2 cm	2-5 cm	5-10 cm	0-1 cm	1-2 cm	2-5 cm	5-10 cm	0-1 cm	1-2 cm	2-5 cm	5-10 cm		
Nematoda	2254	1602	891	160	852	759	1269	339	883	836	1064	113	11022	95.40
Copepoda	58	5	2		46	33	20	2	31	23	12	1	233	2.02
Nauplii	32	1	1		11	16	17	2	19	5	4		108	0.93
Polychaeta	17		1		12	5	21	2	4	6	3		71	0.61
Kinorhyncha	5				4	7	2			5	1		24	0.21
Ostracoda	4		1		2	4	7				3	3	24	0.21
Oligochaeta	1	1	6		1	2	4	2	1	1	4		23	0.20
Gastrotricha	2	1			3	2	2	1	4				15	0.13
Sipunculida	3				3		1		1				8	0.07
Bivalvia	3				1	1			1	1			7	0.06
Halacarida						1			2	2		1	6	0.05
Turbellaria	2						2						4	0.03
Rotifera	2										1		3	0.03
Cumacea									1	1			2	0.02
Tanaidacea					1		1						2	0.02
Amphipoda	1												1	0.01
Isopoda									1				1	0.01
Total	2384	1610	902	160	936	829	1347	348	953	879	1091	115		100.00

Figure 18: Relative representation of the most dominant nematode genera at Sta. 148

1061 nematodes have been identified, from which most could be identified up to the genus level (table XVI).

Molgolaimus is the most abundant genus, although it reaches its maximum abundance in deeper strata of the sediment (fig. 18). Other subdominant genera, like *Neotonchus*, *Sabatieria* and *Paralongicyatholaimus* are mainly confined to the deeper strata. Dominant genera of the upper layers of the sediment are *Microlaimus*, *Desmoscolex* and *Halalaimus*.

The most dominant feeding type (Wieser, 1953) of this community is 1A, the selective deposit feeders. They range between 33 and 54 % of the nematode community, with highest average proportion in the 1-2 cm horizon (fig. 19). The non-selective deposit feeders (1B) range between 17 and 23%; the epistrate grazers (2A) between 15 and 40%. Feeding type 2B (predators and omnivores) are the least presented (between 3 and 4%).

Figure 19: Average feeding type on the nematode community at Sta. 148
1A : selective deposit feeders ; 1B : non-selective deposit feeders ; 2A : epistrate grazers ; 2B : predators/omnivores ; ? : unknown feeding guild
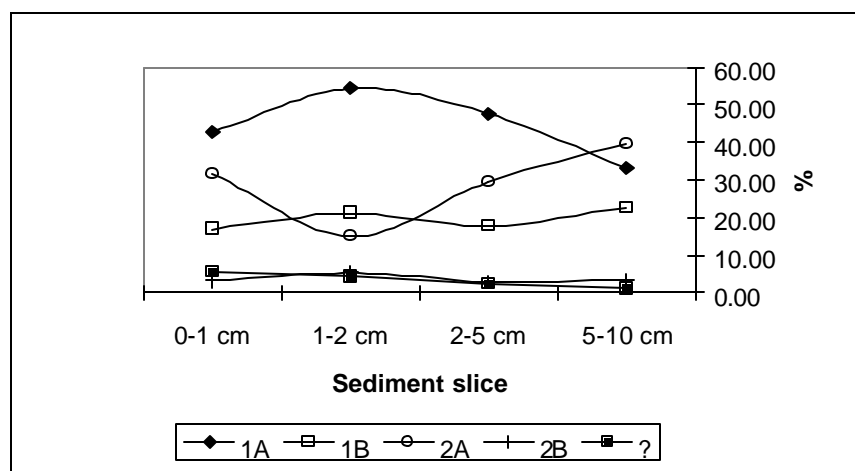
The natural isotope $^{13}C/^{12}C$ ratio's of the nematodes (between −25.5 and −23.5‰, table XVII) were comparable with the earlier observations in the Bransfield Strait, and appeared different between two replica's. In replica ½ no clear differences were found between natural nematode and natural detrital ^{13}C-signals. In replica 2/4 isotopic shift between detritus and nematodes were higher in the upper two sediment layers (e.g. with a difference up to 2‰), compared with the deeper layers (e.g. with a difference lower than 1‰).

Table XVII : Natural isotope ratios $^{13}C/^{12}C$ at Sta. 148 (EASIZ III, Bransfield Strait). Numerical values in parentheses stand for the number of nematode specimens used.

	0-1 cm	1-2 cm	2-5 cm	5-10 cm
MUC ½	-24.43 (472)	-24.74 (500)	-24.55 (500)	-24.13 (18)
MUC 2/4	-23.46 (500)	-23.99 (500)	-23.63 (668)	-25.47 (74)

Table XVI: Station 148: Average percentage composition of the nematode community

Genus	Total	percentage 0-1 cm	1-2 cm	2-5 cm	5-10 cm
Molgolaimus	8.56	5.21	28.33	27.66	19.08
Acantholaimus	6.61	6.70	0.70	1.41	0.62
Halalaimus	6.55	6.36	6.28	2.81	1.31
Desmoscolex	6.17	5.79	6.02	3.86	3.06
Microlaimus	4.58	9.45	3.11	1.41	1.56
Monhystera	4.53	5.34	4.96	0.71	3.93
Cervonema	4.13	5.03	2.42	1.06	0.33
Daptonema	3.99	4.95	4.83	2.47	0.33
Cyatholaimidae	3.77	3.61	1.10	0.70	1.41
Quadricoma	3.65	3.39	3.30	4.22	1.41
Oxystomina	3.34	4.49	1.45	0.00	
Actinonema	2.95	2.48	1.85	0.35	1.85
Sabatieria	2.54	0.41	4.39	11.61	14.72
Leptolaimus	2.30	2.40	0.33	0.70	0.36
Halichoanolaimus	2.08	1.96	2.84	1.05	0.36
Amphimonhystrella	2.07	1.60	2.11	0.00	1.68
Chromadorita	1.84	2.06	0.00	0.00	0.36
Neotonchus	1.79	0.41	1.37	4.91	16.16
Theristus	1.72	1.72	2.45	0.70	0.00
Camacolaimus	1.53	1.21	1.50	1.06	0.00
Diplopeltula	1.52	1.26	1.04	0.71	0.00
Anticoma	1.51	1.57	0.35	1.06	1.02
Paralongicyatholaimus	1.48	0.00	0.71	8.07	8.29
Cyartonema (Southernia?)	1.31	1.21	0.00	0.00	0.00

Genus	Total	percentage 0-1 cm	1-2 cm	2-5 cm	5-10 cm
Xyalidae	1.27	2.45	0.66	0.35	1.99
Spilophorella	1.20	2.45	1.43	0.35	0.33
Aegialoalaimidae	0.94	0.88	0.00	0.00	0.00
Neochromadora	0.93	1.18	0.33	0.35	0.00
Draconema	0.89	0.83	0.00	0.00	0.00
Terschellingia	0.75	0.00	0.00	4.17	4.59
Laimella	0.66	0.00	0.37	3.15	4.63
Southerniella	0.53	1.25	0.00	0.00	0.00
Leptolaimoides	0.51	0.79	0.33	0.35	0.00
Paramesacanthion	0.51	0.39	0.00	0.00	1.33
Desmodora	0.50	0.00	0.37	4.21	1.28
Cobbia	0.50	0.44	0.00	0.35	0.00
Leptolaimidae	0.50	0.44	0.00	0.00	0.62
Nemanema	0.48	0.39	0.35	0.00	0.36
Enoplida	0.47	0.44	0.00	0.00	0.00
Haliplectidae	0.47	0.44	0.00	0.00	0.00
Araeolaimus	0.45	0.79	0.00	0.00	0.00
Chromadoridae	0.45	0.79	0.00	0.00	0.00
Epsilonema	0.45	0.39	0.37	0.00	0.00
Pontonema	0.42	0.39	0.00	0.00	0.00
Hopperia	0.38	0.00	0.33	2.11	2.28
Gammanema	0.25	0.41	0.68	1.41	0.62
Pareudesmoscolex	0.25	0.00	2.07	0.71	0.00
Sphaerolaimus	0.22	0.00	1.36	0.35	1.23

Genus	Total	percentage 0-1 cm	1-2 cm	2-5 cm	5-10 cm
Comesomatidae	0.19	0.00	1.39	0.70	0.00
Thalassolaimus	0.13	0.00	0.70	0.35	0.62
Aegialoalaimus	0.09	0.00	0.70	0.00	0.33
Chaetonema	0.09	0.41	0.33	0.35	0.00
Filitonchus	0.09	0.00	1.06	0.00	0.00
Amphimonhystera	0.06	0.00	0.75	0.00	0.00
Desmodoridae	0.06	0.00	0.00	0.00	0.66
Antomicron	0.03	0.00	0.33	0.00	0.00
Cricolaimus	0.03	0.41	0.00	0.00	0.00
Elzalia	0.03	0.00	0.37	0.00	0.00
Gnomoxyala	0.03	0.00	0.33	0.00	0.00
Linhomoeidae	0.03	0.00	0.00	0.35	0.00
Metacyatholaimus	0.03	0.00	0.33	0.00	0.00
Metalinhomoeus aff.	0.03	0.00	0.00	0.35	0.00
Paralinhomoeus	0.03	0.00	0.00	0.35	0.00
Paramonhystera	0.03	0.00	0.00	0.35	0.00
Praeacanthonchus	0.03	0.41	0.00	0.00	0.00
Praeacanthonochus	0.03	0.00	0.00	0.35	0.00
Prochromadorella	0.03	0.00	0.37	0.00	0.00
Pseudocella	0.03	0.00	0.00	0.00	0.33
Spiliphera	0.03	0.00	0.00	0.35	0.00
Tylenchidae	0.03	0.00	0.37	0.00	0.00
Vasostoma	0.03	0.00	0.00	0.35	0.00
Viscosia	0.03	0.00	0.35	0.00	0.00
?	4.22	5.03	2.45	1.75	0.98

5.3.2 Environmental conditions

A summary of the environmental properties in the EASIZ II- stations is given in table XVIII.

Table XVIII : Summary of the environmental variables in the EASIZ-II stations.

	Locality (°S, °W)	depth	substrate type (% pellite)	Chl-a (µg/g)	Carbon %	Nitrogen %	CN
KN	70°52,1' 10°29,3'	245	Bryozoan mat + coarse silt (63%)	36 ± 30.0	0.7 ± 0.33	0.03 ± 0.009	23
KN	70°49,8' 10°38,0'	298	Sponge spicule mat + coarse silt (53%)	4± 5.1	0.4 ± 0.15	0.06 ± 0.013	7
KG (BS)	62°20,1' 58°38,8'	606	Bare fine silt (81%)	216 ± 293.9	0.3 ± 0.07	0.03 ± 0.007	10
KG (DP)	61°20,6' 58°15,1'	2009	Bare medium silt (60%)	8± 3.2	0.6 ± 0.03	0.06 ± 0.004	10
KG (DP)	61°26,7' 58°06,6'	1028	Bare fine silt (94%)	37 ± 37.6	0.3 ± 0.04	0.04 ± 0.007	8
KG (DP)	61°53,3' 59°06,9'	218	Bare coarse silt (53%)	97 ± 101.8	0.4 ± 0.12	0.03 ± 0.023	10

The sediment of station 148 consisted of fine sand and the silt content (sediment grains between 4 and 63µm) ranged between 27 and 51%. This station was situated in an area with strong bottom currents (caused by the Weddell Sea gyre from the Antarctic Coastal Current) (Knox 1994). Chemical analysis of the near bottom water revealed it was located near a putative methane seep (Weber, pers. comm.). The sediment surface was rather scarcely covered by epifauna. Some bioturbation traces were visible. The content of organic carbon and nitrogen of the sediment ranged respectively between 0.3-0.6 and 0.03-0.17 mass %. C/N ratios ranged between 3 and 11. The figures agree with other studies in the region (table XIX).

Table XIX : Sediment mass% C, N and C/N data from other studies in the region.

Study	Location	Depth (m)	Season	%C	%N	C/N
Schlüter (1991)	SE-Weddell Sea	422-4707	Summer	<0.5		
Herman & Dahms (1992)	SE-Weddell Sea Halley Bay	339-1985	Summer	0.18-0.59		5.54-9
Vanhove et al. (1995)	SE-Weddell Sea Kapp Norvegia	211-2080	Summer	0.2-0.5	0.0-0.1	7.5-9.3
Present study	Bransfield Strait	227-234	Autumn	0.34-0.55	0.03-0.17	3.3-10.5

The natural detrital ^{13}C isotopic ratios ranged between −26.00 and −24.10‰.

	0-1 cm	1-2 cm	2-5 cm	5-10 cm
MUC ½	-24.11	-24.10	-24.55	-24.59
MUC 2/4	-24.65	-26.00	-24.16	-24.60

The natural ^{15}N isotopic ratios of the suspended particulate matter ranged between 3 and 4‰.

	$^{15}N/^{14}N$	%N
MUC1	3.66	0.36824
MUC2	3.18	0.36807
MUC3	3.94	0.36834

5.3.3 The role of nematodes in the carbon flux of Antarctic sediments: incubation experiment

The algal cells settled rapidly and a distinct green layer was visible on the sediment surface within less then 10 minutes, and organic matter in the sediments was successfully enriched in ^{13}C after 5 days (table XX). No clear transport of the organic matter (i.e. increase of C or N, or change in C/N value) out of the 0-1 cm layer was visible during the time-course of the experiment (fig. 20). This is confirmed by the high ^{13}C enrichment at the surface, though much lesser and almost no isotopic change in deeper layers (at 1-2 to 2-5 cm and 5-10 cm, respectively). Food was fresher in the first two sediment slices (e.g. CN-values were lower at 0-1 and 1-2 cm). In additon, no clear time-trend in organic matter was visible at any depth interval. CN ratio's grew slightly with time, indicating that some degradation might have occurred during the experiment. Patchy distribution of organic matter in the sediments might have masked downcore penetration.

carbon/nitrogen ratio

Organic carbon

Organic nitrogen
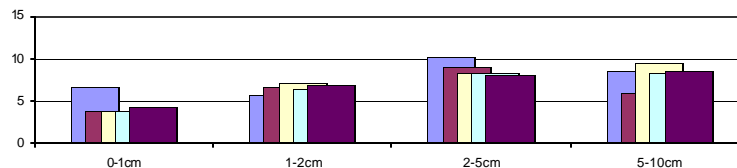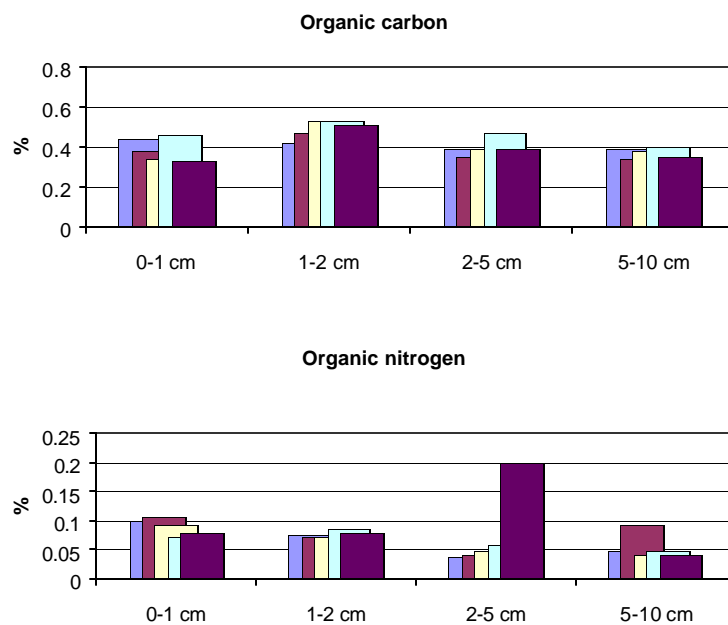
Figure 20: Time-dependent organic matter variation at the four sediment intervals. Each cluster represents the values from the five subsamplings (respectively day 0, 5, 9,13,16)

Table XXI: Isotopic $^{12}C/^{13}C$ ratio's in nematodes during the experiment

		0-1 cm	1-2 cm	2-5 cm	5-10 cm
29/04/00 (day 5)	MUC 1/1	-22.99	NA	-24.83	-26.29
29/04/00	MUC 2/1	-15.46	-21.82	-22.57	-23.25
29/04/00	MUC 3/1	-29.04	-20.16	-23.94	-23.59
03/05/00 (day 9)	MUC 1/3	NA	-22.9	-25.57	-24.86
03/05/00	MUC 2/3	-11.91	-22.65	-22.59	-22.97
03/05/00	MUC 3/2	-22.19	-22.64	-24.40	-24.09
03/05/00	MUC 2/5	3.8	-19.48	-24.14	-22.24
07/05/00 (day 13)	MUC ¼	-7.12	-24.59	-23.56	-24.31
07/05/00	MUC2/6	0.01	-22.89	NA	-23.19
07/05/00	MUC 3/3	-17.37	-22.60	-24.90	-24.62
07/05/00	MUC 2/7	NA	-14.75	-19.87	-21.41
10/05/00 (day 16)	MUC 1/6	NA	-22.81	-19.95	-26.18
10/05/00	MUC 2/8	-10.69	-16.58	-25.08	-23.62
10/05/00	MUC ¾	-21.25	-25.26	NA	-25.06
10/05/00	MUC 2/9	NA	14.56	-18.02	-12.49
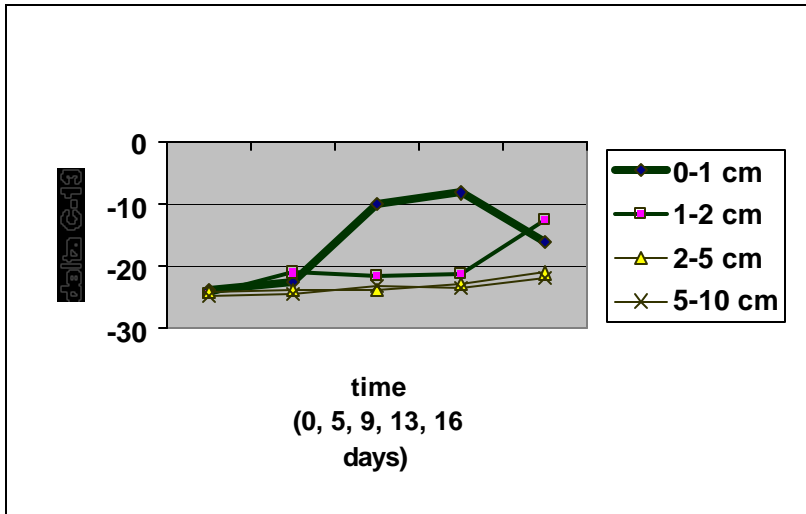
Figure 21 : Temporal variation in ^{13}C isotpic content in the nematodes during the incubati on experiment.

Assimilation of ^{13}C label by nematodes started to a low level at day 5 and was clearly visible after 9 days in the upper cm (fig 21). Enrichment in the upper layer nematodes continued until day 13. In general, enrichment was far below the level of organic enrichment of the sediments (table). Nematodes in the next layer (1-2 cm) were little enriched (compared to day 0 and to detrital ratios) after 13 days and later. In the deepest layers nematode ^{13}C did not change during the incubation and were comparable with detrital and natural isotopic signals.

5.4 DISCUSSION

Methodology. Meiofauna form a key role in the transfer of organic matter within benthic food webs (Coull and Bell 1979). However, in spite of their numerical importance and despite extensive (conventional) assessments on feeding habits in free-living marine nematode communities (Wieser 1953; Alongi and Teitjen 1980; Romeyn and Bouwman 1983; Schiemer 1984; Jensen 1987; Moens and Vincx 1997), there is still a high uncertainty about the diet of those organisms. Recent progress in isotope biogeochemistry may help to meet urgent requirments. This approach is based on the close relationship between the stable isotope composition of a consumer and its food (Fry and Sherr 1984). However, some methodological constraints restricted our study.

We attempted to use a dual isotope (carbon and nitrogen) approach (Fry 1988). An enrichment of ^{15}N is widespread among most animals, irrespective of trophic levels, habitat, form of nitrogen excreted and growth rate. It averages +3.4 $\pm$ 1.1‰ for a single feeding process (Minagawa and Wada 1984), and an average d^{15}N increase of 3.3 $\pm$ 0.2‰ per trophic level is known in Antarctic ecosystems (Wada et al. 1987). ^{15}N measurements are thus useful in defining the trophic position of organisms in systems where feeding relationships are not known. Conversely, d^{13}C are generally only weakly enriched with increasing trophic level (about 1‰); ^{13}C.values of nematodes will be identical or little higher then ^{13}C values of their potential food sources. The use of d^{13}C may provide insights on the sources of organic matter (benthic or planktonic) that are actually assimilated over a long period of time.
Isotopic carbon ratio measurements were rather easily obtained in our study (although adequate replication was not possible). In contrast, signals of isotopic nitrogen were below detection level. As free-living nematodes have low nitrogen

content, a fairly large number of specimens is needed to reach that detection level (e.g. isotopic nitrogen signals from 600 specimens were still below the detection level of the instruments). Such treatmens are too time-consuming because of the small size of deep-sea nematodes, and far from evident as often not enough debris-free specimens could be extracted because of low densities.

Isotopic carbon composition of nematodes under different ecological conditions. Meiobenthic nematodes (the dominant taxon within the meiofauna) mainly consist of grazers adapted to ingestion of specific microbial food items such as bacteria and microalgae (Montagna 1995). Other feeding modes have, however, been proposed for many nematode taxa (Moens and Vincx 1997, and references therein). The evidence regarding whether meiofaunal populations ingest more microbial or algal carbon is, however, conflicting. Whatever preferences they make, communities of nematodes living under different ecological conditions will have different feeding habits depending on the availabilty of the food sources (Wieser 1953). Such differences should be interpretable from stable isotope research.

In estuaries, labile organic matter, as derived from microphytobenthos and settled phytoplankton, constitute an important carbon source for nematodes, but also detrital *Spartina* is assimilated (Couch 1989; Schwinghammer et al. 1983; Middelburg et al. 2000; Moens et al. *subm*). $d^{13}C$ values in estuarine nematodes were found between −18.5 and -14.0‰. Within coastal mud flats microphytobenthos may be predominant in the diet of meiofauna (Schwinghamer et al 1983; Riera et al. 1996). Isotopic ratios of -16.4 to -15.3 ‰ $d^{13}C$ and 8.9 to 9.3 ‰ $d^{13}N$ were mentioned (Riera et al. 1996). Meiofaunal nematode abundances in the deep sea are highest in the top layer of the sediment and decrease rapidly with sediment depth, suggesting that they depend strongly on the input of fresh POM (Vanreusel et al. 1995 and references therein). From traditional descriptive methods it was concluded that the meiofauna communities in Antarctica were primarily related to phytoplankton blooms and associated sedimentation pulses (Vanhove et al. 1995). Nematodes in the deep sea do not depend solely on POM directly. Carnivory or feeding on nanobiota such as bacteria or fungi were considered as alternative feeding strategies. Isotopic ratios of -16.9 ‰ $d^{13}C$ and 12.8 to 15.9 ‰ $d^{13}N$ were mentioned (Goering et al. 1990; Iken et al. *in press*).

The carbon stable isotope abundances in Antarctic nematodes (this study) occurs within a large range of variation between −26.5 and −22.5‰ and are situated closely to the natural detrital signals (e.g. between −26.00 and −24.10‰). The $d^{13}C$ set of Weddell Sea nematodes lies well below carbon isotope values from the earlier mentioned ecosystems in the northern hemisphere. This is in accordance with the significant lower $d^{13}C$ values in the high-latitude Southern Ocean (Sackett et al. 1965; Biggs et al. 1988; Wada et al. 1987; Fischer 1989; Rau et al. 1991b). This unique isotopic signature might be caused by temperature, light, nutrient availability, species composition and other factors (see below). The nematode $d^{13}C$ range are close to the values (-33.2 to −23.9‰) reported for Southern Ocean pelagic invertebrates (Wada *et al.* 1987; Fischer 1989; Rau et al. 1991a).

Nematodes in the isotopic structure of the Antarctic ecosystem. The stable isotope ratios of nitrogen and carbon for biogenic substances were investigated elsewhere to describe the isotopic structure of the Antarctic ecosystem (table XXII).

Table XXII : Isotopic fractioning in the Southern Ocean

	(‰)	SPOM	Plankton	Sediment	Sediment traps
1	$d^{15}N$	0.4 to 0.5	0.6 to 9.8	4.9;5.2;5.5	-3.0 to 0.86
	$d^{13}C$	-27.4 to -26.4	-32.3 to -26.6	-20.5;-25.3;-25.4	-27.9 to -25.6
2	$d^{13}C$	-31.9 to −20.1			
3	$d^{13}C$				-30.5 to –23.2
4	$d^{13}C$	Sea ice: -18 to –20 Open water : -28			
5	$d^{13}C$	−29.7 to −21.9			
6	$d^{15}N$				-2.1 to 7.8
	$d^{13}C$				-30.8 to –27.2
7	$d^{15}N$		1.8 to 3.3		
	$d^{13}C$		-26.7 to −22.8		
8	$d^{15}N$	-5.4 to 41.3			
	$d^{13}C$	-30.4 to −16.7			
9	$d^{13}C$	-1.1 to 1.74			

Data obtained from 1)Wada et al. 1987: Southern Ocean Australian Sector; south of the Polar Front, Nov.Febr; 2) Kopczynska et al. 1995: Prydz Bay, Southern Ocean Australian Sector, Jan/Feb; 3) Bathmann et al. 1991: Jan/Feb; 4) Fischer 1989: Weddell Sea, Summer; 5) Dehairs et al. 1997: Circumpolar Current and Polar Front, spring and early summer; Biggs et al. 1988: Weddell abyssal plain, Maud Rise, Dronning Maud Land margin, South Orkneys, summer; 7) Handa et al. 1992: Breid Bay, Dec/Feb; 8) Rau et al. 1991b: Weddell Sea, Nov/Dec/March/June; 9: Archambeau et al. 1998: South Africa to Antarctica, Feb/March

Summarized, fluctuations of the isotopic abundances in the food web mainly result from the variation of ^{15}N and ^{13}C contents in phytoplankton thrive in a narrow range (-1.6 to 1.9°C) of ambient water temperature, and grown under different nutrient (nitrate and ammonium) and high pCO_2 conditions during austral summer. $d^{13}C$ thus exhibits a large range of low values compared to elsewhere in the marine environment, ranging from −32.3 to −16.7‰ (references in Table and Handa et al. 1992). $d^{13}C$ values of phytoplankton may correspond to changing biomass and different types of species assemblages from larger microplanktonic diatom cells over smaller nanoflagellates to the smallest picoplankton. In Prydz Bay, for example, high $d^{13}C$ values of −20.1 to −22.4‰ may be determined by pennate diatoms such as *Nitzschia* and *Thallassiosira* spp*.* Whereas *Phaeocystis* and naked flagellates (*Cryptomonas* and *Pyramimonas* spp) + diatoms are the likely major determinants of the lower $d^{13}C$ values (-24.5 to −26.7‰). Lowest values (-29.8 to −31.9) were due to the dominance of naked flagellates and *Phaeocystis* spp. Dinoflagellates and pennate diatoms fractionate carbon less (higher $d^{13}C$ signature) than centrics (Kopczynska et al. 1995).

Less is known about the variation of the $^{15}N/^{14}N$ in upper ocean plankton, and relatively little work has been done in te Southern Ocean. Water column organic matter $d^{15}N$ has been found to range from 0.4 to 41.3‰ (references in table XXII), often lower than commonly encountered in lower-latitude waters.

Our investigations were carried out along the continental shelf to the deeper slopes at three different distant localities (e.g. Kapp Norvegia, southern Drake Passage around King George Island and Bransfield Strait around King George Island) and in different substrates (bryozoan debris and sponge spicule covered soft sediments and silty bottoms). The distinction between localities suggest much variation in phytoplankton community structure. Plankton provide a significant proportion of suspended particulate organic matter (SPOM) in the ocean (Rau et al. 1990b), belonging to the well-known "microbial loop". However, still a significant proportion

settles down to serve as food for the bottom dwelling organisms. Yet, differences in primary production will also affect settling organic matter.

At Kapp Norvegia austral summer variations in organic particle fluxes may occur at very short time scales. Sedimentation pulses to the bottom are highly dependent on biological processes associated with the receding ice edge and the advection of possible different water masses. This results in a pronounced isotopic shift related to a sudden change of the organic matter source due to retreating sea-ice. For example, first sedimentation pulses were mainly due to sinking neritic diatoms (e.g. *Nitzschia*, *Actinocyclus* and *Thalassiosira*) and rapidly settling (between 126 and 862 m day^{-1}, Abelmann and Gersonde 1991) krill fecal strings with an average d^{13}C-composition of −24.2‰ and C/N ratio of 8.4. The high 13C values were indicative for sea-ice organisms and ice-associated diatoms. One week later dense packed round pellets consisted mainly of the large *Corethron criophylum* with an average d^{13}C value of −29.7‰ and C/N ratio of 8.6 (Bathmann et al. 1991). According to Wada et al. (1987) and Fischer (1989), high Chl *a* content in the sea-ice was correlated with heavy d^{13}C values of about −18 to -20‰ due to a limited exchange with the surrounding seawater and a reduced CO_2 availability in the sea-ice. As soon as these algae were released and grow in open water, isotopes shift to more negative (lighter) values around -28‰

The isotopic d^{13}C composition (-23.5 and −24.5‰) of the nematodes in Kapp Norvegia range midway between the heavy values of ice algae and oceanic diatom (*Corethron*) filled fecal pellets in sediment traps on the one hand, and lighter values of open water diatomaceous surface phytoplankton on the other hand. They fit quite well with d^{13}C values (-24 ‰) from fecal strings with ice algae such as *Nitzschia*, *Actinocyclus* and *Thalassiosira* diatom spp. Such particulate matter is transported rapidly from the ice-edge and sedimented as rather undigested cells in krill feces with only limited biochemical degradation (Bathmann et al. 1991). In our study, the C/N ratio of organic matter in the sponge spicule mats (6.9) is close to the Redfield value (6.6), and pore-water sillicate is high (1870-2740 µg.l^{-1}), suggesting that healthy growing plankton may account for a major fraction of the sediment organic matter, and serve directly as food for heterotrophic bottom dwelling organisms, such as the nematodes. In all cases around Kapp Norvegia phytoplankton distribution is strongly related to the retreat of the sea ice edge (Bathmann et al. 1991). As seasonal variation in sea ice coverage is an important factor for this part of the marine Antarctic ecosystem, nematode diet may vary considerably during the year.

Further, variation in d^{13}C signatures between the two sites studied may be attributed to changes in biomass of phytoplankton and to the availability of unknown potential food sources (reflected by differences in Chl-*a* concentrations and CN ratios). Finally, shifts in nematode community structure in the bryozoan and sponge spicule mats might be responsible for the (narrow) difference in d^{13}C signatures of nematodes.

The "Bransfield Strait" is characterized by plankton rich surface water masses, dominated by *Phaeocystis*, large *Corethron* spp. and *Chaetoceros* diatoms (Leventer 1991). d^{13}C values (24.5‰) of the nematodes in the strait do not correspond with the heavy d^{13}C - signals (up to about 32‰) of those plankton species. Therefore, *in situ* surface production seems not the probable trophic source for the nematodes.

An alternative explanation might be inferred from time series sediment trap studies. Traps deployed in the strait show highest diatom flux rates from neritic and open ocean environments of the Antarctic Ocean, though are rarely filled with aggregates

of the *in situ* produced biogenic components (Abelmann and Gersonde 1991). In contrast, pennate diatoms, krill feces and also macroalgal debris (larger than 1 mm and derived from brown and red macroalgae) were frequently found in high concentrations. This material in trap material and surface sediments of the strait can be interpreted as indicators of lateral and near-bottom transport resuspended from the slopes of the surrounding islands and from nearby shelf areas (Reichardt 1987; Wefer et al. 1988; Rutgers van der Loeff and Berger 1991; Abelmann and Gersonde 1991). This is supported by the occurrence of strong bottom currents during our period of study.

With this in mind, the nematode diet in the sediments of the Bransfield Strait might consist of similar, highly seasonal occurring food items as in the Kapp Norvegia region (*e.g.* healthy sinking neritic diatoms and fecal strings with an average $d^{13}C$-composition of –24.2‰).

Primary production of planktonic algae is usually considered to be the ultimate energy source for benthic life in the deep sea. However, a contribution of macroalgae (with bacterial colonization) may have been an additional energy source for the nematodes in the Bransfield Strait.

The "Drake Passage" samples near King George Island correspond with zone I (ice-free waters of the Drake Passage and Scotia Sea) from v. Bodungen et al. 1986. Phytoplankton biomass in this region is composed mainly by silicoflagellates (*Distephanus* spp.) and nannoflagellates, and by oceanic and neritic diatoms (*Corethron* spp., *Nitzschia kerguelensis* and small pennates) and radiolarians. Zooplankton grazing pressure is relatively high, so that a large portion of the biosiliceous material occurs in faecal pellets or aggregates (Abelmann and Gersonde 1991). Particulate matter of such material is generally depleted in $d^{13}C$ (values of - 31.9 to –29.7‰ were mentioned for flagellates and *Corethron*-bearing feacal pellets; Bathmann et al. 1991; Kopczynska et al. 1995).

Nematode $d^{13}C$ signals in this region are also amongst the most negative values (-24.9, –24.8, -26.5) measured, though the difference between nematode and planktonic food (amounting roughly to 5‰) is too large to be explained only by the metabolic enrichment in ^{13}C, which is close to 1‰ and occurs during the assimilation of food (Hobson and Welch 1992).

First of all, POM $d^{13}C$ values from Antarctic marine sediments are often higher (to - 18‰) than observed in POM from the overlying water column (Wada et al. 1987). It was speculated that ice algae could be an important source of ^{13}C-enriched sediment POM. Second, within the water column there is a general trend to lower values with increasing depth (Archambeau et al. 1998). Many factors interact to alter the composition of the settling assemblages. The ^{13}C enrichment in POM with increasing depth is the consequence of a selective loss of ^{12}C during metabolism and degradation of POM once it is removed from the euphotic layer (Rau et al. 1991b). Sinking phytodetrital aggregates are thus heavily colonized by numerous microorganisms I concentrations 2 to 5 orders of magnitude higher than in the surrounding water (Prezelin and Alldredge 1983). Mechanical breakdown of the frustules of larger species, such as *Corethron* spp., is a second source of variation. It is particularly important in the Peninsula region, where high standing stocks of grazing zooplankton are responsible for the production of large numbers of fecal pellets comprised of organic material and fragmented diatom valves (Dunbar 1984). Subsequent breakdown by benthic bacteria at the sediment-water interface leads to a further modification of the $d^{13}C$ value of the settled material. C-13 enrichments of

up to 3-4‰ may occur at the sediment-water boundary layer (Fischer 1991). Some, though not clear, degradation signals were observed from the variation in d^{13}C along the sediment profile. Deeper sediment layers (5-10 cm in MUC2/4 from Sta. 148) had higher values.

Finally, the contribution of such bacteria in the diet of nematodes might explain the balance in the d^{13}C value between nematodes and original produced phytoplankton.

In this attempt values have to be regarded with some caution and additional aspects should be taken into account. For example, the isotopic values of different potential food sources may overlap (as seen by Couch 1989) and the nematode diet can be balanced between several food sources. The influence of substrate type will certainly affect the food availability. In our study, higher d^{13}C values were found in the bryozoan debris and, especially, spong spicule mats. Possibly the suspension feedersin this area act as a first filter for depositing organic matter, so that meiofaunal nematodes rely on a sedimentary pool of organic carbon that is partly processed by microbes. Finally, a high nematode diversity in the Weddell Sea (Vanhove et al. 1999) enlarges complexity of interpretation. Still our results may provide interesting new insights into the feeding strategies of Antarctic deep-sea nematodes.

The ecological significance of free-living marine nematodes from the Antarctic as determined by ^{13}C labelling experiments. Sedimentation of organic material from phytoplankton blooms represent a considerable fraction of the annual benthic organic matter (see Graf 1992 for a review). This is especially true in the Weddell Sea (Arntz et al. 1994), and in the particular case of the Bransfield area of the Southern Ocean where daily flux rates are among the highest observed for the Southern Ocean (Liebezeit and v. Bodungen 1987). Settling bloom material is a major driving force for the benthic communities in the Weddell Sea (Jarre-Techmann et al. 1997). Nevertheless, a significant portion of organic matter from lateral near-bottom transport adds to this substantial food export (Wefer et al. 1988).

In recent years, nematodes have been found to be dominant members of the Antarctic meiobenthic communities. They attain high densities and standing stocks (respectively 5.10^6 ind.m² and 1g dwt.m²) during summer as communities from similar depths elsewhere (Vanhove et al. 1999). Observations document a probable direct uptake of primary food sources by the dominant epistratum feeders (see above and Vanhove et al. 1995). This would support the calculations on trophic flows in the benthic shelf community of the Weddell Sea, where roughly 20% more phytoplankton was consumed in the Weddell Sea system than detritus (Jarre-Techmann et al. 1997).

By increasing the decomposition and remineralisation rates of this organic material, nematodes play an important role in this detrital food web (Giere 1993 and references herein). These aspects infere a closer investigation on the share of the nematodes in the C-flux in the Antarctic benthic ecosystem.

Our observations indicate that labile carbon entering the benthic system can be rapidly processed. Within 9 days nematodes ingested already a fraction of the added carbon. Reports on the direct utilization of deposited algal cells from the pelagial by meiobenthic communities in the field (Fleeger et al. 1989; Gooday et al. 1996; Webb 1996; Olafsson and Elmgren 1997) and in mesocosm experiments (Gee and Warwick 1985; Webb and Montagna 1993; Austen and Warwick 1995; Widbom and

Frithsen 1995; Gullberg et al. 1997; Olafsson et al. 1999; Moens et al. *subm.*) are often contradictory. Our observed response time is situated within the range observed in reports where a tight link was found between fresh organic input and abundance/biomass increase of the meiofauna.

Apart from a rapid response, our results demonstrate a distinct segregation between nematodes living in the upper layers (clear response to administered algal carbon) and counterparts dwelling in deeper layers (with a seemingly low preference for fresh material). Although deeper living nematodes showed a delayed response, they were never as enriched as upper layer nematodes (when compared to background detrital carbon isotope signals). These results would partly support Rudnick's hypothesis that meiobenthic animals react in 2 ways to phytoplankton sedimentation, with surface feeders directly assimilating sedimented phytoplankton, while subsurface feeders experience a more stable food supply and rely indirectly on sedimented phytoplankton by feeding on decomposing organic matter with associated bacteria (Rudnick 1989). Nevertheless this assumption is contradicted by others (Olafsson et al. 1999; Moens et al. *subm*) and we should not role out the importance of pore water influence and sediment mixing rates on the $d^{13}C$ of small benthic organisms (Rathburn et al. 1996; McCorkle et al. 1997). One should, for example, notice the very low transport of organic detritus in our experiment.

Evidence has accumulated that, as in many low sublittoral settings, the deep sea is often characterized by a high seasonal regime (Tyler 1988; Asper et al. 1992). In accordance, Weddell Sea particle flux shows an extremely episodic, intense and patchy character of the seasonal varying phytodetritus supply (Clarke 1988; Fischer et al. 1988, Gutt et al. 1998). This implies a rapid response of the fauna directly dependent on euphotic production. The observed rapid and segregated response of the Antarctic nematodes in our incubation experiment paste well into this context. It confirms our earlier suggestion that the meiobenthos responds rapidly and efficiently to the episodic food supply characteristic for this part of the Southern Ocean (Vanhove et al. 1995).

As to finish this discussion, one should take caution in interpreting the observed uptake rates (e.g. 9 to 14 days): [1] allochtonous algal cells were added to the upper water from intact sediment cores. This may be the reason for the relatively low enrichment in the nematodes compared to the background detrital levels. Obviously responses to *in situ* natural material might be much higher depending on the selectivity of the colonizing nematodes. The abundant epistrate grazers in these substrates of the Weddell Sea might be more affected than the non-selective deposit feeders; [2] the amount of added carbon to the experiments should also be taken into consideration. 34.4 mg C/m² (30% algal carbon) was added, situated within the range of daily organic carbon flux in the whole Antarctic. However blooms in the Bransfield are amongst the highest in Antarctica reaching levels of 8 to132! mg C $m^{-2}d^{-1}$. So, one can expect even stronger responses when using higher concentrations of added carbon. Lower amounts were used in this study to prevent anoxic conditions; [3] the experimental design was situated on the low resolution of a total nematode assemblage. The study did not allow for a further breakdown even of the dominant meiobenthic nematodes, as diversity in these sediments is very high (Vanhove et al. 1999). Certainly, the uptake of labeled carbon varies greatly among nematode taxa (Olafsson et al. 1999).

5.5 CONCLUSIONS

Strong benthic-pelagic coupling may be expected in high-latitude areas because these are often characterized by high levels of 'new primary production' attributed to large phytoplankton, especially diatoms, which have high sinking rates. Substantial amounts of organic carbon and biogenic opal may sink as a result of the high plankton death rates, current activity and melting processes in the vicinity of ice-shelves. Moreover, the sedimentation of faecal pellets originating from the grazing activity of protozoans, copepods and krill is sometimes the main process for the transport of material from the surface to the sea floor in the Weddell Sea. However, despite temporary high inputs, and supposedly low bacterial activity, carbon is not accumulated in the sediments.

Observations within the benthic nematode communities in the deep Weddell Sea document a probable direct uptake of primary food sources by the dominant epistrate feeders (Vanhove et al. 1995). This would support the conclusions resulting from trophic flow studies by Jarre-Teichmann et al., (1997), namely that the benthic shelf community of the Weddell Sea consumes roughly more plankton than detritus calculations on trophic flows in (Jarre-Teichmann et al. 1997). The question thus remains whether the nematodes from the Weddell Sea preferentially incorporate fresh food sources or whether they rely on a mixture of different food sources (as is generally the case for fee-living marine nematodes). Therefore, the current stable isotope study focussed on the contribution of the meiobenthos community (and especially the most abundant taxon of the nematodes) in the carbon flux of the Antarctic benthic ecosystem.

The carbon and nitrogen isotopic composition of the free-living Antarctic nematodes collected during the EASIZ II and III of R.V. *Polarstern* to the Weddell Sea was studied in a comparative and experimental way. Signals of isotopic nitrogen were below detection level, even when a large number of specimens (e.g. 600 specimens) were used. Yet, we failed to observe the trophic position of the nematodes in the Weddell Sea food chain. Carbon stable isotope abundances occurred within a large range of variation between -26.5 and -22.5‰ and were situated closely to the natural signals of detritus in the sediments (e.g. between -26.00 and -24.10‰). On the provision that the $d^{13}C$ signature of food is retained in the animal (Fry and Sherr 1984), fresh pennate diatom algae from the settled pelagic phytoplankton and krill faecal strings were indeed proposed as the main carbon source for the nematodes in the Weddell Sea. However, a probable addition of other trophic items could not be excluded. For instance, diagenetic modification was proposed as possible source of variation in these deep sediments.

Our earlier suggestion that the meiobenthos responds rapidly (within 9 days a first response was observed) and efficiently (as shown by the high standing stock of meiobenthic communities in the deep Weddell Sea) to the episodic food supply characteristic for this part of the Southern Ocean was supported by the incubation experiment.

6

GENERAL CONCLUSIONS

Primary productivity is the basic resource that fuels life on Earth. It is therefore reasonable to assume that productivity is correlated with standing stock and diversity in many situations. The extremely seasonal input of food from the ice and water column is increasingly considered to be of great importance. Episodic availability of food requires adaptive responses, which impose specific constraints on the types of organisms able to exploit such resources. Here we report on the coupling of the meiobenthos to the seasonal nature of food production in the Antarctic coastal zone (study 1). Distinct peak abundances, lagging with a few weeks behind peak diatom production, and lower stocks during most of the year with immediate and lagged responses to lower quality nanophytoplankton input were observed within the meiofauna communities. Strong reduced stocks with a short duration in mid winter were found when food availability was at its lowest. This seasonal response was, however, variable from year-to-year. Such characteristic makes Antarctic meiofauna less predictable as would be expected. The observed up-side-down control suggest that meiobenthos is strongly influenced by the year-to-year variations in the timing, intensity and duration of phytoplankton blooms.

Despite comparable high meiofaunal abundances in similar circumstances of seasonal food input, fundamental differences were found between the meiofauna communities from Rothera and Signy. Latitudinal differences, such as the Polar Front nearby the South Orkneys, were proposed to be at the base of the variability between high and low Antarctic nematode communities.

A second important ecological agent structuring the Antarctic benthic realm is the disturbance activities related to calving and moving icebergs. Large areas of the sea floor are thus subjected to spatial and temporal disturbances on scales ranging from centimetres to tens of kilometres and from days to decades or longer. Some 15 to 20% of the world's oceans are affected by this phenomenon, yet measurements of the extent of biological destruction from iceberg impacts and subsequent recovery are very rare. Assessing the rates and processes involved in the destruction and recolonisation by in situ fauna is one of the more recent aims of biological investigations as to marine mineral exploitation and the dumping of radioactive and other chemical wastes. Moreover, with reference to the global warming, the calving of icebergs may be a more frequent phenomenon in the future. Moreover, the wide scales of disturbance intensity are thought to add to the overall high levels of Antarctic benthic biological diversity. We studied the impact of iceberg scouring on Antarctic meiofauna, both in the low subtidal and on the deeper shelf near the Antarctic continent. Data here indicate that the scouring led to more than a 95% decrease in meiofaunal abundance in both areas. The return of major meiofauna groups was accomplished in 30 days in the low subtidal. In spite of this catastrophic destruction, parameters related to nematode community structure, e.g. dominance rank, generation structure, trophic composition and life-traits (r- vs. K-selection) were not affected by the iceberg impact in this area.

Because of major differences of ecological condition between shallow coastal and deep-water habitat, complete nematode community restoration in the latter may take at least some years. An extremely low diversity and a fundamental change in nematode generic composition due to scouring elucidate that the diverse nematode community from the shelf of the Weddell Sea is very fragile against iceberg disturbance. This is in contrast to the findings in the low subtidal where the nematode communities are well adapted to ice disturbance. It was finally concluded that the combined effect of various physical disturbance agents (such as wave action) are structuring the nematode communities at shallow Antarctic coasts while only iceberg disturbance primarily influences the nematode communities in the deep Weddell Sea.

The study of food and feeding habitats of Antarctic benthos has received considerable attention, since they may explain part of the discrepancies between 1) seasonally limited food resources and the existence of a rich benthic life and 2) a low organic carbon content of the Antarctic sediments, despite important sedimentation pulses in summer. Both show that the benthic community, composed of organisms living on and within the sediments of the deep ocean floor, may be an important sink. In particular the meiofauna exhibits high standing stocks in low subtidal and deep sea. Although many fluctuations may be due to factors of unknown nature (for example physical disturbance by storm, macrofaunal activity, biological interactions within the meiofauna etc.) a distinct impact of food supply, as a result of benthic pelagic coupling, is observed in both ecosystems (coastal and deep sea).

Although it is generally accepted that meiofauna as a group are capable of consuming a broad range of microbial food and non-living detrital material, and that meiofauna may specialize on or have preferences for different types of food resources, relatively little is known about how these feeding strategies are manifested under natural conditions. Neither there is exist decisive evidence about the quantitative role of meiofauna in marine food webs. Thus, despite observations of a probable direct uptake of primary food sources by the dominant Epistrate feeding nematodes, the question thus remains whether the nematodes from the Weddell Sea preferentially incorporate fresh food sources or whether they rely on a mixture of different food sources (as is generally the case for fee-living marine nematodes).

Therefore, the current stable isotope study focussed on the contribution of the meiobenthos community (and especially the most abundant taxon of the nematodes) in the carbon flux of the Antarctic benthic ecosystem. The carbon and nitrogen isotopic composition of the free-living Antarctic nematodes collected during the EASIZ II and III of R.V. *Polarstern* to the Weddell Sea was studied in a comparative and experimental way. Carbon stable isotope abundances occurred within a large range of variation between −26.5 and −22.5‰ and were situated closely to the natural signals of detritus in the sediments (e.g. between −26.00 and −24.10‰). On the provision that the $d^{13}C$ signature of food is retained in the animal, fresh pennate diatom algae from the settled pelagic phytoplankton and krill faecal strings were indeed proposed as the main carbon source for the nematodes in the Weddell Sea. However, a probable addition of other trophic items could not be excluded. Our earlier suggestion that the meiobenthos responds rapidly and efficiently (as shown by the high standing stock of meiobenthic communities in the deep Weddell Sea) to the episodic food supply characteristic for this part of the Southern Ocean was supported.

7

<div style="border:2px solid black; padding:10px">

REFERENCES

</div>

Abelmann, A. and Gersonde, R. 1991. Biosiliceous particle flux in the Southern Ocean. Mar. Chem. 35 : 503 – 536.

Alongi, D.M. and Tietjen, J.H. 1980. Population growth and trophic interactions among free-living marine nematodes. In: Marine benthic dynamics. Tenore, K.R. and Coull, B.C. (Eds), University of South Carolina Press, Columbia : 151 – 166.

Archambeau, A.-S., Pierre, C., Poisson, A. and Schauer, B. 1998. Distributions of oxygen and carbon stable isotopes and CFC-12 in the water masses of the Southern Ocean at 30°E and South Africa to Antarctica: results of the CIVA1 cruise. J. Mar. Syst 17 : 25 – 38.

Arntz, W.E. and Gallardo, V.A. 1994. Antarctic benthos: present position and future prospects. In: Antarctic Science. Hempel, G. (ed). Springer-Verlag, Berlin Heidelberg: 243 - 277.

Arntz, W.E., Brey, T. and Gallardo, V.A. 1994. Antarctic zoobenthos. Oceanogr. Mar. Biol. Ann. Rev. 32 : 241 - 304.

Asper, V.L., Deuser, W.G., Knauer, G.A. and Lohrenz, S.E. 1992. Rapid coupling of sinking particle fluxes between surface and deep ocean waters. Nature 357 : 670 – 672.

Austen, M.C. and Warwick, R.M. 1995. Effects of manipulation of food supply on estuarine meiobenthos. Hydrobiologia 311: 175 – 184.

Barnes, D.K.A. and Clarke, A. 1994. Seasonal variation in the feeding activity of four species of Antarctic bryozoan in relation to environmental factors. J. Exp. Mar. Biol. Ecol. 181: 117 - 133.

Bathmann, U.V., Fisher, G., Müller, P.J. and Gerdes, G. 1991. Short term variation in particulate matter sedimentation off Kapp Norvegia, Weddell Sea, Antarctica: relation to water mass advection, ice cover, plankton biomass and feeding activity. Polar Biol, 11(3) : 185 – 195.

Biggs, D.C., Berkowitz, S.P., Altabet, M.A., Bidigare, R.R., DeMaster, D.J., Dunbar, R.B., Leventer, A., Macko, S.A., Nottrouer, C.A. and Ondrusek, M.E. 1988. A coopereative study of upper-ocean particulate fluxes in the Weddell Sea. In : Proceedings of the Ocean Drilling Program, 113. Initial reports, Weddell Sea, Antarctica. Stewart, N.J. (Ed.), College station, Texas, A & M University : 77 - 86.

Bodin, P. and Boucher, G. 1983. Évolution à moyen terme du méiobenthos et des pigments chlorophylliens sur quelques plaged pollutéed par les Hydrocarbures avec utilizatin d'un dispersent. Acta Oecol 3 : 263 - 280.

Bongers, T. 1990. The maturity index: an ecological measure of environmental disturbance based on nematode species composition. Oecologia 83: 14 - 19.

Bongers, T., Alkemade, R. and Yeates, G.W. 1991. Interpretation of disturbance-induced maturity decrease in marine nematode assemblages by means of the Maturity Index. Mar Ecol Prog Ser 76: 135 - 142.

Brylinsky, M and Gibson, J. 1994. Impacts of flounder trawls on the intertidal habitat and community of the Minas Basin, Bay of Fundy. Can J Fish Aquat Sci 51: 650 - 661.

Carey, A.G. Jr and Montagna, P.A. 1982. Arctic sea ice faunal assemblage: first approach to description and source of the under-ice meiofauna. Mar.Ecol. Prog. Ser. 8 : 1 - 8.

Clarke, A. 1988. Seasonality in the Antarctic marine environment. Comp. Biochem. Physiol.. 90B : 461 - 473.

Clarke, A. 1990. Faecal egestion and ammonia excretion in the Antarctic limpet *Nacella concinna* (Strebel, 1908). J. exp. Mar. Biol. Ecol. 138 : 227 – 246.

Clarke, A. and Leakey, R.J.G. 1996. The seasonal cycle of phytoplankton, macronutrients and the microbial community in a nearshore Antarctic marine ecosystem. Limnol. Oceanogr. 41(6) : 1281 - 1294.

Clarke, A., Holmes, L.J. and White, M.G. 1988. The annual cycle of temperature, chlorophyll and major nutrients at Signy Island, South Orkney Islands, 1969-82. Br. Antarctic Survey Bull. 80 : 65 - 86.

Conlan, K.E., Lenihan, H.S., Kvitek, R.G. and Oliver, J.S. 1998. Ice scour disturbance to benthic communities in the Canadian High Arctic. Mar Ecol Prog Ser 166: 1- 16.

Couch, C.A. 1989. Carbon and nitrogen stable isotopes of meiobenthos and their food resources. Est. Coast. Shelf. Sci. 28 : 433 – 441.

Coull, B.C. 1969. Hydrographic control of meiobenthos in Bermuda. Limnol Oceanogr 14: 953 - 957.

Coull, B.C. and Bell, S.S. 1979. Perspectives in meiofaunal ecology. In : Ecological processes in coastal and marine systems. Livingston, R.J. (ed). Plenum Press, New York : 189– 216.

Cross, W.E. 1982. Under-ice biota at the Pond Inlet Edge and in adjacent fast ice areas during Spring. Arctic 35(1) : 13 - 27.

Dehairs, F., Kopczynska, E., Nielsen, P., Lancelot, C., Bakker, D.C.E., Koeve, W. and Goeyens, L. 1997. d^{13}C of Southern Ocean suspended organic matter during spring and early summer: regional and temporal variability. Deep-Sea Res. II 44(1-2) : 129– 142.

De Man, M. 1998. Trofische interacties in het meiobenthos van de Noordzee en de Westerschelde. Eindwerk Katholieke Hogeschool Sint-Lieven, Afdeling Gent

Doake, C.S.M. and Vaughan, D.G. 1991. Rapid disintegration of the Wordie Ice Shelf in response to atmospheric warming. Nature 350: 328 - 330.

Dunbar, R.B. 1984. Sediment trap experiments on the Antarctic continental margin. Ant. J. of the U.S. 19 : 70 – 71.

Elmgren, R., Hansson, S., Larsson, O., Sundelin, B. and Boehm, P.D. 1983. The Tsesis oil spill: acute and long-term impact on the benthos. Mar Biol 73: 161 - 172.

Fabiano, M. and Danovaro, R. 1999. Meiofauna distribution and mesoscale variability in two sites of the Ross Sea (Antarctica) with contrasting food supply. Polar. Biol. 22 : 15 – 123.

Fischer, G., Fütterer, D., Gersonde, R., Honjo, S., Ostermann, D. and Wefer, G. 1988. Seasonal variability of particle flux in the Weddell Sea and its relation to ice cover. Nature 335 : 426– 428.

Fischer, G. 1989. Stabile Kohlstoff-Isotope in partikularer organischer Substanz aus dem Südpolarmeer (Atlantischer Sektor). Thesis, Univ. of Bremen.

Fleeger, J.W., Shirley, T.C. and Ziemann, D.A. 1989. Meiofaunal responses to sedimentation from an Alaskan spring bloom.I. Major taxa. Mar. Ecol. Prog. Ser. 57 : 137 – 145.

Fry, B. 1988. Food web structure on George Bank from stable C, N and S isotopic compositions. Limnol. Oceanogr.33 : 1182 – 1190.

Fry, B. and Sherr, E.B. 1984. d^{13}C measurements as indicators of carbon flow in marine and freshwater ecosystems. Contrib. Mar. Sci. 27 : 13 - 47.

Fukuchi, M., Tanimura, A. and Otsuka, H. 1984. Seasonal change of chloropfyll *a* under fast ice in Lützow-Holm Bay, Antarctica. Mem. Natl. Inst. Polar Res., Spec. Issue 32 : 51 - 59.

Gammie, F. 1995. Breakaway iceberg 'due to warming'. Nature 374: 108.

Gee, J.M. and Warwick, R.M. 1985. Effects of organic enrichment on meiofaunal abundance and community structure in sublittoral soft sediments. J. Exp. Mar. Biol. Ecol. 91 : 247 – 262.

Gerdes, D. 1990. Antarctic trials with the multi-box corer, a new device for benthos sampling. Polar Rec 26: 35 - 38.

Gerdes, D., Klages, M., Arntz, W.E., Herman, R.L., Galéron, J. and Hain, S. 1992. Quantitative investigations on macrobenthos communities of the southeastern Weddell Sea shelf based on multibox corer samples. Polar Biol. 12: 291 - 301.

Giere, O. 1993. Meiobenthology. The microscopic fauna in aquatic sediments. Springer-Verlag Berlin Heidelberg : 328p.

Gilbert, N.S. 1991a. Microphytobenthic seasonality in near-shore marine sediments at Signy Island, South Orkney Islands, Antarctica. Estuar. Coast. Shelf S. 33 : 89 - 104.

Gilbert, N.S. 1991b. Primary production by benthic microalgae in near-shore marine sediments of Signy Island, Antarctica. Polar Biol. 11 : 339 - 346.

Goering, J., Alexander, V. and Haubenstock, N. 1990. Seasonal variability of stable carbon and nitrogen ratios of organisms in a North Pacific bay. Est. Coast. Shelf Sci. 30 : 239 – 260.

Gooday, A.J., Pfannkuche, O. and Lambshead, P.J.D. 1996. An apparent lack of response by metazoan meiofauna to phytodetritus deposition in the bathyal north-eastern Atlantic. J. Mar. Biol. Assoc. U.K. 76 : 297 – 310.

Graf, G. 1992 Benthic-pelagic coupling : a benthic view. *Oceanogr. Mar. Biol. Ann. Rev.*30 : 149 - 190.

Grainger, E.H. and Hsiao, S.I.C. 1990. Trophic relationships of the sea ice meiofauna in Frobisher Bay, Arctic Canada. Polar Biol. 10: 283 - 292.

Gullberg, K.R., Goedkoop, W. and Johnson, R.K. 1997. The fate of diatom carbon within a freshwater benthic community – a microcosm study. Limnol. Oceanogr. 42 : 453 – 460.

Gutt, J., Starmans, A. and Dieckmann, G. 1996. Impact of iceberg scouring on polar benthic habitats. Mar Ecol Prog Ser 137: 311 - 316.

Gutt, J., Starmans, A. and Dieckmann, G. 1998. Phytodetritus deposited on the Antarctic shelf and upper slope: its relevance for the benthic system. J. Mar. Syst. 17 : 435 – 444.

Gutt, J. (*in press*) On the direct impact of ice on benthic communities, a review. Polar Biol.

Handa, N., Nakatsuka, T., Fukuchi, M., Hattori, H. and Hoshiai, T. 1992. Vertical fluxes and ecological significance of organic materials during the phytoplankton bloom during austral summer in Breid Bay, Antarctica. Mar. Biol. 112 : 469 – 478.

Heip, C., Vincx, M. and Vranken, G. 1985. The ecology of marine nematodes. Oceanogr. Mar. Biol. Ann. Rev. 23: 399 - 489.

Herman, R.L. and Dahms H.U. 1992. Meiofauna communities along a depth transect off Halley Bay (Weddell Sea -Antarctica). Polar Biol. 12 : 313 - 320.

Higgins, R.P. and Thiel, H. 1988. *Introduction to the study of meiofauna*. Smithsonian Institution Press, Washington, DC London, 488 p.

Hill, H. 1973. Diversity and evenness: a unifying notation and its consequences. Ecology 54: 427 - 432.

Hobson, K.A. and Welch, H.E. 1992. Determination of trophic relationships within a high Arctic marine food web using $d^{13}C$ and $d^{15}N$ analysis. Mar. Ecol. Prog. Ser. 84 : 9 – 18.

Hofmann, E.E. and Priddle, J. 2000. Interannual variability in the Southern ocean : summary report of a workshop, Cambridge, United Kingdom, 2-7 August 1999. In : SCAR bulletin 138 : 4– 6.

Iken, K., Brey, T., Wand, U., Voigt, J. and Junghans, P. *in press*. Food web structure of the benthic community at Porcupine Abyssal Plain (NE Atlantic): a stable isotope analysis.

Jarre-Teichmann, A., Brey, T., Bathmann, U.V., Dahm, C., Dieckmann, G.S., Gorny, M., Klages, M., Pagés, F., Plötz, J., Schnack-Schiel, S.B., Stiller, M. and Arntz, W.E. 1997. Trophic flows in the benthic shelf community of the eastern Weddell Sea, Antarctica. In : Antarctic communities: species, structure and survival. Battaglia, B., Valencia, J. and Walton, D.W.H. (Eds.). University Press, Cambridge : 118 – 134.

Jensen, P. 1987. Feeding ecology of free-living aquatic nematodes. Mar. Ecol. Prog. Ser. 35 : 187 – 196.

Jørgensen, B.B. 1982. Mineralization of organic matter in the sea bed - the role of sulphate reduction. Nature (London) 296: 643 - 645.

Kauffman, T.A. 1977. *Seasonal changes and disturbance in an Antarctic benthic mud community*. PhD thesis, Unviversity of California, 136 p.

Kopczynska, E., Goeyens, L., Semeneh, M. and Dehairs, F. 1995. Phytoplankton composition and cell carbon distribution in Prydz Bay, Antarctica: relation to organic particulate matter and its $d^{13}C$ values. J. Plankton Res. 17(4) : 685 – 707.

Knox, G.A. 1994. The biology of the Southern Ocean. University Press, Cambridge, 444 p.

Leakey, R.J.G., Fenton, N. and Clarke, A. 1994. The annual cycle of planktonic ciliates in nearshore waters at Signy Island, Antarctica. J. Plankton Res., 16(7) : 841 - 856.

Lee, H.J., Gerdes, D., Vanhove, S. and Vincx, M. *in press a*. Response of meiofauna to disturbance by iceberg scouring on the Antarctic continental shelf at Kapp Norvegia (Weddell Sea).

Lee, H.J., Vanhove, S., Peck, L.S. and Vincx, M. *in press b.* Recolonisation of meiofauna after a catastrophic iceberg scouring in shallow Antarctic sediments. Polar Biol.

Liebezeit, G. and v. Bodungen, B. 1987. Biogenic fluxes in the Bransfield Strait: planktonic versus micralgal sources. Mar. Ecol. Prog. Ser. 36: 23– 32.

Lien, R., Solheim, A., Elverhøi, A. and Rokoengen, K. 1989. Iceberg scouring and seabed morphology on the eastern Weddell Sea shelf, Antarctica. Polar Res 7: 43 - 57.

Matsuda, O., Ishikawa, S. and Kawaguchi, K. 1987. Seasonal variation of downward flux of particulate organic matter under the Antarctic fast ice. Proc. NIPR Symp. Polar Biol. 1 : 23 – 34.

McCorkle, D.C., Corliss, B.H. and Farnham, C.A. 1997. Vertical distributions and stable isotopic compositions of live (stained) benthic foraminifera from the North Carolina and California continental margins. Deep-Sea Res. I 44(6) : 983 – 1024.

Meyer-Reil, L.A. 1983. Benthic response to sedimentation event during autumn to spring at a shallow water station in the western Kiel Bight. Mar. Biol. 77: 247 - 256.

Minagawa, M. and Wada, E. 1984. Stepwise enrichment of ^{15}N along food chains: further evidence and the relation between d^{15}N and animal age. Geochim. Cosmochim. Acta 48 : 1135 – 1140.

Moens, T. and Vincx, M. 1997. Observations on the feeding ecology of estuarine nematodes. J. Mar. Biol. Assoc.U.K. : 211 – 227.

Moens, T., Luyten, C., Middelburg, J.J., Herman, P.M.J. and Vincx, M. *subm*. Tracing organic matter sources of estuarine tidal flat nematodes with stable carbon isotopes.

Montagna, P.A. 1993. Radioisotope technique to quantify *in situ* microbivory by meiofauna in sediments. In: Handbook of methods in aquatic microbial ecology, (Kemp, P.F., Sherr, B.F., Sherr, E.B. and Cole, J.J. (Eds). Lewis publishers, Boca Raton, FL : 745 - 753.

Montagna, P.A. 1995. Rates of meiofaunal microbivory: a review. Vie Milieu 45 : 1 – 10.

Montagna, P.A., Coull, B.C., Herring, T.L. and Dudley, W. 1983. The relationship between abundance of meiofauna and their suspected microbial food (diatoms and bacteria). Estuar. Coast. Shelf S. 17 : 381 -394.

Moodley, L., Boschker, H.T.S., Middelburg, J.J., Pel, R., Herman, P.M.J., de Deckere, E., Heip, C.H.R. *in press.* The ecological significance of benthic Foraminifera as determined by ^{13}C labelling experiments ?

Murphy, E.J., Clarke, A., Symon, C. and Priddle, J. 1995. Temporal variation in Antarctic sea-ice : analysis of a long-term fast-ice record from the South orkney islands. Deep-Sea Res. 42(7) : 1045 – 1062.

Nedwell, D.B., Walker, T.R., Ellis-Evans, J.C. and Clarke, A. 1993. Measurement of seasonal rates and annual budgets of organic carbon fluxes in an Antarctic coastal environment at Signy Island, South Orkney Islands, suggest a broad balance between production and decomposition. Appl. Envir. Microbiol. 59 : 3989 - 3995.

Neilson, R., Boag, B. and Palmer, L.F. 1996. The effect of environment on marine nematode assemblages as indicated by the maturity index. Nematologica 42 : 232 - 242.

Nöthig, E-M and v. Bodungen, B. 1989. Occurence and vertical flux of faecal pellets of probably protozoan origin in the southeastern Weddell Sea (Antarctica). Mar. Ecol. Prog. Ser. 56 : 281 – 289.

? lafsson, E. and Elmgren, R.1997. Seasonal dynamics of sublittoral meiobenthos in relation to phytoplankton sedimentation in the Baltic Sea. Estuar. Coast. Shelf. Sci. 45 : 149 – 164.

? lafsson, E., Modig, H. and van den Bund, W.J. 1999. Species specific uptake of radio-labelled phytodetritus by benthic meiofauna from the Baltic Sea. Mar. Ecol. Prog. Ser. 177 : 63 - 72.

Peck, L.S., Brockington, S., Vanhove, S. and Beghyn, M. 1999. Community recovery following catastrophic iceberg impacts in a soft-sediment shallow-water site at Signy Island, Antarctica. Mar Ecol Prog Ser 186: 1 - 8.

Pearson, T.H. and Rosenberg, R. 1987. Feast and famine: structuring factors in marine benthic communities. In : Organization of communities past and present, Gee, J.H.R. and Giller, P.S. (Eds), Blackwell Scientific Publications, Oxford: 373 - 395.

Peterson, B.J. and Fry, B. 1987. Stable isotopes in ecosystem studies. Ann. Rev. Ecol. Syst. 18 : 293 – 320.

Platt, H.M. and Warwick, R.M. 1988. Free-living marine nematodes. Part 2. British Chromadorids. Pictural key to world genera and notes for the identification of British species. Synopses of the British fauna, New Series 38, Leiden. 98 p.

Rathbun, A.E., Corliss, B.H., Tappa, K.D. and Lohmann, K.C. 1996.Comparisons of the ecology and stable isotopic compositions of living (stained) benthic foraminifera from the Sulu and South China Seas. Deep-Sea Res. I 43(10) : 1617 – 1646.

Rau, G.H., Teyssie, J.-L. Rassoulzadegan, F. and Fowler, S. 1990. C-13/C-12 and N-15/N-14 variations among size-fractioned marine particles : implications for their origin and trophic relationships. Mar. Ecol. Prog. Ser. 59 : 33-38.

Rau, G.H., Hopkins, T.L. and Torres, J.J. 1991a. $^{15}N/^{14}N$ and $^{13}C/^{12}C$ in Weddell Sea invertebrates : implications for feeding diversity. Mar. Ecol. Prog. Ser. 77 : 1 – 6.

Rau, G.H., Sullivan, C.W. and Gordon, L.I. 1991b. $\delta^{13}C$ and $\delta^{15}N$ variations in Weddell Sea particulate organic matter. Mar. Chem. 35 : 355 – 369.

Reichardt, W.T. 1987. Burial of Antarctic macroalgal debris in bioturbated deep-sea sediments. Deep-Sea Res. 34(10) : 1761 – 1770.

Riera, P., Richard, P., Grémare, A. and Blanchard, G. 1996. Food source of intertidal nematodes in the Bay of Marennes-Oléron (France), as determined by dual stable isotope analysis. Mar. Ecol. Prog. Ser. 142 : 303 – 309.

Romeyn, K. and Bouwman, L.A. 1983. Food selection and consumption by estuarine nematodes. Hydrobiol. Bull. 17 : 103 - 109.

Rudnick, D.T. 1989. Time lags between the deposition and meiobenthic assimilation of phytodetritus. Mar. Ecol. Prog. Ser. 50 : 231 – 240.

Rudnick, D.T., Elmgren, R. and Frithsen, J.B. 1985. Meiofaunal prominence and benthic seasonality in a coastal marine ecosystem. Oecologia (Berlin), 67: 157 - 168.

Rutgers van der Loeff, M. and Berger, G.W. 1991. Scavenging and particle flux: seasonal and regional variations in the Southern ocean (Atlantic sector). Mar. chem. 35 : 553 – 567.

Sackett, W.M., Eckelmann, W.R., Bender, M.L. and Be, A.W.H. 1965. Temperature dependence of carbon isotope composition in marine plankton and sediments. Science 148 : 235 – 237.

Sasaki, H. and Hoshiai, T. 1986. Sedimentation of microalgae under the Antarctic fast ice in summer. Mem. Natl. Inst. Polar. Res., Spec. Issue 40 : 45 – 50.

Schiemer, F. 1984. Comparative aspects of food dependence and energetics of free-living nematodes. Oikos 41 : 32 – 42.

Schizas, N.V. and Shirley, T.C. 1996. Seasonal changes in structure of an Alaskan intertidal meiofaunal assemblage. Mar. Ecol. Prog. Ser. 133 : 115 - 124.

Seinhorst, J. 1959. A rapid method for the transfer of nematodes from fixative to anhydrous glycerin. Nematologica 4 : 67 – 69.

Schlüter, M. 1991. Organic carbon flux and oxygen penetration into sediments of the Weddell Sea : indicators for regional differences in export production. Mar.Chem. 35 : 569 – 579.

Schwinghamer, P., Tan, F.C. and Gordon, Jr D.C. 1983. Stable carbon isotope studies on the Pecks Cove mudflat ecosystem in the Cumberland Basin, Bay of Fundy. Can. J. Fish. Aquat. Sci. 40 : 262 – 272.

Sherman, K.M. and Coull, B.C. 1980. The response of meiofauna to sediment disturbance. J Exp Mar Biol Ecol 46: 59 - 71.

Smetacek, V. 1984. The supply of food to the benthos. In : *Flows of energy and materials in marine ecosystems*, Fasham, M.J.R. (Ed*),* Plenum Press, New York : 517 - 547.

Soetaert, K. and Heip, C. 1995. Nematode assemblages of deep-sea and shelf break sites in the North Atlantic and Mediterranean Sea. Mar Ecol Prog Ser 125: 171 - 183.

Sokal, R.R. and Rohlf, F.J. 1981. *Biometry,* second edition, Freeman, W.H. and company, New York, 859 p.

Tenore, K.R., Cammen, L., Findlay, S.E.G., Phillips, N. 1982. Perspectives of research on detritus : do factors controlling the availability of detritus depend on its source? J. mar. Res. 40 : 473 – 490.

Tyler, P.A. 1988. Seasonality in the deep sea. Oceanogr. Mar. Biol. Annu. Rev. 26 : 227 – 258.

Tyson, R.V 1995. *Sedimentary organic matter. Organic facies and palynofacies.* Chapman & Hall, London, 615 p.

Vanaverbeke, J., Soetaert, K., Heip, C. and Vanreusel, A. 1997. The metazoan meiobenthos along the continental slope of the Goban Spur (NE Atlantic). J Sea Res 38: 63 - 107.

Vanhove, S., Wittoeck, J., Desmet, G., Van den Berghe, B., Herman, R.L., Bak, R.P.M., Nieuwland, G., Vosjan, J.H., Boldrin, A., Rabitti, S. and Vincx, M. 1995. Deep-sea meiofauna communities in Antarctica : structural analysis and relation with the environment. Mar. Ecol. Prog. Ser. 127 : 65 - 76.

Vanhove, S., Wittoeck, J., Beghyn, M., Van Gansbeke, D., Van Kenhove, A., Coomans, A. & Vincx, M. 1997. Role of the meiobenthos in Antarctic ecosystems. In : Marine biogeochemistry and ecodynamics. Scientific rresults of phase III (1992-1996) of the Belgian research programme on the Antarctic, volume I, 59p.

Vanhove, S., Lee, H.J., Beghyn, M. Van Gansbeke, D., Brockington, S. and Vincx, M. 1998. The metazoan meiofauna in its biogeochemical environment : the case of an Antarctic coastal sediment. J. Mar. Biol. Assoc. U.K. 78 : 411 – 434.

Vanhove, S., Arntz, W. and Vincx, M. 1999. Comparative study on the nematode communities on the southeastern Weddell Sea shelf and slope (Antarctica). Mar. Ecol. Prog. Ser. 181 : 237 – 256.

Vanhove, S., Beghyn, M., Van Gansbeke, D. Bullough L.W. and Vincx, M. 2000. A seasonally varying biotope at Signy Island, Antarctic: implications for meiofaunal structure. Mar. Ecol. Prog. Ser. 202 : 13 - 25.

Vanreusel, A., Vincx, M., Bett, B.J. and Rice, A.L. 1995. Nematode biomass spectra at two abyssal sites in the NE Atlantic with a presumed contrasting food supply. Int. Revue ges. Hydrobiol. 80(2) : 287 – 296.

v. Bodungen, B., Smetacek, V.S., Tilzer, M.M. and Zeitzschel, B. 1986. Primary production and sedimentation during spring in the Atlantic Peninsula region. Deep-Sea Res. 33(2) : 177 - 194.

Wada, E., Terazaki, M., Kabaya,Y. and Takahisa, N. 1987. [15]N and ^{13}C abundances in the Antarctic Ocean with emphasis on the biogeochemical structure of the food web. Deep-Sea Res 34 (5/6) : 829 – 841.

Walker, T.R. 1993. *Benthic microbial activity in an Antarctic coastal sediment.* Thesis Master of Philosophy, University of Essex, UK, 115 p.

Webb, D.G. 1996. Response of macro- and meiobenthos from a carbon-poor sand to phytodetrital sedimentation. J. Exp. Mar. Biol. Ecol. 203 : 259 – 271.

Wefer, G., Suess, E., Balzer, W., Liebezeit, G., Müller, P.J., Ungerer, C.A. and Zenk W. 1982. Fluxes of biogenic components from sediment trap deployment in circumpolar waters of the Drake passage. Nature 299 (5879) : 145 – 147.

Wefer, G., Fisher G., Fütterer, D.K. and Gersonde, R. 1988. Seasonal particle flux in the Bransfield Strait, Antarctica. Deep-Sea Res 35 : 891 – 898.

Wefer, G., Fisher G., Fütterer, D.K., Gersonde, R., Honjo, S. and Ostermann, D. 1990. Particle sedimentation and productivity in Antarctic waters of the Atlantic sector. In : Geological history of the Polar Oceans : Arctic versus Antarctic. Bleil, U. and Thiede, J. (Eds). Kluwer academic publishers : 363 – 379.

Wefer, G. and Fisher, G. 1991. Annual primary production and export flux in the Southern Ocean from sediment trap data. Mar. Chem. 35 : 597 – 613.

Whitaker, T.M. 1982. Primary production of phytoplankton off Signy Island, South Orkneys, the Antarctic. Proc. R. Soc. London B214 : 169 - 189.

White, M.G., Smith, G.A., Guckert, J.B. and Nichols, P.D. 1993. Nearshore benthic marine sediments. In*: Antarctic Microbiology*, Wilney-Liss : p 219 - 240.

Widbom, B and Frithsen, J.B. 1995. Structuring factors in a marine soft bottom community during eutrophication – an experiment with radio-labelled phytodetritus. Oecologia 101: 156 – 158.

Wieser, W. 1953. Die Beziehung zwischen Mundhöhlengestalt, Ernährungsweise und Vorkommen bei freilebenden marinen Nematoden. Arkiv für Zoologi 2(4) : 439 – 484.

Wormald, A.P. 1976. Effects of a spill of marine diesel oil on the meiofauna of a sandy beach at Picnic Bay, Hong Kong. Envir Pollut 11: 117 - 130

ACKNOWLEDGEMENTS

STRUCTURAL AND ECOFUNCTIONAL BIODIVERSITY OF THE AMPHIPOD CRUSTACEAN BENTHIC TAXOCOENOSES IN THE SOUTHERN OCEAN

C. DE BROYER

G. CHAPELLE

P.-A. DUCHESNE

R. MUNN

F. NYSSEN

Y. SCAILTEUR

F. VAN ROOZENDAEL and

P. DAUBY

INSTITUT ROYAL DES SCIENCES NATURELLES DE BELGIQUE

LABORATOIRE DE CARCINOLOGIE

Rue Vautier, 29

B-1000 Brussels

Belgium

CONTENTS

ABSTRACT

Within the Antarctic Coastal and Shelf Ecosystem (ACSE) the peracarid crustaceans constitute the most diverse animal group in terms of species richness, life styles, trophic types, habitats and size spectra.

Using as a model group the amphipod crustaceans –in turn the richest taxon among peracarids with more than 850 species in the Southern Ocean– this study aimed at describing and evaluating the role of the biodiversity of the vagile macrobenthos in the structure and functioning of the Antarctic Coastal and Shelf Ecosystem.

In the framework of the SCAR EASIZ programme some key structural and ecofunctional aspects of biodiversity were investigated.

Different structural biodiversity features were characterised, namely faunal composition, geographic and bathymetric distribution, habitats and microhabitats, bio-ecological traits. Comparative investigations were performed in two EASIZ benthic reference sites, the eastern Weddell Sea Shelf Community in the High Antarctic, and the Maritime Antarctic sublittoral community of Admiralty Bay, King George Island. In the latter site, species abundance was followed during a complete year cycle, allowing to evidence strong seasonal variations.

Gammaridean amphipods appeared ubiquitous in the shelf communities of the eastern Weddell Sea. Their specific habitats were investigated by comparing catches from different collecting gears and by ethological observations in aquaria. Six main habitats were distinguished: endobenthic, epibenthic, hyperbenthic, benthopelagic, pelagic and cryopelagic. Among epibenthic species, which form the bulk of the fauna, three different strata were detected, together with four symbiotic microhabitats.

The ecofunctional role of biodiversity was approached through the study of trophic diversity and trophodynamics and the significance of the unusually wide size spectra of the Antarctic amphipod crustaceans.

The trophic preferences of 40 dominant amphipod species of the eastern Weddell Sea benthos were deduced from both stomach content analyses and behaviour observations in aquaria. These combined approaches revealed at least eight different feeding types: suspension-feeding, deposit-feeding, deposit-feeding coupled with predation, opportunistic predation, micropredatory browsing, macropredation coupled with scavenging, opportunistic necrophagy and true necrophagy. This feeding type diversity was corroborated by a preliminary analysis of

the carbon and nitrogen stable isotopes. Among these eight types, no particular one was dominant. In the same way, types involving microphagy and macrophagy were equally represented. Predatory types (opportunistic or exclusive) accounted for 64% of the analyzed species, while scavenging types (facultative or obligate) accounted for 60%. The overlap suggests that many amphipod species have a wide dietary spectrum and are able to take advantage of different food resources.

The impact of the amphipod community on the eastern Weddell Sea shelf ecosystem was approached using feeding type results and biomass data. It appeared that sedimenting plankton particles, crustaceans and fish carrion were the 3 main items consumed by these crustaceans, accounting respectively for 10-27, 22-32, and 5-18% of the biomass. In addition, a extensive bibliographic investigation was performed in order to estimate the significance of amphipods in the diet of higher trophic levels: 33 species of invertebrates, 48 of birds, 101 of fish and 10 of mammals are regular consumers of amphipods, the share of this type of prey reaching up to 99%.

As the Antarctic amphipod size spectrum appeared to be the widest, after Baikal Lake, precise length data were gathered about more than 2,000 amphipod species from 15 sites world wide, from polar to tropical, and from marine to freshwater environments. It was shown that gigantism was not directly related to water temperature as often stated, but instead to oxygen availability. Maximum size increases dramatically with oxygen, modal size increases less, and minimum size does not increase at all.

To contribute to a more accurate assessment of the Southern Ocean biodiversity new synthetic tools for compiling, increasing, managing, and disseminating biodiversity information were developed, in particular a "Biodiversity Reference Centre", devoted to Antarctic amphipod crustaceans. It is comprised of comprehensive databases (organising the taxonomic, biogeographic and bio-ecological information), validated and operational reference collections, and a network of contributing specialists engaged in the taxonomic revision of the Antarctic amphipod fauna and the preparation of new conventional and electronic identification guides. These efforts will facilitate monitoring biodiversity in selected EASIZ reference sites.

1. INTRODUCTION

Biodiversity, at its different integration levels –from genes to species and to ecosystems– is a critical element in the evaluation of the resilience of natural systems to environmental changes. In addition, understanding the patterns and processes of biodiversity in relation to production is of fundamental importance for the sustainable management of marine living resources.

Within the Southern Ocean, the Antarctic Coastal and Shelf Ecosystem (ACSE) is the most complex and productive, the richest in species, and likely the most sensitive to global environmental changes. In order to improve our understanding of the ACSE structure and dynamics within the perspective of the global environmental changes, the Scientific Committee on Antarctic Research (SCAR) recently elaborated the programme "*Ecology of the Antarctic Sea-Ice Zone*" (EASIZ). This programme pays a particular attention to these features that make the biology of this ice-dominated ecosystem so distinctive and to understand seasonal, inter-annual, and long-term changes. For a decade, EASIZ proposed an integrated study of the ice, water column and benthic sub-systems focussing on key processes and key organisms in key communities, in a network of study sites (SCAR, 1994).

In the ACSE, the Antarctic macrozoobenthos is characterized by a relatively high species diversity and richness. Several zoological groups, namely the sessile suspension-feeders such as Porifera and Bryozoa and the endo- or epibenthic Polychaeta and Peracarida, are rich in species. Moreover, a high degree of species endemism has been recorded for many taxa (White, 1984), attaining up to 85% in the case of benthic Amphipoda (De Broyer & Ja d ewski, 1993; 1996). Some groups, however, show a moderate species richness (like Bivalvia and Gastropoda), while other groups remain either absent (Stomatopoda, reptant Decapoda) or under-represented (Cirripedia, natant Decapoda) on the Antarctic shelf bottom (Arntz et al., 1997). Circumpolarity in species distribution and extended range of eurybathy (Brey et al., 1996) are common features, as are often high levels of population abundance or biomass. Detailed information on the Antarctic zoobenthos and its diversity can be found in the recent syntheses of Arntz et al. (1994; 1997).

But the latitudinal and vertical patterns of the Antarctic macrobenthos biodiversity in a global perspective, its spatial and temporal variations and the causes of its particular traits remain poorly understood, as well as its roles in the structure and functioning of benthic systems, in particular their productivity and their resilience in the global warming and ozone depletion context.

In the Antarctic benthic communities, in the quasi-absence of decapods, the peracarid crustaceans (Amphipoda, Isopoda, Tanaidacea, Cumacea, Mysidacea,...) are by far the most species-rich group (De Broyer and Jazdzewski, 1996) and probably one of the most diversified in terms of trophic types, modes of life, habitats and size spectra, thus making a good model group for biodiversity studies. The most numerous, the amphipods, comprise more than 850 species in the whole Southern Ocean, 741 of which are benthic species. It was suggested that this high specific diversity could be related to a high heterogeneity of habitats and a variety of ecological roles which remain to be described and understood.

Amphipod habitats and distribution

Recent observations by still and video underwater cameras, coupled with analyses of benthos samples, have allowed a rather precise description of the variety of benthic assemblages from the eastern Weddell Sea shelf (e.g. Galéron et al. 1992; Gutt and Starmans 1998; Gutt and Schickan 1998). The continental shelf, to a depth of more than 600m, is colonised in many places by species-rich assemblages of abundant, diverse and multistratified suspension feeders, like sponges, bryozoans, cnidarians, hydrozoans, holothurians and crinoids. However, there is a gradient of species-rich assemblages of suspension feeders, mostly in the Kapp Norvegia region, to extremely poor detritus feeder's assemblages, in the southernmost part of the Weddell Sea. The shelf bottom cover appears mostly patchy and ranges from a few percent to 100% of the bottom surface. The patchy, diverse and multistratified sessile benthos offers a high diversity of potential microhabitats to small vagile invertebrates.

Gammaridean amphipods, often collected in benthic samples, seem to be ubiquitous in the benthic communities of the eastern Weddell Sea where they constitute an often abundant and always diverse group (Voß, 1988; De Broyer and Klages, 1990; Klages, 1991; De Broyer et al., 1997, 1999; De Broyer et al., 2001). Some species also occur in the pelagic zone where they are usually outnumbered by hyperiid amphipods (*e.g.* Boysen-Ennen and Piatkowski, 1988). They have been so far exceptionally recorded in cryopelagic habitats, at the undersurface of the sea-ice (Günther and Dieckmann, pers. com.). The precise habitat has been described in details only for a few species (Klages, 1991; 1993; Kunzmann, 1992).

At King George Island (South Shetland Islands, Antarctic Peninsula), on the other hand, although the general distribution of the amphipod fauna has been investigated in Admiralty Bay by Jazdzewski et al.(1992), a detailed account of the species habitats and depth range is still lacking. Useful comparison can be made

with the neighbouring sites of the Magellan region (De Broyer and Rauschert, 1999) or of Maxwell Bay and Fildes Strait where Rauschert (1991) studied the distribution of 103 amphipod species, not all of them occurring in Admiralty Bay.

Roles in trophic webs

Our knowledge of the ecofunctional, and specifically the trophodynamic role of the Antarctic amphipods is still very limited, despite the pioneering studies of Richardson (1977), Oliver and Slattery (1985), Slattery and Oliver (1986), Coleman (1989$_{a,b,c}$; 1990$_{a,b}$), and Klages and Gutt (1990$_{a,b}$). Less than 10% of amphipod species have been studied, with very little quantitative work done. Moreover, for the most important groups of Antarctic amphipods (namely Eusiroidea and Lysianassoidea), the feeding type cannot often be deduced with certainty from the feeding appendage morphology. Some necrophagous lysianassoids, however, show a particular mandibular structure, with a specialised molar process, which is a clear indication of their feeding mode (see *e.g.* De Broyer and Thurston, 1987).

The benthic crustaceans (comprising peracarids and natant decapods), despite their low biomass, are a dominant group in terms of energy fluxes in the Weddell Sea shelf ecosystem (Jarre-Teichmann et al.,1997). Amphipods, on the other hand, provide an important food resource to many Southern Ocean demersal and benthic fishes (*e.g.* Gon and Heemstra, 1990; Kock, 1992; Olaso et al., 2000), and to a number of benthic invertebrates (*e.g.* Dearborn, 1977; McClintock, 1994), seabirds (*e.g.* Jazdzewski, 1981; Rauschert, 1991; Cherel and Kooyman, 1998) and seals (*e.g.* Dearborn, 1965; Green and Burton, 1987).

Size spectrum and gigantism

Amphipods are known to have large sized representatives at high latitudes (Barnard, 1962; De Broyer, 1977), which makes the Antarctic amphipods size spectrum rather distinctive when compared to other marine areas. This higher frequency of big specimens, both at the species and the individual level has probably an impact on the ecofunctional role of the amphipod community as a whole.

Although well recognised, this polar gigantism is still poorly understood, due to a lack of thorough analyses. Suggested limiting factors are both physiological and ecological and include temperature, growth rate, resource availability, predation pressure and mortality (Atkinson,1996; Atkinson and Sibly,1997), with most of them tested only at the species level.

Biodiversity assessment tools

Comprehensive and easily accessible biodiversity information is crucial to an accurate assessment of the Southern Ocean biodiversity in the context of global change and of the requirements of the "Global Biodiversity Assessment" (UNEP, 1995). Although the high diversity of the Antarctic peracarid crustaceans and in particular the amphipods is well established, the level of knowledge of their taxonomy, distribution and ecology is insufficient to allow a accurate assessment of the Antarctic marine biodiversity (Barnard and Karaman, 1991; De Broyer and Jazdzewski, 1996). Synthetic biodiversity information tools and efficient identification tools are still totally lacking. In taxonomically difficult groups, these deficiencies handicap both the accurate studies of patterns, processes and role of biodiversity and the development of monitoring programmes linked to global changes. New technologies to describe, analyse and disseminate the biodiversity information allow today new developments (*e.g.* Pankhurst, 1991; Dallwitz et al., 1993; Schalk and Los, 1993; Olivieri et al. 1995).

The present paper reports the results of the research activities conducted in the framework of the Belgian Scientific Research Programme on the Antarctic (Phase IV) and focussing on the description and evaluation of the role of the biodiversity of the macrobenthic peracarid crustaceans in the structure and functioning of the Antarctic Coastal and Shelf Ecosystem (ACSE), in particular in two reference sites of the EASIZ programme (Admiralty Bay, King George Island, and the eastern Weddell Sea). Different structural aspects of the Antarctic peracarid biodiversity were investigated (faunal composition, spatial distribution, habitats…) as well as some ecofunctional features of this diversity (trophic diversity and trophodynamics, size spectra). In addition, the development of the "Biodiversity Reference Centre" for Antarctic Amphipoda including comprehensive databases is presented.

2. MATERIALS AND METHODS

2.1 Study sites

The reference benthic communities belong to two EASIZ Programme key-sites, for which a background knowledge already exists and from which important study material is available:

2.1.1 *The Eastern Weddell Sea Shelf Community* (Figure 1) in the High Antarctic (see e.g. Voß, 1988; Klages, 1991; Galéron et al., 1992; Gerdes et al., 1992), investigated with the collaboration of the Alfred-Wegener-Institut für Polar- und Meeresforschung (AWI), Bremerhaven, Germany.
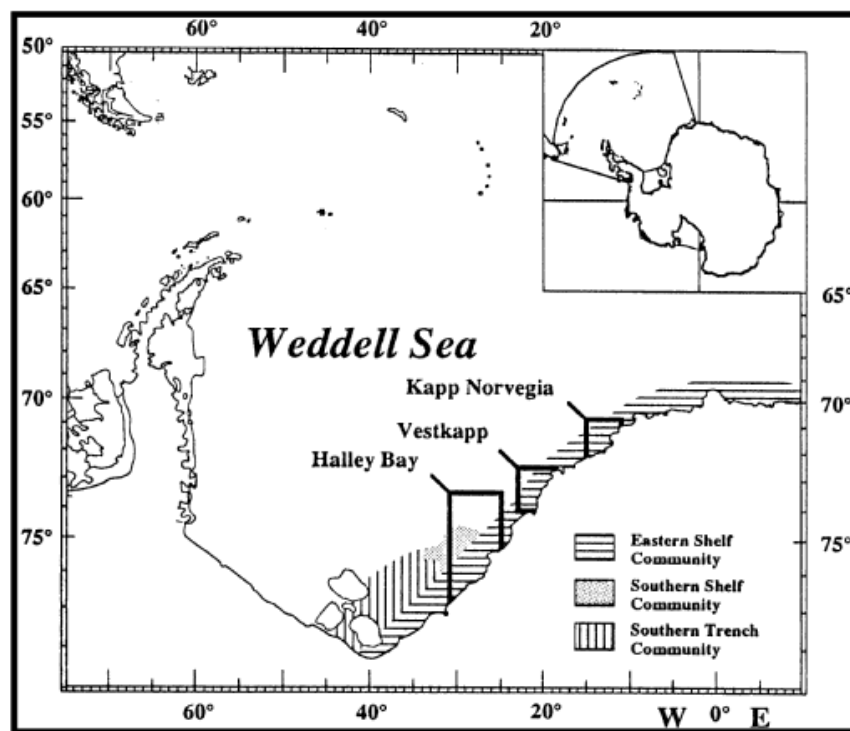
Figure 1: *Location of the sampling areas, Weddell Sea eastern shelf (from Voß, 1988).*

2.1.2. *Admiralty Bay*, King George Island, West Antartic (Figure 2) (see *e.g.* Rakusa-Suszczewski, 1993, Jazdzewski and Sicinski, 1993), investigated in co-

operation with University of Lodz, the Polish Academy of Sciences and the Brazilian Antarctic Programme.
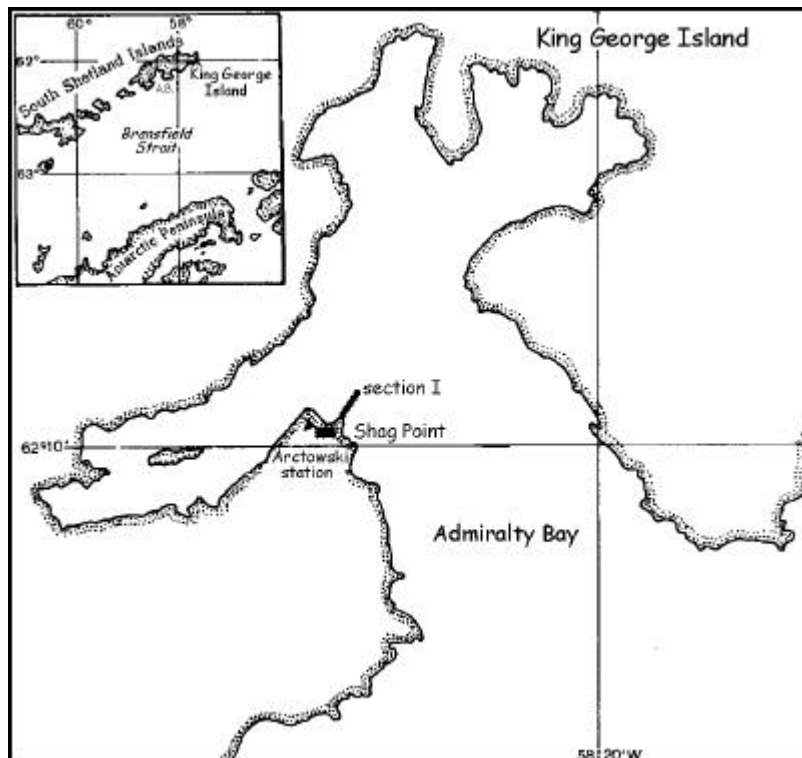
Figure 2: *Location of the main sampling area (section I), Admiralty Bay, King George Island (South Shetland Islands)*

2.2. Field sampling

2.2.1. *Admiralty Bay:* A large amount of peracarid samples were collected between 0 and 500 m by the Polish-Belgian and Brazilian-Belgian missions 1987-1994, by trawls, dredges, grabs, traps or by SCUBA diving. Two series of year-round monthly samples (1988 and 1993) simultaneously collected by traps and trawls at 4 different depths (15 to 300 m) as well as another series of quantitative upper sublittoral samples (1997) were used for studies on life history and seasonal and inter-annual variations of abundance and distribution.

One reference transect, from 0 to 300 m (corresponding to the section I in Figure 2), has been chosen to follow both qualitatively and quantitatively the temporal variations of spatial distribution but also the taxonomic composition, the relative abundance of species, and the population structure. An annual series of monthly samples taken simultaneously by trawl and trap at 15, 30, 50, 90 and 150 m was collected with the co-operation of University of Łódź. An additional series was taken

at 0m at the sublittoral fringe of a stony beach which habitat consisted of cobbles lying on sand and gravel

2.2.2. *Eastern Weddell Sea*: Amphipods were collected from benthic and suprabenthic samples taken during three Antarctic summer cruises of R.V. *Polarstern*: EPOS Leg 3 (ANT VII/4, 1989; Arntz et al., 1990), EASIZ I (ANT XIII/3, 1996; Arntz & Gutt, 1997) and EASIZ II (ANT XV/3, 1998; Arntz & Gutt, 1999). In total 130 catches provided about 80.000 specimens of amphipods from water depths of 60 to 2554 m. Collecting gears included Agassiz, benthopelagic and bottom trawls, dredges, epibenthic sledges, TV grabs, giant and multi– boxcorers, and baited traps (±48 h deployments). Most of the specimens were caught by trawls, the mesh size of which (15 mm) did not retain very small species.

2.3. Habitat characterisation

General information on Weddell Sea bottom habitats came from an interpretation of bottom pictures and ROV videos taken by J. Gutt (AWI) during *Polarstern* cruises and from published habitat descriptions (e.g. Ekau and Gutt, 1991; Gutt and Starmans, 1998; Farhbach et al., 1992; Galéron et al., 1992; Bathmann et al., 1991)

Characterisation of the amphipod habitats in the eastern Weddell Sea was based on a comparative analysis of catches taken by different gears: grabs and corers for the endobenthos (and in smaller extent epibenthos), trawls, dredges, sledges and traps for the epibenthos (and partly endobenthos), epibenthic sledges for the hyperbenthos and RMT (Rectangular Midwater Trawl) for the water column. Identification of microhabitats was based on aquarium and incidental catches observations during the cruises as well as on published records (Kunzmann, 1992).

Ethological observations (habitat choice, food detection and capture, mobility patterns) were performed on living specimens of more than 40 species kept in a cool container on board and afterwards in a cool laboratory at IRScNB, Brussels. Amphipods were maintained at −1°C (±1°C) in aquaria with volumes of 2 to 30 l. Aquaria were provided with different kinds of substrates, according to the known or suspected life style of studied species. A large aquarium with a "reconstituted natural bottom" (30 cm high) was used to study the species behaviour. This "reconstituted" bottom was composed of a mosaic of mixed (fine/coarse) sediment, of sponge spicule mat, of stones and of different common sessile organisms like sponges, cnidarians, hemichordates and bryozoans. Observations were qualitative and

movements and position of amphipods in aquaria were checked at least twice a day for periods ranging from 10 to 56 days. Typical behaviours were video-recorded.

2.4. Trophic type determination and impact on the ecosystem

Feeding experiments were performed in the same aquaria as described above, using different living organisms (like crustaceans, echinoderms or plankton) or dead material (such as pieces of amphipods, fishes or squid) placed on the bottom or presented with forceps. Reactions to odour stimuli were tested using drops of a fluid made of crushed fresh amphipods (the "amphipod juice").

Amphipod gut content analyses were performed mainly on specimens fixed (immediately after sampling) in 4% formaldehyde or, sometimes, on fresh individuals. Dissections (about 1000 individuals) were conducted under a binocular dissecting microscope (Leica MZ12), using forceps and scissors. The digestive tract was cut at the oesophagus level and extracted together with midgut glands from the body. The digestive tract was then separated from midgut glands, opened and the content was spread on a micro-slide. Stains (Serva blue G, fuchsin, Bengal pink) were added depending on detected material. The whole slide surface was examined under optical microscope (Leitz Diaplan) equipped with reflection contrast system. Some digestive tract contents (or parts of them) were explored by SEM techniques.

The amount of food in stomach (C_s) and gut (C_g), respectively, was coded with arbitrary scores (4: 75 to 100% of the volume is filled; 3: 50 to 75%; 2: 25 to 50%; 1: 0 to 25%). Every item present in the digestive tract was determined to the lowest possible taxonomic group, and its proportion was coded using a similar coefficient (P_s, P_g = 1, 2, 3 or 4). A semi-quantitative approach, related to the 'percentage points' method (Hynes, 1950; Williams, 1981), has been adopted using the formulas:

$$I(i) = \sum_{n=1}^{x} C_s(n) * P_s(n) + C_g(n) * P_g(n) \tag{1}$$

where *I(i)*, dimensionless, is the importance of item i in the diet of a given species, and *x* the number of specimens dissected;

$$R(i) = \left[\frac{I(i)}{\sum_{n=1}^{y} I(n)} \right] * 100 \tag{2}$$

where *R(i)*, in %, represents the relative importance of item i in the total diet of a given species, and *y* the number of different items.

Beside gut content analyses, a tentative approach was performed based on lipid class analyses (Graeve et al., 2001) and on natural stable isotope abundances (carbon and nitrogen) as tracers of amphipod position in the Weddell Sea food web (Nyssen et al., 2000). This abundance was measured by isotope-ratio mass spectrometry (IRMS) on muscle tissue of eight species representative of different trophic types. Isotopic ratios were expressed in δ notation as the proportional deviation (in parts per thousand, ‰) of the sample isotope ratio from that of an international standard according to the following formula:

$$\delta X = [(Rsample/Rstandard) - 1] * 1000 \qquad (3)$$

where X is ^{13}C or ^{15}N, R is $^{13}C/^{12}C$ or $^{15}N/^{14}N$. The appropriate standards were Vienna-Peedee-Belemnite (V-PDB) and atmospheric nitrogen for carbon and nitrogen, respectively. Experimental precision (based on the standard deviation of replicates of an atropina standard) was 0.5 and 0.4‰ for carbon and nitrogen, respectively.

The trophic impact of these amphipod species on the eastern Weddell Sea ecosystem was approached by coupling feeding preferences and relative species abundance with the basic formula:

$$T(i) = \sum_{sp = 1}^{x} \frac{\overline{N}_{sp}}{\overline{N}_{tot}} * R(i)_{sp} \qquad (4)$$

where *T(i)* is the trophic impact on food item *i* (in %), *x* the number of analysed species, and $\overline{N}$ the mean number of individuals of a defined species (*sp*) and of all the *x* analysed species (*tot*) for all the samples of a cruise. Only classical benthic sampling devices (trawls and box-corers) were taken into account for evaluating $\overline{N}$, as baited traps for instance do not reflect the actual instantaneous abundance of a species in a defined sampling area.

In order to evaluate the feeding rates of Antarctic amphipods, some experiments were performed at King George Island with 4 different species. After sampling and identification, animals were placed in aquaria and starved out for periods of 9 to 15 days. During this fast, faeces and exuvia were removed daily. Despite animals did not receive any food, the lack of filter on the water circuit might allow suspended particulate matter to be provided in aquariums and this organic matter could eventually be used by amphipods. After starvation, a calibrated food item (piece of squid or alga) was introduced every day (during periods of 7 to 28

days) in the aquarium. Uneaten food was removed after 24 hours, rinsed with freshwater, drained on filter and dried at 60°C during 24 to 48 hours. Results are expressed as $g_{food-DW}.animal^{-1}.day^{-1}$ or $g_{food-DW}.g_{animal-DW}^{-1}.day^{-1}$. The latter expression, if better, does not allow to compare precisely the ingestion rates between species as they can differ in their skeleton calcification rate.

Egestion rates were also estimated after some feeding experiments. After the 24 hours nutrition period, animals were placed in nylon gauze baskets hung a few mm over the bottom of 25 ml jars. The basket mesh size (2 mm) allowed the faecal pellets to pass through, so avoiding coprophagy. Faeces collection was performed twice a day. Dissection of some individuals, after experiment, gave information about the emptiness of digestive system. As for food remains, faeces were dried at 60°C during 48 hours and weighed.

Finally, an attempt was made to evaluate the importance of amphipods as food source for the higher trophic levels in the Southern Ocean (invertebrates, fishes, birds and mammals). This approach was done by collecting information from an exhaustive survey of existing literature (>300 scientific papers).

2.5. Analyses of size spectra

Adult length from 1853 amphipod species were collected in the literature and from sampled material. These data produced detailed size spectra for 15 sites, including 5 from the Southern Ocean, from polar to tropical and marine to freshwater environments. Only benthic species were included and analyses were restricted to 250 m depth (mean continental shelf depth) except for Antarctic data, which include species to 500 m, as the continental shelf is depressed by the Antarctic icecap. Sites with less than 50 described species were not analysed.

Southern Ocean data (Magellanic region, Subantarctic Islands, South Georgia, West and East Antarctica) were compiled from several hundred references quoted in a check-list (De Broyer and Jazdzewski, 1993). Other data came from regional fauna lists: Madagascar (Ledoyer,1982), Mediterranean Sea (Ruffo, 1982-1998), Black Sea (Mordukhai-Boltovskoi et al., 1969), Caspian Sea (Birstein and Romanova, 1968), British Islands (Lincoln, 1979), Barents Sea (Bryagzin, 1997) and Lake Baikal (Bazikalova, 1945). This important data set also allowed the comparison of maximum size within species, thanks to the presence of many species in more than 1 of the 15 sites.

To approach gigantism, a focus on the right hand extreme of the size distribution of the regional taxocoenosis is needed. However, maximum size itself

was not used because of potential sampling bias at some sites. Instead, the threshold size separating the 95% smallest species from the 5% largest (TS 95/5) has been used (allowing the use of the Titicaca Lake value, for which there is no available size spectrum).

2.6. Biodiversity database development

A comprehensive database on taxonomy, distribution and bio-ecology of the Southern Ocean amphipods was developed as a part of the "Biodiversity Reference Centre" for Antarctic amphipoda. The conception of the relational database was a four-steps' operation. In the first step, the database objectives were defined *i.e.* to integrate all relevant information on the biodiversity of the Southern Ocean amphipods useful for an accurate assessment and monitoring of the Antarctic marine biodiversity, the management of specimen collections, the taxonomic revision of the fauna and the preparation of identification tools. Analysis of the logical database structure was the second step and aimed at identifying the different kinds of data and at building a model, a logical scheme that reflects, as close as possible, the actual investigations, including their inter-connections. The third step consisted in designing the forms, the queries and the reports that help the database users to encode, visualise and treat the data. Behind the design of these three main objects, the point was to identify precisely all the programming processes and procedures that answer to the flows of actions the application could encounter. The final step consisted in the technical and practical construction of the database according to the previous steps' requirements.

To perform the analyses and relational schemes two case tools were used: the software DBMain developed by the Computer Science Institute of the University of Namur (Anon., 1998) and the software Visio 5® (Microsoft®). The conceptual framework for this application relied on several sources: Fortuner (1993); the comprehensive model of biodiversity database named "Recorder 2000" (Copp, 1998); the study of the Committee on Computerization and Networking from the Association of Systematics Collections (ASC, 1992); the project "Data Faune Flore" from the University of Mons (Barbier, 1998); the Global Biodiversity Assessment recommendations (Olivieri et al., 1995); the Systematics Agenda 2000 recommendations (SA2000, 1994); the BIOTA program (Colwell, 1996); the Platypus program (http://www.ento.csiro.au/platypus/platypus.html); and the "Information Model for Biological Collections" (Berendsohn et al., 1996).

Developed in Microsoft® Access® 97, the database should move in a near future to an Oracle® data server and should be made accessible through the WWW.

3. RESULTS AND DISCUSSION

3.1. STRUCTURAL BIODIVERSITY

3.1.1. Composition of the peracarid taxocoenoses

3.1.1.1. Admiralty Bay. The detailed faunistic investigations on the Malacostraca allowed to identify so far 127 spp of amphipods, 59 spp of isopods, 14 spp of mysids, 13 spp of cumaceans and 12 spp of tanaids (Table I). Despite an important material still under analysis, the crustacean fauna of Admiralty Bay appears one of the best known in Antarctica. Several new species with ecological importance (Amphipoda: *Orchomenella n.sp., Eusirus n.sp., Oradarea n.sp., Schisturella n.sp.,…*) have been discovered and are under description. This rich material also allowed undertaking taxonomic revision of poorly known species.

Table I: *Number of malacostracan taxa collected in Admiralty Bay*

	Species	Genera	Families	References
Leptostraca	2	2	1	De Broyer, unpubl.
Mysidacea	14	5	3	Konopko, unpubl.
Cumacea	13	7	4	Blazewicz and Jazdzewski, 1995
Tanaidacea	12	8	3	Blazewicz and Jazdzewski, 1996
Isopoda	59	29	19	Arnaud et al., 1986; Teodorczyk, unpubl.
Amphipoda	127	75	30	Jazdzewski et al., 1992; De Broyer and Jazdzewski, 1993; Munn, unpubl.
Euphausiacea	5	2	1	Stepnik, 1982
Decapoda	2	2	2	Arnaud et al., 1986

3.1.1.2. Eastern Weddell Sea. The EPOS, EASIZ I and EASIZ II *Polarstern* campaigns allowed to collect more than 80.000 specimens of amphipods which were identified to the genus or the species level. Due to this efforts, the gammaridean and caprellidean amphipod fauna from the Weddell Sea amounts today more than 237 spp among which about 50 species are considered new to science (before the *Polarstern* investigations only 26 amphipod spp were known from the Weddell Sea).
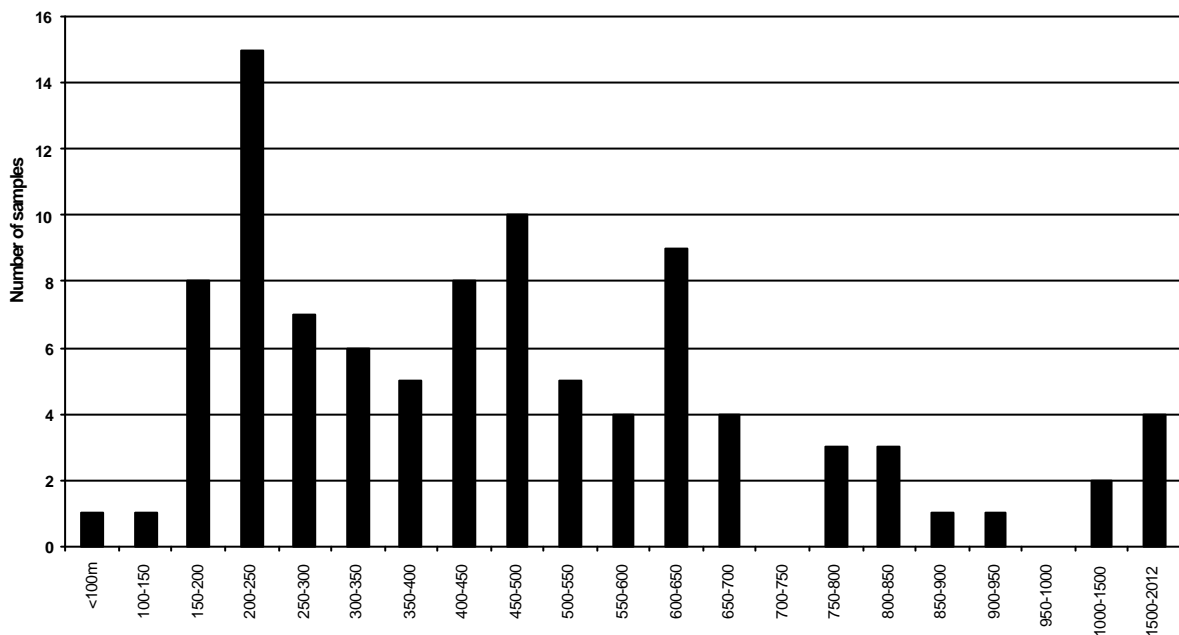
Figure 3: Benthos sampling effort in relation with depth for the three EPOS, EASIZ I and EASIZ II cruises in the eastern Weddell Sea. Gears used were bottom- or Agassiz trawls, dredges, baited traps, TV- grabs and epibenthic sledges.

In a attempt to evaluate the present state of faunal survey of the eastern Weddell Sea and its geographic, bathymetric and ecological coverage, a compilation was made of benthos sampling operations in the eastern Weddell Sea during the benthos-dedicated EPOS and EASIZ I (Gutt et al., 2000) and II campaigns. This compilation indicated the more intensively prospected sectors (Kapp Norvegia) and bathymetric zones: for instance, 80% of the benthos sampling effort was made on the shelf between 150 and 700m (Figure 3). It also revealed the under-sampling of some habitats like the under-surface of the sea ice in the neritic zone where bentho-pelagic, pelagic and cryopelagic species can be found.

3.1.2. Bathymetric distribution and seasonal variations in Admiralty Bay

Spatial and bathymetric distribution of the amphipod fauna was recorded in Admiralty Bay and the temporal variations of the spatial distribution, taxonomic composition, relative abundance of species and population structure were followed quantitatively along the reference transect, from 0 to 150m (section I in Figure 2).

At 0 m, on a stony beach, the macrozoobenthos samples taken during a complete annual cycle appeared to be very rich in vagile fauna settled between and under stones. Macrobenthos consisted mainly of amphipods (ca. 85% of total number), gastropods (11%) and nemerteans (3%). Abundance of the whole macrofauna ranged up to over 50,000 ind.m^{-2} and its biomass over 600 gm^{-2} (FW). Seven species of Amphipoda and four species of Gastropoda were found. Amphipoda were dominated by *Gondogeneia antarctica* (over 70% of all amphipods) and *Paramoera edouardi* (over 20%), whereas among gastropods *Laevilitorina antarctica* prevailed (over 70%). Unexpectedly high abundance and biomass of Amphipoda were observed in the first half of winter (May - July), surpassing otherwise important summer amphipod abundance (Figure 4). This phenomenon could be due to the high autumn abundance of decaying algae on the beach in the tidal zone providing detritus that are probably the main food source for Amphipoda (Jazdzewski et al., 2001)
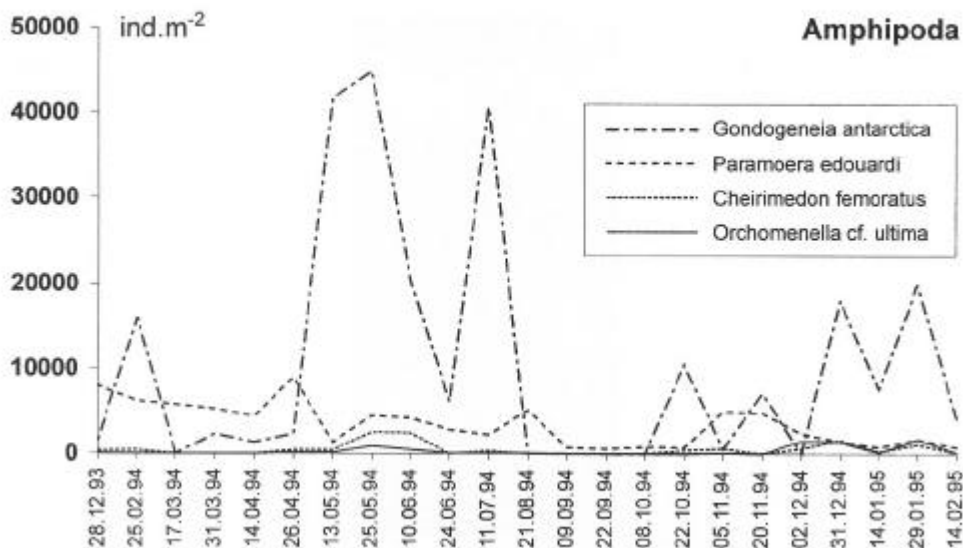
Figure 4*: Year-round abundance fluctuations of the most common amphipod species in the upper sublittoral fringe of Admiralty Bay.*
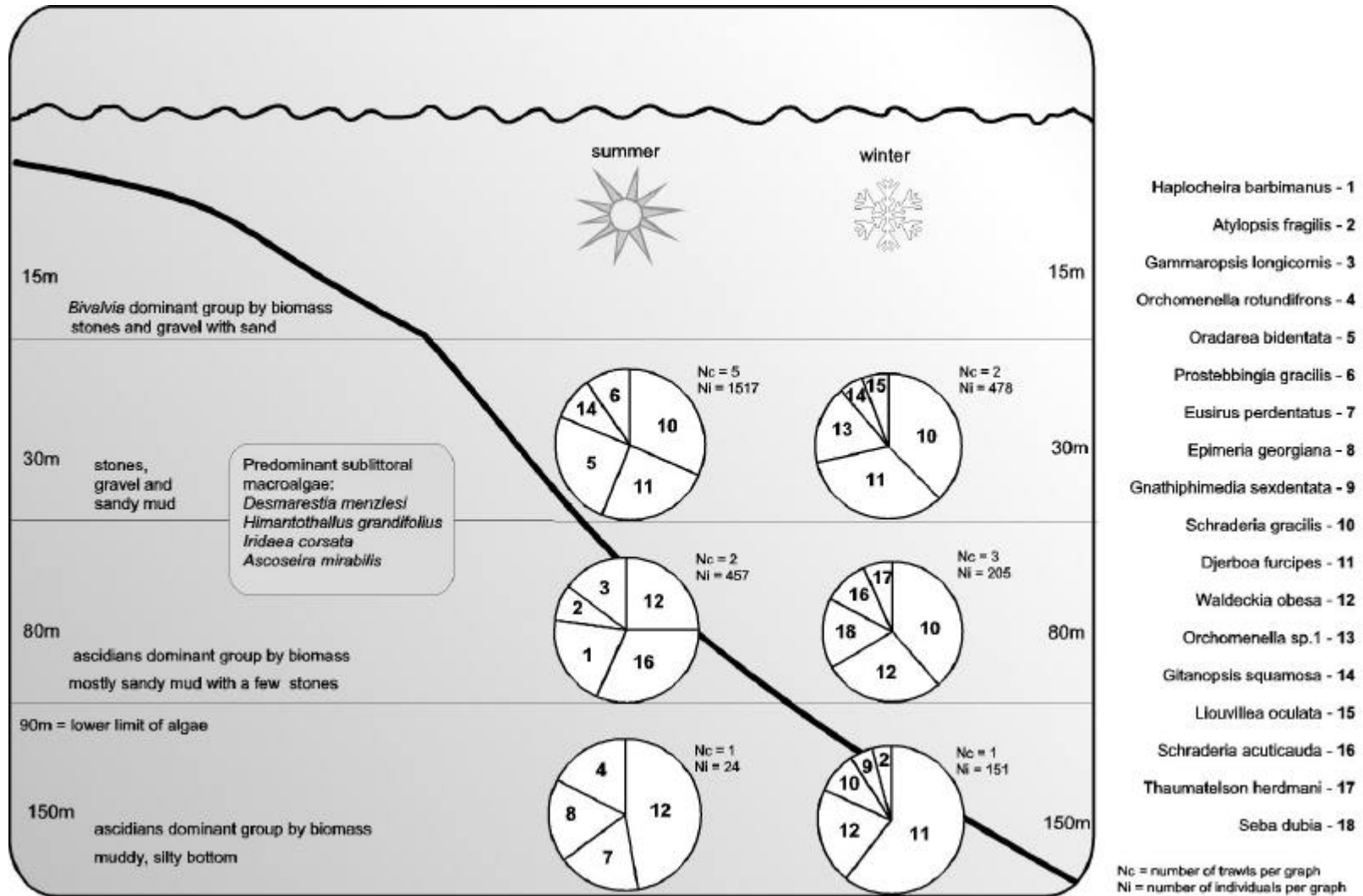
Figure 5: *Seasonal bathymetric variations of benthic amphipods assemblages along section I, Admiralty Bay.*

The material of the monthly time series from the deeper part of the reference transect (15-150m) amounted more than 24.000 specimens in total and 76 spp were identified. The relative abundance in trawls of the top five species from each depth per season is represented on Figure 5. Although the number of samples and individuals was low, it is nevertheless possible to note some patterns. For example, the herbivorous *Schraderia gracilis* and *Djerboa furcipes* were among the five most abundant species for both seasons at 30m. At other depths they were among the top five but only in the winter. This was the first time that *Djerboa furcipes* was collected at 150m, well below the phytal zone, and this relatively deep occurrence may be due to the attraction to the drifted decaying algae found at these depths as indicated by the preliminary examination of stomach contents. Some species are common to more than one assemblage and have high relative abundance at more than one depth. Overall, there are clearly different assemblages corresponding to different depths (Munn et al. 1999).

3.1.3. Vertical distribution in the Weddell Sea

The EASIZ I and II campaigns allowed to add substantial data on the depth distribution range and preferendums between 65 and 2500 m. This is partly due to the extensive and systematic utilisation for the first time of an autonomous trap system which also allowed to detect a probable faunal limit – at least for the scavengers - on the upper slope between 800 and 1000m (De Broyer et al., 1999$_a$) (Figure 6).

3.1.4. Habitats and microhabitats in the Weddell Sea

Comparative analysis of catches allowed to distinguish six major amphipod habitats in the neritic zone (Figure 7). The *endobenthic habitat* is constituted of the first centimetres of the sediment and occupied by sedentary tube- or "cell"-dwellers of the family Ampeliscidae and by permanent burrowers belonging to the Oedicerotidae and Phoxocephalidae and temporary burrowers of the Lysianassoidea. The *epibenthic habitats* with three strata described in more details hereafter, is colonised by numerous free-living species, the most abundant being the Epimeriidae, Eusiridae *s.l.*, Iphimediidae and Lysianassoidea. Among the epibenthos, several *symbiotic* and *inquilinous microhabitats* are occupied mainly by some Colomastigidae, Dexaminidae, Leucothoidae, Lysianassoidea, Sebidae, Stenothoidae and Stilipedidae.
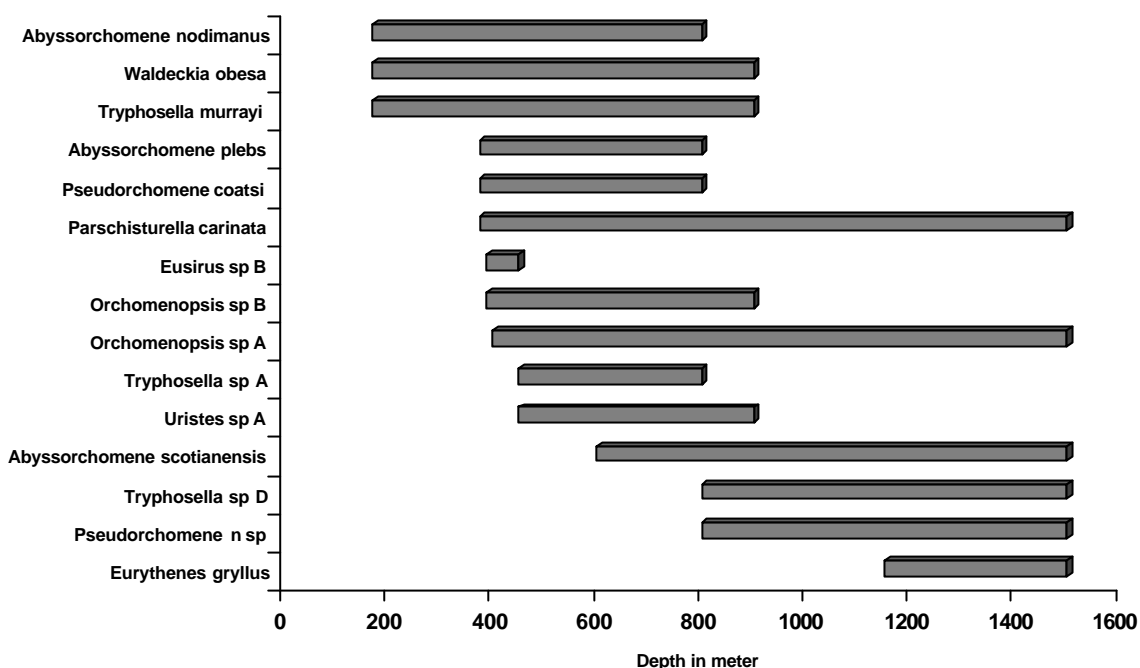
Figure 6*: Vertical distribution of the main amphipod scavenging species in the eastern Weddell Sea shelf and upper slope.*

The Benthic Boundary Layer forms the *hyperbenthic* (or suprabenthic) habitat of some swimming Eusiridae *s.l.* and Lysianassoidea. Along the upper slope off Vestkapp and Halley Bay between 1054 and 1983 m, 32 species (one quarter new to science) from 15 families have been collected at about 1.0 m above the bottom by an epibenthic sledge (Andres, pers. comm.).

Rather few Epimeriidae, Eusiridae *s.l.*, Lysianassoidea and Stegocephalidae occupy the neritic water column showing either a *benthopelagic* or a purely *pelagic* life-style. With the exception of *Eusirus propeperdentatus*, which appeared mostly in the deepest layer of the surface water, the amphipods showed no clear preference for one of the strata (300-200 m, 200-50 m, 50-0 m) (Boysen-Ennen and Piatkowski, 1988). Part of the species found in the water column at several tens or hundreds of meters above the bottom were also found on the bottom, in particular in baited traps. These species are considered *benthopelagic* spending part of their time or part of their life close to or on the bottom in particular for feeding purposes.

The *cryopelagic* habitat *-i.e.* the under-surface of the sea ice- constitutes an habitat for a specialized cryopelagic flora, the sea-ice algae, and a cryopelagic fauna

of krill, harpacticoid and calanoid copepods, and nematodes. Only three species of cryopelagic amphipods have been incidentally recorded so far in the eastern Weddell Sea at Drescher Inlet: one lysianassoid, one eusiroid and surprisingly one stenothoid (Rauschert, pers. comm.).
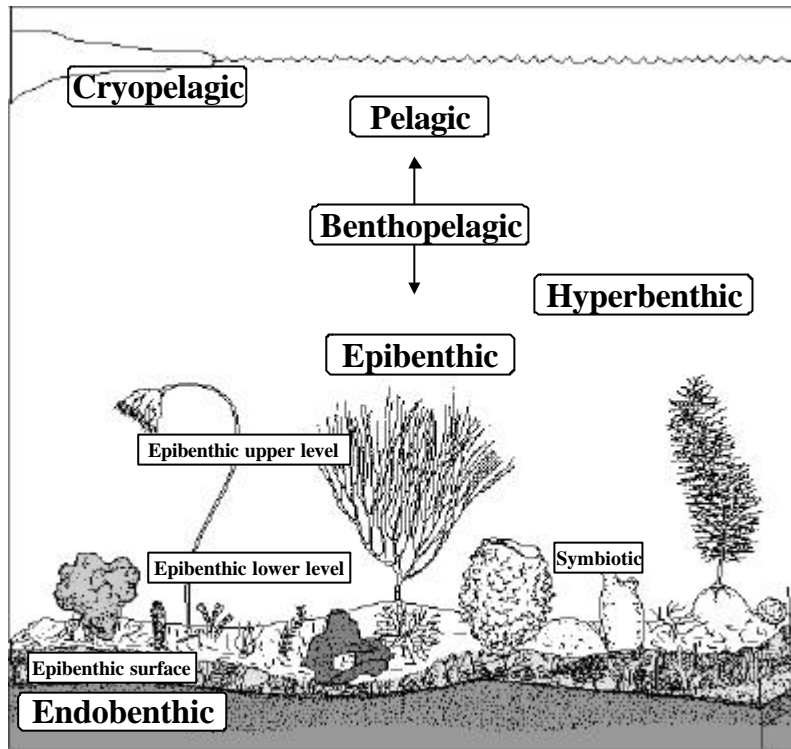
Figure 7: *Scheme of the amphipod macrohabitats in the eastern Weddell Sea neritic zone.*

3.1.4.1. Epibenthic habitats:

The epibenthic layer of the eastern Weddell Sea shelf includes all habitats from the sediment surface level up to the top of sessile organisms which offer secondary substrates to colonisers. Its thickness can reach about 1m as shown by bottom pictures and the size of the biggest sessile invertebrates collected. Amphipods appear distributed on the bottom in three different strata: the sediment surface and the lower and upper strata of the sessile epibenthos.
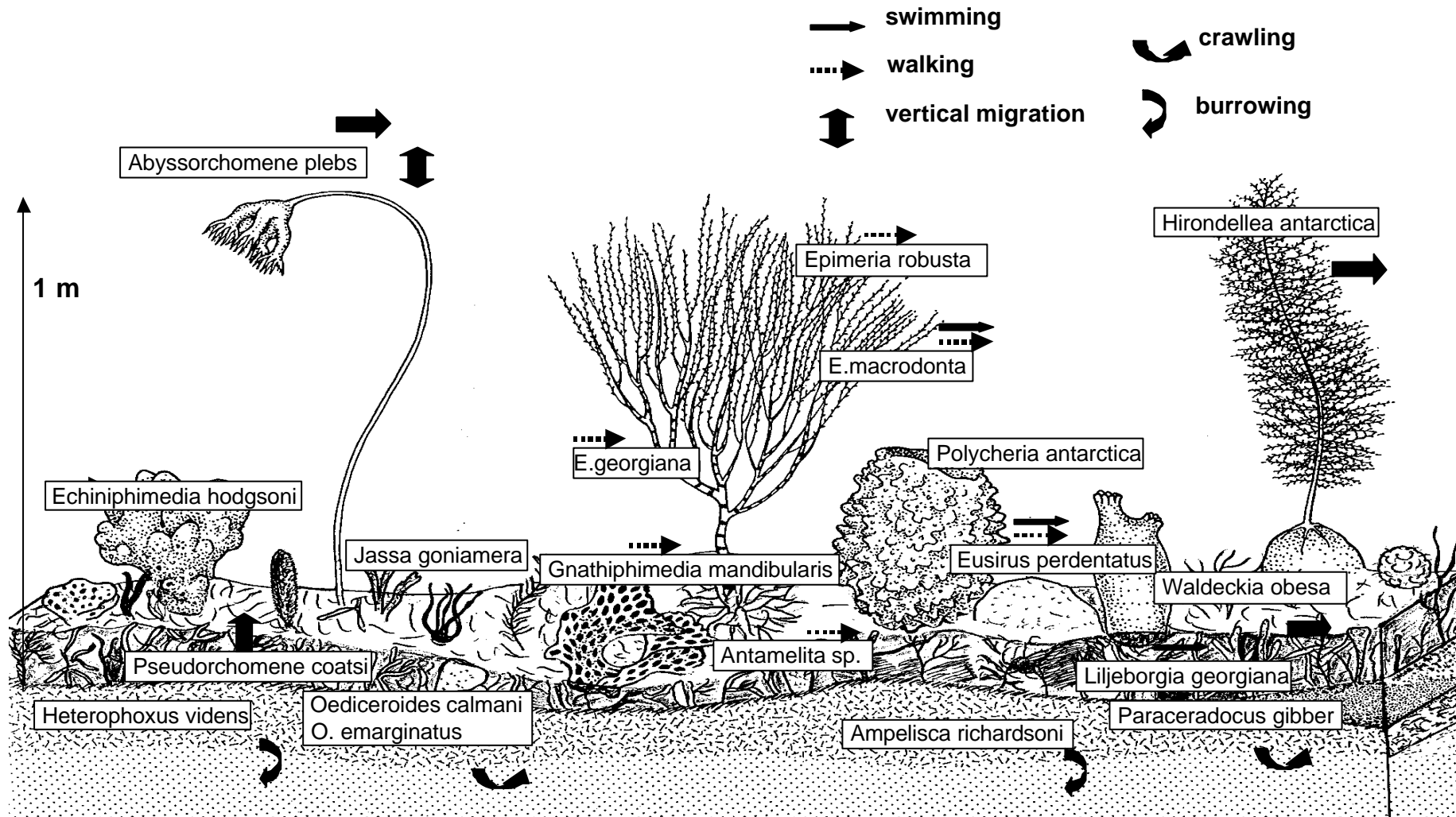
Figure 8: Scheme of habitats occupied by representative amphipod species on the eastern Weddell Sea shelf.

3.1.4.1.1. The sediment surface

Heterogeneous in its composition, structure and thickness, the sediment surface varies from the soft type like sand and mud to the detritic type like coarse bryozoan debris or sponge spicule mats. Dropstones from icebergs can be mixed with this soft or coarse sediment. This very heterogeneous sediment surface often with cracks, interstices and holes offers a great variety of microhabitats to a number of small vagile invertebrates like amphipods (Figure 8). Some amphipod species live only temporarily in this biotope, looking for transitory substrate and protection. Representative species include: Lysianassidae: *Waldeckia obesa*, *Uristes gigas* and *U. adarei*, *Abyssorchomene scotianensis*, *Lepidecreella sp A*, *Orchomenella acanthura*, *Orchomenella pinguides*, *Parschisturella carinata*, *Tryphosella murrayi*.

Other amphipods appear sedentary finding there shelter and food. Representative species from the soft sediment surface include: Melitidae n. sp., *Melphidippa antarctica* and *Epimeria georgiana*; from coarse or mixed sediment surface: *Liljeborgia georgiana* and *Paraceradocus gibber*.

3.1.4.1.2. The lower level of sessile epibenthos

Covering the bottom by patches or in continuous layers, the diverse assemblages of hexactinellids and demosponges (Barthel and Gutt 1992), the various bryozoans and the multiple cnidarians and hydrozoans form highly heterogeneous structures including multiple cavities. This sessile epibenthos provides numerous substrates for amphipods. According to their feeding type, many amphipods also find there food in abundance (Coleman 1989$_{b,c}$, 1990; Klages and Gutt 1990$_b$; Dauby et al., 2001$_a$). Aquarium observations indicated that some species occupied preferably the lower part of the erected substrates, whereas others occurred on the upper part or showed no apparent preference and occurred in both levels and sometimes also on the sediment surface. Representative species typically found in this substrate include several Iphimediidae e.g. *Echiniphimedia hodgsoni*, *E. scotti*, *Gnathiphimedia mandibularis*, *Iphimediella cyclogena* and *Maxilliphimedia longipes*; Epimeriidae: *Epimeria rubrieques*; Eusiridae: *Eusirus perdentatus*; Ischyroceridae: *Jassa goniamera*.

3.1.4.1.3. The upper level of sessile benthos

ROV video records of the sessile suspension-feeder community showed a succession of ball-like, urn- or finger- shaped sponges, tree-like hydrozoans or flower-shaped gorgonians or bryozoans. The canopy of these assemblages, composed of a mixture of delicate and strong organisms, constitutes a secondary

bottom colonised by other invertebrates, the most obvious being echinoderms (e.g. the crinoid *Promachocrinus kerguelensis,* several *Ophiurolepis*), and by fish (*Artedidraco skottsbergi, Trematomus scotti*) (Gutt and Schickan, 1998). Amphipods are suspected to be also present in this layer, but, due to their size, are usually not visible on pictures. The family Epimeriidae comprises typical representatives of this habitat with at least four common species: *Epimeria macrodonta, E. robusta, E. similis* and *Epimeriella walkeri*. Additional representative species are: *Hirondellea antarctica* (Lysianassoidea), a good swimmer also found in the water column, and *Alexandrella mixta* (Stilipedidae)*.*

3.1.4.2. The symbiotic and inquilinous habitats

Among amphipods living on sessile invertebrates, some species, usually sedentary, have established different symbiotic relationships with their hosts which remain to be described.

Species associated with **sponges**: no less than 16 spp of amphipods were recorded on common hexactinellids and demosponges by Kunzmann (1996), who did not established any host-specific relationships. Among her material, four species appear frequently and in relatively high numbers in some sponges: *Seba antarcica, Polycheria antarctica s.l., Colomastix simplicicauda* and *Andaniotes linearis.* They can be considered preferential spongicolous species, but not exclusive as *S. antarctica and P. antarctica s.l.* have also been recorded on ascidians. According to Kunzmann (1996), *S. antarctica* and *P. antarctica* are ectoparasites eating the host tissues and using the sponge as a shelter from predators. In our material, *P. antarctica* was found in holes in the surface tissues of the demosponge *Crella crassa*. Stomach content analysis revealed no sponge spicules but only small particles (less than 100 μm) of unidentifiable organic matter, diatoms fragments and mineral grains (Dauby et al., 2001) which do not confirm Kunzmann's observation of ectoparasitism. In addition, a new species of *Scaphodactylus* (Stenothoidae) was found on an unidentified demosponge.

Species associated with **ascidians**: species of the families Leucothoidae, Lysianassoidea, Stegocephalidae or Stenothoidae have been found in the branchial cavity of different ascidians. *Leucothoe sp.* was found in *Corella eumyota*. The lysianassoid *Orchomenyx sp.* was found in *Ascidia challengeri* and an unidentified species in a "large red ascidian". Stegocephalids have been found in *Ascidia challengeri* and in *Eugyrioides polyducta*. *Metopoides* sp.nov.2 (Stenothoidae) was recorded in *Ascidia challengeri* at depths of 600 and 710 m*.* Preliminary examination indicated no apparent host specificity.

Species associated to **hydrozoans**: two new stenothoid species of the genus *Torometopa* were found on *Oswaldella billardi*. *Thaumatelson* sp. (Stenothoidae) was found on a unidentified hydrozoan. The stolons produced by *Tubularia ralphii* and *Oswaldella antarctica* on several stones from the underwater hilltop of Four Seasons Inlet (NE of Kapp Norwegia) host a few hundreds of stenothoids from 2 spp, which could however not be associated with the hydrozoans but simply shelter in this tri-dimensional substrate (Gili et al., 1999; De Broyer et al., 1999$_a$).

Species associated to **gorgonarians**: one stenothoid species of the genus *Torometopa* was found on *Primnoella* sp. at 400 m while *Polycheria* sp. (Dexaminidae) occurred on a unidentified gorgonarian host.

Precise habitat determination at shelf depths has strong methodological limitations. Bottom pictures and video records have been particularly useful for characterising the habitats of fishes (Ekau and Gutt, 1991) or conspicuous macrobenthos (*e.g.* holothurians: Gutt, 1991; shrimps: Gutt et al., 1991; sponges: Barthel and Gutt, 1992) but are of little help for the small and often hidden amphipods. Analysis of trawl catch contents is of limited or no value to indicate the potential habitat of collected amphipods because of the usually disturbed state of the catch (often a mixture of sediments, stones and diverse fauna) and also the usual high patchiness of sampled assemblages (see e.g. Gutt and Koltun, 1995). They can however be informative in case of homogeneous bottom catches or symbiosis on well-preserved hosts for instance. On the contrary, undisturbed bottom samples from corers and large grabs (which should be more systematically checked) can provide useful epibenthic habitat indications. Aquarium observations can provide information on the general behaviour (see *e.g.* Enequist, 1949; Klages and Gutt, 1990$_{a,b}$) and on the species ability to select a particular habitat (*e.g.* Coleman, 1989$_a$). On the other hand, extrapolations on the basis of similar morphologies to infer similar habitats can be hazardous, as shown for instance by the *Eusirus* case: *Eusirus perdentatus* is a typically epibenthic animal, walker and poor swimmer (Klages, 1993) although its sister species *Eusirus propeperdentatus* is a purely pelagic animal (Andres, 1979; De Broyer & Jazdzewski, 1993).

From a preliminary comparison with the other amphipod macrohabitats in the eastern Weddell Sea, the epibenthic zone, here subdivided in three different levels, appears the most heterogeneous and the richest in species. The presumed habitats of some representative epibenthic species are presented schematically on Figure 8. Each epibenthic strata from the heterogeneous sediment surface to the top of the erected sessile benthos offers to amphipods different habitats characterised by some physical parameters and by nature and availability of food. Some species find there a

temporary substrate or a shelter, others forage in this habitat, in some cases at the expense of the living substrate itself. The comparatively high number of "walker-climber" species (mainly belonging to the Iphimedioidea, with more than 50 spp), mostly found on the different levels of the rich suspension feeder assemblages, seems unique to the eastern Weddell Sea. It is most probably linked to the diversity of microhabitats and the abundance of food offered by the rich epibenthos to these specialised micropredatory grazers or unspecialised predators (feeding types according to Coleman, 1989[b,c]; Klages and Gutt, 1990[b]; Dauby et al., 2001[a]).

Aquarium observations have indicated two possible levels of amphipod distribution on the sessile epibenthos substrates, which require confirmation. It seems nevertheless possible to differentiate the environmental conditions of the two levels. At the top of the epibenthic substrates, the upper level strata can be more exposed to strong currents (a current of 40 cm/sec was recorded in Kapp Norvegia at 5m above the bottom at a depth of 676m; Fahrbach et al., 1992). This seems *a priori* a favourable position for the free-living suspension-feeders (Ischyroceriidae…) to collect the organic rain from the above water column and from lateral advection. Currents can also carry carrion smell and this place could be advantageous for scavengers like Lysianassoidea (see Ingram and Hessler, 1983). These trophic advantages are balanced, however, by a greater exposure to predators. Benthic fish stomachs contents (*Trematomus spp., Pogonophryne spp., Artedidraco orianae*…) for instance frequently revealed *Epimeria* species supposed to stay at this level (Olaso, 1999; Olaso et al., 2000).

The selected species undoubtedly represent the most conspicuous and the most common ones in the epibenthic catches so far analysed. But most specimens have been caught by trawls with a 15 mm mesh size which do not always allow adequately collecting small species, which can be numerous judging from the preliminary analysis of material from small mesh-sized dredge (Rauschert, unpubl.). The diversity of symbiotic and inquilinous habitats is probably highly underestimated. Only sponge habitats have been systematically investigated (Kunzmann, 1996) so far. Ascidians remain to be more systematically checked for their inquilinous fauna. Potential associations with cnidarians and hydrozoans should draw more attention. A number of small species, among which the numerous Stenothoidae, might have developed preferential relationships with some hosts. They could represent an important part of the specific diversity of the eastern Weddell Sea amphipods.

3.2. ECOFUNCTIONAL BIODIVERSITY

3.2.1. Trophic diversity in the Weddell Sea

Almost all known feeding types can be encountered in the amphipod benthic communities of the eastern Weddell Sea shelf. A notable exception is the macroherbivory which is apparently lacking, probably due to the apparently complete absence of macroalgae in that ice-covered deep shelf area. On the basis of both diet analyses (*i.e. R(i)*'s distribution in species' digestive tract contents, see M&M) and ethological observations in aquarium, the following eight feeding types can be distinguished (Figure 9) (Dauby et al., 2001ₐ).

A. *Suspension–feeding type.* Amphipods of this group are typically epibenthic and feed on particulate organic matter (plant or animal, dead or alive) from the water column, such as plankton or micronekton organisms or by-products (*e.g.* faecal pellets), and advected material. The main amphipod families of that type are Ampeliscidae, Melphidippidae, Dexaminidae and Ischyroceridae. These animals are always weakly motile, or sedentary. Depending upon the strategy used for taking food, different behavioural categories can be distinguished:
* *active suspension-feeders*, which either improve the collection of food by moving part of their body or by creating a water current (*e.g. Ampelisca richardsoni*), or which seize or trap sinking material by the way of their antennae (*e.g. Jassa goniamera*).
* *passive suspension-feeders*, which stay motionless upside-down on the bottom, feeding on sinking particles (*e.g. Melphidippa antarctica*);
Analyses of the stomach and gut content of these organisms revealed the prevalence of plankton-originating items and of miscellaneous detrital bodies.

B. *Deposit–feeding type.* Also typically epibenthic, these amphipods feed on relatively large particles collected on the seafloor, originating either from the water column or from the breakdown of benthic biota. Families Epimeriidae, Melitidae or Gammaridae (*Ceradocus* group) have representatives of that type, with common Antarctic species *Epimeria georgiana, Antamelita sp., Paraceradocus gibber.* Gut contents of these amphipods usually show a wide variety of organic debris: sponge spicules, worm setae, echinoderm ossicles, crustacean appendages, or plankters, associated with mineral particles.

C. *Deposit–feeding / predatory type.* Amphipods of this trophic type, mainly belonging to Liljeborgiidae and Oedicerotidae, are weakly motile endo- or epibenthic forms. They feed on the same kind of items as those of the previous type, but also complement their diet with small living benthic preys such as polychaetes and tiny

amphipods. Crustacean fragments represent a significant share of the gut content. Common representative species: *Oediceroides emarginatus, O. calmani, Liljeborgia georgiana.*

D. *Opportunistic predatory type.* Amphipods of this trophic type are epibenthic and belong mainly to Epimeriidae (*Epimeria macrodonta, E. robusta, E. rubrieques*). They feed on miscellaneous small material that they detect with antennae and capture with gnathopods. They are weakly motile but can walk on the seafloor in search of food. Analyses of gut contents reveal a wide diversity of animal food items (hydrozoan, gorgonian, sponge, polychaete, holothuroid and crustacean parts) and some plankton-originated stuffs.

E. *Micropredatory browsing type.* Animals of this feeding type collect small food elements from sedentary organisms which are unable to flee. Browsers (or "grazers") use to eat only part of each prey item without killing it. Eastern Weddell Sea browsing amphipods specialized in grazing on colonies of different benthic invertebrates. Organisms of this type are also known as "surface microphagous browsers", "carnivorous browsers", or "micropredatory grazers". Grazers on periphyton ("microherbivorous browsers"), albeit existing, are not selective and can conveniently be classed in deposit-feeders. Micropredatory browsing behaviour has been developed in different families of Antarctic amphipods (Epimeriidae, Iphimediidae or Lysianassidae *s.l.*). These are typically epibenthic, and are moreover usually feeding preferentially on one kind of prey: *Epimeria similis* and *Hirondellea antarctica* graze on cnidarian colonies, *Echiniphimedia hodgsoni* on sponges, *Gnathiphimedia mandibularis* on bryozoans, *Bathypanoploea schellenbergi* on gorgons.

F. *Macropredatory / opportunistic scavenging type.* This trophic type, mainly predatory, embraces a large number of species belonging to various families: Epimeriidae (*Epimeriella walkeri*), Eusiridae (*Eusirus perdentatus, E. antarcticus, Rhachotropis antarctica*), Phoxocephalidae (*Heterophoxus videns*) or Stilipedidae (*Alexandrella mixta*). Members of the group are endo- or epibenthic, and feed on a wide variety of prey. Prey differs from one species to another, and a site-dependent intraspecific variability is apparent. Non selective feeding is usual, but some members of this feeding type display diet preferences for particular animal groups such as polychaetes, other amphipods or ophiuroids. Different predatory behaviours (active searching, ambushing) are also encountered in this group.
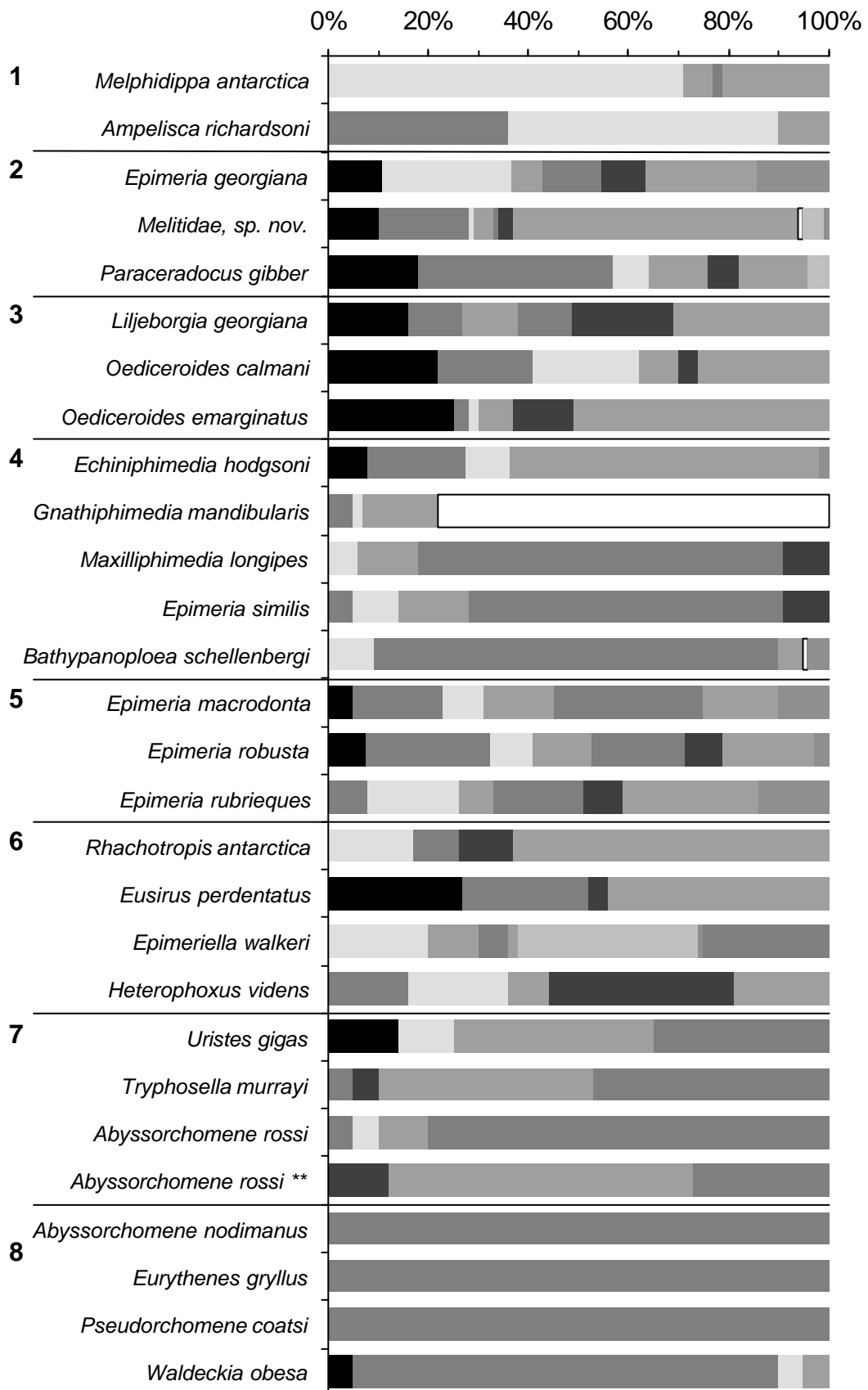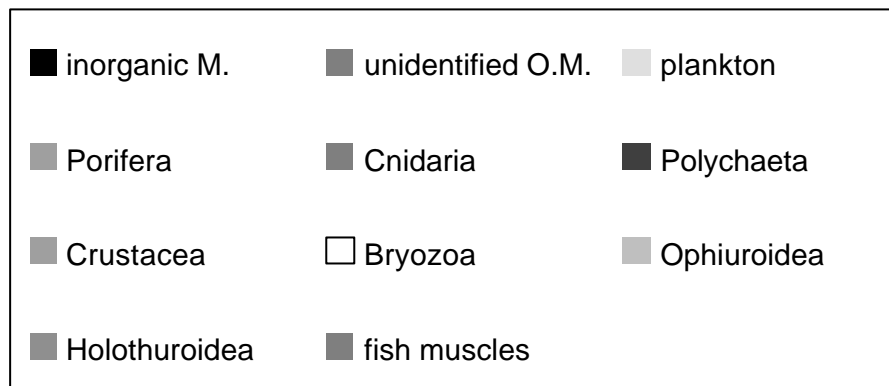
Figure 9: *Mean proportions [R(i)'s] of the different food items in the digestive tract of different Weddell Sea amphipods. Numbers refer to trophic types (see text).*

G. *Opportunistic necrophagy type.* Amphipods of this trophic type, mainly epibenthic, are commonly found in traps baited with meat or dead fish. Analyses of digestive tract contents and observations made in aquaria show that carrion constitutes only a fraction of the diet. These species are able to kill preys, the size of which ranges from copepods to small fishes. The relative importance of both feeding behaviours is likely to depend upon potential food availability, which is spatially and seasonally dependent. Common representative species (all belonging to the Lysianassidae family) are: *Tryphosella murrayi, Uristes gigas, Abyssorchomene rossi, A. plebs.*

H. *Necrophagy type.* This vast group of epibenthic, benthonectonic or benthopelagic amphipods frames most of its diet with pieces of muscle or other tissues from dead animals, either vertebrates or invertebrates. Representatives of this trophic type all belong to the Lysianassoidea superfamily: *Abyssorchomene nodimanus, Pseudorchomene coatsi, Parschisturella carinata, Eurythenes gryllus, Waldeckia obesa.* These forms are ubiquitous, highly motile, and always abundant. Experiments carried out in aquarium show that olfaction is the main process involved in the detection of carrion.

3.2.2. Stable isotope approach

Specific $\delta^{13}C$ and $\delta^{15}N$ values in amphipods are presented in Figure 10. *Ampelisca richardsoni* is completely isolated from other amphipods with the lowest δ

for the carbon and for the nitrogen (δ^{13}C = -27.1 ± 0.9‰; δ^{15}N = 6.6 ± 0.6‰). These values are the closest to those displayed for SPOM and are significantly different from values of all the other species (ANOVA *p* < 0.01) except for the δ^{13}C of *Epimeria similis* and *Iphimediella cyclogena*. *Eusirus perdentatus* and *I. cyclogena* present similar δ^{13}C but their nitrogen ratios are significantly different from each other (ANOVA *p* = 0.0005). *E. perdentatus* δ^{15}N values differ significantly from all other species nitrogen ratios except from *E. similis* single value. Unlike its δ^{13}C, *I. cyclogena* δ^{15}N values belong to the highest with those of *Orchomenella* cf. *pinguides*, *Waldeckia obesa*, *Tryphosella murrayi* and *Parschisturella carinata*. Furthermore the four latter species stable isotope ratios are not significantly different from each other, neither for the carbon nor for the nitrogen (Nyssen et al., 2000).
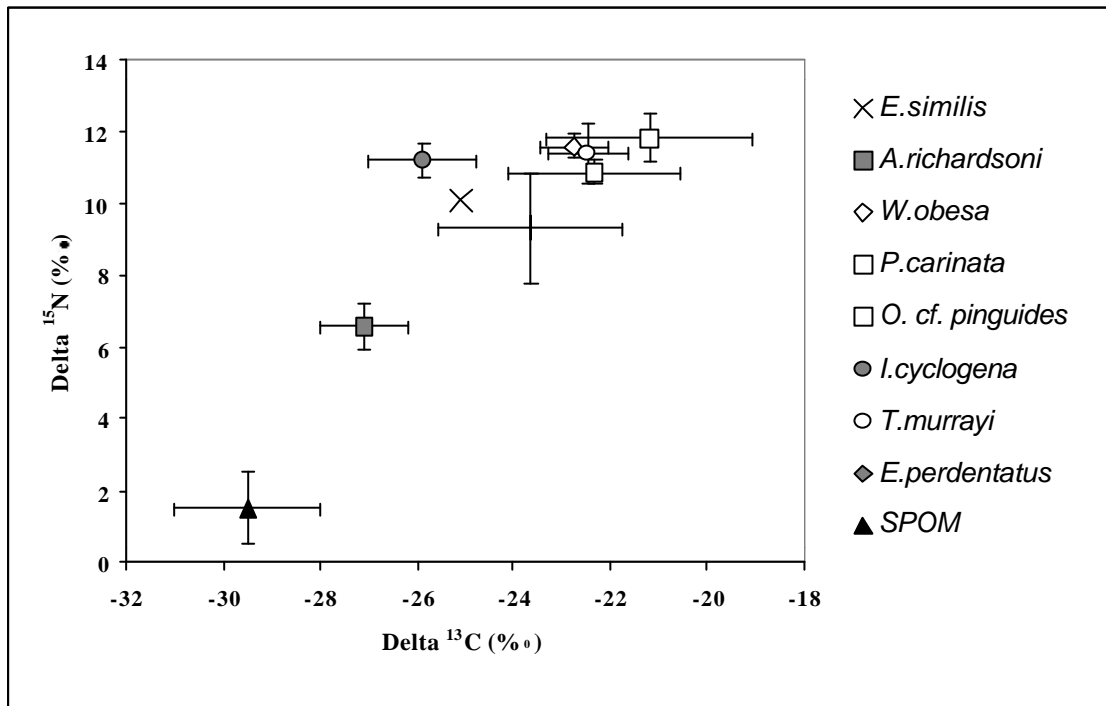
Figure 10: *d*^{13}*C versus* *d*^{15}*N values of SPOM and of 8 amphipod species from the eastern Weddell Sea.*

3.2.3. Impact of amphipods on the benthic ecosystem

The mean relative abundance (*R(i)*, in %) of the different food items in the digestive tract of the most important Weddell Sea amphipod species was presented in Figure 9. The analysed species were chosen on the basis of their relative abundance, each one representing at least 0.4%, on the average, of the total

amphipod population collected during each cruise. For the EPOS cruise (1989), these species represent 52.8% of total amphipods (58% of all the samples have been analysed), while, for the EASIZ I cruise (1996), they represent 70.9% of total amphipods (82% of the samples have been investigated) (Dauby et al., 2001[b]).

The amphipod trophic impact on the different available food items [$T(i)$, see M&M] of the Weddell sea is presented in Figure 11, for the EPOS and the EASIZ I cruises, respectively.

For the EPOS samples, crustaceans appear to be the most frequently consumed items (32%), followed by fish carcasses (18%). If we do not take into account the unidentified organic matter (unrecognizable organic bodies without any specific features like cnidocysts, or without any hard structures like chitinous plates or spicules), particles of planktonic origin represents the third most common item. Sponges, cnidarians and worms (polychaetes and nematodes) are about equally consumed (5 to 7%), while bryozoans and echinoderms represent only a tiny fraction of the amphipod diet.
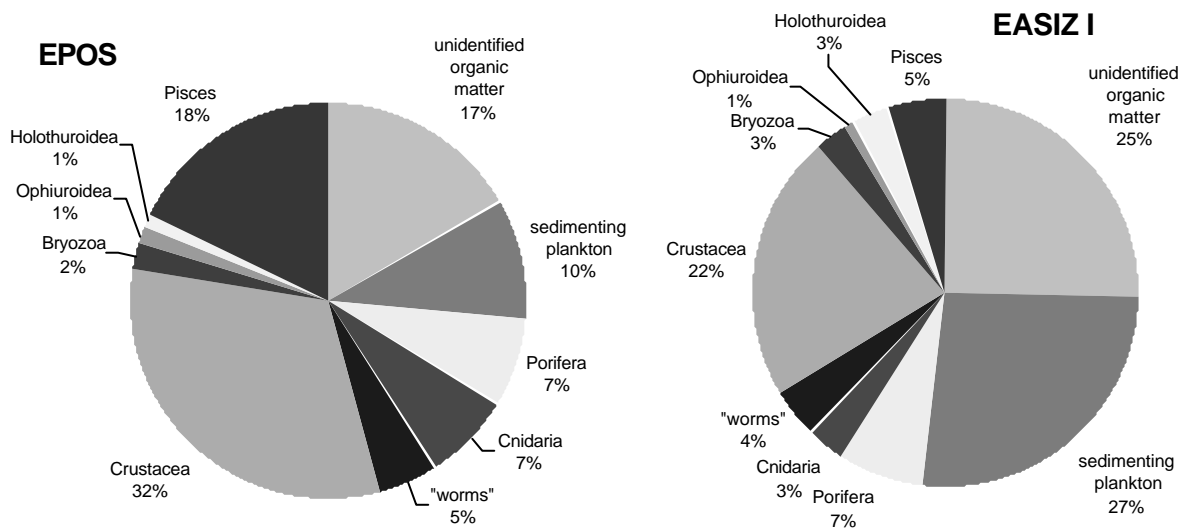
Figure 11: Mean relative trophic impacts [T(i)] (in %) of the eastern Weddell Sea benthic amphipod community on the different potential food sources, during the EPOS (1989) and EASIZ I (1996) cruises. Inorganic material (sediment grains) were omitted for calculation.

Results from the EASIZ I cruise are rather different. Plankton-originating cells (together with the unidentified matter) are the main dietary component (27%), before crustaceans (22%). Fish flesh constitute only a small fraction (5%), of the same order

of occurrence as worms, bryozoans or holothuroids. Sponges, with 7%, are the third item in importance in the amphipod diet.

3.2.4. Amphipod feeding rates

Eight species, representative of different trophic types (herbivory, omnivory, necrophagy), were used to try to evaluate the Antarctic amphipod feeding (FR), egestion (ER) and thus assimilation (AR) rates. These specific mean rates are presented in Table II.

Table II: Mean feeding rates ($g_{food-DW} \cdot g_{animal-DW}^{-1} \cdot day^{-1}$), egestion and assimilation rates (% of ingested food) for the different analysed amphipod species.

species	given food	FR ($\%.day^{-1}$)	ER (% food)	AR (% food)
Djerboa furcipes	algae	6.2	54	46
Eurymera monticulosa	squid	3.0	13	87
	algae	2.4	n.d.	n.d.
Gondogeneia redfearni	squid	15.7	10	90
Prostebbingia brevicornis	squid	9.5	44	56
Abyssorchomene nodimanus	squid	3.8	n.d.	n.d.
Parschisturella carinata	squid	2.2	n.d.	n.d.
Tryphosella murrayi	fish	2.1	n.d.	n.d.
	squid	1.4	n.d.	n.d.
Waldeckia obesa	fish	3.1	33	67
	squid	2.2	n.d.	n.d.

It clearly appears that feeding rates present large variations (one order of magnitude) with respect to amphipod species. But, for a given species, these rates, albeit slightly different, are not strongly influenced by the kind of offered food.

It must be pointed out that the data presented in Table II are average values over several feeding experiments, and that results from each experiment are average values over several days (cfr. M&M). An example of the day-to-day variations in the feeding rate during an experiment with *A. nodimanus* is shown in Figure 12. Feeding

Abyssorchomene nodimanus
feeding rate on squid meat
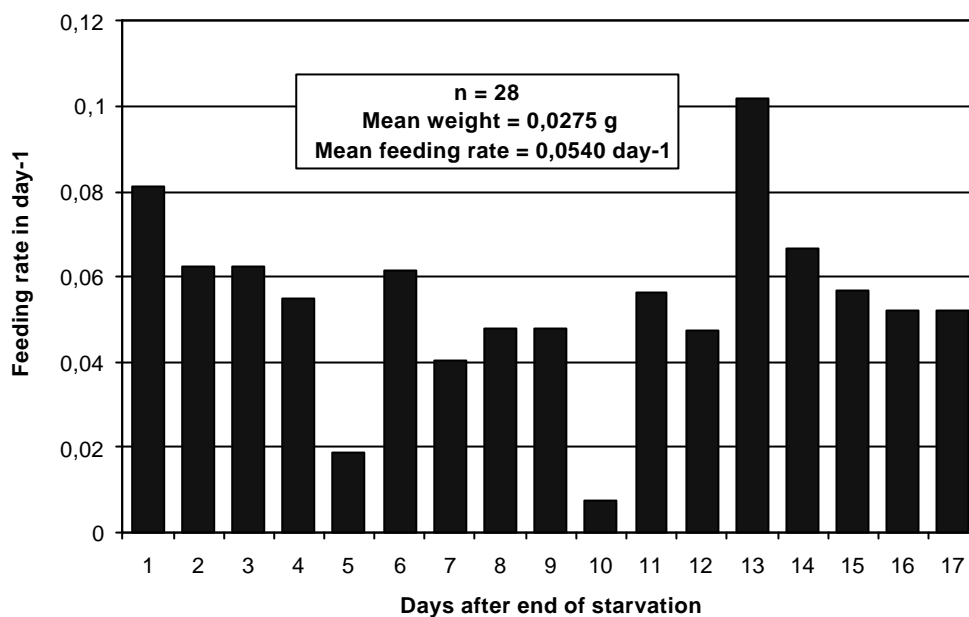
Figure 12: Example of the day-to-day variation of the feeding rate of
Abyssorchomene nodimanus *fed on squid.*

Waldeckia obesa
Feeding rates
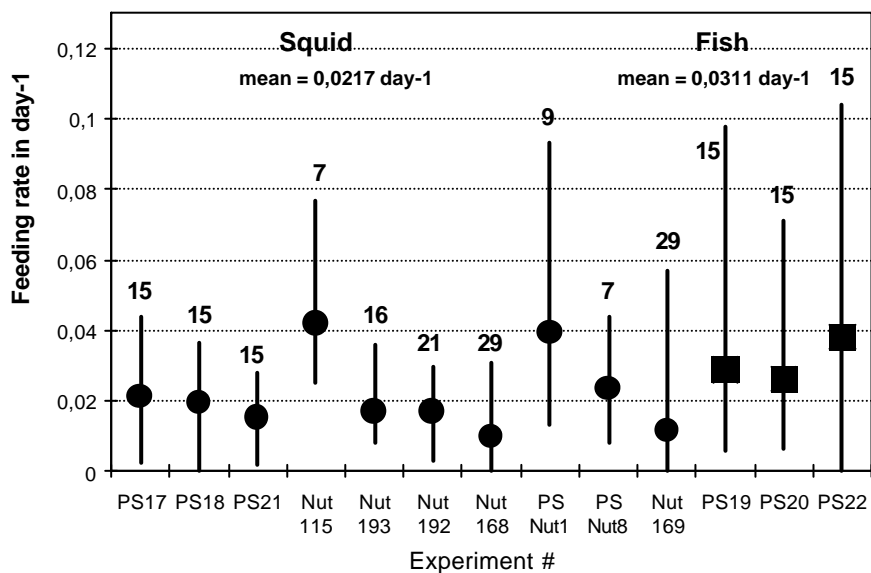
*Figure 13: Feeding rates (mean + day-to-day variations) of*Waldeckia obesa *fed with*
squid (circles) or fish (squares) during different experiments. Numbers above bars
indicate numbers of specimens used for each experiment.

is obviously not constant, and a kind of cycle (rhythm?) is observed with periods of intense activity and periods of quasi fasting, maybe corresponding to the digestion time. A high feeding rate is always noticed at the beginning of experiment, after the starvation phase. In the same way, rather important differences can be seen when comparing the rates estimated for distinct experiments (example of *W. obesa* in Figure 13), as results may vary by a factor of 4 to 5.

3.2.5. Amphipod as food source for higher trophic levels

An exhaustive survey of the Antarctic literature allowed to record 192 different known predators on pelagic and benthic amphipods in the Southern Ocean. A summary of these records is given in Table III.

Table III: Overview of the amphipod predators in the Southern Ocean (bibliographic data). "Groups" refers to the number of different predator families (fishes and birds) or orders (invertebrates and mammals), species to the predator species number, and citations to the total number of recorded pairs [amphipod-predator].

	"groups"	species	citations
Invertebrates	12	33	69
Fishes	19	101	798
Birds	11	48	529
Mammals	2	10	39

The exploitation of this dataset is, however, rather difficult. In the early Antarctic literature, most of the data about amphipods in predators' digestive tracts were in the presence/absence form. From the mid 20th century, some quantitative information became available, mainly as "frequency of occurrence". But it is only since the 1980's that were published valid data in the form of preyed amphipod mass and/or volume percentages in predator diets. Moreover, even in recent papers, most authors have not tried to determine amphipod species, making the information less useful.

Notwithstanding, a tentative inventory of predators for which amphipods represent a significant share in the bulk of their diet was established; some of these are listed in Table IV. For most of the other recorded predators, amphipods constitute a smaller dietary fraction (in the order of few percents). As shown in Table IV, hyperiid species (mainly *Themisto gaudichaudii*) are largely consumed by predators feeding in the water column (myctophid fish, petrels, penguins and

group		species	habitat	%	amphipods
Annelida	Polychaeta	*Harmothoe spinosa*	B	→ 99	GAM
Crustacea	Amphipoda	*Bovallia gigantea*	B	→ 99	GAM
Pisces	Artetidraconidae	*Artetidraco orianae*	B	→ 80	GAM
		Pogonophryne permitini	B	→ 73	GAM
	Channichthyidae	*Champsocephalus gunnari*	P	→ 86	HYP
	Harpagiferidae	*Harpagifer bispinis*	B	→ 98	GAM
	Myctophidae	*Electrona carlsbergi*	P	→ 27	HYP
	Nototheniidae	*Gobionotothen gibberifrons*	B	→ 38	GAM
		Lepidonotothen larseni	B-P	→ 40	GAM-HYP
		Notothenia coriiceps	B	→ 88	GAM
	Rajidae	*Bathyraja maccaini*	B	→ 58	GAM
Aves	Oceanitidae	*Oceanites oceanicus*	P	→ 45	HYP
	Procellariidae	*Pachyptila belcheri*	P	→ 70	HYP
		Pachyptila turtur	P	→ 60	HYP
	Sphenicidae	*Eudyptes chrysolophus*	P	→ 37	HYP
		Pygoscelis adeliae	P (B)	→ 58	HYP-GAM
Mammalia	Cetacea	*Balaenoptera borealis*	P	→ 45	HYP

Table IV*: Mass percentages of amphipods in the diet of some Antarctic predators (from various sources).*
B: benthic species; P: pelagic species; GAM: gammarids; HYP: hyperiids.

whales), while gammarids abound in the diet of benthic predators (invertebrates and notothenioid fish).

3.2.6. Size diversity and polar gigantism

To determine the significance of big Antarctic species, size spectra have been established in various sites, from polar to tropical latitudes, and from freshwater to marine sites. At all 15 sites, these size spectra are right skewed; however, skewness increases as temperature decreases (Figure 14). Thus, mode, mean and maximum size all increase with decreasing temperature whereas minimum size does not change.

Gigantism itself is addressed by the TS95/5: when plotted against mean water temperature for marine sites, this parameter increases curvilinearly as temperature decreases (Figure 15 A).

However, non marine sites do not fit this pattern. Lake Baikal (salinity: 0‰), and less conspicuously, the Caspian (13‰) and Black Sea (17‰), lie above the relationship for marine sites, and the discrepancy increases as salinity decreases. The Lake Baikal TS95/5 is x1.8 the marine value for the same temperature. On the other hand, the high altitude Lake Titicaca value lies under the relationship.

Re-plotting the TS95/5 values against water dissolved oxygen content removes the discrepancy between marine and other environments (Figure 15 B). The produced relationship covers all sites, is linear and accounts for >97% of the variance in the data:

$$TS95/5= -43.4 + 0.244\ AE2\quad (N = 13;\ r2=0.97) \qquad (4)$$

Thus the factor controlling TS95/5 is oxygen availability. When data (not shown) for TS90/10, TS80/20, TS50/50 and TS20/80 are regressed against mean environmental oxygen the fit of the relationships improves as TS value increases, indicating that oxygen becomes more important and other ecological factors reduce in effect as size increases. Furthermore the relationship between TS95/5 and temperature for marine sites in Figure 15 A is curvilinear, reflecting the non-linear relationship between seawater oxygen content and temperature (Chapelle and Peck, 1999; Peck and Chapelle, 1999; Chapelle, 2001).
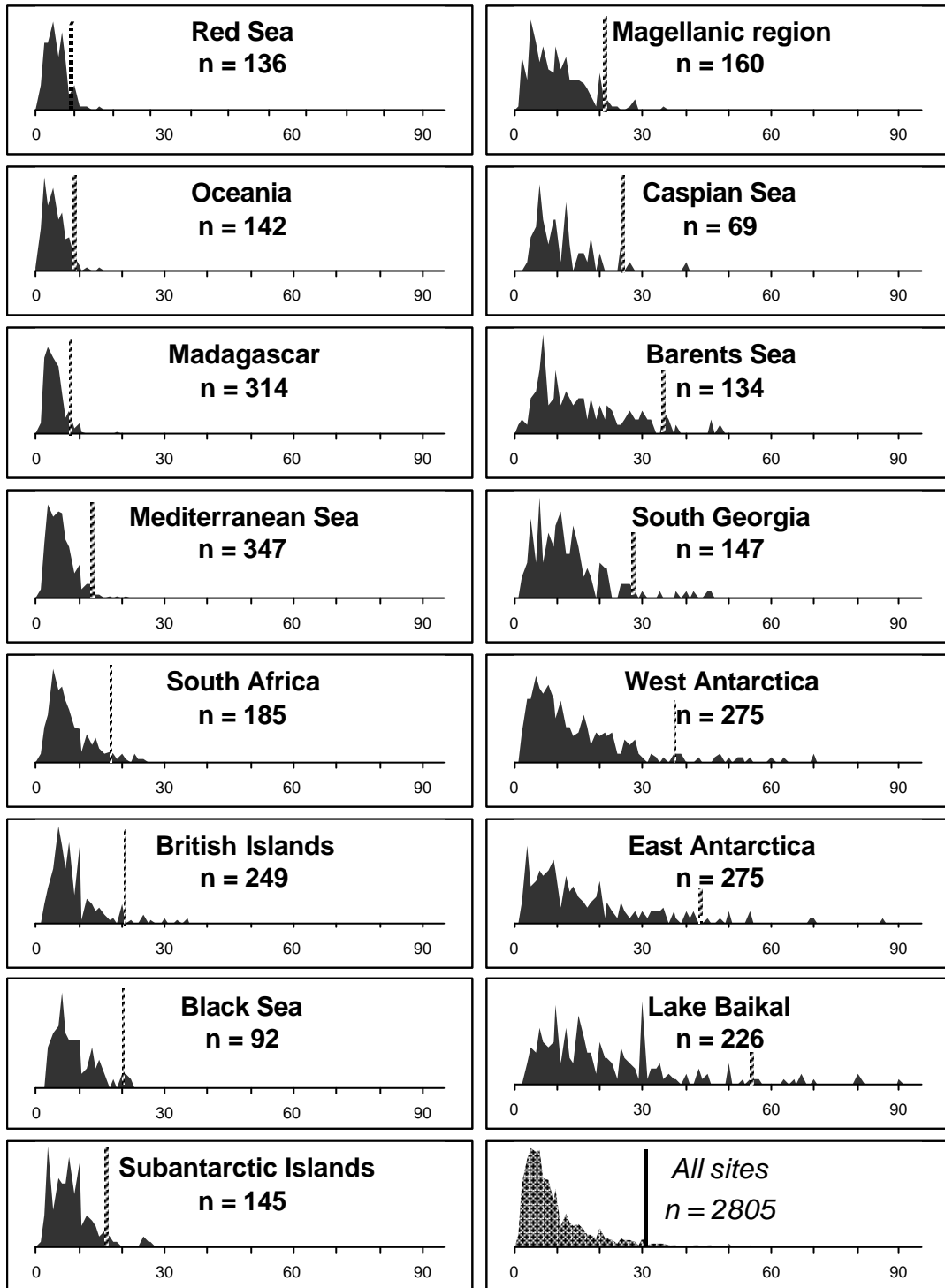
Figure 14: *Amphipod crustacean size spectra for the 15 selected sites (12 marine and 3 brackish or freshwater). The order follows the absolute oxygen concentration gradient. The last graph pools all the other ones. For each spectrum, n= number of species and the bar indicates the TS95/5 value.*
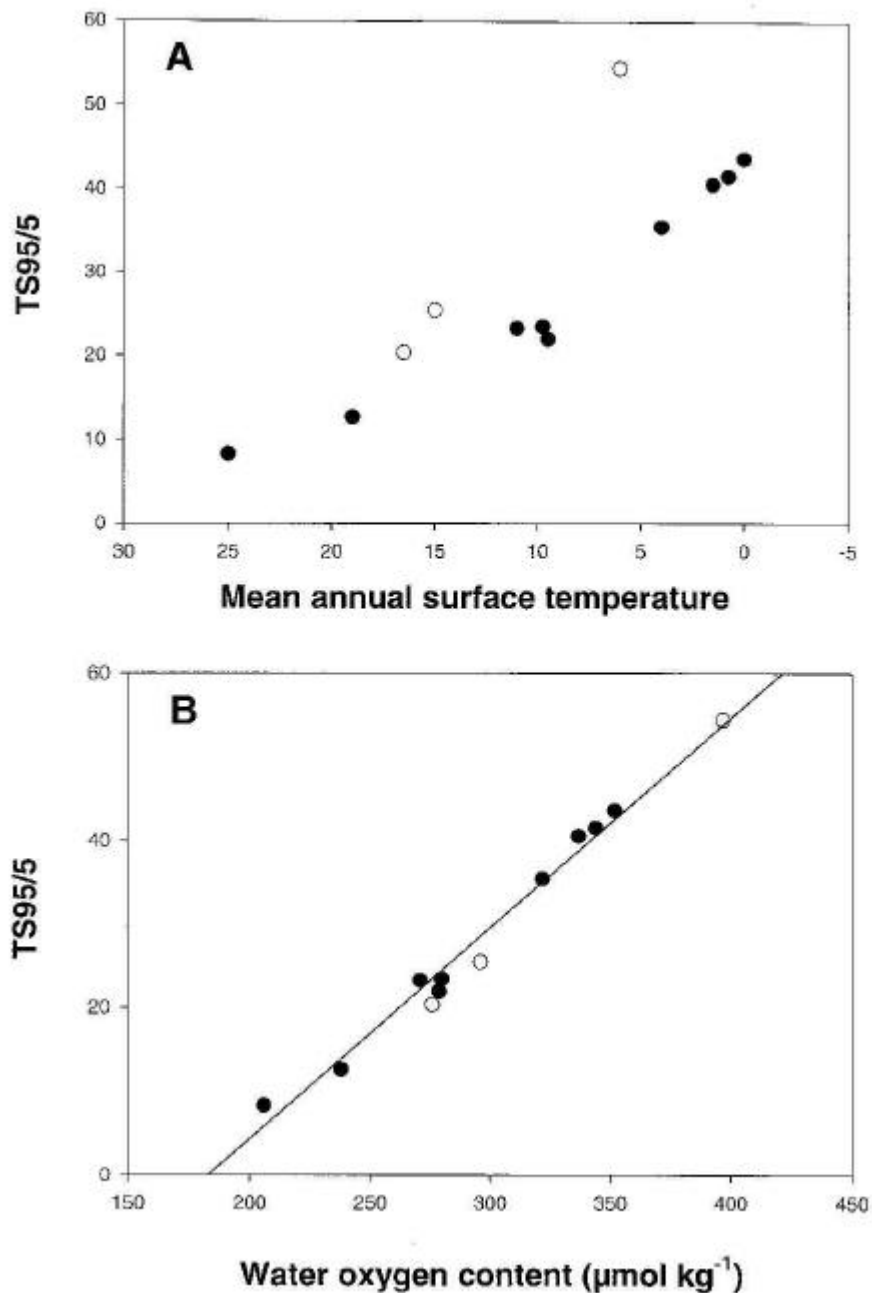
Figure 15: *Effects of (A) temperature and (B) oxygen availability on the biggest amphipod crustacean sizes for 9 marine (filled circles) and 3 reduced salinity sites (open circles). (A) 95%/5% threshold size (TS95/5) vs mean annual water temperature (inverted scale). (B) TS95/5 vs calculated dissolved oxygen content at saturation (µmol kg*$^{-1}$*), based on the surface water mean temperatures and salinity. Although not every habitat in the considered sites will experience permanent high oxygen saturation, this 100% value represents the optimal conditions for species to attain large size.*

TS95/5 in the equation *(4)* reaches zero when mean environmental oxygen is 183 µmol.kg^{-1}. This could indicate an environmental limit for amphipods. A variety of hot and/or highly saline conditions could produce 183 µmol.kg^{-1} of oxygen. No amphipods are found in such hot brine areas which are inhabited by organisms including brine shrimp and ostracods.

Surprisingly, minimum size does not vary significantly, either with temperature (Pearson correlation coefficient (PCC)=-0.019, P=0.952), or environmental oxygen (PCC=0.402, P=0.195). Clearly oxygen availability is not an overall selective pressure towards increased size for all species, but sets upper limits to maximum attainable size for the largest species (MPS).

Our data also show this increase of maximum size with oxygen to exist at the superfamily, family and genus level. Furthermore, comparing the size of the species present in more than one ecosystem revealed a similar trend within species (569 pairs analyzed).

If modal size corresponds to optimal size for a given body design, then optimal amphipod size increases with oxygen availability. However, minimum size is independent of environmental oxygen, temperature or salinity within the range of the investigated sites. Thus MPS increases dramatically with oxygen, modal size increases less and minimum size not at all, and the overall effect widens the size spectrum.

Having established that MPS in amphipods is tightly linked to environmental oxygen we now examine underlying mechanisms potentially underpinning this limitation: 1) the metabolic rate relationship with temperature. 2) haemolymph oxygen carrying capacity and 3) external oxygen availability,

1. Ectothermal basal metabolic rate rises with temperature, increasing tissue maintenance costs (Clarke, 1991; Ivleva, 1980). Although body size tends to decrease with increased temperature at marine sites, the largest amphipods were not found in our coldest sites (high Antarctic, 0°C), but in Lake Baikal (+6°C). Temperature-dependent trade-offs between tissue synthesis and catabolism apparently do not limit MPS, as the observed increase in MPS at freshwater sites despite the enhanced osmoregulatory costs would require an unlikely increase in resource acquisition.

2. Oxygen enters amphipod blood through a low-efficiency gill (Wolvekamp and Waterman, 1960), and is transported both by passive diffusion and bound to haemocyanin. Marine amphipod haemolymph contains 10-20 mg.cm3 haemocyanin (Spicer, 1993), which is low for crustaceans. Data from the Antarctic

giant isopod *Glyptonotus antarcticus* (Whiteley et al., 1997), also showing a relatively low haemocyanin level, suggest that Antarctic amphipods carry about 60-70% of their circulating oxygen in solution, whereas tropical species carry about 30-40% and Lake Baikal amphipods carry about 60-70% (as they have haemolymph osmotic concentrations around 340-360 mOsm, although being freshwater species). This reduces the haemolymph dissolved oxygen content of Baikal amphipods at 6°C to similar levels to marine species at 0°C. Thus Lake Baikal and Antarctic species should be similar sizes, instead of which TS95/5 is 54.4 mm for Baikal amphipods and 43.6 mm for Antarctic. This suggests saturation levels of haemolymph dissolved oxygen must increase from tropical to polar, and marine to freshwater environments, and the critical factor dictating MPS is gill efficiency.

3. According to Fick's law a key parameter determining oxygen uptake across a gill is the partial pressure difference between the external medium and the circulating haemolymph. For similar external partial pressure and gill efficiency, more oxygen will enter the blood at sites with low temperature and salinity, and thus higher absolute oxygen concentrations. Thus the saturation levels and absolute concentrations of oxygen in the blood will be higher at low temperature and salinity sites and amphipod MPS will reflect this in the way observed.

The above arguments indicate MPS is limited by oxygen concentration in the external water, mediated by a less than 100% efficient gill. Thus large size will occur at high concentrations, because a greater mass of oxygen will pass across the gills, increasing the possible path length for oxygen in the circulatory system.

The strong relationships we obtained were between external oxygen concentration and length, not body mass. However amphipods, like other groups showing large size at low temperatures and especially in Antarctica (e.g. pycnogonids and nemerteans) have a restricted circulatory system with few lateral branches. In other groups a stronger relationship with body mass would be expected. Whether MPS is reached will depend on several factors. In any environment with many species selection pressures will drive them into as many niches as possible and both large and small size will be exploited.

Oxygen supply has been suggested as the reason for Carboniferous insect gigantism, because during this period atmospheric oxygen was 30-35% (Graham et al., 1995). Their demise when oxygen content fell could indicate that large species are susceptible to such change and the giant amphipods described here would disappear first following elevated temperatures or other global oxygen reducing events. Being close to the critical limit for MPS in a given oxygen environment may

be a specialisation making giant species more prone to extinction over geological time.

If the increasing skewness shown by the spectra on Figure 14 reflects the adult size distribution, it is not very relevant to evaluate the amphipod trophic impact as a whole for a given time and surface. A size histogram with all cohorts would reveal for all ecosystems, including Antarctica, an even bigger predominance of the small specimens (for example smaller than 20 mm), as the juveniles and immatures for big species would also be part of that fraction. On the other side, it is precisely the higher part of this histogram (thus bigger than 20 mm), which would distinguish the Antarctic amphipod taxocoenosis from the other marine ones, as the size range of their prey is expected to match this large size. Although no accurate data exist, the density of at least some of the biggest Antarctic species seems to be important (e.g. *Ampelisca richardsoni, Eusirus perdentatus, Abyssorchomene plebs* or *Tryphosella murrayi,* see Klages 1993, Vo 1988). This might explain the small number of benthic shrimp species in general, and the very low density of the smaller species in particular : from the 5 Weddell Sea species, *Chorismus antarcticus, Nematocarcinus longirostris* and *Notocrangon antarcticus* are abundant, but with an adult size of about 100 mm not overlapping amphipod size range while a potential competition with the commonest giant amphipods might explain the scarcity of *Lebbeus antarcticus* and *Eualus kinzeri*, both with a size comprised between 100 and 25 mm (Sieg & Wagele, 1990; Gorny, 1999).

3.3. DEVELOPMENT OF A BIODIVERSITY REFERENCE CENTRE FOR THE SOUTHERN OCEAN AMPHIPOD CRUSTACEA

The development of some new tools for the assessment and the identification of the whole Southern Ocean amphipod biodiversity has been undertaken.

A « Biodiversity Reference Centre » for Antarctic Amphipoda (ANT'PHIPODA) was set up at IRScNB. (Figure 16). It comprises on one hand a comprehensive database on taxonomy, geographic and bathymetric distribution, ecology (habitats, trophic type,…) and biology (size, reproduction,…) of the 850 Southern Ocean species. In addition, it assembles a specialised documentation referenced in a searchable bibliographic database and a large iconographic file for species identification purposes (De Broyer et al., 1999b, 2000).
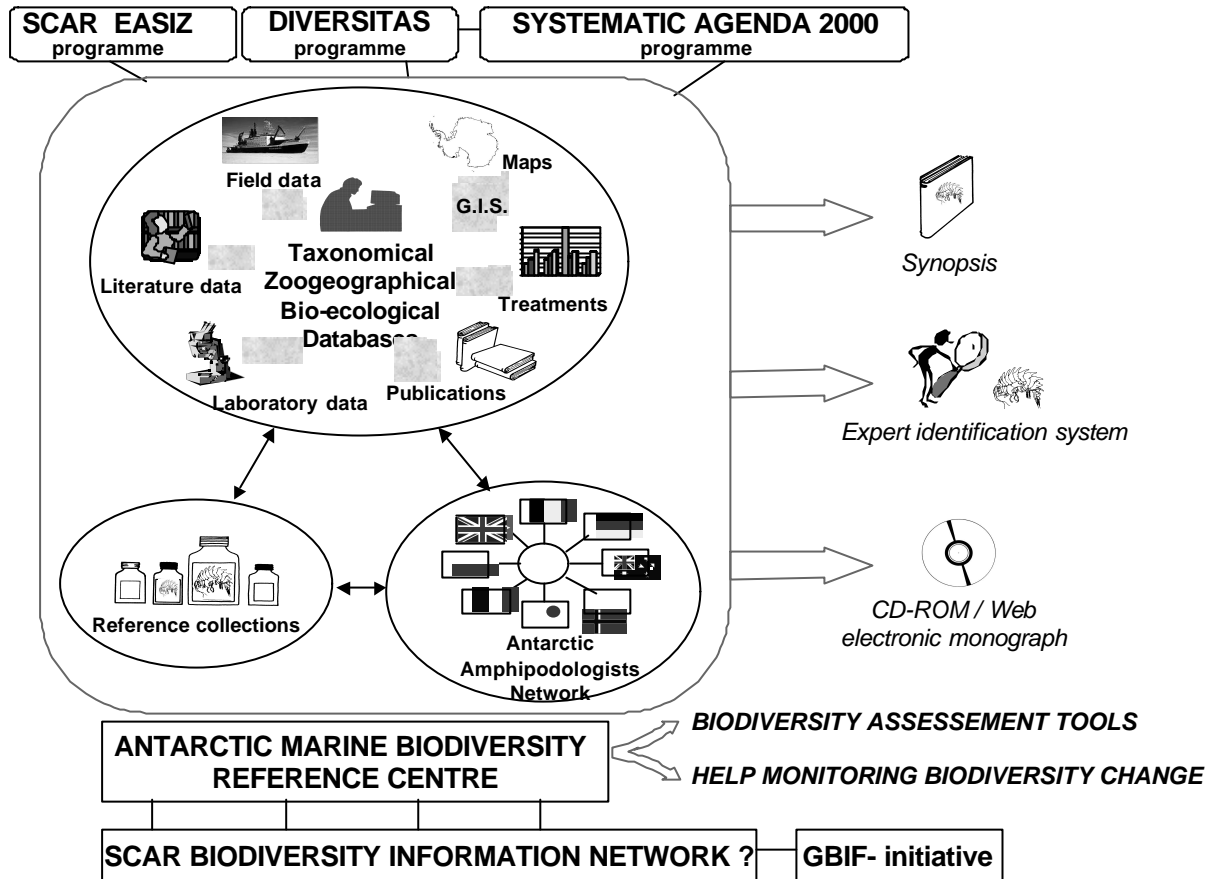
Figure 16: *Scheme of the stucture of the "Biodiversity Reference Centre" for Antarctic Amphipoda (ANT'PHIPODA).*

On the other hand, the reference centre also includes extensive reference collection (400 000 specimens) of the Southern Ocean amphipod fauna provided by the Belgian Antarctic Expeditions and the Belgian participation in other Antarctic campaigns in the Weddell Sea, Queen Maud Land, Antarctic Peninsula region, Kerguelen Islands, Tierra del Fuego, or contributed by the «Antarctic Amphipodologist Network » or the Antarctic programmes of Argentina, Brazil, Chile, France, Germany, The Netherlands, New Zealand, Poland, Russia, U.K. and U.S.

A network of 13 specialists from 9 countries (the «Antarctic Amphipodologist Network ») was established to undertake the coordinated revision of the Antarctic amphipod fauna (see *e.g.* Berge et al., 2000; Berge, 2001[a,b]) and the preparation of identification guides and an expert system for identification. The network includes : H.G. Andres (Hamburg); D. Bellan-Santini (Marseille); J. Berge (Tromsø); C.O. Coleman (Berlin); K. Conlan (Ottawa); C. De Broyer (Brussels, coordinator); M. Hendrycks (Ottawa), T. Krapp-Schickel (Bonn), K. Ja d ewski (ód); J.K. Lowry

(Sydney); M. Rauschert (Berlin); I. Takeuchi (Matsumaya) and M.H. Thurston (Southampton).

In paralell with the development of the reference centre « ANT'PHIPODA », a database (the « ABBED » database) on the benthos biodiversity of Admiralty Bay, King George Island, was set up in collaboration with the University of   ód , Poland. Focussing on some representative groups (Crustacea, Echinodermata and Polychaeta), the ABBED database will integrate the abundant data collected during 25 years of study on the taxonomy, distribution and ecology of the Admiralty Bay benthos by Polish, Brazilian, German, Dutch and Belgian teams. It would contribute to manage and disseminate the biodiversity information and to monitor the benthic biodiversity change in this reference site of the SCAR EASIZ programme.

Finally, a web site devoted to « ANT'PHIPODA » has been created, at the URL:
http://www.naturalsciences.be/amphi

4. CONCLUSIONS

This study attempted to contribute to a better knowledge of the biodiversity of a nearly pristine area of the world, the Southern Ocean, and to a better understanding of the role of biodiversity in the Antarctic Coastal and Shelf Ecosystem.

In the present study, several key aspects of the structural and ecofunctional biodiversity of the peracarid crustaceans were investigated : composition of the taxocoenoses, spatial and quantitative distribution, specialisation with respect to ecological niches, roles in ecosystem trophodynamics and size distribution.

They were approached by field studies at the level of two reference sites of the SCAR EASIZ programme (Eastern Weddell Sea and Admiralty Bay, King George Island) and by a general study of the whole Southern ocean amphipod fauna.

The project first allowed some substantial additions to the inventory of the Antarctic benthic amphipods and to the knowledge of their precise habitats. New extensive data on their geographic and bathymetric distribution were collected, as well as detailed information on their ecological characteristics. New abundance and biomass data, which were still sparse at the amphipod group level and extremely limited at the species level in both reference sites, were gathered. Much effort has been devoted so far to the study of the eastern Weddell Sea reference community where particularly intensive and innovative sampling over several seasons provided a wealth of material. This effort also enhanced the crucial need for an intensification of comparable collection sets obtained with reliable quantitative samplers such as box-corers, in order to get accurate estimations of benthos biomasses and distribution over the whole Antarctic.

Rarely performed so far in the Antarctic, systematic observations of living animals in cool labs allowed new insights on the ecology and biology of a number of individual species. In particular, the behavioural observations and the gut contents analyses conducted on several hundreds of specimens of the most common amphipod species from the eastern Weddell Sea shelf clearly showed that these crustaceans have developed a wide range of trophic types, from suspension-feeding to carnivory, and feed on a large variety of food, from plankton to carrion. The only

trophic type apparently lacking is macroherbivory, which can be explained by the absence of benthic macroalgae on shelf bottoms. Such a trophic diversity could probably be compared, and in some cases related to the diversity of benthic microhabitats. This large habitat diversity was demonstrated through the analysis of pictures got by still and video cameras, by observations in aquaria, and by sampling. Diverse symbiotic associations of amphipods with various invertebrates were also documented and appeared to be more common than expected.

Among the different feeding types noticed for the studied species, almost 50% deal with particulate organic matter (sinking or resuspended), the remainder being focussed on animal tissue consumption, either living (micro- and macropredatory) or dead (necrophagy). These trophic types, however, do not seem to be well defined for several species, some amphipods being likely able to shift from a diet to another (in a limited range of food size) with respect to environmental conditions and food availability. Taking into account the direct importance of particulate organic matter for detritivore and suspensivore amphipods, and its indirect importance as food source for the benthic invertebrates preyed by predator amphipods, it appears that the Weddell Sea benthic amphipod community is more closely dependent on primary production than previously thought. Many species are likely to suffer the seasonal variations of the latter, and could develop wintering strategies, such as diet change, reserve constitution or starvation. Necrophagy, for instance, could be a more exploited trophic way.

The role of the amphipod community in the global Antarctic food web, and in particular as prey for higher trophic levels, was approached through an extensive bibliographical survey. Amphipods are consumed by more than 190 different species of invertebrates, fishes, seabirds and marine mammals. They can represent almost 100% of the diet of some predators, either benthic or pelagic.

Another topic investigated in this project was the significance of the Antarctic amphipod size spectrum, gigantism and species richness. The arguments exposed in the results section indicate that Maximum Potential Size (MPS) is limited by oxygen concentration in the external water, mediated by a less than 100% efficient gill. Thus large size will occur at high concentrations, because a greater mass of oxygen will pass across the gills, increasing the possible path length for oxygen in the circulatory

system. Whether MPS is reached will depend on several factors. In any environment, selection pressures will drive species into as many niches as possible and both large and small size will be exploited. It is clearly the case in Antarctica, where the minimum size for amphipod species is the same as in the tropics. If the number of such small species is still relatively low, taxonomic description of new small species is now increasing quickly (notably in the highly diversified family Stenothoidae) and this would allow a more accurate assessment of the size spectra.

Regarding this trend to use as many niches as possible, it is worth mentioning that the Antarctic species larger than 20mm show a wide trophic type diversity; macro-herbivores, detritivores, suspension-feeders, scavengers, micro- and macro-predators are all represented by giant species (Dauby et al., 2001_a). The selective pressures having driven these species to their large size are complex and related to many factors such as life style, fecundity, foraging range, competition and predation pressure to name a few. As such, they remain to be identified through careful case studies.

To contribute to a more accurate assessment of the Antarctic marine biodiversity, the "Biodiversity Reference Centre for Antarctic Amphipoda" has been initiated at the Royal Belgian Institute of Natural Sciences in Brussels with comprehensive databases, specimen collections and specialised documentation. In relation with the reference centre, an international group of specialists, the "Antarctic Amphipodologist Network" has been established and has started to revise the whole Antarctic amphipod fauna and to prepare new conventional identification tools and a expert system for identification.

In connection with the reference centre, the "Admiralty Bay Benthos Biodiversity Database" was designed through Belgian-Polish co-operation to compile and manage the pertinent data on benthos biodiversity, benthic environment and benthos-related biological and physical data. It remains to be implemented to contribute to assess and monitor the benthos biodiversity in a long studied reference site of the EASIZ programme, in the context of the global environmental changes.

ACKNOWLEDGMENTS

REFERENCES

Andres, H.G. 1979. Gammaridea (Amphipoda, Crustacea) der Antarktis-Expedition 1975/76. Auswertung der Dauerstation südlich von Elephant Island. Meeresforsch. 27: 88-102.

Anonymous 1998. Analyse de l'information et conception de bases de données, Séminaires DB-MAIN et DB-MAIN/Objectif 1. FUNDP, Namur, 200 pp.

Arnaud, P.M., Jazdzewski, K., Presler, P. and Sicinski, J. 1986. Preliminary survey of benthic invertebrates collected by Polish Antarctic Expeditions in Admiralty Bay (King George Island, South Shetland Islands). Pol. Polar Res. 7: 7-24.

Arntz, W. and Gutt, J. 1997. The expedition ANTARKTIS XIII/3 (EASIZ I) of "Polarstern" to the Weddell Sea in 1996. Ber. Polarforsch. 249: 1-148.

Arntz, W. and Gutt, J. 1999. The Expedition ANTARKTIS XV/3 (EASIZ II) of "Polarstern" to the Eastern Weddell Sea and the Antarctic Peninsula 1998. Ber. Polarforsch. 301: 1-229.

Arntz, W., Ernst, W. and Hempel, I. 1990. The expedition ANTARKTIS VII/4 (EPOS Leg 3) and VII/5 of the R/V *Polarstern* in 1989. Ber. Polarforsch. 68: 1-214.

Arntz, W., Brey, T. and Gallardo, V.A. 1994. Antarctic zoobenthos. Oceanogr. Mar. Biol. Annu. Rev. 32: 241-304.

Arntz, W., Gutt, J. and Klages, M. 1997. Antarctic marine biodiversity: an overview. In: B. Battaglia, J. Valentia & D.W.H. Walton (eds.), Antarctic Communities: Species, Structure and Survival. Cambridge University Press: 3-14.

ASC, 1992. An information model for Biological Collections [The ASC Model]. Report of the Biological Collections. Data Standards Workshop, August 18-24, 1992. Association of Systematic Collections, Committee on Computerization and Networking. gopher://kaw.keil.ukans.edu:70/11/standards/asc.

Atkinson, D.1996. On the solutions to a major life-history puzzle. Oikos 77: 359-365.

Atkinson, D., Sibly, R.M. 1997. Why are organisms usually bigger in colder environments ? Making sense of a life history puzzle. Trends Ecol. Evol. 12: 235-239.

Barbier, Y., 1998. Nouvelles méthodes de gestion des données biogéographiques avec application aux Hyménoptères Sphécides de France, de Belgique et des régions limitrophes (Hymenoptera, Sphecidae). Thèse Doctorat, Univ. Mons-Hainaut, Belg., 162 pp.

Barnard, J.L. 1962. South Atlantic abyssal amphipods collected by R.V. Vema. In: Vema Research Series I, Abyssal crustacea. Barnard, J.L., Menzies, R.J. and Bacescu, M.C. (Eds). Columbia Univ. Press, New York, 1-78.

Barnard, J.L. and Karaman, G.S. 1991. The families and genera of marine Gammaridean Amphipoda (except marine Gammaroids) – Part I and Part II. Rec. Aust. Mus. 13: 1-866.

Barthel, D. and Gutt, J. 1992. Sponge association in the eastern Weddell Sea. Antarct. Sci. 4: 137-150.

Bathmann, U., Fischer, G., Muller, P.J. and Gerdes, D. 1991. Short-term variations in particulate matter sedimentation off Kapp Norvergia, Weddell Sea, Antarctica: relation to water mass advection, ice cover, plankton biomass and feeding activity. Polar Biol. 11: 185-195.

Bazikalova, A.Y. 1945. Lake Baikal amphipods. Tr. Baykal'sk. Limnol. St. 11, 1-440.

Berendsohn, W. G., Anagnostopoulos, A., Hagedorn, G., Jakupovic, J., Nimis, P.L. and Valdés, B. 1996. The CDEFD Information Model for Biological Collections. Proc. Eur. Sci. Found. Workshop "Disseminating Biodiversity Information", Amsterdam.

Berge, J., 2001$_a$. Revision of the amphipod (Crustacea: Stegocephalidae) genera *Andaniotes* Stebbing, 1897 and *Metandania* Stephensen, 1925. J. nat. Hist., in press.

Berge, J., 2001$_b$. Revision of *Stegosoladidus* Barnard and Karaman, 1987 (Crustacea: Amphipoda: Stegocephalidae), redescription of two species and description of three species. J. nat. Hist., in press.

Berge J., De Broyer C. and Vader W., 2000. Revision of the Antarctic and sub-Antarctic species of the family Stegocephalidae (Crustacea : Amphipoda) with description of two new species. Bull. Inst. r. Sci. nat. Belg. 70: 217-233.

Birstein, J.A. and Romanova, N.N. 1968. In: Atlas bespozvonochnykh Kaspiiskogo moria (Atlas of invertebrates from Caspian sea) Pishchevaia Promyshlennost, Moscow, 241-290.

Blazewicz, M. and Jazdzewski, K., 1995. Cumacea (Crustacea, Malacostraca) of Admiralty Bay, King George Island: a preliminary note. Pol. Polar Res. 16: 71-86.

Blazewicz, M. and Jazdzewski, K., 1996. A contribution to the knowledge of Tanaidacea (Crustacea, Malacostraca) of Admiralty Bay, King George Island, Antarctic. Pol. Polar Res. 17: 213-220.

Boysen-Ennen, E. and Piatkowski, U. 1988. Meso- and macrozooplankton communities in the Weddell Sea, Antarctica. Polar Biol. 9: 17-35.

Brey, T., Dahm, C., Gorny, M., Klages, M., Stiller, M. and Arntz, W. 1996. Do Antarctic benthic invertebrates show an extended level of eurybathy. Antarct. Sci. 8: 3-6.

Bryazgin, V. 1997. Diversity, distribution and ecology of benthic amphipods (Amphipoda, Gammaridea) in the Barents Sea sublittoral. Pol. Polar Res. 18: 89-106.

Chapelle, G. and Peck, L. 1999. Polar gigantism dictated by oxygen availability. Nature 399: 114-115.

Chapelle G. 2001. Antarctic and Baikal amphipods : a key for understanding polar gigantism. Thèse Doctorat, Univ. cathol. Louvain, Belg.

Cherel, Y. and Kooyman, G.L. 1998. Food of emperor penguins (*Aptenodytes forsteri*) in the western Ross Sea, Antarctica. Mar. Biol. 130: 335-344.

Clarke, A. 1991. What is cold adaptation and how should we measure it? Amer. Zool. 3: 81-92.

Coleman, C.O. 1989a. On the nutrition of two Antarctic Acanthonotozomatidae (Crustacea: Amphipoda). Gut contents and functional morphology of mouthparts. Polar Biol. 9: 287-294.

Coleman, C.O. 1989b. Burrowing, grooming and feeding behaviour of *Paraceradocus,* an Antarctic amphipod genus (Crustacea). Polar Biol. 10: 43-48.

Coleman, C.O. 1989c. *Gnathiphimedia mandibularis* K.H. Barnard 1930, an Antarctic amphipod (Acanthonotozomatidae, Crustacea) feeding on Bryozoa. Antarct. Sci. 1: 343-344.

Coleman, C.O. 1990a. Two new Antarctic species of the genus *Epimeria* (Crustacea: Amphipoda: Paramphithoidae), with description of juveniles. J. r. Soc. N.-Z. 20: 151-178.

Coleman, C.O. 1990b. *Bathypanoploea schellenbergi* Holman & Watling, 1983, an Antarctic amphipod (Crustacea) feeding on Holothurioidea. Ophelia 31: 197-205.

Colwell, R.K. 1996. Biota, the Biodiversity Database Manager. Sinauer associates, Inc., Publishers, Sunderland, Massachusetts, 374 pp.

Copp, C. J. T. 1998. The Recorder Project. Systems Analysis. Environmental Information Management. In HTML or RTF @ http://www.nbn.org.uk/projects/recorder/.

Dallwitz, M.J., Paine, T.A. and Zurcher, E.J. 1993. Delta System: a general system for processing taxonomic descriptions. CSIRO.

Dauby P., Scailteur Y. and De Broyer C., 2001$_a$. Trophic type diversity within the eastern Weddell Sea amphipod community. Hydrobiologia 443: 69-86.

Dauby P., Scailteur Y., Chapelle G. and De Broyer C. 2001$_b$. Potential impact of the main benthic amphipod on the eastern Weddell Sea shelf ecosystem (Antarctica). Polar Biol. 24: in press.

Dearborn, J.H., 1965. Food of Weddell seals at McMurdo Sound, Antarctica. J. Mammal. 46: 37-43.

Dearborn, J.H., 1977. Foods and feedings characteristics of Antarctic asteroids and ophiuroids. In: Llano G.A. (Ed.): Adaptations within Antarctic Ecosystems. Proc. 3rd SCAR Symp. Antarct. Biol. Smitsonian Institution, Washington, 293-326.

De Broyer, C. 1977. Analysis of the gigantism and dwarfness of Antarctic and Subantarctic Gammaridean Amphipoda. In: Llano G.A. (Ed.): Adaptations within Antarctic Ecosystems. Proc. 3rd SCAR Symp. Antarct. Biol. Smitsonian Institution, Washington, 327-334.

De Broyer, C. and Jazdzewski, K. 1993. Contribution to the marine biodiversity inventory. A checklist of the Amphipoda (Crustacea) of the Southern Ocean. Doc. Trav. Inst. r. Sci. nat. Belg. 73: 1-155.

De Broyer, C. and Jazdzewski, K. 1996. Biodiversity of the Southern Ocean: towards a new synthesis for the amphipoda (crustacea). Boll. Mus. civ. St. nat. Verona 20: 547-568.

De Broyer, C. and Klages, M. 1990. The role of the gammaridean amphipods in the eastern Weddell Sea benthic communities. Belg. J. Zool. 120: 20-21.

De Broyer C. and Rauschert M. 1999. Faunal diversity of the benthic amphipods (Crustacea) of the Magellan region as compared to the Antarctic (Preliminary results). Sci. Mar. 63 (suppl.1): 281-293.

De Broyer, C. and Thurston, M.H. 1987. New Atlantic material and redescription of the type specimens of the giant abyssal amphipod *Alicella gigantea* Chevreux (Crustacea). Zool. Scr. 16: 335-350.

De Broyer C., Rauschert M. and Chapelle G. 1997. Trophodynamics, Biodiversity and Gigantism of the Amphipod Crustacea Taxocoenoses. In : Arntz W.and

Gutt J., The Expedition ANTARKTIS XIII/3 (EASIZ I) of « Polarstern » to the Eastern Weddell Sea in 1996. Ber. Polarforsch. 249: 76-79.

De Broyer, C., Rauschert, M. and Scailteur, Y. 1999$_a$. Structural and ecofunctional biodiversity of the benthic amphipod taxocoenoses. In : Arntz W.and Gutt J., The Expedition ANTARKTIS XV/3 (EASIZ II) of « Polarstern » to the Eastern Weddell Sea and the Antarctic Peninsula 1998. Ber. Polarforsch. 301: 163-174.

De Broyer C., Van Roozendael F., Jazdzewski K., Chapelle G., Munn D.R. and Scailteur Y. 1999$_b$. An "Antarctic Marine Biodiversity Reference Centre" devoted to amphipod crustaceans. In : Repelewska-Pekalowa J. (Ed.). Polish Polar Studies, XXVI Polar Symposium, Lublin, Poland, 341.

De Broyer, C., Duchesne, P.A., Vander Linden, Ch., Van Roozendael, F., Jazdzewski, K., Sicinski, J., Jamar, C., Chapelle, G., Dauby, P., Kuyken, T., Nyssen, F. and Robert, H., 2000. ANT'PHIPODA, the Biodiversity Reference Centre devoted to Antarctic amphipods (Crustacea): a tool for developing and managing Antarctic marine biodiversity information. Pol. Arch. Hydrobiol. 47: 657-669.

De Broyer, C., Scailteur, Y., Chapelle, G. and Rauschert, M. 2001. Diversity of epibenthic habitats of gammaridean amphipods in the eastern Weddell Sea. Polar Biol. in press.

Ekau, W. and Gutt, J. 1991. Notothenoid fishes from the Weddell Sea and their habitat, observed by underwater photography and television. Proc. NIPR Symp. Pol. Biol., Tokyo, 4: 36-49.

Enequist, P., 1949. Studies of the soft-bottom amphipods of the Skagerak. Zool. Bidr. Uppsala 28: 297-492.

Fahrbach, E., Rohardt, G. and Krause, G. 1992. The Antarctic Coastal Current in the southeastern Weddell Sea. Polar Biol. 12: 171-182.

Fortuner, R. 1993. Advances in computer methods for systematic biology : artificial intelligence, databases, computer vision. Johns Hopkins Press, London, 560 pp.

Galéron, J., Herman, R.L., Arnaud, P.M., Arntz, W.E., Hain, S. and Klages, M. 1992. Macrofaunal communities on the continental shelf and slope or the southeastern Weddell Sea, Antarctica. Polar Biol. 12: 283-290.

Gerdes, D., Klages, M., Artnz, W.E., Herman, R.L., Galéron, J. and Hain, S. 1992. Quantitative investigations on macrobenthos communities of the souteastern Weddell Sea shelf based on multibox corer samples. Polar Biol. 12: 291-301.

Gili, J.M., Arntz, W.E., Filipe, P., Lopez, P., Orejas, C., Ros, J. and Teixido, N. 1999. The role of benthic suspension feeders in Antarctic communities. In: Arntz, W.E. and Gutt, J. (Eds). The expedition ANT XV/3 (EASIZ II) of RV "Polastern" in 1998? Ber. Polarforsh. 301: 30-83.

Gon, O. and Heemstra, P.C. (Eds). 1990. Fishes of the Southern Ocean. J.L.B. Smith Inst. Ichthyol., Graham, 462 pp.

Gorny, M. 1999. On the biogeography and ecology of the Southern Ocean decapod fauna. Sci. Mar. 63 (suppl.1): 367-382.

Graeve, M., Dauby, P. and Scailteur, Y. 2001. Combined lipid, fatty acid and digestive tract content analyses: a penetrating approach to estimate feeding modes of Antarctic amphipods. Polar Biol. in press.

Graham, J.B., Dudley, R., Aguller, M. and Gans, C. 1995. Implications of the late Palaeozoic oxygen pulse for physiology and evolution. Nature, 375: 117-120.

Green, K. and Burton, H.R., 1987. Seasonal and Geographical Variayion in the Food of Weddell Seals, Leptonychotes weddelii, in Antarctica. Austr. Wildl. Res. 14: 475-489.

Günther, S., George, K.H. and Gleitz, M. 1999. High sympagic metazoan abundance in platelet layers at Drescher Inlet, Weddell Sea, Antarctica. Polar Biol. 22: 82-89.

Gutt, J. 1991. On the distribution and ecology of holothurians in the Weddell Sea (Antarctica). Polar Biol. 11: 145-155.

Gutt, J. and Koltun, 1995. Sponges of the Lazarev and Weddell Sea, Antarctica: explanations for their patchy occurrence. Antarct. Sci. 7: 227-234.

Gutt, J. and Schickan, T. 1998. Epibiotic relationships in the Antarctic benthos. Antarct. Sci. 10: 398-405.

Gutt, J. and Starmans, A. 1998. Structure and biodiversity of megabenthos in the Weddell and Lazarev Seas (Antarctica): ecological role of physical parameters and biological interactions. Polar Biol. 20: 229-247.

Gutt, J., Gorny, M. and Arntz, W.E. 1991. Spatial distribution of Antarctic shrimps (Crustacea: Decapoda) by underwater photography. Antarct. Sci. 3: 363-369.

Gutt J., Sirenko B.I., Arntz W.E., Smirnov I.S. and De Broyer C. (with contributions of 27 taxonomists from Russia, Spain, Belgium, U.K. and Germany), 2000. Biodiversity of the Weddell Sea : list of macrobenthic species (forams and fish included) sampled during the expedition ANT XIII/3 (EASIZ I) with RV « Polarstern ». Ber. Polarforsch. 372: 1-103.

Hynes, H.B.N. 1950. The food of freshwater sticklebacks (*Gasterosteus aculeatus* and *Pygosteus pungitius*), with a review of the methods used in studies of the food of fishes. J. Anim. Ecol. 19: 36-58.

Ingram, C. and Hessler, R.H. 1983. Distribution and behaviour of scavenging amphipods from the central North Pacific. Deep-Sea Res. 30: 683-706.

Ivleva, I.V. 1980. The dependence of crustacean respiration on body mass and temperature. Int. Rev. Ges. Hydrobiol. 65: 1-47.

Jarre-Teichmann, A., Brey, T., Bathmann, U.V., Dahm, C., Dieckmann, G.S., Gorny, M., Klages, M., Pagés, F., Plötz, J., Schnack-Schiel, S.B., Stiller, M. and Arntz, W.E. 1997. Trophic flows in the benthic community of the eastern Weddell Sea, Antarctica. In: Antarctic communities: species, structure and survival. Battaglia B., Valencia J. and Walton D.W.H. (Eds.).Cambridge University Press, 118-134.

Jazdzewski, K. 1981. Amphipod crustaceans in the diet of pygoscelid penguins of the King George island, South Shetland Islands, Antarctica. Pol. Polar Res. 2: 133-144.

Jazdzewski, K. and Sicinski, J. 1993. 12. Zoobenthos. In: The Maritime Antarctic Coastal Ecosystem of Admiralty Bay. Rakusa-Suszczewski, S. (Ed.). Dept of Antarctic Biology, Polish Academy of Sciences, Warsaw. p.83-95.

Jazdzewski, K., De Broyer, C., Teodorczyk, W. and Konopacka, A. 1992. Survey and distributional patterns of the amphipod fauna of Admiralty Bay, King George Island, South Shetland Islands. Pol. Polar Res. 12: 461-472.

Jazdzewski K., De Broyer C., Pudlarz M. and Zielinski D. 2001 Seasonal fluctuations of vagile benthos abundance in the sublittoral fringe of a maritime Antarctic fjord. Polar Biol. in press.

Klages, M. 1991. Biologische und populationdynamische Untersuchungen an ausgewählten Gammariden (Crustacea: Amphipoda) des südöstlichen Weddellmeeres, Antarktis. Dissertation Univ. Bremen, Deutch., 240 pp.

Klages, M. 1993. Distribution, reproduction and population dynamics of the Antartic gammaridean amphipod *Eusirus perdentatus* Chevreux, 1912 (Crustacea). Antarct. Sci., 5: 349-359.

Klages, M. and Gutt, J. 1990[a]. Observations on the feeding behaviour of the Antarctic gammarid *Eusirus perdentatus* Chevreux, 1912 (Crustacea: Amphipoda) in aquaria. Polar Biol. 10: 359-364.

Klages, M. and Gutt, J. 1990[b]. Comparative studies on the feeding behaviour of high Antarctic amphipods (Crustacea) in laboratory. Polar Biol. 11: 73-79.

Kock, K.H. 1992. Antarctic fish and fisheries. Cambridge Univerity Press, 359 pp.

Kunzmann, K. 1992. Die mit ausgewahlten Schwammen (Hexactinellida und Demospongiae) aus dem Weddellmer, Antarktis vergesellschaftete Fauna. Diss. zur Erlang. Dokt., Univ. zu Kiel. 108pp.

Kunzmann, K. 1996. Die mit ausgewählten Schämmen (Hexactinellida und Demospongia) aus dem Weddellmeer, Antarktis, vergesellschaftete Fauna. Ber. Polarforsch. 210: 1-93.

Ledoyer, M. 1982. Faune de Madagascar. 59 (1). Crustacés amphipodes gammariens. Familles des Acanthonotozomatidae à Gammaridae. Ed. CNRS, Paris, 598 pp.

Lincoln, R.J. 1979. British marine amphipoda: Gammaridea. British Museum, Natural History, London.

McClintock, J.B. 1994. Trophic biology of antarctic shallow-water echinoderms. Mar. Ecol. Prog. Ser. 111: 191-202.

Mordukhai-Boltovskoi, F.D., Greze, I.I. and Vassilenko, S.V. 1969. Determination guide of the fauna from Black and Azov seas, Tome 2, free-living invertebrate crustaceans [in Russian], 440-494.

Munn, D.R., De Broyer, C., Sicinski, J. and Dauby, P. 1999. Seasonal variation of distribution and new records of benthic amphipods (Crustacea) from Admiralty Bay, King George Island, West Antarctic. In : Repelewska-Pekalowa J. (Ed.). Polish Polar Studies, XXVI Polar Symposium, Lublin, Poland, 371-378.

Nyssen, F., Brey, T., Lepoint, G., Bouquegneau, J. M., De Broyer, C., and Dauby P. 2000. Use of stable isotopes to delineate amphipod trophic status in Antarctic food webs. Pol. Arch. Hydrobiol., 47: 579-584.

Olaso, I. 1999. The pelagic fish food web. In Arntz, W.E. and Gutt, J. (Eds) The expedition ANTA XV/3 (EASIZ II) of RV "Polarstern" in 1998. Ber. Polarforsch. 301: 110-118.

Olaso, I., Rauschert, M. and De Broyer, C. 2000. Impact of the family Artetidraconidae (Pisces) on the eastern Weddell Sea benthic communities. Mar. Ecol. Prog. Ser. 194: 143-158.

Olivieri, S., Harrison, J., Busby, J.R. 1995. Data and information management and communication. In : Heywood, V.H. (Ed.), Global Biodiversity Assessment. Cambridge University Press, 607-670.

Oliver, J.S. and Slattery, P.N. 1985. Effects of crustacean predators on species composition and population structure of soft-bodied infauna from McMurdo Sound, Antarctica. Ophelia 24: 155-175.

Pankhurst, R.J. 1991. Practical taxonomic computing. Cambridge University Press, 202 pp.

Peck, L. and Chapelle, G. 1999. Reply to "Spicer J.L. and Gaston K.J. - Amphipod gigantism dictated by oxygen availability?". Ecol. Lett. 2: 401-403.

Rakusa-Suszczewski, S. (Ed.) 1993. The Maritime Antarctic Coastal Ecosystem of Admiralty Bay. Department of Antarctic Biology, Polish Academy of Sciences, Warsaw, 216pp.

Rauschert, M. 1991. Ergebnisse des faunistischen Arbeiten im Benthal von King George Island (Sudshetlandinselm, Antarktis). Ber. Polarforsch. 76: 1-75.

Richardson, M.G. 1977. The ecology (including physiological aspects) of selected Antarctic marine invertebrates associated with inshore macrophytes. PhD Thesis, University of Durham (U.K.), 163 pp.

Ruffo, S. 1982, 1989, 1993, 1998. The Amphipoda of the Mediterranean. Mem. Inst. Oceanogr. Monaco. 13: 1-959.

SA2000, 1994. Systematics Agenda 2000: Charting the Biosphere, Technical Report. Produced by Systematics Agenda 2000, 34 pp.

SCAR, 1994. Coastal and Shelf Ecology of the Antarctic Sea-Ice Zone (CS-EASIZ), a SCAR programme of marine research for the coastal and shelf ecosystem of Antarctic. SCAR Rep. 10: 1-20.

Schalk, P.H. and Los, W. 1993. The application of interactive multimedia software in taxonomy and biological diversity studies.

Sieg, J. and Wägele, J.W. 1990. Fauna der Antarktis. Paul Parey, Berlin, 197 pp.

Slattery, P.N. and Oliver, J.S. 1986. Scavenging and other feeding habits of lysianassid amphipods (*Orchomene* spp.) from McMurdo Sound, Antarctica. Polar Biol. 6: 171-177.

Spicer, J.I. 1993. Oxygen binding by amphipods (Crustacea) haemocyanins. Mar. Behav. Physiol. 24: 123-136.

Stepnik, R. 1982. All-year population studies of Euphausiacea (Crustacea) in the Admiralty Bay (King George Islands, South Shetland, Antarctic). Pol. Polar Res. 3: 49-68.

UNEP, 1995. Global biodiversity assessment. Cambridge University Press, 1140 pp.

Voß, J. 1984. Verbreitung und Okophysiologie des Makrozoobenthos in der sudlichen und sudostlichen Weddell See. Ber. Polarforsch. 19: 106-115.

Voß, J. 1988. Zoogeographie und Gemeinscheftsanalyse des Makrozoobenthos des Weddellmeeres (Antarktis). Ber. Polarforsch. 45: 135-144.

White, M.G. 1984. Marine benthos. In : R.M. Laws (Ed.), Antarctic Ecology. Academic Press, London: 421-461.

Whiteley, N.M., Taylor, E.W., Clarke, A., El Haj A.J. 1997. Haemolymph oxygen transport and acid-base status in *Glyptonotus antarcticus* Eights. Polar Biol. 18: 10-15.

Williams, M.J. 1981. Methods for analysis of natural diet in portunid crabs (Crustacea: Decapoda: Portunidae). J. exp. mar. Biol. Ecol. 52: 103-113.

Wolvekamp, H.P., Waterman, T.H. 1960. Physiology of Crustacea, Respiration. In: The Physiology of Crustacea. Waterman T.H. (ed), Academic Press, New York, vol. 1, 35-100.

AN INTEGRATED APPROACH TO ASSESS CARBON DYNAMICS IN THE SOUTHERN OCEAN

BELCANTO

F. Dehairs[1], C. Lancelot[2], L. André[3], M. Frankignoulle[4], E. Deleersnijder[5]

S. Becquevort[2], D. Cardinal[3], T. Cattaldo[1], B. Delille[4], M. Elskens[1], N. Fagel[3-6], H. Goosse[5], E. Hannon[2], J. Navez[1-3], G. Probst[5], V. Schoemann[2] with the collaboration of E. Kopczynska[7] and A. Kostianoy[8]

1- Vrije Universiteit Brussel, Analytische Chemie (Brussels, Belgium)
2- Université Libre de Bruxelles, Ecologie des Systèmes Aquatiques (Brussels, Belgium)
3- Royal Museum for Central Africa, Department of Geology (Tervuren, Belgium)
4- Université de Liège, Unité d'Océanographie Chimique (Liège, Belgium)
5- Université Catholique de Louvain, Unité d'Astronomie et de Géophysique (Louvain, Belgium)
6- University of Liège, Silicoclastic Sedimentology and Clay Geology (Liège, Belgium)
7- Polish Academy of Sciences, Department of Antarctic Ecology (Warszawa, Poland)
8- Institute of Oceanology P.P. Shirshov, Ocean Experimental Physics Laboratory (Moscow, Russia)

TABLE OF CONTENTS

ABSTRACT

During this study we investigated on the physical, chemical and biological factors and processes that control primary production and export production in different functional environments of the Southern Ocean. A major output of the study is a 1D mechanistic biogeochemical model that reproduces quite accurately the features of Southern Ocean phytoplankton blooms and predicts magnitude and fate of exported carbon. The overwhelming influence of light, mixing and iron availability on plankton productivity is confirmed. Export production was experimentally assessed using different approaches, based on water column and sedimentary proxies, and an overall convergence of results was observed. The importance of organic matter mineralization in the ocean's interior was evaluated from direct measurements of bacterial activity and accumulation of the mesopelagic Ba_{xs}-barite proxy. Finally, the impact of the biological pump on air to sea flux of CO_2 was assessed for different regions of the Southern Ocean.

1. INTRODUCTION

The Global Ocean plays an important role as a buffer to global warming by absorbing some 40% of the CO_2 released annually (Battle et al., 2000). Specifically the Southern Ocean, because of its unique hydrodynamical and ecological features, appears as a potential major CO_2 sink. This is not just because of its large size (18% of the World Ocean), but mainly as a result of physical and biological processes including cooling and sinking of surface waters, biological uptake and export of organic carbon from the surface layer.

Dissolved CO_2 in surface waters is taken up by photosynthesising algae which require nutrients (phosphate, ammonium/nitrate, and dissolved silica) and trace elements such as iron for their growth. Because of a sustained supply of essential nutrients (N, P, Si) through deep-water upwelling, the Southern Ocean has great potential to further enhance CO_2 uptake via the biological pump. However, in the HNLC (High Nutrient Low Chlorophyll) waters of the modern Southern Ocean this does not necessarily occur because of iron limitation (e.g. de Baar et al., 1995; de Baar and Boyd 1999), since this ocean benefits put poorly from inputs by continental erosion (Kumar et al., 1995). There seems to be little doubt today that iron plays a pivotal role in ecosystem structure and food-web export. Iron-enrichment experiments conducted in the HNLC waters of the Southern Ocean, both shipboard (e.g. de Baar et al. 1990, Martin et al. 1990, Buma et al. 1991) and *in situ* (Boyd et al., 2000) resulted in the stimulation of the large class of algae, in particular chain-forming diatoms (de Baar and Boyd 1999), more prone to sustain carbon export.

Thus, depending on the phytoplankton community and the associated food-web structure, the organic carbon produced is either retained in the surface layer through fast microbial respiration or exported to the deep-ocean as phytoplankton cells, plankton debris or faecal pellets. In the latter case more carbon is retained by the ocean and less returns to the atmosphere. This flux of carbon to the deep ocean is called the biological carbon pump. Its efficiency relies on the one hand on light and nutrient controls of phytoplankton and ecosystem structures and on the other hand on the mineralisation rate of exported carbon when sinking from the surface layer towards the sediment. Mineralisation of sinking organic carbon, in combination with deep ocean circulation, ultimately determines the extent of carbon storage by the ocean. At most of the deep ocean stations where sediment traps were deployed, only few percent of the originally exported carbon arrived in the ocean's interior (below 1000 m) with the major fraction remineralised by bacterial activity during settling (e.g. Berger et al., 1988).

The importance of organic carbon mineralisation in the mesopelagic layer (100-1000 m) is still poorly known and its prediction requires the full understanding of the mechanisms regulating bacterial degradation of the sinking material as well as the strategy by which bacteria compete for organic matter in these HNLC waters. Quantification of organic carbon mineralisation in the mesopelagic layer can be estimated by comparing the particulate organic carbon (POC) fluxes recorded by deep sediment traps with the primary production and the export flux of carbon at the base of the surface layer, as reconstructed from specific algorithms (e.g. Bishop, 1988). Overall, this approach suffers from a lack of reliability due to the fast and large degradation of the exported organic matter. However, more refractory proxies of organic carbon, such as bio-Ba, barite have been identified (because of their refractory nature) (e.g. Dymond et al., 1992; François et al., 1995). Nevertheless, all approaches based on proxies are potentially affected by biological processes and are also particularly sensitive to spatial and seasonal patterns of POC/proxy ratios (e.g. Dymond and Collier, 1996; Rutgers van der Loeff, 1997; Dehairs et al., 2000a).

In the present study we aimed at elucidating the main factors and processes controlling primary production in different functional environments of the Southern Ocean and at evaluating the impact of this process on atmosphere - ocean exchange of CO_2. To further evaluate the efficiency of this biological carbon pump, we also focused our attention on the export of organic carbon to the ocean's interior and on its mineralisation. Finally, a coupled physical biogeochemical model was elaborated to reproduce the inter-linkage between the whole of the physical, chemical and biological processes that are in control of the carbon fluxes.
The applied research methodology involved and combined: (i) Direct estimates of CO_2 air-sea exchange and identification of sink-source regions in the Southern Ocean; (ii) Studies of the physico-chemical and biological mechanisms controlling the dominance of key components of the phytoplankton community; (iii) Estimates of the export of organic carbon from the surface mixed layer and the microbial degradation in the subsurface and the deeper water column and (iii) Numerical development of a 1D mechanistic biogeochemical model.

During the duration of the project several Antarctic expeditions have been conducted in collaboration with scientists from other countries. It has, however, not been possible to address all research objectives during single cruises, merely because of limited access, in terms of personnel, on board research vessels of the host countries. As a result, the different fieldwork tasks of the project had to be split up between different expeditions:

- CO_2 surveys were done during two major expeditions (SAZ'98: summer 1998, *R/V Aurora Australis*; ANTARES-4: summer 1999, *R/V Marion Dufresne*) plus dedicated or logistical cruises (OISO3 cruise and *R/V Marion Dufresne* and R*/S Astrolabe* logistical cruises from 1998 to 2000). The eastern and western basins of the Indian Ocean were covered and Subtropical, Subantarctic, Polar Front and Antarctic Circumpolar Current regions investigated.

- The AESOPS expedition (summer 1998, *R/V Nathaniel B. Palmer*) covered the continental shelf area in the Ross Sea and was dedicated to the study of biogenic matter aggregation, sedimentation and bacterial degradation.

- Phytoplankton assemblages, new production and export production were investigated during the SAZ'98 and ANTARES 4 expeditions. SAZ'98 expedition crossed the Subantarctic and Polar Front Zones south of Tasmania, while ANTARES-4 was a meso-scale study in the vicinity of the Subtropical and Subantarctic zones north-west of the Kerguelen archipelago.

- Finally, the effect of iron and light on phytoplankton growth was studied in the Polar Front Zone and the Antarctic Circumpolar Current in the Atlantic sector during the ANTX-VI/3 expedition (summer 1999, *R/V Polarstern*).

2. METHODOLOGY

A. Site description and hydrographical features of expeditions conducted during this study

During this 4-year project it has not been possible to address all research objectives during single cruises, merely because of limited access, in terms of personnel, on board the research vessels of the host countries. As a result the different research tasks were tackled mostly during different expeditions, as outlined below.

A.1. The coastal and the continental shelf system: The Ross Sea Continental Shelf during AESOPS 1997 expedition

We participated in the fourth U.S. JGOFS Antarctic Environment and Southern Ocean Process Study (AESOPS) Cruise of the *R/V Nathaniel B. Pa*lmer to the Ross Sea continental shelf (5 November to 16 December 1997). Four successive transects were realised along the AESOPS Ross Sea line at 76°30'S from 175°W to 168°E in the Ross Sea polynya in 1997, aboard the R.V. *Nathaniel B. Palmer* (**Figure 1**). The transects were: Transect 1, stations 402 to 406 (17 – 21 November); Transect 2, stations 412 to 423 (21 – 27 November); Transect 3, stations 425 to 429 (27 November – 01 December); and transect 4, stations 430 to 437 (6 – 12 December). The results of US-JGOFS AESOPS cruises are publishing in two special issue of Deep-Sea Research (2000, 2001). The Ross Sea is a high-latitude, nutrient-rich continental shelf system that exhibits one of the most predictable and spatially extensive phytoplankton blooms in the Southern Ocean (Sullivan et *al.*, 1993, Arrigo and McClain, 1994). The stratification of the water column resulting from freshwater lenses generated from receding ice edge is initiated early in October within the polynya, generating an environment that is favourable for phytoplankton growth (Smith *et al*., 2000). In fact the region in the central polynya became ice-free due to the advective influence of winds, whereas to the east and west, ice disappeared largely due to in situ melting (Smith *et al*., 2000). Nutrient concentrations reflected phytoplankton uptake, and reached their seasonal minimal in early February. Chlorophyll concentrations were maximal in early January, whereas productivity was maximal in late November (Smith *et al*,. submitted). The Ross Sea appears to have two dominant phytoplankton assemblages (the first being dominated by diatoms and the second by the colonial haptophyte *Phaeocystis antarctica*) that are often spatially distinct (Arrigo *et al*,. 1999).
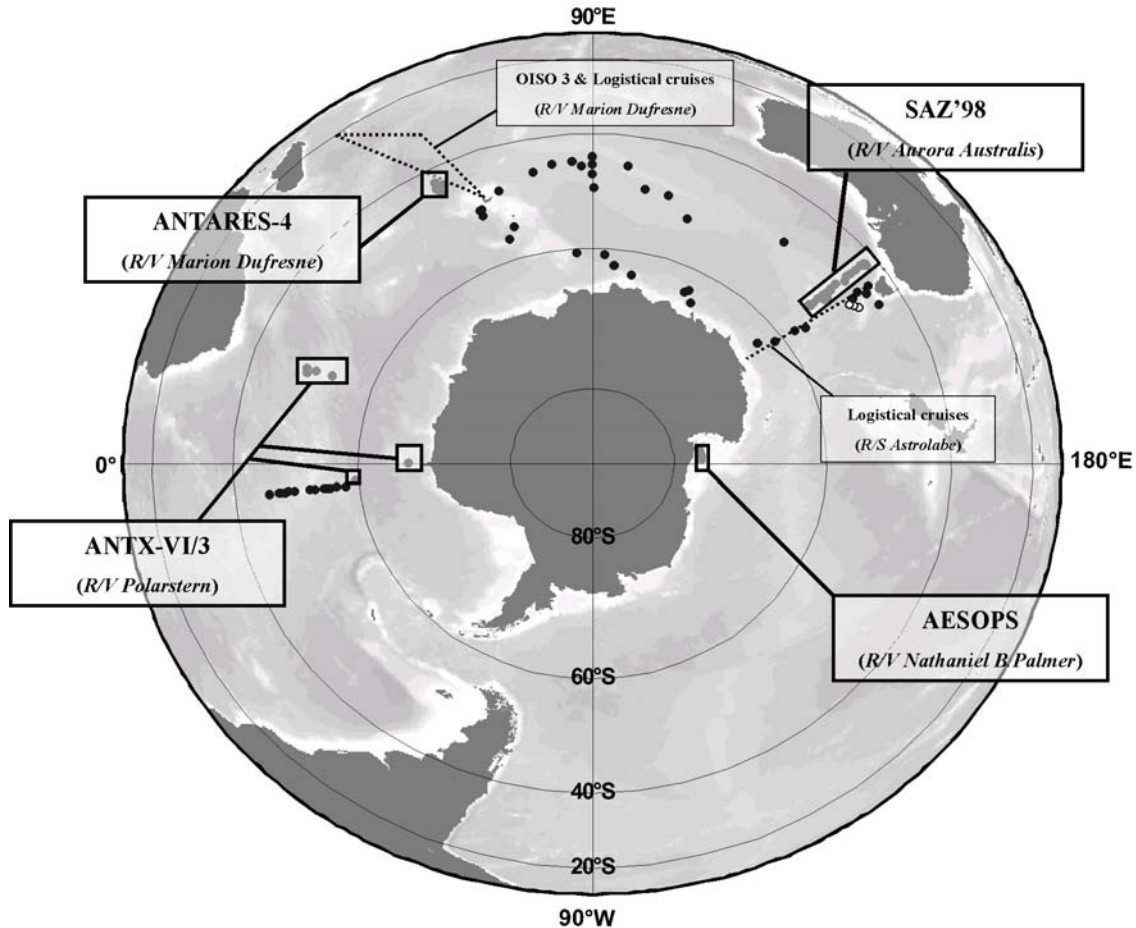
Figure 1: General map of expeditions conducted during this project. Sampling areas for AESOPS (1997), SAZ'98 (1998), ANT-XVI/3 and ANTARES-4 (1999) are represented by rectangles. pCO$_2$ surveys performed during OISO 3 and logistical cruises are represented by shaded lines. Black dots symbolize the core tops and sediment traps from other expeditions (ANT-X/6, 1992; APSARA, 1984, 1988 and 1994; KH94-4, 1994 and 147GCO, 1995) used in this study.

A.2. The Subantarctic and Polar Front zones and the Antarctic Circumpolar Current area

Three expeditions were conducted in Southern Atlantic and Indian Oceans (**Figure 1**): SAZ '98 south of Tasmania, ANT XVI/3 between Africa and Antarctica and ANTARES-4 in the Kerguelen – Crozet area. The main feature of the Southern Ocean is its conspicuous frontal banding consisting of several circumpolar quasi-uniform belts divided by fronts, comparatively narrow zones of sharp changes in vertical structure, temperature, salinity and nutrients. It has become an accepted terminology to call Subantarctic Zone the region bordered by the Subtropical Front (STF) on the north, and the Polar Front (PF) on the south. The observations indicate

that at the surface the transition from the Subantarctic Zone (SAZ) to the Antarctic Zone occurs in two distinct steps rather than one, the so-called Subantarctic Front (SAF) and the Polar Front proper. Frontal structures may present striking regional differences particularly in the Indian Ocean (Belkin and Gordon, 1996). A more detailed description of the Southern Ocean circumpolar circulation and fronts is given in Whitworth (1988), Orsi *et al*. (1995) and Belkin and Gordon (1996).

The SAZ '98 expedition

The SAZ'98 expedition took place from February 28th to April 2nd 1998 on board *R/V Aurora Australis* in the Australian sector of the Southern Ocean. The cruise provided an opportunity to investigate the whole SAZ along the WOCE SR3 transect between Subtropical waters and the Polar Front (42°-55°S, 141.5°-143°E; **Figure 1**). The STF is usually considered as the poleward boundary of subtropical water. According to Rintoul *et al*. (1997), who studied the main frontal systems for the same study area, the position of the STF coincides with the 11°C isotherm at 150 m, which is at 42°S in our case (**Figure 2**). Due to its high spatio-temporal variability, the SAF is less well defined. Definitions vary considerably between authors and geographical locations.
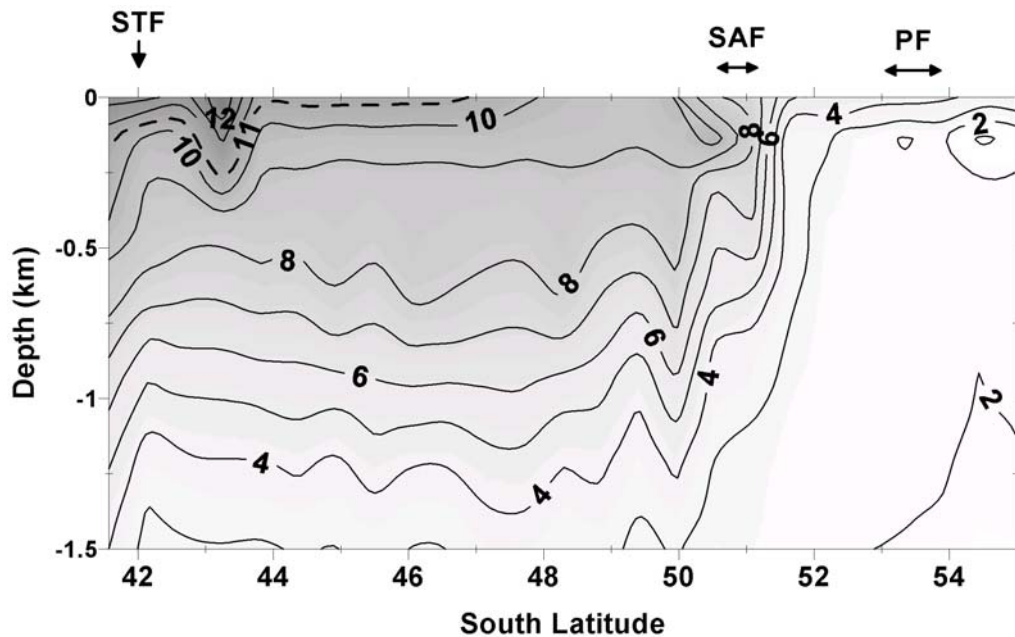

Figure 2: Potential temperature (°C) distribution for upper 1500m on the SAZ'98 meridional section along 142°E. STF, SAF and PF represent respectively Subtropical, Subantarctic and Polar Fronts.

Park *et al*. (1993) state that temperature and salinity gradients of 4°-8 °C and 34.1-34.5 ‰ at 200 m are the subsurface expressions of the SAF. Accordingly, during SAZ'98 the SAF was located between 50.5°S and 51.3°S. The Polar Front (PF) can be identified on the basis of the northernmost extent of remnant Antarctic Winter Water expressed by a subsurface temperature minimum of 2°C as a result of spring

and summer heating. As previously seen by Rintoul *et al*. (1997) for the same area, the PF is located between 53° and 54°S (**Figure 2**). Surface water temperatures range from about 12°C at 43°S to 3°C in the PF. The strong horizontal temperature gradient between 50.5° and 52°S clearly indicates the position of the SAF.

Moreover, five sediment traps were deployed from September 1997 to March 1998 at three latitudes along 140°E: at 47°S (1000, 2000, 3800m) within the Sub Antarctic Zone, at 51°S, the Sub Antarctic Front, (3300m) and at 54°S in the Polar Front Zone (800 and 1500m). Full sample details (collection, processing, chemical treatment) are given in Bray *et al*. (2000) and Trull *et al*. (2001).

The ANT-XVI/3 cruise

The ANT-XVI/3 cruise took place in the Atlantic sector of the Southern Ocean (**Figure 1**) on board *R/V Polarstern* between 18th March and 10th May 1999.

Stations were sampled in the Polar front (Stn 161 and 167), the Antarctic Circumpolar Current (Stn 190 and 198) and in the Antarctic coastal current close to the edge of the Antarctic continent (Stn 182 and 185) between 49°S 20°E and 70°S 6°W (Bathmann *et al.*, 2000).

The ANTARES-4 expedition

The ANTARES-4 cruise on board *R/V Marion Dufresne* (January 4th– Feburary 23th 1999) consisted in a study at mesoscale of the confluence of the Agulhas, Subtropical and Subantarctic Fronts (AF, STF and SAF respectively) in the Crozet Basin (**Figure 1**).

The Crozet Plateau area is characterized by the confluence of several fronts (**Figure 3**). The SAF is deflected northwards at 62°5 E and converges within the STF (Gamberoni *et al.*, 1982; Park *et al.*, 1991). East of 62°E, the Agulhas Front (AF) reaches the STF/SAF to form a triple frontal system AF/STF/SAF (Belkin and Gordon, 1996); referred as the "Crozet Front", one of the strongest in the world ocean. We observed this feature during ANTARES-4 cruise. At the surface, temperature and salinity gradients give the position of the fronts. Around 45.4°S - 62.7°E, the STF and SAF merged into only one structure. This structure extended northwards and was deflected eastward while approaching the AF (44.5°S - 64°E). The AF was encountered at 41°S - 62°E. Furthermore pCO_2 survey of the area of SAZ'98 and ANTARES-4 cruises have been completed in spring by measurements made through OISO 3 cruise (Indian Ocean Observatory Service - INSU) and logistical cruises onboard the *R/V Marion Dufresne* (Nov 98 and Dec 98) and the *S/V. Astrolabe* (Oct and Dec 99) (**Figure 1**).
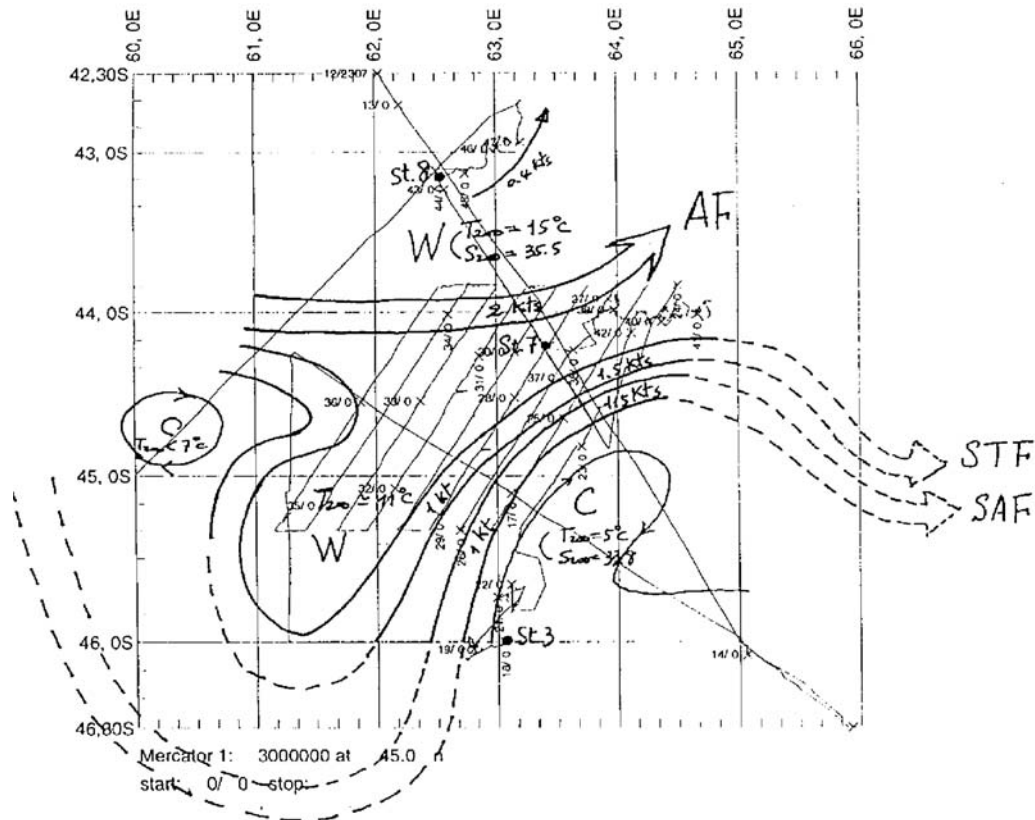
Figure 3: Schematic circulation in the frontal zone studied during ANTARES-4. AF: front associated to the Agulhas Return Current. STF: Subtropical Front. SAF: Subantarctic Front. C and W are for cold and warm surface waters, $\Theta<7°C$ and $\Theta>15°C$ respectively. Figure taken from ANTARES-4 cruise report.

Finally, the role of coastal area with regard to the budget of air-sea exchange of CO_2 of the subantarctic ocean have been investigated in the Kerguelen archipelago in 1996, 1997 et 1999 through monitoring of diel and seasonal changes of pCO_2 and related parameters in various sites of the archipelago (**Figure 1**).

B. Materials and methods

B.1. pCO_2, pH and Talk measurements

During ANTARES-4, SAZ'98, OISO 3 and other logistical cruises, underway parameters (pCO2, salinity, temperature) were measured with a sampling frequency of 1 mn, using a fully computerised acquisition system, connected to the non-toxic seawater supplies of the ships. , Underway partial pressure of CO_2 was measured directly using an equilibrator coupled to an infra-red analyser (Li-Cor[7] 6262). The

13

equilibrator consists in a vertical plexiglas tube (height: 80 cm, diameter: 10 cm) which is filled up with marbles in order to increase the surface exchange and reduce the air volume (Frankignoulle *et al.*, 2001). Seawater reaches the equilibrator (3 l.min^{-1}) by the top of the tube and a closed air circuit (3 l.min^{-1}) ensures circulation through the equilibrator (from the bottom to the top) and the analyser. The barometric pressure inside the equilibrator is kept equal to the atmospheric one using a 30m fine plastic tube open to the atmosphere outside the ship. Both the barometric pressure and temperature are monitored in the air circuit. The Li-Cor[7] analyser was calibrated routinely versus CO_2 in air standards with nominal mixing ratios of 0 and 345 $\forall$ 1 μatm supplied by *Air Liquide Belgium*. Once a day, atmospheric pCO_2 was measured with The Li-Cor[7] from an air circuit which input were situated at the bow of the ship. Dissolved Inorganic Carbon during the ANTARES-4 cruise and punctual pCO_2 for the Kerguelen monitoring in 1999, were calculated from measurements of pH and Total Alkalinity (TAlk). TAlk was measured using the classical Gran electrotitration method (Gran, 1952) on 100ml GFC filtered samples. The reproducibility of measurements was 4μeq.kg^{-1}. pH was measured using commercial combination electrodes (Ross type, Orion[7]). The electrode was calibrated using Tris buffer, as proposed by Dickson (1993), on the total proton scale (pH(SWS)). The reproducibility of pH measurement was 0.2 mV, which corresponds to an error of 0.004 pH units. CO_2 speciation was calculated using the CO2SYS Package (Lewis and Wallace 1998) and according to the pH(SWS) scale (total proton, Mole.kg^{-1}) using the CO_2 acidity constants of Roy et al. (1993), the CO_2 solubility coefficient of Weiss (1974) and the borate acidity constant of Hanson (1973). The total borate molality was calculated using the Culkin (1989) ratio to salinity. The errors in pCO_2 and DIC were 14 µatm and 9 µmole.kg^{-1} respectively. During the monitoring of the Kerguelen archipelago in 1996 and 1997, DIC and pCO_2 were measured with a similar method with the exception of the pH calibration; the electrode was calibrated according to the NBS scale. Thereafter, speciation have been calculated using the CO_2 acidity constants of Mehrbach *et al.* (1973) refit by Dickson and Millero (1987).

Bacterial abundance (during Kerguelen monitoring)

Bacterial abundance was determined by acridine orange direct counts (AODC) (Hobbie *et al.*, 1977). A minimum of 300 fluorescing cells with a clear outline and definite cell shape was counted as bacterial cells in 10 random microscope fields.

Chlorophyll (during Kerguelen monitoring)

Phytoplankton was studied using chlorophyll a concentration. All samples were prefiltered through a 200 µm mesh to remove detritic material and larger biota, then filtered by gentle vacuum filtration of 1l of seawater through a Whatman® GF/F glass-fiber filter. The measurements of chlorophyll a were carried out using the

spectrofluorometric method developed by Neveux and Panouse (1987). Fluorescence was measured on a Perkin-Elmer® MPF 66 spectrofluorometer.

Nutrients (during Kerguelen monitoring)

Water samples were filtered through a Whatman® GF/F glass-fiber. The filtrates were subsequently frozen at -20°C until laboratory analysis. Nitrate + nitrite concentrations were assayed using a Skalar® AutoAnalyser and the method of Tréguer and Le Corre (1975). The accuracy of the analyses was assured by calibration with standard salts in low-nutrient sea water. The analytical accuracies were ± 0.1µmol.l^{-1} for nitrate.

B.2. Radiotracer (^{14}C-bicarbonate, ^{55}Fe) uptake experiments

Three kinds of incubations with radiotracers were performed in order to relate Fe uptake with the phytoplankton photosynthesis, growth and respiration in function of the ambient Fe concentration for the different encountered autumnal phytoplankton communities. All the material used for sampling and during the incubation experiments was treated according to the recommended ultraclean methods to avoid trace metal contamination (Nolting and de Jong, 1995).

Sampling

Water samples were collected in the Atlantic Sector of the Southern Ocean between 49°S and 70°S. Sampling was carried out using pre-cleaned Go-Flo bottled either mounted on the Teflon coated rosette frame or attached to a kevlar wire. The Go-Flo bottles were closed by means of Teflon messengers. They were emptied and the samples further treated in a pressurised class 100 clean cooled container (NIOZ) or in class 100 laminar flow bench. Sub-samples were taken for running the radiotracer incubation experiments as well as for measuring the following associated parameters.

Chemical and biological parameters

Dissolved Fe concentrations were measured on samples filtered with 0.1-µm Nuclepore polycarbonate membrane filters by flow injection analysis (de Jong *et al.*, 1998). Nutrients were determined in 0.45 *µ*m membrane (Sartorius cellulose-acetate) filtered seawater according to the methods described in Grasshoff *et al.* (1983). Chlorophyll *a* retained on 0.8-µm Nuclepore membrane was measured by fluorometry after acetone extraction in the dark at 4°C. Phytoplankton abundance was determined by inverted microscopy in samples fixed with a 1% lugol-glutaraldehyde solution after a 12-h sedimentation in Utermöhl chambers (Hasle, 1978).

Radiotracer incubation experiments

Before starting the radiotracer incubation experiment, all samples were kept in the dark for at least 4 hours allowing the cells to reach their basal metabolism.

- Photosynthesis

In order to determine the photosynthetic parameters -the photosynthetic efficiency, α; the index of photoinhibition, β; the maximal specific rate of photosynthesis normalized to Chl*a*, P^B_{max}, the maximum realized photosynthesis rate, P_m, and the light adaptation parameter, E_k- P/E curves were determined from the measurement of ^{14}C-bicarbonate assimilation in a temperature controlled "photosynthetron" as described by MacIntyre *et al.* (1996). Seawater samples of 1ml were spiked with 5 µCi of $H^{14}CO_3$ and incubated at different light intensities (0-600 µmol quanta $m^{-2}.s^{-1}$) for 2-2.5 hours. After incubation, the excess inorganic ^{14}C was degassed for 24 h after addition of 6N HCl. Radioactivity was determined by liquid scintillation (scintillation cocktail Ecolume) with a Packard (Tri-carb 160 CA) analyzer. The photosynthetic parameters were estimated from the photosynthesis-irradiance curves fitted with the nonlinear fitting method of Marquardt-Levenberg using Platt's equation (Platt *et al.*, 1982).

- Carbon and iron (extra- and intracellular) uptake rates

Parallel long-term time-course incubations of ^{14}C and ^{55}Fe were conducted at 100 µmol quanta m^{-2} s^{-1} at *in situ* temperature and mimicking the *in situ* day length. These experiments were performed with natural phytoplankton assemblage and Fe-enriched (addition of 0.25, 0.5, 1.0 and 2.5 nM of $FeCl_3$ during 48 hours) natural samples. In order to determine the initial concentration of "available" dissolved Fe and to identify accidental contamination, concentrations were measured directly after having enriched with $FeCl_3$. At each incubation time, 250-450 ml was filtered using Whatman GF/F (^{14}C) or Nuclepore membranes (^{14}C, ^{55}Fe). ^{14}C-Whatman GF/F were acidified (HCl 0.1N) to eliminate excess inorganic carbon and then frozen at –18 ºC. The ^{14}C labeled cellular material collected on filters were sequentially solubilized as described in Lancelot and Mathot (1985) in order to distinguish between carbon assimilated into 4 pools of cellular constituents: small metabolites, lipids, polysaccharides and proteins. The ^{14}C radioactivity was determined by liquid scintillation with a Packard (Tri-Carb 160 CA) analyzer. Two ^{55}Fe-filtrations were processed at each incubation time to distinguish between total Fe uptake (adsorption + intracellular) and intracellular Fe uptake. The latter was isolated by applying, during the filtration, the leaching method of Hudson and Morel (1989) based on the use of Ti complexed with citrate and EDTA. The extracellular uptake rate was estimated by subtracting the intracellular uptake rate from the total uptake rate. The radioactivity on the filters was determined by liquid scintillation after the addition of scintillation
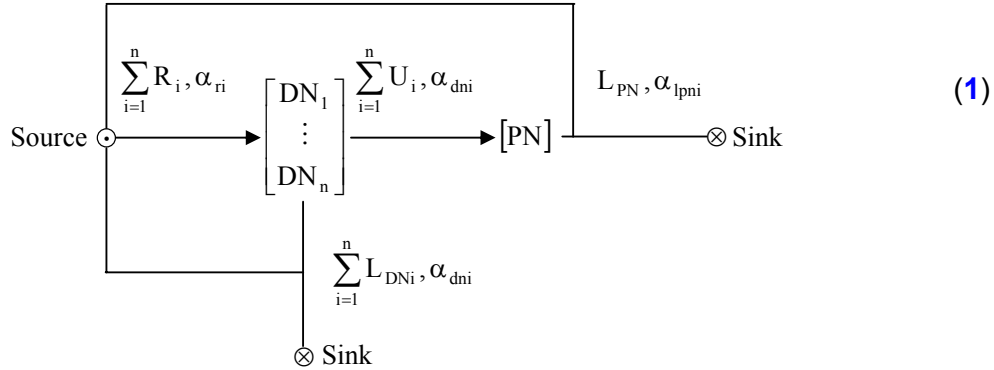
16

cocktail (Ready Safe). The relative uptake was calculated based on the activity of the particles collected on the filters divided by the total activity (filter + solution) at a given time. Molar uptake rates were then estimated from the initial dissolved concentrations of Fe.

B.3. Assessment of ^{15}N uptake

Ammonium and urea concentrations were determined aboard according to Koroleff (1969) and Goeyens *et al*. (1999), respectively. Samples for nitrate and dissolved organic nitrogen (DON) were taken in polystyrene bottles and frozen until analysis in the home laboratory. Suspended matter for particulate organic carbon (POC) and particulate nitrogen (PN) determinations was collected on precombusted (450°C) Whatmann GF/F filters, dried at 60°C and stored in polystyrene Petri dishes until analysis in the home lab. Experiments for the determination of nitrogen uptake rates (nitrate, ammonium and urea) were launched by addition of labelled (^{15}N and ^{13}C 99 %) into 2 liter polycarbonate incubation bottles. ^{15}N tracer additions resulted in increases of the concentration, which are similar to the analytical detection limit, i.e. approximately 0.1 and 0.05 µM for nitrate, ammonium and urea, respectively. ^{13}C tracer additions resulted in increases of the dissolved inorganic carbon concentration (DIC) by about 5% of the ambient level. All incubations were carried out during 12 hours under natural light conditions in an on-deck incubator, thermostated with running seawater. PN, collected on Whatmann GF/F filters after incubation, is converted to dinitrogen by a modified Dumas combustion technique and ^{15}N abundance is determined by emission spectrometry (Fiedler and Proksch, 1975) using JASCO NIA-1 and NIA-151 ^{15}N analysers. Sub-samples for ^{13}C abundance are analysed with a C-N analyser (Carlo-Erba NA 1500) coupled to the inlet system of a dual inlet Isotope Ratio Mass Spectrometer (Delta E Finnigan Mat).

N-uptake conditions were studied with the aim: (i) to analyse relative importance of new versus regenerated production by the so-called (*f*-ratio) in function of the coupling between uptake and regenerative processes, the plankton community structure and ammonium and dissolved iron concentrations and (ii) compare estimates of new production with estimates of export production based on the Ba-barite proxy. The data discussed here were gathered during SAZ'98 expedition in summer 1998 (north south transect from 42°S to 55°S and 141°30'E).

The transfer of ^{15}N tracer into different particulate (PN) and dissolved (DN$_i$ for i = 1…n) nitrogen pools during an incubation experiment with natural planktonic assemblages can be outlined as follows (**scheme 1**):

$$\text{Source} \odot \xrightarrow{\sum_{i=1}^{n} R_i, \alpha_{ri}} \begin{bmatrix} DN_1 \\ \vdots \\ DN_n \end{bmatrix} \xrightarrow{\sum_{i=1}^{n} U_i, \alpha_{dni}} [PN] \xrightarrow{L_{PN}, \alpha_{lpni}} \otimes \text{Sink}$$

$$\sum_{i=1}^{n} L_{DNi}, \alpha_{dni} \quad \otimes \text{Sink}$$

(1)

Where α_i is the isotopic enrichment (ratio of ^{15}N: $^{14+15}N$) associated with the corresponding nitrogen flux rates: R_i = regeneration, U_i = uptake, L_{DNi} = DN_i loss, and L_{PN} = PN loss. Loss rates from the dissolved and particulate nitrogen pools are source-sink processes with respect to the equation for N-mass conservation. The source term represents all processes giving rise to a regeneration of the dissolved nitrogen pools during the incubation, such as excretion and release of organic and inorganic nitrogen substrates by the planktonic community, bacterial transformations from one nitrogen source to another, e.g. ammonification, nitrification, denitrification... The sink term represents all processes responsible for missing nitrogen within the time span of incubation, such as adsorption of nitrogen to clay particles or to container walls, uptake by bacteria that passed through the GF/F filters used in ^{15}N-studies, and breakage of cells containing ^{15}N due to filtration stress.

The N-flux rates and f-ratio were computed from refined mass and isotopic balance equations with an inverse least square technique (Elskens, 1999 and Elskens *et al*., submitted). The procedure enables us to yield error forecasts and criteria for the valuation of the field data. Furthermore, an experimental design based on controlled ammonium additions, and a general procedure for the derivation of "simple" relationships in non-linear regression models was used to study the sensitivity of the f-ratio relative to perturbations of the regenerated nutrient supply.

B.4. Aggregate degradation studies

Seawater was sampled at one (in the surface mixed layer, between 10 and 40 m) or two depths (in the surface mixed layer and at 100 m deep), making use of the "Marine Snow Catcher" large volume sampling bottle (100L, MSC; Southampton Oceanography Center Technology, England) (Lampitt *et al*., 1993). The MSC is simply a large (1.5 m tall and 30 cm in diameter), polyethylene cylinder equipped with Niskin-like closure devices at each end. It collects 100 L of water. Water passage through the device during descent is through large diameter terminal apertures

constructed to minimize turbulence. After recovery, 5 liters of water are sampled, and the device placed in a rack upright on deck for two h to allow particles to settle. The top 90 L were then gently drained through a spigot, and the bottom section of the water bottle, containing 5 L of water and any particles that had settled, was then collected and processed. Chlorophyll a, particulate organic carbon, microorganism composition and enumeration, and bacterial ectoenzymatic activities and production were measured in sub-samples from this concentrated sample. The MSC was used both to concentrate rare marine particles and to estimate the particle sinking rates.

B.4.I. Plankton, biomass and composition

Chlorophyll a was measured using standard JGOFS procedures (JGOFS, 1996). Particulate organic carbon was analysed with a Carlo Erba NA 2000 elemental analyzer.

Composition and enumeration of planktonic organisms including bacteria, protozooplankton and phytoplankton was determined by epifluorescence microscopy.

Bacterial abundance
Whole water samples were preserved with formaldehyde (2% final concentration). Five to ten ml of sample were filtered through a 10 µm-pore size Nuclepore polycarbonate membrane to separate free-living bacteria from bacteria attached to microphytoplankton and its derived particles. Numbers of phytoplankton-attached bacteria were estimated directly over phytoplankton or derived aggregates. Possible overestimation of attached bacteria due to scavenging of the free-living bacteria by particles during filtration was considered. Ten µm prefiltered samples (5 mL aliquots) were filtered through 0.2 µm Nuclepore membrane to estimate abundance and biomass of free-living bacteria. Bacterial numbers were determined by epifluorescence microscopy after DAPI staining following the procedure of Porter and Feig (1980).

Protist abundance
Protists numbers were determined by epifluorescence microscopy after Proflavin staining following the procedure of Haas (1982). Autotrophic species were distinguished from heterotrophs by the red autofluorescence of chlorophyll a observed under blue light excitation.

Aggregate density
Aggregates were preserved with 1% (final concentration) Lugol-gluteraldehyde solution and stored at 4°C in the dark until analysis for a maximum of 6 months prior to examination. Aggregate densities were measured microscopically. The major

phytoplanktonic taxa in aggregates were determined using an inverted microscope (Leitz Fluovert) after concentration in settling chambers (Hasle, 1978). We recognize that extremely fragile aggregates may be disrupted by this process, but most aggregates in the Ross Sea appear to be rather robust (Asper and Smith, submitted).

B.4.II. Sinking Rate Estimates

Mean particle sinking rates were determined based from the change in the vertical distribution of both chlorophyll a and POC after two hours in the MSC. The MSC was used as a SETCOL proposed by Bienfang (1981). This method allows for the determination of sinking rates in a non-turbulent field and is not indicative of in situ sinking rates. They do, however, provide a means to compare sinking rates of particles as they change through time and in space. Chlorophyll a was used as the phytoplankton biomass index to calculate total phytoplankton sinking rates, and POC was measured as a total community index to calculate total particle sinking rates. Taxon-specific rates were determined from the temporal changes in the vertical distribution of taxon densities. Sinking rates (w) were calculated according the following equation:

$$w = \frac{\left(V_s b_s - V_s(b_{0,0} + b_{0,t})/2\right)}{V_t(b_{0,0} + b_{0,t})/2}\left(\frac{l}{t}\right) \quad \textbf{(1)}$$

Where V_s is the volume of settled fraction $b_{0,0}$
　　　　V_t is the total volume of sample in the MSC
　　　　$b_{0,0}$ is the total biomass initially within MSC volume
　　　　$b_{0,t}$ is the total biomass analyzed at the end of the trial
　　　　b_s is the total biomass settled during trial time
　　　　t is the duration of the measurement (Bienfang, 1985).

B.4.III. Microbial activities

Bacterial processes of particle-attached and free-living bacteria were estimated using the procedures of Becquevort *et al.* (1998). Reverse filtration through a 10 μm pore sized polycarbonate membranes (Nuclepore) as proposed by Dodson and Thomas (1978) was used to distinguish between the free-living bacteria and the total bacterial community. The activity of the total bacterial community was measured on the unfiltered water sample, whereas the activity of free-living bacteria was measured in the filtrate. The activity of particle-attached bacteria was then estimated by the difference.

Potential ectoenzymatic activity

Potential ectoenzymatic activity was measured at 20°C after adding a saturating concentration of artificial substrates that produce fluorescent products when hydrolyzed by ectoenzymes present. In the optimal conditions of temperature and substrate, this activity can be used as a measure of the amount of ectoenzymes rather than to simulate *in situ* rates (Billen, 1991). The aminopeptidase activity does not follow the same dependency as bacterial growth, showing an exponential relationship (with Q_{10} of 2.3) up to 20°C in the Antarctic waters (Billen, 1991). Two ectoenzymes were tested: ectoprotease and ecto-β-glucosidase. The former was measured because it has been suggested as being a constitutive property of bacteria in aquatic environments (Billen, 1991), and the latter because it is an indicator of the degradation of *Phaeocystis*- derived material through the specific cleavage of β-glucoside linkages characteristic of the *Phaeocystis* gel-producing polysaccharides (Thingstad and Billen, 1994; Lancelot and Rousseau, 1994).

- Ectoprotease activity

  L-leucyl-2β-naphthylamide hydrochloride (LLβN) was used as substrate for proteolytic ectoenzymes, as it produces fluorescent naphtylamine after hydrolysis of the peptide-like bond. The experimental procedure was that of Somville and Billen (1983).

- Ectoglucosidase activity

  4-methylumbelliferyl-β-glucoside (MUF-GLU) was used as substrate for β-glucosidase, which produces fluorescent 4-methylumbelliferone after hydrolysis of β-linked (1-2, 1-3, 1-4, 1-6) disaccharides of glucose, celluhexose, and carboxymethylcellulose (Barman, 1969). The procedure was adapted from the protocol of Hoppe (1983) and Somville (1984).

Bacterial production

Bacterial production was estimated by incorporation of ^{3}H-thymidine at *in situ* temperatures (-1.9 to 0°C) (Fuhrman and Azam, 1982). Thymidine incorporation was converted into bacterial production using conversion factors of Ducklow *et al.* (1999) established for the Ross Sea bacterial communities (i.e., 8.6×10^{17} bacteria produced per mole of thymidine incorporated in the cold TCA insoluble material). The conversion factors for attached bacteria are assumed to be the same as those estimated for free-living bacteria. Bacterial carbon demand was estimated assuming bacterial carbon content per cell of 20 fg C cell^{-1} and a bacterial growth efficiency (BGE) of 15 %. The estimated BGE in the Ross Sea ranges between 9 and 38% (Carlson *et al.*, 1999).

B.5. Barium and Strontium uptake experiments

In order to assess the uptake of Ba, Sr by phytoplankton and particles, we conducted on-board isotope dilution experiments using Southern Ocean seawater samples with natural plankton community composition and *in-vitro* cultures of diatoms (*Chaetoceros lauderi*) or prymnesiophytes (*Phaeocystis pouchetti*). The effect of algal and bacterial activity was studied during short-term (<130 hours) and long-term (>80 days) incubations. The long-term incubations were aimed at understanding the barite precipitation process, while with the short-term incubations we focussed on the link between algal activity and elemental uptake.

On-board incubations

Incubation experiments were run during the SAZ'98 (Subantarctic Zone), the AESOPS (Ross Sea) and the ANTARES-4 (Subtropical and Subantarctic zones) cruises. For sampling, we used the MSC described in **§B.4**. Samples were taken at surface (maximum of fluorescence; usually 20-30 m) and subsurface at the bottom of the mixed layer (100-200 m). Large particles were preconcentrated in the lower retrievable part of the bottle by leaving the latter for 2h upright on deck, before any sampling. The bulk of the water was then drained and the entire sample from the retrievable cell was recovered and used for incubations. About 2.5 litre were immediately filtered (0.4 μm polycarbonate membrane) and were used for assessing the natural isotopic composition (T_0, *Original*, see **Scheme 2**).
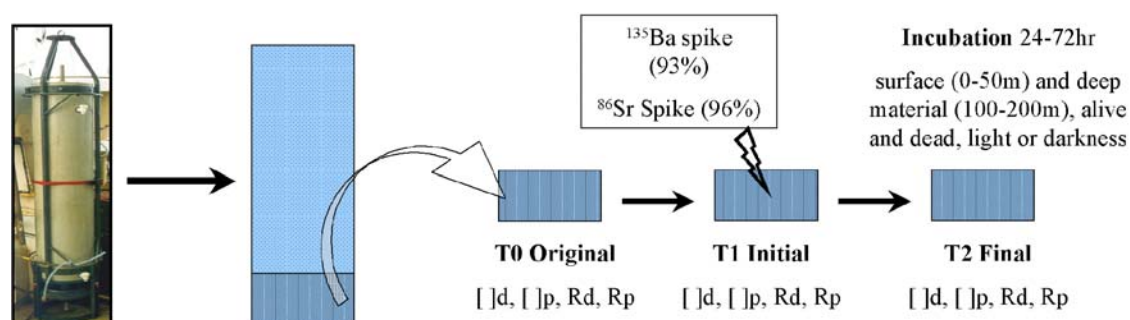
Scheme 2: General procedure used for incubations during expeditions AESOPS, SAZ'98 and ANTARES-4.

The remaining volume was spiked with ^{86}Sr and ^{135}Ba isotopes (T_i, *Initial*). Usually, surface samples were incubated for 12 to 48 hours under natural illumination and temperature using an on-deck flow-through incubator continuously fed with surface ocean water while subsurface samples were left for 70 to 125 hours in darkness at the temperature of surface water (T_f, *Final*). Occasionally, surface samples were incubated in darkness and subsurface samples under light conditions. Some experiments on dead phytoplankton (killed by addition of $HgCl_2$) were also

performed. At the end of the incubation, samples were filtered (0.4 µm polycarbonate membranes).

For each incubation, three solute samples (*Original*, before incubation; *Initial*, just after spiking and *Final*, at the end of the incubation) and two suspended particles samples (*Original* and *Final*) were analysed. Prior to analysis, filtered material was treated as discussed for suspended matter in **§B.6-II** while the incubation solutions were diluted about 30 times with Milli-Q grade water. Isotopic ratios ($^{88}Sr/^{86}Sr$ and $^{138}Ba/^{135}Ba$) and concentrations (Sr and Ba) were measured by ICP-MS (VG PlasmaQuad PQ2 Plus). Mass bias, during isotopic ratio measurements was corrected from periodic measurements of original solutions with natural isotope abundances. For the dissolved phase, *Initial* and *Final* values were averaged as no significant difference between the two is expected.

The factor F which represents the change of the isotopic ratio in particles after exchange with seawater was calculated as follow (example with the Ba case):

$$[Ba]_{p,f} \cdot \left(^{138}Ba \Big/ _{135}Ba \right)_{p,f} = [Ba]_{p,i} \cdot \left(^{138}Ba \Big/ _{135}Ba \right)_{p,i} + \Delta [Ba]_d \quad \textbf{(2)}$$

with $[Ba]_{p,i} = [Ba]_{p,f} - \Delta[Ba]_{d,i}$

And

$$F = \frac{\Delta.[Ba]_d}{[Ba]_{p,f}} = \frac{\left(^{138}Ba \Big/ _{135}Ba \right)_{p,f} - \left(^{138}Ba \Big/ _{135}Ba \right)_{p,i}}{\left(^{138}Ba \Big/ _{135}Ba \right)_{d,f} - \left(^{138}Ba \Big/ _{135}Ba \right)_{p,i}} \quad \textbf{(3)}$$

With [Ba] = barium concentration
  Δ [Ba] = decrease of Ba in the solution
  $(^{138}Ba/^{135}Ba) = {}^{138}Ba / {}^{135}Ba$ isotopic ratio
  d and p represent dissolved and particulate phases respectively
  i and f represent initial and final time conditions

In vitro incubations

Diatoms (*Chaetoceros lauderi*) and prymnesiophytes (*Phaeocystis pouchetti*) were cultured *in-vitro* in 10L of seawater previously filtered (polycarbonate membrane of 0.4 µm porosity) and sterilised. Nutrients and vitamins were added and the culture was set in a cool room at 5°C under light (12h/day), with constant and gentle shaking. Once the optimal culture growth was reached (after about 1 month) the culture suspension was split into culture batches submitted to different treatments:

(1) light with cells alive; (2) in the dark with cells alive; (3) in the dark and cells killed by azide addition. ^{86}Sr and ^{135}Ba spikes were added to all cultures. About 1 litre was sampled after an incubation period of 3h40', 7h00' and 13h25' (diatoms cultures) or 1h30', 4h00' and 26h00' (*Phaeocystis* cultures). Cultures were filtered immediately after sampling on polycarbonate membrane filters (0.4µm). Chemical and analytical procedures are identical to those described above for *on-board* incubations, except that mass bias was corrected using the isotopic composition of an artificial standard of Sr and Ba with natural isotopic composition.

Long-term uptake kinetics

The following *in-vitro* experiments were conducted to study the barite precipitation process in degrading phytoplankton:

Diatom cultures were prepared as described above for short-term incubations. Once the optimal culture growth reached (after ~1 month) two batches were prepared (3-4 L each): (1) addition of antibiotics to stop bacterial activity (*i.e.* axenic environment); (2) no antibiotics added. Both cultures were then spiked with ^{135}Ba and ^{86}Sr isotopes in order to change drastically the dissolved isotopic ratio.

For *Phaeocystis*, 3 batches (5.5 L each) were spiked with ^{135}Ba and treated as follows: (1) addition of azide in order to kill phytoplankton and bacterial activity (2) addition of antibiotics and (3) degradation in normal conditions.

Cultures were then left in the dark at 5°C under gentle shaking. Algal activity progressively stopped because of absence of light and nutrients and formation of aggregates was observed especially for non-axenic cultures. Presence or absence of barite was checked regularly (every 5-10 days) on aliquots of the detritus by scanning electron microscopy (SEM).

B.6. Elemental analysis of suspended matter, sediment trap and sediments

B.6.I. Sample Origin

Suspended matter (SAZ'98 and ANTARES-4) was sampled using 12 litre Niskin bottles. In general 12 depths were sampled in the upper 600m of water column to focus on the mesopelagic Ba maximum. Seawater was transferred to 12 litre gauged perspex filtration units and filtered on polycarbonate membranes of 0.4 µm porosity using pressure of filtered air (0.4 µm porosity filters). On board filters were dried at 50°C and stored in sealed plastic petri dishes.

The detail of sampling for SAZ'98 sediment traps are detailed in Bray *et al.* (2000) and Trull *et al.* (2001).

Core tops from the Atlantic Sector (1992 ANT-X/6 cruise), Indian Sector (APSARA cruises in 1984, 1988 and 1994) and from the Tasmanian shelf (KH94-4 and 147GCO cruises in 1994 and 1995) were analyzed for Ba accumulation to assess the reliability of the excess Ba (Ba_{xs}) signal in surface Southern Ocean sediments as a proxy for paleoproductivity of the upper water column. Locations of these samples are given in **Figure 1**.

B.6.II. Trace and major analysis

In the laboratory, filtered material (1/4-1/2 of original filter or 50-100mg of sediments) was dissolved overnight in a clean room using teflon bombs by concentrated acids (3ml HCl / 2ml HNO_3 / 1ml HF; all Suprapur grade) and heating at 90°C in sealed Teflon$^®$ vials in a clean pressurized room. After evaporation to dryness, the residue was dissolved in 2% HNO_3 and made to volume (10-15 ml) with Milli-Q water type (Cardinal *et al.*, 2001). For sediments the acid digestion is preceded by the addition of 0.5-3 ml of H_2O_2 10% during 1-3 days at 40°C to remove the organic matter. The digestions of the core tops from the Atlantic and Indian sectors were done using HCl, HNO_3 and $HClO_4$ acids as detailed in Fagel *et al.* (accepted). The SAZ sediment traps were digested at WHOI by S. Bray (Bray *et al.*, 2000; Trull *et al.*, 2001).

Blanks were processed in the same conditions as samples and their analytical signals were subtracted. Trace elements were analysed by ICP-MS (VG Elemental PQ2 Plus). The following isotopes were measured in triplicate: ^{88}Sr, ^{90}Zr, ^{138}Ba, ^{139}La, ^{140}Ce, ^{141}Pr, ^{146}Nd, ^{157}Gd, ^{163}Dy, ^{165}Ho, ^{166}Er, ^{172}Yb, ^{232}Th and ^{238}U. Oxides were minimised by checking that ThO is less than 2% of a total Th in an artificial standard solution. A correction of the $^{141}Pr^{16}O$ interference has been applied on ^{157}Gd. Matrix and instrumental drift effects were continuously monitored and corrected by measuring the fluctuations of four internal standards (^{99}Ru, ^{115}In, ^{185}Re and ^{209}Bi) added to the samples. Major elements (Al, Fe, Mg, Ca, Mn, Na, P, S, K and Ti) were measured by ICP-AES (Thermo Optek Iris Advantage). The ICP-AES was also used to analyse samples with high concentrations in Ba and Sr or for comparison with the ICP-MS measurements. Y and Au internal standards were used to correct the instrumental drift during ICP-AES analysis. For trace and major elements external calibrations were performed using artificial standard solutions and dilute mineralised natural rock standards (e.g., BHVO-1, MAG-1, SGR-1, CCH-1, DWA, SDC-1, JLs-1; Govindaraju, [1994]).

The Detection Limits (DL: calculated as 3 times the standard deviation of the blank) in solution fluctuate between 0.5 pg/g (Heavy REE) and 40 pg/g (Ba) for trace elements and between 1 mg/g (Mn) and 140 mg/g (P) for major elements (Cardinal *et al.*, 2001). Data below DL have been excluded. The precision of barium and

strontium analyses was also controlled by replicates on twelve samples using isotope dilution (^{135}Ba and ^{86}Sr spikes). Isotope dilution and external calibration results did not differ by more than 2.5%.

B.6.III. Corrections to Ba data

Correction for lithogenic Ba supply
Biogenic Ba, Ba$_{xs}$, was obtained by correcting total Ba for the contribution of lithogenic Ba, following Dymond *et al.* (1992) and using Post Archean Australian Shale Ba/Al or Ba/Ti ratios as the lithogenic reference (Taylor and McLennan, 1985). The difference between the two calculations (Al, Ti) is generally less than 10% (Cardinal *et al.*, 2001). Because a better accuracy was obtained on Al analyses, we preferred the correction based on Ba/Al ratios. Ba$_{xs}$ generally represents 95 ± 5 % of the total Ba but minimum Ba$_{xs}$ values in the range of 75 - 88 % have been recorded in some samples especially at SAZ'98 45.0°S, and to a lesser extent at SAZ'98 46.8°; 49.5° and 51.0°S.

Moreover, the measured Ba$_{xs}$ accumulation rate might be different from the Ba$_{xs}$ rain rate in sediments, because of *(1)* partial dissolution of barite at the seawater-sediment interface, before burial and *(2)* post-depositional sediment redistribution (focusing/winnowing).

Correction for barite dissolution at sediment water column interface (1)
Dymond et al. (1992) estimated the Ba$_{xs}$ preservation rate as a function of the sediment mass accumulation rate (in µg/cm^2/yr) using the following algorithm:

$$(FBa_{xs}) = (AR\ Ba_{xs}\ measured) / degree\ of\ preservation\ (\%) \qquad (\mathbf{4})$$

$$Where\ degree\ of\ preservation\ (\%) = 20.9\ log\ (MAR) - 20.3 \qquad (\mathbf{5})$$

This algorithm has been widely applied in paleoproductivity reconstructions from Ba$_{xs}$ sediment geochemistry (see Gingele *et al.*, 1999). Its prediction has been invalidated by data only in a few studies, where preservation efficiencies could be related to a diagenetic remobilization of Ba (Paytan *et al.*, 1996; McManus *et al.*, 1999). Eq. (**4**) assumes that bottom waters are undersaturated with respect to barite. We emphasized in our study (Fagel *et al.*, accepted) that a correction for dissolution through application of Eq. (**5**) may not always be justified but should depend on water column depth. This was deduced from the observed anti-correlation between Ba$_{xs}$ contents and water depth below 2500 m in the Atlantic sector of the Southern Ocean (**Figure 4**). This suggests that above 2000 m no significant dissolution of barite may

occur. This is in accordance with the thermodynamic study of Monnin *et al.* (1999) on barite saturation index as evidenced in **Figure 4**.
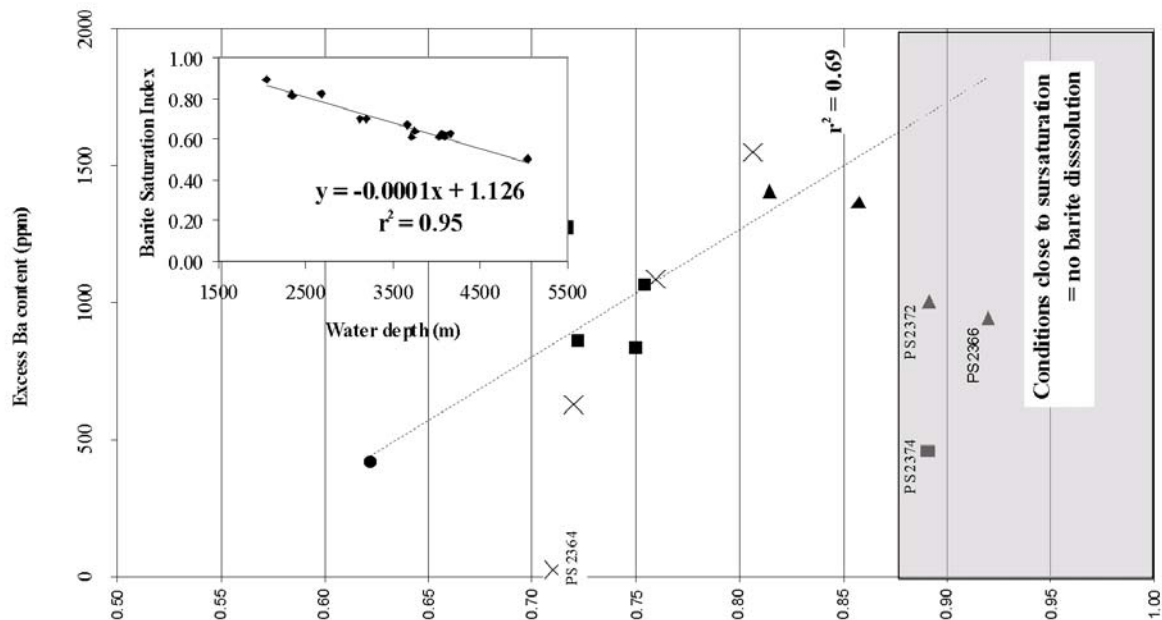

Figure 4: Ba$_{XS}$ content reported as a function of the local barite saturation index (SI). SI were calculated from the regression line with water depth shown in the upper part of the diagram. The thermodynamical calculations of SI are based on ANT-X/6 data (Monnin *et al.*, 1999). Barite should not dissolve in waters characterized by SI index close or higher than 1 (shaded area).

Therefore the dissolution correction (Eq. **5** and **6**) has been applied only to sediments with a barite saturation index lower than 0.80 for ANT-X/6 core tops. As no barite saturation index data are available in the Indian sector, APSARA samples have been corrected only for core tops deeper than 2500 m (Fagel *et al.*, submitted). For the same reasons, core tops from the Tasmanian shelf have also been corrected.

Correction for post-depositional sediment redistribution (2)

It was suggested that the highest sedimentary mass accumulation rates are due, at least partly, to lateral advection. Such a process is common in the Southern Ocean due to strong abyssal currents linked with the Antarctic Circumpolar Current and the Antarctic Bottom Current (Francois *et al.*, 1993; Kumar, 1994; Frank *et al.*, 1996). Therefore the ^{230}Th$_{xs}$ content was measured in surface sediments to quantify the post-depositional sediment redistribution. Samples were prepared by a standard method at WHOI (Anderson and Fleer, 1982; Frank *et al.*, 1996; Fagel *et al.*, submitted). The post-depositional sediment redistribution by bottom current was corrected mainly by normalizing Ba$_{xs}$ fluxes to excess ^{230}Th activity in sediments as follows (Francois *et al.*, 1993):

Preserved Ba_{xs} rain rate (mg/cm²/kyr) = (p x Z x [Ba_{xs}]) / [$^{230}Th_{xs}$] (**6**)

with p = production of ^{230}Th in the water column=2.63 dpm/cm^2/kyr for a 1000m water column
Z = water depth in km,
[Ba_{xs}] = measured content in the surface sediment in µg/g
[$^{230}Th_{xs}$] = measured activity in the surface sediment in dpm/g

This method is based on the assumption of a constant flux of ^{230}Th to the sediment, which is equal to the rate of production from ^{234}U in the water column. It assumes there is no ^{230}Th removal during the lateral transport (boundary scavenging). François *et al.* (1997) estimated the accuracy of the reconstructed fluxes at 40%, due to this boundary scavenging effect. The $^{230}Th_{xs}$ results and their subsequent focusing correction are discussed in Fagel *et al.* (submitted).

B.6.IV. Sequential leaching on sediment

Based on the pioneer work of Church (1970), Paytan *et al.* (1993) have set up a leaching methodology for the isolation of barite achieving a phase purity of more than 90 %. Our aim in this study was to set up a technique of barite separation useful for the geochemical identification of barite using a smaller quantities of sediment (<<1g) for samples such as sediment traps. Several Southern Ocean sediments and several leaching procedures (various acids and concentrations) were studied and we will present here only one experiment. All different tests came to similar conclusions. Leachings were conducted following five kinds of operations:
(1) 0.1 g of sediments, crushed in an agate mortar is put in a clean 20 ml Teflon centrifuge tube in which all the leaching steps are performed (2) after the addition of the leaching reagent (~5 ml) the tube is placed in a warm (~ 50°C) ultrasonic bath (45'-1h30'). (3) The sample is centrifuged and, after saving the supernatant, washed carefully with water in between every leaching step by three successive ultra-centrifugations. The leachate is then transferred to a clean polypropylene vial after each rinse. (4) Centrifuge tube with solid residue is dried overnight at 105°C before the addition of the next reagent. (5) After each acid step the residue is weighed and the amount of sediment leached measured by weight loss. Except for ultra-centrifugation and drying operations, the full procedure is conducted in a pressurised clean room. All reagents were Suprapur grade and water was Milli-Q grade. The five following reagents were used in order to dissolve the different sedimentary components: H_2O_2 10 % (organic material removal), HCl 0.05N (carbonate dissolution), HF 0.1N (partial removal of oxide coatings and clays), HNO_3 0.5N (barite dissolution) and HF 40 % (diatoms and lithogenic component dissolution). Sequential leachings on ~0.1g sample have been performed on two aliquots from PS2361 sediment (ANT-X/6, 3-5cm depth, 8.8 % CaCO3 and 79.6% opal, 1830ppm Ba) and

28

three aliquots of PS2376 (3-5cm depth, 33.6% $CaCO_3$, 55.5% opal, 1630ppm Ba) respectively. Six tubes (labelled A-F) were used and have been processed as shown in **Table I**.

Table I: Details of the leaching procedure.

Tube	A	B	C	D	E	F
	PS2361 3-5	PS2361 3-5	PS2376 3-5	PS2376 3-5	PS2376 3-5	Blank
Step	0.11 g	0.11 g	0.13 g	0.13 g	0.11 g	0
1			5 ml H_2O_2 10 %			
2 $acid_{xs}$ = 0.50	1.0 ml	1.0 ml	HCl 0.05 N 4.45 ml	4.45 ml	3.9 ml	2.0 ml
3 $acid_{xs}$ = 0.75	0.52 ml	0.52 ml	HCl 0.05 N 2.2 ml	2.2 ml	1.95 ml	1.0 ml
4 $acid_{xs}$ = 1.0	0.52 ml	0.52 ml	HCl 0.05 N 2.2 ml	2.2 ml	1.95 ml	1.0 ml
5 $acid_{xs}$ = 1.5	1.0 ml	0	HCl 0.05 N 4.45 ml	4.45 ml	0	2.0 ml
6 $acid_{xs}$ = 2	1.0 ml	0	HCl 0.05 N 4.45 ml	4.45 ml	0	2.0 ml
7			5 ml HF 0.1 N			
8			5 ml HNO_3 0.5N			
9			5 ml HF 40%			

Each reaction was performed during 45' within an ultrasonics bath at ~50°C for all steps except the duration of steps 1 and 4 (1h30'). Centrifugations after every step were performed 3 times, during 1h at 25,000 rpm, except tubes A & B in step 1 that were centrifugated 5 times.

The dilute HCl step was split into 3 or 5 successive steps. We calculated the excess acid as follows:

$$HCl_{xs} = 100 \times n_{HCl} / n_{CaCO3} \quad (\mathbf{7})$$

With n_{HCl} the cumulative mole number of acid added to the sample from the first HCl step,
n_{CaCO3} the total mole number of $CaCO_3$ in the 0.1 g sediment aliquot (based on calcite X-ray micro-diffractometry results).
A HCl_{xs} of 1 corresponds to a dissolution reaction requiring 1 mole HCl for 1 mole $CaCO_3$.

Details regarding the site location and sediment composition are given in Fagel et al. (submitted) and Cardinal *et al.* (submitted) as well as in **§B.6–I** of this volume.

B.6.V. Barite solubility in acid

Figure 5 gives the cumulative fraction of some representative elements vs. successive sequential step
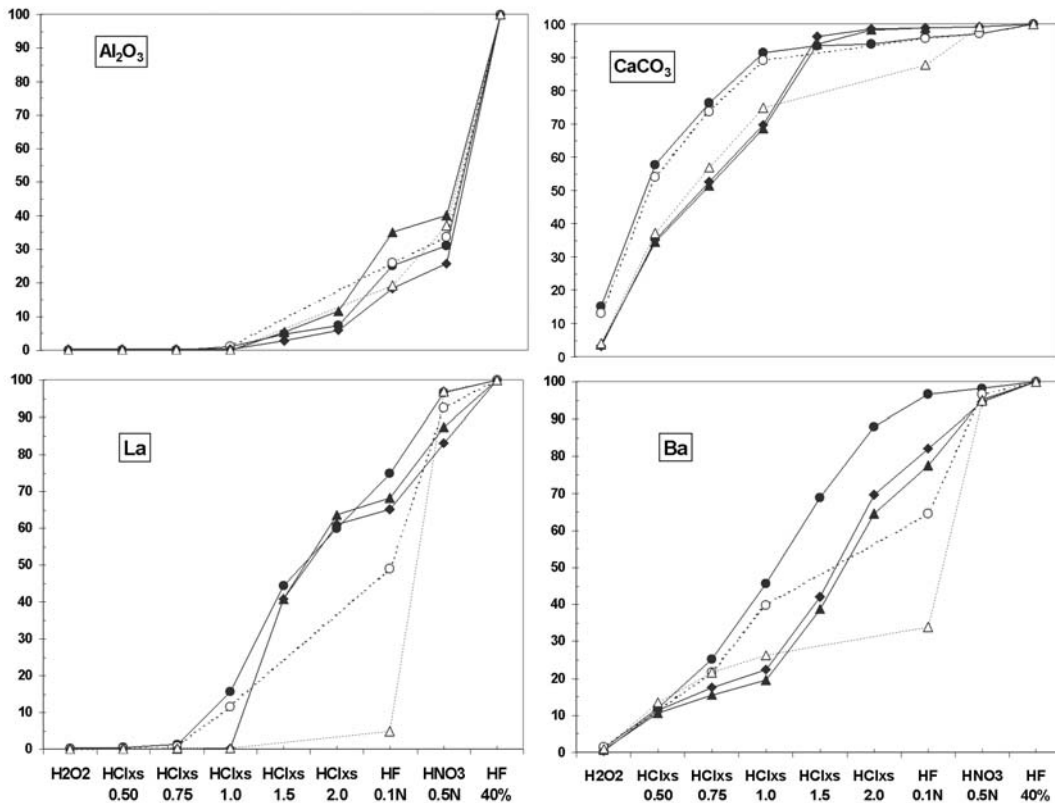
Figure 5: Cumulated % of element leached vs. step. PS2361: Tube A: filled circles, Tube B: open circles. PS2376: Tube C: filled triangles, Tube D: filled diamonds, Tube E: open triangles

A large amount of Ba is leached during the early steps of our experiment. The solid phases leached contain at this stage ~4000 ppm and ~1400 ppm of Ba for PS2361 and PS2376 respectively. **Figure 6** shows the similarity between Ba and S contents of the leachates and points towards a barite dissolution process. This is confirmed by the following calculation of the theoretical Ba contribution from the other phases at for instance the first HCl step. Except barite, the other sources of Ba in sediment can be detrital (clays, feldspars), carbonates (mainly foraminiferas and coccoliths), opal silica (diatoms) and authigenic ferro-manganese oxy-hydroxides (e.g., Gingele and Dahmke, 1994). We exclude organic matter fraction in the Ba budget as its contribution can be neglected in such sediments (Cardinal *et al.*, to be submitted).
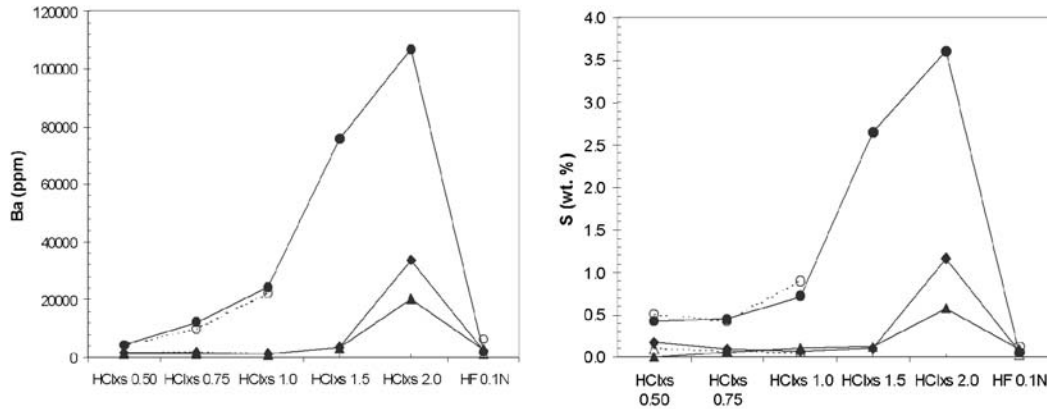
Figure 6: Ba and S contents of the solid phases leached during HCl and HF 0.1 N steps. PS2361: Tube A: filled circles, Tube B: open circles. PS2376: Tube C: filled triangles, Tube D: filled diamonds, Tube E: open triangles.

The Ba content of diatom opal is below 30 ppm (Collier and Edmond, 1984) and its contribution can be excluded too, as Si was not significantly leached in the first leaching steps. The average Ba upper crustal content is 550 ppm (Taylor & McLennan, 1985) and the Ba content of foraminifera and coccoliths is less than 13 ppm for (Lea & Boyle, 1990, 1991; Stoll, pers. comm., 1999). The affinity of Ba for Fe-Mn-oxyhydroxides is high, especially for MnO_2 (Li *et al.*, 1984) that can contain large but variable amounts of Ba (700 - 4000 ppm; Piper and Williamson, 1977; Dymond *et al.*, 1984). However, in the first dilute HCl leaching steps no Fe was detected and the amount of Mn leached (less than 0.1 % of the leachate) is very low. Based on these average Ba contents and our major element analyses, the highest Ba contribution coming from other sources but barite in the Ba budget during the HCl steps would be 3 % only (1 % on average). These results show that barite is dissolved from the beginning of the dilute acid leachings (HCl 0.05N) and onwards. This solubility is much higher than the theoretical value (Handbook of Chemistry and Physics, 1975), which should have dissolved only 5 % and 1 % of Ba for PS2376 and PS2361 respectively at HCl_{xs} of 1.0 (our experimental values are 25 % and 46 % respectively).

A possible explanation for this large underestimation of marine barite solubility in acid could be the very small size of marine barites (<5 μm) and the resulting large specific surface that would facilitate dissolution. We also performed several leaching experiments with acetic acid 0.2-1 N and evidenced the dissolution of the barite with this acid as well (Cardinal *et al.*, submitted). A similar leaching experiment on trap material showed that more than 80 % of Ba dissolved (Cardinal *et al.*, submitted).

These results have the two following implications on the use of Ba in pale-oceanography:

Underestimation of barite contents

A pure barite phase cannot be isolated by dilute acid leaching on small amounts of sediment (~0.1g) because barites are rapidly dissolved. The Paytan et al. (1993) procedure for barite isolation requires several strong acid leachings at room temperature on a much larger amount of sediment (10g). Jacot des Combes *et al.* (1999a,b) used the Lyle *et al.* (1984) procedure that also involves acid leaching. Both these studies ascribe the residual Ba signal to barite. Gingele *et al.* (1999) proposed a weak acetic acid leaching before XRD-analyses of barite in carbonated sediments to assess barite contents in sediment. For the same reason the leaching experiment on trap material by Dymond *et al.* (1992), beginning with acetic acid leaching has most likely dissolved some barites too. Our data clearly indicate that acid leachings on sediments or trap material can completely dissolve the authigenic barite and thus the application of any weak acid leaching for barite separation is questionable in the light of our results. We then suspect that some barite fraction could have been dissolved resulting in a probable underestimation of barite content in sediments and especially in trap material studies, although performed at room temperature.

Geochemistry of barite

The belief that marine barite is non-sensitive to acid and is a "highly refractive chemical species" (Gingele *et al.*, 1999) can yield erroneous interpretations. For instance, Lerche and Nozaki (1998) also applied several acid leachings on trap material. They discussed REE patterns and Ce anomaly variations in the various phases and claimed that the positive Ce anomaly observed in the final digestion might due to an authigenic barite signature. However our results show that the Ce anomaly variations in this phase can hardly be ascribed to barite signature after using such acid leaching because barite may have been dissolved in the earlier steps.

C. Numerical experimentation

C.1. Description of the Ice-Ocean hydrodynamic model (CLIO-1D)

C.1.I. Model description

The 1D version of the CLIO model has been derived from the 3D version of CLIO (Goosse et al., 2000) by performing some modifications and simplifications in the initial code (for details, see Probst, 2000a). It can be described briefly as follows.
A 3-layer model thermodynamic sea-ice model (Fichefet and Gaspar, 1988) simulates the changes of snow and ice thicknesses and heat content in response to

the surface and bottom heat fluxes. The variations of ice compactness due to thermal processes are determined following the approach proposed by Häkkinen and Mellor (1990). The ice model also incorporates a parameterisation of the latent heat storage in brine pockets and a simple scheme for snow-ice formation.

The ice-ocean stress is taken to be a quadratic function of the difference between the ice velocity and the ocean surface velocity. Following McPhee (1992), the sensible heat flux from the ocean to the ice is taken to be proportional to the temperature difference between the surface layer and its freezing point and to the friction velocity at the ice-ocean interface. Finally, the mass exchanges between ice and ocean are represented in terms of an equivalent salt flux.

The ocean component is a primitive-equation model resting on the usual set of assumptions, i.e., the hydrostatic equilibrium and the Boussinesq approximation. It is assumed in this 1-D version that the horizontal advection and diffusion terms can be neglected as a first approximation or taken into account in a simple way (see below). The parameterisation of vertical mixing (Goosse et al., 1999) is based on a simplified version of the Mellor and Yamada's (1982) level-2.5 model. In this parameterisation, one differential equation is solved to obtain the vertical profile of turbulent kinetic energy (TKE). The TKE is then used to derive vertical diffusivities and viscosities using algebraic formulas.

The model is dynamically driven by the wind stresses, which can be either directly prescribed or either derived form the wind velocities, using a quadratic law. The surface fluxes of heat are determined from atmospheric data by using classical bulk formulas described in Goosse (1997). Input fields consist of surface air temperatures, cloud fractions, air relative humidities, and surface wind speeds. To compute the freshwater input at surface, evaporation/sublimation is derived from the turbulent flux of latent heat and precipitations are prescribed. The solid precipitations are deduced from the total amount of precipitation and the surface air temperature following Ledley (1985).

In the standard configuration, the vertical grid cells have constant thickness (1m) from 1 to 100 m, then, the thickness increases by 10 % of the value of the preceding step until the bottom of the ocean.

Parameterisation of three-dimensional effects

In order to achieve a reasonable simulation of the seasonal cycle of the ice cover, a series of modifications has been introduced. The goal of these modifications is to take the horizontal processes into account.

- First, we have introduced a parameterisation of the effect of divergence of the sea-ice velocity in the model (for details, see Probst, 2000b). The latter has been deduced from the general law of conservation

$$\frac{\partial \Psi}{\partial t} = -\vec{\nabla}.\left(\vec{u}_i \Psi\right) + D\nabla^2\Psi + S_\Psi \qquad (\textbf{8})$$

where Ψ represents a variable that is transported with the ice, as for example the snow volume, the ice volume, the ice concentration; S_Ψ represents the changing rate of Ψ due to the thermodynamic effects already treated in the thermodynamics part of the model and D represents a horizontal diffusion coefficient.

Neglecting D and assuming that the horizontal variation of Ψ are weak, the following expression can be obtained after discretization:

$$\Psi^{t+1} = \Psi^t + dt\left(1 - \Psi^t\right)\vec{\nabla}.\vec{v} \qquad (\textbf{9})$$

Where $\vec{\nabla}.\vec{v}$ is the ice velocity divergence $[\text{s}^{-1}]$ (hereafter referred to as cdiv) and dt is the time step $[\text{s}]$.

- Secondly, a restoring term on the temperature and the salinity crudely parameterises the horizontal transport in the ocean. Indeed, the 3D oceanic circulation in the ocean generally supplies heat and salt to the water column below the mixed layer coming from northern regions. This has two consequences. First, this heat can be used to melt ice or to slow down its formation. Secondly the inflow of salty, dense water at depth helps to maintain the stratification of the water column. If the influence of this circulation is neglected, the deep ocean slowly looses its heat and the mixed layer deepens with time. This restoring effect on temperature is expressed as follows

$$\frac{\partial T}{\partial t} = F - k\left(T - T_{obs}\right) \qquad (\textbf{10})$$

Where T is the temperature, F represents all terms in the equation except the restoring, T_{obs} is the observed temperature and k represents the inverse of a time scale.

Thus, we obtain after discretisation:

$$T^{t+1} - T^t = F\,dt - k\left(T^t - T_{obs}\right)dt \qquad (\textbf{11})$$

C.1.II. Model calibration

In order to test the model, we conducted simulations at three points located in the Southern Ocean. They have the same longitude (18° W) but differ by their latitudes (73.5°S, 70.5°S, and 67.5°S). The atmospheric forcing is deduced form monthly

mean climatologies (for more details about those climotologies, see Goosse, 1997). For each point, four simulations are performed in order to assess the influence of both the restoring and the divergence of the ice transport. In the first one, no restoring and no ice divergence are included. The restoring is included in the other three experiments with values of cdiv ranging from 0 to 0.01 s^{-1}. It must be stressed that the value of cdiv should ideally vary with time and location. Nevertheless, a value constant trough time is retained here for simplicity. Because of the potentially large impact of the value of cdiv on the simulation, the sensitivity of model results to change of this parameter has to be tested at each location where the model is applied. Indeed, it allows selecting a value that is associated with a reasonable simulation of the seasonal cycle of the ice cover.

Figures 7-9 show that the impact of the restoring tends to be stronger in the northern parts of the section that in the Southern part. This seems natural since the oceanic temperatures are higher in those regions. On the other hand, a high value of cdiv is necessary in the Southern part of the section in order to reach a stable seasonal cycle of the ice cover, particularly at 73.5°S where the southerly winds transport to the north large amounts of ice.

When using restoring on temperature and salinity as well as the parameterisation of the effect of the ice transport divergence, the date of complete melting of the ice cover simulated by the model is in reasonable agreement with the satellite observations (Gloersen et al, 1992). On the other hand, the ice begins to form too late in the model: the sea-ice appears around June instead of May for the point located at 67.5°S, around February instead of April for the point located at 70.5°S and around mid February instead of March for the point located at 73.5° S. In addition, the ice thickness simulated by the model tends to be a little too low. These differences between the simulations and the observations can be due to various factors, including the forcing, the 1-D approximation or the use of a time-invariant value for cdiv. An important point is certainly the absence of ice convergence in the model. Indeed, at the end of summer and at the beginning of autumn, ice can be transported to an ice free-zone from permanently ice-covered regions or from one where the ocean begins to be ice-covered earlier. Then, ice can maintain even if the local production would only begin later since sea ice absorbs much less solar radiation than the ocean because of its high albedo. Furthermore, the ice transport is associated with a negative transfer of latent heat that cools the area and thus helps the sea-ice formation. Unfortunately, as we assume in the parameterisation of the ice transport that the horizontal variation of the variables associated with the ice is weak, this effect could not be taken into account in the model.
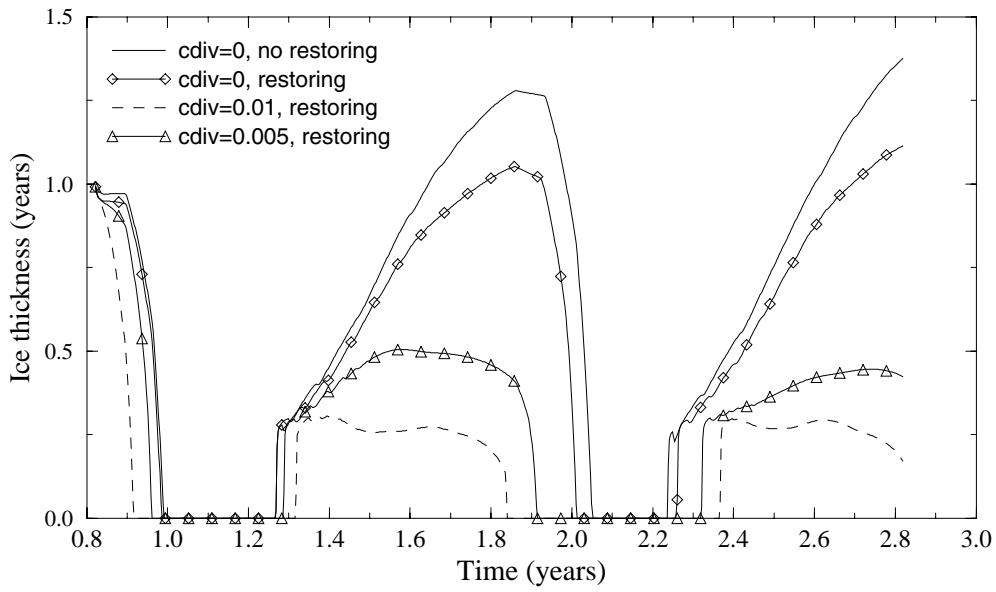
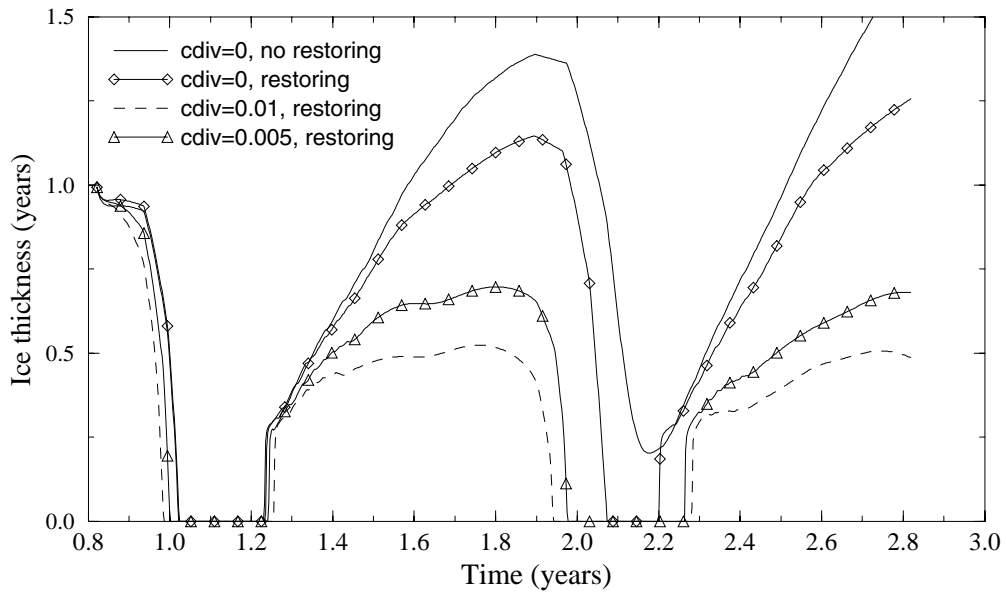**Figure 7**: Temporal evolution of the sea-ice thickness at 67.5 °S

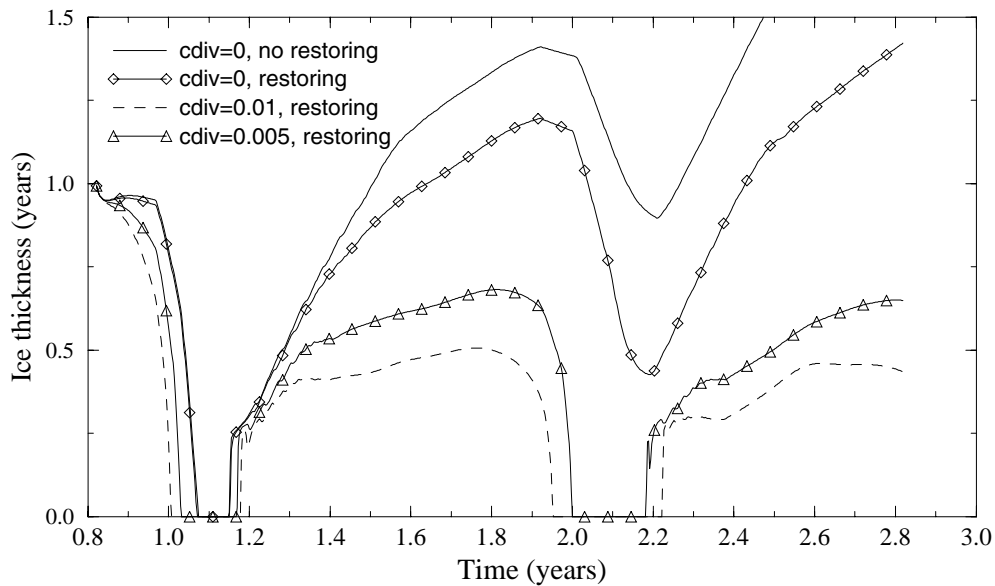**Figure 8**: Temporal evolution of the sea-ice thickness at 70.5 °S

Figure 9: Temporal evolution of the sea-ice thickness at 73.5 °S

After this validation of CLIO-1D under a climatological forcing, it is now necessary to test the model behaviour with an atmospheric forcing that has a greater temporal variability. Unfortunately, the long series of mixed layer depth in ice-covered regions are not easily available to validate the model. Therefore, we compared the mixed layer simulated by CLIO-1D with the one simulated by the model of Veth (1991) in the Scotia Sea (47°S). This model has already been validated during many campaigns in the Southern Ocean and so the comparison constitutes a good test for CLIO-1D. Both models use the same atmospheric forcing (except for the precipitation data) as well as initial temperature and salinity profiles. In CLIO, the mixed layer boundary has been diagnosed as the depth at which the turbulent diffusion coefficient becomes lower than 5.10^{-4} m^2s^{-1}.

Figure 10 shows that the evolution of the mixed layer depth in CLIO is pretty close to that predicted by the model of Veth under the same atmospheric forcing. Both models mainly respond to fluctuations of the wind stress with deep mixed layers when the wind is strong and shallower ones when the wind is weak. Nevertheless, the two models tend to differ for very shallow mixed layer. When the wind is very weak, the mixed layer in CLIO is virtually zero while it is always of a few meters when using the model of Veth.
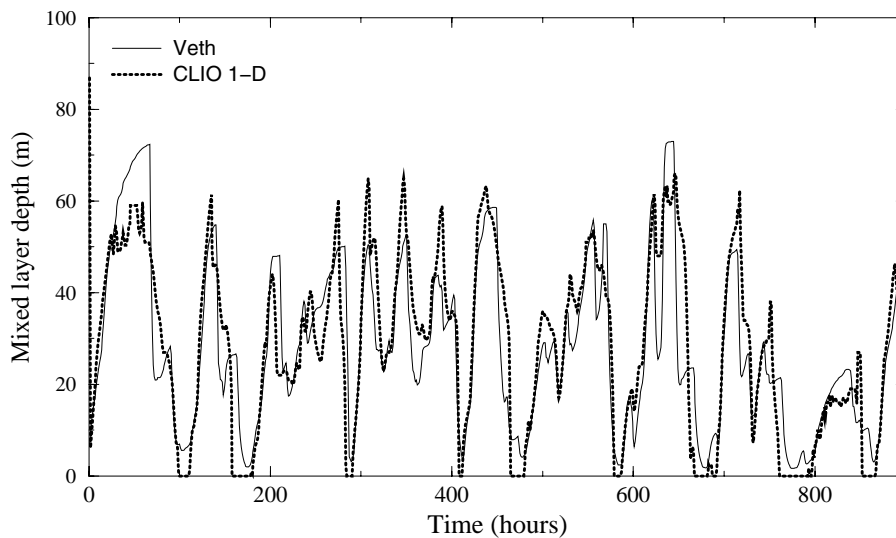
Figure 10: Comparison between mixed layer generated by CLIO-1D model and Veth's model at 47°S

C.2. Biogeochemical model SWAMCO

C.2.I. Model description

The biogeochemical model SWAMCO (Sea Water Microbial Community) of the C, N, Fe cycling through the Antarctic planktonic system, implemented during phases II and III of the Belgian Research Programme on the Antarctic (Lancelot et al., 1991a,b, 1993, 1997), was further developed for application at the scale of the Southern Ocean. The SWAMCO model upgrading included: integration of P and Si cycling; improvement of iron and grazing parameterisation; coupling with a chemical model of the carbonate system and air-sea exchange of CO_2; implementation of a parameterisation describing phytoplankton aggregation and sinking rate. Basics of the new SWAMCO parameterisations are shortly described below. Details can be found in Lancelot et al. (2000) and Hannon et al. (2001).

Biogenic elements

The biogeochemical description of the SWAMCO model was extended for considering explicitly (as discrete state variable) 3 major biogenic elements (N, P, Si) and dissolved iron (DFe). This biogeochemical resolution (**Figure 11**) allows for considering the nowadays well-admitted key role of iron in driving phytoplankton community dominance and related food-web structures and biogeochemical cycles in the Southern Ocean, and for simulating any nutrient limitation condition and shift

38

between limiting nutrients (including iron). P and Si parameterisation (nutrient uptake rates and cellular elemental ratios) was derived from literature and is reported in Lancelot *et al*. (2000). Current knowledge on nutrient co-limitation is also considered in the new SWAMCO version. For instance the observed increase of diatom silicification in response to iron-stress (Takeda, 1998); Hutchins and Bruland, 1998) is expressed by an empirical formulation relating the diatom Si:C elemental ratio to iron concentration. Also the ammonium inhibition of phytoplankton nitrate uptake is described by a non-competitive inhibition equation (Harrison et al., 1996) parameterised by Elskens et al. (1997). Both parametrisations can be found in Lancelot *et al*. (2000).

Parameterisation of iron limitation

One basic statement of SWAMCO is the distinction between two phytoplankton groups diatoms and autotrophic nanoflagellates (**Figure 11**) characterized by their own Fe physiology, i.e. cellular Fe requirements and kinetics parameters of Fe assimilation. This allows describing the observed ability of nanophytoplankton to outcompete large diatoms in the low-iron waters of the Southern Ocean, due to their higher affinity for dissolved iron uptake and their lower biochemical iron requirements (Sunda and Huntsman, 1995; Hutchins, 1995). The half-saturation constant for iron assimilation by autotrophic nanoflagellates is set to 0.3 nM. This value was derived from shipboard iron-enrichments (Boyd *et al*., submitted) in the Australasian sector, and recent laboratory-controlled studies of algal iron uptake mechanisms (M. Maldonado, pers. comm.). The half-saturation constant of diatom iron uptake (1.2 nM) was calculated from Fe-enrichment experiments conducted in the Atlantic sector of the Southern Ocean (Scharek et al., 1997) when assuming that Fe supply in a low Fe environment stimulates only the diatom component of the phytoplankton community. In agreement a concentration of 1.12 nM Fe was recently measured for cultivated Antarctic chain-forming diatoms (*Chaetoceros dichaeta*; Timmermans et al., 2001) suggesting that the kinetics of iron assimilation by micro-size Antarctic diatoms can be characterised by an half-saturation constant of 1-1.2 nM. Cellular Fe requirements (Fe:C) were estimated from literature (Morel, 1990; Brand, 1991; Sunda, 1991, Muggli et al., 1996) and fixed at 0.2 and 0.0025 mmol:mol for diatoms and autotrophic nanoflagellates respectively.

Sinking rate and aggregation processes

The previous version of the model (Lancelot et al., 1997) was implemented in a upper mixed layer physical frame. In this code, sinking of diatom and detrital particulate matter from the surface layer to the mesopelagic was expressed as a loss term and parameterised by a first-order constant. The upgraded SWAMCO model

now explicitly describes the downward transport of particles (diatoms, biogenic silica and detrital particles) through the water column, allowing simulation of vertical fluxes of particles. The standard version of the model considers a constant sinking rate of 1.0 m day^{-1}, based on mean sinking rates measurements of micro-size Antarctic diatoms (e.g. Waite and Nodder, 2001). Other parameterisations were implemented to explore possible mechanisms accelerating the downward carbon export from the upper ocean. On the one hand, the possible impact of iron stress on diatom sinking rates (Muggli et al., 1996) and the subsequent change in the magnitude of organic carbon export was investigated making use of different formulations (Hannon et al., 2001) derived from field measurements of iron replete and iron-depleted diatom sinking rate (Waite and Nodder, 2001). The role of diatom aggregation on the downward export of biogenic particles was on the other hand investigated (Hannon et al., 2001) by implementing the model of Kriest and Evans (1999) based on the model of Jackson (1990). Conceptually, this approach relies on an independent treatment of diatom cell abundance and biomass, each obeying its own conservation law. Average size and sinking rate of diatom-particle change as particles aggregate or the largest particles sink out. The size distribution of the diatom-derived aggregates is assumed to follow a hyperbolic law, whose exponent is a function of the average particle size.

Grazing parameterisation

Two formulations have been used to describe nanoflagellate and microzooplankton feeding (respectively on bacteria and nanoflagellates). The Holling-II (Michaelis-Menten function) formulation with a prey threshold was used in Lancelot *et al*. (2000). In the current version (Hannon *et al*., 2001) the Holling-III sigmoid function was preferred because it was shown to provide robust stabilization of low phytoplankton biomass typical of HNLC areas outside bloom period. Both formulations were parameterised according to a synthesis of grazing experiments for the Atlantic and Indian sector of the Southern Ocean (Becquevort, 1999).

Model of carbonate system and air-sea exchange of CO_2

A physico-chemical module describing the carbonate system in sea-water and air-sea exchange of CO_2 (Hannon et al., 2001) was coupled to the SWAMCO model (Lancelot et al., 2000) in order to estimate the efficiency of the biological pump of atmospheric CO_2 in the Southern Ocean. The module computes the speciation of the carbonate system, from dissolved inorganic carbon (DIC) and alkalinity of the surface water. The former is constrained by net carbon production i.e. the balance between net primary production and mineralisation. The calculated ΔpCO_2 (difference of CO_2 partial pressure between the atmosphere and the sea surface) and the wind velocity

drive the air-sea exchange of CO_2, following the Wanninkhof's (1992) relationship. The DIC budget is closed by a term of up-welling.
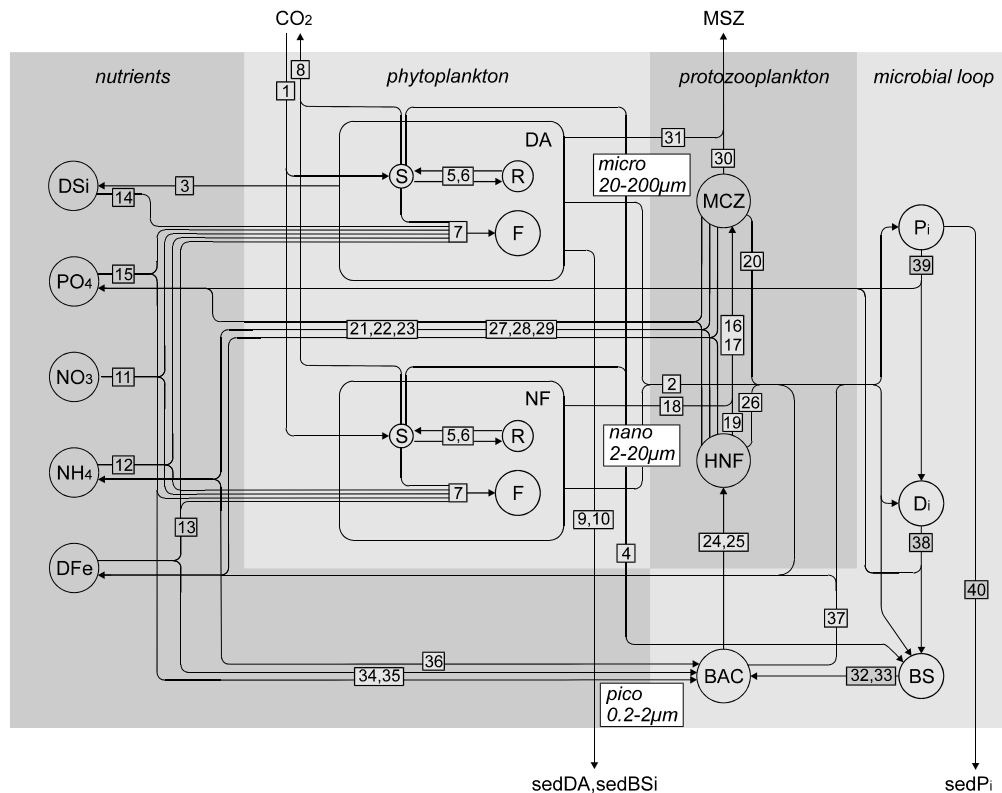

Figure 11: Structure of the biogeochemical SWAMCO model

C.2.II. Model runs

The SWAMCO model was first validated throughout its application to relevant polar expeditions such as the SO-JGOFS expedition ANT-X/6 and the *in situ* Southern Ocean Iron RElease Experiment (SOIREE). The ANT X/6 cruise of *R.V. Polarstern*), part of the Southern Ocean JGOFS programme, took place in the Atlantic sector (6°W) in austral spring 1992 (from early October to late November). The cruise investigated phytoplankton spring bloom development and related biogeochemical fluxes in different water masses: the Polar Frontal region, the open-ocean zone of the southern Antarctic Circumpolar Current, its boundary with the Weddell Gyre, and the marginal ice-zone. Addressed questions focused on the relative roles of physical stability, iron limitation, and grazing pressure in constraining phytoplankton development and associated export production and drawdown of atmospheric CO2 (Smetacek et al., 1997). The *in situ* mesoscale Southern Ocean iron-release experiment (SOIREE) was conducted in the Australasian-Pacific sector at 61°S, 140°E (south of the Polar Front and north of the southern Antarctic Circumpolar

Current Front), over 13 days in February 1999. The main issue of that cruise was the investigation of the response of pelagic biota to increased iron supply (Boyd et al., 2000). The experiment consisted in the iron fertilisation of an area of ~50km^2 and the subsequent monitoring of dissolved iron, auto- and heterotrophs and grazers biomass as well as biogeochemical parameters to assess the food-web response to iron enrichment, and biogeochemical implications (macro-nutrients and CO2 depletions, downward particle export).

For this purpose SWAMCO was implemented in an 'off-line' physical frame providing at each time step the depth of the upper mixed layer. The physical and chemical forcing functions and initial conditions used for these simulations were extracted from *in situ* observations.

The validated SWAMCO model was further 'on-line'coupled to the 1D-CLIO model of sea-ice and water column dynamics to simulate annual cycles of carbon and biogenic elements in different regions of the Southern Ocean with contrasted climatological conditions (**Table II**). A typical winter Fe concentration of 0.5 nM extracted from the existing data base of de Baar and de Jong (in press) was chosen as initial conditions. Ice-covered iron concentration of up to 1-5 nM were used for considering the surface water iron enrichment observed at the time of ice melting (Sedwick *et al*., 2000). The prediction capability of 1D-SWAMCO was first assessed through its application to the KERFIX site where biogeochemical time-serie data are available. As part of the French-JGOFS program, the time-serie station KERFIX, located in the Indian sector of the Southern Ocean south of the Polar Frontal Zone, 60 miles south-west of the Kerguelen Islands (50°40'S 68°25'E), was monthly sampled between January 1990 and March 1995 for the measurement of current hydrological and biogeochemical parameters (see description in Jeandel *et al*., 1998). This open ocean station was first implemented to assess interannual variability of parameters related to the carbon cycle in the Southern Ocean. This unique data set can be further used for testing the capability of biogeochemical models to reproduce the observed seasonal and interannual variability of CO_2 exchange at the sea-atmosphere interface.

Finally model scenarios and sensitivity analysis were conducted to investigate the relative role of wind, ice, iron, grazing on the functioning of the biological pump of atmospheric CO_2 in the Southern Ocean.

Table II: Selection of Southern Ocean sites for annual runs.

Site	latitude S	longitude W
KERFIX (Indian sector)	51°	291°
Ice-free Weddell Sea area	59°	49°
Seasonal ice zone of the Ross Sea	70°	180°

3. RESULTS AND DISCUSSIONS

A. CO_2 air-sea exchange

A.1. pCO_2 dynamics around the Kerguelen Archipelago

Until recently, coastal seas have been assumed to play a minor role in the global carbon cycle. However, the potential importance of this region at a global scale has been emphasized by numerous studies extensively reviewed by Walsh (1988), Wollast (1998) and Gattuso *et al.* (1998). In spite of the increasing interest for the role of coastal seas with regards to the increasing atmospheric concentration of carbon dioxide (CO_2), the question is whether the coastal sea is a net source or sink of atmospheric CO_2 is still a matter of debate (Smith, 1981; Wollast, 1983; Cleveland *et al.*, 1983; Walsh, 1991; Wollast, 1991; Smith and Hollibaugh, 1993). In fact, complexity and heterogeneity of the numerous and contrasted ecosystems of the coastal seas, as well as the sparsity of data sets, still stand in the way of settling the question once and for all. In the Southern Ocean, the question of the role of coastal area is even less assessed. However, coastal areas of the southern ocean (both Antarctic and Subantarctic) are productive with large phytoplanktonic blooms. This enhanced coastal primary production can strongly affect pCO_2 (Poisson *et al.*, 1993; Metzl *et al.*, 1995). However, with the exception of the works of Metzl *et al.* (1991), Poisson *et al.* (1993), Delille *et al.* (1997), Louanchi *et al.* (1999) and Delille *et al.* (2000b) around the Kerguelen archipelago and the study of Gibson and Trull (1999) in Antarctica, as far as we know there is no other study of pCO_2 in the coastal waters of the Southern Ocean.

We report here a budget of the annual air-sea exchange of CO_2 of the nearshore waters around Kerguelen Archipelago with the atmosphere. Attention has been paid to cover various sites from waters within fjords and semi-enclosed bay of the archipelago to offshore waters. In the same way, the role played by giant kelp beds of the archipelago has been examined and taken into account to budget annual fluxes of CO_2.

Seasonal changes of pCO_2 in the shallow waters of the Morbihan Gulf
In 1996 and 1997 seasonal evolutions of pCO_2 and related parameters have been investigated within shallow waters of the Morbihan Gulf near the base of Port aux Français (**Figure 12**).
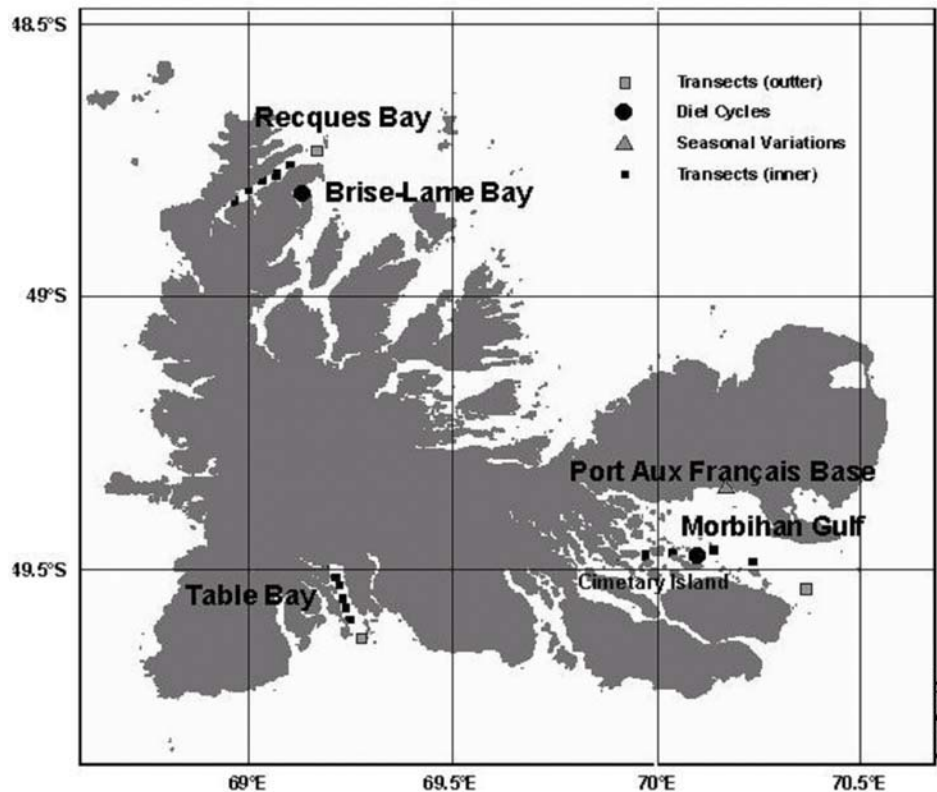
Figure 12: Sampling sites around the Kerguelen archipelago.

Biological parameters exhibit seasonal patterns, which allow one to distinguish the successive steps of the yearly biological turnover (**Figure 13**). The phytoplanktonic spring bloom is well marked and leads to a large depletion of NO_3^-+NO_2^- in October. This depletion is limited in time and mineralization start just after the end of spring phytoplanktonic bloom. From February to April, bacterial abundance reaches its highest level and the associated strong respiration leads to a strong increase of NO_3^-+NO_2^- concentration. This increase is weaker in winter, in good agreement with the decrease of bacterial abundance. But mineralization continues till the next bloom. In spite of an important temporal variability at the meso time-scale, partly due to physical processes or riverine inputs, pCO_2 variations over the year are large and exhibit seasonal patterns in which the different steps of the annual biological turnover are well marked (**Figure 13**).
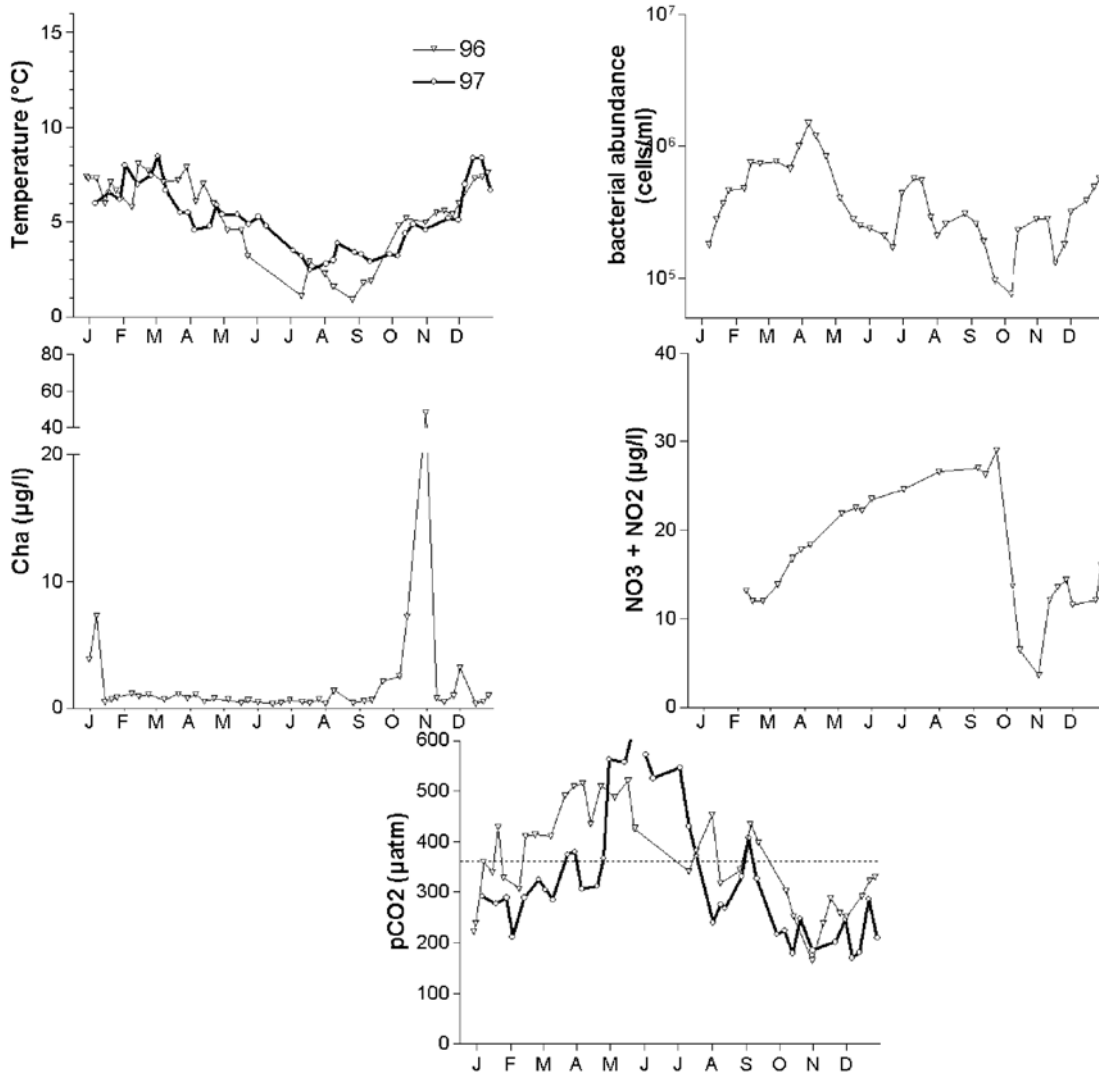
Figure 13: Seasonal changes of temperature, Cha, bacterial abundance, $NO_3^- + NO_2^-$ and pCO_2.

Development of phytoplanktonic blooms in spring and summer is responsible to marked undersaturations of pCO_2 (as low as 160 µatm) while decay of organic matter lead to large oversaturations (up to 640 µatm) in autumn and winter which illustrate the close coupling of pCO_2 and microbial activity in the shallow water of the archipelago and possible development of resuspension mechanisms.

Physical processes could greatly influence pCO_2 (particularly air- sea exchange which is enhanced by strong winds encountered in the archipelago), but, with the exception of winter time, influence of temperature variations and air-sea exchanges on pCO_2 are hidden by the magnitude of variations due to biological processes.

Thus, shallow waters of the Morbihan Gulf appear to be highly productive (both primary production and mineralization). This biological activity plays a leading role on inorganic carbon dynamics almost all the year.

Diel cycles over a Macrocystis kelp bed

A substantial proportion of coastlines of the Kerguelen archipelago is occupied by highly productive giant kelp bed *Macrocystis pyrifera*. These macroalgae are one of the largest and grow up to 50m in length, forming undersea forests in hard-bottom subtidal areas of subantarctic islands (Sfriso *et al.*, 1987; Lavery and McComb, 1991; Hanisak 1993). Macroalgae have great potential for biomass production and CO_2 uptake (Smith, 1981; Wilcox and North, 1988; Gao and McKinley, 1994). Smith (1981) pointed out that the coastal marine macrophyte ecosystems, including both macroalgae and seagrasses, occupy only about 2×10^6 km^2 but could act as an effective carbon sink. However, with the exception of the work by Frankignoulle and Distèche (1984, 1987) and Frankignoulle and Bouquegneau (1987, 1990) little is known on the influence of macrophytes on pCO_2 and their quantitative significance in the global carbon cycle is still poorly known (Gattuso *et al.*, 1998). Furthermore, in contrast to the numerous studies on the biology and primary productivity of polar microalgae, high latitude macroalgae have been little studied, although dense population of highly productive seaweeds are known from the Southern Ocean (Dunton and Dayton, 1995). Previous studies of pCO_2 dynamics above macrophytes have shown marked diel cycles (Frankignoulle and Distèche, 1984; Frankignoulle and Bouquegneau, 1990; Delille *et al.*, 1997). We have investigated in 1997 diel cycles of pCO_2 above some macrocystis kelp bed in the Morbihan Gulf and in the Brise-Lame Bay.

Figure 14 shows diel changes of pCO_2 normalized to a constant temperature of 5°C and a constant salinity of 33.4. The pCO_2 pattern inside the kelp beds exhibits clear trends excepted in winter.
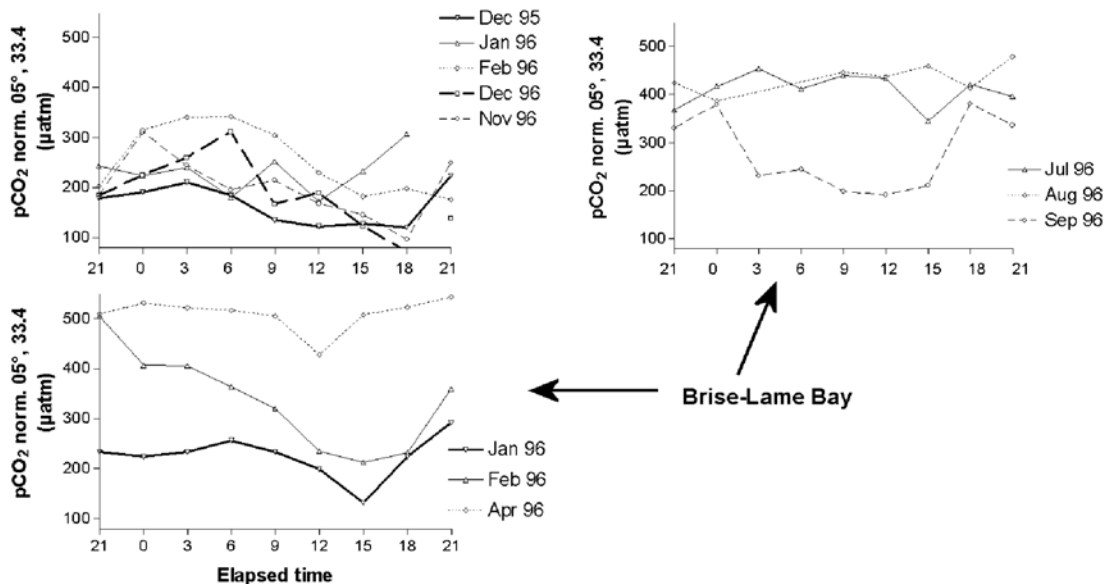

Figure 14: Diel cycle of normalized pCO_2 over Macrocystis kelp bed of Cemetery Island and Brise-Lame Bay.

From September to April, pCO_2 decreases during the day to reach a minimum at 12 p.m. or 3 p.m. and increases sharply at twilight. These diel pCO_2 oscillations illustrate the strong influence of the macrophyte's photosynthetic activity on pCO_2. In winter, when primary production of kelp bed is at its weakest, this control does not appear. Largest magnitudes of diel cycles of pCO_2 have been observed in December at the maximum of solar irradiance. High primary production leads to large changes in Dissolved Inorganic Carbon content (DIC) of the water above the macrocystis kelp bed. Maximum decrease of DIC is observed in December (up to 600 $\mu mol.kg^{-1}.d^{-1}$). Taking into account the height of water column (6m), this uptake of DIC corresponds to a gross primary production around 40 $gC.m^{-2}.d^{-1}$ (data not shown). In the same way, weekly measurements in front of the Port aux Français base yield to net primary production up to 4.2 $gC.m^{-2}.d^{-1}$ (Delille *et al.*, 2000b).

Seasonal changes of pCO₂ around the archipelago

In 1999, transects have been realized in three bays around the archipelago at different seasons. We present here average values corresponding of the five inner and the two outer sampling stations of each bay.

Seasonal changes of pCO_2 around Kerguelen Archipelago (**Figure 15**) range from 270 µatm to 580 µatm.
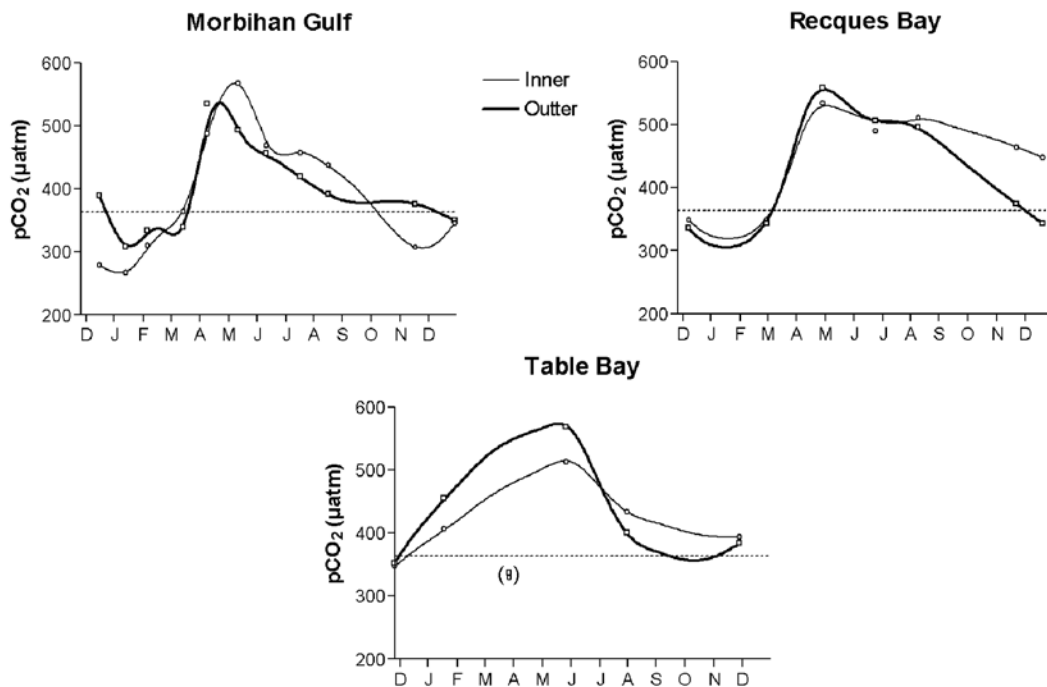
Figure 15: Seasonal changes of pCO_2 around the Kerguelen archipelago (thin line : inner stations, thick line : outer stations).

In the Morbihan Gulf, the seasonal pCO_2 pattern for inner stations is consistent with those obtained in 1996 and 1997 for the shallow waters of the Morbihan Gulf (**Figure 15**). Outside the Morbihan Gulf, the variability is weaker and minimal of pCO_2 values are reached later. In the same way, the overall pattern in the Recques Bay is similar to the one observed outside the Morbihan Gulf with a delayed bloom associated and subsequent decrease of pCO_2. Magnitude of seasonal changes is weaker inside than outside the bay. Table Bay can be submitted to large inputs of terrestrial fresh water as in March 1999 (values in brackets) where salinity was below 20 for the whole bay. Summer decrease of pCO_2 seems to be weaker for the Table Bay than for the other sampling sites. Magnitudes of seasonal changes are obviously weaker inside the bay than outside.

The Morbihan Bay appears to be the most productive site, with primary production starting earlier in the season. In the other sites, oversaturation of CO_2 is encountered for the larger part of the year and seasonal changes seem to be more marked outside the bays.

Annual air-sea exchange of CO_2

Table III shows the annually integrated air-sea fluxes computed from the wind speed at the meteorological station of Port aux Français. To compute these fluxes, we used the interpolated seasonal evolution of seawater pCO_2, water temperature and atmospheric CO_2 measured at Amsterdam Island (V.Kazan, personal communication). Since the choice of an algorithm for computation of air-sea fluxes of CO_2 is still a matter of debate, budget of CO_2 fluxes have been calculated using the different formulations in current use, i.e. Liss and Merlivat (1986), Wanninkhof (1992), Wanninkhof and McGillis (1999) and Nightingale *et al.* (2000).

Intensive surveys of pCO_2 of the waters surrounding the archipelago from Nov.1998 to Jan.1999 by way of underway measurement of pCO_2 have shown that the beginning of phytoplanktonic blooms and subsequent decrease of pCO_2 occur by the middle of December in the water outside the Morbihan Gulf (Delille *et al.*, 2000a). Thus, in spite of the lack of measurements from October to November 1998, our budget is probably only slightly biased. On the other hand, the phytoplanktonic bloom occurs in spring inside the Morbihan gulf and this season has been poorly covered in 1999. Hence our budget in the Morbihan gulf is probably overestimated. With the exception of shallow waters with annual air-sea exchange close to zero, waters of the Morbihan gulf appear to act as a net source of CO_2. In the same way, annual budget of CO_2 fluxes in the Recques Bay and Table Bay shows net efflux of CO_2 towards the atmosphere. On contrary macrocystis kelp beds appear to be a net sink of CO_2. Even if the integrated budget of CO_2 uptake above macrophytes of the archipelago appears to be of minor importance with regard to overall budget of the archipelago,

this uptake must be considered taking into account the world surface occupied by macrophytes i.e. $2*10^6$ km^2 (Smith, 1981).

Table III: Average flux (top) and net annually integrated air-sea echange (bottom) of CO_2 around the Kerguelen archipelago computed using the Liss and Merlivat (1986), Wanninkhof (1992), Wanninkhof and McGillis (1999) and Nightingale *et al.* (2000) formulations of the CO_2 exchange coefficient.

Site	Year	Liss & Merlivat (86) gC/m^2/yr	Wanninkhof (82) gC/m^2/yr	Wanninkhof & McGillis (99) gC/m^2/yr	Nightingale *et al.* (00) gC/m^2/yr
Morbihan Gulf - Cimetary island - Shallow waters	96	3.5	14.0	2.0	1.1
Deep waters (inner/outer)	98	19.8 - 21.2	40.4 - 43.6	57.7 - 63.3	26.7 - 28.6
Recques Bay (inner/outer)	99	58.5 - 43.9	120.7 - 90.3	177.9 - 131.8	79.2 - 59.3
Table Bay (inner/outer)	99	44.8 - 53.4	91.3 - 107.4	130.2 - 148.3	60.1 - 71.0
Macrocystis kelp bed	96	-9.5	-16.0	-15.4	-13.1
		MtC/yr	MtC/yr	MtC/yr	MtC/yr
Morbihan Gulf		0.012	0.026	0.037	0.017
South		0.018	0.036	0.05	0.024
East		0.023	0.048	0.068	0.031
North		0.094	0.194	0.285	0.127
West		0.014	0.03	0.043	0.02
Macrocystis kelp bed		-0.009	-0.016	-0.015	-0.013
Kerguelen Archipelago (bays and shelf above 50m)		**0.0152**	**0.317**	**0.468**	**0.206**

Many factors are susceptible to cause uncertainties in our calculations, however, seasonal patterns of pCO$_2$ in 1999 and integration of fluxes allow us to assess that on the whole nearshore (depth<50 m) waters surrounding the archipelago behave as a source of CO_2. This result is unexpected since the Southern Ocean is considered to be a sink of CO_2 (Metzl *et al.*, 1995; Takahashi *et al.*, 1997; Metzl *et al.*, 1999). Furthermore, the area near the Polar Front is generally considered as one of the most productive ones of the Southern Ocean and this production is enhanced in the plume of the Kerguelen archipelago. Taking into account that the average wind speed is rather constant over the year, succession of primary production and decay of organic matter, increase and decrease of temperature should lead to an annual budget close to zero. Therefore, this net imbalance of the annual budget of CO_2 fluxes is probably due to a large input of inorganic carbon. We have observed that terrestrial freshwater has a low content of DIC and that its run-off leads to strong decrease of pCO$_2$ (Delille *et al.*, 2000b). However, a terrestrial input of Particulate Organic Carbon (POC) or Dissolved Organic Carbon (DOC) could represent a substantial input of DIC, through mineralization, in the water column. But taking into

account that Delille and Perret (1991) have shown that terrestrial material is hardly mineralized in the water column, it appears that an input of inorganic carbon through the advection of offshore waters rich in CO_2 could be a valuable explanation of the imbalance. This enrichment could be due to an enhanced winter mixing as well as possible upwelling activity.

A.2. Distribution of pCO_2 in the Subantarctic zone of the Indian Ocean during spring and summer

The Southern Ocean is often assumed to be a significant CO_2 sink because it is an area where surface waters are cooled, air-sea exchange is enhanced by the regional high wind velocity and its surface area is large. The Subantarctic Ocean (both Subantarctic Zone -SAZ- and Polar Frontal Zone -PFZ-) is one of the most productive areas of the Southern Ocean. Primary production in spring and summer leads to strong decrease of pCO_2. Hence, the Subantarctic Ocean acts as a strong sink of CO_2 and its contribution to the overall uptake of CO_2 by the whole Southern Ocean appears to be essential. However, numerical models which investigate the global fate of CO_2 disagree significantly about the location and magnitude of the major sink areas. Furthermore, high biological activity of the Subantarctic ocean is likely to cause discrepancies in the estimates of CO_2 by the models. Therefore, assessment of CO_2 uptake by the Southern Ocean still requires direct measurement of pCO_2 as well as a better understanding of the major processes controlling the CO_2 distribution in the Subantarctic-Ocean.

From 1997 to 1999, six cruises have been undertaken (international JGOFS cruises, OISO cruise and several logistical cruises (**Table IV**) during spring and summer time in the Subantarctic zone (Crozet Basin) and south of Australia.

Table IV: Open ocean cruises in the period 1997 to 1999.

	Oct-Nov.	Dec.	Jan-Feb.	Mar.
Crozet Basin	**LC** (Logistical Cruise) *R/V Marion Dufresne*	**OISO 3** *R/V Marion Dufresne*	**ANTARES-4** *R/V Marion Dufresne*	
South Australia	**LC** *S/V Astrolabe*	**LC** *S/V Astrolabe*		**SAZ'98** *R/V Aurora Australis*

In early November, the Subtropical zone appeared to be undersaturated with respect to atmospheric pCO_2 and the lowest value was observed north of the Subtropical Front (STF) (**Figure 16**). A sharp decrease of CO_2 was also observed across the SAF, north of the Crozet archipelago. pCO_2 tended to increase southward and passed the threshold of saturation (~364 µatm) near the Kerguelen archipelago where the lowest values of SST were observed. However, in late December, the Kerguelen plateau appeared to be strongly undersaturated, undersaturation of the SAZ was enhanced and the Subtropical zone became oversaturated. Similarly, South of Australia, the Subantarctic Zone (SAZ) appeared to be undersaturated (320~340 µatm) in late summer. pCO_2 slightly increased across the SAF (340~350 µatm in the Polar Frontal Zone) to exceed saturation across the Polar Front (PF). In summer, oversaturation of Subtropical waters was enhanced, in contrast with the Subantarctic waters whose CO_2 content tended to decrease, reaching as low as 310 µatm. However, a patch of oversaturation was still present near the Crozet archipelago, as well as over the Kerguelen Plateau situated to the east of the plume of the archipelago. Furthermore, the strongest undersaturation (less than 295 µatm) has been observed north of the Agulhas Front (AF). South of Australia, both SAZ and PFZ were undersaturated. The undersaturation was enhanced in the SAZ, while pCO_2 increased towards the Polar Front. Nevertheless, pCO_2 in the SAZ tended to increase during March.

Observations in the Crozet Basin and South of Australia showed a similar pattern. pCO_2 was remarkably anti-correlated with SST and therefore varied contrary to thermodynamically constraint. Thus pCO_2 was quite sensitive to changes of water masses probably through their biological productivity. From spring to summer SAZ appeared to be strongly undersaturated. This undersaturation was enhanced from October to January and tended to decrease in March. Strongest undersaturation was observed just north of the AF. The PFZ appeared less undersaturated than the SAZ, and even in summer, oversaturation has been observed near the Crozet Island as well as in the eastern part of the Kerguelen Plateau. We feel that local physical (coastal upwelling activity) or biological processes at the continental margin or above the shelf might have a strong influence on pCO_2 content close to the Subantarctic coast.
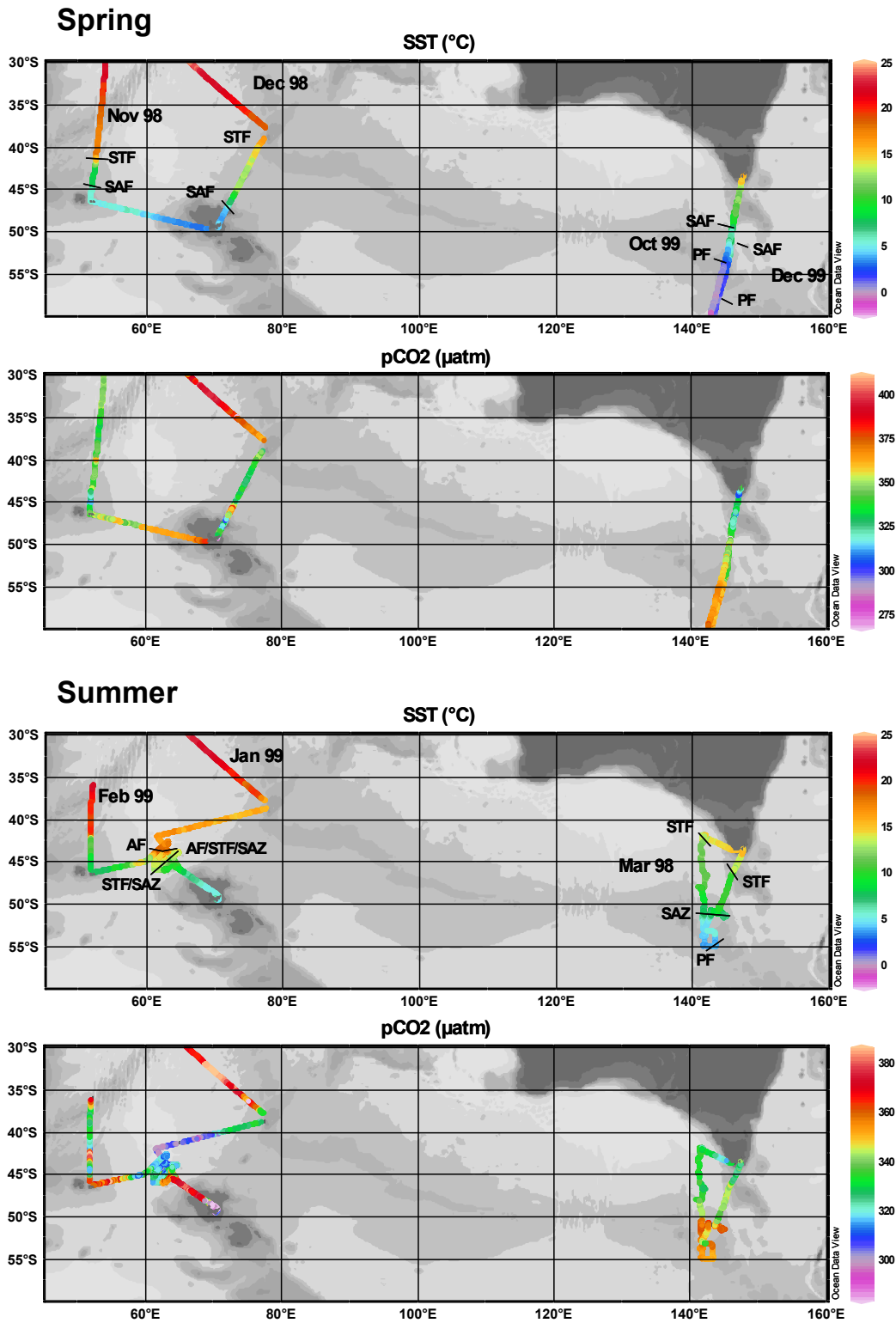
Figure 16: Distribution of SST and pCO2 during spring (top) and summer (bottom) in the Indian sector of the Southern Ocean

Mesoscale distribution of pCO_2

The Crozet Plateau area is characterised by the confluence of several fronts. The SAF is deflected northwards and converges with the STF. East of 50-52°E, the Agulhas Front (AF) joins the STF/SAF to form a triple front AF/STF/SAF. This front is referred as the "Crozet Front", which stands as one of the strongest fronts in the world ocean.

The ANTARES-4 cruise offered the opportunity to study the confluence of the three fronts at a resolution around 20km. pCO_2 (**Figure 17**) ranged from a slight oversaturation (up to 370 µatm) to a net undersaturation (down to 300µatm) with respect to atmospheric concentration of CO_2 (around 365 µatm).

pCO_2 distribution was obviously correlated to temperature and salinity. Meanders of the SAF/STF as well as AF appeared also clearly in the pCO_2 pattern. The SAF/STF defined a net decrease of the pCO_2 from saturation (360-370µatm) to undersaturation (320-325µatm). pCO_2 decreased northward to reach a minimum of 300 µatm across the AF. In subtropical waters, two small tongues of warmer water correspond to an increase of pCO_2 suggesting that pCO_2 increased towards the North accordingly to increase of temperature. It is worth to note that all the hydrological structures at meso-scale are remarkably well reproduced in the pCO_2 pattern. For example, it was perceptible in the south-eastern part of the studied area where a tongue of colder and less saline Subantarctic water is associated with an increase of pCO_2.

Figure 18 shows subsurface temperature, salinity, inorganic carbon concentration and related parameters along a cross frontal section. According to the definitions of Park *et al.* (1993) STF corresponds to a T-S range of 8-12°C and 34.6-35.0 at 200m with axial values of 10°C and 34.8, while SAF corresponds to a T-S range of 4-8°C and 34.1-34.5 at 200 m with axial values of 6°C and 34.3. In the studied zone, STF joined SAF and it is quite difficult to distinguish each other. Merged fronts extended from around 44°2S to 44°7S and were marked by strong gradients in temperature and salinity. From σ_t, we estimate that the pycnocline was situated around 80 m and 50 m (south and north of the fronts, respectively).
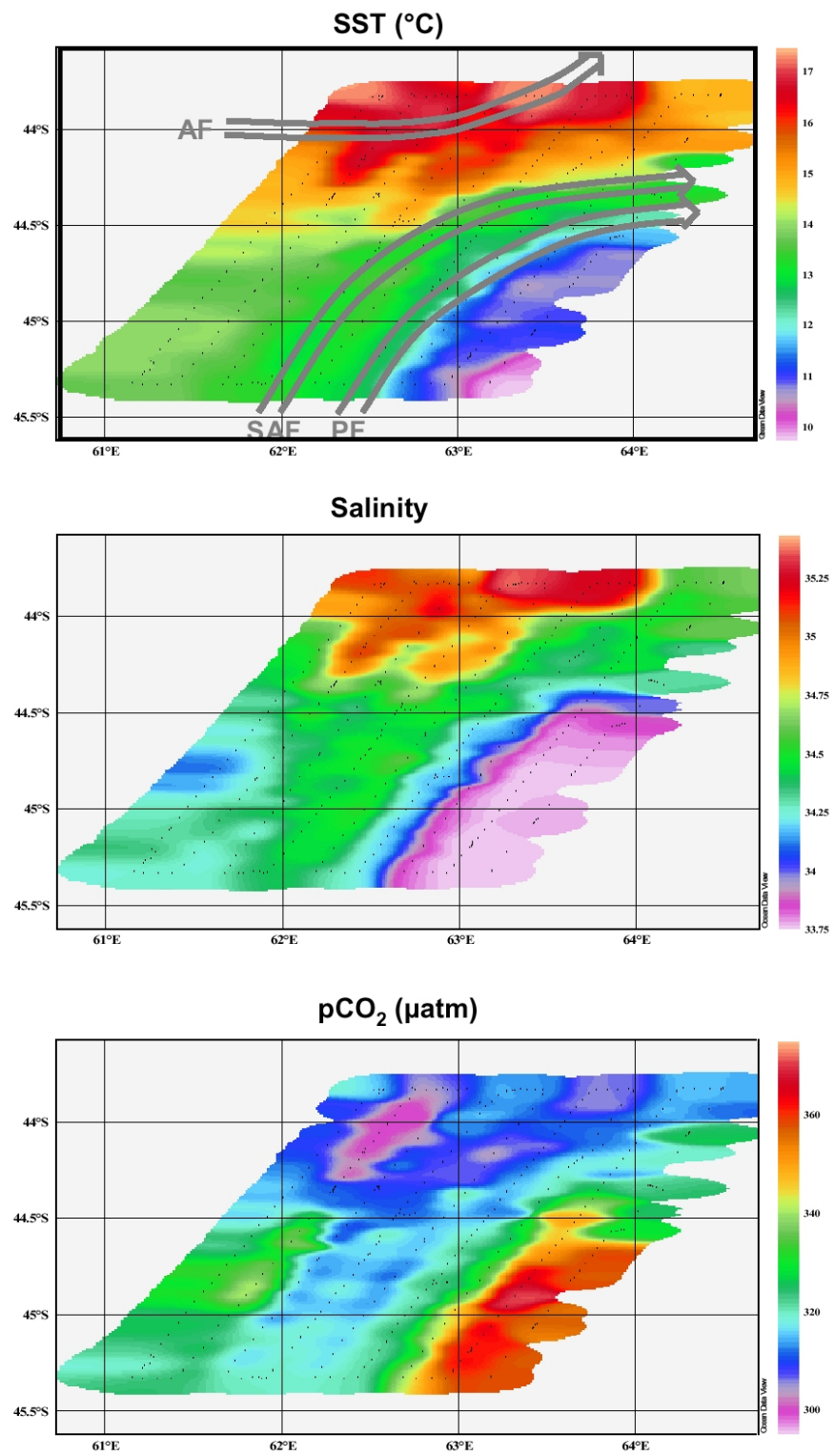
SST (°C)

Salinity

pCO$_2$ (µatm)

Figure 17: SST, Salinity and pCO$_2$ distributions for the ANTARES-4 studied area
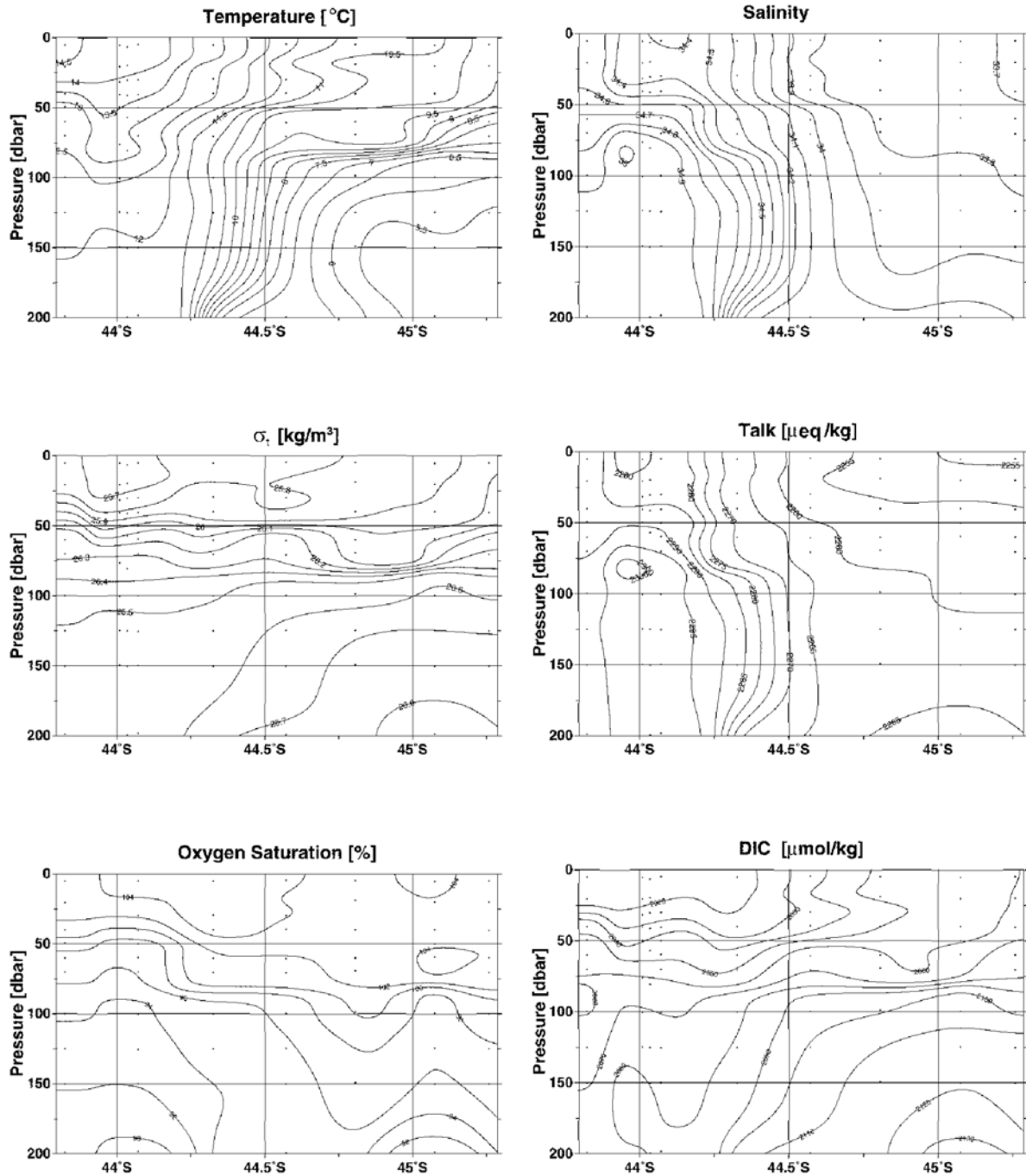
Figure 18: Vertical distribution of temperature, salinity, DIC and related parameters along a cross frontal transect.

As for surface distribution, the TAlk vertical profile is well superimposed upon the salinity pattern down to 800m (data not shown). This suggest that calcification/dissolution of carbonate is weak in surface water of the area. This is in accordance with a limited concentration of coccolithophorids susceptible to influence TAlk. In contrast DIC exhibits a different pattern with regard to salinity and TAlk.

Frontal structure was less marked and DIC decreased southward while salinity and TAlk increased. North and south of the front, one could notice marked gradients around the pycnocline depth. Vertical distribution of oxygen saturation exhibited a similar pattern with a transition from oversaturation to undersaturation at the pycnocline depth. This leads to believe that both increase of DIC and decrease of oxygen saturation is brought about through enhanced degradation of organic detritus at the depth of the pycnocline. Latitudinal distribution of DIC reflected the surface observation. Decrease of both DIC and pCO_2 towards the north is then probably due to phytoplankton blooming in spring and summer.

SST distribution and seasonal evolution of the fronts

The southward succession of distinct hydrological zones surrounding the Antarctic is a major characteristic of the Southern Ocean. The boundaries between these areas are clearly marked from a hydrological as well as a biogeochemical point of view. Hence, clear and detailed mapping of the Subantarctic Zone and in the Indian Sector was of vital importance in the way of assessment of budget of air-sea exchange of CO_2. Basic frontal zones are identifiable in the SST gradient field throughout the year. This gives an advantage in simultaneous viewing of the frontal pattern in the whole basin basing on satellite sea surface temperature (SST) data. SST from weekly global Advanced Very High Resolution Radiometer (AVHRR) data for the period of 1997-1999 is used to investigate seasonal variability of large-scale oceanic frontal zones in the Southern Indian Ocean delimited by 30-60°S and 20-150°E. Furthermore, SST fields have been used to establish pCO_2 fields from SST/pCO_2 relationships and thereafter to assess the air-sea exchange of CO_2 for the whole Subantarctic part of the Indian Ocean. Furthermore, from SST fields, SST gradients fields have been computed and used in order to investigate for the first time the structure and seasonal variability of the complete frontal system all over the Southern Indian Ocean based on the SST data.

Figure 19 presents the average position of the fronts estimated from SST gradient fields. This scheme in general corresponds to the known scheme presented by Belkin and Gordon (1996), but some details are different. Both the AFZ quasi-stationary meanders located at 26-27°E and at 32-33°E are not visible, because both are located in between the longitudes chosen for the analysis. From the other side the southward directed meander of the PFZ located directly at 30°E (Belkin and Gordon, 1996) for sure was not detected by the SST analysis. Their scheme shows that the North Subtropical Zone (NSTFZ) starts (or separates from the AFZ) at 50-60°E, but in the present analysis it was drawn from 40°E and far apart from the AFZ. Moreover the part of this frontal zone westward of 40°E is unclear due to low SST gradients observed. Sometimes it can be traced along latitude 34-35°S farther westward, where it reaches the AFZ rounding the coast of Africa. In other cases it
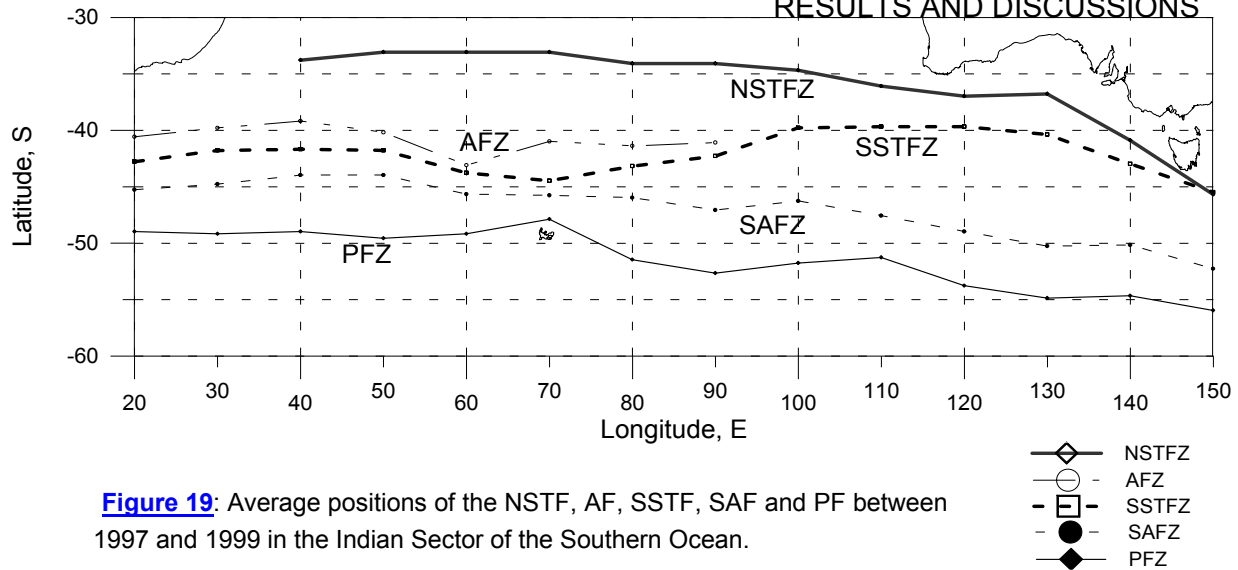
Figure 19: Average positions of the NSTF, AF, SSTF, SAF and PF between 1997 and 1999 in the Indian Sector of the Southern Ocean.

looks like merging the AFZ at the 30-35°E. At 50-60°E the AFZ, SSTFZ (South Subtropical Front) and SAFZ forms the single frontal zone called the "Crozet Front".

At Kerguelen longitude (70°E) a northward deflection of the AFZ from the Crozet Front was observed with the PFZ being northward from Kerguelen as an average position. It is close enough to the SSTFZ and Subantarcic Front Zone (SAFZ), for this triple (or quadruple in the case when the AFZ does not split out) frontal zone to be called the "Kerguelen Frontal Zone" in analogy with the Crozet Frontal Zone. From weekly maps, PFZ appears sometimes divided in two branches rounding Kerguelen Island; it was also occasionally located south of the island, and may even cross it. Such a behavior of the PFZ is in agreement with analogous cases described by Belkin and Gordon (1996). Moore *et al.* (1999) mapped the SST expression of the PFZ generally southward of Kerguelen, which may be explained by different years (1987-1993) analyzed and by the automatic method for the frontal zone mapping applied.

Farther eastward the frontal zones separate and only the AFZ, previously deflected from the Crozet Frontal Zone, merge with the SSTFZ between 90 and 100°E, which is a little bit far than mentioned by Belkin and Gordon (1996) The last difference between schemes concerns the merging region of the NSTFZ and SSTFZ and tracing of the resulting single Subtropical Frontal Zone. From the SST analysis they are well apart till 140°E (even the standard deviation bars are crossing out), which is 20-30° eastward than mentioned by Belkin and Gordon (1996).

Linear trends have been calculated for variations of the frontal zones position, SST, and SST gradients at every chosen longitude in 1997-1999. Trends in position may reach 0.0035^{o}lat./day for example for the AFZ at 90°E, which means that during three years an average position of the frontal zone shifted more than 3.5^{o}lat. It's interesting that all frontal zones exhibit such significant trends, but at different places and

sometimes with different signs. The same is valid for the SST trends showing in three years in average a change of $3^{o}C$. It's difficult to estimate the significance of the trends in the SST gradients due to their high variability, which reaches more than 50% of its mean value.

The inter-annual (1997-1999) linear trend (slope b) of the average position and of the average SST of the AFZ, NSTFZ, SSTFZ, SAFZ and PFZ in the Southern Indian Ocean at each chosen longitude have been establish in order to detect general motion of the frontal zone system northward or southward due to a climatic change in these years. It was surprisingly observed that in the western and eastern parts of the Southern Indian Ocean the trends of the frontal zones position differ significantly (are higher) with respect to its central part. This is better seen for the SST trends, where trends are positive at both sides of the region and negative in the central part, which represents a wave-like structure. This means that in the present case there is no usually expected northward or southward movement of the frontal zones due to a climatic change, but a signature of a planetary wave was observed probably. Such a planetary wave called the Antarctic Circumpolar Wave does exist (White and Peterson, 1996. The characteristic feature of the wave is a propagation of the anomalies eastward with the circumpolar flow with a period of 4-5 years and taking 8-10 years to round the pole. The wave was detected in our study using a different approach.

Integrated air-sea exchanges of CO_2

Scarcity of pCO_2 data is one of the main difficulties for computing overall air-sea exchanges. A simple solution involves finding a relationship between pCO_2 and other oceanic properties for constraining continuous pCO_2 fields. In this context, the pCO_2/SST relationship appears useful since SST is one of the only oceanic parameter available on weekly and planetary scale. Tans *et al.* (1990) and Metzl *et al.* (1995) use pCO_2/SST relationship and SST climatology to construct seasonal pCO_2 fields.

Our dataset allows us to focus on two seasons (spring and winter). **Figure 20** presents our overall observations made from 1997 to 1999. To extract a large-scale structure we have eliminated the data for the coastal regions (Crozet and Amsterdam Island, Kerguelen plateau, Tasmania). We applied these equations to the monthly SST fields obtained from remote sensing with a $0.2° \times 0.2°$ resolution. Then we computed monthly air-sea fluxes fields using monthly wind speed fields obtained from ERS 2 scatterometer, whose measurements are consistent with wind speed measurements from Carioca buoys deployed in the SAZ Indian sector (Merlivat, personal communication). We used the gas transfer coefficients of Liss and Merlivat (1986), Wanninkhof (1992), Wanninkhof and McGillis (1999) and Nightingale *et al.* (2000).
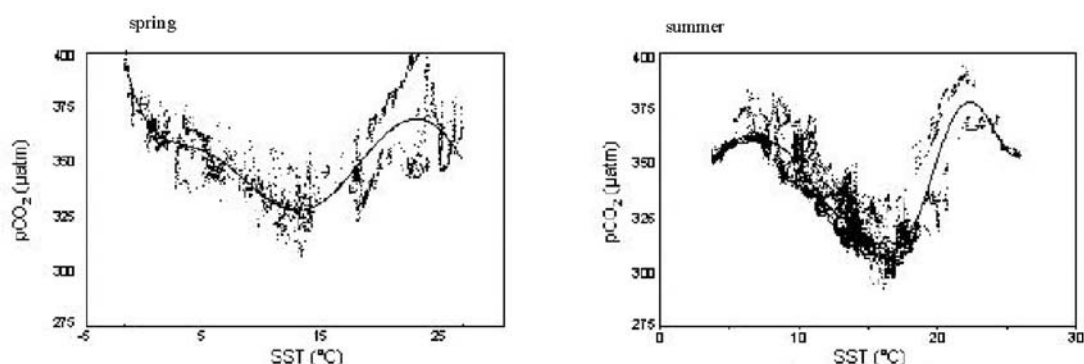
Figure 20: pCO$_2$ versus SST diagrams for open ocean environments (left: spring – right: summer). The regression is also shown.

Table V presents the average fluxes. For the whole region 50°S-35°S, the mean air-sea flux of CO$_2$ computed using the gas transfer coefficient of Liss et Merlivat (1986) is around –2.26 mmol.m^{-2}.d^{-1} in summer. This result agrees well with the fluxes computed for the same area by Metzl et al. (1995) in January-February 1991 (-2.8 mmol.m^{-2}.d^{-1}) and in January 1992 (-2.7 mmol.m^{-2}.d^{-1}).

Table V: Averaged and integrated air-sea flux of CO$_2$ over the different zones of the subantarctic ocean. Fluxes were computed using the gas transferts coefficients of Liss and Merlivat (1986), Wanninkhof (1992), Wanninkhof and McGillis (1999) and Nightingale *et al.* (2000).

Average Flux (mmol/m^2/d)	Liss & Merlivat (86)		Wanninkhof (82)		Wanninkhof & McGillis (99)		Nightingale *et al.* (00)	
	Spring	Summer	Spring	Summer	Spring	Summer	Spring	Summer
STZ	-1.05	-0.55	-2.01	-1.04	-2.00	-1.06	-1.39	-0.72
NSAZ	-2.46	-2.15	-4.86	-4.13	-6.12	-4.58	-3.27	-2.82
SSAZ	-3.27	-3.09	-6.75	-6.24	-9.87	-8.61	-4.45	-4.14
PFZ	-1.32	-0.56	-2.86	-1.19	-4.74	-1.91	-1.85	-0.77
POOZ	0.16	-1.14	0.33	-2.48	0.47	-4.19	0.22	-1.61
35°-50°S	-2.53	-2.26	-5.14	-4.46	-7.14	-5.58	-3.41	-3.00
Integrated Flux (GtC)								
NSAZ	-0.022	-0.019	-0.044	-0.036	-0.055	-0.040	-0.029	-0.025
SSAZ	-0.020	-0.019	-0.042	-0.039	-0.061	-0.053	-0.027	-0.026
PFZ	-0.007	-0.003	-0.015	-0.006	-0.025	-0.010	-0.010	-0.004
35°-50°S	-0.051	-0.045	-0.102	-0.089	-0.141	-0.111	-0.068	-0.060

Furthermore, we distinguished different areas through analysis of SST fields and computed an average and overall air-sea exchange for each of them i.e. the STZ; north of the NSTF, the North Subantarctic Zone (NSAZ); north of the SSTF, the South Subantarctic Zone (SSAZ); north of the SAF, the PFZ) north of the PF, and the POOZ south of the PF. Since we have only partly sampled the Subtropical Zone

(STZ and POOZ, average fluxes for both areas must be considered with care and no integration was attempted.

With the exception of the PFZ and POOZ, differences between spring and summer time are weak. STZ, NSAZ, SSAZ, act as net CO_2 sinks. This sink is enhanced towards the SAF.

On the whole, the overall flux of CO_2 for the 35°S~50°S band of the southern ocean (from 20°E to 150°E) depends mainly on the gas transfer coefficient used and ranges from **-0.051 to -0.141 Gt** in spring and from **-0.045 to -0.111 Gt** in summer.

B. The Biological pump

The efficiency of the biological pump in extracting carbon from the surface waters and in translocating this carbon to deeper waters is set not only by the level of primary production, but also by the dominant phytoplanktonic groups which affect the structure of the pelagic food web (carbon retention -microbial food-web versus export-classical linear food chain).

Nowadays there is little doubt that iron availability plays a pivotal role in structuring the phytoplankton community of the Southern Ocean. Low Fe supply is indeed limiting the growth rate of large diatoms while still sufficient for the development of pico-and nanosized cells, which are better competitors at low nutrient concentrations. Besides iron, light, silicon and to some extent ammonium availability are currently reported as important co-limiting factors of phytoplankton growth (Armstrong, 1999; Boyd et al., 2000).

The relative importance of new versus regenerated production as a function of plankton community structure, as well as ammonium-iron interactions in regulating phytoplankton N-uptake conditions (*f*-ratio) were investigated in the Subantarctic and Polar Front Zones along 142°E, south of Australia, during summer 1998 (chapter **B.2**). The iron and light interactions with phytoplankton growth have been investigated in the PFZ and the ACC of the Atlantic sector, during autumn 1999 (see chapter **B.1**).

B.1. Light and Iron control of phytoplankton growth

The Fe and light control of phytoplankton growth were studied by means of radiotracer incubation experiments during *ANT XVI/3* expedition (summer 1999). Photosynthesis, growth and Fe uptake were measured for the different autumnal

phytoplankton communities encountered at Stations 185, 190 and 198 experiencing dissolved Fe concentrations between 0.15 nM and 0.33 nM (**Table VI**).

Table VI: Description of the sampled stations.

	Station 185	**Station 190**	**Station 198**
Sampling Date	21 April	25 April	3 May
Position	67°00'S, 00°01'E CC Marginal Ice Zone	54°02'S, 19°58'E ACC Open Ocean Zone	51°29'S, 20°01'E ACC Open Ocean Zone
Sampling depth (m)	40 Upper mixed layer	40 Upper mixed layer	60 Upper mixed layer
Chl$a$ (µg liter^{-1})	0.12	0.28	0.51
Dissolved Fe (nM)	0.33	0.30	0.15
Total Phytoplankton abundance (10^3 cells liter^{-1})	73	130	357
Phytoplankton>10µm abundance (10^3 cells liter^{-1})	3.5	5.0	97.2

Iron assimilation and the carbon metabolism are interrelated by several ways (see Geider and La Roche, 1994, for review). Iron is an essential micronutrient for phytoplankton growth. It is found in the active sites of many photosynthetic and respiratory electron carriers, including cytochromes, hemes, and Fe-sulfur proteins such as ferredoxin. Several steps in the synthesis of chlorophyll are iron-dependent. It is essential in nitrogen acquisition systems as a component of nitrate and nitrite reductases and nitrogenase. Fe-containing proteins are also needed in other biosynthetic and degradative reactions, including those involved in detoxification of O_2 radicals.

Iron chemistry in seawater is complex and still not fully understood. Moreover, phytoplankton species may have different Fe uptake strategies: the uptake of Fe' by membrane bound porter sites (Hudson and Morel, 1990), the uptake of Fe-siderophore chelates (Trick *et al.*, 1983), extracellular reduction (Maldonado and Price, 1999), excess (or luxury) uptake and storage (Sunda and Huntsman, 1995), and solid-phase Fe acquisition (Kuma *et al.*, 1999). The finding that more than 99% of dissolved Fe is complexed by organic ligands in natural seawater (Gledhill and van den Berg, 1994; Rue and Bruland, 1995) implies that inorganic Fe concentrations are not sufficient to sustain growth of even small phytoplankton species (Wells *et al.*, 1995) so that other chemical forms of Fe should be available. Both the lack of

knowledge of Fe chemistry in seawater combined to the diversity in the phytoplankton Fe uptake strategies render it impossible nowadays to quantify bioavailable Fe. In this work, we consider dissolved Fe (organic and inorganic) as an approximation of the potential available Fe.

B.1.I. Characterization of the sampled stations

In this report we focus on the comparison of the results obtained at Station 185 (**Table VI**), located in the Antarctic Coastal Current close to the edge of the Antarctic continent, and at Stations 190 and 198 sampled in the Antarctic Circumpolar Current. Chlorophyll *a* as well as the phytoplankton abundance were the lowest at Station 185 and the highest at Station 198 (**Table VI**). The phytoplankton community was essentially composed of nanophytoplankton <10µm (>95% in terms of abundance) dominated by Chrysomonadales at Station 185 and Station 190. At Station 198, the larger phytoplankton species (>10µm) represented as much as ca. 30% of the total phytoplankton abundance and were dominated by *Pseudonitzschia helmii*.

B.1.II. C and Fe metabolism of autumn phytoplankton

Photosynthesis

Photosynthesis-irradiance data are shown in **Figure 21** and the photosynthetic parameters given in **Table VII**. These parameters are within the range of values previously observed in the Southern Ocean (Smith and Sakshaug, 1990; Mathot, 1993).
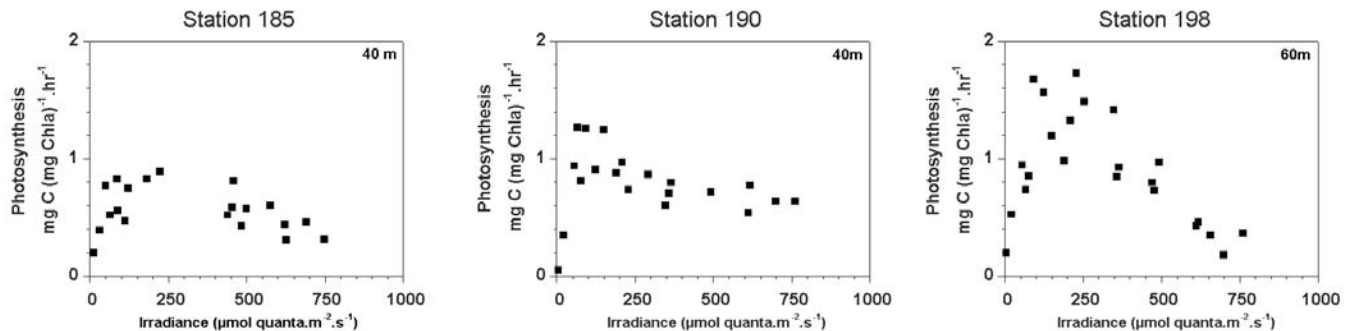
Figure 21: Photosynthesis-irradiance relationships at Station 185, Station190 and Station 198.

The maximum realized photosynthesis rate, P_m, were similar at Stn 185 and Stn 190 and was relatively higher at Stn 198. Similar photosynthetic efficiencies were found at Stn 185 and 198. It was relatively higher at Stn 190. The susceptibility to photoinhibition was very intense for the phytoplankton community collected at Stn 198 compared to those observed at Station 185 and 198. All these samples were collected in the upper mixed layer (**Table VII**).

Table VII: Photosynthetic parameters at the sampled stations.

		Station 185	Station 190	Station 198
Pmax	mg C $(mg\ Chla)^{-1}\ hr^{-1}$	1.09	1.18	9.7
α	mg C $(mg\ Chla)^{-1}\ hr^{-1}(mmol\ quanta\ m^{-2}s^{-1})$	0.016	0.038	0.022
β	mg C $(mg\ Chla)^{-1}\ hr^{-1}(mmol\ quanta\ m^{-2}s^{-1})$	0.0016	0.0012	0.0432
Pm	mg C $(mg\ Chla)^{-1}\ hr^{-1}$	0.79	1.02	1.46
Ek	$\mu mol\ quanta\ m^{-2}\,s^{-1}$	49	27	66

Under Fe-limited conditions, the photosynthetic performance of phytoplankton cells may decline. Cells show a decrease in their pigment content and photosynthetic efficiency (van Leeuwe and Stefels, 1998). Fe limitation can also lead to the suppression of the synthesis of photoprotectors resulting in the absorption of excess excitation energy under high light conditions. Superoxide radicals can then be formed, inducing the formation of aggressive H_2O_2. Moreover, the catalase necessary for the breakdown of H_2O_2 also demands Fe (Geider and LaRoche, 1994). Consequently, the exposure to high light intensities can induce photodamage in Fe-limited cells.

Larger phytoplankton is more susceptible to Fe limitation. Small cells have larger surface area to volume ratios and better diffusional characteristics which make them more competitive under low Fe concentrations than the larger cells (Sunda and Huntsman, 1995). K_m values for growth of small cells of diatoms were found to be about three orders of magnitude lower than for larger diatoms (Timmermans *et al.*, 2001).

The strong photoinhibition observed at Stn 198 could reflect Fe limitation of the present phytoplankton community which is composed of relatively more species >10μm than Station 185 and 190 and experienced lower dissolved Fe concentrations (**Table VI**). The relatively high Chl*a* concentration observed at this station combined with the relatively low dissolved Fe concentration suggest that Station 198 sampling corresponds to a post-bloom situation.

Fe uptake and growth

The mechanisms of Fe uptake were studied in relationship to light and ambient concentrations of Fe. Two pools of Fe are linked to the phytoplankton cells: the extracellular Fe, linked to the external side of the cellular membrane and the assimilated intracellular Fe. The Fe assimilation was measured simultaneously to the carbon assimilation into four pools of cellular constituents (lipids, small metabolites, polysaccharides and proteins). Proteins constitute a good index of phytoplankton growth (Cuhel *et al.*, 1984; Lancelot *et al.*, 1986). One of the objectives of this

experiment was to determine if the Fe assimilation and the C fixation into the proteins are interrelated. Additional enrichment experiments were performed in order to test the importance of Fe limitation for the collected phytoplankton assemblage. The Fe:C fixed into proteins ratios were estimated and their variation studied in function of light and the dissolved Fe concentrations.

- Kinetic experiments

The total and intracellular Fe uptake was linear in relation to the incubation time both in the light and in the dark for all the experiments. **Figure 22a and 22b** show the results of the experiment conducted at Station 185 as a typical example.

Even if both total and intracellular uptake continued in the darkness, their uptake rates decreased in the dark compared to those in the light. The intracellular uptake rates in the dark represented only 40 to 50% of the uptake in the light for all the experiments (Station 185, 190 and 198). On the contrary, whereas the extracellular uptake rates in the dark only represented 10 to 20% of the one in the light at Station 185 and Station 190, at Station 196, the extracellular uptake rates stayed relatively high in the dark (70% compared to light).
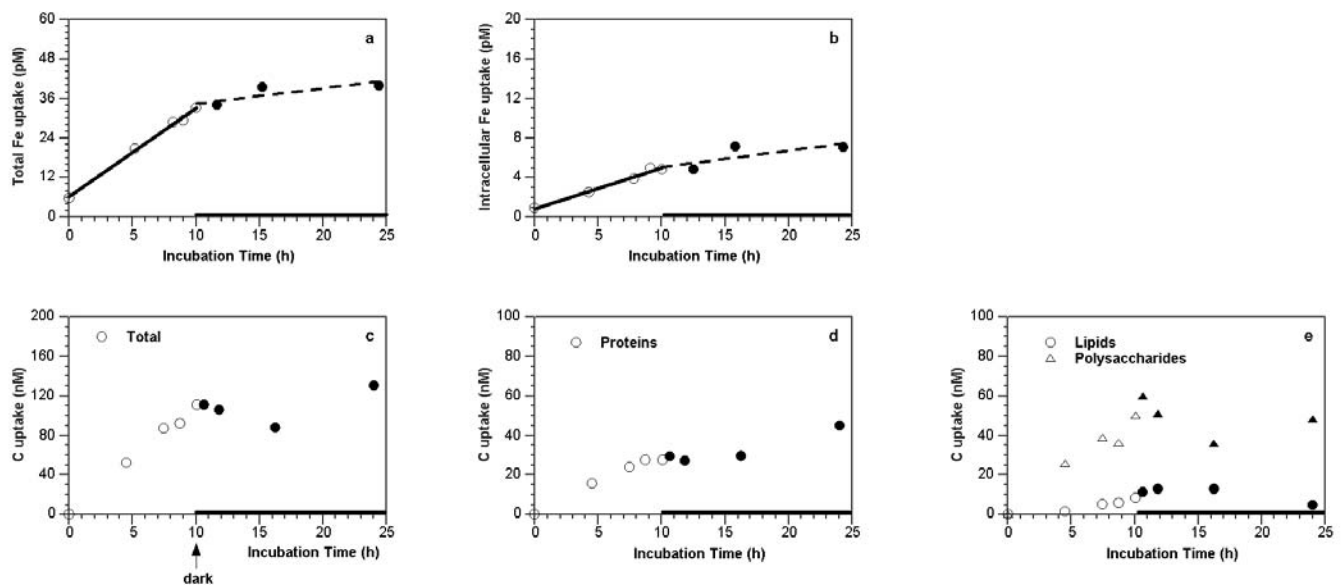
Figure 22: Uptake at Station 185 of the total Fe uptake (a), intracellular Fe uptake (b), total carbon, (c), carbon into proteins (d) and carbon into lipids and polysaccharides (e) in relation to incubation time on a 10h:14h light:dark cycle.

At Station 198, most of the extracellular uptake (ca. 80%) was due to phytoplankton >10µm. Only 20% of the extracellular uptake was attributed to phytoplankton sizing between 0.8 and 10µm, as shown by the fractionation on 0.8 and 10µm filters (**Figure 23**). At Station 185 and 190, most of this extracellular uptake occurred in the

smaller fraction (60 to 70 %). The extracellular Fe uptake could depend on Fe speciation and on its bioavailability. On one hand, Fe is photoreduced in the light which can increase its availability to the cells (Sunda, 1994). On the other hand, some phytoplankton species have reductases on the external surface of their membrane (Volker and Wolf-Gladrow, 1998). By this mechanism, the larger phytoplankton species of Station 196 could have access to much Fe under light and dark conditions. The results of the total carbon fixed and the carbon bound specifically to proteins, lipids and polysaccharides are shown for Station 185 in **Figure 22 (d and e)**. For the assimilation of Fe, the phytoplankton maintains incorporation of carbon into proteins (**Figure 22d**) in the dark at the expense of polysaccharides and lipids (**Figure 22e**), which are well known storage products used to maintain protein synthesis (Lancelot *et al.*, 1986).

Station 185	Station 190	Station 198

Intracellular Uptake

Extracellular Uptake
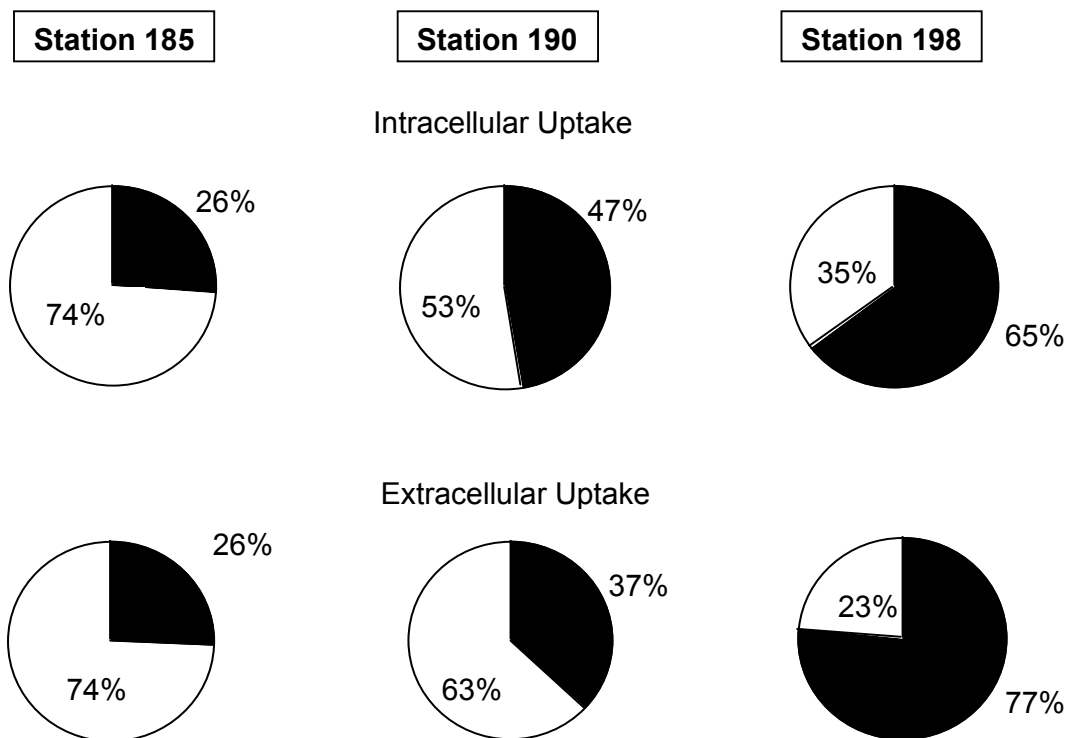
Figure 23: Intracellular and extracellular percentages of the Fe uptake by small nanoflagellates (<10µm) in white and larger phytoplankton (>10µm) in black at Station 185, 190 and 198.

- Response to Fe enrichment
Results of the Fe uptake for the enrichment experiments at Station 185 and Station 198 are shown in **Figure 24 (a to d)**. Contrary to the results obtained at Station 198, where a steep linear increase of the total and intracellular uptake is observed for the tested concentrations (up to 1 nM), no clear increase was observed for the

experiment at Station 185. As a consequence of the data points scatter, the half saturation constant for the Fe assimilation at Station 185 is estimated between 0.3 and 0.8 nM dissolved Fe. These results suggest that in contrast to the phytoplankton assemblage collected at Station 185 which is essentially composed of small species of phytoplankton (<10μm), the phytoplankton community, constituted by larger species >10μm, at Station 198 was limited by the ambient dissolved Fe concentration (0.15nM, see **Table VII**).
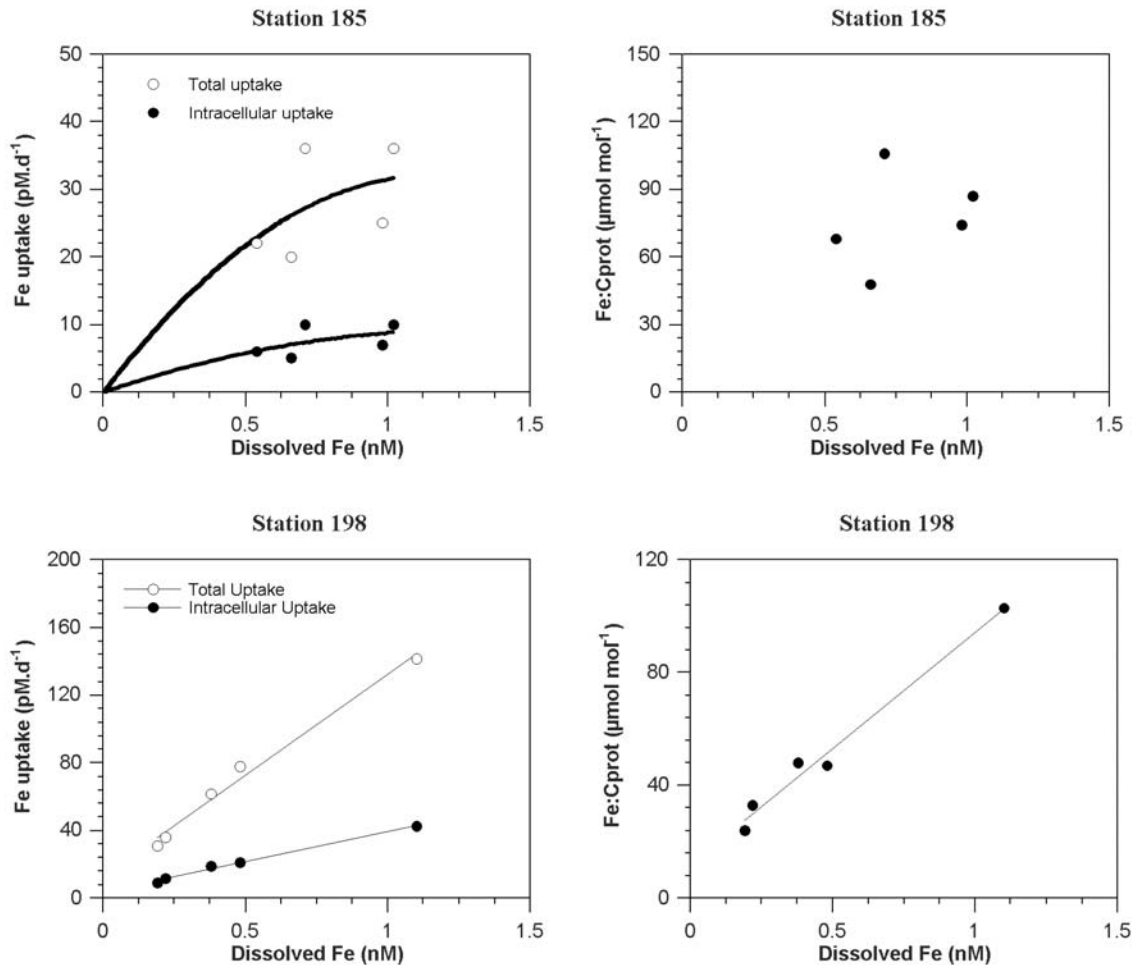
Figure 24: Effects of Fe addition on the Total and intracellular Fe uptake at stations 185 (a) and 198 (b) and Fe:C into proteins ratios at stations 185 (c) and 198 (d).

- Fe:C uptake ratios
The Fe:C cellular ratios were estimated on a cell protein basis (Fe:C-prot, **Table VIII**). Similar ratios were observed at Station 185 and 190, whereas lower ratios were estimated at Station 198. No increase was observed after Fe enrichment at the

former station (**Figure 24c**). On the contrary, these ratios increased linearly with the added dissolved Fe at Station 198, suggesting Fe limitation here. Relatively close values of these ratios were calculated in the light and in the dark (**Table VIII**) indicating that intracellular Fe uptake could be directly linked to the C assimilated into proteins and consequently to the phytoplankton growth.

Table VIII: Fe: C fixed into proteins uptake ratios at station 185, 190 and 198.

Fe:Cprot (µmol:mol)	Station 185	Station 190	Station 198
Light	127	156	32
Dark	156	116	42

B.2. Nitrogen uptake regime: f-ratio and new production

In this section we present the results concerning the late summer, early fall nitrogen-uptake regime as observed in the Subantarctic and Polar Front Zones south of Australia, during the SAZ'98 expedition.

Assuming no regeneration of nitrogen and no loss of dissolved and particulate nitrogen during the incubations (i.e. a simplified steady state approach), the uptake rate of a nitrogen compound can be expressed as follows (Dugdale and Goering (1967):

$$\overline{U}_i = \frac{PN_t.(\alpha_{pni,t} - \alpha_n)}{t.(\alpha_{dni,0} - \alpha_n)} \qquad (12)$$

where is uptake rate of nitrogen compound i (nitrate, ammonium or urea); $\alpha_{pni,t}$ the isotopic abundance in the particulate phase at the end of the incubation; α_n, the natural ^{15}N abundance; t, the duration of the incubation; $\alpha_{dni,0}$, the initial isotopic abundance in the solution at time zero.

In **Figure 25** we compare observed conditions of nutrient and PN concentrations at incubation stop with calculated conditions based on the simplified steady state approach of Dugdale and Goering (1967). In this comparison, the principal interest is the identification of systematic errors that can occur when the underlying assumptions of the steady state approach are not completely valid, as would be the case if (i) substrate pools show a net change over time as a result of consumption and production, and (ii) decrease of nitrogen from the substrate pools is not balanced by an equal increase of nitrogen in the particulate pool.
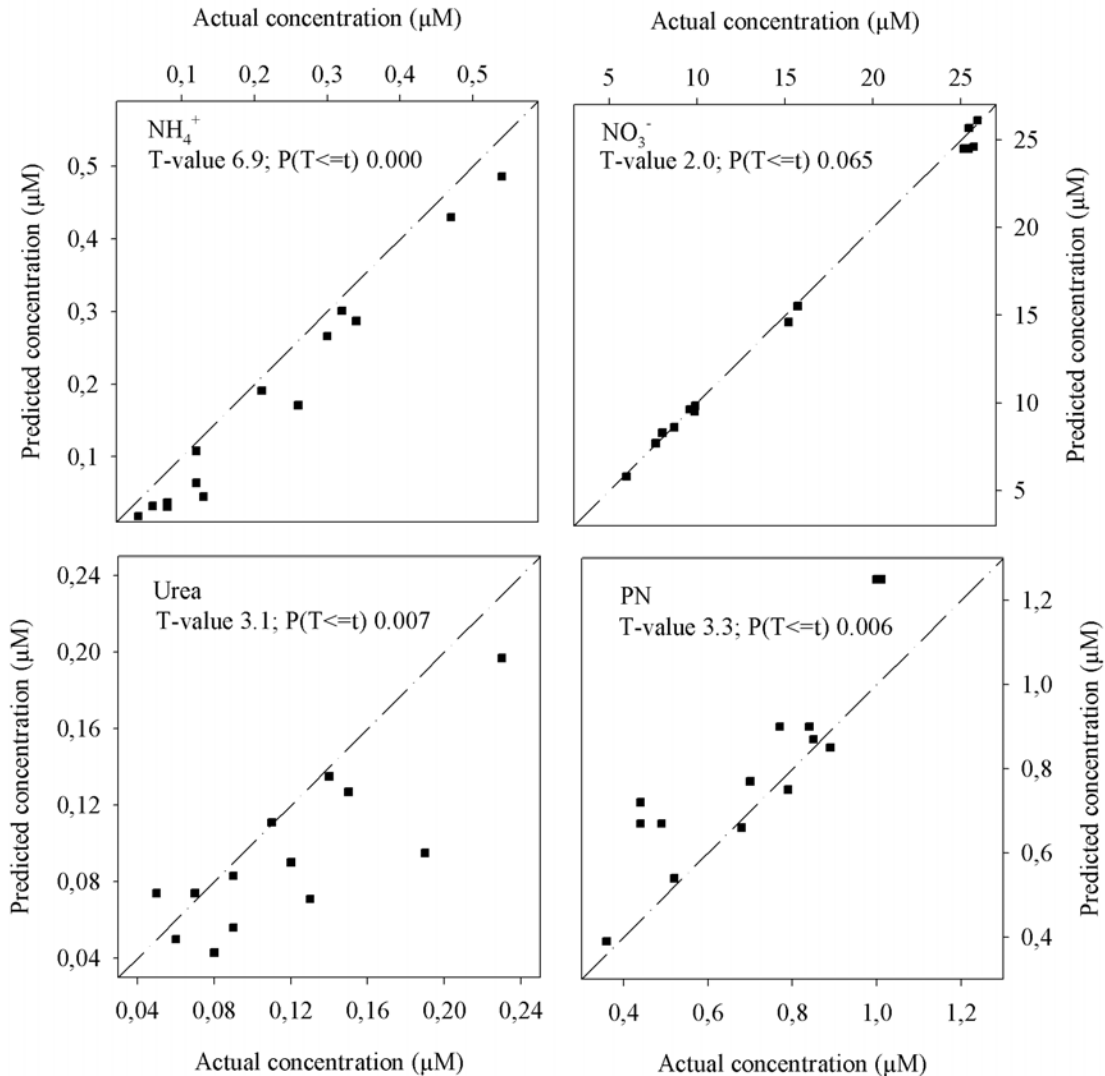
Figure 25: Plots of actual nitrogen concentrations *versus* predicted values as derived from the equation of Dugdale and Goering (1967). The dashed line shows 1:1 relationship. Text gives the results of a paired *t*-test (alpha = 0.05) and the related probability

As shown in **Figure 25**, mass balance was not achieved in most uptake experiments. For ammonium and urea, predicted concentrations were consistently lower than observed ones, suggesting that regeneration and loss rates from the dissolved nitrogen pools were not negligible. Conversely, the budget for nitrate was reasonably achieved. This result is supported by field experiments indicating that nitrification in the upper mixed layer of the studied area was likely negligible (B. Popp, pers. comm.). Finally, the calculated PN concentrations were higher than observed ones suggesting nitrogen was lost from cells. To improve on this situation, uptake rates were computed with the extended model (Elskens *et al.*, submitted). One of the important strengths of the technique developed is the ability to evaluate the accuracy (trueness and precision) of the estimates by calculating error propagation on the

measured variables. Results suggest that the largest potential bias on computed N-flux rates is due to the presence of varying fractions of detrital nitrogen in natural suspended matter.

N-flux rates and f-ratio

A synopsis of the N-uptake conditions in the average surface stratum (5-30 m) is shown in **Figure 26**.
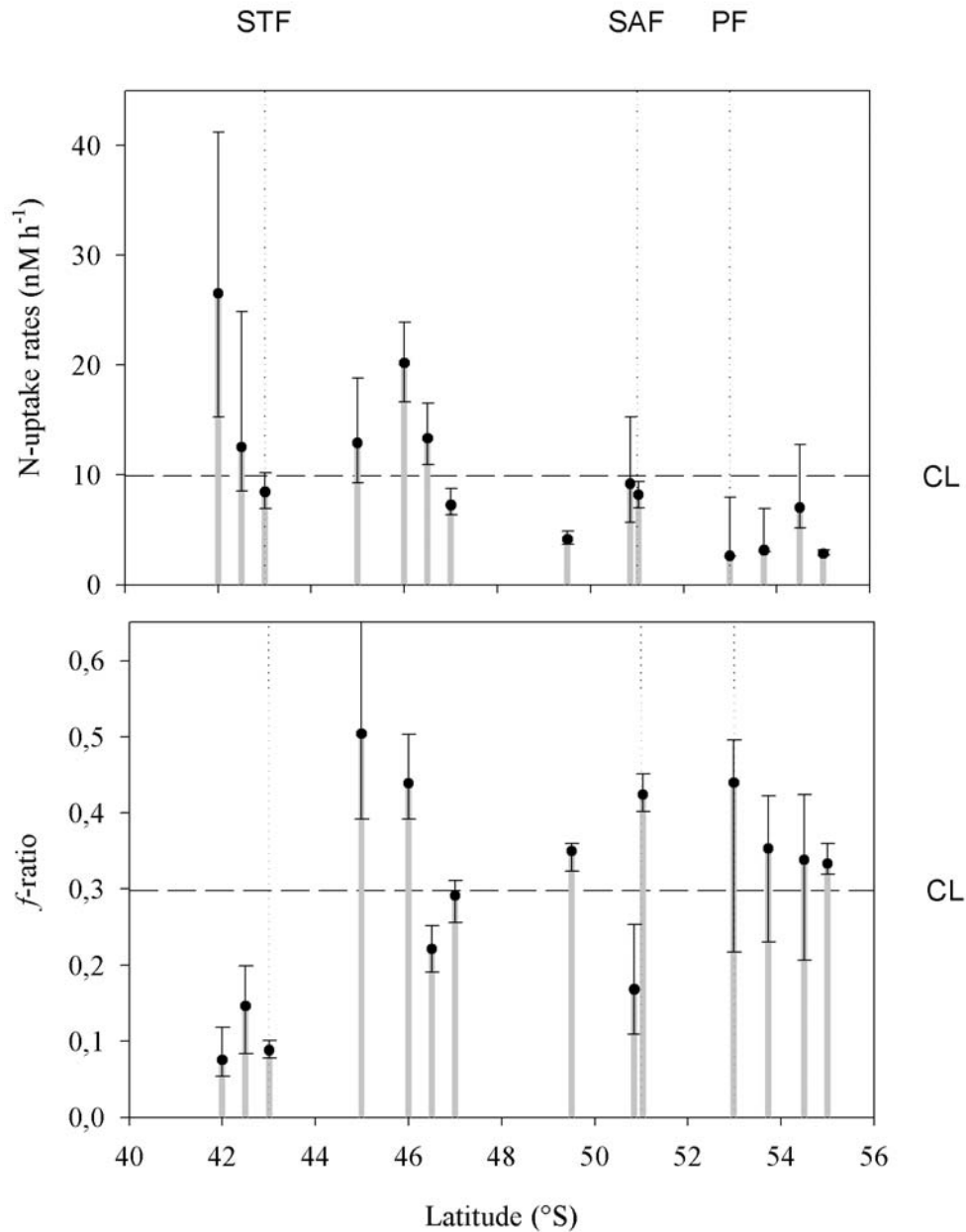
Figure 26: Regional variations of the N-uptake conditions in surface waters. Bars represent random errors on the estimates. STF = Sub-Tropical Front, SAF = Sub-Antarctic Front, PF = Polar Front and CL = mean estimate.

The surveyed section along 141°30'E-143°E crosses the Subtropical Front (STF), the Sub-Antarctic Front (SAF) and the Polar Front (PF). Stations located north of the STF were characterised by uptake rates above the mean estimate, low values of f-ratio (0.08-0.14), and by the presence of a regenerative, well growing community. The phytoplankton assemblage was mainly composed of flagellates and dinoflagellates with the latter contributing most to the carbon biomass. It attracted the highest concentration of microzooplankton (Kopczynska et al., submitted). South of the STF, the f-ratio increased to 0.43–0.51 with uptake rates up to 20 nM h^{-1}. The shift in the nitrogen uptake conditions apparently did not coincide with marked changes in the phytoplankton community structure, but there was evidence for advection of lithogenic material and associated iron at 45°S (Cardinal *et al.*, accepted), perhaps reflecting inputs from Tasmania's southern continental shelf by westward-flowing currents. Between latitudes 47°S and 55°S, the f-ratio oscillated between 0.16 and 0.44 with uptake rates below the mean estimate. The phytoplankton assemblage of lower cell densities than in the north showed a southward increasing contribution of diatoms and cocolithophorids to carbon biomass (Kopczynska *et al.*, accepted). Along the entire transect, the f-ratio estimates suggest a system running mainly on regenerated production except at 45°S-46°S. Overall, ammonium was the dominant nitrogen source used by phytoplankton (47%), followed by nitrate (32%) and urea (21%).

Net changes of the dissolved and particulate nitrogen pools over the incubation period (i.e., the balance between production and consumption processes) are illustrated in **Figure 27**. A cusum analysis (i.e., the sum of the deviations between the individual data and the overall mean carried out forward cumulatively) suggests the following trends. For Ammonium, demand exceeds regeneration (-5.3 nM h^{-1}) at stations located north of the STF, while the reverse is found on the remaining part of the transect (+1.5 nM h^{-1}). This transient unbalance of fluxes is corroborated by an observed increase of ammonium concentration from 0.1 up to 0.6 μM between 44°S and 54°S. It should be noted, however, that with a net production rate of +1.5 nM h^{-1} on average, an ammonium build-up of 0.1 μM would require at least 3 days, all other conditions remaining the same. Nitrate regeneration is of minor importance, and thus consumption prevails over the whole transect, but with an exceptional event at 45-46°S (mean process change from –1.4 to –7.3 nM h^{-1}). This might possibly reflect the enrichment of surface waters in dissolved iron from a background concentration of 0.1 up to 0.4 nM (Sedwick, per. com.).
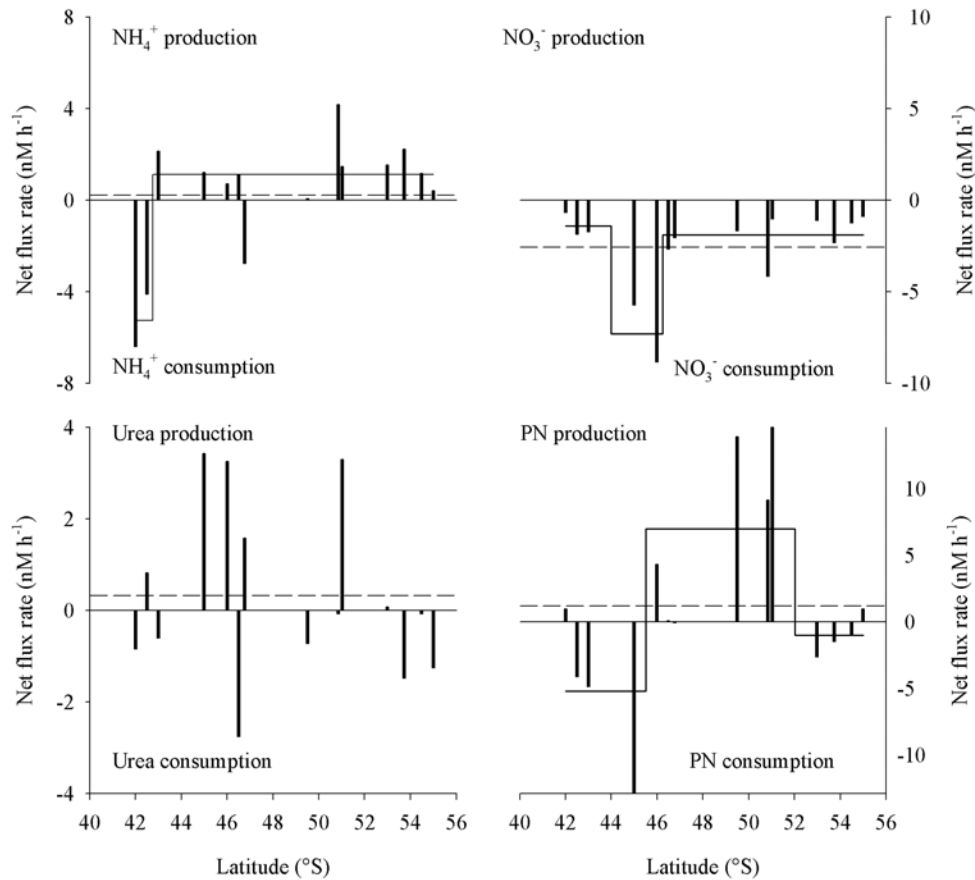
Figure 27: Analysis of the variability in *f*-ratio in response to small perturbations (0.1-0.2 µM) of the ambient ammonium concentration.

For urea, the points fluctuate randomly around a mean estimate of +0.32 nM h^{-1} with no discernible patterns in the data except an increase in process variability between latitudes 45-52°S. For PN, the mean balance of the processes shows an increase from –5.2 up to +7.0 nM h^{-1} around 45-46°S, followed by a decrease to –1 nM h^{-1} further south around 51-52°S. The highest release of nitrogen from PN occurs north of 45°S and coincides with the highest concentration of microzooplankton (Kopczynska *et al.*, accepted), thus suggesting that grazing processes are responsible for the trend.

Analysis of the variability in f-ratio: sensitivity to ammonium concentration
The N-uptake conditions depend largely on the efficiency of nitrogen regeneration in the surface layer, and its variation in space and time. Because ammonium is known to affect the uptake of nitrate, it was used as a perturbing agent for investigating the variability in *f*-ratio. Ammonium up to 1 µM was added to each of the batch incubation experiment, and N-flux rates were computed as described above. Overall, the

additions resulted in significantly enhanced ammonium and lowered nitrate uptake rates, while there were no significant effects on the uptake of urea with rates fluctuating randomly within the estimated precision limits (Anova Analysis). Also important is the fact that the uptake of nitrate was never totally suppressed even at ammonium up to 1µM. The maximum apparent inhibition of nitrate uptake ranging from 33 to 81% is similar to observations by others (e.g. Dortch, 1990; Harrison *et al.*, 1996).

Because the observed relationships between *f*-ratio and ammonium treatment were variable, ranging from linear to convex shaped curves, they were fitted to rational functions of the form:

$$f = \frac{f^{\circ} + a.x}{1 + b.x} + \varepsilon \qquad \textbf{(13)}$$

Where f° is the *f*-ratio at ambient concentration, x the amount of ammonium added, a, b the parameters to be estimated, and ε the residual term. Such variability in the observed trends is not unusual and has been reported previously by several authors (Dortch, 1990, Wheeler and Kokkinakis, 1990; Armstrong, 1999 and references therein). Differentiating **Eq. 13** with respect to x yields the slope of the tangent at the curve, i.e. the variation in *f*-ratio expected for a given perturbation (x) of the ambient ammonium concentration. The slope was calculated for x increasing up to 0.2 µM, as larger values are unlikely under conditions depicted in **Figure 28**. Slopes varied considerably from 0.07 to 7.8 but with steepest values found in water masses showing enrichment in dissolved iron and low ambient ammonium (**Figure 28**). A factorial analysis revealed close interactions between ammonium and iron in regulating N-uptake conditions, meaning that the effect of both factors was not merely additive, in agreement with model results of Armstrong (1999). This interaction term might possibly explain the various trends reported above, being linear in areas of iron stress, and becoming non-linear with increasing iron availability. On average, the N-uptake conditions appeared rather stable ($\partial_x f / f$ < 18%; open symbols) excepted for the area between 45-46°S ($\partial_x f / f$ up to 50%; closed symbols). At these latitudes, the *f*-ratio can shift rapidly between 0.21 and 0.77 in response to small ammonium perturbations ($\pm$ 0.1 µM), as may occur for instance during the nycthemeral cycle. Thus in HNLC areas, versatility versus stability of *f*-ratio seems closely linked with progress of the season: the system is versatile in the early phase of the growth season, or when submitted to pulsed inputs of macro- and micro-nutrients, whereas it is stable later in the season under conditions of iron stress and high ammonium availability (Goeyens *et al.*, 1995; 1998 and references therein).
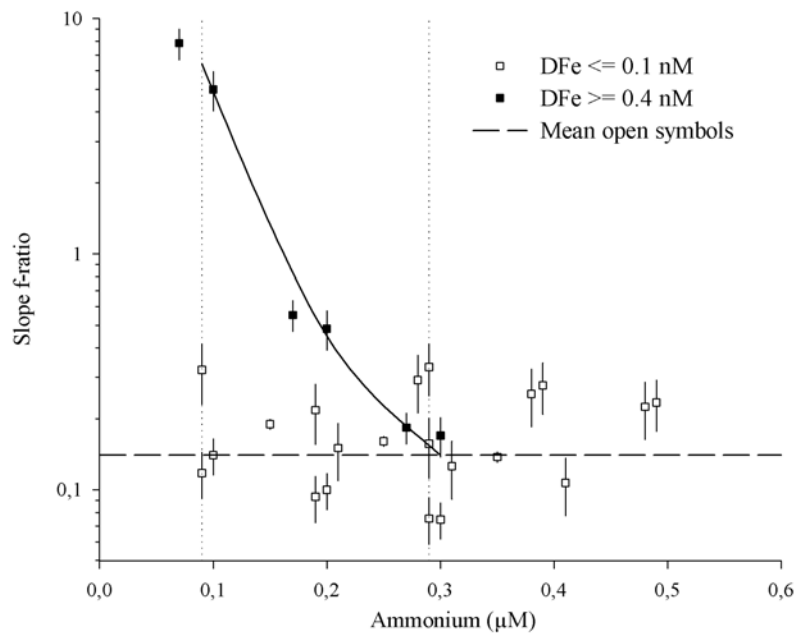
Figure 28: Analysis of the variability in *f*-ratio in response to small perturbations (0.1-0.2 µM) of the ambient ammonium concentration.

Since ecosystem maturity is a property that increases as the degree of ecosystem perturbations decreases (Platt *et al.*, 1992), the variability of *f*-ratio is in some way a diagnostic of the level of disturbance to which the system is subject.

B.3. Nano/micro-plankton composition and nitrogen uptake regime during fall

For details on phytoplankton and microzooplankton species we refer to Kopczynska *et al.* (accepted). In the present report we limit the discussion to the subject of phytoplankton community variability and production parameters
Phytoplankton cell densities in surface waters (5-30 m) decreased from STZ over SAZ (46°S) to the PFZ (**Figure 29**). The predominance along the entire transect of nano-size cells representing different taxonomic groups suggests a stage of regenerative production stretched between 42°-55°S, the more so, that the scene takes place in March at the end of the austral summer when an enhanced availability of ambient ammonium can be expected. Regenerative production is often, but not always, characterized by predominance of smaller cells (see Goeyens *et al.*, 1991; Semeneh *et al.*, 1998) which tend to satisfy their nitrogen requirement by assimilation of ammonium (Koike *et al.*, 1986; Probyn and Painting, 1985; Owens *et al.*, 1991).

73
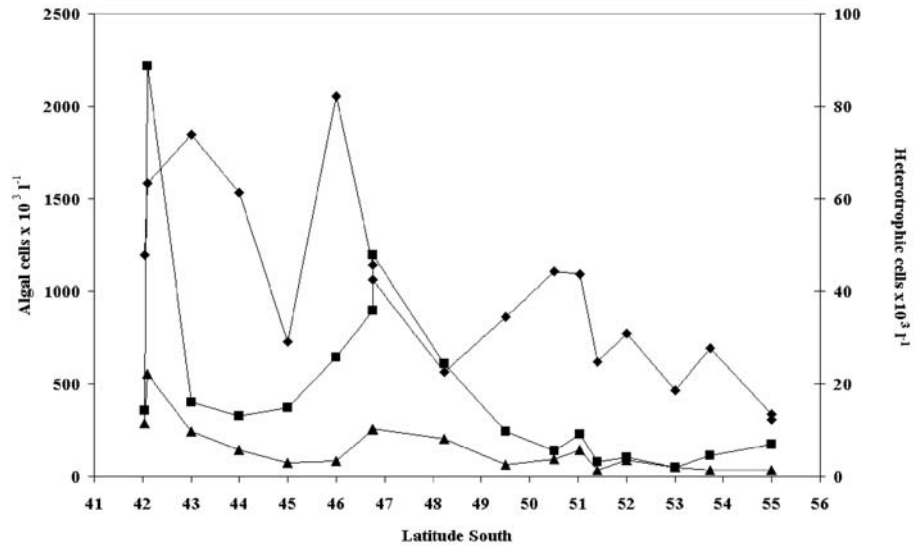
Figure 29: Latitudinal distribution of phytoplankton and microzooplankton. Cell densities of algae and heterotrophic dinoflagellates represent average values for the 5-30m surface water stratum. Ciliates, which in the PF are found mainly at 90m, represent average values for the water column. Large heterotrophic dinoflagellates have been excluded from phytoplankton cell densities. Diamonds, phytoplankton; squares, heterotrophic dinoflagellates; triangles, ciliates.

The distribution of cell-carbon concentration shows less latitudinal variation for algal and heterotrophic dinoflagellate cells, with the latter showing lower concentrations than the former (**Figure 30**). Ciliate C-biomass, on the contrary, was observed to exceed algal and heterotrophic dinoflagellate C-biomass at 42°, 47° and 48°S.
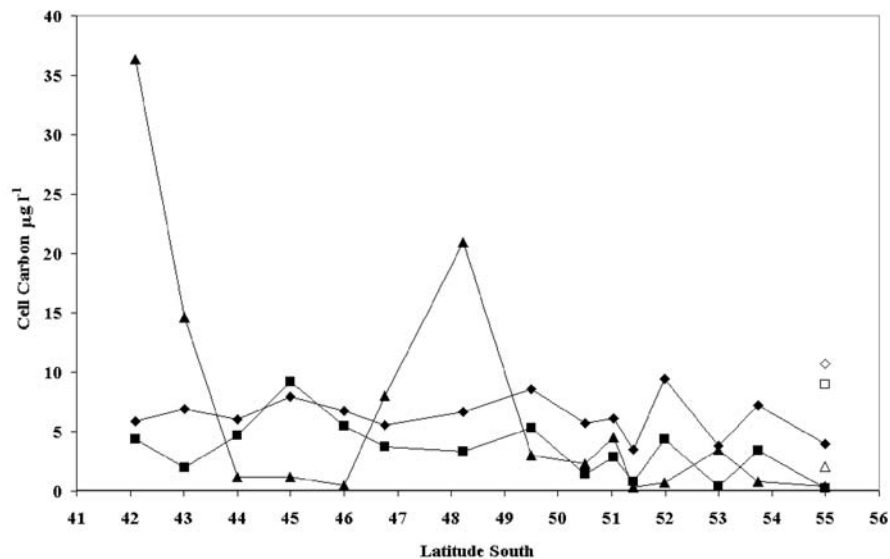
Figure 30: Latitudinal variation of phytoplankton and microzooplankton carbon biomass. The values represent averages for the upper 90m of the water column. Filled diamonds, squares triangles, respectively phytoplankton, heterotrophic dinoflagellates and ciliates at 141°E. Open diamond, square and triangle, respectively phytoplankton, heterotrophic dinoflagellates and ciliates at 143°E.

74

From the ^{15}N uptake rate data (*f*-ratios) discussed by Elskens *et al.* (see **§B.2.I** and submitted) it can be concluded that the phytoplankton assemblages along the transect represent different (at least three) stages with variable importance of regenerative and new production. These are: the STC region (42°-43°S); the Subantarctic Zone (45°-47°S) with its additional frontal feature at 46.7°S and the Polar Front Zone. Many of the extreme values of productivity related parameters occur at the STC.

- The Subtropical zone is characterised by the highest cell counts, carbon biomass and chlorophyll *a* encountered in the surface waters along the transect. Elskens *et al.* (see **§B.2** and submitted) observed that here *f*-ratios are lowest (between 0.08 and 0.14), suggesting large predominance of regenerative production. Furthermore, they observed rates of nitrogen uptake (i.e. ammonium + nitrate + ureum) to be the highest (up to 27 nM h^{-1}) resulting in the lowest ambient NH_4^+ concentrations measured for the whole transect (**Table IX**). The maximum column integrated primary production values (up to 98 mg C m^{-2} d^{-1}; F.B. Griffiths, unpublished results) are also found in this northern part of the SAZ transect. This situation undoubtedly provides good nutritional conditions for the development of the highest concentration of protozooplankters such as dinoflagellates and ciliates (**Figure 29**). Phytoplankton carbon is mainly attributed to dinoflagellates, which are represented there by more species than in the southern part of the transect.

Table IX: Physico-chemical data for SAZ' 98; average values for upper 100m of water column.

CTD	Latitude	Longitude	Temperature (°C)	Salinity	Phosphate mmol l^{-1}	Nitrate+Nitrite mmol l^{-1}	Ammonium nmol l^{-1}*	Silica mmol l^{-1}
4	42.09	141.89	12.48	34.895	0.69	7.9	55	1.5
9	42.05	141.89	12.20	34.800	0.66	7.9	24	0.6
18	43.01	141.42	11.11	34.577	0.78	10.4	198	0.5
19	43.99	141.50	11.00	34.590	0.78	10.4	268	0.4
22	44.99	141.51	10.84	34.614	0.80	10.6	405	1.0
23	46.00	141.51	10.93	34.605	0.79	10.7	353	0.8
24	46.76	142.07	11.05	34.644	0.75	9.1	220	0.5
29	46.77	142.00	11.08	34.629	0.73	9.5	169	0.8
41	48.23	141.40	9.67	34.434	0.99	13.5	116	1.7
43	49.51	141.78	9.06	34.334	1.08	14.7	208	1.4
46	50.52	141.77	7.33	33.976	1.43	20.8	236	3.5
49	51.03	141.76	7.55	33.964	1.42	20.3	458	2.6
76	51.41	142.80	7.69	33.957	1.38	20.3	470	1.9
66	51.99	141.77	4.88	33.800	1.61	24.9	353	3.0
58	53.73	141.80	3.56	33.828	1.73	25.9	339	6.7
65	52.99	141.76	4.12	33.804	1.69	25.8	388	4.8
73	54.99	141.74	3.62	33.817	1.64	25.5	563	2.9
74	54.99	143.50	2.98	33.831	1.75	26.0	576	7.5

data are from M. Rosenberg and T. Trull (pers. comm.); * data from R. Watson (pers. comm.)

- The subantarctic area between *45° and 47°S* appears to represent a different functional zone. Elskens et al. (submitted) observed that here *f*-ratios are highest, reaching 0.51 at 45°S and 0.43 at 46.7°S and thus reflecting increased importance of new production

The productivity is slightly decreased relative to the situation at 42°S with primary production reaching 80 mg C m^{-2} d^{-1} at 46.7°S (G.B. Griffiths, unpublished results) and nitrogen uptake reaching 20 nM h^{-1} at 46°S (Elskens *et al.*, see **§B.2** and submitted). Heterotrophic cell numbers show a broad maximum between 46° and 48°S with heterotrophic dinoflagellates largely in excess of ciliates (**Figure 29**). Numbers, however, remain inferior to those observed at 42°S. The autotrophic carbon biomass is mainly accounted for by dinoflagellates and nanoflagellates, but there is an increased contribution of coccolithophorids and larger diatoms (*Pseudonitzschia* spp.; *Fragilariopsis* spp.; *Thalassiothrix* spp.).

It is interesting to note that the upper water column (500m) in the entire area between 40° and 45°S has been reported to have higher levels of the dissolved micronutrients Fe and Mn, relative to the area further south (Sedwick *et al.*, 1997). Furthermore, Cardinal et al. (submitted) observed higher contents of particulate Fe and Mn in the upper 500m at 45°S relative to stations further south and north. These observations might point towards an input of Fe and Mn from the Tasmanian slope and shelf region located to the east of the investigated transect. It appears, however, that while these conditions possibly contribute to shaping the nitrogen uptake regime (Elskens *et al.*, see **§B.2** and submitted), they do not appear to strongly affect the plankton community composition.

- Between 47° and 55°S *f*-ratios are lower and do not exceed 0.45 but tend to increase southward. Primary production does generally remain below 60 mg C m^{-2} d^{-1} and shows a southward decreasing trend (Griffiths *et al.*, submitted). Furthermore, uptake rate of nitrogen is low and does not exceed 10 nM h^{-1} (at 51°S; Elskens *et al.*, see **§B.2** and submitted). The phytoplankton is characterised by lower cell densities and contains more diatoms both with regard to number of cells and species. In the vicinity of the SAF (50°-51°S) cell numbers exhibit intermediate maxima at 5 and 30m as does carbon biomass at 5m. In the PF region at 90m diatom carbon exceeds the carbon biomass of dinoflagellates. This is also reflected in the highest chlorophyll *a* content at 90 to 120m in the PF region (max. = 0.69 µg l^{-1} at 100m, 53.7°S; S. Wright, pers. Comm.) suggesting that the cells are still in a healthy condition.

Our data point out to a sinking diatom bloom at the PF with accumulation of matter in the subsurface waters. The many empty diatom cells observed in the entire PFZ indicate past bloom conditions and suggest that diatoms were more important in the

community earlier in the summer season. The empty frustules may result from sexual reproduction (Crawford, 1995; Crawford *et al.*, 1997), or dinoflagellate grazing (Jacobson and Anderson, 1986). Slightly increased numbers and carbon biomass (the latter especially at 55ºS, 143ºE) of heterotrophic dinoflagellates suggest the latter process. The very low silica concentrations found along the transect were probably limiting for diatom growth (see Jacques, 1983) for some time preceding sampling. Thus we have phytoplankton in a near bloom situation in the north thriving under ammonium-based regenerative production at the STC, while further south in the SAZ and PFZ the relative importance of new production is higher and reaches a maximum at 45°-46°S, possibly supported there by iron supply. However, except for the situation at 45°S, the N-uptake regime does never switch entirely to predominance of new production. The inverse relationship between heterotrophs cell carbon (or numbers) and *f*-ratio (**Figure 31**) suggests that the N-uptake regime is controlled by the activity of the heterotrophs and the excretion of ammonium associated with grazing activity. The frequently encountered senescent colonies of *Phaeocystis* in the STZ and SAZ suggest an earlier bloom of at least this one species. About half of our observations indicate that the matrices of *Phaeocystis* are colonised, probably by heterotrophic nano-cells as suggested for North Sea *Phaeocystis* (Rousseau *et al.*, 1994) and larger free-living microheterotrophs, dinoflagellates and ciliates are commonly encountered.
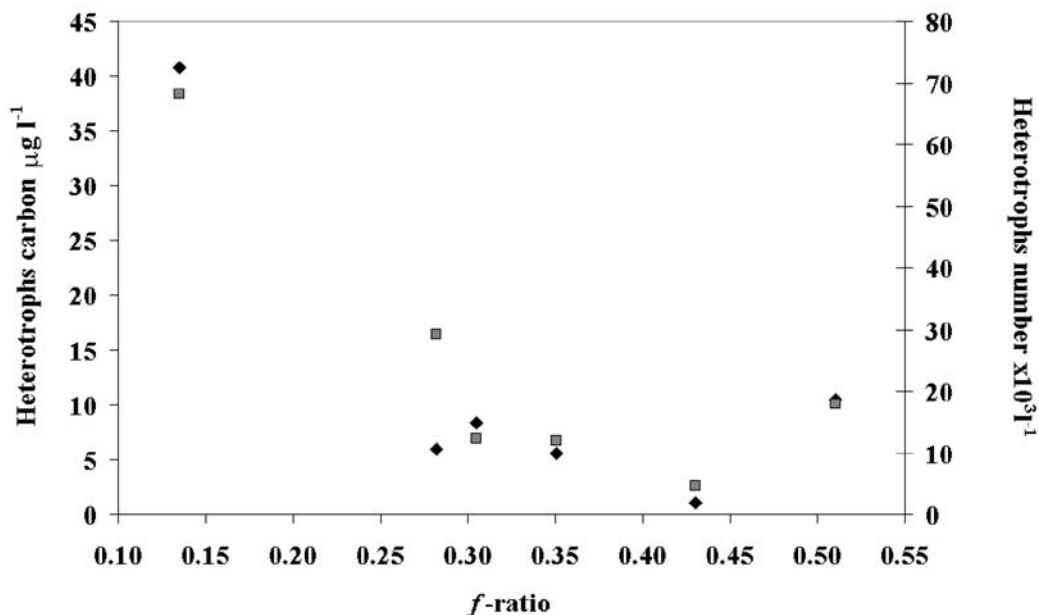
Figure 31: Latitudinal distribution of microzooplankton versus *f*-ratios (the latter from Elskens *et al.*, submitted). Squares, diamonds, respectively, heterotrophic cell numbers and carbon content.

The maximum values of microzooplankton cell densities and carbon biomass obtained in this study are within the highest ranges reported from the Southern Ocean (see Burkill *et al.*, 1995; Archer *et al.*, 1996). Our results suggest that microzooplankton are the major grazers along the transect that substantially control the size of phytoplankton populations present and contribute significantly to the N-nutrient cycling and carbon flow. This view is supported by the relatively high numbers and biomass of ciliates and dinoflagellates, their spatial distribution associated with phytoplankton peaks, and recent information on the importance of microzooplankton grazing (Archer *et al.*, 1996). It should be emphasized that the populations of protozooplankton along the transect have been underestimated, since a great number will also be found among nano-size flagellates and dinoflagellates (see Becquevort *et al.*, 1992; Becquevort, 1997; Bjornsen and Kuparinen, 1991); these were not distinguished because of the counting method used. In our samples peaks of dinoflagellate and ciliate numbers coincide in surface waters and appear to be associated with maximum phytoplankton cell numbers (**Figures 29 and 32**).

Plot with regression equation $y = 0.2206x + 1.8459$ and $R^2 = 0.7761$. Y-axis: Ciliate cells x 10^3 l^{-1}. X-axis: Dinoflagellate cells x 10^3 l^{-1}.
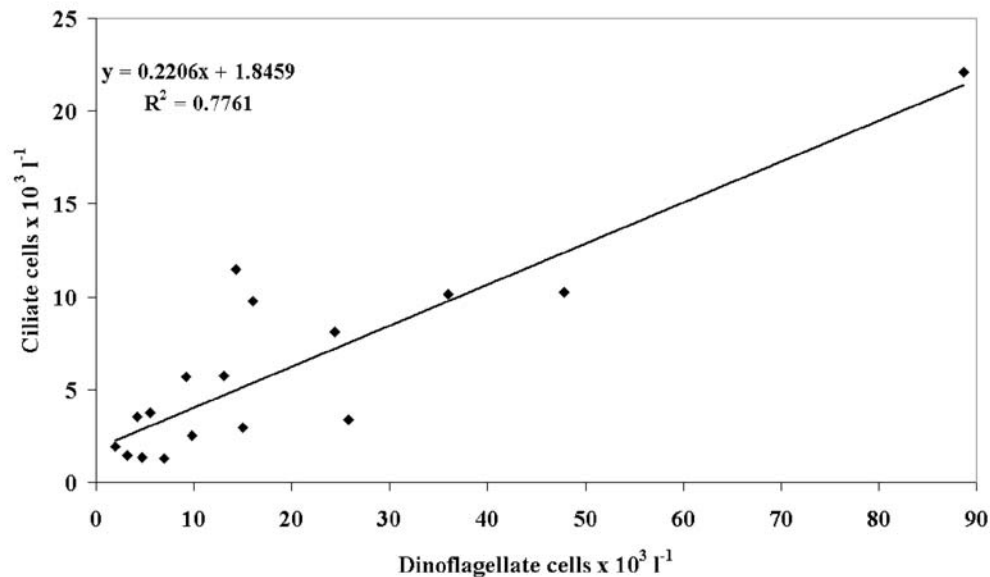
Figure 32: Co-variation between ciliate and heterotrophic dinoflagellate cell numbers.

C. Export production: functioning and yield of the biological pump

Carbon export can be estimated via different approaches. These include the direct measurement of processes that govern carbon export, such as aggregation of phytoplankton-derived material mineralisation, aggregate sinking rates and bacterial degradation of aggregates. These processes have been investigated in the Ross Sea

Polynya during austral spring 1997 (see chapter C.1).

Other approaches consist in estimating carbon export production from water column POC fluxes and POC accumulation in the sediments. However, because of the highly labile character of organic matter (for oceanic systems only about 1% of the organic carbon synthesised in surface waters finally reaches the sediment; Berger; 1989), POC flux itself is not the ideal tracer or proxy of export production. Therefore, considerable research efforts went into identifying useful tracers or proxies of carbon export production. One of the proxies with great potential to resolve the export flux is biogenic Ba, occurring mainly as microcrystals of barite formed during the aggregation and mineralisation of biogenic detritus (see chapter **C.2**). The particulate bio-Ba proxy has been investigated during two cruises: SAZ'98 (March 1998) along 142°E in the Subantarctic and Polar Front Zones, south of Australia and ANTARES-4 (January - February 1999) in the Subantarctic Zone of Indian sector (Kerguelen - Crozet area). In section **C.2.I.1**, particulate Ba data are compared with dissolved Ba profiles, to discuss possible mechanisms of bio-Ba formation. In section **C.2.III** the water column Ba proxy results are confronted with two other approaches used for assessing export production: i.e. new production based on *f*-ratio and bio-Ba fluxes recorded by SAZ'98 sediment traps. Finally, export productions reconstructed from bio-Ba accumulation in surface sediments of the Australian, Indian and Atlantic sectors of the Southern Ocean are discussed in section **C.2.IV**.

C.1. Aggregation, sedimentation and bacterial degradation of phytoplankton material in the Ross Sea

The export of particulate matter from the surface to the deep ocean results from the balance between sinking and dissolution/remineralization of particulate matter during transfer within the water column. Sediment traps are often used to measure the export of particulate matter, but the possibility of hydrodynamic bias in collection remains (Gardner, 1999; Yu *et al.,* 2001). Moreover, short-term events in the upper ocean (such as diurnal events) are not resolved in time and space by deep, moored sediment traps. As an alternative, carbon export can be estimated from the direct measurements of processes that govern carbon export. These are aggregation, sinking rates and bacterial mineralisation of phytoplankton-derived material. Such processes were investigated in the Ross Sea Polynya during austral Spring 1997. This site was chosen because of the spatially variable occurrence of *Phaeocystis* and diatom spring blooms, two phytoplankton groups with reported contrasted export significance. Indeed, the mesozooplankton-palatable diatoms contribute significantly to export, resisting microbial degradation in the surface waters owing to their high potential to aggregate (Riebesell, 1993) and sink, as well as their likelihood of being ingested with the subsequent production of fecal pellets. In contrast, *P. antarctica*

colonies experience little grazing pressure by mesozooplankton (Weisse *et al.,* 1994) or microzooplankton (Caron *et al.*, 2000). The fate of a senescent *Phaeocystis* sp. bloom varies regionally, and is determined by the physical and biological characteristics of the ecosystem in which it occurs (Wassmann, 1994). *P. antarctica* cells can be exported during periods of rapid growth (Ditullio *et al.*, 2000), or material derived from the bloom can sink after maximum biomass is attained (Wassmann *et al.*, 1990; Riebesell *et al.*, 1995; Smith and Dunbar, 1998). Cells also can be lysed in the surface layer and subsequently remineralised without significant sedimentation (van Boeckel *et al.*, 1992; Becquevort *et al.*, 1998).

C.1.I. Aggregation and sedimentation

Aggregation has been reported an important mechanism enhancing vertical flux (Jackson, 1990; Kiorboe and Hansen, 1993). Indeed, during the phytoplankton bloom, aggregates can quickly form and sink out of the mixed layer (Alldredge and Gotschalk 1989, Riebesell 1991). The factors regulating aggregation are still unclear (Alldredge and Jackson 1995). Particle concentration, size distribution, surface stickiness, phytoplankton-bacteria interactions and the intensity of the physical processes such as shear are factors proposed in the literature as controlling the process of aggregation (Alldredge and Jackson 1995. As reported elsewhere (Jackson 1990, Riebesell 1993), the appearance of aggregates in the Ross Sea polynia (defined as particles with a diameter > 0.5 mm) corresponded with the increase in chlorophyll a and POC concentration. During the earliest occupation (November 17 to 27), no aggregates were recorded. At that time the phytoplankton biomass was relatively modest ($\overline{ChlA}$ = 1.05 μg L^{-1}, range 0.29 - 2.39 μg L^{-1}; $\overline{POC}$ = 226 μg C L^{-1}, range 63 - 506 μg C L^{-1}; **Figure 33 and 34**) and the assemblage was dominated by naked nanoflagellates and autotrophic dinoflagellates. By the end of November, the chlorophyll a and POC concentrations had increased substantially, and by the middle of December they had reached 14 μg L^{-1} and 725 μg C L^{-1}, respectively. At that time, *Phaeocystis* colonies dominated the phytoplankton community but the presence of diatoms resulted in the enhanced formation of aggregates. Nevertheless, the density of aggregates recorded (0.25 and 0.49 L^{-1} at Station 36, 76°30'S, 170°E, 11 December and station 37, 76°30'S, 169°E, 12 December, respectively) remained low throughout the investigated period, despite an observed increase in chlorophyll of order one order of magnitude (**Figure 33**). However, as suggested by higher records of aggregates (> 0.5 µm) abundance and sinking rates in January 1996 (Asper and Smith, submitted) the contribution of aggregation to export production in the Ross Sea might be significant during summer.
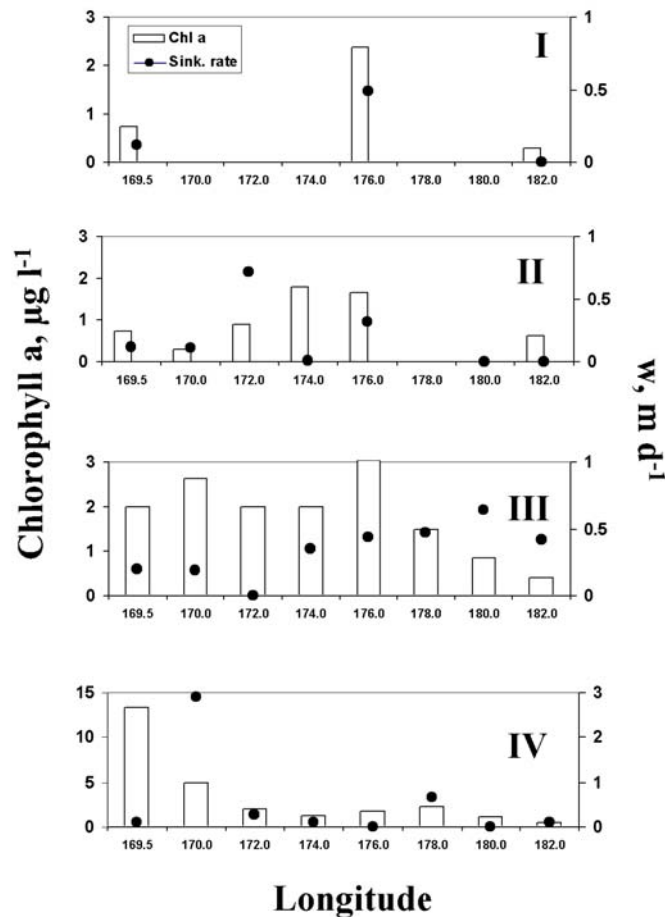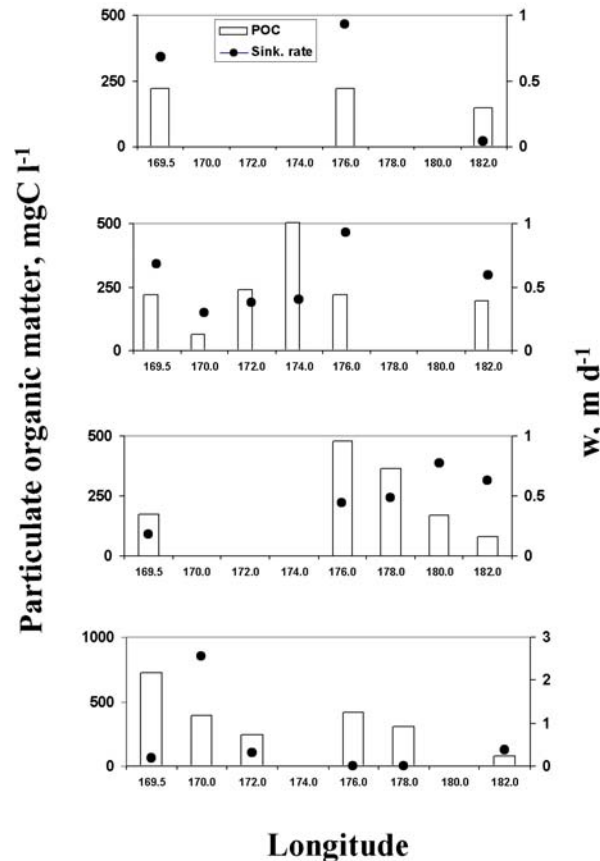
Figure 33: Spatio-temporal distributions of sinking rates (w) estimated from chlorophyll a within the upper mixed layer along 76°30'S. Transect numbers indicated in upper corner. Note biomass scale changes in different panels. The aggregate density was 0.25 and 0.49 L^{-1} at Stations 36 (76°30'S, 170°E, 11 December) and 37 (76°30'S, 169°E, 12 December), respectively.

The sinking rates measured in this study were within the low range of rates previously observed in the ocean. Daily sinking rate (w) of healthy phytoplankton (Chl.a-based sinking rate; **Figure 33**) and total living and detrital biogenic particles (POC sinking rate; **Figure 34**) varied over time and ranged between 0.01 and 3 m d^{-1} (**Figures 33 and 34**). The maximum sinking rate of both Chla-particles (0.7 m d^{-1}) and POC (3 m d^{-1}) was observed during the last occupation of the section at 170°W. At this station, aggregates were observed. The sinking rates estimated from chlorophyll a and POC changes were positively correlated (R^2 = 0.71, n=19), with significantly higher sinking rates of particulate carbon. No significant linear relationships were observed between sinking rates and chlorophyll a and POC concentrations (for chlorophyll a: R^2 = 0.04 and for POC: R^2 = 0.03). Published values of sinking rates of aggregates show variations between 1 and 200 m d^{-1} (Alldredge, 1979; Bodungen *et al.,* 1986; Billet *et al.*, 1983; Alldredge and Silver 1988; Shanks and Trent, 1980; Asper, 1987; Jackson,

1990; Tiselius and Kuylenstierna, 1996; Pilskaln *et al.*, 1998). For individual cells reported sinking rates vary between 0 and 10 m d^{-1} (Bienfang, 1985; Riebesell, 1989; Muggli *et al.*, 1996), with most recent estimates being ca. 1 m d^{-1} or less.

Figure 34: Spatio-temporal distributions of sinking rates (w) estimated from POC concentrations within the upper mixed layer along 76°30'S. Transect numbers indicated in upper corner. Note biomass scale changes in different panels. The aggregate density was 0.25 and 0.49 L^{-1} at Stations 36 (76°30'S, 170°E, 11 December) and 37 (76°30'S, 169°E, 12 December), respectively.

Thus our estimate of sinking rates falls well within the low range of reported values, and strongly suggests that vertical fluxes via passive sinking were insignificant during austral spring. However, such estimates based on Chl-a and POC changes are averages and could mask massive sedimentation rates of some individual cells as occasionally observed in the Southern Ocean (Crawford, 1995; di Tullio et al, 2000). In accordance, we found taxon-specific differences in sinking behaviour (**Table X**). Phytoplankton cells, sorted as diatoms and dinoflagellates (colonial forms, *Gyrodinium* spp.) had the highest sinking rates, with the highest average value (0.18 m d^{-1}) being observed for centric diatoms. The *P. antarctica* colonies sinking rates

averaged 0.05 m d^{-1} and always were less than 0.19 m d^{-1}. In the case of heterotrophic cells, an unidentified protozoan exhibited high sinking rates (up to 16.8 m d^{-1}). Both auto- and heterotrophic dinoflagellates had the same mean sinking rate (0.05 m d^{-1}). Furthermore, within each taxon, large spatial and temporal variations in sinking rate were observed. Indeed, the sinking rates of individual cells are not only determined by physical factors associated with cell size and shape, but also by their physiological state (Waite *et al.,* 1992, 1994), which in turn results from a dependence of sinking rate on nutrient concentrations and ambient irradiance (Bienfang, 1984; Moore and Villareal, 1996). Particularly, the iron-status of diatoms has a dramatic effect on its sinking rate, causing a 5-fold increase of the sinking rates of Fe-depleted cells relative to Fe-replete ones (Muggli *et al.*, 1996; Waite and Nodder, 2001). However, growth rates remained high throughout our cruise (Smith *et al.*, 2000), and independent studies suggest that iron limitation occurs later in summer (Sedwick *et al*., 2000; Olson *et al*., 2000).

Table X: Average and range of sinking rates of total phytoplankton assemblage, the total community and individual taxa (m d^{-1}).

Group	Average (m d^{-1})	Min. – Max. (m d^{-1})
Total Phytoplankton		
chl a-based	0.64 *(10 m)* 0.23 *(100 m)*	0 – 3.02 *(10 m)* 0 – 1.43 *(100 m)*
Biogenic and detrital particle	0.71 *(10 m)*	0 – 2.55 *(10 m)*
	2.35 *(100 m)*	0.45 – 7.86 *(100 m)*
Autotrophic cells		
Pennate diatoms	0.06	0 – 0.83
Centric diatoms	0.18	0 – 1.07
Dinoflagellates (colonial forms)	0.05	0 – 0.88
Phaeocystis sp. colonies	0.05	0 – 0.19
Heterotrophs		
Dinoflagellates (colonial forms)	0.05	0 – 0.9
Choanoflagellates	0.05	0 – 0.2
Unidentified protozoa	2.16	0 – 16.8

C.1.II. Biodegradation of phytoplankton-derived material

Microbial degradation of phytoplankton-derived material depends on the activities of free-living bacteria as well as those of particle-attached bacteria. Phytoplankton and/or phytoplankton-derived aggregates often are microhabitats highly enriched in bacteria that display intense biological activity relative to the surrounding water (Simon *et al.*, 1990; Smith *et al.*, 1995). These bacteria actively participate in the remineralization and enzymatic dissolution of particulate organic matter in the surface waters and during sinking to the deep ocean (Cho and Azam, 1988; Smith *et al.*, 1992). Therefore, particle-attached bacteria can modify the efficiency of the oceanic carbon pump. Based on the reported low growth rates but high ectoenzymatic activity of attached bacteria, Azam (1998) suggested that most of hydrolysates produced by ectoenzymatic activities could diffuse from particles without being used by attached bacteria, thus reducing the sinking flux and increasing dissolved organic matter concentrations available to unattached heterotrophs. In order to test this hypothesis in the Southern Ocean we conducted measurements of abundance, enzymatic (ectoprotease, ecto-β-glucosidase) activities and production of free-living vs. particle-attached bacteria.

Bacterial abundance and activity were very low until the end of November, and increased slowly by the middle of December. Bacterial abundance varied from 0.03×10^9 to 0.50×10^9 cells L^{-1}. Until the end of November, the bacterial community was largely free-living, but thereafter the percentage of particle-attached bacteria increased, especially in the western part of the transect. However, the proportion of attached bacteria remained less than 7% of the total bacterial abundance throughout the entire cruise. The contribution of particle-attached bacteria to the heterotrophic activities was more significant. Bacterial production ranged between 0.11 and 3.06×10^6 cells L^{-1} h^{-1}. The last occupation of the transect showed markedly increased bacterial production, and in parallel the contribution of attached-bacteria to the total bacterial production increased from 0 to 18%. This percentage is low compared to other *Phaeocystis*-dominated ecosystems such as for instance the Southern Bight of the North Sea where the cellular production by attached bacteria has been shown to contribute to 60% (Laanbroek *et al.*, 1985) and 68% (Becquevort *et al.*, 1998) of total bacterial production.

The ectoproteasic and ecto-β-glucosidasic activities ranged between 0 and 15.9 nmol L^{-1} h^{-1} ($\overline{X}$ = 4.64 nmol L^{-1} h^{-1}) and between 0 and 0.36 nmol L^{-1} h^{-1} ($\overline{X}$ = 0.07 nmol L^{-1} h^{-1}), respectively. Protease activity was ten to one hundred times larger than glucosidase activity. In parallel to the observed *P. antarctica* colonial biomass increase, a sharp increase of ecto-β-glucosidasic activity was observed at the beginning of December. During the last occupation of the transect, the contribution of

attached bacteria to the total enzymatic activities reached 19 and 24% for ectoprotease and ecto-β-glucosidase, respectively. The contribution of particle-attached bacteria to enzymatic activities was in the same range as the proportion of particle-attached bacteria to total production. As such, the degradation of the phytoplankton-derived organic matter and its utilization by particle attached bacteria were coupled, contrasting with the conceptual model of Azam (1998). Moreover, all cell-specific activities (growth rates and ectoenzymatic activities) of particle-attached bacteria were significantly higher than those of free-living bacteria. Mean cell-specific ectoenzymatic activities (ectoprotease and ecto-β-glucosidase) were significantly (t-test, $p < 0.005$ for ectoprotease and $p < 0.05$ for ecto-β-glucosidase) higher (by 4-7 times) for particle-attached bacteria than for free-living bacteria (**Table XI**). The average ratio between both enzymatic activities was similar (0.03); but, the values for free-living bacteria were more variable (varying by one order of magnitude). The growth rate of attached bacteria was on average two times higher than that of free-living bacteria. The observed difference in the activity per cell in ambient water and on particles may be caused by a difference in the percentage of bacteria actively expressing a distinct enzyme and/or by different bacterial species compositions.

Table XI: Average and range (in brackets) of bacterial growth rate, specific ectoproteasic activity (EPA), specific ecto-β-glucosidasic activity (EGA) and EGA/EPA ratio for free-living bacteria and particle-attached bacteria.

Parameter	Free-living bacteria Average [Min. – Max.]	Attached bacteria Average [Min. – Max.]
Growth rate (h^{-1})	0.009 [0.001– 0.025]	0.012 [0.001-0.045]
Specific ectoproteolytic activity (EPA) (10^{-18} mol cell^{-1} h^{-1})	36.93 [4.79 – 134.80]	181.05 [33.69 – 366.23]
Specific ecto-b-glucosidasic activity (EGA) (10^{-18} mol cell^{-1} h^{-1})	0.61 [0.19 – 1.41]	4.26 [1.41 – 8.64]
EGA/EPA Ratio	0.03 [0.01- 0.10]	0.03 [0.01– 0.04]

There are numerous reports that indeed suggest that a considerable fraction (up to 50%) of the free-living bacterial assemblage is in some kind of dormant state (e.g., Hoppe, 1976; del Giorgio and Scarborough, 1995; Choi *et al.*, 1996). Furthermore, some evidence based on the use of specific indicator of cell viability suggests that particle-associated bacteria could be proportionally more active (higher percentage of 5-cyano-2,3-ditolyl tetrazolium chloride positive cells) compared to free-living cells

(Sherr *et al.*, 1999). Finally, comparative phylogenetic evidence suggests that particle-attached bacterial assemblages may differ in composition from those inhabiting the surrounding water column (DeLong *et al.,* 1993; Bidle and Fletcher, 1995).

C.1.III. Potential sedimentation vs. remineralisation during spring in the Ross Sea

From the daily sinking rates and mean POC concentration, daily potential fluxes through the 100 m horizon were estimated and compared to daily primary productivity. Daily potential fluxes at 100 m ranged from 6 to 1000 mg C m^{-2} d^{-1} ($\overline{X}$ = 137 mg C m^{-2} d^{-1}) (**Table XII**), which represents a low proportion of the daily primary productivity (from 1.4 to 38.5%; $\overline{X}$ = 14.2%; **Table XII**). In contrast to the primary production, which increased from mid-November to mid-December, there was little variation in the average proportion of primary production potentially being exported.

Table XII Ross Sea, spring 1997; average and range (in brackets) of POC flux at 100 m, daily primary productivity (PP), potential export (% of PP), total bacterial carbon demand (% of PP) and particle-attached bacterial carbon demand (% of PP). n.d. = not detectable.

Transect	POC flux at 100 m (mg C m^{-2} d^{-1})	Primary Productivity (mg C m^{-2} d^{-1})	Potential export (% of PP)	Total bacterial carbon demand (% of PP)	Attached bacterial carbon demand (% of PP)
I (17-21 Nov.)	120 [6 – 205]	957 [408 – 1512]	12.7 [1.4 – 21.6]	1.9 [0.8 – 2.5]	n.d.
II (21-27 Nov.)	110 [19 – 204]	722 [408 – 972]	15.1 [4.7 – 26.6]	2.5 [1.5 – 3.7]	n.d.
III (27 Nov. – 1 Dec.)	119 [31 – 211]	772 [336 – 960]	15 [3.8 – 22.8]	2.9 [0.5 – 6.0]	0.2 [n.d. – 0.7]
IV (6 – 12 Dec.)	205 [24 – 1001]	1432 [336 – 2604]	14.1 [2.7 – 38.5]	4.9 [1.7 – 11.6]	0.7 [n.d. – 1.9]

A maximal potential sedimentation from the euphotic zone (39% of the primary production) was estimated during the last occupation of the transect. These data are consistent with what is known about bloom evolution in the Ross Sea Polynya. The bloom reaches maximum biomass in mid-December and decreases to much lower levels throughout January and February (Arrigo *et al.*, 1998, Smith *et al.*, 2000; Smith and Asper, 2001). A delay between production and export is another consistent feature of the Ross Sea (Smith and Dunbar, 1998; Asper and Smith, 1999; Collier *et al.*, 2000). Flux is low during the early phases of the phytoplankton bloom, but as the bloom's biomass reaches its maximum and growth begins to decrease, large aggregates are formed which in turn exhibit increased sinking rates and settle from the euphotic zone (Asper and Smith, 1999).

If we assume that bacterial growth efficiency was 15% (Carlson *et al.*, 1999), we can estimate from bacterial growth rate the amount of carbon metabolized by bacteria relative to the percentage of the primary production. We estimate that the total bacterial carbon demand represented from 0.5 to 11.6% of primary production (**Table XII**). Furthermore, less than 2% of primary production would be metabolized by particle-attached bacteria during spring. It might be possible that the contribution of particle–attached bacteria increased later in summer. The maximum total (free-living and particle attached) bacterial production in the Ross Sea was indeed observed in January-February (Ducklow *et al.*, in press). However, in the Ross Sea increases of bacterial biomass and production remain small relative to change of phytoplankton biomass and productivity (Carlson *et al.* 1998). The low bacterial production was attributed to the low dissolved organic matter supply during the height of *Phaeocystis antarctica* bloom, resulting in a net organic C fixation that was efficiently channeled and retained in the particulate organic carbon pool (Carlson *et al.* 1998).

Moreover, krill concentrations in the Ross Sea, especially the Southern portion, are low (Marr, 1962). *P. antarctica* generally is not grazed by mesozooplankton (Weisse *et al.*, 1994), and in the Ross Sea it is grazed by microzooplankton at only low rates (Caron *et al.*, 2000).

In summary, the early spring plankton community in the Ross Sea was dominated by active phytoplankton growth and accumulation in the surface waters, with generally low and constant rates of sedimentation. In mid-December aggregates were observed and were correlated with increased potential sedimentation (up to 39% of the primary production). Low percentages of phytoplankton production were mineralised by free-living and particle-attached bacteria. Thus, the net losses of photosynthetically generated organic matter in the early stages of the seasonal bloom are quantitatively minor, and the accumulation of organic material in the water column closely parallels the growth dynamics of phytoplankton.

C.2. The barium-barite proxy of export production

Today it is well known that particulate Ba fluxes through the water column and accumulation in the sediments are related with productivity [e.g. *Dymond et al*., 1992; *François et al*., 1995; *Paytan et al*., 1996; *Nürnberg et al*., 1997]. Furthermore, other studies have emphasised that particulate Ba contents in mesopelagic waters, while reflecting productivity, show a better correlation with bacterial degradation of exported organic matter [*Dehairs et al*., 1980, 1997]. Furthermore, *Dehairs et al*. [1997] observed a response time for mesopelagic Ba to changes in surface productivity in the order of a few weeks to a month.

C.2.I. Validation of the Ba-barite proxy: biogeochemical processes acting on the distribution and the trace element content of the Ba proxy

C.2.I.1. *From dissolved to particulate Ba*

Biological subtraction of dissolved Ba

The complex association of barium with phytoplankton activity (Dehairs *et al.,* 1980; Stroobants *et al.,* 1991 and Dehairs *et al.*, 1992) results in a distribution where the dissolved barium is generally depleted in the surface ocean and enriched in the deep ocean (Wolgemuth and Broecker, 1970; Li *et al.*, 1973). The depletion in surface waters should reflect the incorporation into biogenic matter and precipitation as barium sulphate inside micro-environments (Dehairs *et al.*, 1980; Bishop, 1988 and Stroobants *et al.*, 1991). Using this characteristic, we estimated the potential particulate flux which should be associated to the dissolved Ba consumption. The calculation was done for the southern ACC using the well documented dissolved Ba section (Cattaldo *et al.*, submitted) from WOCE/I6 CIVA-1 (44-70°S, 30°E) where a systematic Ba concentration gradient between the surface mixed layer and winter water (i.e. temperature minimum water, stations 2 to 26, 55.7°-69°S) was observed (**Figure 35**). We calculated the loss function required to account for the Ba utilisation in the surface layer. We have written the mass balance for Ba bringing into account Ba transport via vertical advection, turbulent diffusion and uptake-sedimentation:

$$J=K(\Delta Ba/\Delta z)_{up}+W[Ba]_{summer}-W[Ba]_{winter} \quad (\mathbf{14})$$

Transport coefficients applied were the same as those used by de Baar *et al.* (1995; turbulent diffusion coefficient, $K= 3.10^{-5}$ m^2 s^{-1}) except that we choose a higher vertical velocity as would occur in the Southern part of the ACC (W=58 to 106 10^{-5} cm s^{-1}; upwelling velocities annually averaged and zonally averaged over 1700km, Hense *et al.*, in prep.). Incoming advective transport was calculated using the Ba concentration found in the winter water layer ($[Ba]_{winter}$) and outgoing advective transport was based on the average Ba concentration in the box with lowest Ba concentrations ($[Ba]_{summer}$). For the eddy-diffusive flux (upward) the concentration gradients between winter water and summer water were considered ($(\Delta Ba/\Delta Z)_{up}$).

Balancing in's and out's allowed to estimate the consumption term *J*. We found Ba fluxes of 5.5±5 to 10.5±9 mg cm^{-2} ky^{-1}, respectively. Assuming that Ba uptake within the upper water layer (~60 m) continues during 1 to 4 months depending on the latitude (length of growth season based on duration of ice-free conditions; Schweitzer, 1995), the high flux of 10.5 mg cm^{-2} ky^{-1} would induce a Ba deficit of 4.2 nmol L^{-1} what is more than twice the observed deficit (1.8 nmol L^{-1}).
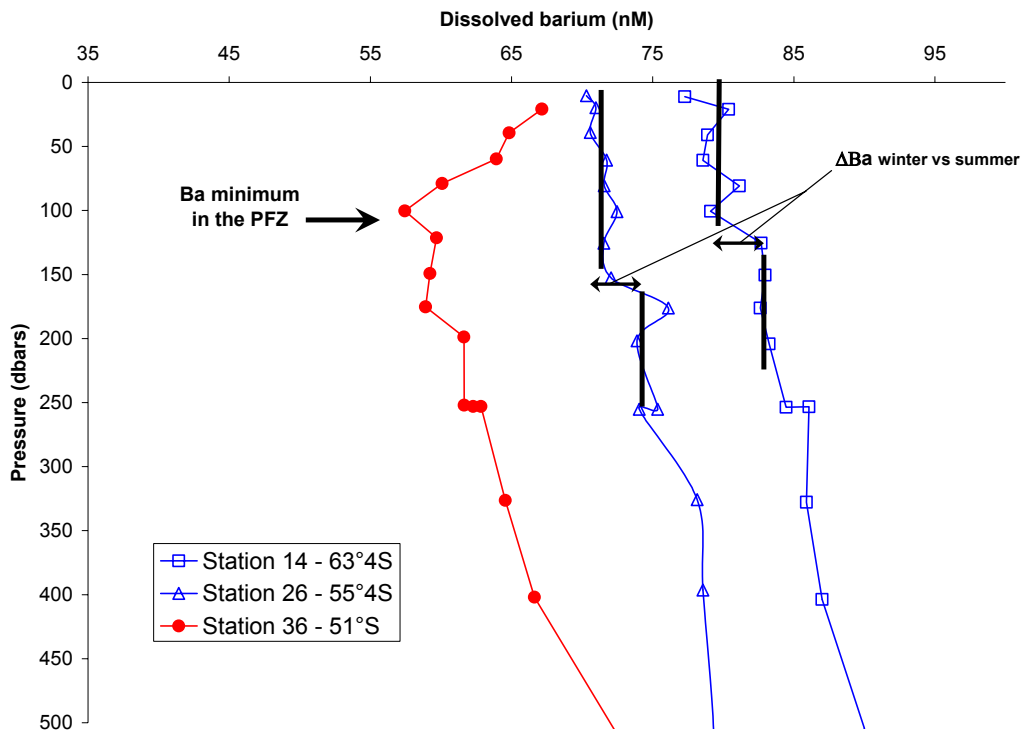
Figure 35: Selected dissolved Ba (nmol l^{-1}) profiles of the upper 500m of the CIVA-1 section at 30°E. Open symbol profiles taken in the ACC show the Ba concentration gradient between summer and winter seawaters. Full circles profile reflects the dissolved Ba minimum observed in the PFZ which results most likely from biological activity (Cattaldo et al., submitted).

Using the lower flux of 5.5 mg cm^{-2} ky^{-1}, calculations show that the observed Ba deficit can be accounted for (calculated Ba deficit 2.2 nmol L^{-1}). Resulting fluxes of particulate Ba around 5.5 mg cm^{-2} ky^{-1} for ACC are of the same order as biogenic Ba vertical rain rates in the PFZ (2.1 mg cm^{-2} ky^{-1}) and in the POOZ (1.7 mg cm^{-2} ky^{-1}) of the Atlantic sector (see **Table XVI, this §**) but suggests a non negligible dissolution of particulate Ba during transit of the particulate matter to the sediments.

Incubation experiments - translocation of Ba from solution to suspended matter and phytoplankton

Ba does not seem to be directly involved in phytoplankton growth or biochemical reactions although its particulate content in the ocean is correlated with the surface biological productivity. By studying and quantifying the Ba uptake by algae we aim to better constrain this link. It is common for uptake experiment studies to compare specific uptake rates (**Eq. 15**).

The relation between specific uptake rates and incubation times should a be linear increasing : For a situation with long incubation times and non-linear uptake shown in

scheme 3, calculations introduce a bias since as it is clear that no incorporation occurs during phase #2.

$$V\ (h^{-1}) = [\ (R_{fp}-R_{np})\ /\ (R_{isw}-R_{np})\ ]\ /dt \qquad (\textbf{15})$$

With R_{fp}=final particles isotopic ratio
   R_{np}=natural isotopic ratio in particles
   R_{isw}=seawater isotopic ratio after addition of spike
   dt=incubation duration (h)
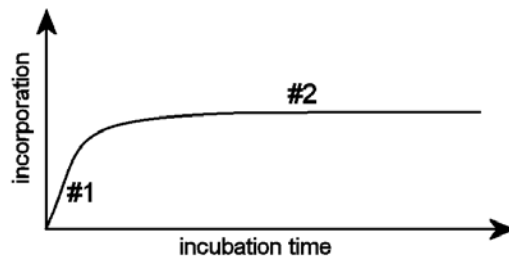
(**3**)

For the major part of our experiments, the phase #1 was very fast (<1hour) and unresolved. Consequently, we avoid the use of uptake rate values and replace them by the Fx100 (**Eq.3**, §2.B.5). This factor which represents the change of the isotopic ratio in particles after exchange with seawater will be used for inter-comparison as an index of isotopic exchange. An F value of 100 indicates that the entire particulate material has exchanged isotopically with ambient solution.

- Barium
Figure 36 summarizes the results for the whole data set of short term Ba incubations (i.e. laboratory diatom or *Phaeocystis* cultures and shipboard experiments).
The largest variations of the isotopic ratio were found for *Phaeocystis* (average F~58%); next largest for diatom cultures (av. F~18%), then for SAZ'98 (av. F~11%) and finally smallest for ANTARES-4 and Ross Sea (av. F~3%). For the natural systems (SAZ'98, AESOPS and ANTARES-4), there was no clear relationship with depth or incubation condition (time, light, dark, live or dead cells). This suggests that the incorporation of Ba is fast and mainly the result of adsorption.
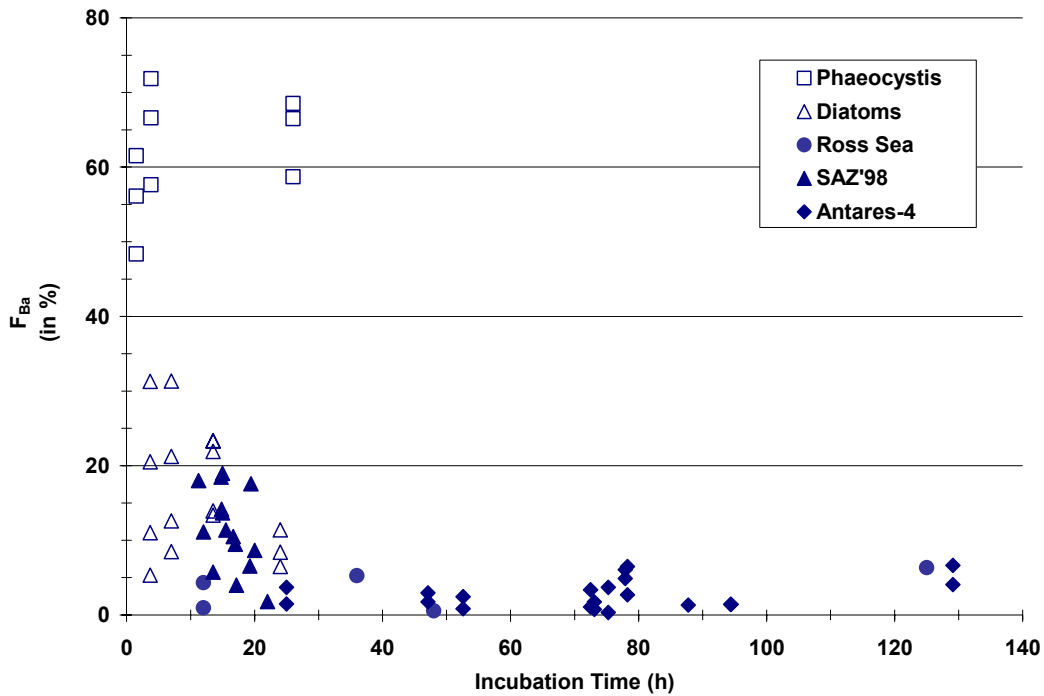
Figure 36: Variations of the ratio $^{138}Ba/^{135}Ba$ (relative to the spiked seawater $^{138}Ba/^{135}Ba$) with incubation time for on-board incubations (Ross Sea, full circles; SAZ'98, full triangles and ANTARES-4, full diamonds) and in-vitro experiments (*Phaeocystis*, open squares and diatoms, open triangles)

However, for *Phaeocystis* and diatom cultures, interesting features were observed: **(1)** For *Phaeocystis* cultures (**Figure 37**), after a fast change of F (0 to 55% in 1hr30'), a further small incorporation (F from 55 to 65%) was observed.
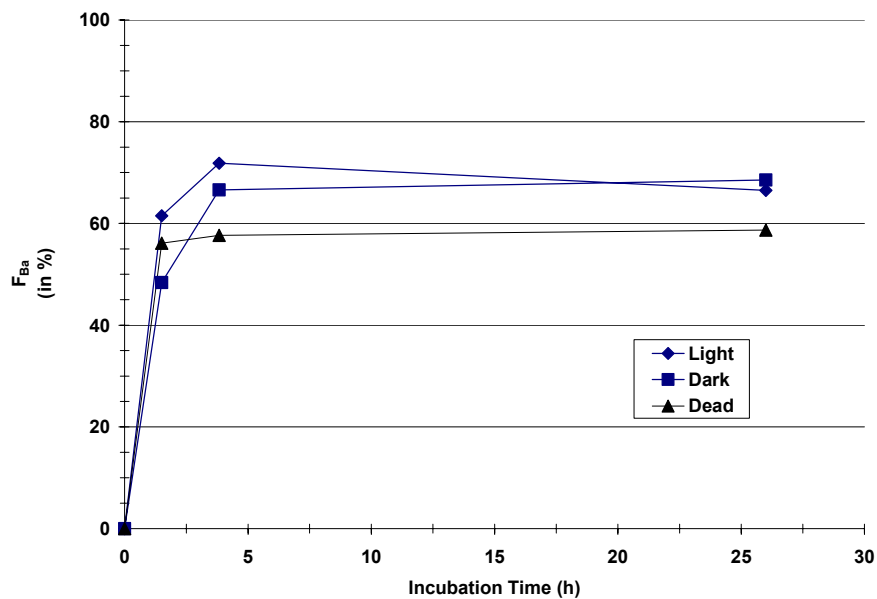
Figure 37: Same as **Fig.36** but *Phaeocystis* experiments only with phytoplankton under light (full diamonds) or dark (full square) conditions or with killed cells (full triangles).

91

Then the process of isotopic homogenisation is stopped and a plateau was reached. The fact that the three experiments, including dead phytoplankton incubations, showed a (significant) incorporation of Ba suggests that this incorporation process is not mainly due to uptake, but rather to adsorption. However, the higher F values for live *Phaeocystis* compared to dead cells and the increase of F between 2 and 4 hours (observed for the live cultures but not for the dead cells) suggests that an active incorporation, although limited, is going on.

(2) Figure 38 shows an inverse relation (r^2=0.78) between F and the total particulate Ba concentration for diatom cultures. This suggests proportionally less exchange for incubations with high original Ba concentrations. This can be explained if we assume that two particulate Ba pools are present in diatoms; one exchangeable, the other not. Hence, the variations of the $Pool_{exchangeable}$ / $Pool_{non-exchangeable}$ ratio will control the variations of F. An F value greater than 50% would mean that the exchangeable pool is the most important and vice-versa.

Our observations suggest that in case of low original Ba concentrations (<1500 pmol/L), the proportions of these two stocks may be close (but the non-exchangeable pool remains the major one, F between 20 and 30%) while for high concentrations (>3500 pmol/L) the non-exchangeable (internal ?) pool will be clearly predominant (F<10%). This feature can be noticed only for the experiments with diatoms for which the range of the particulate Ba concentrations was large.
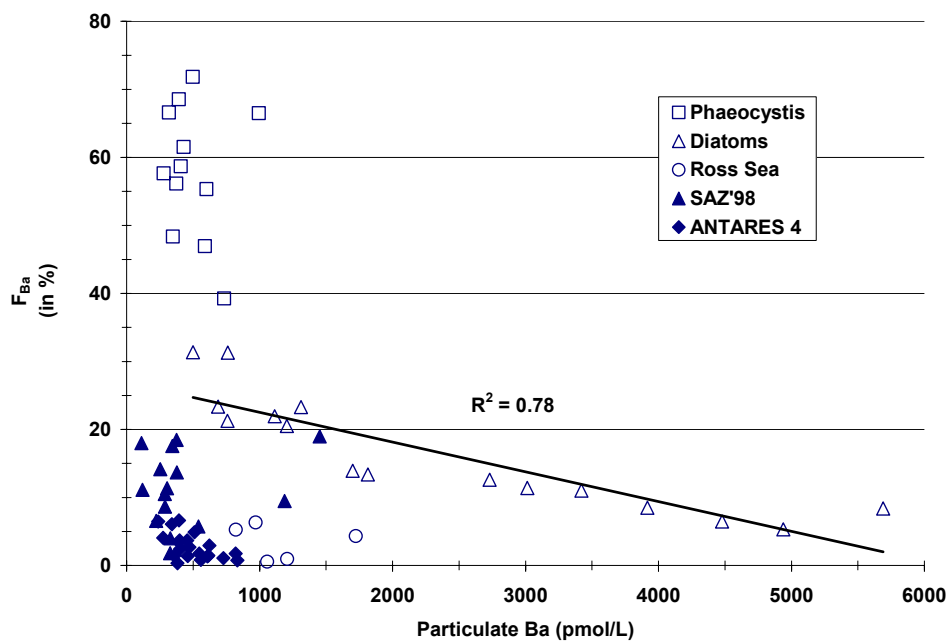
Figure 38: Same as **Fig.36** excepted that F is expressed versus total particulate Ba concentration for on-board incubations (Ross Sea, full circles; SAZ'98, full triangles and ANTARES-4, full diamonds) and in-vitro experiments (*Phaeocystis*, open squares and diatoms, open triangles). Regression line applied for diatoms only.

- Strontium

Exchanges between seawater and natural Southern Ocean particles are clearly higher for Sr than for Ba, with an average value for F around 47% (**Figure 39**). For all experiments, a large variability of F is observed (21-100% for diatom cultures, 16-82% for SAZ'98 and 17-74% for ANTARES-4). As expected, an increase of the incubation time seems to result in an increase of the exchange between seawater and particles (see full diamonds, **Figure 39**). In general, however, the deeper samples, having smaller Sr contents, were incubated over longer periods (because we assumed reduced biological activity at greater depth). Thus, as for Ba (see **Figure 38**), F might be inversely related with Sr content (**Figure 40**), rather than with incubation time.
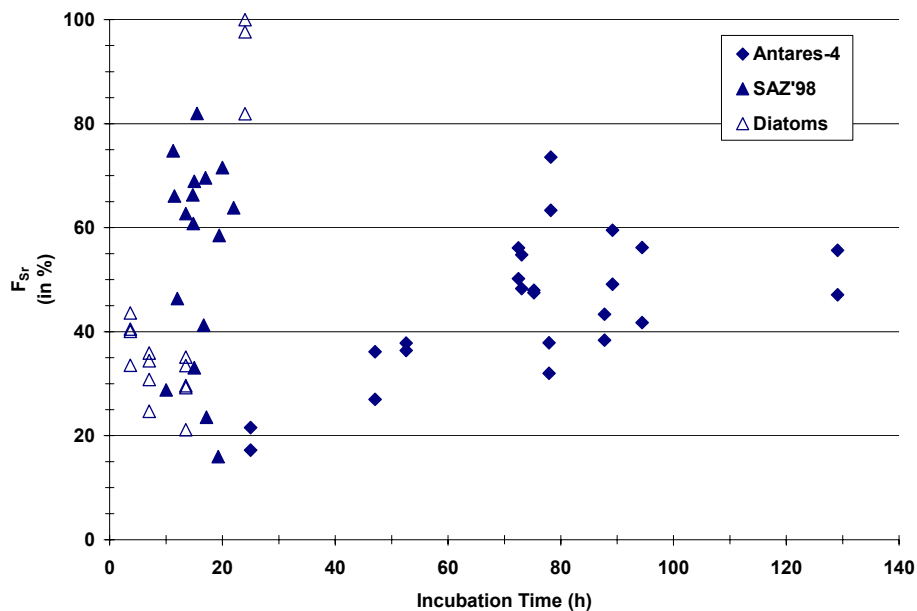
Figure 39: Variations of the ratio $^{88}Sr/^{86}Sr$ (relative to the spiked seawater $^{88}Sr/^{86}Sr$) versus incubation time for on-board incubations (SAZ'98, full triangles and ANTARES-4, full diamonds) and in-vitro experiments (diatoms, open triangles).

As outlined previously, there is probably a close inverse link between F and the relative contribution of a non- or a poorly-exchangeable Sr pool. This is evidenced for in-situ experiments (**Figure 41**): the exchange is larger in deep (full symbols; smaller Sr content) than in surface samples (open symbols; larger Sr content). This condition can be related to the nature or quality of suspended matter present at these two depth levels: in surface waters the main non-exchanging pool would be associated with skeletal material ($CaCO_3$ and/or $SrSO_4$) or with organic matter while at greater depth, the exchanging pool becomes relatively more important due to a partial dissolution of the skeletal material or to the organic matter microbial degradation.
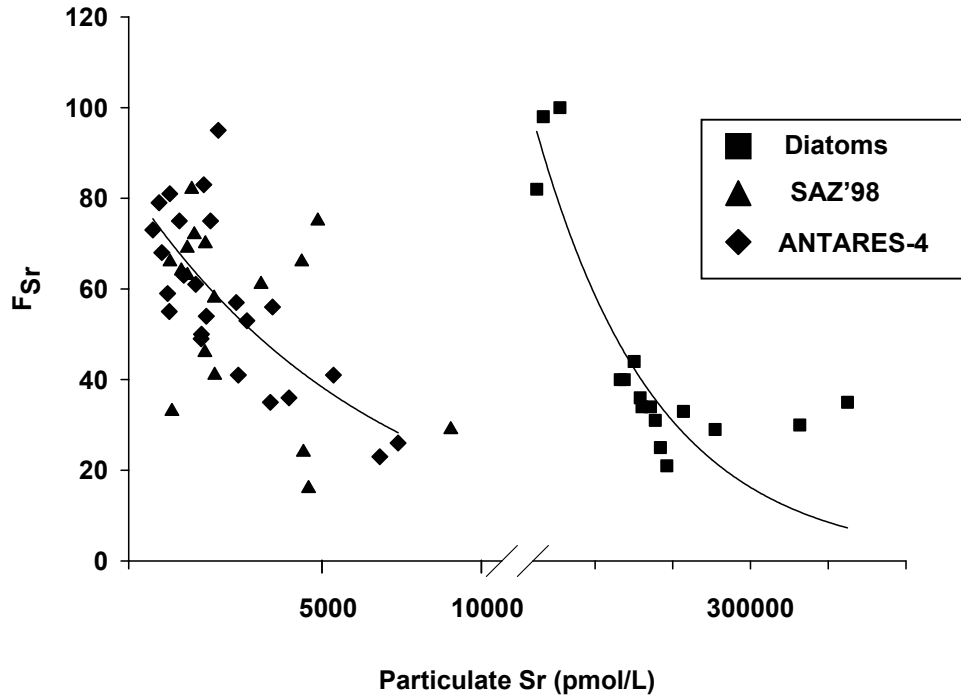
Figure 40: Same as **Fig.39** excepted that F is expressed versus particulate Sr concentration for on-board incubations (SAZ'98, full triangles and ANTARES-4, full diamonds) and in-vitro experiments (diatoms, full squares).
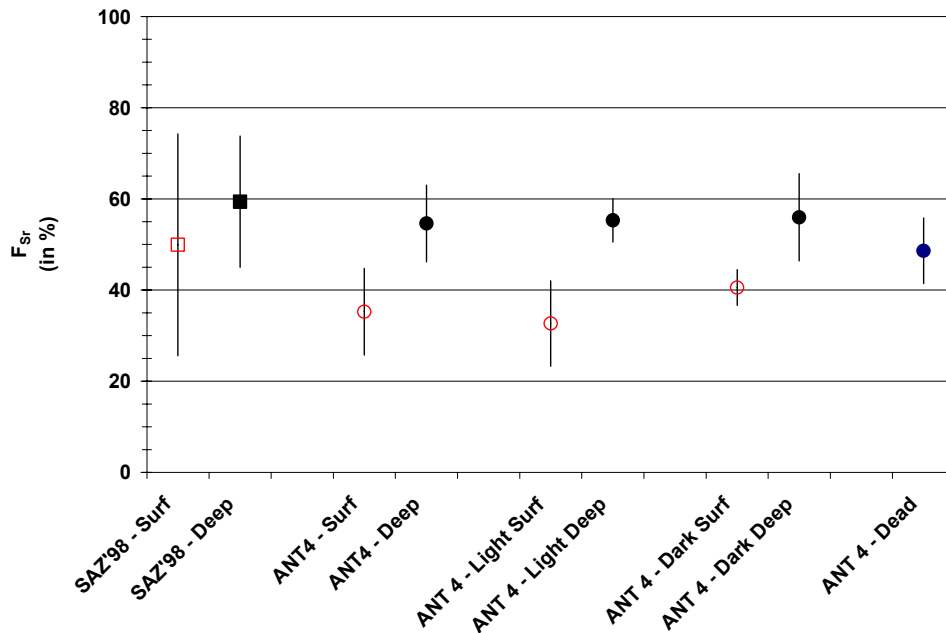
Figure 41: Variations of the ratio F_{Sr} for surface (~30m, open symbols) and deep (100 to 200m, full symbols) on-board experiments during SAZ'98 and ANTARES-4.

-Long term incubations

Results are summarized in **Table XIII**. For diatoms, after 84 incubation days, F values for Ba range from 13% (axenic cultures) to 18% (alive material) which is similar to the ones obtained at the end of short term cultures (F ~ 14-22%). This indicates that the transfer of Ba from dissolved to particulate phase during long term incubations is limited and again supports the assumption of a coexistence of a fast exchanging and a non-exchanging refractory pools: a short incubation period is sufficient to saturate the small (external) pool with the [135]Ba provided by the spike. Isotopic equilibrium is installed quickly by continuous renewal of already exchanged atoms while the internal pool remains mostly unchanged.

Table XIII: F values obtained for long term in-vitro degradations.

Phytoplankton	Incub. Type	Incub. Time days	F Ba %	F Sr %
Diatoms	Axenic	84	18	88
Diatoms	Dark	84	13	76
Phaeocystis	Alive	1 (26hr)	66	-
Phaeocystis	Dark	1 (26hr)	69	-
Phaeocystis	Dead	1 (26hr)	59	-
Phaeocystis	Alive	57	55	-
Phaeocystis	Dark	57	39	-
Phaeocystis	Dead	57	47	-

A decrease of F is observed for *Phaeocystis* cultures between short and long-term experiments (from 65% at T=26 hours to 46% at T=57 days, in average). These lower final signals can be explained by assuming a relative decrease of the exchangeable stock (with isotopic ratio largely modified) compared to the non-exchangeable one (with isotopic ratio that remains natural) during degradation. It seems plausible to observe this decrease only for *Phaeocystis* because they are not protected by skeletons and can be easily degraded: the early adsorbed Ba with modified isotopic signature will be progressively lost during the remineralisation (i.e. dissolution) of the algae on a long-term scale.

In non-axenic diatom culture, formation of large aggregates was observed, probably as a result of bacterial activity. Numerous barite crystals were observed by SEM after 84 days in an aggregate (**Picture 1**). At the same time no evidence of barite was found in the culture kept under axenic conditions. In contrast, for *Phaeocystis* cultures, a few isolated barites were observed in the axenic culture after 56 days (photo). Although our SEM aliquots were probably not perfectly representative of the cultures, this gives insight that the precipitation of barite is a long and complex process (weeks-months) that can hardly be reproduced in *in vitro* experiments. Yet, the presence of bacteria and diatoms seem to favour the precipitation of barite.

Three Ba sources could be involved for barite formation: (1) the Ba adsorbed on the particulate phase; (2) the Ba from the ambient solution and (3) the original internal Ba not affected by isotopic exchange. Since no increase of F was observed after barite precipitation (as dated by SEM), hypothesis (1) and (2) can be rejected. Further investigation should focus on which form Ba is incorporated within the skeleton to facilitate the barite precipitation, especially the likelihood of micro barites (<< 1µm) should be investigated.
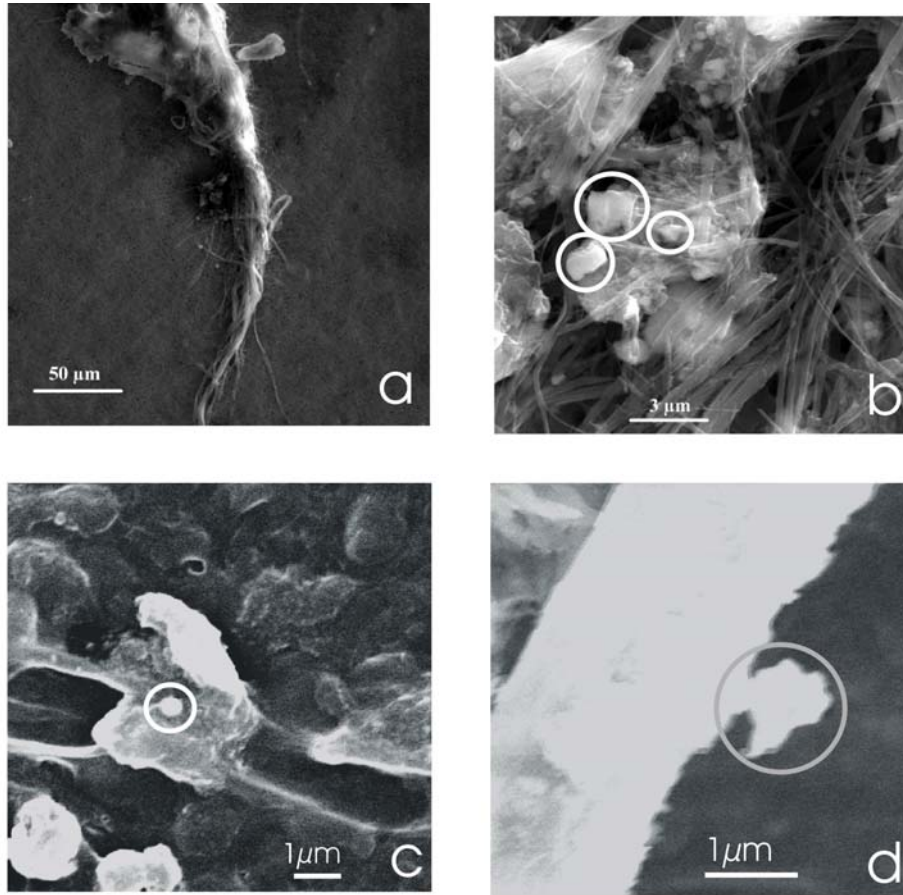
Picture 1: SEM-MEP pictures of material depredated during long term incubations: aggregates (a) and barites within this aggregate (b) are from non axenic diatom cultures after 84 days. (c) and (d) represent isolated barites in *Phaeocystis* cultures after 57 days.

- Summary

Our results suggest that the exchange between solution and particles is mainly due to adsorption processes. In case the adsorbed Ba finally leads to barite, these findings are in agreement with Bishop's observation (1988) that barite is apparently not actively formed by marine plankton. Incubations with high original particulate Ba

and Sr concentrations are characterized by the lowest relative exchange. As a consequence, high concentrations of particulate Ba and Sr seem largely associated with non-exchanging reservoirs. We hypothesize that the total particulate stock consists of two pools. Differences between experiments can be explained if there is some control by the nature of the incubated material:

(1) High exchange for Ba in case of *Phaeocystis* (F~58%) and low exchange in case of diatoms: *Phaeocystis* is a naked flagellate representing an easily exchanging substrate because it forms large gelatinous colonies and thus probably favors adsorption. On the contrary, the skeleton of diatoms (and probably also coccolithophorids) can play the role of non-exchanging phases, with Ba directly incorporated in the skeleton or present as micro-barite (<<1 μm) associated within the skeleton.

(2) High Ba and Sr exchanges for SAZ'98 compared to ANTARES-4: there are indications that dinoflagellates and coccolithophorids (= poorly exchanging pools?) dominate the phytoplankton distribution at ANTARES-4, while at SAZ'98 nanoflagellates and picoflagellates were predominant in terms of cell numbers. Clearly further work is required on this aspect.

(3) The pool which is not exchanging with the ambient solution could be isolated from undersaturated seawater and, therefore, it would be the ideal site for barite formation and preservation. This is reflected also by the relation between mesopelagic Ba and diatom abundance, described in this **§, section C.2.III.1 and Figure 47**.

C.2.I.2. Barite Characterization: Morphology and REE content

SEM – Morphologies
Scanning Electronic Microscope investigations on SAZ'98 (45°S) and ANTARES-4 (station #8) filtered particles showed that barite microcrystals are present throughout the water column (10 - 3200m). The barite crystals from the upper hundred meters size often less than 1μm and exhibit irregular shapes although well crystallized and larger (1-3μm) particles can be present (**Picture 2**). In contrast, deeper barites are usually more than 2 μm. The comparison between SAZ'98 and ANTARES-4 barites did not show differences between Sub Tropical Indian and Sub Antarctic Australian sectors nor between shallow and deep morphotypes. However, the assumption that barite precipitation occurs within barite saturated microenvironments created by the degradation process of organic material, is in accordance with the shape of the particulate Ba profiles described above.

Composition - REE in barites
Ce contrasts with the other LREE by having two oxidation states (IV and III). Hence, focusing on REE and especially on the Ce anomaly (Ce/Ce* = 2[Ce/Ce$_{PAAS}$] /

[La/La$_{PAAS}$ + Pr/Pr$_{PAAS}$]) that expresses the difference in behaviour between Ce and other REE, can provide insight into (1) adsorption-desorption processes through the water column; (2) particle sources and (3) redox processes (e.g., Sholkovitz *et al.*, 1994; Lerche and Nozaki, 1998; Tachikawa *et al.*, 1997, 1999).
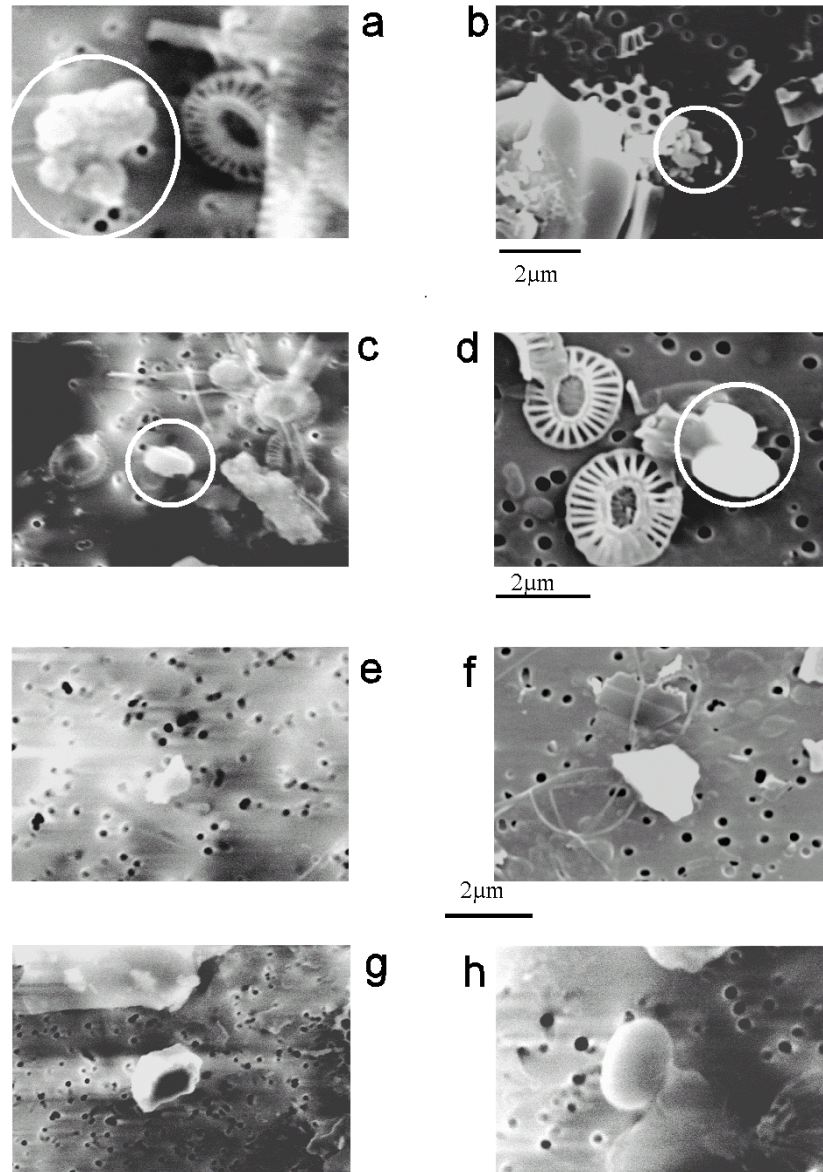
Picture 2: SEM-MEP pictures of suspended matter samples from ANTARES-4 and SAZ'98 expeditions. (a) and (b) aggregates of barites (resp. ~1µm, station 8, 150m, ANTARES-4 and 45°S, 200m, SAZ'98) (c) to (h) isolated crystals of barites: (c) ~1µm, station 8, 150m (ANTARES-4) (d) 45°S, 200m (SAZ'98) (e) ~1.5 µm, station 8, 3200m (ANTARES-4) (f) 45°S, 200m (SAZ'98) (g) ~3.5 µm, station 8, 3200m (ANTARES-4) (h) ~2 µm, station 8, 3200m (ANTARES-4)

The normalised REE patterns of successive leachates (**Figure 42**) show that all but HNO$_3$ leachates are REE depleted, especially for the first four steps.
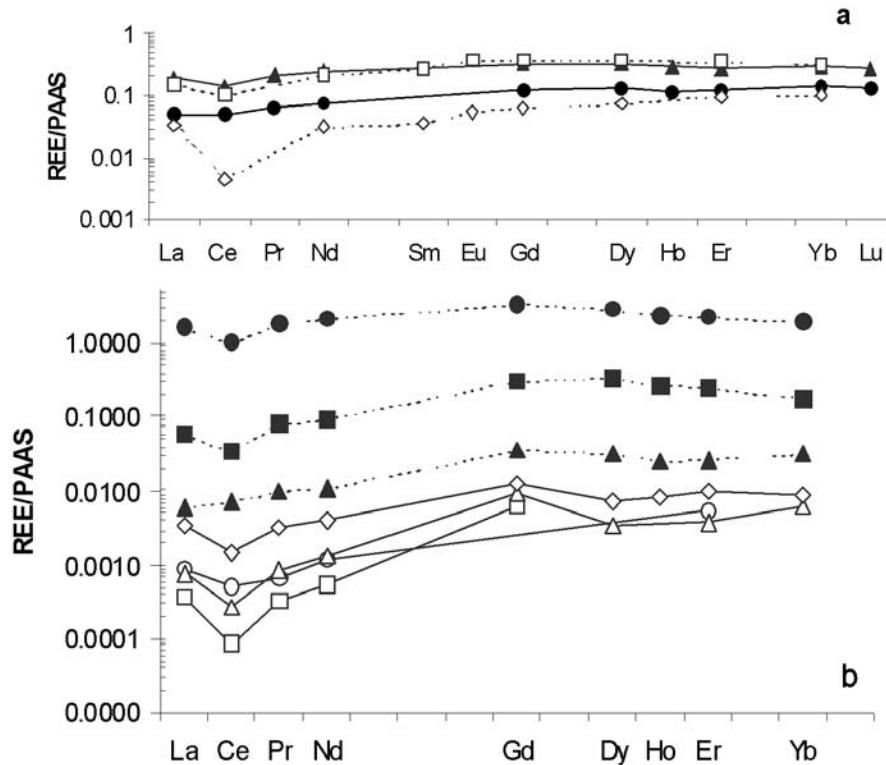
Figure 42: PAAS normalised REE patterns. a) Bulk sediments and associated phases. Bulk PS2376: closed triangles. Bulk PS2361: closed circles. Diatoms: open squares (Elderfield et al., 1981). Foraminiferas: open diamonds (Elderfield et al., 1981). b) Leachates of tube E (PS2376). Step 1: H_2O_2 (open circles). Step 2: HCl_{XS} 0.5 (open squares). Step 3: HCl_{XS} 0.75 (open triangles). Step 4: $HCl_{XS}1$ (open diamonds). Step 5: HF 0.1N (filled squares). Step 6: HNO_3 0.5N (filled circles). Step 7: HF 40% (filled triangles).

It probably identifies the involvement of essentially two end-members in the suspended matter. The first one is REE depleted and bears a negative Ce anomaly,typical of carbonate phase, (Piper, 1974a, b; Elderfield et al., 1981; Nath et al., 1992, 1997). The second pole is less depleted to slightly enriched in REE with a less negative Ce/Ce* signal (i.e. higher contribution of detrital phases). In case the barite Ce/Ce* signature is not significantly different from the range defined by the mixing of the carbonate and the lithogenic poles and/or in case barites contribute but to a very low extent to the REE content in the total leachate budget, compared to the one of these phases, it is not possible to identify the barite anomaly signal.

Piper (1974a) observed La content in barite was enriched by a factor of 5 compared to shales. Guichard et al. (1979) found that marine barites were also REE enriched, especially for La (10-326 ppm). More recently, Martin et al. (1995) and Fagel et al. (1997) found REE enrichment in barite concentrates too. Although Guichard et al. (1979) checked the purity of the barite (90-100 %), they also observed anatase or rutile (TiO_2) impurities. The purity of barite phase is "only" 5-23 % in Fagel et al. (1997) and they identified via SEM investigation some contamination with Ti and Al

oxides in these barite concentrates. Nd isotopic data of Martin et al. (1995) are not consistent with the hypothesis of Nd enriched barites. They concluded that the barite phase has been contaminated by Nd from accessory minerals (zircons, sphenes, rutile) that could be REE enriched (Becker and Dietze, 1986) and that pure barite Nd content is much less than 4 ppm. These oxides could be involved in a REE contamination of the barite rich phases of Guichard et al. (1979) and Fagel et al. (1997) as well.

In order to contribute towards the assessment of the barite REE contents we calculated the Nd balance taking into account the Nd contribution from Mn oxy-hydroxides (Elderfield et al., 1981) and carbonates (Palmer, 1985). All the Nd leached in the early steps of our leaching experiment could be explained by these two phases with no significant contribution of barite as discussed in details in Cardinal et al. (submitted). Hence, our study is in agreement with Martin et al. (1995) indicating barites contain a very small amount of REE, probably even less than a few ppm.

C.2.II. *Particulate Ba$_{xs}$ profiles*

The stock of Ba$_{xs}$ in mesopelagic waters has been shown to reflect the input and the (bacterial) degradation of surface water organic matter (Dehairs *et al*., 1990, 1997). The usefulness of mesopelagic Ba$_{xs}$ as a proxy for carbon input and heterotrophic POC respiration derives from the role played by biogenic detritus as the micro-environment concentrating and conveying excess-Ba to mesopelagic waters. This Ba$_{xs}$ is released to the ambient fine suspended matter pool as barite micro-crystals and the seasonal build up of this signal in the mesopelagic waters is thought to reflect the intensity of organic carbon transfer and degradation (*Dehairs et al*., 1990, 1992a, 1997).

Figure 43 shows the sampling zones during SAZ'98 and ANTARES-4 expeditions and particulate Ba$_{xs}$ depth distributions are shown in **Figure 44**.

Excepted the profile at 46.8°S, there is a surface Ba$_{xs}$ minimum (< 200pmol l^{-1}) followed by an increase in the 100-200 m depth range. Between 150 and ~500 m a broad mesopelagic maximum is observed, followed by a slight decrease in concentration below. These features are best expressed by the ANTARES-4 G2 and G4 and the SAZ'98 51.0°S and 53.0°S profiles. Such Ba$_{xs}$ profiles and the observed concentrations are in agreement with earlier observations for Subantarctic and PFZ areas (*Poisson et al*., 1990; *Dehairs et al*., 1991, 1997; F. Dehairs, unpublished results) as discussed in Cardinal *et al.* (in press).
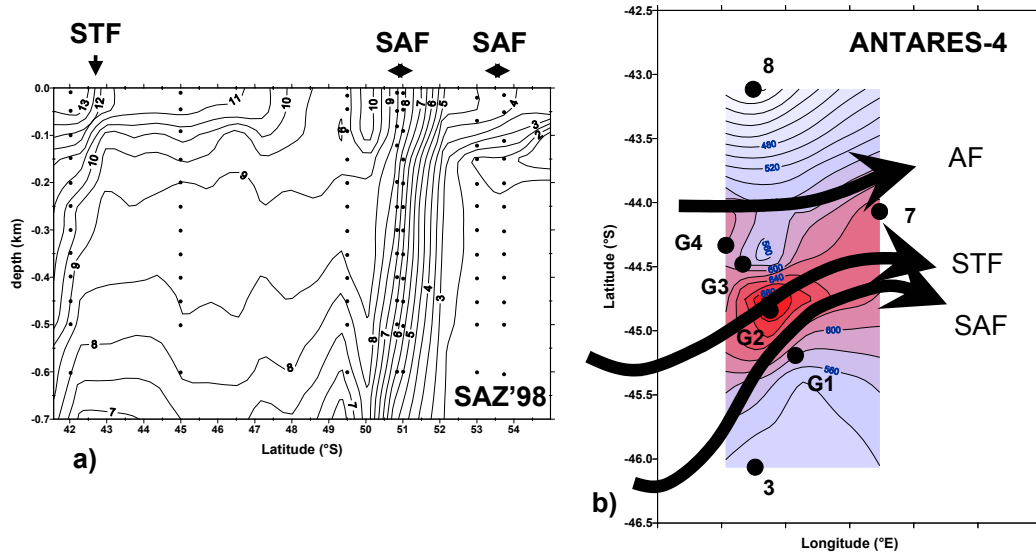
Figure 43: (a) SAZ'98 temperature section (contour plot) and particulate Ba samples (dots) taken during this cruise. Subtropical, Subantarctic and Polar Fronts are also reported (b) particulate Ba sampling stations (dots), mesopelagic Baxs (contour plot) and simplified frontal system (from H.Y. Park, pers. comm.) during ANTARES-4.

However for some stations, the particulate Ba_{xs} profiles are less smooth (e.g. ANTARES-4, stations 7 and 3) or the subsurface maximum is less apparent (e.g., SAZ'98 42.0° and 47.0°S). The SAZ'98 profile at 45.0°S, is peculiar and will be discussed further (see section *advection* in this §). We calculated the mesopelagic Ba_{xs} content at each station by considering the depth weighted average Ba_{xs} concentration for the depth interval between 150 and 450m where the mesopelagic Ba maximum appears (**Figure 44**).

For the SAZ'98 stations there is a trend of increasing mesopelagic Ba_{xs} with increasing latitude south of 46.8°S (**Figure 45**).

Simultaneously, the average particulate REE and Ca contents decrease southward and this is explained respectively by (i) a lower contribution of lithogenic components from Tasmanian shelf and (ii) the larger contribution of diatoms to phytoplankton biomass. This southward increase of mesopelagic Ba_{xs} has already been observed during earlier cruises for the SAZ and PFZ (Dehairs *et al*., 1990; *Poisson et al*., 1990, F. Dehairs, unpublished results) as discussed in Cardinal *et al.* (in press). Subtropical and Subantarctic waters during SAZ'98 have lower mesopelagic Ba_{xs} contents, barely exceeding a background Ba signal of about 160 pmol l^{-1} observed for depths > 1000 m (e.g. Indigo 3 cruise; *Dehairs et al*., 1990). On the contrary, going south from the Subantarctic zone across the PFZ we observe in general a sharp increase in Ba_{xs} content reaching maximum values, slightly exceeding 600 pmol l^{-1} at the southern edge of the PF.
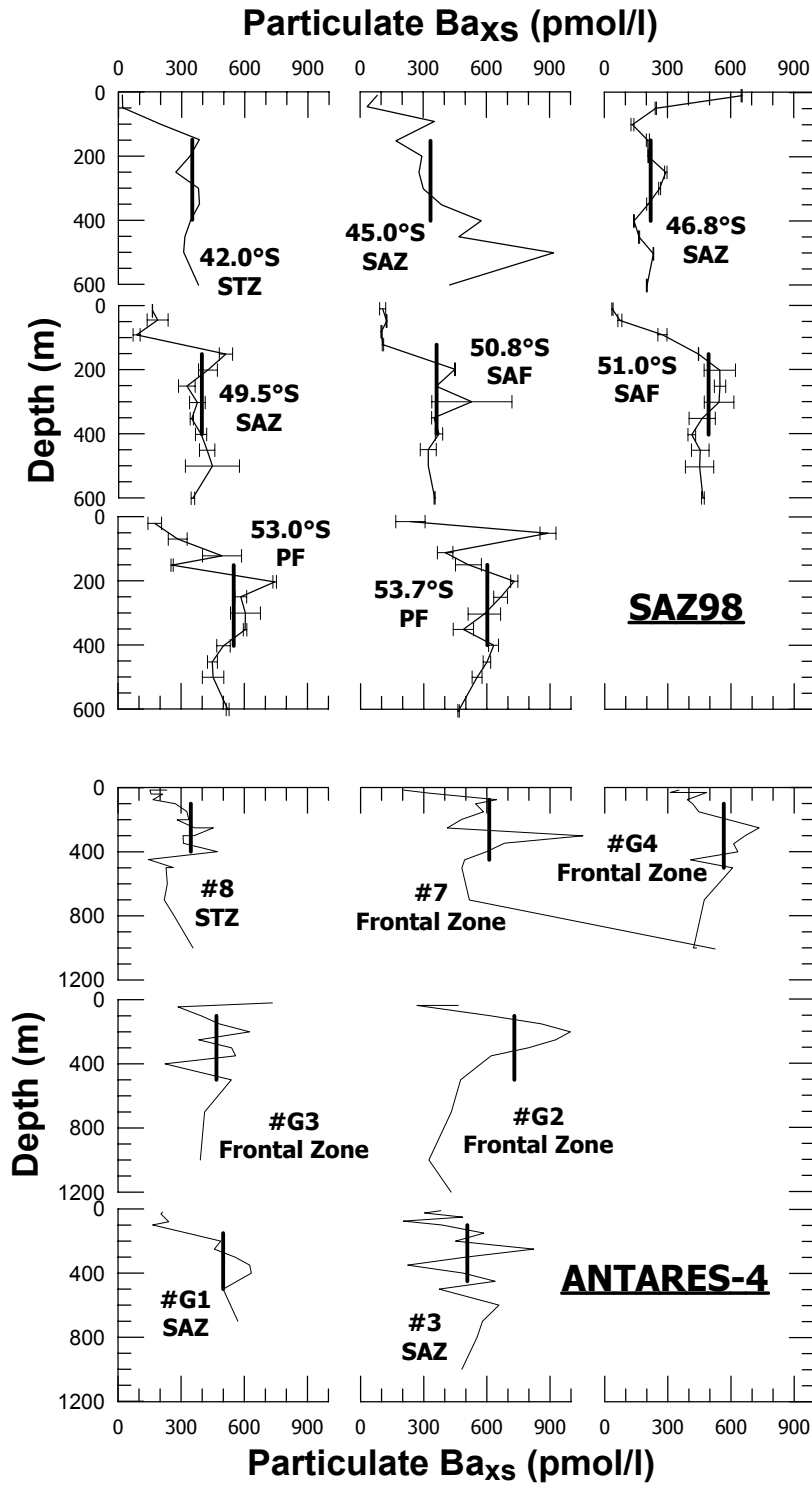
Figure 44: Particulate Ba$_{XS}$ profiles during SAZ'98 and ANTARES-4. The vertical lines represent the mesopelagic Ba$_{XS}$: average of Ba$_{XS}$ throughout the depth layer indicated.
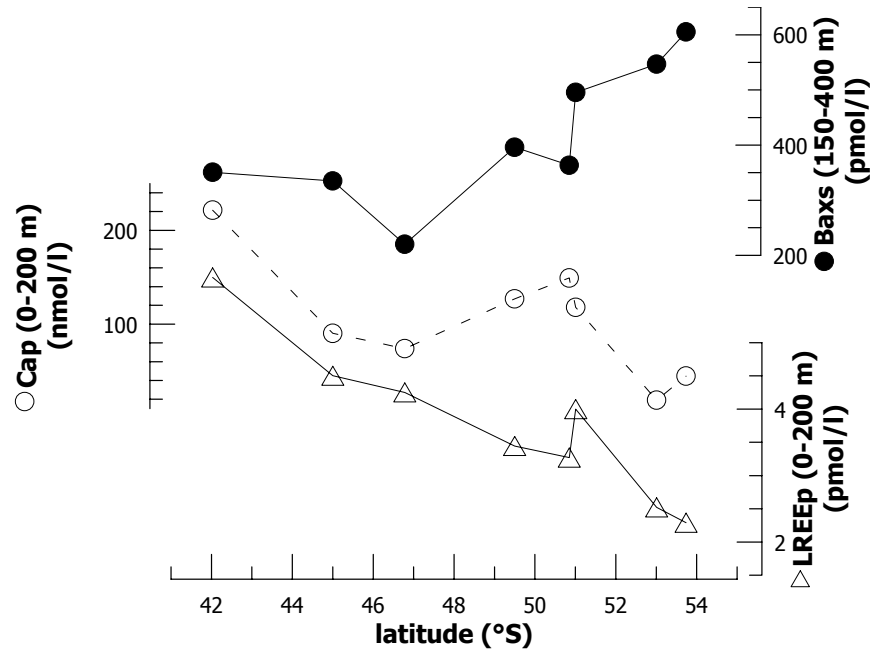
.

102

Figure 45: Mesopelagic Ba$_{xs}$ (filled circles), 0-200 m average particulate Ca (open circles) and 0-200 m average particulate ΣLREE (open triangles) vs. latitude during SAZ'98.

Our observations would emphasise the ubiquitous character of the mesopelagic excess-Ba signal as well as the importance of the PFZ and the Southern Antarctic Circumpolar Current as areas of enhanced export and mesopelagic mineralisation of exported organic matter. Latitudinal trend of mesopelagic Ba$_{xs}$ also coincides with the one of increasing *f*-ratios (see **section *N-flux rates and f-ratio* in §B.2**). The *f*-ratio (ratio of phytoplankton NO_3 uptake over the sum of nitrate, ammonium and ureum uptake) reflects the ratio of new over total production and is an instantaneous image of the potential export production (Elskens *et al.*, submitted). Thus there is an internal consistency between the potential of the production system for export and the observed breakdown of organic matter in mesopelagic waters suggesting that in general the daily production rates are representative of longer periods (weeks).

ANTARES-4 stations located south of the SAF, in the PFZ, show mesopelagic Ba$_{xs}$ contents (500 to 550 pM) similar to those observed in the PFZ region of the Australian sector during SAZ'98. Station 8, north of the Agulhas Retroflection Front shows low mesopelagic Ba$_{xs}$ (300 pM). On the contrary, stations 7, G4, G3, G2, located in the zone squeezed between the converging AF, STF and SAF have high mesopelagic Ba$_{xs}$ contents, with station G2 showing the maximum value (800 pM) observed during this study (**Figure 43**). Clearly, the areas studied during ANTARES-4 and SAZ'98 highlight that frontal systems are characterized by higher export production rates.

Advection

At SAZ'98 45.0°S, concentrations of Al, Zr, Ti, REE, Mn and Th increase between 250 and 600m (**Figure 46**). The increase is not observed for elements that have a large non-lithogenic fraction (Sr, Ca, U) except for Ba. This station is close to the Tasmanian continental shelf and intermittent northeast - southwest subsurface currents have been observed in the area (Rintoul and Sokolov, submitted) as well as unusually high total-dissolvable Fe contents (Sedwick *et al.*, 1997).
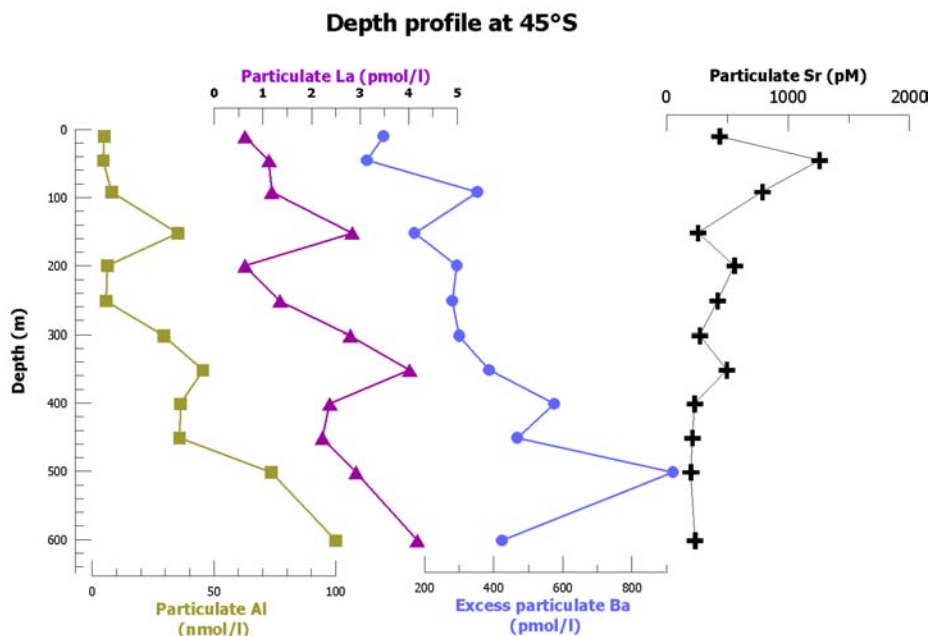

Figure 46: Al (nM), La (pM), Ba$_{xs}$ (pM) and Sr (pM) profiles at 45°S, 142°E (SAZ'98).

We hypothesize that resuspended sediments from the Tasmanian shelf and slope were advected to the site of sampling. Our data emphasise that the analysis of specific elements such as Al, Zr, Ti, Th and REE are useful to identify such advective input of particles disturbing the vertical signal.

At 45°S, we also observe a continuous increase of Ba$_{xs}$ between 300 and 500 m to a maximum of 1000 pmol l^{-1}. At 600 m Ba$_{xs}$ has decreased again to the level observed at the other stations. At first sight the link between high Ba$_{xs}$ (assumed to result from a 100 % in-situ authigenic process) and high loads of lithogenic elements is not obvious. A similar situation, however, was observed in the North East Atlantic, where sediment traps at intermediary depths, close to the margin, showed evidence of contribution of advected material including Ba$_{xs}$ (Fagel *et al.*, 1999; Dehairs *et al.*, 2000). While reducing conditions in shelf sediments would preclude preservation of barite (Von Breymann *et al.*, 1992; McManus *et al.*, 1998), it is possible that this advected matter represents nepheloid layer particles, which might be enriched in

Ba$_{xs}$ or reflects higher levels of Ba$_{xs}$ generated in the water column by higher productivity in shelf waters.

C.2.III. Confronting the Ba-barite proxy and new/export production

C.2.III.1. *Conditional relationship between new production and mesopelagic particulate barium*

New production, as estimated from ^{15}N tracer incorporation experiments carries information about the degree of coupling between processes in the surface box and deeper layers (Eppley and Peterson, 1979). When dealing with new production, however, the matter of scale is of critical importance and it is only under genuine steady state conditions, that new and export production can be compared (Platt *et al.*, 1992). In most cases ^{15}N-tracer incorporation experiments provide only an estimate of daily new production unless time-series observations are available. However, in **§B.2** and in Elskens *et al.* (submitted) it is argued that a low sensitivity of *f*-ratio for perturbations of ammonium availability is characteristic for systems in apparent steady state. Thus stability of *f*-ratio was interpreted to reflect a relatively stable ecosystem in an advanced stage of the growth season. Thus, in systems characterised by a low versatility of the N-uptake conditions values for daily new production rates would possibly also hold for longer time scales (e.g. weeks to months) and would thus provide reliable estimates of carbon export from the photic zone. We took advantage of this peculiarity to explore the relationship between the mesopelagic barium signal and new production estimates. The ultimate goal being the development of an accurate transfer function, linking particulate barium and export production at the base of the photic zone, and forecast the organic carbon mineralisation flux and profile in the mesopelagic water column (200 to 600m).

A model approach was developed and applied to new production and water column particulate Ba$_{xs}$ data collected during the SAZ'98 cruise (February-March 1998) between the Subtropical Front and the Polar frontal zone, south of Australia (142°E). In **§B.2.I** and in Elskens *et al.* (submitted) we discussed that *f*-ratio perturbance by increased ambient ammonium was mostly low during SAZ'98, except for a section between 45° and 46°S where surface waters have been reported to be enriched in dissolved iron. This apparent stability of *f*-ratio thus warrants the extrapolation of new production values to longer time scales and allows for a comparison of new production and water column particulate Ba$_{xs}$ stocks. From this direct comparison it appears, however, that new production predictions, conditional on the site-corresponding Ba predictor variable, were not significantly improved over a constant mean prediction, i.e. assuming a single zonal average mesopelagic Ba signal. While primary productivity decreased in north-south direction during SAZ'98 (F.B. Griffiths

et al., unpublished data, 2001), we observed that mesopelagic Ba_{xs}, on the contrary, increased from the Subantarctic Zone to the Polar Front parallelling a north-south increase of diatom contribution to carbon biomass in the upper 100m (see **§B.2** and **§C.2.II**, and Kopczynska *et al.,* Cardinal *et al.*, in press). When plotting the ratio of new production over mesopelagic Ba versus % carbon biomass carried by diatoms, it appears clearly that with increasing relative contribution of the latter, the NP over meso-Ba_{xs} decreases (**Figure 47**). In other words, the decay of a given amount of exported and decayed organic matter does not result in a constant amount of mesopelagic Ba, but would depend also on the relative abundance of diatoms in the original phytoplankton community. By categorizing the NP/meso-Ba_{xs} ratios with respect to the relative abundance of diatoms, the ratios are much closer to the local means than to the overall mean and the within group standard deviation are noticeably smaller than the overall standard deviation (**Figure 47**).
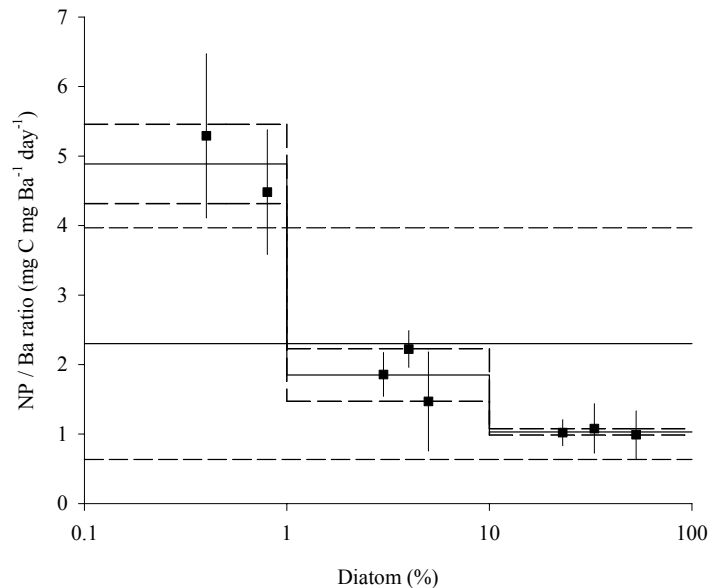
Figure 47: Ratio of new production over mesopelagic Ba versus % carbon biomass carried by diatoms along the SAZ'98 transect.

A possible way to alleviate the diatom-effect on the NP versus meso-Ba_{xs} regression is to consider an interactive regression model in which the level of the Ba-predictor variable is tuned by additional variables through linear combinations. To create a set of additional variables, n-1 contrast codes are required considering n possible levels of the categorical variable diatom%. These are readily obtained by using the Helmert contrasts [*Judd and McClelland*, 1989]:

n levels

$$\begin{matrix} \lambda_{1,i} \\ \lambda_{2,i} \\ \vdots \\ \lambda_{n-1,i} \end{matrix} \begin{pmatrix} n-1 & -1 & \cdots & -1 & -1 \\ 0 & n-2 & \cdots & -1 & -1 \\ \vdots & \vdots & \vdots & \vdots & \vdots & \vdots \\ 0 & 0 & 0 & 1 & -1 \end{pmatrix}$$

where $\lambda_{k,i}$ are the code values for n levels of the categorical variable diatom%. Then the predictor variables to be included in the regression equation (**Eq. 16**) can be written in the following general form:

$$\begin{cases} X_{0,i} &= Ba_i \\ X_{1,i} &= \lambda_{1,i}.X_{0,i} \\ \vdots & \vdots & \vdots \\ X_{n-1,i} &= \lambda_{n-1,i}.X_{0,i} \end{cases}$$

with $Y_i = \beta_o.X_{o,i} + \beta_1.X_{1,i} + \cdots + \beta_{n-1}.X_{n-1,i} + \varepsilon_i = (\beta_o + \beta_1.\lambda_{1,i} + \cdots + \beta_{n-1}.\lambda_{n-1,i})Ba_i + \varepsilon_i$ (**16**)

with Y_i, the ith new production estimate, ε_i, the ith residual assumed to be independent and normally distributed, and β the unknow parameters to be estimated by minimizing the sum of the squared residuals. In the present study, the goodness of fit is satisfactory with three levels of variation only.

In conclusion it can be said that mesopelagic Ba_{xs} indeed reflects the magnitude of the exported carbon flux and its partial mineralisation in mesopelagic waters. However, one must carefully assess the composition of the phytoplankton community, since, clearly, the sensitivity of the Ba-tracer towards exported carbon is greater when diatoms contribute significantly to the phytoplankton community.

C.2.III.2. *Relationship between new production POC, Ba_{xs} fluxes recorded by sediment traps*

Daily new production was estimated by multiplying the column integrated primary production data from F.B. Griffiths (unpublished data) with the *f*-ratio values obtained from the ^{15}N incubation work (**Table XIV**; see **§B.2.I** and Elskens *et al.*, submitted). These new production values were compared with export production estimates calculated from the POC fluxes recorded by the sediment traps moored at 47°, 51° and 55°S (Trull *et al.*, submitted) using the algorithms proposed by Sarnthein et al. (1988) and Martin *et al.* (1987) (**Table XV**). Export production was also recalculated from the Ba_{xs} sediment trap flux (Cardinal, unpublished data, 2001) by combining the algorithm describing the evolution of POC/Ba ratio with depth in the oceanic water

column given by François et al. (1995), and the above mentioned algorithms relating POC flux at depth with export production.

Table XIV: SAZ'98 latitudinal distribution of new production ($mgC.m^{-2}.d^{-1}$) calculated from integrated primary production ($mgC.m^{-2}.d^{-1}$, from F.B. Griffiths, unpublished data) and *f*-ratio (this study) and export production ($mgC.m^{-2}.d^{-1}$) based on Sarnthein *et al.* (1988) and François *et al.* (1995) equations.

Latitude °S	PP $mgC.m^{-2}.d^{-1}$	NP (1) $mgC.m^{-2}.d^{-1}$	EP (2) $mgC.m^{-2}.d^{-1}$	*f*-ratio	st.dev. *f*-ratio
42	374	35		0.09	0.04
45 (STF)	308	150		0.49	0.10
47 (SAZ)	220	56	45, 69, 50	0.25	0.04
49	208	73		0.35	0.02
51 (SAF)	133	57	48	0.43	0.03
53	83	37		0.45	0.15
54	117	41	33, 29	0.35	0.11
55 (PFZ)	96	32		0.33	0.02

(1) = PP x f-ratio

(2) calculated following footnote (2) in Table **XV**

Table XV: For three SAZ'98 mooring sites and six depths, comparison of export production estimations based on POC or Ba fluxes approaches and on different algorithms (see footnotes). POC data from Trull *et al.* (submitted).

Station	Trap depth m	Corg µmol/m²/d	Corg µg/cm²	FBa µg/cm²	POC/Ba	Ex Prod (1) mg/m²/d	Ex Prod (2) mg/m²/d	Ex Prod (3) mg/m²/d	Ex Prod (4) mg/m²/d
47°S	1000	522	75	1.82	40.9	26	45	28	47
	2000	465	81	2.83	28.4	42	69	51	82
	3000	312	57	2.19	26.2	36	50	50	67
51°S	3300	328	60	2.09	28.8	41	48	56	65
54°S	800	346	63	1.33	47.5	19	33	20	33
	1500	171	32	1.24	25.9	13	29	16	34

(1)   Export production calculated as : $ExP = F_{POC} / (a\,Z^{c})^{(1/b)}$, (based on Sarnthein et al., 1988)

(2)   Export production calculated as : $ExP = F_{Ba}\,(d\,Z^{e}) / (a\,Z^{c})^{(1/b)}$, (based on Sarnthein et al., 1988 and François et al., 1995)

(3)   Export production calculated as : $ExP = F_{POC} / (Z / Z_{100})^{f}$, (based on Martin et al., 1987)

(4)   Export production calculated as : $ExP = F_{Ba}\,(d\,Z^{e}) / (Z / Z_{100})^{f}$, (based on Martin et al., 1987 and François et al., 1995)

with Z = sediment trap depth; Z_{100} = 100m, i.e. the depth horizon through which the C-export occurs

a = 8.93; b = 0.926; c = -0.542; d = 4816; e = -0.614; f = -0.760

Export production deduced from Ba_{xs} fluxes slightly exceed those based on POC flux, but, in general, differences between the two approaches remains within a factor two. We can conclude that for the SAZ'98 expedition there is a ramarkable consistency between three proxies of carbon export flux (new production,

mesopelagic Ba_{xs} and sediment trap flux) despite the fact that these integrate information over quite different time scales (sediment trap time scale > mesopelagic Ba_{xs} > new production). This is an encouraging situation, as it allows to better constrain export production and provides perspectives for assessing mineralisation of exported organic matter in the intermediate and deep ocean.

C.2.IV. Sedimentary Baxs and export production

The barite as paleoproductivity proxy relies on the observed correlation between biological productivity in surface waters and Ba content in recent and past marine sediments (e.g., Goldberg and Arrhenius, 1958; Church, 1970; Schmitz, 1987). Algorithms relying on the vertical evolution of the POC/Ba_{xs} ratio in sediment trap material were proposed to quantify export production from Ba_{xs}. The POC/Ba_{xs} ratio depends on the dissolved Ba concentration (Dymond et al., 1992) or is linked to the water depth (François et al., 1995; Nurnberg et al., 1997). Considering only open oceanic sediment trap data outside influence of slope regions, Francois et al. (1995) established an empirical relationship relating the year averaged POC/Ba flux ratios to depth. This reflects the fact that organic carbon breakdown and barite formation is a homogenous process worldwide and further allows to calculate export production only from Ba_{xs} fluxes. Export production (EP) may be estimated as a function of the water column Ba_{xs} flux (FBa_{xs} in g/cm²/yr) and water depth (Z in m) as given in **Table XV** (we used equation 2 in this case). With FBa_{xs} corresponding to the wet vertical Ba_{xs} flux or Ba_{xs} rain rate. The approach assumes there is no advective supply of Ba_{xs}. However advection of Ba_{xs} has been recently evidenced along the NE Atlantic Margin (Fagel et al., 1999) and probably also in the SAZ section close to the Tasmanian shelf (see **§C.2.II, section *advection*** and Cardinal *et al.*, in press). This approach can also be applied for the sedimentary environment. In that case, FBa_{xs} is the net vertical Ba_{xs} flux or rain rate of Ba_{xs}. To access Ba_{xs} rain rates from sedimentary Ba_{xs} accumulation, we need to correct sediment focusing / winnowing and probable barite dissolution. Vertical rain rate can be calculated from $^{230}Th_{xs}$. Correction of partial dissolution of barite at the seawater-sediment interface, before burial is done as discussed in Fagel *et al.* (accepted).

Export production estimate in the Atlantic sector
Ba_{xs} Vertical Rain Rates (i.e. corrected from focusing/winnowing and for the potential dissolution) are given in **Table XVI**. The estimates of export production vary by a factor of five along the ANT-X/6 transect (1.8 to 10gC/m^2/yr). They are stable in the PFZ (mean = 4.94 gC/m²/yr) but vary by a factor 2 to 3 in the area further south. The accuracy of the export production estimates is affected by the accuracy of the ^{230}Th-correction. On the one hand, the ^{230}Th correction may not be particularly

straightforward in the POOZ due to intense boundary scavenging effect. This area is under the influence of the outflow of dissolved Th-enriched Weddell Sea water (Walter, 1998). The dissolved ^{230}Th enrichment results from a low scavenging rate in the Weddell Sea caused by the local low particle flux (Rutgers van der Loeff and Berger, 1983, Walter *et al.*, 1997). Consequently, in the POOZ the vertical flux of ^{230}Th is higher than the production rate, potentially leading to an underestimation of export production by up to a factor of 2 (R. van der Loeff, pers. comm.). On the other hand, the constant ^{230}Th flux model requires that redistributed particles come from an area characterized by a similar rain rate, i.e. from an area with similar water depth (François *et al.*, 1993; R. Francois, pers. comm.). If the redistributed sediment was initially deposited in a shallower area, before being transported to its final site of deposition, its lower excess ^{230}Th content will dilute the local excess. The error on the vertical flux ranges between 10 and 40% (underestimation of focusing effect and thus overestimation of Ba_{xs} flux and export production), depending on the depth difference between the initial and final deposition site (R. Francois, pers. comm.). For instance, such a sediment supply from a shallow area has been reported for the region in vicinity of Maud Rise (Abelmann and Gersonde, 1991). Thus, irregular seafloor topography (presence of mid-oceanic Antarctica- America ridge) favors advective supply of ^{230}Th from adjacent shallower water depth. The boundary scavenging effect would lead to an underestimation of the Ba_{xs} flux and subsequently to an underestimation of the export production. Our export production estimates from sedimentary Ba_{xs} fluxes may be compared with estimates based on other approaches (primary production, consumption of oxygen, ^{234}Th deficit, suspended particulate Ba, modeling), using data from the same ANT-X/6 cruise or different cruises in the same region (**Table XVII**). All the water column proxies record the highest C export production values in the Polar Front. For instance, Nurnberg (1995) measured the trapped Ba fluxes in the PF (600 and 3200m) and in the POOZ (360 m) and recalculated export productions at 100 m of 5.6 gC/m^2/yr and 1.3 gC/m²/yr respectively. Correcting these values for trapping efficiencies of 67 and 47 % for the upper and lower traps, respectively in the PFZ (100% in POOZ) the estimate in the PFZ for both traps increases to 9.9-10.2 gC/m^2/yr. Rutgers van der Loeff *et al.* (1997) observed a significant enhancement of ^{234}Th adsorption in PFZ (ANT-X/6; 6°W) surface waters during the bloom development, resulting in an estimated carbon export production of 3.6 to 9.6 gC/m^2 during the one-month bloom event. For the POOZ, they observed a lower ^{234}Th-based export production of 1.8-3.6 gC/m^2. Model results of the seasonal bloom development during the ANT-X/6 cruise (Lancelot *et al.*, 2000 and this volume, see Results and Discussion, §D) produce similar export production values for the bloom period (PFZ: 1-7.6 gC/m²/yr; POOZ: 1.2 gC/m²/yr).

Table XVI: Location, geochemistry and export production estimates from studied core tops. 147GCO MAR are calculated from LGM depths and DBD (Connell & Sikes, 1997), KH94-4 MAR are from Ikehara et al. (2000); * sample not taken into account in the mean..

Sample	Environment	Latitude	Longitude	Water depth	Ba_{xs}	MAR	Focusing	VRR Ba_{xs}	Export Production
		°S	°W	m	ppm	mg/cm²/yr	%	mg/cm²/kyr	gC/m²/yr
Atlantic sector (ANT-X/6)									
PS 2368	PFZ	46.5	6.0	3756	832		90	1.8	4.0
PS 2363	PFZ	48.0	6.0	4040	860		90	2.0	4.5
PS 2376	PFZ	48.3	6.0	4091	1272		93	2.2	5.3
PS 2367	PFZ	49.0	6.0	3712	1068		90	2.3	5.8
	mean PFZ							**2.1**	**4.9**
PS 2366	POOZ	50.6	6.0	2060	944		73	1.4	2.9
PS 2362	POOZ	53.0	6.0	2688	1368		80	2.0	4.7
PS2372	POOZ	53.6	6.0	2341	1004		83	1.0	1.8
PS2365	POOZ	55.0	6.0	3117	1410		80	2.3	6.0
	mean POOZ							**1.7**	**3.8**
PS 2361	SIZ	55.1	6.0	3194	1550		82	2.3	6.0
PS 2369	SIZ	55.5	6.0	4059	628		87	2.2	5.5
PS 2364*	SIZ	56.0	6.0	4156	28*		87	0.10*	0.05*
PS 2371	SIZ	57.0	6.0	3660	1083		87	3.5	10.9
	mean SIZ							**2.7**	**7.5**
PS 2370	WG	58.3	6.0	5039	421		91	1.2	2.1
Indian sector (APSARA)									
MD 9406	SAZ	44.7	90.1	3315	799	4.0	71	1.8	3.9
MD 94109	SAZ	44.7	90.1	3315	893	4.0	71	2.0	4.7
KR 8801	SAZ	46.7	79.5	2925	698	2.6	45	2.1	5.0
KR 8802	SAZ	45.8	82.9	3480	657	5.1	81	1.2	2.1
MD 9402	SAZ	45.6	86.5	3572	1017	8.8	90	1.6	3.3
	mean SAZ					**4.9**	**72**	**1.7**	**3.8**
MD 94104	PFZ	46.5	88.1	3460	1221	7.2	90	1.5	3.0
KR 8803	PFZ	46.1	90.1	3400	1018	3.7	70	2.1	5.2
MD 88770	PFZ	46.0	96.5	3290	748	4.6	70	1.9	4.3
MD 94107	PFZ	47.8	90.2	3525	1038	5.7	84	1.7	3.7
KR 8804	PFZ	49.9	100.1	3350	1010	3.2	17	5.4	21.0
MD 88772	PFZ	50.0	104.9	3240	1402	2.7	62	3.0	8.6
MD 9404	PFZ	50.4	90.3	4036	1002	2.3	63	1.8	4.0
MD 88774	PFZ	52.9	109.9	3330	735	6.4	81	1.6	3.4
	mean PFZ							**2.4**	**6.7**
									4.6 if 1 sple excld.
MD 88795	POOZ	50.8	68.0	1950	950	1.9	90	0.2	0.2
KR 8805	POOZ	52.9	109.9	3510	1153	2.6	90	0.6	0.8
MD 84551	POOZ	55.0	73.3	2230	911	3.3	60	1.2	2.3
	mean POOZ							**0.7**	**1.1**
KR 8815	SIZ	63.3	141.9	3880	1014	1.2	-19	3.5	11.0
KR 8822	SIZ	64.7	119.5	3140	594	1.7	-182	6.4	27.4
	mean SIZ							**5.0**	**19.2**
Tasmanian shelf									
147GCO			°E						
4	SAZ	44.1	145.2	2981	778	2.5	61	1.5	3.8
31	SAZ	44.3	149.0	2981	722	3.5	81	0.9	2.2
7	SAZ	45.1	146.2	3307	788	2.7	70	1.2	3.0
14	SAZ	46.3	145.1	3360	1149	1.6	33	2.6	6.5
17	SAZ	47.5	145.5	3001	813	2.5	51	2.0	5.1
KH94-4									
TSP-1	SAZ	47.7	147.5	1301	255	1.2	-75	1.2	3.3
TSP-2	SAZ	48.1	146.9	2283	525	1.2	-3	1.4	3.8
TSP-3	SAZ	48.6	146.4	2897	417	1.2	-30	1.5	3.8
	mean SAZ							**1.5**	**3.9**

147GCO MAR are calculated from LGM depths and DBD (Connell & Sikes, 1997)

KH94-4 MAR are from Ikehara et al. (2000)

(a)   data from Walter et al., 1997

(b)   estimation from Frank et al., 1996

*   sample not taken into account in the mean

Table XVII: Comparison of export production estimates for the Atlantic and the Indian sectors of the S.O. (see text for discussion).

	Material	Proxy		Export production (gC/m^2/yr)			
				SAZ	PFZ	POOZ	SIZ
Atlantic sector							
ANT-X/6	surface sediment	[1] Ba$_{xs}$	aver. (min. - max.)	-	4.9 (4.0 - 5.8)	3.8 (1.8 - 6.0)	7.5 (5.5 - 11)
ANT-X/6	particulate Ba	[2] consumption O$_2$	EP (200-400m)	-	2.73	1.74	1.09
ANT-X/6	particulate matter	[3] ^{234}Th	max EP (gC/m²/bloom)	-	9.6	3.6	-
PF3	traps	[4] Ba$_{xs}$	EP (100m)	-	5.6	1.3	-
		[5]	EP (100m)	-	9.9-10.2	1.3	-
ANT-X/6	modelisation	[6] SWAMCO model	max EP(gC/m²/bloom)	-	7.6	1.2	-
12°-4°E transect	Holocene sediment	[7] Ba$_{xs}$		2.6	7 - 10	14	4.5
Atlantic sector	Holocene sediment	[8] Ba$_{xs}$		3 - 4	5 - 10	15 - 24	5
Indian sector							
APSARA cores	Holocene sediment	[1] Ba$_{xs}$	aver. (min. - max.)	3.8 (2.1 - 5.0)	6.7 (3.0 - 21) 4.6 (1 sple excluded)	1.1 (0.15- 2.33)	19
Indian sector	Holocene sediment	[8] Ba$_{xs}$		-	-	22	-
ANT-X/6	C primary production	[9]	PP gC/m²/yr	-	37.4	8.5	-

[1] This work [2] Dehairs et al., 1992 [3] Rutgers van der Loeff et al., 1997 [4] Nurnberg, 1995 [5] modified from Nurnberg, 1995
[6] Lancelot et al., in press [7] Frank, 1996; Frank et al., 1996 [8] Francois et al., 1997

For the same Atlantic transect (ANT-X/6) export production could also be estimated from mesopelagic organic carbon oxidation rates calculated from dissolved oxygen consumption rates or from the amount of mesopelagic Ba$_{xs}$ built up since the beginning of the growth season (Dehairs *et al.*, 1997). The latter estimate should be smaller than the export production, since it represents only a fraction (although large) of the downward carbon flux from the mixed surface layers. It appears that, for the PFZ, 2.7 gC/m^2/yr are respired in the subsurface water layer between 200 and 400 m. This value reduces to 1.7 gC/m^2/yr for the POOZ and, to only 1.1 gC/m^2/yr for the SIZ. Despite variability of the export production estimates based on different proxies and approaches (**Table XVII**) results indicate generally that export production is at least 1.5 higher in the Polar Front Zone than in the Permanently Open Oceanic Zone.

It is important to note that export productions reported in literature and obtained from dissolution-corrected ^{230}Th normalized sedimentary excess Ba fluxes give much higher export production estimates in the POOZ (14-24 gC/m²/yr), with values at least twice higher than those estimated in PFZ (5-10 gC/m²/yr - Frank *et al.*, 1996; Francois *et al.*, 1997). There is evidence that the maximum export production values occur in the high opal-flux belt of the Atlantic sector, located south of the PF. However, it remains unclear to what extent these massive opal depositions result from the local high productivity, or are enhanced by sedimentary focusing (Rutgers van der Loeff *et al.*, 1997). Indeed, our estimates of export production, based on sedimentary Ba$_{xs}$ fluxes, are much closer to those based on water column proxies, especially in the POOZ. Such observation emphasizes that south of the PF barite

preservation may be underestimated when using the Dymond *et al.* (1992) algorithm. Only a comparison between trap material and bottom sediments could help to accurately assess preservation rate.

Export production estimates in the Indian sector

In the Indian Sector, the mean export production estimate in the PFZ (4.6 gC/m²/yr, one value > 20 gC/m²/yr excluded) is quite similar to the mean estimate for the Atlantic sector (4.9 gC/m2/yr). For the POOZ, the export production values are lower than for the PFZ (0.15-2.33 gC/m²/yr), and usually lower than the values reported for the Atlantic sector. Francois *et al.* (1997) reported a quite high export production value of 22 gC/m^2/yr (**Table XVII**) for the Antarctic Zone in the Indian sector.

This estimate was based on dissolution-corrected ^{230}Th normalized Ba$_{xs}$ flux of one single surface sediment sample in the POOZ close to Kerguelen Island. Two processes may contribute to the overestimation of the export production: (1) the barite preservation rate may be higher than indicated by the Dymond *et al.* (1992) algorithm and (2) the advective supply of ^{230}Th from sites with a shallower water column could dilute the ^{230}Th$_{xs}$ due to production in the local water column and lead to an overestimation of the Ba$_{xs}$ flux. In the SIZ, the two surface sediments give also a high export production of 11 and 27 gC/m²/yr. However, those samples are collected in the eastern part of the studied area and we have no other data for direct comparison. Furthermore, the sampled location is characterized by intense winnowing (focusing factor < 1). The preservation rates, as deduced from Dymond *et al.* (1992), are thus minimum values and the export production estimates are maximum. Finally, we can note that the SAZ average estimate from the Indian Sector (3.80 gC/m²/yr) is very similar to the one obtained for SAZ core tops from Tasmanian Shelf (3.93 gC/m²/yr).

To conclude, export production estimates from sediment Ba$_{xs}$ give similar values in the PFZ for both the Atlantic and the Indian sector of the SO (4.9 and 4.6 gC/m²/yr, respectively). The mean export production estimate in the Indian sector represents only ~ 30% of the Atlantic sector estimate. Both sectors record their highest export production values in the SIZ (mean: 7.5 and 19 gC/m²/yr, respectively). In the Atlantic sector, our export production estimates from sediment are in agreement with other studies based on other proxies measured during the ANT-X/6 cruise, with higher export production in the PFZ than in the POOZ. In POOZ, our results are much closer to the estimates deduced from water column proxies than previous calculations based on dissolution-corrected ^{230}Th normalized sedimentary Ba$_{xs}$ fluxes. This observation suggests that barite could in fact be better preserved in the sediments of the POOZ than suggested by the Dymond *et al.* algorithm (1992).

D. Physical, chemical and biological mechanisms controlling the CO2 uptake in the Southern Ocean: results from the one dimensional-SWAMCO model

D.1. Validation of the SWAMCO model

The ability of the SWAMCO model to reproduce seasonal biogeochemical features of the surface waters of the Southern Ocean and estimate the CO_2 exchange at the air-sea interface was first assessed by applying the model to specific sites where relevant time-series biogeochemical observations are available. These are: the Spring 1992- JGOFS – ANT X/6 expedition of *R/V Polarstern*, which sampled the Polar Frontal Zone and the sea-ice associated S-ACC at 6°W (Lancelot et al., 2000); the Southern Ocean Iron RElease Experiment (SOIREE; Boyd et al., 2000), conducted in the Australasian sector in late summer 1999 (Hannon et al., 2001); and the monitoring station KERFIX located in the Indian sector of the Southern Ocean (50°40'S 68°25'E).

D.1.I. SO-JGOFS cruise ANT-X/6 of *R.V. Polarstern* (Oct.-Nov. 1992)

The predictions of the model, driven by *in situ* physical and chemical conditions observed during the 1992 cruise ANT-X/6 of *R/V Polarstern*, were successfully compared with chemical and biological observations (Lancelot et al., 2000). In particular the model properly simulates the diatom bloom recorded in the iron-enriched Polar Frontal region as well as the lack of ice-edge phytoplankton bloom in the marginal ice zone (MIZ) of the ACC area (**Figure 48a**). Also well predicted is the depletion of surface silicic acid (**Figure 48b**) and dissolved inorganic carbon (**Figure 48c**), concomitant to the diatom bloom.

The carbon budget calculated from model predictions over the cruise period (40 days) shows a marked difference between the PFr and the MIZ (**Figure 49a and 49b**). This is clearly due to quantitative difference in primary production and its fates (accumulation, export, mineralisation). Spring primary production is one order of magnitude higher in the PFr, reaching a total of 1900 mmol C m^{-2}. From this 43% is exported out of the surface layer, 30% is re-mineralised and 27% accumulates in the surface layer (**Figure 49a**). The fate of the latter (mineralisation and/or export) remains undetermined at the time-scale of the model runs (40 days). As a consequence the biotic uptake of TCO_2 (1331 mmol C m^{-2}) in the PFr overwhelms the TCO_2 increase associated to the upwelling of CO_2 saturated waters, leading to a strong under-saturation of the surface waters, and a subsequent sink of atmospheric CO_2 (**Figure 48c**). In contrast, remineralization rate is relatively important (~50% of primary production) in the low production MIZ (**Figure 49b**), resulting in a biotic uptake of TCO_2 (92 mmol C m^{-2}) slightly lower than the upward transport of TCO_2.

Hence the biotic uptake does not compensate the cumulative effect of seasonal warming and upward transport of CO_2 in over-saturating the surface waters, resulting in a net source of CO_2 to the atmosphere in the MIZ (**Figure 49b**).

These model results agree perfectly with the estimations of CO_2 exchange across the air-sea interface based on interpolated pCO_2 from field measurements during the successive transects of the ANT-X/6 cruise (Bakker et al., 1997).
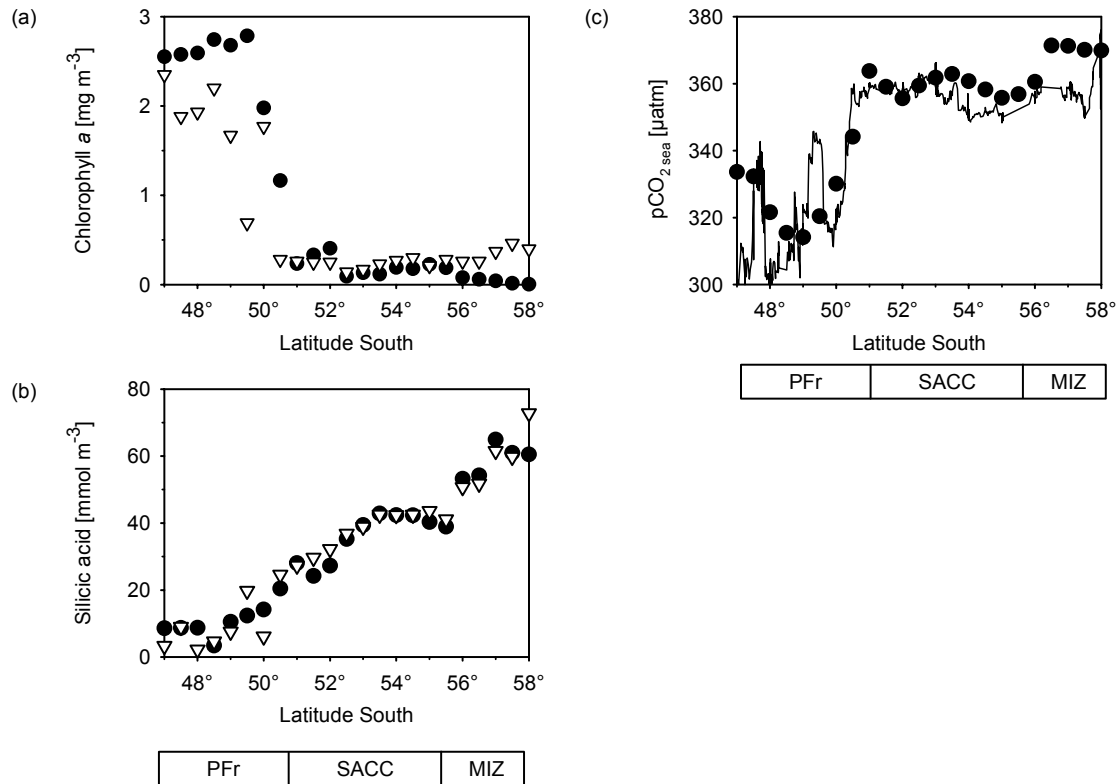
Figure 48: SWAMCO model predictions (•) vs. field observations (∇, ——) along transect 11 of the ANT X/6 cruise: Chlorophyll a (a), silicic acid (b), $pCO_{2\,sea}$ (c).
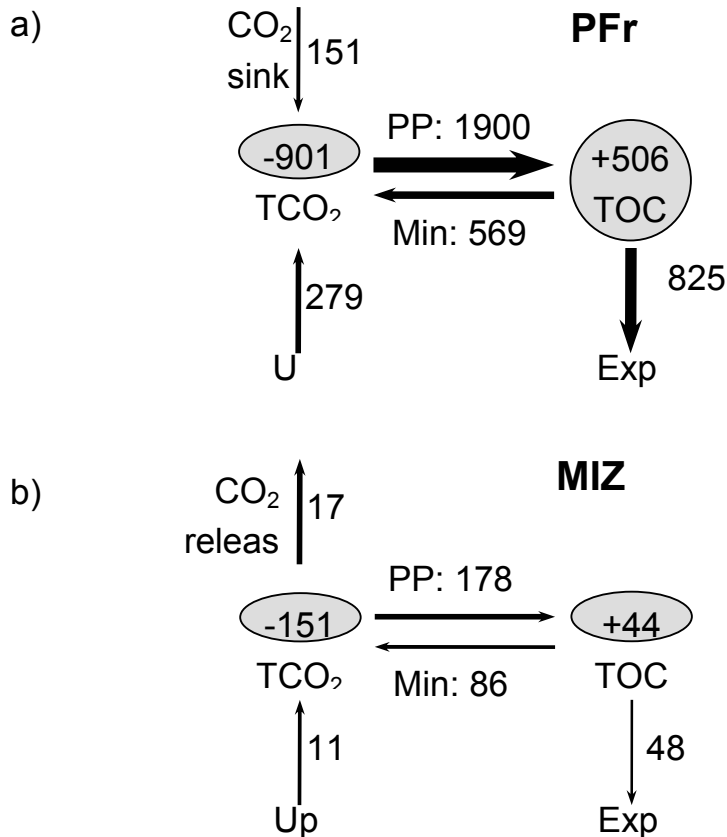
Figure 49: Carbon budget predicted by the SWAMCO model for the period of the JGOFS – ANT-X/6 cruise (Oct. - Nov. 1992) in the Polar Frontal region (PFr) and Marginal Ice Zone (MIZ) of the SACC (Atlantic sector). PP: net primary production; Min: mineralisation; Up: TCO_2 change due to vertical transport; Exp: POC export production. Fluxes and variations of the standing stocks of TCO_2 and TOC are given in mmol C m^{-2}.

D.1.II. Southern Ocean Iron RElease Experiment (SOIREE, Feb. 1999)

As a second validation experiment, the SWAMCO model was applied to the SOIREE site and further used to investigate the impact of a mesoscale *in situ* iron enrichment experiment (SOIREE) on the planktonic ecosystem and biological pump in the Australasian-Pacific sector of the Southern Ocean (Hannon et al., 2001). For this purpose model simulations were run over a period of 60 days (longer then the site occupation of SOIREE, 13 days), allowing focusing on both the early and late impacts of the intended iron fertilisation. A control run (without iron enrichment) was carried out in parallel, and corresponded to the situation out of the fertilised patch. The hydro-meteorological forcing of these simulations, similar for the patch (IN) and the surrounding waters (OUT), was extracted from *in situ* observations for the SOIREE period (13 days) and from archived meteorological data for the period following the site occupation.

Model predictions of chlorophyll a associated to diatoms and nanoflagellates state variables were successfully compared with *in situ* size-fractionated chlorophyll a recorded both inside and outside the patch, during the 13 days period of SOIREE (Fig. 3). Predicted diatom-Chl a, which remains at very low levels outside the patch (Chl *a* > 20μm ~ 0.05 μg l^{-1}) dominates the phytoplankton inside the patch, as observed during SOIREE (Gall *et al*., 2001). As shown by the 60 d simulation, the dominance of diatoms inside the patch increases after the end of SOIREE (**Figure 50b and 50d**) peaking at 3.4 μg Chl a l^{-1} around day 23. SWAMCO predictions of chlorophyll a stocks after day 13 could be successfully compared with those estimated from SeaWiFS ocean colour (Abraham et al., 2000). The composite image obtained 42 days after the onset of SOIREE (mid March 1999) shows a 230 km^2 region with chlorophyll a >1 μg l^{-1}, and maximum concentrations of >2 μg Chl a l^{-1} (based on algorithm). Our model predicts around day 42 a mean chlorophyll a of 1.33 μg l^{-1} that corresponds to the decline phase of the iron-stimulated bloom.
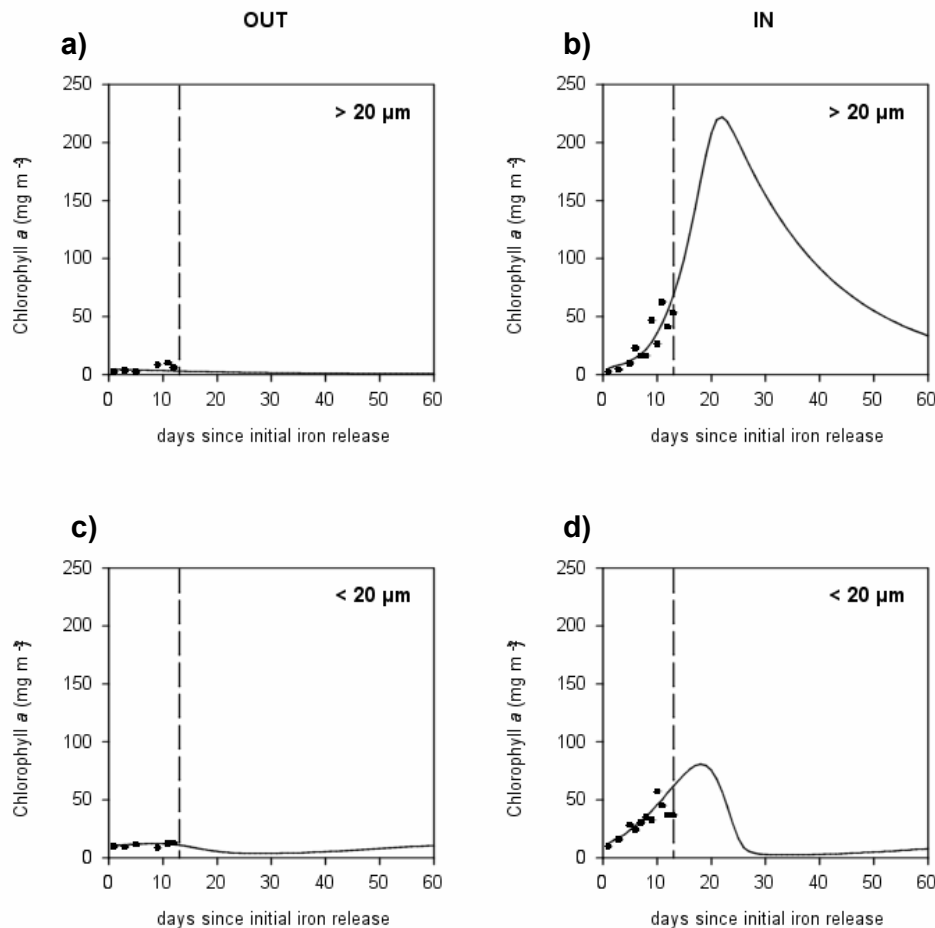
Figure 50: SOIREE: time-series of chlorophyll a integrated over the mixed-layer, outside (OUT) and inside (IN) the fertilized patch, for the large (>20μm) and small (<20μm) algae: SWAMCO modeling (line) vs. field observations (dots). The dashed line indicates the end of the SOIREE site occupation.

The 60d SWAMCO runs predict inside the fertilised area a delay of about 2 weeks between the maximum of chlorophyll a concentration in the upper layer and those of POC export flux out of the mixed-layer (34 mmol C m^{-2} d^{-1}; **Figure 51b**), and surface ΔpCO2 (~79 µatm; **Figure 51a**).
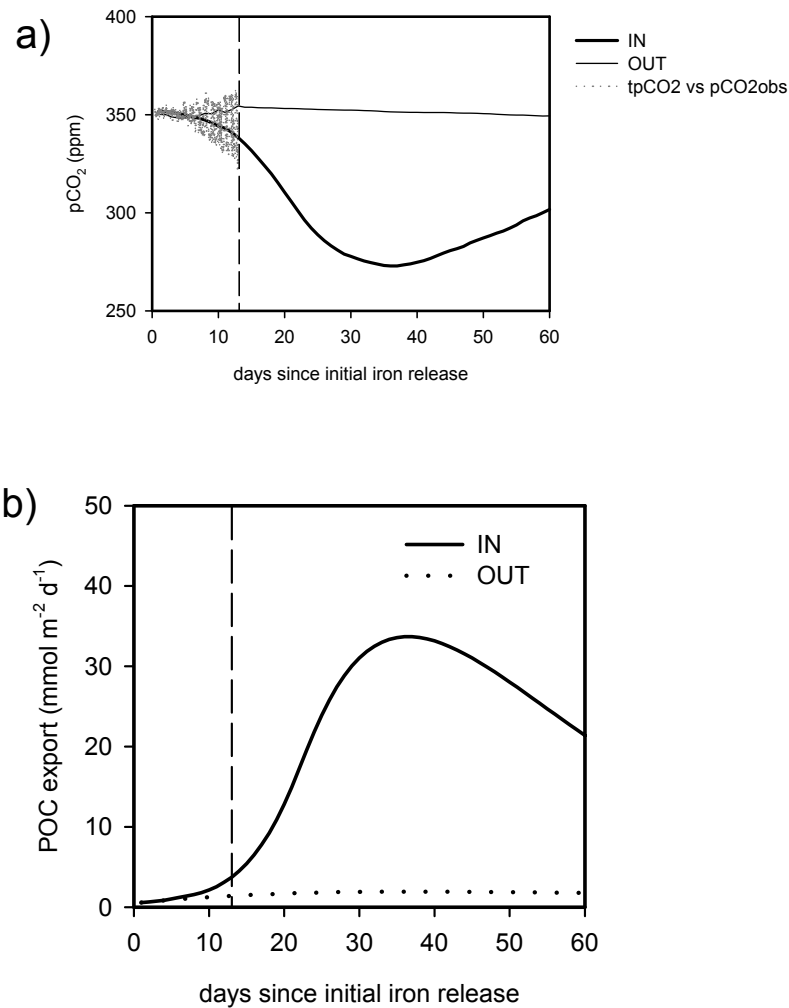
Figure 51: SOIREE: time-series of surface water pCO2 (a), POC export production flux at the base of the mixed-layer (b), outside (OUT) and inside (IN) the patch, predicted by the SWAMCO model. Under-way observations of pCO2 are shown on plot (a); variations of the under-way signal reflect the ship movements crossing the patch center and the surrounding waters.

This high under-saturation of the surface water within the fertilised patch predicts for the 60d period an atmospheric CO$_2$ sink of 1204 mmol C m^{-2} (**Figure 52**). The latter

value almost exactly corresponds to the POC export production over the same period (**Figure 52**).
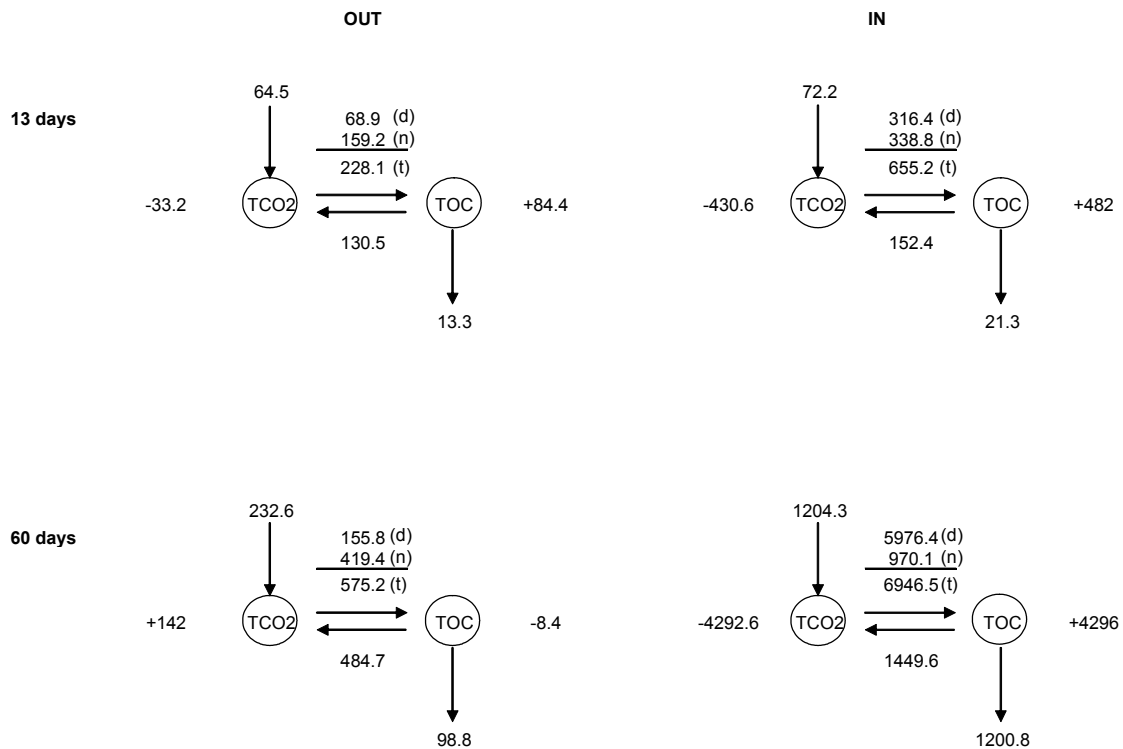
Figure 52: SOIREE: carbon budget outside (OUT) and inside (IN) the fertilised patch, integrated over 13 and 60 d, predicted by the SWAMCO model. Uptake of atmospheric CO2, size-fractionated and total primary production (d: diatoms; n: nanoflagellates, t: total phytoplankton), mineralisation, export (POC) production, changes of the standing stocks of dissolved inorganic carbon and total organic carbon. Unit : mmol C m^{-2}.

These model results complete the field observations collected during the 13 days following the initial iron release, and confirm the role of iron as a major control of the biological pump efficiency in the remote HNLC waters of the Southern Ocean. One main benefit of this numerical experiment consists in the extrapolation of the impact of the iron fertilisation at the bloom time-scale, from the onset to the decline, which could not be completely monitored during the 13 d site occupation of SOIREE. The model notably reveals that samples collected from sediment-traps deployed during SOIREE, which showed no significant difference of particle export inside and outside the fertilised area (Nodder and Waite, 2001; Trull, 2001), could not be conclusive, because of the time-scale of the experiment. One may notice that even the 60 d model runs, do not answer the question of the fate of the primary production, since 78% of the net carbon production is maintained in the surface waters standing stock at the end of the period. This result must be considered carefully due to low

parameterisation of processes related to the bloom decline and termination (mesozooplankton grazing, aggregation and sedimentation). This latter issue is discussed in the section "sensitivity analysis" below.

D.1.III. KERFIX

As third validation experiment, SWAMCO runs were conducted at latitude of the KERFIX time-series station (Jeandel *et al.*, 1998) in order to test the model capability for reproducing observed seasonal trends. For this purpose SWAMCO was coupled 'on line' to the 1D-CLIO model (1D-SWAMCO) and run under meteorological conditions of 1998 for several years up to steady state. The latter was achieved for all physical and biological state variables from the 3^d-year simulation (not shown). For validation assessment, 3^d-year predictions of diatom- and nanoflagellate- Chla were compared with observed size-fractionated chlorophyll a (Fiala et al., 1998). The comparison (**Figure 53**) shows a reasonable agreement between diatom-Chla predictions and observations, both in timing and magnitude.
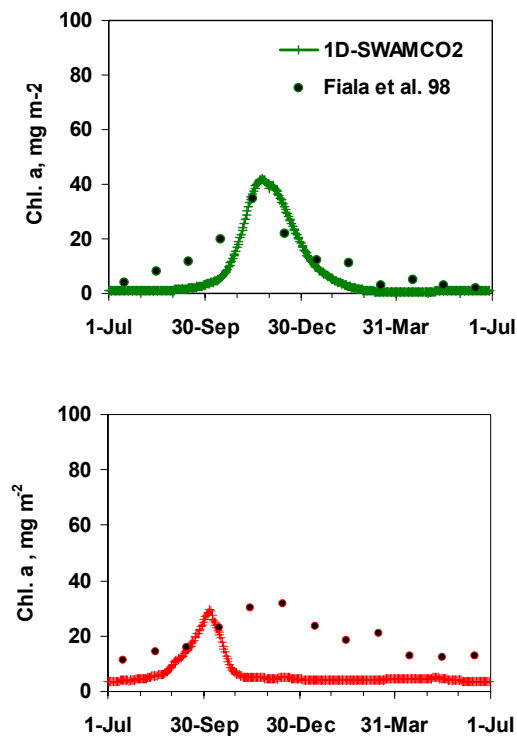
Figure 53: 1D-SWAMCO predictions of Diatom- (a) and nanoflagellate- (b) Chla and observations at KERFIX time-series station.

Less agreement is observed for predicted nanoflagellate-Chla concentration that, although of good order of magnitude, is peaking too early and fast when compared to observations (**Figure 53b**) due to model closure terms (no explicit description of

mesozooplankton feeding which could modulate the control of nanoflagellates by microzooplankton grazing pressure). Predicted seasonal evolution of pCO_2 (**Figure 54**) shows a net sink in October-November which corresponds with a peak of diatom production at low temperature of ~ +3°C. From summer to late fall, 1D-SWAMCO runs predict a net source of CO_2 at the KERFIX latitude which corresponds to temperature increase and low primary production. On an annual base, the model predicts that the portion of Southern Ocean in the KERFIX area would act as a source of CO_2 (**Table XVIII**).

D.2. Seasonal and regional variability of CO_2 uptake by the Southern Ocean

As a first step to address the question of when and where the Southern Ocean acts as a sink for atmospheric CO_2, annual 1D-SWAMCO runs were conducted on a selection of contrasted Southern Ocean sites [with respect to their meteorological and sea-ice conditions (see **Table II** in Methodology section) and iron availability]. Initial winter dissolved iron concentration of 0.5 nM (after the review by de Baar and de Jong, 2001) was assumed for standard runs. Additional runs were conducted at the Weddell and Ross Sea location for mimicking observed elevated iron concentration either due to continental inputs or release of ice-deposited iron at sea-ice melting (Sedwick and Di Tullio, 1996; Westerlund and Ohman, 1991). For these model runs sea-ice biological production and subsequent CO_2 exchange at the atmosphere-sea ice interface were neglected. Results (**Figure 54; Table XVIII**) clearly show the dual influence of temperature and light/iron driven primary production on the timing and magnitude of the CO_2 uptake by the Southern Ocean. In low iron (0.5nM) ice-free areas (**Figure 54**; 50°S, 59°S), the model simulates a net sink of CO_2 in September-October which corresponds to the spring phytoplankton bloom period. On the contrary in the summer period when surface temperature is higher and primary production iron-limited, the Southern Ocean acts at these latitudes as a CO_2 source (**Figure 54**). Annual budgets estimate a net source of CO_2 at the KERFIX latitude and a net sink at latitude 59°S explained more by the lower surface temperature at the latter latitude than a higher primary production. At higher latitude such as 70°S, 1D-SWAMCO predict a significant CO_2 sink in December-February (**Figure 54**). This seasonal shift compared to lower latitudes is clearly explained by the late development of primary production driven by light availability under the double control of global solar radiation and ice coverage. The increased vertical stability of the surface layer at the time of ice melting provides phytoplankton cells with optimal light conditions explaining its blooming and the resulting high oceanic CO_2 uptake. On an annual base, a higher CO_2 sink is predicted at latitude 70°S compared to the lower latitudes tested (**Table XVIII**). Additional 1D-SWAMCO runs conducted at latitudes 59°S and 70°S with higher initial iron condition show both

121

a net increase of the CO_2 sink in response to iron addition (**Table XVIII**). Surprisingly the model predicts a significantly higher increase of the CO_2 sink in response to iron addition at latitude 59°S, most probably due to the higher duration of the spring season. Indeed, due to the latitudinal effect, the period of sufficient light for phytoplankton growth is limited to 3 months at latitude 70°S.
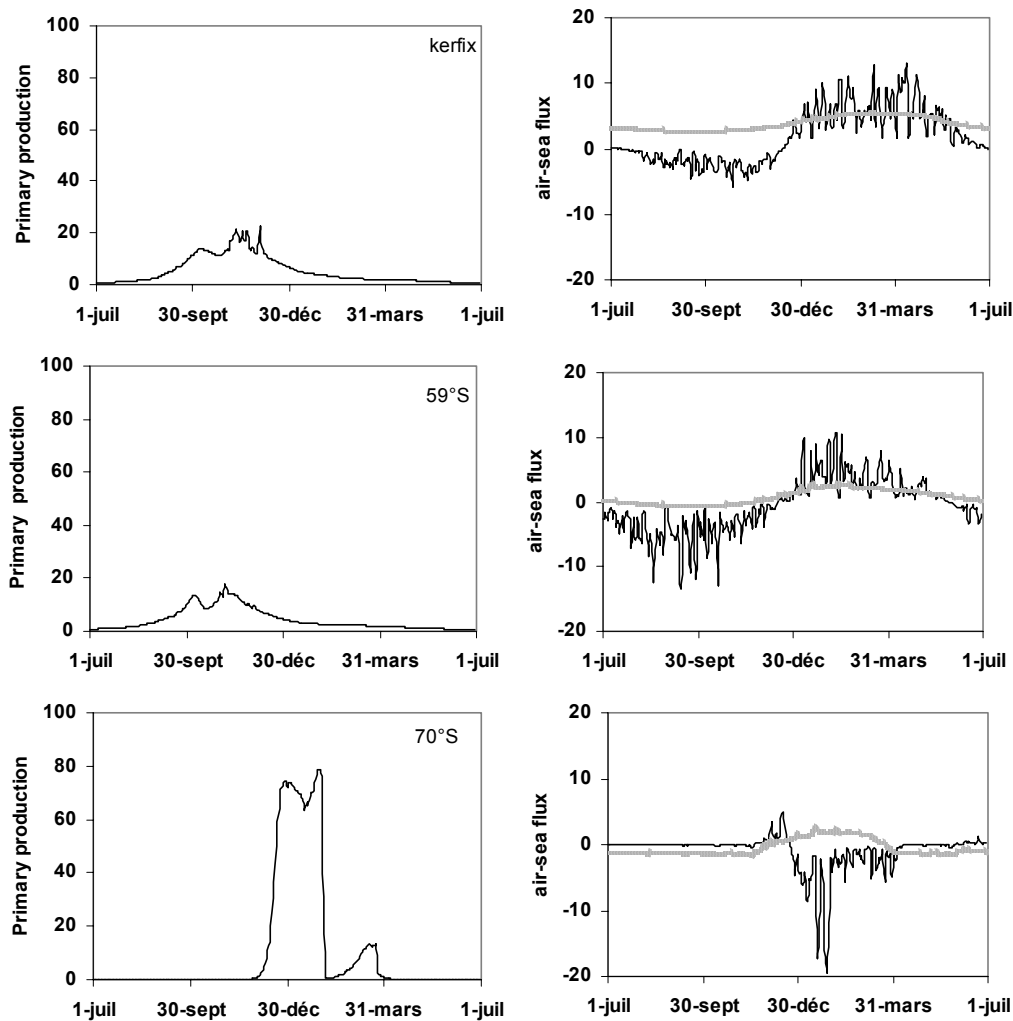

Figure 54: 3[d]-year 1D-SWAMCO simulation of primary production and seasonal temperature (grey band), air-sea CO_2 exchange at 50°S (KERFIX), 59°S (Weddell Sea) & 70°S (Ross Sea latitude) for winter DFe of 0.5nM. Unit: mmole C m^{-2} d^{-1}

Table XVIII: Annual sea-air flux (gCm^{-2}year^{-1}) estimated from 1D-SWAMCO simulations in the surface layer (100m).

Latitude	Winter dissolved iron, nM		
	0.5	1	2.5
50°S (Kerfix)	7.66		
59°S (Weddell)	-2.48	-7	-17.5
70°S (Ross Sea)	-4.21	-5.26	-6.85

D.3. Sensitivity testing based on SWAMCO model scenarios

Model scenarios were conducted to explore the relative importance of physical (wind, sea-ice, mixing regime), chemical (iron) and biological (grazing) factors in controlling the efficiency of the biological pump. Furthermore the sensitivity of the model response to key parameterisation of carbon export production was investigated, highlighting further directions in biogeochemical modelling.

D.3.I. Sensitivity to forcing conditions

Model scenarios with varying physical (wind, ice, solar radiation, mixing-regime) and chemical (iron) forcing were conducted to better understand the dual role of light climate and iron in driving the efficiency of the biological pump of atmospheric CO_2 in the Southern Ocean.

Iron availability

The sensitivity of the net carbon production and air-sea exchange of CO_2 to iron availability was first investigated by running several SWAMCO model simulations with increased fluxes of iron from dust deposition (in the range 0-100 mg m^{-2} yr^{-1}). These run were performed at the SO-JGOFS-ANT-X/6 site (all the controls, except iron, were fixed to their in situ value). Results (Lancelot et al., 2000; Hannon et al., submitted) predict a significant increase of carbon production in response to the iron enrichment, over the whole range of Fe deposition values, and for both the PFr and MIZ (**Table XIX**). However, the net C production in the MIZ is kept one order of magnitude lower than in the PFr, even with the highest iron deposition. This results from the difference of light climate between these two regions with deep-mixing events being more frequent and intense in the MIZ (Lancelot et al., 2000). As a consequence a clear enhancement of the atmospheric CO2 sink is predicted in the PFr in response to increased iron deposition (**Table XIX**).

Table XIX: Sensitivity of the SWAMCO model predictions of air/sea exchange of CO_2 and net carbon production to iron enrichment from aeolian deposition in the Polar Frontal region (PFr) and the Marginal Ice zone (MIZ) of the Southern ACC. Other forcing functions (wind, air temperature, global radiation, ice-cover, major nutrients concentration) are unchanged (kept to their in situ value). Rates are integrated over 5 weeks (ANT-X/6 site, austral spring 1992). Units: mmol C m^{-2}.

	CO_2 exchange		C production	
	PFr	**MIZ**	**PFr**	**MIZ**
no Fe deposition	-151	176	1331	92
+ 20 mg m^{-2} yr^{-1}	-177	169	1649	177
+ 50 mg m^{-2} yr^{-1}	-211	165	2117	225
+ 100 mg m^{-2} yr^{-1}	-244	162	2557	262

In the MIZ, the net source of CO_2 is only very slightly decreased by the higher iron deposition (**Table XIX**). These results stress the interplay between the iron and the light climate in driving the efficiency of the biological pump.

Wind, light climate

The influence of the light climate on the response of the phytoplankton to iron availability was assessed by conducting four simulations with increasing mixed-layer depth (40, 65, 100, 120 m), applied to the iron-fertilised SOIREE site (the mean observed mixed-layer depth during the SOIREE experiment was ~65m). Model predictions (**Figure 55**) show that, under these iron-enriched conditions a shallow mixed layer of 40 m favors the development of a large autotrophic nanoflagellates biomass (**Figure 55b**), without significantly modifying the diatom bloom (**Figure 55a**), relative to the standard conditions (65 m). This is due to a rapid growth of autotrophic nanoflagellates under optimal light and sufficient iron and the delayed-response of the micrograzers, as revealed by the grazing:growth ratio (**Figure 55c**). The more favorable the light regime is, the later the grazing:growth ratio reaches 1, which defines the end of the algal biomass increase, and the beginning of the bloom decline (**Figure 55c**). As a consequence of this floristic shift the stimulated primary production predicted for a shallow mixed layer of 40 m is not reflected in the magnitude of POC export. The latter is lower than the export production predicted for the standard 65 m simulation (Hannon et al., 2001). These SWAMCO scenarios suggest that the magnitude of the diatom bloom stimulated by the SOIREE experiment was primarily controlled by the iron supply, whereas light more than iron was the bottom-up control of autotrophic nanoflagellates growth.

At the opposite, deep mixed-layers of 100m and more prevent development of both diatoms and autotrophic nanoflagellates (**Figure 55a and 55b**), indicating that reduced light levels negate the effect of the iron addition. These model scenarios

indicate that wind is a major factor driving the biological production in the Southern Ocean, through the control it exerts on the light climate within the water column. Wind also directly controls the flux of CO_2 at the air-sea interface (whatever the direction of this flux is), making its impact on the pump of atmospheric CO_2 more complex. Such an effect was investigated by testing the response of the net carbon production and air-sea exchange of CO_2 to changing wind velocity.
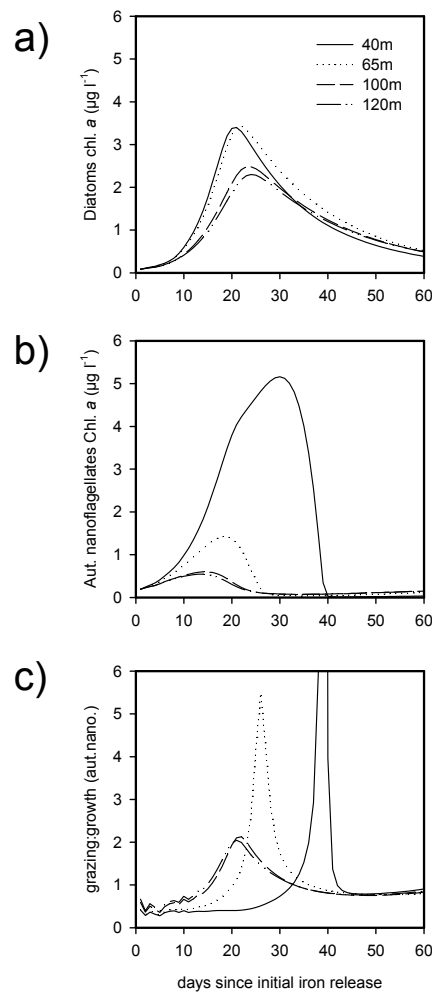
Figure 55: SOIREE, sensitivity of the diatoms chlorophyll a (a), autotrophic nanoflagellates chlorophyll a (b), and grazing:growth rates ratio (c) of the autotrophic nanoflagellates to the mixing regime (mixed-layer depth from 40 to 120 m), predicted by the SWAMCO model.

Two different scenarios were explored: a constant wind between 4-20 m s^{-1}, and two situations mimicking periodic storms (up to 20 and 30 m s-1) around an average wind

as *in situ*. These scenarios were conducted at the SO-JGOFS-ANT-X/6 site (PF). Results are summarised in **Table XX**. The highest carbon productions are predicted for the "moderate" storm scenario (<20 m s-1), and for a constant wind of 16 m s^{-1}. Other scenarios (strong storms, constant wind velocity other than 16 m s^{-1}) generate carbon productions ~50% lower than this predicted at in situ wind conditions (**Table XX**). This reflects the fact that high wind (constant, or periodic storms), by deepening the mixed-layer depth supplies in the surface waters with required iron to sustain a substantial biological production. This effect is counteracted by light limitation when constant wind velocity is too high (20 m s^{-1}) or storms are too strong (>20 m s^{-1}). The response to wind scenarios of the air-sea exchange of CO_2 does not exactly display the same pattern as the net carbon production; due to the effect of the wind on the gas exchange at the sea surface [see Wanninkhof's (1992) relationship]. Thus the highest carbon production does not necessarily lead to the highest sink of atmospheric CO_2, as illustrated by the comparison between the "in situ" standard, and the "moderate storms" (<20 m s^{-1}) scenario (**Table XX**).

From these model results, it appears that the efficiency of the biological pump of atmospheric CO_2 in the Southern Ocean is ultimately favoured by a succession of calm periods (allowing algal biomass accumulation) and storms (relieving the iron deficiency by the mixing with sub-surface waters).

Table XX. Sensitivity of the model predictions of air-sea exchange of CO_2 and net carbon production to the wind regime. Other forcing functions (air temperature, global radiation, ice-cover, major nutrients and dissolved iron concentrations) are those met in the Polar Frontal region (PFr) during the ANT-X/6 cruise (austral spring 1992). Rates are integrated over 5 weeks. Units: mmol C m^{-2}.

		CO_2 exchange	C production
variable wind	in situ wind (mean = 11 m s^{-1})	-151	1331
	11 m s^{-1} + storms (<20m s^{-1})	-169	1159
	11 m s^{-1} + storms (<30m s^{-1})	-110	726
constant wind	4 m s^{-1}	-3	518
	8 m s^{-1}	-66	564
	11 m s^{-1}	-179	700
	16 m s^{-1}	-247	1251
	20 m s^{-1}	-148	659

D.3.II. Sensitivity to model parameterisation

Iron physiology parameterisation

Considering the key role of Fe in regulating diatom blooms and export production, several SWAMCO runs were conducted at the Polar Frontal region to explore the model response to changing values of the half-saturation constant for iron assimilation and the cellular Fe content [Fe:C]. Results of these scenarios are annualised in terms of diatom production and POC export production (**Table XXI**). The magnitude of the diatom bloom and the POC export production are not much dependent on the half-saturation constant for Fe uptake in the range 0.18-1.8 µmol Fe m^{-3}. More sensitive is the dependence on the iron to carbon stoichiometry which shows a +22 and -35% variation of the SWAMCO reference diatom production with tested values of Fe:C between 0.02 and 0.2. Furthermore model scenarios show that the exported fraction of carbon production is positively related to the cellular iron content. Similar scenarios related to silicon parameterisation, notably investigating the dependence of the diatom silicification level on ambient iron (Lancelot et al., 2000), clearly evidence the complex interplay of Si and Fe limitation in regulating diatom blooms and the associated biogeochemical cycles in the Southern Ocean, as already suggested by laboratory and field observations (Takeda et al., 1998; Hutchins and Bruland, 1998; de Baar et al., 1999). These SWAMCO scenarios strongly indicate that more investigations on the nutrient dynamics of phytoplankton are needed to understand mechanisms driving export production events in the Southern Ocean. They indicate as well that simple models based on a limitation of phytoplankton production by a single element are not suitable to investigate the carbon cycle in the Southern Ocean.

Table XXI: Sensitivity of the SWAMCO model to iron physiology parametrization (cellular elemental ratio, half-saturation constant for iron assimilation); Diatom production, POC export production, in the upper 100 m, integrated over the period of the ANT X/6 cruise (austral spring 1992, Polar Frontal region).

		Diatom production [mol C m^{-2}]	POC export [mol C m^{-2}]
Fe:C [mol:mol]	0.02	2.53	1.06
	0.1	2.08	0.98
	0.2*	**1.35**	**0.82**
K$_{Fe}$ [µmol m^{-3}]	0.18	1.5	0.95
	1.2*	**1.35**	**0.82**
	1.8	1.26	0.75

* data in bold : reference simulation

Aggregation and sedimentation

The importance of different sedimentation mechanisms in determining the magnitude of the downward flux of phytoplankton was explored by testing different parameterisations of diatom sedimentation and aggregation. Specifically, a possible link between iron depletion and diatoms sinking rate (see Muggli et al., 1996) was considered and the importance of cell chain formation and particle aggregation was investigated using the model of Kriest and Evans (1999).

Figure 56 shows how iron-mediated sinking rates can affect the bloom decline and the downward flux of particles.
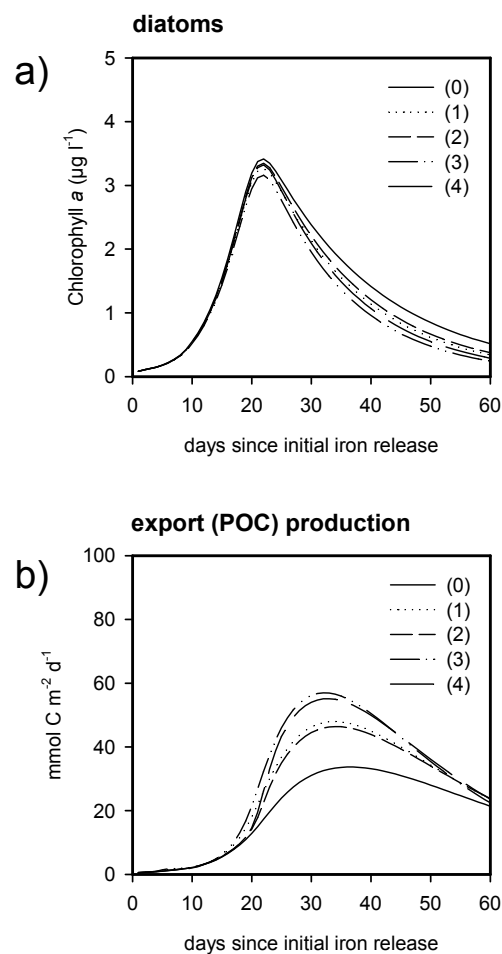
Figure 56: SOIREE: Sensitivity of diatoms chlorophyll a (a) and POC export production (b) to the sinking rate r_s in relation with iron availability: (0) standard: r_s=1.0 m d^{-1};
(1) $r_{s\ max}$=1.7 m d^{-1}, linear shape; (2) $r_{s\ max}$=1.7 m d^{-1}, exponential shape; (3) r_{smax}=2.3 m d^{-1}, linear shape; (4) $r_{s\ max}$=2.3 m d^{-1}, exponential shape. See details in Hannon et al. (2001)

Four different relationships linking the sinking rate to the ambient iron concentration were tested, on the basis of sinking rates measurements on dominant blooming species during SOIREE (*Fragilariopsis kerguelensis*; Waite and Nodder, 2001). The four parameterisations differ by the maximum sinking rate (characterising iron-depleted diatoms) and the shape of the function relating sinking rate to algal iron stress (linear, or inverse exponential). For each case, we considered a minimum sinking rate of 1 m d-1 for replete iron conditions. Although the decline of the diatom biomass is barely affected (**Figure 56a**), prediction of POC export production is considerably enhanced when relating sinking rate to algal iron stress (**Figure 56a**). Scenarios (3) and (4) (maximum sinking rate = 2.3 m d^{-1}) induce a 50% increase of the integrated POC export, over 60 days (Hannon et al., 2001). The impact of the aggregation process on the downward flux of POC was investigated by implementing in SWAMCO the simple parameterization of phytoplankton aggregation recently developed by Kriest and Evans (1999) and based on the model of Jackson (1990). This approach relies on an independent treatment of cells abundances and biomass, each obeying its own conservation law. Essentially two parameters are determinant in this aggregation model: the stickiness factor (s) characterizing the probability that two colliding particles will aggregate, and the probability that two dividing cells will separate (p). Four pairs of values for these two parameters were tested (**Figure 57**), and the resulting prediction of diatoms chlorophyll a and POC export production were compared to the standard run. Small values of p (scenarios 1 and 2) result in substantial diatom aggregation and correspondingly a higher export production than predicted by the standard run (**Figure 57b**), but maintain the diatom biomass at low values (< 2µg Chl a l^{-1}, **Figure 57a**). Varying the value of s in this case does not change much the export flux, nor the diatom biomass (**Figure 57**). On the contrary, a high value of p (scenarios 3 and 4) results in fewer aggregates and hence more diatom biomass is predicted to accumulate in the mixed-layer, up to chlorophyll a concentrations similar to the one predicted by the standard run (**Figure 57a**). In this case, low or high stickiness (scenarios 3 and 4) respectively slow down or accelerate the diatom bloom decline (**Figure 57a**). Interestingly, the combination of high p and s (scenario 4) induces a short but massive export event occurring only a few days after the diatom peak (**Figure 57**). This leads to a POC export flux accounting for 61% of primary production (compared to 20% in the standard SOIREE run). Finally it may be noticed that none of these scenarios predict significant export production during the 13 d simulation (i.e. time period of the SOIREE observations). A longer period of observation at the site would have been needed to detect a signal in export production.

These exploratory scenarios show the importance of the aggregation processes on the bloom decline and the subsequent downward flux of particles to the deep ocean. In particular they point out the importance of diatom cell characteristics such as cell

size, chain forming and stickiness on the intensity and duration of export events. Unfortunately little is known on these aspects of diatom physiology and deserve further research.

diatoms

export (POC) production
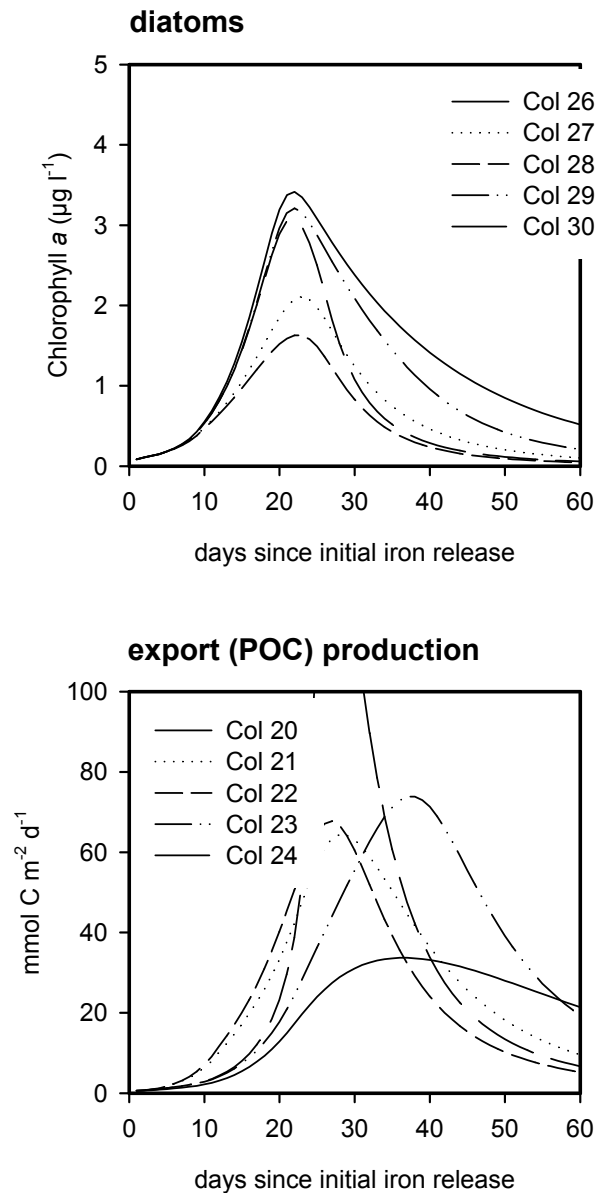
Figure 57: SOIREE: Sensitivity of diatoms chlorophyll a (a) and POC export production (b) to the parameterization of the aggregation process: (0) standard; (1) p = 0.15, s = 0.05; (2) p = 0.15, s = 0.2; (3) p = 0.3, s = 0.05; (4) p = 0.3, s = 0.2.
(p: probability of separation of the cells; s: stickiness factor)
See details in Hannon et al. (2001).

4. SYNTHESIS AND EVALUATION OF RESEARCH RESULTS RELATIVE TO ORIGINAL OBJECTIVES – OVERALL CONCLUSIONS

This work confirms the crucial bottom-up control of phytoplankton production by Fe availability. Our observations for the Atlantic sector confirm the greater sensitivity to Fe limitation for plankton communities composed of larger species, compared to communities with predominance of small cells. Fe limitation appears to be the common condition for the Southern Ocean waters studied, except for specific areas in the vicinity of shelves and influenced by advective input of Fe, such as the Ross Sea and the northern part of the SAZ, west of Tasmania.

Settling rates of individual, autotrophic and heterotrophic cells, colonies and detrital particles during early season in the Ross Sea were ≤ 8 m d^{-1}, similar to observations elsewhere. During mid-summer some increase of export was noticed associated with increased aggregate formation. Since the biomass associated with such slowly sinking particles is relatively large, the carbon fluxes involved become significant and in any case larger than observed for the other Southern Ocean areas. The degradation of sinking particles appeared mainly controlled by attached bacteria. Degradation was relatively low in spring, but it is likely that bacterial activity would have increased with advancing season. Indeed, for a late summer situation in the SAZ and PFZ regions south of Australia, production of ammonium generally exceeded demand, reflecting a decaying bloom with dominance of regenerated production (*f*-ratios <0.5), and probable enhanced bacterial activities.

Inhibition of nitrate uptake and resulting decrease of *f*-ratio due to ambient ammonium increase was high for phytoplankton originally thriving in low ammonium (<0.1 μM) and high iron (>0.4 nM) waters, while it was low, to non-significant in conditions of low Fe (<0.1 nM). Thus, on from a certain level of Fe-depletion the phytoplankton is insensitive to increasing availability of ammonium, as would occur generally along the growth season. In this case, *f*-ratios obtained from short term incubations can be considered as representative for longer time scales, probably of the order of days to weeks, an interesting aspect when trying to link new production to export production.

POM mineralises quickly in the water column and POC flux itself might therefore not be the best parameter to assess export production. Recent publications, in general, emphasise the good potential of excess-Ba – barite is a proxy for organic carbon, and results from this study confirm this. Although full detail about the biogeochemical processes involved with Ba uptake and barite synthesis could not be resolved here, it appeared that phytoplankton uptake of Ba from solution is essentially via adsorption. This adsorbed Ba adds to an original pool of excess Ba in the plankton that does not

seem to exchange with the solution and which we suspect to consist of micro-crystalline barite, a mineral we observed to be an ubiquitous component of the Southern Ocean suspended matter. Diatoms appear to carry a larger pool of excess Ba and adsorb proportionally less additional Ba from the solution. This observation was also confirmed from SAZ and PFZ field data, showing a co-variation between water column excess particulate Ba and diatom abundance. Thus, under diatom dominance a given POM unit produces more excess Ba, than under conditions of *Phaeocystis* dominance, for instance. When using the Ba proxy to assess export production, this condition must be taken into account via appropriate algorithms.

During the present study it was possible to compare several conceptually and technically entirely different methodologies to assess carbon export from the surface mixed layer (i.e. upper 100m). Direct assessment of the carbon flux was possible from the settling rates of individual, autotrophic and heterotrophic cells, colonies and detrital particles and from new production measurements based on *f*-ratio and primary production. Carbon export flux obtained from these methods would reflect the short term situation (i.e. days to a few weeks). Seasonally or annually averaged export productions were derived from particulate organic C and Ba_{xs} fluxes in sediment traps and from sedimentary Ba_{xs} rain rates. Clearly, export production estimates obtained from narrow time windows (generally spring and summer) are larger than those based on broader time windows, since the latter have also integrated the signals for the weakly, to non-productive, winter period. It is nevertheless remarkable that the different approaches based on very different and independent methodologies provide converging export production values for the main Southern Ocean areas investigated. Highest export productions are observed for the Antarctic Shelf (Ross Sea) and the Seasonal Ice Zone (80 to 200 mgC m^{-2} d^{-1}). The Polar Front Zone (PFZ) in the Indian sector has greater export production than the Permanently Open Ocean Zone (37 and 10 mgC m^{-2} d^{-1}, respectively). For the Atlantic sector (6°W), differences between PFZ and POOZ are less pronounced. For the Subantarctic Zone to the west, southwest of Tasmania, export production is higher (70 to 150 mgC m^{-2} d^{-1}) than for the PFZ (30 mgC m^{-2} d^{-1}), but this might me a peculiar situation due to iron repletedness resulting from the proximity of the Tasmanian shelf. Furthermore, for the PFZ and ACC in the Atlantic sector, comparison of the export production values predicted by the SWAMCO-1D CLIO model with the estimates based on proxy flux (sedimentary Ba_{xs} rain rate) show good agreement, providing further weight to the magnitude of the calculated export productions.

In spring and summer, the area between 35° and 50°S in the Indian and Australian sectors was estimated to be a net sink for atmospheric CO_2, amounting to between 27 and 86 mgC m^{-2} d^{-1} equivalent to 0.045 and 0.141 GtC, respectively. The fact that such net air to sea fluxes are of the same order of magnitude as the carbon export

flux from the surface mixed layer, emphasises the important role of the biological pump, at least during the bloom period, in redistributing atmospheric carbon into the ocean. However, when giving these data a closer look, the question is raised on how to reconcile them with the observation of low *f*-ratios (<0.5; at least for late summer in the SAZ), which suggest less than 50% of primary production is available for export. Clearly, such a comparison requires further improvement of the spatio-temporal resolution of the production process and the export production regime in the Southern Ocean.

REFERENCES

Abelmann, A. and Gersonde, R. 1991. Biosiliceous particle flux in the Southern Ocean. Mar. Chem. 35: 503-536.

Abraham, E.R., Law, C.S., Boyd, P.W., Lavender, S.J., Maldonado, M.T. and Bowie, A.R. 2000. Importance of stirring in the development of an iron-fertilized phytoplankton bloom. Nature 407: 727-730.

Alldredge, A.L. 1979. The chemical composition of macroscopic aggregates in two neritic seas. Limn. Oceanogr. 24: 855-866.

Alldredge, A.L. and Silver, M.W. 1988. Characteristics, dynamics and significance of marine snow. Progr. Oceanogr. 20: 41-82.

Alldredge A.L. and Gotschalk, C. 1989. Direct observations of the flocculating of diatom blooms: characteristics, settling velocities and formation of diatom aggregates. Deep-Sea Res. I. 36: 59-171.

Alldredge, A.L. and Jackson, G.A. 1995. Preface: aggregation in marine systems. Deep-Sea Res. II. 42: 1-7.

Anderson, R.F. and Fleer, A. 1982. Determination of natural actinides and plutonium in marine particulate material. Anal. Chem. 54: 1142-1147.

Anderson, R.F. and Kumar, N. 1995. Late Quaternary changes in the biological productivity of the Southern Ocean. Internat. Symp. on Carbon Fluxes and Dynamic Processes in the Southern Ocean: Present and Past, Brest (France) 1995 (Abstract).

Arrigo, K.R. and McClain, C.R. 1994. Spring phytoplankton production in the western Ross Sea. Science. 266: 261-263.

Arrigo, K.R., Weiss, A.M. and Smith, W.O.Jr. 1998. Physical forcing of phytoplankton dynamics in the western Ross Sea. J. Geophys. Res. 103: 1007-1022.

Arrigo, M.R., Robinson, D.H., Worthen, D.L., Dundar, R.B., DiTullio, G.R., van Woert, M. and Lizotte, M.P. 1999. Phytoplankton community structure and the drawdown of nutrients and CO_2 in the Southern Ocean. Science. 283: 265-267.

Asper, V.L. 1987. Measuring the flux and sinking speed of marine snow aggregates. Deep-Sea Res. 34: 1-17.

Asper, V.L. and Smith, W.O.Jr. 1999. Particles fluxes during austral spring and summer in the southern Ross Sea (Antarctica). J. Geophys. Res. 104: 5345-5360.

Azam F. and Cho, B.C. 1987. Bacterial utilisation of organic matter coupling on marine aggregates. In: Ecology of microbial communities. Fletcher, M., Gray, M. and Jones, T.R.G. (Eds.). Cambridge University Press, Cambridge: 261-281.

Azam, F. 1998. Microbial control of oceanic carbon flux: the plot thickens. Nature 280: 694-696.

de Baar, H.J.W., de Jong, J.T.M., Bakker, D.C.E., Loscher, B.M., Veth, C., Bathmann U.V. and Smetacek, V. 1995. Importance of iron for plankton blooms and carbon dioxide drawdown in the Southern Ocean. Nature, 373, 412-415.

de Baar, H.J.W. and Boyd, P.W. 1998. The role of iron in plankton ecology and carbon dioxide transfer of the Global Oceans. In: JGOFS symposium, IGBP Books Series. Cambridge University Press.

de Baar,H.J.W., de Jong, J.T.M., Nolting, R.F., Timmermans, K.R., van Leeuwe, M.A., Bathmann, J., Rutgers van der Loeff, M. and Sildam, J. 1999. Low dissolved Fe and the absence of diatom blooms in remote Pacific waters of the Southern Ocean. Mar. Chem., 66: 1-34.

Bakker, D.C.E., de Baar, H.J.W. and Bathmann, U.V., 1997. Changes of carbon dioxide in surface waters during spring in the Southern Ocean. Deep-Sea Res. 44: 91-127.

Barman, T.E. 1969. Bacterial utilisation of organic matter in the sea. In Microbial Enzyme in Aquatic Environments. Chrost, R. (Ed). Springer Verlag, Berlin: 43 pp.

Bareille, G. 1991. Flux sédimentaires: Paléoproductivité et paléocirculation de l'Océan Austral au cours des 150,000 dernières années. Ph. D. thesis No 604. Université de Bordeaux I, Talence.

Bareille, G., Labracherie, M., Labeyrie, L., Pichon, J.J. and Turon, J.L. 1991. Biogenic silica accumulaion rate during the Holocene in the southeastern Indian Ocean. Mar. Chem. 35: 537-551.

Bareille, G., Labracherie, M., Labeyrie, L., Mortlock, R. and Froelich, P. 1993. Late Pleistocene Opal Accumulation Rates in the Circum-Polar Antarctic (Southern Ocean). EOS Transactions, AGU (Abstract).

Bareille, G., Labracherie, M., Bertrand, P., Labeyrie, L., Lavaux, G. and Dignan, M. 1998. Glacial-Interglacial changes in the accumulation rates of major biogenic components in Southern Ocean sediments. J. Mar. Systems. 17: 527-539.

Bates, N.R., Hansell, D.A., Carlson, C.A. and Gordon, L.I. 1998. Distribution of CO_2 species, estimates of net community production, and air-sea CO_2 exchange in the Ross Sea polynya. J. Geophys. Res. 103: 2883-2896.

Bathmann, U.V., Scharek, R., Klaas, C., Smetacek., V. and Dubischar, C.D. 1997. Spring development of phytoplankton biomass and composition in major water masses of the Atlantic sector of the Southern Ocean. Deep-Sea Res. II. 44: 51-68.

Bathmann, U.V., Smetacek, V. and Reinke, M. 2000. The expeditions ANTARKTIS XVI/3-4 of the Research Vessel "Polarstern" in 1999. Berichte zur Polarforschung. 135-236.

Becker, S. and Dietze, H.J. 1986. Massenspektrographische konzentrations-bestimmung der seltenen-erder-elemente an schwermineralfraktionen der ostsee-strandsifen. Z. Angew. Geol. 32: 299-301.

Becquevort, S., Rousseau, V. and Lancelot, C. 1998. Major and comparable roles for free-living and attached bacteria in the degradation of Phaeocystis-derived organic matter in Belgian coastal waters of the North Sea. Aquat. Microb. Ecol. 14: 176, 39-48.

Belkin, M. and Gordon, L.A. 1996. Southern Ocean fronts from the Greenwich meridian to Tasmania. J. Geophys. Res. 101: 3675-3696.

Bellerby, R.G.J., Turner, D.R. and Robertson, J.E. 1995. Surface pH and pCO$_2$ distributions in the Bellingshausen Sea, Southern Ocean, during the early Austral summer. Deep-Sea Res. 42: 1093-1107.

Biddanda, B.A. 1985. Microbial synthesis of macroparticulate matter. Mar. Ecol. Prog. Ser. 20: 241-251.

Bidle, K.D. and Fletcher, M. 1995. Comparison of free-living and particle-associated bacterial communities in the Chesapeake Bay by stable low-molecular-weight RNA analysis. Appl. Environ. Microbiol. 61: 944-952.

Bienfang, P.K. 1981. SETCOL - A technologically simple and reliable method for measuring phytoplankton sinking rates. Can. J. Fish. Aquat. Sci. 38: 1289-1294.

Bienfang, P.K. 1984. Size structure and sedimentation of biogenic microparticulates in a subarctic ecosystem. J. Plankt. Res. 6: 985-995.

Bienfang, P.K. 1985. Size structure and sinking rates of variuos microparticulate constituents in oligotrophic Hawaiian waters. Mar. Ecol. Progr. Ser: 23: 143-151.

Billen, G. and Servais, P. 1988. Modélisation des processus de dégradation bactérienne de la matière organique en milieu aquatique. In: Micro-organismes dans les écosystèmes océaniques. Masson. Bianchi et coll. (Eds): 219-245.

Billen, G. 1991. Protein degradation in aquatic environments. In: Enzymes in Aquatic Environments. Chrost, R. (Ed). Springer Verlag, Berlin: 122-142.

Billett, D.S.M., Lampitt, R.S., Rice, A.L. and Mantoura, R.F.C. 1983. Seasonal sedimentation of phytoplankton to the deep-sea benthos. Nature. 302: 520-522.

Bishop, J.K. 1988. The barite-opal-organic carbon association in oceanic particulate matter. Nature. 332: 341-343.

Bodungen, B.V., Smetacek, V.S., Tilzer, M.M. and Zeitzschel, B. 1986. Primary production and sedimentation during spring in the Antarctic Peninsula region. Deep-Sea Res.I. 33: 177-194.

Boehme, S.E., Sabine, C.L. and Reimers, C.E. 1998. CO$_2$ Fluxes from a coastal transect: a time-series approach. Mar. Chem. 49-67.

Bolter, M. and Dawson, R. 1982. Heterotrophic utilization of biochemical cmpounds in Antarctic waters. Neth. J. Sea Res. 16: 315-332.

Borges, A.V. and Frankignoulle, M. 1999. Daily and seasonal variations of the partial pressure of CO$_2$ in surface seawater along Belgian and southern Dutch coastal areas. J. Mar. Sys. 251-266.

Boyd, P.W. and coll. 2000. A mesoscale phytoplankton bloom in the polar Southern Ocean stimulated by iron fertilisation. Nature, 407:695-702.

Boyd, P.W., Crossley, A.C., Di Tullio, G.R., Griffiths, F.B., Hutchins, D.A., Quéguiner, B., Sedwick, P.N. and Trull, T.W. submitted Effects of iron supply and irradiance on phytoplankton processes in subantarctic waters south of Australia. J. Geophys. Res..

Brand, L.E. 1991. Minimum iron requirements of marine phytoplankton and the implications for biogeochemical control of new production. Limnol. Oceanogr. 36: 1756-1771.

Bray, S., Trull, T. and Manganini, S. 2000. SAZ Project moored sediment traps: Results of the 1997-1998 deployments. Antarctic CRC Res. Rep. N°15, Hobart, Australia.

Cardinal, D., Dehairs, F., Cattaldo, T. and André, L. Geochemistry of suspended particles in the Subantarctic and Polar Front Zones south of Australia: Constraints on export and advection processes. J. Geophys. Res. accepted.

Cardinal, D., Fagel, N. and André, L. Sequential leaching experiment on two Southern Ocean sediments: Implications on the Sr and REE geochemistry of marine barite. Mar. Geol. To be submitted.

Carlson, G.A., Ducklow, H.W., Hansell, D.A. and Smith, W.O. 1998. Organic carbon partitioning during spring phytoplankton blooms in the Ross Sea polynya and the Sargasso Sea. Limnol. Oceanogr. 43: 375-386.

Carlson, C.A., Ducklow, H.W., Hansell, D.A. and Smith, W.O. 1998. Differences in ecosystem dynamics between spring blooms in the Ross Sea Polynya and the Sargasso Sea reflected by contrasts in dissolved and particulate organic carbon partioning. Limnol. Oceanogr. 43: 375-386.

Carlson, C.A., Bates, N.R., Ducklow, H.W. and Hansell, D.A. 1999. Estimation of bacterial respiration and growth efficiency in the Ross Sea, Antarctica. Aquat. Microb. Ecol. 19: 229-244.

Caron, D.A., Dennett, M.R., Lonsdale, D.J., Moran, D.M. and Shalapyonok, L. 2000. Microzooplankton herbivory in the Ross Sea, Antarctica. Deep-Sea Res. II 47: 3249-3272.

Cattaldo, T., Dehairs F., Metzl, N., Monnin, C., and Jeandel, C. Hydrological and Biogeochemical control of dissolved Barium in the Southern Ocean along 6°W and 30°E. Submitted to J. Geophys. Res.

Charles, C.D., Froelich, P.N., Zibello, M.A., Mortlock, R.A., and Morley, J.J. 1991. Biogenic opal in Southern Ocean sediments over the last 450,000 years: Implications for surface water chemistry and circulation. Paleoceanography. 6: 697-728.

Cho, B.C. and Azam, F. 1988. Major role of bacteria in biogeochemical fluxes in the ocean's interior. Nature 332: 441-443.

Choi, W.J., Sherr, E.B. and Sherr, B.F. 1996. Relation between presence/absence of a visible nucleoid and metabolic activity in bacterioplankton cells. Limnol. Oceanogr. 41: 1161-1168.

Church, T.M., 1970. Marine barite, Ph.D. Thesis, University of California, San Diego.

Cleveland, W.S., Freeny, A.E., and Graedel, T.E. 1983. The seasonal Component of atmospheric CO_2: Information from new approaches to the decomposition of seasonal time series. J. Geophys. Res. 934-946.

Collier, R. and Edmond, J. 1984. The trace element geochemistry of marine biogenic particulate matter. Prog. Oceanog. 13: 113-199.

Collier, R., Dymond, J., Honjo, S., Manganini, S., Francois, R. and Dunbar, R. 2000. The vertical flux of biogenic and lithogenic material in the Ross Sea: moored sediment trap observations. Deep-Sea Res. II 47: 3491-3520.

Comiso, J.C., McClain, C.R., Sullivan, C.W., Ryan, J.P. and Leonard, C.L. 1993. Coastal zone color scanner pigment concentrations in the Southern Ocean and relationships to geophysical surface features. J. Geophys. Res. 98: 2419-2451.

Connell, R.D. and Sikes, E.L. 1997. Controls on Late Quaternary sedimentation of the South Tasman Rise. Aust. J. Earth Sci. 44: 667-675.

Copin-Montegut, C., 1988. A new formula for the effect of temperature on the partial pressure of carbon dioxide in seawater. Mar. Chem. 25: 29-37.

Crawford, R.M. 1995. The role of sex in the sedimentation of a marine diatom bloom. Limnol. Oceanogr. 40: 200-204.

Cuhel, G.F., Ortner, P.B., and Lean, D.R.S. 1984. Night synthesis of protein by algae. Limnol. Oceanogr. 29 : 731-744.

Culkin, F., 1989. Salinity: definitions, determination and standards. Sea Technology, 47-49.

Cullen, J. J., Yang, X. and MacIntyre H.L., 1992. Nutrient limitation of marine photosynthesis, p. 123-137. In Falkowski, P. G. & Woodhead, A. D. [Eds.], Primary productivity and biogeochemical cycles in the sea. Plenum Press.

Davidson, A.T. and Marchant, H.J. 1992. Protist abundance and carbon concentration during a Phaeocystis-dominated bloom at Antarctic coastal site. Polar Biol. 12: 387-395.

Dehairs, F., Chesselet, R. and Jedwab, J. 1980. Discrete suspended particles of barite and the barium cycle in the open ocean. Earth Planet. Sc. Lett. 49: 528-550.

Dehairs, F., Goeyens, L., Stroobants, N., Bernard, P., Goyet, C., Poisson, A. and Chesselet, R., 1990. On suspended barite and the oxygen minimum in the Southern Ocean. Global Biogeochem. Cy. 4: 85-102.

Dehairs, F., Stroobants, N. and Goeyens, L. 1991. Suspended barite as a tracer of biological activity in the Southern Ocean. Mar. Chem. 35: 399-410.

Dehairs, F., Baeyens, W. and Goeyens, L. 1992a. Accumulation of suspended barite at mesopelagic depths and export production in the Southern Ocean. Science. 258: 1332 - 1335.

Dehairs, F., Goeyens, L., Stroobants, N. and Mathot, S. 1992b. Elemental composition in the Scotia-Weddell Confluence area during spring and summer 1988 (EPOS Leg 2). Polar Biol. 12: 25-33.

Dehairs, F., Shopova, D., Ober, S., Veth, C. and Goeyens, L. 1997. Particulate barium stocks and oxygen consumption in the Southern Ocean mesopelagic water column during spring and early summer: relationship with export production. Deep-Sea Res.II. 44: 497-516.

Dehairs, F., Fagel, N., Antia, A.N., Peinert, R., Elskens, M. and Goeyens, L. 2000. Export production in the Bay of Biscay as estimated from barium-barite in settling material: A comparison with new production. Deep-Sea Res.I. 47: 583-601.

de Jong, J.T.M., den Das, J., Bathmann, U., Stoll, M.H.C., Kattner, G., Nolting F.G. and de Baar, H.J.W., 1998. Dissolved iron at subnanomolar levels in the Southern Ocean as determined by ship-board analysis. Anal. Chim. Acta 377: 113-124.

del Giorgio, P.A. and Scarborough, G. 1995. Increase in the proportion of metabolically active bacteria along gradients of enrichment in freshwater and marine plankton: implications for estimates of bacterial growth and production rates. J. Plankt. Res. 17: 1905-1924.

De Long, E.F., Franks, D.G. and Alldredge, A.L. 1993. Phylogenetic diversity of aggregate-attached vs. free-living marine bacteria assemblages. Limnol. Oceanogr. 38: 924-934.

Delille, B., Delille, D., Fiala, M., Gleizon, F., and Frankignoulle, M. 2000a. Distribution and variations of pCO_2 in subantarctic waters of the Kerguelen Archipelago. The southern Ocean: Climate changes and the cycle of carbon, Southern Ocean JGOFS symposium, Brest 8-12 July 2000.

Delille, B., Delille, D., Fiala, M., Prevost, C., and Frankignoulle, M. 2000b. Seasonal changes of pCO_2 over a subantarctic Macrocystis kelp bed. Polar Biol.

Delille, D., Marty, G., Cansemi-Soullard, M., and Frankignoulle, M. 1997. Influence of subantarctic Macrocystis bed in diel changes of marine bacterioplankton and CO_2 fluxes. J. Plankton Res.9: 1251-1264.

De Master, D. J., 1981. The supply and accumulation of silica in the marine environment. Geochim. Cosmochim. Acta. 45: 1715-1732.

De Master, D.J., Dunbar, R.B., Gordon, L.I. Leventer, A.R., Morrison, J.M. and Nelson, D.M. 1992. Cycling and accumulation of biogenic silica and organic matter in high-latitude environments: the Ross Sea. Oceanography. 5: 146-153.

Dickson, A.G. and Millero, F.J. 1987. A comparison of the equilibrium constants for the dissociation of carbonic acid in seawater media. Deep-Sea Res. 1733-1743.

Dickson, A.G., 1993. pH buffers for sea water media based on the total hydrogen ion concentration scale. Deep-Sea Res.I. 40: 107-118.

DiTullio, G.R., Grebmeier, J.M., Arrigo, K.R., Lizotte, M.P., Robinson, D.H., Leventer, A., Barry, J.P., Van Woert, M.L., and Dunbar, R.B. 2000. Rapid and early export of Phaeocystis antarctica blooms in the Ross Sea, Antarctica. Nature. 404: 595-598.

Dodson, A.N. and Thomas, W.H. 1978. Reverse filtration. In: Phytoplankton manual. Monographs on Oceanographic Methodology. Sournia, A. (Ed). UNESCO, Paris: 104-106.

Ducklow, H., Carlson, C. and Smith, W. 1999. Bacterial growth in experimental plankton assemblages and seawater cultures from the Phaeocystis antarctica bloom in the Ross Sea, Antarctica. Aquat. Microb. Ecol. 19: 215-227.

Dunton, K.H. and Dayton, P.K. 1995. The biology of high latitude kelp. 499-507. Elsevier Science B.V.

Dortch, Q. 1990. The interaction between ammonium and nitrate uptake in phytoplankton. Mar. Ecol. Prog. Ser. 61: 183-201.

Dugdale, R.C. and Wilkerson, F.P., 1986. The use of ^{15}N to measure nitrogen uptake in eutrophic oceans: experimental considerations. Limnol. Oceanogr. 31: 673-689.

Dugdale, R.C. and Wilkerson, F.P. 1990. Iron addition experiments in the Antarctic: a re-analysis. Global Biogeochem. Cy. 4: 13-19.

Dymond, J., Lyle, M., Finney, B., Piper, D.Z., Murphy, K., Conard, R. and Pisias, N. 1984. Ferromanganese nodules from MANOP Sites H, S, and R- Control of mineralogical and chemical composition by multiple accretionary processes. Geochim. Cosmochim. Acta. 48: 931-949.

Dymond, J., Suess, E. and Lyle, M. 1992. Barium in deep-sea sediment: a geochemical proxy for paleoproductivity. Paleoceanography. 7: 163-181.

Elderfield, H., Hawkesworth, C.J., Greaves, M.J. and Calvert, S.E. 1981. Rare earth element geochemistry of oceanic ferromanganese nodules and associated sediments. Geochim. Cosmochim. Acta. 45: 513-528.

El-Sayed, S. Z., Biggs, D. L. and Holm-Hansen, O. 1983. Phytoplankton standing crop, primary productivity and near-surface nitrogenous nutrient fields in the Ross Sea, Antarctica. Deep-Sea Res. 30: 871-886.

Elskens, M., Baeyens, W. and Goeyens, L., 1997. Contribution of nitrate to the uptake of nitrogen by phytoplankton in an ocean margin environment. Hydrobiologia. 353: 139-152.

Elskens, M., Goeyens, L., Dehairs, F., Rees, A., Joint, I., and Baeyens, W., 1999. Improved estimation of f-ratio in natural phytoplankton assemblages. Deep-Sea Res.I. In press.

Elskens, M., Baeyens, W., Cattaldo, T., Griffiths, B. and Dehairs, F. N-Uptake conditions during summer in the Sub-Antarctic and Polar frontal zones of the Southern Ocean (Australian sector). Submitted to J. Geophys. Res.

Fagel, N., André, L. and Dehairs, F. 1999. Advective excess Ba transport as shown from sediment and trap geochemical signatures. Geochim. Cosmochim. Acta. 63: 2353-2367.

Fagel, N., Dehairs, F., André, L., Bareille, G. and Monnin, C. Export production estimation from sedimentary Ba content: A comparison between Atlantic and Indian sectors of the Southern Ocean. Paleoceanography. Submitted (Apr. 2000).

Fagel, N., André, L. and Debrabant, P. 1997. Multiple seawater-derived geochemical signatures in Indian oceanic pelagic clays. Geochim. Cosmochim. Acta. 61: 989-1008.

Fahl, K. and Kattner, G. 1993. Lipid content and fatty acid composition of algal communities in sea-ice and water from the Weddel Sea (Antarctica). Polar Biol. 13: 405-409.

Fichefet, T. and Gaspar, P. 1988. A model study of upper ocean-sea ice interactions. J. Phys. Oceanogr. 18: 181-195.

Fichefet, T. and Goosse, H. 1999. A numerical investigation of the spring Ross Sea polynya. Geophys. Res. Let. 26: 1015-1018.

Fiedler, R. and Proksch, G., 1975. The determination of nitrogen-15 by emission and mass spectrometry in biochemical analysis: a review. Anal. Chim. Acta. 78: 1-62.

Francois, R., Bacon, M. P., Altabet, M. A. and Labeyrie, L. 1993. Glacial/interglacial changes in sediment rain rate in the SW Indian sector of Subantarctic waters as recorded by ^{230}Th, ^{231}Pa, U, and δ^{15}N. Paleoceanography. 8: 611-629.

Francois, R., Honjo, S., Manganini, S. and Ravizza, G. 1995. Biogenic barium fluxes to the deep sea: implications for paleoproductivity reconstructions. Global Biogeochem. Cy. 9: 289-303.

Francois, R., Altabet, M.A., Yu, E.-F., Sigman, D.M., Bacon, M.P., Frank, M., Bohrmann, G., Bareille, G. and Labeyrie, L. 1997. Contribution of Southern Ocean surface-water stratification to low atmospheric CO_2 concentrations during the last glacial period. Nature. 389: 929-935.

Frank, M., 1995. Reconstruction of late quaternary environmental conditions applying the natural radionuclides ^{230}Th, ^{10}Be, ^{231}Pa and ^{238}U: A study of deep-sea sediments from the eastern sector of the Antarctic Circumpolar Current System. Doctoral Dissertation, Heidelberger Akademie für Wissenschaften, Berichte zur Polarforschung, 186, 136 pp.

Frank, M., Gersonde, R., Rutgers van der Loeff, M., Kuhn, G. and Mangini, A. 1996. Late Quaternary sediment dating and quantification of lateral sediment redistribution applying ^{230}Th$_{ex}$: a study from the eastern Atlantic sector of the Southern Ocean. Geol. Rundsch. 85: 554-566.

Frankignoulle, M. 1988. Field measurements of air-sea CO_2 exchange. Limnol. Oceanogr. 313-322.

Frankignoulle, M. and Bouquegneau, J.-M. 1987. Seasonal variations of the diel carbon budget of a marine macrophytes ecosystem. Mar. Ecol. Prog. Ser. 197-199.

Frankignoulle, M. and Bouquegneau, J.-M. 1990. Daily and yearly variations of total inorganic carbon in a productive coastal area. Est. Coast. Shelf. Sci. 79-89.

Frankignoulle, M. and Distèche, A. 1984. CO_2 chemistry in the water column above a *Posidonia* seagrass bed and related air-sea exchanges. Oceanol. Acta 209-219.

Frankignoulle, M. and Distèche, A. 1987. Study of the transmission of the diurnal CO_2 concentration changes observed above a *Posidonia* seagrass bed. A method to determine the turbulent diffusion coefficient in a 8 meters water column. Cont. Shelf Res. 67-76.

Frankignoulle, M., Borges, A. and Biondo, R. 2001. A new design of equilibrator to monitor carbon dioxide in highly dynamic and turbid environments. Water Res., 35/5, 1344-1347

Furhman, J.A. and Azam, F. 1982. Bacterioplankton secondary production estimates for coastal waters of British Columbia, Antarctica, and California. Appl. Environ. Microb. 39: 1085-1095.

Gall, M., Boyd, P.W., Hall, J., Safi, K., Chang, H. 2001. Phytoplankton processes: Part 1 Community structure in the Southern Ocean and changes associated with the SOIREE bloom. Deep-Sea Res. II (in press)

Gambéroni, L., Géronimi, J., Jeanin, P.F. and Murail, J.F. 1982. Study of frontal zones in the Crozet-Kerguelen region. Oceanol. Acta. 5: 289-299.

Gao, K. and McKinley, K.R. 1994. Use of macroalgae biomass production and CO_2 remediation: a review. J. Appl. Phycol 45-60.

Gardner, W.D. 1999. Sediment trap sampling in surface waters. In: The Changing Ocean Carbon Cycle. Hanson, R.B., Ducklow, H.W. and Field J.G. (Eds). Cambridge University Press, Cambridge: 240-283.

Gattuso, J.-P., Frankignoulle, M., and Wollast, R. 1998. Carbon and carbonate metabolism in coastal aquatic ecosystems. Ann. Rev. Ecol. Syst. 405-433.

Geider, R.J. and La Roche, J. 1994. The role of iron in phytoplankton photosynthesis and the potential for iron-limitation of primary productivity in the sea. Photosynthesis Res. 39: 275-301.

Gibson, J.A.E. and Trull, T.W. 1999. Annual cycle of fCO_2 under sea-ice and in open water in Prydz Bay, East Antarctica. Mar. Chem.3-4: 187-200.

Gingele, F.X. and Dahmke, A. 1994. Discrete barite particles and barium as tracers of paleoproductivity in South Atlantic sediments. Paleoceanography. 9: 151-168.

Gingele, F.X., Zabel, M., Kasten, S., Bonn, W.J. and Nürnberg, C.C. 1999. Biogenic barium as a proxy for paleoproductivity: Methods and limitations of application. In:

Use of proxies in paleoceanography: Examples from the South Atlantic. Fischer, G. and Wefer, G. (Eds). Springer-Verlag, Berlin: 345-364.

Gledhill, M. and van den Berg, C.M.G. 1994. Determination of complexation of iron (III) with natural organic complexing ligands in seawater using cathodic stripping voltametry. Mar. Chem. 47: 41-54.

Gloersen, P., Campbell, W.J., Cavalieri, D.J., Comiso, J.C., Parkinson, C.L. and Zwally, H.J. 1992. Arctic and Antarctic sea ice, 1978-1987: satellite passive-microwave observations and analysis. NASA SP-511.,Washington, D.C, 290pp.

Goeyens, L., Dehairs, F., Tréguer, P., Baumann, E.M. and Baeyens, W. 1995. The leading role of ammonium in the nitrogen uptake regime of Southern Ocean marginal ice zones. J. Mar. Syst. 6: 345-361.

Goeyens, L. Kindermans, N., Abu Yusuf, M. and Elskens, M. 1998. A room temperature procedure for the manual determination of urea in seawater. Estuar. Coast. Shelf S. 47: 415-418.

Goeyens, L., Semeneh, M., Elskens, M., Shopova, D., Baumann, M.E.M. and Dehairs, F. 1998. Phytoplankton nutrient utilisation and nutrient signature in the Southern Ocean. J. Mar. Syst. 17: 143-157.

Goeyens, L., Tréguer, P., Lancelot, C., Mathot, S., Becquevort, S., Morvan, J., Dehairs, F. and Baeyens, W. 1991. Ammonium regeneration in the Scotia-Weddell confluence area during spring 1988. Mar. Ecol. Progr. Ser. 78: 241-252.

Goldberg, E.D. and Arrhenius, G.O.S. 1958. Chemistry of Pacific pelagic sediments. Geochim. Cosmochim. Acta. 13: 153-212.

Goosse, H. 1997. Modelling the large-scale behaviour of the couped ocean–sea-ice system. Ph.D. thesis. Univ. Cat. Louvain, Louvain-la -Neuve, Belgium.

Goosse, H., Deleersnijder, E., Fichefet, T. and England, M.H. 1999. Sensitivity of a global coupled ocean-sea ice model to the parameterization of vertical mixing. J. Geophys. Res. 104: 13,681-13,695

Goosse, H., Campin, J.M., Deleersnijder, E., Fichefet, T., Mathieu, P.P., Morales Maqueda, M.A. and Tartinville, B. 2000. Description of the CLIO model Version 3.0. Scientific Report 2000/3, Institut d'Astronomie et de Géophysique G. Lemaître, Louvain-la-Neuve, Belgium, 49pp. http://www.astr.ucl.ac.be/tools/clio.html.

Goosse, H., Campin, J.M. and Tartinville, B. 2001. The sources of Antarctic Bottom Water in a global ice-ocean model. Ocean Modelling 3(1-2), 51-65.

Gordon, L.I., 1994. Patterns of nutrient distributions in the Ross Sea during austral summer, 1990 and 1992. EOS Transactions. Amer. Geophys. Union. 75: 138 (Abstract).

Govindaraju, K., 1994. Special Issue of Geostandards Newsletter.18, 158pp.

Gran, H.H., 1931. On the conditions for the production of plankton in the sea. Rapp. Cons. Int. Expl. Mer. 75: 37-46.

Goyet, C., Millero, F.J., O'Sullivan, D.W., Eischeid, G., McCue, S.J., and Bellerby, R.G.J. 1998. Temporal variations of pCO_2 in surface seawater of the Arabian sea in 1995. Deep-Sea Res. I 609-623.

Gran, H.H., 1931. On the conditions for the production of plankton in the sea. Rapp. Cons. Int. Expl. Mer. 75: 37-46.

Gran, G. 1952. Determination of the equivalence point in potentiometric titration, part II. Analyst 661-671.

Guichard, F., Church, T.M., Treuil, M. and Jaffrezic, H. 1979. Rare earth in barites: distribution and effects on aqueous partitioning. Geochim. Cosmochim. Acta. 43: 983-997.

Haas, L.W. 1982. Improved epifluorescence microscopy for observing planktonic microorganisms. An. Inst. Océanogr. 58: 261-266.

Häkkinen, S. and Mellor, G.L. 1990. One hundred years of Arctic ice cover variations as simulated by a one-dimensional, ice-ocean model. J. Geophys. Res. 95: 15959-15969.

Hanisak, M.D. 1993. Nitrogen release from decomposing seaweeds: species and temperature effects. J. Appl. Phycol 175-181.

Hannon, E., Stoll, M.H.C., de Baar, H.J.W., Veth, C. and Lancelot C. in prep. Control of the CO2 drawdown in the Southern Ocean by iron and wind: a modeling study.

Hannon, E., Boyd, P.W., Silvoso, M., and Lancelot, C. 2000. Modeling the bloom evolution and carbon flows during SOIREE: Implications for future in situ iron-enrichments in the Southern Ocean. Deep Sea Res. II (in press).

Hannon, E., Boyd, P.W., Silvoso, M., Lancelot, C. 2001. Modeling the bloom evolution and carbon flows during SOIREE: Implications for future in situ iron-enrichments in the Southern Ocean. Deep-Sea Res. II. (in press).

Hansson I 1973. Determination of the acidity constant of boric acid in synthetic seawater media. Acta. Chem. Scand 924-930.

Harrison, W.G., Harris, L.R. and Irwin, B.D., 1996. The kinetic of nitrogen utilization in the oceanic mixed layer: nitrate and ammonium interactions at nanomolar concentrations. Limno. Oceanogr. 41: 16-32.

Hasle, G.R., 1978. The inverted microscope method. In: Monographs on Oceanographic Methodology, Phytoplankton Manual. Sournia R. (Ed). UNESCO, Paris: 6: 88-96.

Hobbie, J.E., Daley, R.J., and Jasper, S. 1977. Use of nuclepore filters for counting bacteria by fluorescence microscopy. Appl. Environ. Microbiol 1225-1228.

Hoppe, H.-G. 1976. Determination and properties of actively metabolizing heterotrophic bacteria in the sea, investigated by means of micro-autoradiography. Mar. Biol. 36: 291-302.

Hoppe, H.-G., 1983. Significance of exoenzymatic activities in the ecology of brackish water: measurements by means of methylumbelliferyl-substrates. Mar. Ecol. Progr. Ser. 11: 299-308.

Hoppema, M., Fahrbach, E., Schröder, M., Wistotzki, A. and de Baar, H.J.W. 1995. Winter-summer differences of carbon dioxide and oxygen in the Weddell Sea surface layer. Mar. Chem. 51, 177-192.

Hudson, R.J.M. and Morel, F.M.M., 1989. Distinguishing between extra- and intracellular iron in marine phytoplankton. Limnol. Oceanogr. 34: 1113-1120.

Hudson, R.J.M. and Morel, F.M.M., 1990. Iron transport in marine phytoplankton: Kinetics of cellular and medium coordination reactions. Limnol. Oceanogr. 35: 1002-1020.

Hutchins, D.A. and Bruland, K.W. 1998. Iron-limited diatom growth and Si:N uptake ratios in a coastal upwelling regime. Nature. 393: 561-564.

Ikehara, M., Kawamura, K., Ohkouchi, N., Murayama, M., Nakamura, T. and Taira, A. 2000. Variations of terrestrial input and marine productivity in the Southern Ocean (48°C) during the last two deglaciations. Paleoceanography. 15: 170-180.

Inoue, H. and Sugimura, Y. 1988. Distribution and variations of oceanic carbon dioxide in the western North Pacific, eastern Indian, and Southern Ocean south of Australia. Tellus. 40: 308-320.

Jackson, G.A. 1977. Nutrients and production of giant kelp, *Macrocystis pyrifera*, off southern California. Limnol. Oceanogr.6: 979-995.

Jackson, G.A., 1990. A model of formation of marine algal flocs by physical coagulation processes. Deep-Sea Res. 37: 1197-1211.

Jacobs, S.S., 1989. Sea ice and oceanic processes on the Ross Sea continental shelf. J. Geophys. Res. 94: 195-211.

Jacot des Combes, H., Caulet J.P. and Tribovillard, N.P. 1999a. Pelagic productivity changes in the equatorial area of the NW Indian Ocean during the last 400 kyr. Mar. Geol. 158: 27-55.

Jacot des Combes, H., Tribovillard, N. and Caulet, J.-P. 1999b. Paleoproductivity and paleoceanographic changes in the Amirante Passage area (Equatorial Indian Ocean): a 200 kyr interval of lower pelagic productivity. Bul. Soc. Géol. France. 170: 899-914.

Jeandel, C. and coll. 1998. KERFIX, a time-series station in the Southern Ocean: a presentation. J. Marine Syst. 17:555-569.

JGOFS, 1996. Protocols for the Joint Ocean Flux Study (JGOFS) measurements. Intergovernmental Oceanographic Commission (Ed) Bergen, Norway: Report No. 19: 170 pp.

Jochem, F.J., Mathot, S. and Quéguiner, B. 1995. Size-fractionated primary production in the open Southern Ocean in austral spring. Polar Biol. 15: 381-392.

Kalnay, E. and XXI others. 1996. The NCEP/NCAR 40-year reanalysis project. Bull. Amer. Meteor. Soc. 77: 437-471

Kiorboe, T., 1993. Turbulence, phytoplankton cell Size, and structure of pelagic food webs. Adv. Mar. Biol. 29: 1-72.

Kiorboe, T. and Hansen, J.L.S. 1993. Phytoplankton aggregate formation: observations of patterns and mechanisms of cell sticking and the significance of exopolymeric material. J. Plankton. Res. 15: 993-1018.

Kirchman, D., K'Nees, F. and Hodson, R. 1985. Leucine incorporation and its potential as a measure of protein synthesis by bacteria in natural aquatic systems. Appl. Environ. Microb. 49: 599-607.

Keir, R.S., 1988. Paleoproduction and atmospheric CO_2 based on ocean modeling. In: Productivity of the Oceans: Present and Past. Berger, W.H., Smetacek, V.S. and Wefer, G. (Eds.) John Wiley & Sons: 395-406.

Knox, F. and Mc Elroy, M. 1984. Changes in atmospheric CO_2: Influence of the marine biota at high latitudes. J. Geophys. Res. 89: 4629-4637.

Koroleff, F., 1969. Direct determination of ammonia in natural waters as indophenol blue. Int. Counc. Explor. Sea. 9: 19-22.

Kriest, I. and Evans, G.T. 1999 Representing phytoplankton aggregates in biogeochemical models. Deep-Sea Research I, 46, 1841-1859.

Kuma, K., Tanaka, J. and Matsunaga, K., 1999. Effect of natural and synthetic organic-Fe(III) complexes in an estuarine mixing model on iron uptake and growth of a coastal marine diatom, Chaetoceros sociale. Mar. Biol. 134: 761-769.

Kumar, N., 1994. Trace metals and natural radionuclides as tracers of ocean productivity. Ph.D. Thesis. Columbia University.

Kumar, N., Anderson, R.F., Mortlock, R.A., Froelich, P.N., Kubik, P., Dittrich-Hannen, B. and Suter, M. 1995. Increased biological productivity and export production in the glacial Southern Ocean. Nature. 378: 675-680.

Laanbroek, H.L., Verplanke, J.C., De Visscher, P.R.M. and De Vuyst, R. 1985. Distribution of phyto- and bacterioplankton growth and biomass parameters, dissolved inorganic nutrients and free amino acids during a spring bloom in the Oosterschelde basin, The Netherlands. Mar. Ecol. Progr. Ser. 25: 1-11.

Lampitt, R.S., Wishner, K.F., Turley, C.M. and Angel, M.V. 1993. Marine snow studies in the Northeast Atlantic: distribution, composition and role as a food source for migrating plankton. Mar. Biol. 116: 689-702.

Lancelot, C. and Mathot, S., 1985. Biochemical fractionation of primary production by phytoplankton in Belgian coastal waters during hort- and long-term incubations with ^{14}C-bicarbonate. I. Mixed diatom population. Mar. Biol. 86: 219-226.

Lancelot, C., Mathot, S. and Owens, N.J.P. 1986. Modelling protein synthesis, a step to an accurate estimate of net primary production: Phaeocystis pouchetii colonies in Belgian coastal waters. Mar. Ecol. Prog. Ser. 32: 193-202.

Lancelot, C., Veth, C. and Mathot, S. 1991a. Modelling ice-edge phytoplankton bloom in the Scotia-Weddell Sea sector of the Southern Ocean during spring 1988. J. Mar. Syst. 2: 333-346.

Lancelot, C., Billen, G., Veth, C., Mathot, S. and Becquevort, S. 1991b. Modelling carbon cycling through phytoplankton and microbes in the Scotia-Weddell Sea area during sea ice retreat. Mar. Chem. 35: 305-324.

Lancelot, C., Mathot, S., Becquevort, S., Dandois, J.-M. and Billen, G. 1993. Carbon and nitrogen cycling through the microbial network of the marginal ice zone of the Southern Ocean with particular emphasis on the northwestern Weddell Sea. In: Belgian Scientific Research Programme on Antarctica. Scientific results of Phase 2 (Feb.1989-Dec.1991). Caschetto, S. (Ed). Science Policy Office, Brussels: 1-103.

Lancelot, C., Mathot, S., Veth, C. and de Baar, H.W.J. 1993. Factors controlling phytoplankton ice-edge blooms in the marginal ice-zone of the north western Weddell Sea during sea ice retreat 1988: field observations and mathematical modelling. Polar Biol. 13: 377-387.

Lancelot, C. and Rousseau, V. 1994. Ecology of Phaeocystis-dominated ecosystems: The key role of colony forms. In: The Haptophyte AlgaeLeadbeater B.S.C. Green, J. (Ed). Publisher Oxford University Press. 51: 229-245.

Lancelot, C., Becquevort, S., Menon, P., Dandois, J.M., Mathot, S. 1997. Ecological Modelling of the Planktonic Microbial Food-Web. In: Belgian Research Programme on the Antarctic. Scientific Results of Phase III (1992-1996). Caschetto, S. (Ed.). Science Policy Office, Brussels: 1-78.

Lancelot, C., Hannon, E., Becquevort, S., Veth, C., and De Baar, H. 1999. Modeling phytoplancton blooms and related carbon export production in the Southern Ocean: application to the Atlantic sector in Austral spring 1992. Deep-Sea Res., submitted.

Lancelot, C., Hannon, E., Becquevort, S., Veth, C. and de Baar, H.J.W. 2000 Modelling phytoplankton blooms and related carbon export production in the Southern Ocean: application to the Atlantic sector in Austral spring 1992. Deep-Sea Res., Part I, 47: 1621-1662.

Lavery, P.S. and McComb, A.J. 1991. Macroalgal-sediment nutrient interactions and their importance to macroalgal nutrition in a eutrophic estuary. Est. Coast. Shelf. Sci. 281-295.

Lea, D.W. and Boyle, E.A. 1990. Foraminiferal reconstruction of barium distributions in water masses of the glacial oceans. Paleoceanography. 5: 719-742.

Lea, D.W. and Boyle, E.A. 1991. Barium in planktonic foraminifera. Geochim. Cosmochim. Acta. 55: 3321-3331.

Ledley, T.S. 1985. Sensitivity of a thermodynamic sea ice model with leads to time step size. J. Geophys. Res. 90: 2251-2260.

Lerche, D. and Nozaki, Y. 1998. Rare earth elements of sinking particulate matter in the Japan Trench. Earth Planet. Sc. Lett. 159: 71-86.

Lewis, E. and Wallace, D. 1998. Program Developed for CO_2 System Calculations, ORNL/CDIAC-105. Carbon Dioxide Information Analysis Center, Oak Ridge, Tenn.

Li, Y.H., T.L. Ku, G.G. Mathieu and K. Wolgemuth, 1973. Barium in the Antarctic Ocean and implications regarding the marine geochemistry of Ba and 226Ra. Earth Planet. Sc. Lett., 19, 352.

Li, Y.-H., Burkhardt, L., Buchholtz, M., O'Hara, P. and Santschi, P.H. 1984. Partition of radiotracers between suspended particles and seawater. Geochim. Cosmochim. Acta. 48: 2011-2019.

Liebig von, J. 1840. Organic chemistry and its application to agriculture and physiology. Taylor and Walton, London.

Liss, P.S. and Merlivat, L. 1986. Air-sea exchange rates: introduction and synthesis. 113-118. Reidel.

Louanchi, F., Ruiz-Pino, D., and Poisson, A. 1999. Temporal variations of mixed-layer oceanic CO_2 at JGOFS-KERFIX time-series station: Physical versus biogeochemical processes. J. Mar. Res 165-187.

Lyle, M., Heath, G.R. and Robbins, J.M. 1984. Transport and release of transition elements during early diagenesis: sequential leaching of sediments from MANOP Sites M and H. Part I. pH 5 acetic acid leach. Geochim. Cosmochim. Acta, 48, 1705-1715.

MacIntyre, H.L., Geider, R.J. and McKay, R.M., 1996. Photosynthesis and regulation of RUBISCO activity in net phytoplankton from Delaware Bay. J. Phycol. 32:718-731.

Maldonado, M.T. and Price, N.M. 1999. Utilization of iron bound to strong organic ligands by plankton communities in the subarctic Pacific Ocean. Deep-Sea Research II 46: 2447-2473.

Mann, K.H. 1982. Ecology of coastal waters. 58-60. Blackwell.

Marr, J.W.S. 1962. The natural history and geography of the Antarctic krill (Euphausia superba Dana). Discov. Rep. 32: 33-464.

Martin, J. H. and Fitzwater, S. E. 1988. Iron deficiency limits phytoplankton growth in the North-East Pacific Subarctic. Nature. 331: 341-343.

Martin, J.H., Gordon, R.M. and Fitzwater, S.E. 1990. Iron in Antarctic waters. Nature. 345: 156-158.

Martin, E.E., Macdougall, J.D., Herbert, T.D., Paytan, A. and Kastner, M. 1995. Strontium and neodynium isotopic analyses of marine barite separates. Geochim. Cosmochim. Acta. 59: 1353-1361.

Mathot, S. 1993. Phytoplankton in the marginal ice zone and its contribution to the annual primary production of the Southern Ocean. Ph.D. thesis. Univ. Libre de Bruxelles.

McCarthy, J.J., Taylor, W.R. and Taft, J.L., 1977. Nitrogenous nutrition of the plankton in Chesapeake Bay. I. Nutrient availability and phytoplankton preferences. Limnol. Oceanogr. 22: 996-1010.

McManus, J., Berelson, W.M., Klinkhammer, G.P., Johnson, K.S., Ciale, K.H., Anderson, R.F., Kumar, N., Burdige, D.J., Hammond, D.E., Brumsack, H.J., McCorkle, D.C. and Rushdi, A. 1998. Geochemistry of barium in marine sediments: Implications for its use as a paleoproxy. Geochim. Cosmochim. Acta. 62: 3453-3473.

McPhee, M G., 1992. Turbulent heat flux in the upper ocean under sea ice. J Geophys Res. 97: 5365-5379.

Mehrbach, C., Culberson, C.H., Hawley, J.E., and Pytkowicz, R.M. 1973. Measurements of the apparent dissociation constants of carbonic acid in seawater at atmospheric pressure. Limnol. Oceanogr. 897-907.

Mellor, G.L. and Yamada, T. 1982. Development of a turbulence closure model for geophysical fluid problems. Rev. Geophys. Spac. Phys., 20: 851-875.

Metzl, N., Beauverger, C., Brunet, C., Goyet, C., and Poisson, A. 1991. Surface water carbon dioxide in the southwest Indian Sector of the Southern Ocean: A highly variable CO_2 source/sink region in summer. Mar. Chem. 85-95.

Metzl, N., Poisson, A., Louanchi, F., Brunet, C., Schauer, B., and Brès, B. 1995. Spatio-temporal distribution of air-sea fluxes of CO_2 in the Indian and Antarctic Ocean. Tellus 56-69.

Metzl, N., Tilbrook, B., and Poisson, A. 1999. The annual fCO_2 cycle and the air-sea CO_2 flux in the sub-Antarctic Ocean. TellusB: 849-861.

Mitchell, B.G. and Holm-Hansen, O. 1991. Observations and modelling of the phytoplankton crop in relationship to mixing depth. Deep-Sea Res.II. 38: 981-1008.

Monnin, C., Jeandel, C., Cattaldo, T. and Dehairs, F. 2000. The marine barite saturation state of the world's ocean. Mar. Chem. 65: 253-261.

Moore, J.K. and Villareal, T.A. 1996. Buoyancy and growth characteristics of three positively buoyant marine diatoms. Mar. Ecol. Progr. Ser. 132: 203-213.

Morel, F.M.M., Rueter, J.G. and Price, N.M. 1990. Iron nutrition of phytoplankton and its possible importance in the ecology of ocean regions with high nutrient and low biomass. Oceanography, 4(2): 56-61.

Mortlock, R.A., Charles, C.D., Froelich, P.N., Zibello, M.A., Saltzman, J., Hays, J.D., and Burckle, L.H. 1991. Evidence for lower productivity in the Antarctic Ocean during the last glaciation. Nature. 351: 220-223.

Muggli, D.L., Lecourt, M. and Harrison, P.J. 1996. Effects of iron and nitrogen source on the sinking rate, physiology and metal composition of an oceanic diatom from the subarctic Pacific. Mar. Ecol. Progr. Ser. 132: 215-227.

Murphy, P.P., Feely, A., Gammon, H., Harrison, D.E., Kelly, K.C. and Waterman, L.S. 1991a. Assessment of the air-sea exchange of CO_2 in the South Pacific during austral autumn. J. Geophys. Res. 96: 20445-20465.

Murphy, P.P., Feely, A., Gammon, H., Kelly, K.C. and Waterman, L.S. 1991b. Autumn air-sea disequilibrium of CO_2 in the South Pacific Ocean. Mar. Chem. 35: 77-84.

Nath, B.N., Roelandts, I., Sudhakar, M. and Plüger, W.L. 1992. Rare earth element patterns of the central Indian basin sediments related to their lithology. Geophys. Res. Lett. 19: 1197-1200.

Nath, B.N., Bau, M., Rao, B.R. and Rao, Ch.M. 1997. Trace and rare earth elemental variation in Arabian Sea sediments trough a transect across the oxygen minimum zone. Geochim. Cosmochim. Acta. 61: 2375-2388.

Navez, J., 1985. Méthodes d'analyse des éléments majeurs dans les roches silicatées basée sur la spectrométrie d'émission dans un plasma a couplage inductif. Mus. Royal Afr. Centr., Tervuren (Belgique), Dept. Geol. Min., Rapport annuel 1983-1984, 87-90.

Nelson, D.M. and Smith, W.O. 1986. Phytoplankton bloom dynamics of the western Ross Sea ice-edge. II. Mesoscale cycling of nitrogen and silicon. Deep-Sea Res.I, 33: 1389-1412.

Nelson, D.M., De Master, D.J., Dunbar, R.B. and Smith, W.O. 1996. Cycling of organic carbon and biogenic silica in the Southern Ocean: Estimates of water-column and sedimentary fluxes on the Ross Sea continental shelf. J. Geophys. Res. 101: 18, 519-18, 532.

Neveux, J. and Panouse, M. 1987. Spectrofluorometric determination of chlorophylls and pheophytins. Arch. Hydrobiol. 567-581.

Nightingale, P.D., Malin, G., Law, C.S., Watson, A.J., Liss, P.S., Liddicoat, M.I., Boutin, J., and Upstill-Goddard, R.C. 2000. n situ evaluation of air-sea gas exchange parameterizations using novel conservative and volatile tracers . Global Biogeochem. Cycles1: 373-387.

Nodder, S.D., Waite, A.M. 2001. Is Southern Ocean carbon and biogenic silica export enhanced by iron-stimulated increases in biological production? Sediment trap results from SOIREE. Deep-Sea Res. II (in press)

Nolting, R.F. and de Jong, J.T.M., 1995. Sampling and analytical methods for the determination of trace metals in surface seawater. Intern. J. Environ. Anal. Chem. 57: 189-196.

Nürnberg, C.C., 1995. Bariumfluss und Sedimentation im Südlichen Südatlantik - Hinweise auf Produktivitätsänderungen im Quartär. Ph.D. Thesis. Universität Kiel. Geomar Report 38, 105 pp.

Nürnberg, C.C., Bohrmann, G. and Schluter, M. 1997. Barium accumulation in the Atlantic sector of the Southern Ocean: Results from 190,000-year records, Paleoceanography, 12, 594-603.

Olson, R.J., Sosik, H.M., Chekalyuk, A.M. and Shalapyonok, A. 2000. Effects of iron enrichment in the Southern Ocean during late summer: active fluorescence and flow cytometric analyses. Deep-Sea Res. II 47: 3179-3199.

Orsi, A., Whitworth III, T. and Nowlin, W.D. 1995. On the meridional extent and fronts of the Antarctic Circumpolar Current. Deep-Sea Res. I. 42: 641-673.

Palmer, M.R., 1985. Rare earth elements in foraminifera tests. Earth Planet. Sc. Lett. 73: 285-298.

Park, Y.-H., Gambéroni, L. and Charriaud, E. 1991. Frontal structure and transport of the Antarctic Circumpolar Current in the south Indian Ocean sector, 40-80°E. Mar. Chem. 35: 45-62.

Park, Y.-H., Gambéroni, L. and Charriaud, E. 1993. Frontal structure, water masses, and circulation in the Crozet basin. J. Geophys. Res. 98: 12361-12385.

Park, Y.-H., Charriaud, E. and Fieux, M. 1998. Thermohaline structure of the Antarctic surface water / winter water in the Indian sector of the Southern Ocean. J. Mar. Syst. 17: 1-23.

Passow, U., 1991. Species-specific sedimentation and sinking velocities of diatoms. Mar. Biol. 108: 449-455.

Paytan, A., Kastner, M. and Chavez, F.P. 1996. Glacial to interglacial fluctuations in productivity in the equatorial Pacific as indicated by marine barite. Science. 274: 1355-1357.

Paytan, A., Kastner, M., Martin, E.E., Macdougall, J.D. and Herbert, T. 1993. Marine barite as a monitor of seawater strontium isotope composition. Nature. 366: 445-449.

Pillsbury, R.D. and Jacobs, S.S. 1985. Preliminary observations from long-term current meter moorings near the Ross Ice Shelf. In: Oceanography of the Antarctic Continental Shelf. Antarctic Research Series. Jacobs, S.S. (Ed). American Geophysical Union, Washington: 43: 87-107.

Pilskaln, C.H., Lehmann, C., Paduan, J.B. and Silver, M.W. 1998. Spatial and temporal dynamics in marine aggregate abundance, sinking rate and flux: Monterey Bay, central California. Deep-Sea Res.I. 45:1803-1837.

Piper, D.Z., 1974. Rare earth elements in the sedimentary cycle: a summary. Chem. Geol. 14: 285-304.

Piper, D.Z., 1974. Rare earth elements in ferromanganese nodules and other marine phases. Geochim. Cosmochim. Acta. 38: 1007-1022.

Piper, D.Z. and Williamson, M.E. 1977. Composition of Pacific Ocean ferromanganese nodules. Mar. Geol. 23: 285-303.

Platt, T., Gallegos, C.L. and Harrison, W.G., 1980. Photoinhibition of photosynthesis in natural assemblages of marine phytoplankton. J. Mar. Res. 38: 687-701.

Platt, T., Harrison, W.G., Irwin, B., Horne, E.P. and Gallegos, C.L., 1982. Deep-Sea Res. 29: 1159-1170.

Poisson, A., Schauer, B. and Brunet, C. 1990. Les Rapports des Campagnes à la Mer, MD 53 / INDIGO 3, à bord du « Marion Dufresne », Fascicule 2, No 87-02. Les Publications de la Mission de Recherche des Terres Australes et Antarctiques Françaises, 269 p.

Poisson, A., Metzl, N., Brunet, C., Schauer, B., Bres, B., Ruiz-Pino, D. and Louanchi, F. 1993. Variability of sources and sinks of CO_2 in the Western Indian and Southern Oceans during the year 1991. J. Geophys. Res. 98: 22 759-22 778.

Poisson, A., Metzl, N., Brunet, C., Schauer, B., Brès, B., Ruiz-Pino, D., and Louanchi, F. 1993. Variability of sources and sinks of CO_2 in the Western Indian and Southern Oceans During the Year 1991. J. Geophys. Res.C12: 22 759-22 778.

Porter, K.G. and Feig, Y.S. 1980. Use of DAPI for identifying and counting aquatic microflora. Limnol. Oceanogr. 25: 943-948.

Probst, G. 1999. Tests de validation de la partie hydrodynamique du modèle CLIO-1D. Progress Report 1999/1, Institut d'Astronomie et de Géophysique G. Lemaître, Louvain-la-Neuve, Belgium, 21pp.

Probst, G.,1999. Validation de la partie glace de mer du modèle CLIO-1D. Progress Report 1999/5, Institut d'Astronomie et de Géophysique G. Lemaître, Louvain-la-Neuve, Belgium, 15pp.

Probst, G. 1999. Test de validation du modèle couplé CLIO-1D / SWAMCO. Progress Report 1999/6, Institut d'Astronomie et de Géophysique G. Lemaître, Louvain-la-Neuve, Belgium, 14pp.

Probst, G., 2000a. Description of the 1D version of the CLIO model. Progress Report 2000/2, Institut d'Astronomie et de Géophysique G. Lemaître, Louvain-la-Neuve, Belgium, 16pp.

Probst, G., 2000b. An integrated approach to assess carbon dynamics in the Southern Ocean – Sea ice and water column 1D modelling. Progress Report 2000/3, Institut d'Astronomie et de Géophysique G. Lemaître, Louvain-la-Neuve, Belgium, 37pp.

Quéguiner, B., Tréguer, P., Peeke, I. and Scharek, R. 1997. Biogeochemical dynamics and the silicon cycle in the Atlantic sector of the Southern Ocean during austral spring 1992. Deep-Sea Res.II. 44: 69-89.

Ratkowsky, D.A., 1990. Handbook of nonlinear regression models. Vol. 107. Owen, D.B. (Ed.). Marcel Dekker, INC, New York, 241 p.

Riebesell, U., 1989. Comparison of sinking and sedimentation rate measurements in a diatom winter/spring bloom. Mar. Ecol. Progr. Ser. 54: 109-119.

Riebesell, U. 1991. Particle aggregation during a diatom bloom. II Biological aspects. Mar. Ecol. Progr. Ser. 69: 281-291.

Riebesell, U., 1993. Aggregation of Phaeocystis during phytoplankton spring blooms in the southern North Sea. Mar. Ecol. Progr. Ser. 96: 281-289.

Riebesell, U., Reigstad, M., Wassmann, P., Noji, T. and Passow, U. 1995. On the trophic fate of Phaeocystis pouchetii (Hariot): VI. Significance of Phaeocystis-derived mucus for vertical flux. Neth. Sea Res. 33: 193-203.

Rintoul, S.R., Donguy, J.R., and Roemmich, D.H., 1997. Seasonnal evolution of upper ocean thermal structure between Tasmania and Antarctica. Deep-Sea Res.I, 44: 1185-1202.

Rintoul, S.R. and Sokolov, S. 2000. Baroclinic transport variability of the Antarctic Circumpolar Current south of Australia (WOCE repeat section SR3). J. Geophys. Res. 106: 2795.

Rousseau, V., Mathot S. and Lancelot, C. 1990. Calculating carbon biomass of Phaeocystis sp. from microscopic observations. Mar. Biol. 107: 305-314.

Roy, R., Roy, L., Vogel, J.C., Porter-Moore, C., Pearson, T., Good, C.E., Millero, F.J. and Campbell, D.M., 1993. The dissociation constants of carbonic acid in seawater at salinities 5 to 45 and temperatures 0 to 45°C. Mar. Chem. 44: 249-267.

Rue, E.L. and Bruland, K.W., 1995. Complexation of iron(III) by natural organic ligands in the Central North Pacific as determined by a new competitive ligand equilibration/adsorptive cathodic stripping voltametric method. Mar. Chem. 50: 117-138.

Rutgers van der Loeff, M. M. and Berger, G.W. 1983. Scavenging of ^{230}Th and ^{231}Pa near the Antarctic Polar Front in the South Atlantic. Deep-sea Res. I. 40: 339-357.

Rutgers van der Loeff, M.M., Friedrich, J. and Bathmann, U.V. 1997. Carbon export during the spring bloom at the Atarctic Polar Front, determined with the natural tracer ^{234}Th. Deep-Sea Res. II. 44: 457-478.

Sabine, C. and Key, R.M., 1998. Controls on fCO_2 in the South Pacific. Mar. Chem. 60: 95-110.

Sarkar, A., Bhattacharya, S.K. and Sarin, M.M. 1993. Geochemical evidence for anoxic deep water in the Arabian Sea during the last deglaciation. Geochim. Cosmochim. Acta. 57: 1009-1016.

Sarmiento, J. and Toggweiler, R. 1984. A new model for the role of the oceans in determining atmospheric pCO_2. Nature. 308: 621-624.

Sarmiento, J.L. and Orr, J.C., 1992. A pertubation simulation of CO_2 uptake in an Ocean circulation model. J. Geophys. Res. 97: 3621-3645.

Scharek, R., van Leeuw, M.A. and de Baar, H.J.W. 1997. Responses of Southern Ocean phytoplankton to the addition of trace metals. Deep-Sea Res.II. 44: 209-228.

Schlitzer, R. 2001. Ocean Data View, http://www.awi-bremerhaven.de/GEO/ODV.

Schmitz, B. 1987. Barium, equatorial high productivity and the northward wandering of the Indian continent. Paleoceanography. 2: 63-77.

Schneider, B. and Morlang, J. 1995. Distribution of the CO_2 partial pressure in the Atlantic ocean between Iceland and the Antarctic peninsula. Tellus. 47: 93-102.

Schweitzer, P.N., 1995. Monthly Average Polar Sea-Ice Concentration. U.S. Geological survey digital data series DDS-27. URL http://geochange.er.usgs.gov/pub/sea_ice/

Sedwick, P.N., Edwards, P.R., Mackey, D.J., Griffiths, F.B. and Parslow, J.S. 1997. Iron and manganese in surface waters of the Australian subantarctic region. Deep-Sea Res.I. 44: 1239-1253.

Sedwick, P.N., DiTullio, G.R. and Mackey, D.J. 2000. Iron and manganese in the Ross Sea, Antarctica: seasonal iron limitation in Antarctic shelf waters. J. Geophys. Res. 105: 321-336.

Semeneh, M., Dehairs, F., Elskens, M., Baumann, M.E.M, Kopczynska, E.E., Lancelot, C. and Goeyens, L. 1998. Nitrogen uptake regime and phytoplankton community structure in the Atlantic and Indian sectors of the Southern Ocean. J. Mar. Syst. 17: 159-177.

Semeneh, M., Dehairs, F., Fiala, M., Elskens, M., Goeyens, L. 1998b. Seasonal variation of phytoplankton community structure and nitrogen uptake regime in the Indian Sector of the Southern Ocean. Polar Biol. 20: 259-272.

Sfriso, A., Marcomini, A., and Pavoni, B. 1987. Relationships between macroalgal biomass and nutrient concentrations in a hypertrophic area of the Venice Lagoon. Mar. Env. Res. 297-312.

Shanks, A.L. and Trent, J.D. 1980. Marine snow: sinking rates and potential role in vertical flux. Deep-Sea Res. I 27: 137-143.

Sherr, B., del Giorgio, P. and Sherr, E.1999. Estimating abundance and single-cell characteristics of actively respiring bacteria via the redox dye, CTC. Aquat. Microb. Ecol. 18: 117-131.

Siegenthaler, U. and Sarmiento, J.L. 1993. Atmospheric carbon dioxide and the ocean. Nature. 365: 119-125.

Simon, M. and Azam, F. 1989. Protein content and protein synthesis rates of planktonic marine bacteria. Mar. Ecol. Progr. Ser. 51: 201-213.

Simon, M., Alldredge, A.L. and Azam, F. 1990. Bacterial carbon dynamics on marine snow. Mar. Ecol. Progr. Ser. 65: 205-211.

Sholkovitz, E.R., Landing, W.M. and Lewis, B.L. 1994. Ocean particle chemistry: The fractionation of rare earth elements between suspended particles and seawater. Geochim. Cosmochim. Acta. 56: 1567-1579.

Smetacek, V., 1985. Role of sinking in diatom life-history cycles: ecological, evolutionary and geological significance. Mar. Biol. 84: 239-251.

Smetacek, V., de Baar, H.J.W., Bathmann, U.V., Lochte, K. and Rutgers van der Loeff, M.M. 1997. Ecology and biogeochemistry of the Antarctic Circumpolar Current during austral spring: a summary of Southern Ocean JGOFS cruise ANT X/6 of R.V. Polastern. Deep-Sea Res.II. 44: 1-21.

Smetacek V., de Baar, H.J.W., Bathmann, U.V., Rutgers van der Loeff, M.M. and Lochte K. 1997. Ecology and biogeochemistry of the Antarctic Circumpolar Current during Austral spring : Southern Ocean JGOFS cruise ANTX/6 of R.V. Polarstern. Deep-Sea Res. II, 44(1-2), 519pp

Smith, S.V. 1981. Marine macrophytes as global carbon sink. Science 838-840.

Smith, W.O. and Nelson, D.M. 1985. Phytoplankton bloom produced by a receeding ice edge in the Ross Sea: spatial coherence with the density field. Science. 227: 163-166.

Smith, D.C., Simon, M., Alldredge, A.L. and Azam, F.1992. Intense hydrolytic enzyme activity on marine aggregates and implications for rapid particle dissolution. Nature. 359: 139-142.

Smith, S.V. and Hollibaugh, J.T. 1993. Coastal metabolism and the oceanic carbon balance. Rev. Geophys. 75-89.

Smith, D.C., Steward, G.F. Long, R.A. and Azam, F. 1995. Bacterial mediation of carbon fluxes during a diatom bloom in a mesocosm. Deep-Sea Res. II 42: 75-97.

Smith, W.O., Nelson, D.M. Ditullio, G.R. and Leventer, A.R. 1996. Temporal and spatial patterns in the Ross Sea: Phytoplankton biomass, elemental composition, productivity and growth rates. J. Geophys. Res. 101: 18,455-18,465.

Smith, W.O. and Gordon, L.I. 1996. Bloom or Bust: Hyperproductivity of the Ross Sea (Antarctica) polynya during Austral Spring. Science. 362: 1322-1328.

Smith, W.O.Jr., and Dunbar, R.B. 1998. The relationship between new production and vertical flux on the Ross Sea continental shelf. J. Mar. Syst. 17: 445-457.

Smith, W.O.Jr., Anderson, R.F., Moore, J.K., Codispoti, L.A. and Morrison, J.M. 2000. The US Southern Ocean Joint Global Flux Study: an introduction to AESOPS. Deep-Sea Res.II. 47: 3073-309

Smith, W.O., Jr., Marra, J. Hiscock, M.R. and Barber. R.T. 2000. The seasonal cycle of phytoplankton biomass and primary productivity in the Ross Sea, Antarctica. Deep-Sea Res. II 47: 3119-3140.

Smith, W.O.Jr. and Asper, V.A. 2001. The influence of phytoplankton assemblage composition on biogeochemical characteristics and cycles in the southern Ross Sea, Antarctica. Deep-Sea Res.I. 48: 137-162.

Somville, M. and Billen, G. 1983. A method for determination exoproteolytic activity in natural waters. Limnol. Oceanogr. 28: 190-193.

Somville, M., 1984. Measurement and study of substrate specificity of exoglucosidase activity in eutrophic water. Appl. Environ. Microb. 48: 1181-1185.

Stroobants N., Dehairs, F., Goeyens, L., Vanderheijden, N. and Van Grieken, R. 1991. Barite formation in the Southern Ocean water column. Mar. Chem. 35: 411-421.

Stefels, J. and van Leeuwe, M.A., 1998. Effects of iron and light stress on the biochemical composition of Antarctic Phaeocystis sp. (Prymnesiophyceae). I. Intracellular DMSP concentrations. J. Phycol. 34: 486-495.

Sullivan, C.W., Arrigo, K.R., Mc Clain, C.R., Comiso, J.C. and Firestone, J. 1993. Distribution of phytoplankton blooms in the Southern Ocean. Science. 262: 1832-1837.

Sunda W.G., Swift, D. and Huntsman, S.A. 1991. Iron growth requirements in oceanic and coastal phytoplankton. Nature, 351: 55-57.

Sunda, W.G., 1994. Trace metal/phytoplankton interactions in the sea, p. 213-247. In Bidoglio, G. & Stumm, W. [Eds.], Chemistry of aquatic systems: local and global perspectives. Kluwer Academic.

Sunda, W.G. and Huntsman, S.A., 1995. Iron uptake and growth limitation in oceanic and coastal phytoplankton. Mar. Chem. 50: 189-206.

Tachikawa K., C. Jeandel and B. Dupré, 1997. Distribution of rare earth elements and neodynium isotopes in settling particulate material of the tropical Atlantic Ocean (EUMELI site), Deep-Sea Research, 44, 1769-1792.

Tachikawa K., C. Jeandel, A. Vangriesheim and B. Dupré, 1999. Distribution of rare earth elements and neodymium isotopes in suspended particles of the tropical Atlantic Ocean (EUMELI site), Deep-Sea Research I, 46, 733-755.

Takahashi T., Olafsson J., Goddard J.G., Chipman D.W. and Sutherland S.C., 1993. Seasonal variation of CO_2 and nutrients in the high-latitude surface oceans: a comparative study, Global Biogeochemical Cycles, 7, 843-878.

Takahashi, T., Feely, A., Weiss, R.F., Wanninkhof, R., Chipman, D.W., and Sutherland, S.C. 1997. Global air-sea flux of CO2: An estimate based on measurment of sea-air pCO2 difference. Proc. natl. acad. sci. USA 8292-8299.

Takeda, S., 1998. Influence of iron availability on nutrient consumption ratio of diatoms in oceanic waters, Nature, 393, 774-777.

Tans P.P., Fung I.Y. and Takahashi T., 1990. Observational constraints on the global atmospheric CO_2 budget, Science , 247, 1431-1438.

Taylor S.R; and McLennan S.M. 1985. The continental crust: its composition and evolution, Blackwell Scientific Publications, 312 pp.

Thingstad T. F. and I. Martinussen, 1993. Are bacteria active in the cold pelagic ecosystem of the Barents Sea ? Polar Research. 13, 45-55.

Thingstad F. and G. Billen, 1994. Microbial degradation of Phaeocystis material in the water column. In: The Ecology of Phaeocystis-dominated Ecosytems, C. Lancelot & P. Wassmann (eds.), J.Mar. Syst., 5, 55-66.

Timmermans, K.R., Gerringa, L.J.A, de Baar, H.J.W., van der Wagt, B., Veldhuis, M.J.W.,de Jong, J.T.M., Croot, P.L.and Boye, M. 2001. Growth rates of large and small Southern Ocean diatoms in relation to availability of iron in natural seawater. Limnol. Oceanogr. 46: 260-266.

Tiselius, P. and Kuylenstierna, M. 1996. Growth and decline of a diatom spring bloom: phytoplankton species composition, formation of marine snow and the role of heterotrophic dinoflagellates. J. Plankt. Res. 18: 133-155.

Tranter D.J., 1982. Interlinking of physical and biological processes in the Antarctic Ocean, Oceanography and Marine Biology, Annual Review, 20, 11-35.

Treguer, P. and Le Corre, P. 1975. Manuel d'analyses des sels nutritifs dans l'eau de mer. Utilisation de l'Auto-analyzer II Technicon. U.B.O.

Tréguer P., L.I. Gordon and D.M. Nelson, 1994. N/Si/P uptake ratios in the surface layer of the Ross Sea during summer, 1990 and 1992, EOS Transactions, AGU, 75(3), 138-139.

Trick, C.G. *et. al.*, 1983. Science.

Trull, T., S. Bray, S. Manganini, S. Honjo and R. François, 2001. Moored sediment trap measurements of carbon export in the Sub-Antarctic and Polar Front Zones of the Southern Ocean, south of Australia. J. Geophys. Res, submitted.

van Boeckel, W. H. M., Hansen, F. C. Riegman, R. and Bak, R. P. M. 1992. Lysis-induced decline of a Phaeocystis spring bloom and coupling with the microbial foodweb. Mar. Ecol. Progr. Ser. 81: 269-276.

van Leeuwe, M.A., Scharek, R., de Baar, H.J.W., Goeyens, L. and de Jong J.T.M. 1997. Iron enrichment experiments in the Southern Ocean : physiological responses of plankton communities. Deep-Sea Res. II , 44(1-2): 189-208.

van Leeuwe, M.A. and Stefels, J., 1998. Effects of iron and light stress on the biochemical composition ofAntarctic Phaeocystis sp. (Prymnesiophyceae). II. Pigment Composition. J. Phycol. 34: 496-503.

Verity P.G., T.A. Villareal and T.J. Smayda, 1988. Ecological investigations of blooms of colonial Phaeocystis pouchetii. II. The role of life-cycle phenomena in bloom termination, J.Plank. Res., 10, 49-66.

Veth C., 1991. The evolution of the upper water layer in the marginal ice zone, austral spring 1988, Scotia-Weddell Sea, J.Mar.Syst., 2, 451-464.

Veth C., C. Lancelot and S. Ober, 1992. On processes determining the vertical stability of surface waters in the marginal ice zone of the north-western Weddel Sea and their relationship with phytoplankton bloom development, Pol.Biol., 12, 237-243.

Völker, C. and Wolf-Gladrow, D.A., 1999. Physical limits on iron uptake mediated by siderophores or surface reductases. Mar. Chem. 65: 227-244.

Von Breymann M.T., K.-C. Emeis and E. Suess, 1992. Water depth and diagenetic constraints on the use of barium as a paleoproductivity indicator, in: Upwelling Systems: Evolution since the Early Miocene, eds. C.P. Summerhayes, W.L. Prell and K.-C. Emeis, Geological Society Special Publication No 64, pp 273-284.

Waite, A., Fisher, A., Thompson, P.A. and Harrison P.J. 1992. Does energy control the sinking rates of marine diatoms? Limn. Oceanogr. 37: 468-477.

Waite, A., Fisher, A. Thompson, P.A. and Harrison, P.J. 1997. Sinking rate versus cell volume relationships illuminate sinking rate control mechanisms in marine diatoms. Mar. Ecol. Progr. Ser. 157: 97-108.

Waite, A. and Nodder, S. 2001.The effect of in situ iron addition on the sinking rates and export flux of Southern Ocean diatoms, Deep-Sea Res. II, in press.

Walsh, J.J. 1988. On the nature continental shelves. 1-520.

Walsh, J.J. 1991. Importance of continental margins in the marine biochemical cycling of carbon and nitrogen. Nature 53-55.

Walter, H-J., M.M. Rutgers van der Loeff, and H. Holtzen, Enhanced scavenging of ^{231}Pa relative to ^{230}Th in the South Atlantic south of the Polar Front. Implications for the use of ^{231}Pa/^{230}Th ratio as a paleoproductivity proxy, Earth Planet. Sci. Lett., 149, 85-100, 1997.

Walter, H-J, Scavenging of ^{231}Pa and ^{230}Th in the South Atlantic: implications for the use of the ^{231}Pa/^{230}Th ratio as a paleoproductivity proxy. Alfred Wegener Institut, Bremerhaven, Report 282, 1998.

Wanninkhof, R. 1992. Relationship between wind speed and gas exchange over the ocean . J. Geophys. Res. 7373-7382.

Wanninkhof, R. and McGillis, W.R. 1999. A cubic relationship between air-sae CO_2 exchange and wind speed. Geophys. Res. Let.13: 1889-1892.

Wassmann, P., Vernet, M. Mitchell, B. and Rey G.F. 1990. Mass sedimentation of Phaeocystis pouchetii in the Barents Sea. Mar. Ecol. Progr. Ser. 66: 183-195.

Wassmann P., 1994. Significance of sedimentation for the dynamics of Phaeocystis blooms, J. Mar. Syst., 5, 81-100.

Wefer G. and G. Fischer, 1991. Annual primary production and export flux in the Southern Ocean from sediment trap data, Mar. Chem., 35, 597-613.

Weiss, R.F. 1974. Carbon dioxide in water and seawater: the solubility of a non-ideal gas. Mar. Chem. 203-215.

Weisse T., K. Tande, P. Verity, F. Hansen and W. Gieskes, 1994. The trophic significance of Phaeocystis blooms, J. Mar. Syst., 5, 67-80.

Wells, M.L., Price, N.M. and Bruland, K.W., 1995. Iron Chemistry in seawater and its relationship to phytoplankton: a workshop report. Marine Chem. 48: 157-182.

Whitworth III T., 1988. The Antarctic Circumpolar Current, Oceanus, 31, 53-58.

Wheeler, W.N. and Druehl, L.D. 1986. seasonal growth and productivity of *Macrocystis integrifolia* in British Columbia, Canada. Mar. Biol., 181-186.

Wilcox, H.A. and North, W.J. 1988. CO2 Reduction and Reforestation. Science 1493-1494.

Wolgemuth, K. and W.S. Broecker, 1970. Barium in seawater. Earth Planet. Sc. Lett, 8, 372.

Wollast, R. 1983. Interactions in estuaries and coastal waters. 385-409. Wiley-Interscience.

Wollast, R. 1991. The coastal organic carbon cycle: fluxes, sources and sinks. 365-382. Wiley.

Wollast, R. 1998. Evaluation and comparison of the global carbon cycle in the coastal zone and in the open ocean.9: 213-252. John Wiley & Sons.

Yu, E.-F., Francois, R. Bacon, M.P. Honjo, S. Fleer, A.P. Manganini, S.J. Rutgers van der Loeff, M.M. and Ittekot, V. 2001. Trapping efficiency of bottom-tethered sediment traps estimated from the intercepted fluxes of ^{230}Th and ^{231}Pa. Deep-Sea Res. II 48: 865-889.

Zwally H.J., Comiso, J.C. and A.L. Gordon, 1985. Antarctic offshore leads and polynyas and oceanographic effects. In: Oceanography of the Antarctic Continental Shelf, Antarctic Research. Series, ed. S.S. Jacobs, AGU, Whashington, 43, 203-226.

RESPONSE OF THE SOUTHERN OCEAN PLANKTON ECOSYSTEM TO PHYSICAL AND TROPHIC CONSTRAINTS: THE CASE OF THE ROSS SEA.

Jean-Henri HECQ[1], Anne GOFFART[1], Cristina BEANS[1], Alain NORRO[2], Giulio CATALANO[3], Letterio GUGLIELMO[4],

1 : Université de Liège, Unité d'Ecohydrodynamique, Institut de Chimie B6c, SART TILMAN B4000 LIEGE.
2 : Management Unit of the North Sea Mathematical Models (MUMM), Gulledelle 100, B1200 BRUSSELS
4 : Istituto Thalassografico, CNR, TRIESTE, Italy
3 : Universita di Messina, Laboratory of Marine Ecology. MESSINA, Italy

TABLE OF CONTENTS

ABSTRACT

The main objective of our studies was to determine the response of the Global Ocean Ecosystem (GLOBEC) to the variability of biotic and abiotic factors.

The purpose of the present contribution was the conceptualization, the parameterization and the validation of a model, which integrates the physical and trophic processes governing the equilibrium and changes of biodiversity in the Ross Sea pelagic ecosystem.

The conceptualisation consists of a multidisciplinary field study of the biodiversity and productivity of the plankton ecosystem in a context of variation of the environmental and climatic conditions. The parametrisation consists of the development, inside an interdisciplinary network of a coupled physical / biological model able to simulate the multiparametric variability of the Ross Sea, with a particular attention to the variability connected with climate.

A choice of results from oceanographic cruises in the Ross Sea were integrated into the model, according to the specificity of each sub-model: 1) physico-chemical information: processes associated with the polynya aperture; origin of water masses and general pattern of nutrient distribution; water column structure and variability; 2) phytoplankton data: spatial and temporal characterization of the autotrophic communities, in term of biomass, production and dominant species; relationship between pigment stocks, nutrient depletions and nitrogen assimilation; 3) zooplankton information: spatial and temporal variability of the dominant species, grazing and excretion by the main taxa.

Thanks to a useful method of High Performance Liquid Chromatography (HPLC), the concentration of phytoplankton pigments and their grazing degraded products were determined in the water column, in the ice, in suspended sediments, in zooplankton and krill digestive systems and in faecal pellets. Pigment values were used as algal tracers of fluxes across the food chain in the upper layers of the water column and as data to parametrize, calibrate and validate ecological models. Cruises carried in the Ross Sea showed that the major part of the Southern Ross Sea is dominated by *Phaeocystis* pigments (mainly 19'-hexanoyloxyfucoxanthin). The fucoxanthin, used as tracer for

diatoms, is the dominant pigment in the coastal areas, where it is present in high concentration in the ice and in the water column, and in the water column of the central Ross Sea, at the northern limit of the polynya. In the diatom-dominated areas, high levels of phaeophorbides indicate high grazing pressure which reduces diatom blooms magnitude. Moreover, the results have completed the picture of distribution of ice-algae pigments in relation with ice retreat and emphasized the temporal succession of various algae groups like Chryptophytes and Prasinophytes and the control of primary production exportation by grazing.

Data obtained during the Ross Sea cruises have confirmed that the most important factors regulating the Antarctic pelagic food chain are physical processes operating within the circumpolar marginal ice zone during the ice melting period. As a typical characteristic of the Ross Sea, the ice free surface of the polynya is propagating from the South to the North, with an increase of the water surface exposed to the sunlight. The diversity of biota assemblages in the Ross Sea seems to be controlled mainly by local constraints rather than by the presence of specific sub-ecosystems. For example, the ice-edge melting is not simultaneous for the whole region, the central and southern parts being opened sooner than the lateral parts; the areas of depth shallower than 500 m seem to be inaccessible to krill which is strongly influences the fate of the primary production and the ice-algae content is higher in the western part of the Ross Sea than in other areas (Hecq et al., 1999).

A mechanistic 1 D ecohydrodynamical model (*ECOHYDRO-MVG*) of the Ross Sea Seasonal Ice Zone plankton ecosystem has been developed to test the influence of the physical constraints on the temporal and variability of the system. The physical model parameterizes explicitly the water column vertical structure and mixing and takes into account the importance of the ice dynamics, the atmospheric constraints and the presence of ice algae. The sea-ice model computes the temperature, the thickness and the surface of the ice deduced from heat exchanged vertically through the ice-air and ice-ocean interfaces and horizontally through the leads.

The biological model computes the seasonal variation of the vertical distribution of principal plankton, bacteria, nutrient and organic matter variables dominating the herbivorous and microbial food webs in the ice and in the water column.

The model has been applied to a set of standard conditions corresponding to the general state characteristics of the Ross Sea. The model have been tested in various local Ross Sea situations and discussed in relation with data acquired during the cruises. A 3D modeling approach of the Ross Sea plankton ecosystem have been developed.

1. INTRODUCTION

1.1 State of the art

The Southern Ocean is more diversified than previously thought and contained a strong variability in the nature and composition of its plankton biota assemblages. Some aspects of the variability of the Southern Ocean plankton ecosystem were identified during the first phases of Belgian Antarctic Programme by the participants of the proposal. In the same time, modeling approaches were developed. The variability of the Southern Ocean results in regional individualization and seasonal succession of sub-ecosystems characterized by specific biota assemblages, identified in diverse areas of the Southern Ocean (Smetacek et al., 1990; Marchant and Murphy, 1994), in the Ross Sea (Hecq et al., 1999; Goffart et al., 2000) and in sub-antarctic areas (Saggiomo et al., 1994).

The dynamics of the Southern Ocean ecosystem is to a large extent determined by its specific environmental features. The variability of the ecosystem results in the spatial individualization of local sub-ecosystems, together with the associated seasonal changes of those sub-ecosystems. Some aspects of the principal processes governing the variability were identified during the first phases of Belgian Antarctic Programme. Further insights into these processes were studied by the participants to the present network as part of a convention with the Italian National Programme of Antarctic Research within the framework of the ROSSMIZE Programme (Italo-American Research Programme on the Ross Sea ice-edge ecosystem). A better definition of biota assemblage distribution in function of spatial and temporal diversity of environmental sub-ecosystems is an expected result.

In actual conditions, numerous physical and trophic processes control simultaneously the variability of the Southern Ocean global ecosystem. The circulation system, coupled to the seasonal changes in the light regime and sea-ice cover, imposes to the Southern Ocean a North-South pattern in its bioproductivity, species composition, distribution of biological resources, pattern of food webs and trophic relationships between marine organisms. The principal physical processes operating within the circumpolar marginal ice zone during the

4

ice melting period were modeled. A better approach of the Ross Sea polynya formation and propagation from the South to the North is expected.

The Antarctic marine food web is unique among oceanic ecosystems in that it is characterized by its large dependence on a single key species, the Antarctic krill *Euphausia superba*, and by the fact that many species are dependent on sea-ice during at least a part of their life history. For these reasons, the Southern Ocean marine ecosystem may be especially vulnerable to perturbations caused by changes in environmental conditions (e.g. climate), pollution stress or exploitation of natural resources. The specific influence of such changes was approached and the potential perturbations and the possible resilience were determined. A better understanding of the key processes governing the ecosystem is expected as a reference for comparison with perturbed systems showing altered processes. Consequently, documentation of natural population fluctuations and understanding of the mechanisms underlying this variability is critical if prediction of the effects of natural, climate or anthropogenic changes on the Antarctic marine ecosystem is expected.

A modeling approach is necessary to investigate the dynamics of Southern Ocean organisms and the interactions of key populations with each other (predation, competition) and with their physical environment, especially with sea-ice dynamics and water circulation. Both of these are sensitive to climate changes. The model is a processes model which provides conceptual hypothesis and the possibility to explore different data sets. By using simple data assimilation methods, it is used to identify what crucial observations are missing and it suggests laboratory and environmental experiments which need to be performed.

Whether the Southern Ocean can be considered a single ecosystem, or a series of interconnected ecosystems, is a moot point. One can consider the sea-ice, the pelagic waters and the sediments as separate ecosystems, and these can be further subdivided on geographic and depth criteria. However, it must be keep in mind that they are all interconnected to a greater or lesser degree. The most difficult question to resolve is the diversity of spatial and temporal scales. The small scale variability of the lower trophic levels of the ecosystem has an influence at larger temporal and spatial scales on the krill dynamics and on the higher trophic levels (birds, fishes and mammals). On the other hand, the higher

trophic levels constraint periodically and locally the lower trophic levels. Finally the long-term and large scale variability of the global ecosystem is controlled by the balanced feed-back exerted by various levels. The model is used to investigate the dynamics of Southern Ocean organisms and the interactions of key populations with each other (predation, competition) and with their physical environment, especially with sea-ice dynamics and water circulation.

1.2 Goals of the research

The research consists of a multidisciplinary study of the biodiversity and productivity of the global ecosystem of the Southern Ocean, in a context of variation of the environmental and climatic conditions. The main objective is to develop inside an interdisciplinary network a coupled physical / biological model able to simulate the multiparametric variability of the Ross Sea, with a particular attention to the variability connected with climate change. The analysis of sub-ecosystems at specific time and space scales and the interconnection of these systems are developed by means of a proper modeling.

The development of the coupled model, based on our previous experience in the Ross and Weddell Seas, needs experimental implementation or parametrization of some specific processes for which extensive developments were enterprise in our groups:
- Experimental study of phytoplankton responses (determined by its pigments content) to the Southern Ocean physical constraints (such as light, nutrient availability, vertical structure of the water column, structural and thermal properties of the ice) and to the trophic control (grazing by zooplankton, biodegradation, bio-sedimentation).
- Parameterization of ice melting and formation and resolution of three-dimensional, time-dependent, non linear Navier-Stokes equations describing the conservation of mass, momentum, temperature and salinity, forcing the Southern Ocean global ecosystem.

The data for forcing functions, initial values of variables and for data assimilation and validation of the model are issued from oceanographic cruises performed by our team during the different phases of the Belgian Scientific Research Programme on the Antarctic and from all literature's data.

The main goals of the project are:

1. To understand how the physical and biological processes coupled at various scales control the functioning and the evolution of the global ecosystem of the Southern Ocean. More specifically, the goal is to quantitatively determine how this ecosystem reacts to the whole to the physical constraints and to the trophic conditions. Expected results are both qualitative (which species or group of species are favored by specific physical constraints ?) and quantitative (what are the biomass and productivity of the dominant species ?).

2. To determine, in a perspective of help to the decision-making process as regards environmental protection, how this system would respond to environmental and climatic changes, natural or anthropogenic.

The strategy is the development of coupled models, the experimental determination of specific key processes and cruises data acquisition and assimilation. The strong coupling between the Antarctic marine food web and the physical environment, especially the dependence on sea-ice, makes the Southern Ocean an ideal environment to test many of the GLOBEC core hypotheses on the role of physical variability on marine animal population dynamics. Many of the scientific objectives of this program are relevant also to those of SCAR and the International Whaling Commission. The complex nature of the Antarctic system argues for a holistic and integrated approach for studying its response to changes. The most difficult task is not really to couple biological and hydrodynamical equations if the processes are at the same scale. The major problem begins when one decides to relate processes from various scales. The strategy we propose is the development of a set of coupled sub-models resolving both physical and biological variables at a determined scale. Each specific scale sub-model will run separately and will be interconnected by step to the others. In a first step the model will run on standard mean conditions to determine an « actual state » or standard run of the whole Southern Ocean global ecosystem, which will serve as a reference for analyses of sensitivity, data assimilation and simulation of climate changes impact.

2. MATERIAL AND METHODS

With the aim of clarifying this chapter, positions and sampling periods of the different oceanographic cruises whom results are used for discussion are presented in sections 3.1.1, 3.1.2 and 3.2.2.

2.1 Hydrographic data

Vertical sampling was carried out on hydrographic stations. Sampling was performed using twelve 10-liter Niskin bottles attached to a CTD rosette or with a SBE 32 Carousel sampler, equipped with twenty-four 12-liter Niskin bottles. In the upper 200 m, standard sampling depths were the surface, 10, 25, 50, 100 and 200 m. Moreover, 2-5 variable depths were added to the hydrological casts according to the stratification and the attenuation of incident PAR.

Continuous depth profiles of temperature and salinity were collected at each station. Density values were computed from these data and are reported in Artegiani et al. (1992) and Russo et al. (1997). Because water-column stability is an important controlling factor for the biomass and structure of phytoplankton communities, E_{max} (m^{-1} x 1000), the stability index of the depth corresponding to the maximum density gradient, was calculated according Mitchell and Holm-Hansen (1991) and Catalano et al. (1997).

2.2 Nutrients

During the 5th Italiantartide expedition (cfr. section 3.1.2), nitrate, nitrite, orthophosphate and silicic acid concentrations were determined on board by means of a Technicon II Autoanalyser (Hansen and Grasshoff, 1983), while during the Rossmize cruise (cfr. section 3.1.2), an Alpkem autoanalyser was adopted according to ALPKEM (1992a-c).

Ammonium was always determined with a Technicon autoanalyzer, according to the indophenol blue method adapted for segmented flow analyzers by Tréguer and Le Corre (1975). Hypochlorite solution was used as chlorine donor; freshly prepared Millipore Milli-Q water served as the blank solution.

Nutrient depletions through the water column characterize the nitrate and silicic acid uptake regimes. Calculated nutrient depletions represent seasonally integrated nutrient removal in the surface layer down to the depth, where the *in situ* nitrate and silicic acid concentrations equal the winter values NiWi and SiWi, respectively. Nitrate depletion (NiDe) values are believed to be associated with « new » production, *sensu* Dugdale and Goering (1967). The silicic acid depletion (SiDe), on the other hand, depicts diatom production. As pointed out by the above cited authors there are some implicit assumptions in using this methodology. Nutrient depletion values can be biased by either physical reintroduction or biological processes such as nitrification (Bianchi et al., 1997), and should therefore be considered as minimal values. Moreover, it must be stressed that NiDe does not reflect total dissolved nitrogen uptake since concomitant uptake of other nitrogenous nutrients such as dinitrogen, ammonium and dissolved organic nitrogen is not negligible (Bronk et al., 1994). Most important is the assumption that vertical and lateral mixing in both the temperature minimum and surface layer are small. This condition is fulfilled; the evidence therefore is that the observed temperature in the remnant winter water is approximately equal to the temperature in the winter surface water (near to the freezing point: all values are $\leq$-1.70 C). Additionally, fluxes due to vertical gradients in the surface layer should be small. Finally, possible nutrient changes due to the addition of melt water from the sea ice should be accounted for by normalization to a constant salinity; a detailed procedure for calculating the depletions is given by Hoppema et al. (2000). However, no corrections for possible dilution by melting ice were introduced in the current investigation, according to Goeyens et al. (1995).

2.3 Phytopigments

Samples of one liter for pigment determination were filtered at low vacuum pressure through Whatman GF/F filters. They were immediately frozen at -25 °C until analysis on board, some hours later. Frozen filters were extracted in 100 % methanol using grinding and refiltration to remove cellular debris. Phytoplankton pigments and their degradation products were separated and quantified by high performance liquid chromatography (HPLC), following the procedures of Mantoura and Llewellyn (1983) and Williams and Claustre (1991), for the 5th Italiantartide and Rossmize cruises, respectively. With this method, zeaxanthin

9

and lutein coelute. Divinyl chl *a* is not resolved from chlorophyll *a* and the sum of both chlorophylls is referred as chl *a*. Diagnostic pigments used in this study and their taxonomic significance are listed in Table 1.

In the Ross Sea, fucoxanthin and 19'-hexanoyloxyfucoxanthin (19'-HF) are used as a chemotaxonomic tool to identify, respectively, diatoms (Jeffrey, 1980; Claustre et al., 1994; Barlow et al., 1998) and prymnesiophytes (Gieskes and Kraay, 1986; DiTullio and Smith, 1995; Jeffrey et al., 1997). Prymnesiophytes are very common in the Ross Sea and consist mainly of *Phaeocystis antarctica* (Innamorati et al., 1990; Marino and Cabrini, 1997).

Table 1: Diagnostic pigments used in this study and their taxonomic significance.

Pigment	Taxonomic significance	References
Chlorophyll *a*	All photosynthetic microalgae (except prochlorophytes)	a
Divinyl chl *a*	Prochlorophytes	b
19'- HF	Haptophyceae (Prymnesiophyceae)	a, j, k
19'- BF	Haptophyceae (Prymnesiophyceae), Chrysophyceae, Pelagophyceae	a, c
Fucoxanthin	Diatoms, Bolidophyceae	a, d, e, f, g, h
Zeaxanthin	Cyanobacteria, Prochlorophytes	a, i
Lutein	Green algae	a

a: Jeffrey et al. (1997) g: Claustre et al. (1994)
b: Goericke and Repeta (1992) h: Barlow et al., 1998
c: Latasa and Bidigare (1998) i: Vidussi et al. (2000)

d: Jeffrey (1980)   j: Gieskes and Kraay, 1986

e: Goffart et al. (2000)   k: DiTullio and Smith.

f: Guillou et al. (1999b)

Among the phaeopigments, phaeophorbides *a* are here considered. They are produced from the breakdown of chl *a* by the enzymatic activity of the zooplankton digestive system, and are utilized here as a quasi-conservative tag for the detection of ingestion of phytoplankton by feeding herbivores (Jeffrey, 1974; Welschmeyer and Lorenzen, 1985; Vernet and Lorenzen, 1987; Jeffrey et al., 1997).

2.4 NITROGEN UPTAKE BY TOTAL PHYTOPLANKTON

Samples for productivity incubations are obtained from depths corresponding to 100, 50, 20, 10, 5, 1 and exceptionnally 0.1 % of PAR with a CTD rosette fitted with 24 Niskin bottles of 12 liters. Nitrogen uptake rates are determined with tracer experiments according to Dugdale and Goering (1967), using the stable isotope ^{15}N and following the JGOFS protocols and the analytical procedures described by Owens (1988) and Owens and Rees (1989). From each depth two subsamples are transferred into 1 L polycarbonate bottles covered with perforated nickel screens to mimic the *in situ* irradiance conditions. The samples are spiked respectively with $Na^{15}NO_3$ (99.9 % ^{15}N) and $^{15}NH_4Cl$ (70.4 % ^{15}N), placed in on-deck incubators and maintained at sea-surface temperature with running seawater. After 24 h of incubation, the samples are filtered on precombusted Whatman GF/F filters (25 mm diameter), rinse with filtered seawater and store frozen until isotope analysis with a continuous flow nitrogen analyser-mass spectrometer (ANCA 20-20 MS, Europa Scientific). Original data on nitrogen uptake are reported in Lipizer and Catalano (1999). Absolute nitrogen uptake (QN, μmol m^{-3} d^{-1}) was calculated according to JGOFS Protocols (1994). Specific uptake rates (ν, in d^{-1}) are defined as the nutrient removed per unit of particulate nitrogen (PN) and per unit of time; absolute uptake rates or transport rates (ρ, in nM d^{-1}) are the products of specific uptake rates and PN concentrations (Wilkerson and Dugdale, 1992). The relative importance of new versus total production is expressed as the *f* ratio (Eppley and Peterson, 1979).

3. RESULTS

3.1. PHYSICO-CHEMICAL INFORMATION ON THE ROSS SEA

3.1.1. Data and Climatologies available for the ROSS SEA

Surface salinity and temperature field for the Ross Sea and surrounding area have been deduced from World Ocean Atlas 1994 (WOA94) (S. Levitus, T. Boyer, R. Burgett, and M. Conkright of the National Oceanographic Data Center. NODC) which presents annual, seasonal and monthly climatologies for the entire world ocean.

In November, very low temperatures are proposed by the WOA94 at locations that are covered by sea ice Nevertheless it should be pointed out that we have no information on the number of used field profiles for regions covered by sea ice.
In the same time as the sea ice melting starts, a more contrasted thermal front appears on the showed climatology inside the Ross Sea. The presence of these frontal structures is confirmed by the salinity and sigma-t fields (figures 1).
The Antarctic convergence is well represented by the SST field.
Less saline water appears during the melting of the sea ice(B,C,D) and a large scale 'plume' is visible in January (C)
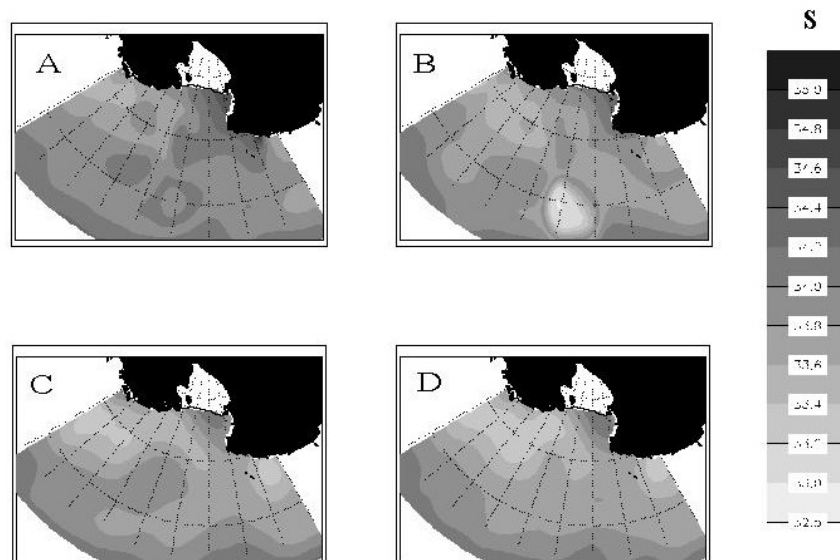
Figure 1: Typical monthly mean sea surface salinity climatology from November (A) to February(D) WOA94. This figure enhances a minimum of salinity as the sea ice is melting (B to D). A tongue of less saline water is observed at large scale in January.

Density is more relevant than temperature or salinity to trace water masses. To be able to extract more information from the hydrological data we calculate surface density fields from the above presented temperature and salinity climatology using Fofonoff and Millard (1983). Density fronts are present in the Ross Sea during the period from November until February, although the validity of the density field is questioned when a sea ice coverage is present. New information can be extracted from the density field such as the gyre visible just out of the Ross Sea in February. That information was not visible in the SST and salinity fields.

The World Ocean Database CD-ROM series are available at the National Oceanographic Data Center (NOAA) and provide an access to quality controlled profile used to compute the presented climatologies. The NODC database include about $5 \ 10^6$ metadata of which 23047 stations concern the Ross Sea sector. Data extracted from that database were used during this research program to focus on some region of interest and to provide initialisation and boundary condition data to the model. Figure Y shows the temporal distribution of the available data. Most of the available data for the Ross Sea sector have been taken between 1955 and 1980 with a maximum of activity centred on 1960. That distribution contrast with one obtained for the Weddell Sea sector that is centred on 1980.
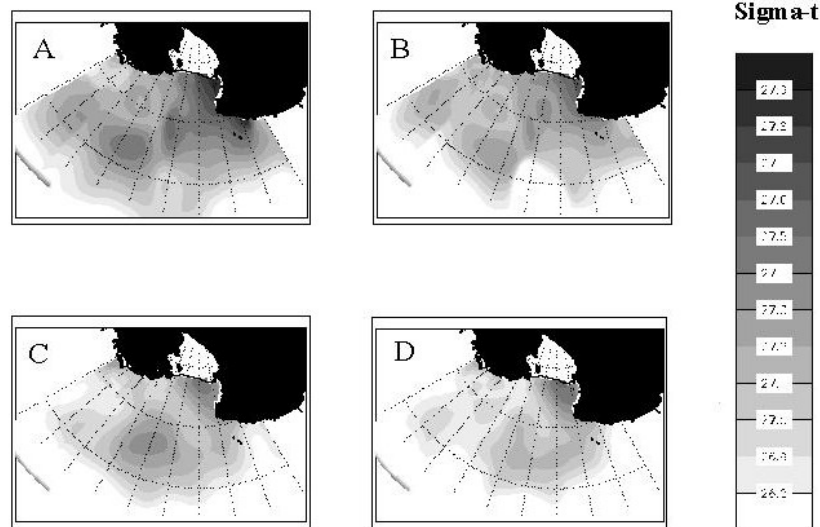
Figure 2: Typical monthly mean climatology of the density (recalculated from temperature and salinity monthly mean using Fofonoff and Millard (1983).

Data sets of current measurement are not numerous in that region of the world. We present data from drifters (Lagrangian data) that have been used to deduce boundary conditions. These data are made available by Donald V. Hansen, Pierre-Marie Poulain, and the Atlantic Oceanographic and Meteorological Laboratory (Miami) for the drifter data. No data track enters the Ross sea and goes below 65 ° of latitude South. Some drifter also have a temperature sensor. No temperature plot from the drifter data is shown here. The data are provided by ocean basin and by year and therefore need to be sorted out for a specific region, the Ross Sea. Example of such data is illustrated below.

Figure 3 shows the long term tracks of three drifters. Such data permits to extrapolate current speed and direction for the hydrodynamic model boundary conditions. As an example, drogue n° 22107 has been tracked during one year. 120 ° of longitude at a mean latitude of 58° S have been covered. This corresponds to a surface current of the order of magnitude of 0.15 m/s.
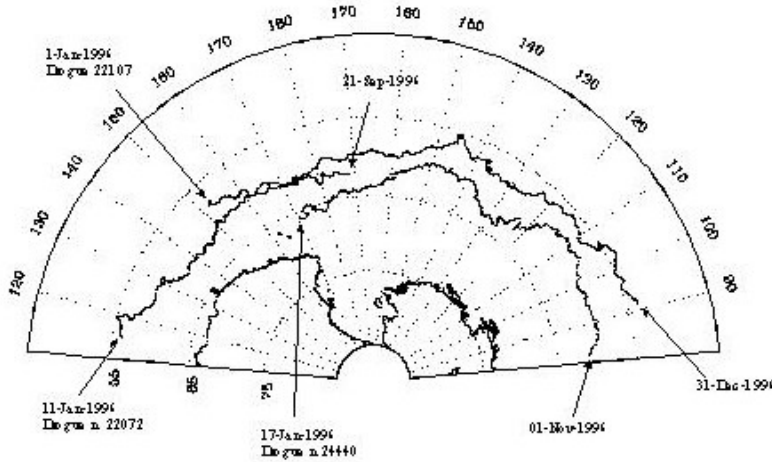
Figure 3: Drifter tracks in the surrounding area of the Ross Sea .Data from Atlantic Oceanographic and Meteorological Laboratory for the drifter data, NOAA.

Pillsbury and Jacobs (1985), Picco et al.,(1999), Manzella et al, (1999) and Picco et al,. (2000) present analyses of current meter data obtained at various location inside western and central the Ross Sea.

Pillsbury and Jacobs (1985) showed annual and quarterly mean current speed ranging from 4 to 11 cm/sec for mooring site close to the Ross ice shelf while maximum value of almost 42 cm/sec has been observed. The general direction of the flow is to the west with a mooring showing water intruding under the Ross Ice Shelf.

That range of value is confirmed by Picco et al,.(1999) for mooring along the Ross sea Ice shelf . Values in excess of 40 cm/sec are also obtained for one mooring.

Open sea measurement ranges to a maximum of about 20 cm/sec for mean value while hourly means values can reach almost 1 m/s of Cape Adare.

High meso-scale variability is observed from the analysis of current-meter time series. (Pillsbury and Jacobs, 1985; Picco et al,. 1999).

Information on the general circulation of the western and central Ross Sea is also given by the analysis of Picco et al,. (1999 & 2000). They showed the existence of a clockwise gyre for the central and western Ross Sea shelf. Furthermore the barotropic character of the flow below 240m is enhanced reflecting the fact that the seasonal cycle of salinity and temperature does not "affect" the flow.

Hellerman-Rosenstein wind stress climatology is used to force the model (Fig 4). (Hellerman and Rosenstein (1983)). Other data set are available for some Antarctic region such as the Weddell Sea (IOC, 1997)

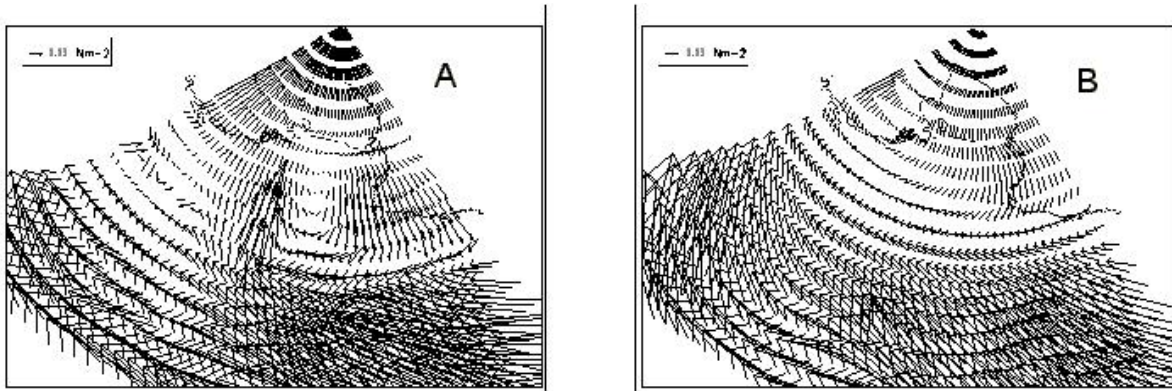Remote sensed data of wind field are available from CERSAT-IFREMER(France).

Figure 4: wind stress Hellerman and Rosenstein (1983) climatology for the Ross Sea and surrounding area. Typical February (A) and typical September (B). Note the gyre on the Ross Sea in February

The bathymetry used by the model is based on the ETOPO5 bathymetry. ETOPO5 have a 1/12° by 1/12° coverage of the entire world.

The Ross Sea is characterised by depth not exceeding 500 m. Just outside the Ross Sea, depth can reach more than 3000 m. The depth of the Ross Sea is an important parameter for controlling some aspect of its biology.

3.1.2 Hydrological and nutrients data from oceanographic cruises

Origin of water masses and general pattern of nutrient distribution in the Ross Sea

The Ross Sea can be considered as the largest Continental Shelf and Coastal Zone (CSCZ) of Antarctica where seawater and continental ice interact directly by ice melting, and thereby modify the characteristics of the water masses involved. In addition, the katabatic winds in the southern and western parts of the Ross Sea make these zones particularly active in producing sea ice and brine.

The following characterization of water masses in the Ross Sea is published in Catalano, Benedetti, Predonzani, Goffart, Ruffini, Rivaro and Falconi et al. (1999). Salinity and temperature ranges corresponding to each water mass are reported in Russo (1999).

On its continental shelf, the Ross Sea is influenced by only one water mass of external origin: the Circumpolar Deep Water (CDW), characterized by relatively high temperature and salinity, high silicic acid and low oxygen concentration. All other water types are derived from modifications of the CDW by mixing, cooling and by inputs from precipitation, melting and brine formation (Jacobs et al. ,1985; Russo, 1999).

The processes responsible for polynya maintenance are also responsible for the modification which leads to the formation of the High Salinity Shelf Water (HSSW), located in the southwestern Ross Sea and at Terra Nova Bay (Jacobs et al., 1985). The HSSW is the most salted and dense water found in the Ross Sea.

Supercooled Deep Ice Shelf Water (DISW) originates from glacial ice melting, operated by the HSSW at the base of the Ross Ice Shelf. Its domain is mainly located in the southern zone of the Ross Sea, near the Ross Ice Shelf edge. It can be detected by a temperature minimum below freezing point, the lowest temperature reached in the Ross Sea. Its density is lower than that of HSSW but higher than that of any other water type in the Ross Sea.

The Low Salinity Shelf Water (LSSW), which is slightly higher in temperature but considerably lower in salinity, is found between the surface Antarctic waters AASW and the HSSW, mainly on the eastern part of the Ross Sea shelf (Jacobs et al., 1985; Russo, 1999).

Another type of bottom water, the Low Salinity Bottom Water (LSBW), is characterized by intermediate properties between those of the CDW portion which intrudes on the continental shelf and of the LSSW. It has been found in some stations carried out during Italian expeditions along the continental slope.

An important modification of the CDW, resulting from the mixing which occurs on the slope front, is its transformation in the Warm Core (WMCO). The WMCO is an intermediate water mass with a temperature above freezing point, and is considered a major factor responsible for the opening of the Ross Sea (Russo, 1999).

The Antarctic Surface Water (AASW) is the most variable water type in the Ross Sea. It is formed during winter and originates from upwelled CDW, which is modified by interactions with atmosphere, ice and surface winter water. Alternatively, AASW can also be produced in summer, on the continental shelf, from the mixing between shelf water and sea-ice meltwater.

During the austral summer, the highest average temperature (0.1°C) and the shallowest mixed layer (12 and 16 dbar) are observed along Victoria Land Coast and Terra Nova Bay, respectively. On the contrary, in the northern Ross Sea, the upper mixed layer on the continental break is characterized by the highest salinity (34.0).

From the nutrient point of view, the Ross Sea is considered as a typical Continental Shelf Coastal Zone (CSCZ) where, during summer, occasional high nutrient consumption occurs, particularly in the Marginal Ice Zone (MIZ) and in some protected coastal areas as Terra Nova Bay. As a part of the ITALIANTARTIDE Polar Research Project, four oceanographic cruises were carried out in late austral spring and in summer in different years (Fig. 5), with the aim to improve the knowledge of spatial and temporal nutrient patterns in the Ross Sea.
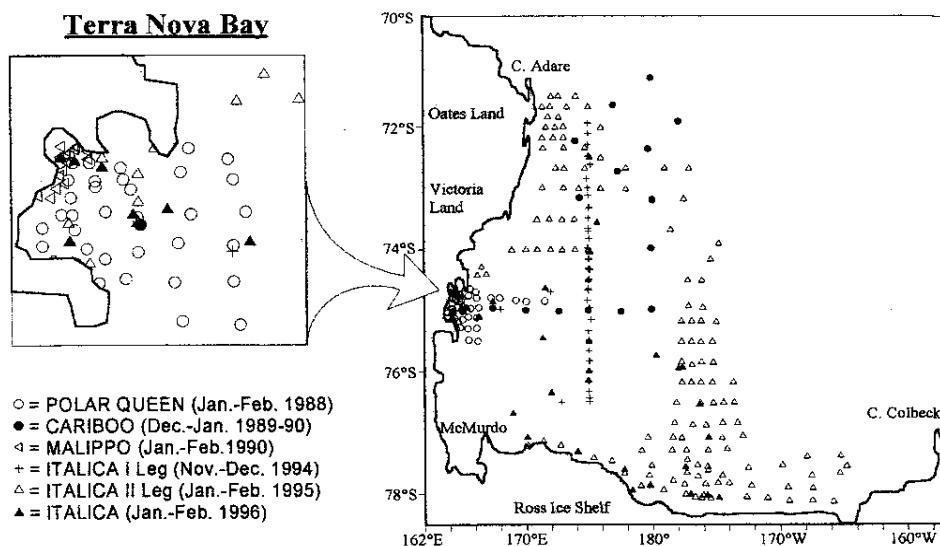
Figure 5: Position of stations where water sampling for nutrient analysis was carried out during the ITALIANTARTIDE expeditions (1988-1996). In the upper 200 m, standard sampling depths were: surface, 10, 20, 50, 100 and 200 m. Other sampling depths were added according to the water column stratification monitored from the CTD profile, the fluorescence maximum and the depth corresponding to 50, 20, 10, 5 and 1% attenuation of incident PAR. Below 200 m, the sampling depth were chosen on the basis of the CTD profile only.

Plots of $Si(OH)_4$, NO_3+NO_2 and PO_4 vs. salinity for the stations where a surface salinity < 34.1 was observed (Fig. 6) and relationships between nutrients for all the stations where CDW was detected (Fig. 7) and are presented as examples.

Synthesis of available information shows that, in the Ross Sea:

1. Low or very low nutrient concentrations are found in the low-salinity melt-water areas during late spring and summer. The data show, however, that dilution by melting ice alone can not account for nutrient concentrations as low as those observed, which must therefore be attributed to enhanced biological assimilation. Thus, the low nutrient content as a consequence of biological uptake characterizes the Antarctic Surface Water (AASW) during spring and summer (Fig. 6), when the increased water column stability and irradiance regime favor phytoplankton blooms, which is rather common in the Marginal Ice Zone (MIZ) and in coastal zones.

19

However the spatial and temporal extent of nutrient depletion in the AASW is highly variable and no mean value can be given.

Extreme situations are observed in Terra Nova Bay and in the northern Ross Sea. The lowest average salinity of the upper mixed layer (33.6), the highest dissolved oxygen concentration (385.4 μM) and the highest nutrient decreases (33.0, 1.0 and 11.1 μM for $Si(OH)_4$, PO_4 and NO_3+NO_2, respectively) are observed in Terra Nova Bay, with nutrients reaching sometimes concentration levels which might be limiting for phytoplankton growth. On the contrary, on the continental break in the northern Ross Sea, the lowest oxygen content (348.0 μM) and nutrient utilization (4.3 μM for $Si(OH)_4$ and no significant depletion for the other nutrients) are detected. This could be to the vicinity of a slope front, where enhanced vertical advection brings deep nutrients to the surface layer.
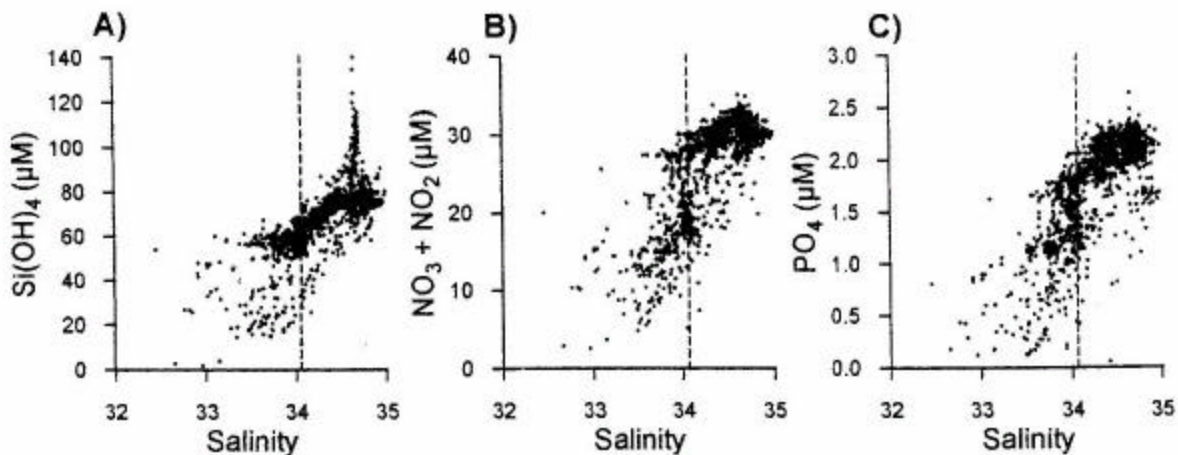

Figure 6: Plots of $Si(OH)_4$ (A), NO_3+NO_2 (B) and PO_4 (C) vs. salinity for the stations where a surface salinity < 34.1 was observed (from Catalano et al., 1999).

2. The dissolved N and P concentrations are linearly related (Fig. 7). This simple relationship is not observed with Si, and both Si/N and Si/P ratios vary non-linearly in the direction of a substantial excess of Si in the nutrient-rich deep waters.

3. Some features linked with hydrological circulation, such as the presence of Circumpolar Deep Water (CDW), and its intrusions on the continental shelf are well reflected by nutrient, oxygen and temperature distributions. These features were especially evident during the Italian cruises in the NW part of Ross Sea, near the continental shelf break.
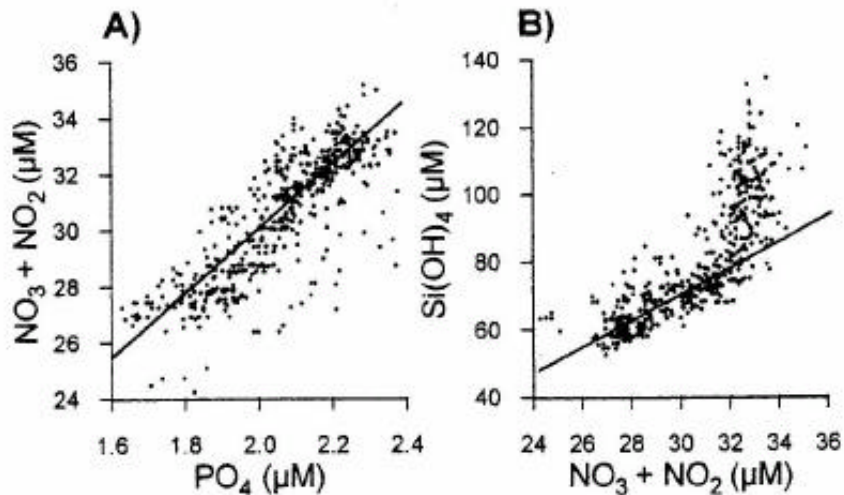
Figure 7: Plots of NO_3+NO_2 vs PO_4 (A) and $Si(OH)_4$ vs NO_3+NO_2 (B) for all the stations where CDW was detected (from Catalano et al., 1999).

4. A particular case of thermal stratification, characterized by surface waters of high salinity, was observed in Terra Nova Bay in 1988. In that year, strong summer heating induced the stratification of surface water as salted as HSSW, in which substantial nutrient assimilation by phytoplankton was clearly detectable.

5. No significant patterns of nutrient distribution were found related to the spreading of HSSW or Low Salinity Shelf Water (LSSW) and Low Salinity Bottom Water (LSBW) on the Ross Continental Shelf. Therefore, these water masses are defined on the basis of T/S data.

6. Iron limitation of phytoplankton growth has been proposed as a factor controlling nutrient depletion. While this problem is beyond the aim of this work, further studies are needed in order to evaluate its relevance for nutrient concentrations in Ross Sea surface waters.

Water column structure and variability in the Ross Sea

Hydrological and nutrient data obtained in the Ross Sea during oceanographic cruises aim at a better understanding of the water masses structure during the different stages of the phytoplankton growth season. Hydrological and nutrient data

presented here as illustration of the water column structure and variability in the Ross Sea are a part of the Goffart, Catalano and Hecq (2000) publication.

Field studies presented here took place as part of the Italian National Antarctic Programme and were conducted in the Ross Sea during cruises in two separate years (Fig. 8, Table 2). The first set of data was collected during the austral summer (5th Italiantartide expedition), along an east to west transect at 75°S, from the open water to the Terra Nova Bay polynya (transect 1). On the « Rossmize » cruise, a south-north section across the Ross Sea polynya was sampled in November at 175°E, following the northward ice retreat (transect 2). The Rossmize cruise represents one of the earliest entries into the Ross Sea polynya during the austral spring by an oceanographic vessel.
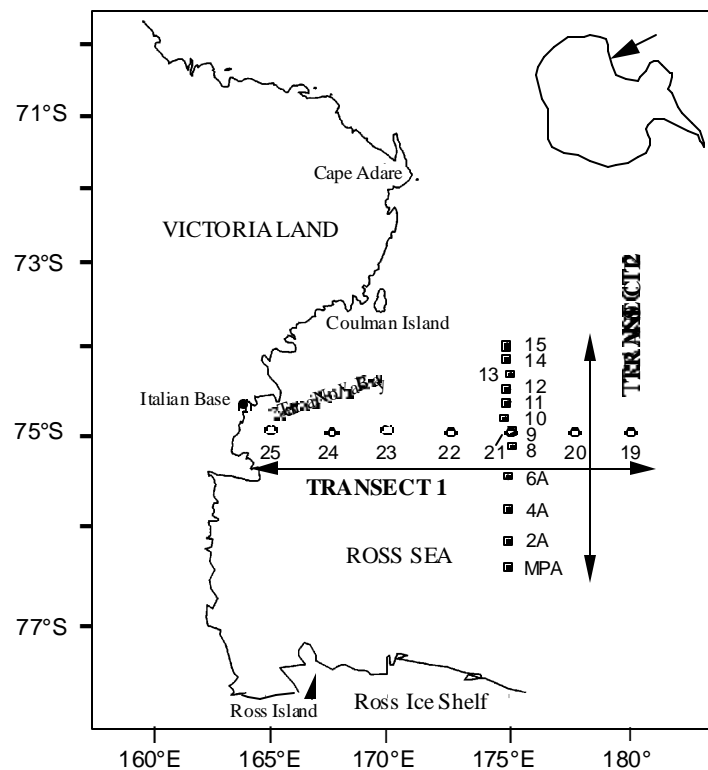

Figure 8: Map of stations location during this study.

Western Ross Sea: transect 1

On the first cruise, transect 1 was situated in a region of open water with drifting ice floes.

Table 2: Position and calendar of the transects used in this study.

Transects	Stations	Latitude	Longitude	Period
Transect 1	19, 20, 21, 22, 23, 24, 25	75°S	165°02' E - 179°56'E	01 - 06 Jan. 90
Transect 2	MPA, 2A, 4A, 6A, 8, 9, 10, 11, 12, 13, 14, 15	76°27'S - 73°59'S	175°E	20 - 26 Nov. 94

The pack-ice edge was located between the coast of Victoria Land and the westernmost station (station 25). The major feature of the hydrographic field was a well-established lens of low-density low-salinity surface water from station 22 to station 25 (Fig. 19). Within this stable surface layer, almost certainly produced by ice melt, a very strong thermohaline gradient was observed, with temperature and salinity varying from values >1°C and <33.4 at the surface to values <1.6°C and >34.5 at 30 m (data from Artegiani et al., 1992). On the whole, a stable upper mixed layer prevailed for the westernmost stations (stations 22 to 25), with E_{max} varying from 21 to 107 m^{-1} x 1000. Lower values of E_{max} in eastern part of the section (7 to 22 m^{-1} x 1000) indicated a less stable water column.

The highly stratified region was an area of pronounced silicic acid and nitrate depletions (Fig. 6) with their concentrations reduced by up to 30% of the winter values (deduced from the values taken immediately below the pycnocline). The most intense nutrient removal occurred for silicic acid, which was reduced by about 65 μM within the surface mixed layer at station 25 (85 μM at 50 meters, 17 μM at 5 meters). At the same station, nitrate was reduced from ca. 30 μM below the pycnocline to < 10 μM at the surface.

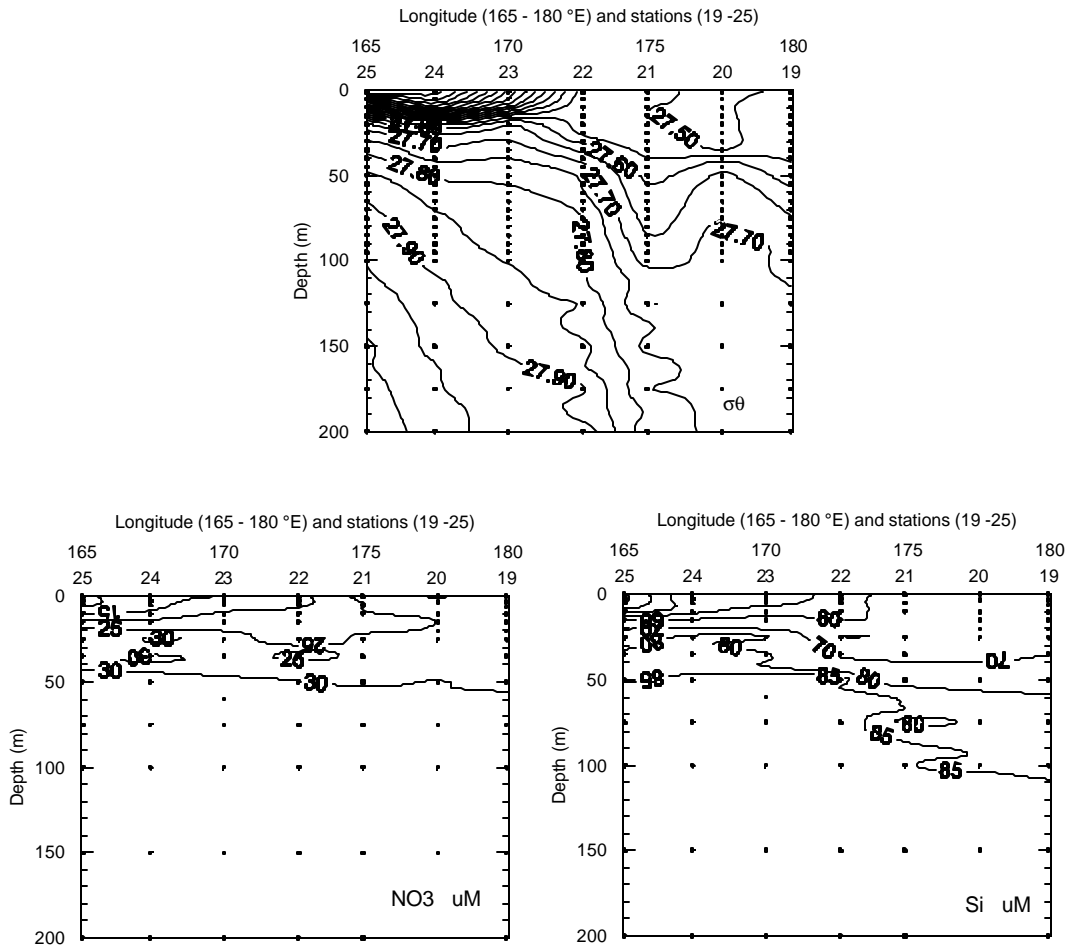Figure 9: Distribution of σ_θ, nitrate (μM) and silicic acid (μM) in the upper 200 m along transect 1. σ_θ data from Artegiani et al. (1992).

South central Ross Sea: transect 2

Along transect 2, the area of investigation can be separated into three main regions based on the different ice conditions encountered: the polynya area (stations MPA - 8), the marginal ice zone (stations 9-12) and the pack-ice zone (stations 13-15). This pattern was also reflected in the physical, chemical and biological variables focused on in this paper (Fig. 10).

In the polynya area, the water column was mostly unstratified (Fig. 7) and its structure reflected a strong vertical mixing, as emphasized by the very low value of the average E_{max} (6 m^{-1} x 1000). Within the marginal ice zone, stratification increased slightly (average E_{max} of 8.5 m^{-1} x 1000), as a result of a small decrease in surface salinity (less than 0.1 % reduction in salinity, data from Russo et al., 1997). Further

north, below the pack-ice, the water column reflected a typical homogeneous winter structure.

During early spring, nitrate+nitrite and silicic acid concentrations in the south central Ross Sea were very high (Fig. 10). Ambient concentrations in the 100 m upper layer ranged from 24.7 μM to 32.0 μM for nitrate+nitrite and from 71.0 to 84.9 μM for silicic acid. The overall nutrient spatial variation was small, with slightly lower concentrations at the ice edge and on the northern side of the transect, below the pack-ice.
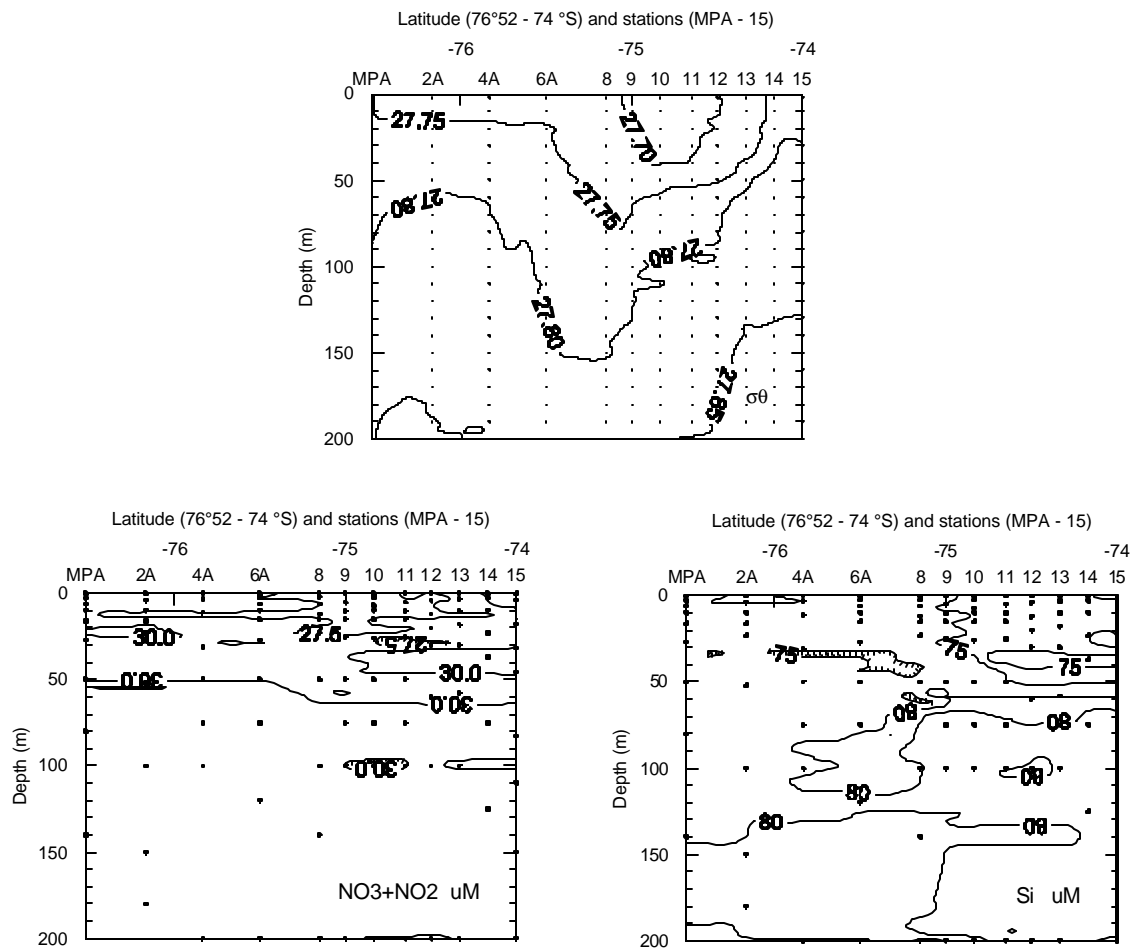
Figure 10: Distribution of σ_θ, nitrate+nitrite (μM) and silicic acid (μM) in the upper 200 m along transect 2. σ_θ data from Russo et al. (1997).

Relationship among vertical stability, estimated nutrient utilization and particulate organic matter

The Ross Sea area, where most of the work during the cruises of the ITALIANTARTIDE project was carried out, is classified as a coastal and continental shelf zone (CCSZ), in which the dynamics of nutrients and phytoplankton are largely controlled by a hydrological structure and irradiance regime (Smetacek and Passow, 1990; Nelson and Smith, 1991). Typical CCSZ phenomena are the marginal ice zones (MIZ), where some consistency in enhanced vertical stability has been observed following the input of less saline and less dense meltwater, together with nutrient depletion and biogenic matter production (e.g. El-Sayed and Taguchi, 1981; Smith and Nelson, 1985; Cota et al., 1992). Therefore, particularly in the MIZ, pycnocline strengthening shows its double effect: it decreases phytoplankton dispersal by vertical mixing and, in a situation characterized by lower nutrient concentrations, it increases phytoplankton buoyancy in the photic layer (Culver and Smith, 1989). During the phytoplankton bloom at the ice edge, the concentration of particulate organic matter increases (Smith and Nelson, 1985) and its biochemical composition changes (Fabiano et al., 1993).

The aim of this study was to investigate the relationships between pycnocline strengthening, which occurs in the MIZ, nutrient removal due to primary production, and the amount and biochemical composition of the particulate organic matter. Results presented here are published in Catalano, Povero, Fabiano, Benedetti and Goffart (1997). They summarize the data collected in the Ross Sea during the austral summers 1987 and 1989-1990.

In order to obtain an estimate of the nutrient anomalies, due to the phytoplankton assimilation, found in the upper mixed layer (UML), the following assumptions are made:

1. The vertical stability E according to Steinhorn (1985):

$$E = \rho^{-1} \, (\delta\rho/\delta z)$$

where ρ is the density of the seawater and z is the depth in m, is used to estimate both the strength of the pycnocline and the lower limit of the mixed layer.

2. The summer formation of the UML, which in the Ross Sea usually occurs within the upper 100 m, is considered to be due to solar heating or to the salinity decrease originating from the pack-ice melting or to both these factors.

3. The salinity and nutrient concentrations determined at the depth immediately below the UML, hereafter called Z(L), are taken as reference values for the winter prior to dilution by the advection of summer ice-meltwater or utilization by phytoplankton.

4. In the upper 100 m, all the depths are expressed in dbar in place of m.

The method suggested by Mitchell and Holm-Hansen (1991) has therefore been followed to establish the strength of the pycnocline between the UML and the already defined depth Z(L) immediately below it. First, E was calculated for every depth, Z, between 0 and 100 dbar from the following equation:

$$E(Z)= \rho^{-1} \text{ x} \left[\gamma T(Z+DZ/2) - \gamma T(Z-DZ/2) \right]/\Delta Z$$

where ? and ? are, respectively, the seawater density, expressed in kg dm^{-3}, and the density anomaly (UNESCO, 1985), T is the temperature in °C, Z is the depth in dbar and ? Z is a selected depth interval (4 dbar in our case).
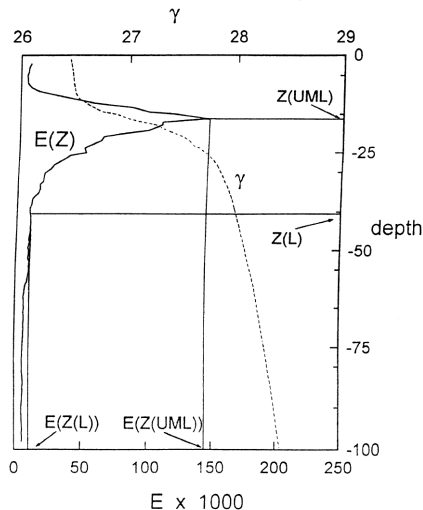

Figure 11: Vertical profile of the stability E (m^{-1} x 1000) and density anomaly ? (kg m^{-3}). From Catalano et al. (1997).

Then, at every station, the vertical profile of E(Z) can be reconstructed and, from this, one can find the maximum value of E and the corresponding depth Z(UML). Finally

Z(L), which is the first depth below Z(UML) where E(Z) becomes low and again nearly constant, can be deduced from the same profile (Fig. 11).

Summarizing, Z(UML) is the depth corresponding to the maximum density gradient, which also corresponds approximately to the middle of the pycnocline; here E reaches its maximum value, which is also taken as a stability index of the mixed layer (i.e. what we have called pycnocline strength). Z(L), on the other hand, is assumed to be the depth of the base of the pycnocline, corresponding to the top of the winter water and considered to be unaffected by the summer dilution or phytoplankton assimilation (Catalano and Benedetti, 1990; Catalano et al., 1991a, b; Fabiano et al., 1993).

From these considerations on vertical stability and from the consequent reduction in vertical mixing, the weighted average consumption of nutrients [nitrate (ΔNW), phosphate (ΔPW) and silicate (ΔSiW), in mmol m^{-3}] in the UML can be calculated. Figure 12 shows the dependence of estimated nutrient depletion on pycnocline strength. Despite the differences in sampling periods and sites, it is clear that for E(Z(UML)) < 25, the increments of utilized nitrate, phosphate and silicate are higher than those for E(Z(UML)) > 25. Furthermore, for E(Z(UML)) > 25, nutrient utilization ratios are more independent of E(Z(UML)). In summary, 49% of the stations are characterized by E(Z(UML)) > 25 and show prevalently a depletion of nutrients of >4, 0.4 and 10 mmol m^{-3} for nitrate, phosphate and silicate, respectively.

Two additional considerations can be drawn from our results. First, it can be seen that the N/P ratios are lower than the expected value of 16 (Redfield et al., 1963), while Si/N ratios are higher than the value of 1 proposed by Richards (1958) for the Atlantic intermediate layer and the value of 0.1 deduced, after Copin-Montegut and Copin-Montegut (1978), for the Indian subantarctic area. Similar features have been found already for the southernmost province of the Southern Ocean. In particular, Copin-Montegut and Copin-Montegut (1978), analyzing the particulate matter from the Antarctic Ocean, found N/P and Si/N ratios ranging, respectively, from 8.9 to 17.1 and from 0.1 to 2.33. Reconsidering now the ratios obtained from our results, it is possible to see that N/P values for the three different cruises in the Ross Sea are fairly constant and in good agreement with the values proposed for Antarctic phytoplankton, while the Si/N ratios vary from 1.7 to 3.4. Furthermore, it can be observed that the higher Si/N ratios are found mostly at stations characterized by a

more stratified water column with higher utilization of nitrogen and silicon and high biomass typical of fresh particulate organic matter of autotrophic origin.
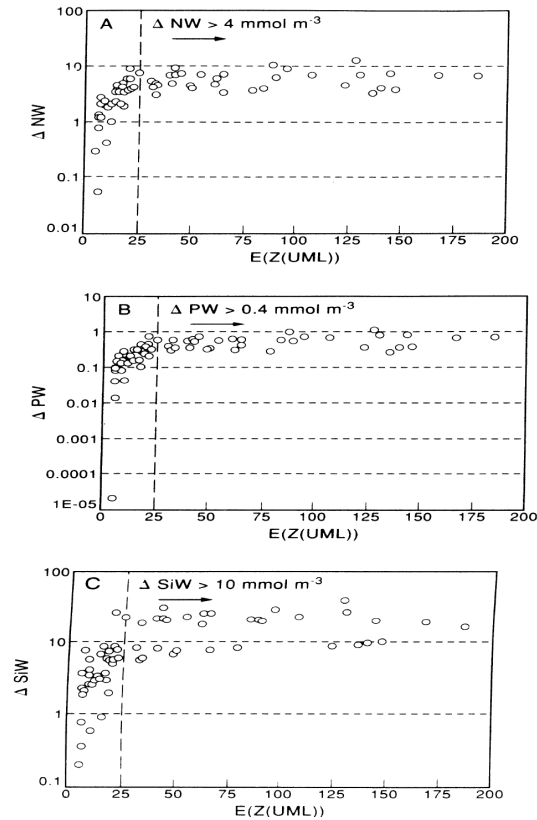

Figure 12: Nutrient utilisation (mmol m^{-3}): (A) nitrate (?NW), (B) phosphate (?PW) and (C) silicate (?SiW) vs the vertical stability E (m^{-1} x 1000). The dashed vertical line represents the threshold for $E(Z(\text{UML}) = 25$ .Above this value the nutrient utilisation is prevalently > 4, 0.4 and 10 mmol m^{-3} for nitrate, phosphate and silicate, respectively (from Catalano et al., 1997).

In addition, our results are in agreement with an « evolutional » model of phytoplankton blooms in pelagic Antarctic waters (Treguer and Jacques, 1992; Hecq et al., 1999). Moreover, we can state that the vertical stability index, expressed as $E(Z(\text{UML}))$, and the calculated nutrient utilization can be used as discriminating criteria to characterize the different phases of the primary production process. The value of vertical stability, $E(Z(\text{UML})) = 25$, represents a threshold for the primary production process. Below this value the significant relationship between vertical stability and nutrient consumption indicates that the vertical stability of the water

column is the main factor influencing primary production. Above this value, nutrient depletion and high biomass (POC concentrations), with little dependence on $E(Z(\text{UML}))$, show that other factors, such as grazing pressure (Smetacek, 1985; Huntley et al., 1991), light limitation (Smetacek and Passow, 1990; Nelson and Smith, 1991) and micronutrient availability (Martin and Fitzwater, 1988; Martin et al., 1990), may play a major role in regulating primary productivity in the upper mixed layer of Antarctic water.

3.2 PHYTOPLANKTON

3.2.1 Phytoplankton data: variability and impact of physical forcing

The spatial and temporal distributions of phytoplankton pigments were investigated in the western and south central Ross Sea during austral spring 1994 and summer 1990. Large gradients in biomass and phytoplankton community composition were observed both in the east-west and south-north directions, in relation to differences in water column structure and stability, which themselves depend on the processes of ice retreat within the different areas.

The first objective is to examine the spatial and temporal distributions of phytoplankton in the western and south central Ross Sea, during the austral spring (November - December) and summer (January), using pigments measured by HPLC as biomarkers. The pigment data are related to nutrient conditions and physical structure of the water column in order to provide insight into the factors controlling the composition of the phytoplankton community. The second objective is to discuss the role that the processes of ice melting, polynya opening, and zooplankton grazing might have on phytoplankton dynamics in the western and south central Ross Sea.

Field studies presented here took place as part of the Italian National Antarctic Program and were conducted in the Ross Sea during cruises in two separate years (Fig. 8, Table 2). Results presented here are a part of the Goffart, Catalano and Hecq (2000) publication.

Western Ross Sea: transect 1

Figure 13 shows the spatial variation of chlorophyll *a* (chl *a*), fucoxanthin, 19'-hexanoyloxyfucoxanthin (19'-HF) and phaeophorbides *a* along transect 1. As regards integrated chl *a* concentrations, a west - east gradient was observed, with a core of biomass over 125 mg chl *a* m^{-2} in the upper 100 m extending seaward for approximately 220 km (stations 25 to 22). Maximum integrated chl *a* reached 358 mg chl *a* m^{-2} at station 22 and was then followed by a drastic decrease of concentrations proceeding eastward. An area of moderate chl *a* concentrations was situated at the eastern end of the transect, around station 20.

Fucoxanthin was the most abundant carotenoid on this transect, and its distribution was similar to that of chl *a* (Fig. 13). Diatom biomass, as estimated from fucoxanthin concentrations, was greatest in the upper 50 m of the western portion of the transect and decreased markedly east of station 22. In the western part of the section, integrated fucoxanthin concentrations in the upper 100 m ranged from 89 - 239 mg m^{-2}, and reached a maximum value at station 22, where chl *a* concentration was maximum.

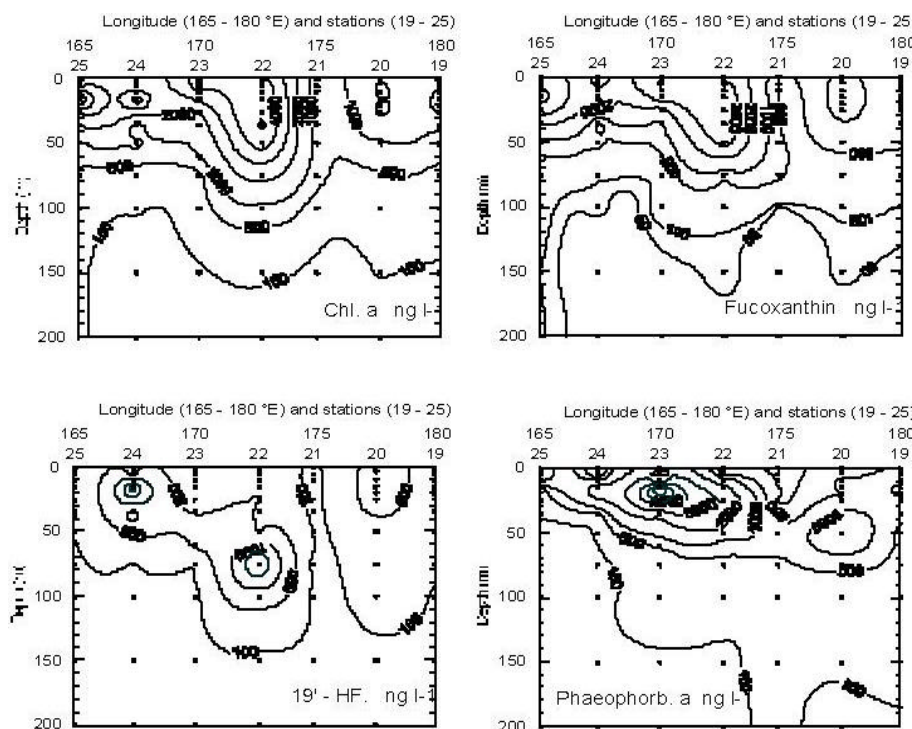Figure 13: Distribution of chl *a*, fucoxanthin, 19'-hexanoyloxyfucoxanthin (19'-HF) and phaeophorbides *a* in the upper 200 m along transect 1 (ng l^{-1}).

Integrated 19'-HF, the second most dominant chromophytic pigment, did not show any clear trend of variation moving along the transect. However, the vertical distribution of 19'-HF exhibited a contrast between the western and the eastern parts of the section. In the western part, maxima of 19'-HF concentrations were generally observed below those of fucoxanthin whereas maxima of 19'-HF and fucoxanthin concentrations coincided in the area of moderate chl. *a* concentrations around station 20 (Fig. 13). Moreover, while fucoxanthin concentration decreased rapidly with depth, the vertical gradient in 19'-HF concentration was less pronounced.

High levels of phaeophorbides *a* were found at the stations where chl *a* concentrations were elevated (Fig. 13). In the western part of the section, the vertical distribution of phaeophorbides *a* followed the patterns of chl *a* and fucoxanthin. The maximum integrated concentration of phaeophorbides *a* was seen in the central part of the diatom bloom, and reached the exceptionally high level of 192 mg . m^{-2} in the upper 100 m at station 23.

The high-biomass region of the bloom was an area of pronounced silicate and nitrate depletions (Fig. 13) with their concentrations reduced by up to 30 % of the winter values (deduced from the values taken immediately below the pycnocline). The most intense nutrient removal occurred for silicate, which was reduced by about 65 μM within the surface mixed layer at station 25 (85 μM at 50 meters, 17 μM at 5 meters). At the same station, nitrate was reduced from ca. 30 μM below the pycnocline to <10 μM at the surface.

South central Ross Sea: transect 2

Similar and moderate standing crops of phytoplankton were found in the polynya and in the ice edge area (Fig. 14). The polynya had integrated values of chl *a* ranging from 58 to 186 mg chl *a* m^{-2} in the upper 100 m while the ice edge area showed integrated chl *a* from 55 to 181 mg chl *a* m^{-2}. Significantly lower levels of chl *a* (20 - 27 mg chl *a* m^{-2}) characterized the pack-ice area.

Along transect 2, 19'-HF was the major contributor to total carotenoid abundance and showed concentrations higher than those of fucoxanthin. The distribution of 19'-HF exactly followed that of chl *a*, indicating that prymnesiophytes, and *Phaeocystis* in particular, were present both throughout the polynya and the marginal ice zone (29 -

132 mg 19'-HF m^{-2} in the upper 100 m). The variation of 19'-HF across the polynya and the marginal ice zone did not show any particular tendency. However, 19'-HF exhibits a drastic decrease in the water under the ice, even though it was dominant in melting-ice region.

On the other hand, fucoxanthin, the pigment second in abundance after 19'-HF, was strictly coupled to the marginal ice zone where it showed marked increases (31 - 67 mg m^{-2} in the upper 100 m) as compared to polynya and pack-ice stations (Fig. 11). The maxima of phaeophorbides *a*, used as grazing tracer, also occurred in the marginal ice zone, where diatoms were most abundant. In that area, an important fraction of phytoplankton production appears to be transferred to higher trophic levels through herbivores, in particular through krill that were present in extremely high concentrations ($\approx$ 29 tons . km^{-2} at station 11; Azzali, personal communication).

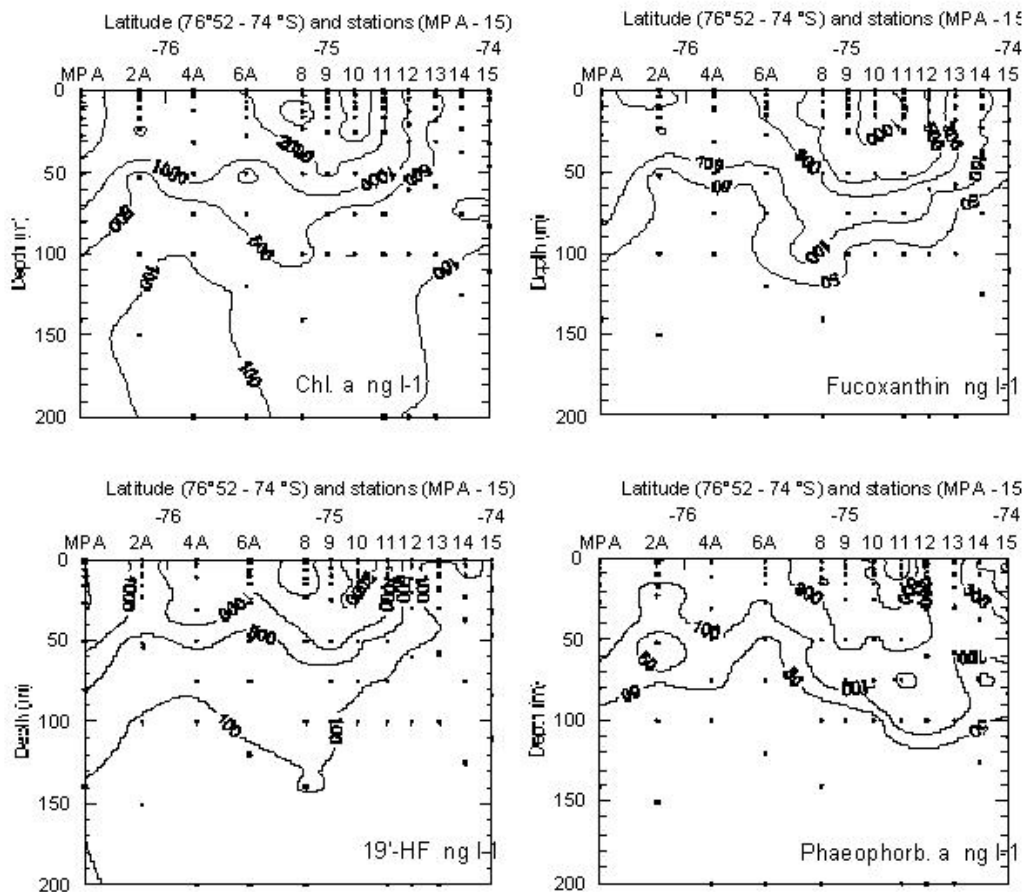Figure 14: Distribution of chl *a*, fucoxanthin, 19'-hexanoyloxyfucoxanthin (19'-HF) and phaeophorbides *a* in the upper 200 m along transect 2 (ng l^{-1}).

Discussion

The range in pigment concentrations we report for transects 1 and 2 confirms the presence of substantial gradients in phytoplankton biomass and species distribution within the western and south central Ross Sea. The distributions of phytoplankton seem to be largely controlled by hydrological structure and water column stratification, which are themselves dependent on the mechanisms which govern the concentration of sea ice within the Ross Sea.

In the western Ross Sea, east of Victoria Land and Terra Nova Bay, the stratification of the water column results primarily from the input of low-salinity meltwater, most likely derived from sea ice which melts near the coast and from coastal glaciers (transect 1). The highest phytoplankton concentrations observed in this study were tightly coupled to the region of meltwater influence and were dominated by diatoms, as indicated by the elevated fucoxanthin concentrations. Typically, *Fragilariopsis curta* is the most abundant species in the sediment record of the western Ross Sea over the past 18000 years (Kellogg and Truesdale, 1979) and dominates the diatom assemblage of other ice edge blooms reported for the western Ross Sea (e.g. Wilson et al., 1986; DiTullio and Smith, 1995). Consequently, its dominance within the ice edge bloom we studied is assumed.

The overall spatial extent and biomass levels of the bloom we observed were similar to previous reported field observations dealing with summer conditions in the western Ross Sea. Our data suggest the annual occurrence of an intense diatom bloom associated with the coastal ice-edge region and allow us to accurately describe its spatial and temporal characteristics. Synthesis of available information (Table 3) suggests that a diatom-dominated ice-edge bloom extends off the coast of Victoria Land from 72°30'S to 77°S, within 100 to 250 km from the coastal ice edge and persists at least from early January to late February. However, pronounced nitrate and silicate depletion observed by early January within the high biomass core of our transect suggests that bloom initiation takes place much earlier in the season. This asumption is confirmed by satellite images, which reveal that substantial chl *a* concentrations exist by mid-December in Terra Nova Bay (Arrigo and Mc Clain, 1994). Although it is difficult to assign a time frame for a process controlled by physical conditions, it seems reasonable to infer that the diatom ice-edge bloom of the western Ross Sea persists on the order of 2.5 - 3 months. Although this estimate

involves a number of uncertainties, it allows an appreciation of the temporal pattern of the bloom based on field observations and emphasizes its potential major role in the functioning of the pelagic ecosystem of the Ross Sea.

The only other carotenoid pigment detected in significant concentration within the area of meltwater influence was 19'-HF, used as marker for prymnesiophytes. The presence of 19'-HF could be attributable to *Phaeocystis*, whose presence in relatively small numbers (60 - 170 10^3 cells l^{-1}) was reported for Terra Nova Bay in January 1990 (Andreoli et al., 1993). The shift between the vertical distributions of fucoxanthin and 19'-HF suggests that 19'-HF containing cells have superior photoadaptative properties, as emphasized by Palmisano et al. (1986), and are able to survive at very low irradiances. For instance, at station 22, maximum of 19'-HF concentration.

Outside of the diatom-dominated ice-edge bloom, chl *a* concentrations were markedly lower until approximately 400 km seaward of the coast, where a secondary, less intense, chl *a* maximum was detected in the open water. The open water chl *a* maximum was different in its pigment composition from the diatom-dominated ice-edge bloom. It contained fucoxanthin and 19'-HF in similar proportions, indicating a mixed community of diatoms and prymnesiophytes. These observations coincide with those reported for the south eastern Ross Sea (76°30'S, 175-180°E) where a secondary chl *a* maximum was found in late January 1990, 2 to 4 weeks after our transect (Nelson et al., 1991). The species composition within this area of moderate phytoplankton biomass was a mixed assemblage of *Phaeocystis* and numerous diatom species, with *Corethron criophilum* and a *Chaetoceros* species the major contributors to the diatom biomass (Leventer unpubl., in Nelson and Tréguer, 1992).

The distribution of phaeophorbides *a*, in relation to chl *a*, indicated that zooplankton grazing and phytoplankton biomass were tightly coupled. Within the diatom-dominated ice-edge bloom, grazing pressure significantly reduced the diatom biomass and transferred a sustained part of algal material to the herbivore trophic level. The most abundant mesozooplanktonic grazers were the thecosome pteropods *Limacina helecina* and copepods (Hecq et al., 1992). Adult and juvenile euphausiids were also observed. Grazing of phytoplankton was maximum in the central part of the bloom, while stations situated closer to the ice-edge were characterized by less grazed and probably younger diatoms based on pigment distributions.

Table 3: Parameters characteristics of the ice edge blooms of the western Ross Sea. All transects were normal to the coastal ice edge. See maps showing sampling locations in the original papers for longitudes.

Latitude	Period	Spatial extension of the bloom	Dominant phytoplankton	Pigment concentration within the ice-edge bloom	Pigment concentration outside the ice-edge bloom	Pigment concentration, average along the transect, including non-blooming area	Reference
72°30'S	12 January–05 February 1990	within the coastal region	Diatoms: *Fragilariopsis curta*, *Fragilariopsis cylindrus*, *Chaetoceros* spp. and *Corethron cryophilum*	3.7 mg chl. a m^{-3} (maximum concentration)	–	–	Smith et al. (1996)
72°30'S	05–28 February 1992	within 150 km of the coast	Diatoms	2.4 mg chl. a m^{-3} (maximum concentration)	–	0.61 mg chl. a m^{-3}	DiTullio and Smith (1995), Smith et al. (1996)
75°S–166°E (Terra Nova Bay) CZCS	10 December 1978–19 February 1979 / 16 January 1979	>8000 km^2		1–10 mg m^{-3} / ≥10 mg m^{-3}	–	–	Arrigo and McClain (1994)
75°S	01–06 January 1990	220 km from the ice edge	Diatoms	6.76 mg chl. a m^{-3} (maximum concentration) 129–358 mg chl. a m^{-2} (0–100 m)	61–115 mg chl. a m^{-2} (0–100 m)	2.10 mg chl. a m^{-3} (0–100 m)	This study
75°S	05–28 February 1992	within 150 km of the coast	Diatoms	3.1 mg chl. a m^{-3} (maximum concentration)	–	2.15 mg chl. a m^{-3}	DiTullio and Smith (1995), Smith et al. (1996)
76°30'S	13 January–05 February 1990	100–150 km from the ice edge	Diatoms: *F. curta* (80–90% of the cells), *F. cylindrus* and *Fragilariopsis closterium*	11.8 mg chl. a m^{-3} (maximum concentration)	–	–	Nelson et al. (1991), Nelson and Tréguer (1992), Smith et al. (1996)
76°30'S	05–28 February 1992	within 250 km of the coast	Diatoms	4.8 mg chl. a m^{-3} (maximum concentration)	–	1.93 mg chl. a m^{-3}	DiTullio and Smith (1995), Smith et al. (1996)
76–77°S	January–February 1983	200–250 km from the ice edge	Diatoms: *F. curta* (70–80% of the cells) and *F. closterium* (5–20% of the cells)	146–322 mg chl. a m^{-2} (0–150 m)	63–107 mg chl. a m^{-2} (0–150 m)	–	Smith and Nelson (1985), Wilson et al. (1986)

Thus, it appears that the stabilization of the upper layer of the water column associated with the receding ice-edge of the western Ross Sea favors diatom growth and accumulation. This is exploited by a classical food web where large herbivorous zooplankton provide the major link to larger animals and play an important role in regulating algal biomass. Moreover, the long duration of this phenomenon must influence substantially the fluxes of biogenic carbon and silica towards apex predators and deep waters.

The physical environment and the water column structure observed in the south central Ross Sea differ markedly from those observed in the western Ross Sea. Physical data along transect 2 demonstrate that very little meltwater had been introduced into the surface layer, even in the marginal ice zone, as referred to also by Smith and Gordon (1997). These observations suggest that direct melting plays only a minor role in the formation and opening of the Ross Sea polynya north of the Ross Ice Shelf. This hypothesis seems supported by the findings of Arrigo et al. (1998) who demonstrate that the mechanisms of the Ross Sea polynya formation are controlled mainly by air temperature in winter, which determine sea ice thickness and integrity. Polynya formation begins only when the temperature rises and the sea ice increases in brine volume, allowing sea ice breakup. Once ice breakup has begun, a set of complex processes interact to govern the concentration within the Ross Sea polynya, including the influence of surface currents and wind stress on sea ice distribution (Arrigo et al., 1998). With the opening of the polynya, the ice-free area is propagating from the south to the north until the beginning of January when the polynya becomes contiguous with the rest of the Ross Sea (Arrigo and McClain, 1994; Hecq et al., 1999).

As a consequence of these mechanisms of ice retreat, the water-column structure of the south central Ross Sea polynya is characterized by a relatively deep mixed layer, a low stability index, and a quite homogenous nutrient distribution. These conditions favor the presence of a bloom dominated by *Phaeocystis*, both in the polynya area and often in the weakly stratified marginal ice zone. *Phaeocystis* dominate in the south central Ross Sea probably because of their ability to maintain near-maximal photosynthetic rates at much lower irradiance levels than can diatoms (Leventer and Dunbar, 1996; Arrigo et al., 1999). By mid to late November, the latitudinal extension of the *Phaeocystis* bloom covered at least the area of the south central Ross Sea

between 76°30'S and 74°50'S (transect 2). Complementary informations are provided by Smith and Gordon (1997) who observed *Phaeocystis* dominance at the same period of the same year along a longitudinal transect perpendicular to the Victoria Land coast at 76°30'S. In both cruises, nutrients and chl *a* concentrations exhibited similar distributions. These results clearly indicate that *Phaeocystis* blooms in early spring in the Ross Sea polynya, when it can outcompete other species in the unstratified or poorly stratified water column.

At the northern limit of the polynya, fucoxanthin concentrations were significantly higher in close proximity to the retreating ice edge than for the open water region where ice had disappeared for some time. A diatom bloom was confined to the slightly stratified area of the marginal ice zone and overlapped with the *Phaeocystis* bloom. However, the spatial extension the diatom-rich band of the south central Ross Sea was quite narrow (c.a. 30 km), corresponding with the reduced width of the slightly-stratified marginal ice zone. Furthermore, fucoxanthin concentrations in the marginal ice zone of the polynya were approximately 3 times lower than within the diatom bloom observed in the western Ross Sea.

In spite of its reduced geographical extent, the marginal ice zone of the south central Ross Sea was an area of increased transformation of chl *a*, mainly through grazing activity as suggested by the greater phaeophorbide levels. The degradation of the algal material appeared to be due to grazing pressure by various types of herbivorous zooplankton, among them the very large amounts of krill. These krill contributed to a total disappearance of the biomass of bloom-forming phytoplankton within two weeks (Hecq et al., 1999). Moreover, the diatom - krill assemblage characterizing the marginal ice zone of the polynya (Hecq et al., 1999) attracted remarkable populations of birds and Minke whales in a period of early production when diatoms are scarce in other areas.

To examine the relationship between water column stratification (itself depending on the mechanism of ice retreat) and diatom or *Phaeocystis* dominance, we plotted E_{max} against integrated fucoxanthin and 19'-HF for each station of transects 1 and 2 (Fig. 15). The depth of integration Z(L) was calculated according to Catalano et al. (1997), assumed to be the depth of the base of the pycnocline. The maximum observed values of integrated 19'-HF were observed in stations with very low E_{max} (< 10 m^{-1} x 1000) corroborating the hypothesis that *Phaeocystis* are well adapted to a mixed

water column (Fig. 15A). These values correspond to the polynya and marginal ice zone stations of transect 2. However, a low E_{max} does not necessarily imply a *Phaeocystis* bloom, as shown for the pack-ice stations of transect 2. In this case, very low irradiance below the pack presumably prevents *Phaeocystis* growth. On the other hand, diatom abundance showed a positive correlation with water column stability (Fig. 15B). Increasing water stability apparently favored the growth and accumulation of diatom standing crops and allowed them to adapt to a particular light regime.

Recently, evidence of seasonal iron limitation in the Ross Sea provided complementary information on the factors controlling biomass and species distribution in Antarctic shelf waters. Sedwick et al. (2000) showed that diatoms bloom only in the ice edge regions, where both light and iron, supplied from melting sea ice, are abundant. In the unstratifed waters, *Phaeocystis* dominated the algal community during spring and early summer in iron-replete conditions (>1 nM dissolved Fe), as a result of iron supply from upwelled bottom waters. Later in the season, very low iron concentrations in the ice-free waters (< 0.2 nM dissolved Fe) limit both *Phaeocystis* and diatom growth.

In summary, it appears that the mechanisms of ice retreat within the Ross Sea (melting in the western Ross Sea and ice breakup and wind stress in the south central Ross Sea) control the water column structure, its stability characteristics and its iron contents. Large-scale melting, like in the western Ross Sea, induces a highly-stratified water column and allows the development of an intense diatom bloom associated with the iron-enriched coastal ice-edge region. On the contrary, in the south central Ross Sea, the processes of polynya formation result in relatively deep mixing and weakly stratified waters. *Phaeocystis*, as opposed to diatoms, appear to be better adapted to a less stable water column and bloom very early in spring in the polynya and the associated marginal ice zone. In addition, within the slightly stratified area of the marginal ice zone, at the northern limit of the polynya, a moderate diatom bloom overlaps with *Phaeocystis*. These typical patterns of phytoplankton distribution within the Ross Sea illustrate the importance of hydrodynamic processes of vertical stabilization which determine largely the dominance of diatom or *Phaeocystis* assemblages in Antarctic shelf waters.
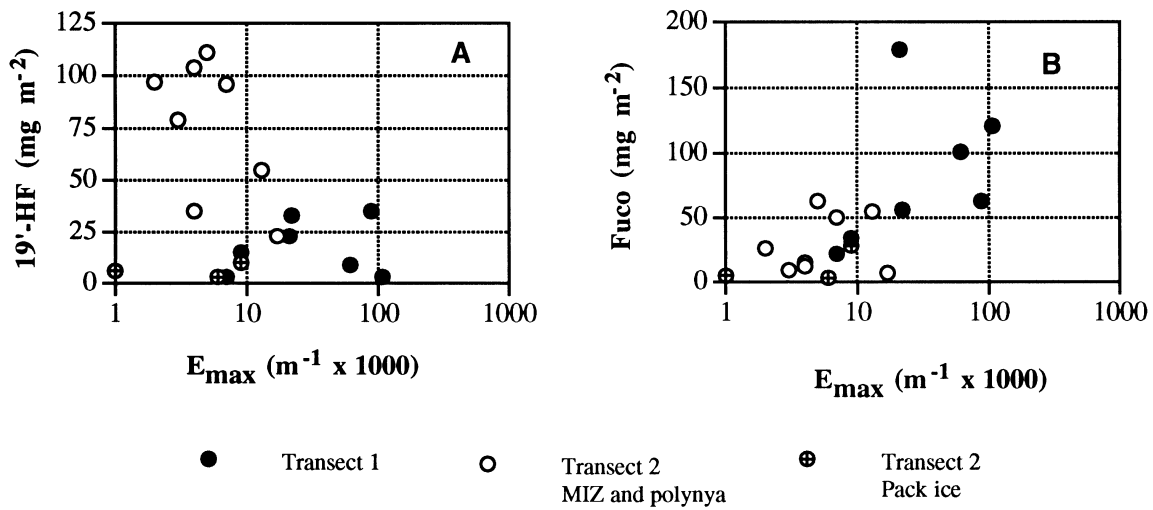
Figure 15: Maximum vertical stability E_{max} (m^{-1} x 1000) vs integrated 19'-HF (A, mg m^{-2}) and fucoxanthin (B, mg m^{-2}) for transects 1 and 2. Depth of integration Z(L) was calculated according to Catalano et al. (1997).

3.2.2 Antarctic spring: the importance of new production

This section intends to contribute to a more accurate evaluation of the importance of phytoplankton production in term of « new » and « regenerated » production in the marginal ice zones of the Ross Sea. Results presented here summarize the Lipizer, Ruffini, Predonzani, Cozzi, Goffart and Catalano (1997) paper.

Sampling was carried out during the 1994/95 Italian Antarctic Expedition in the Ross Sea from November 14 to December 15, 1994. 29 stations were sampled along 175°E, from 76 to 71°S, following the northward ice retreat.

In terms of phytoplankton nutrient uptake, NO_3 uptake was elevated in the polynya. In the polynya stations, the daily absolute uptake (QNO_3) exceeded 50 $\mu mol . m^{-3} d^{-1}$. When integrated between the surface and the depth corresponding to 1% PAR, the obtained value was 4.9 $mmol . m^{-2} d^{-1}$. On the other hand, the pack ice stations exhibited low QNO_3, with a integrated value of 0.9 $mmol . m^{-2} d^{-1}$. The highest values usually occurred in subsurface layers, at depth corresponding to 30-50% PAR. In many polynya stations, where the phytoplankton community was *Phaeocystis* dominated, uptake rates at 1% PAR were higher than surface values, suggesting that *Phaeocystis*, as opposed to diatoms, are able to photosynthesize at very low light intensities.

The same trend was evidenced for absolute NH_4 uptake (QNH_4). The polynya stations were characterized by QNH_4 higher than 40 $\mu mol\,m^{-3}\,d^{-1}$, while maximum absolute NH_4 uptake values were measured in the marginal ice zone area, with a water column integrated value of 2.0 $mmol\,m^{-2}\,d^{-1}$. In the pack ice stations, QNH_4 were < 40 $\mu mol\,m^{-3}\,d^{-1}$.

With the marginal ice zone, our averaged nitrogen uptake rates integrated from the surface to 1% PAR penetration (in $mmol\,m^{-2}\,d^{-1}$) are close to those reported for the MIZ in other seas (Table 2 in Lipizer et al., 1997). QNH4, on the other hand, appears slightly lower, resulting, as a consequence, in a higher f ratio, which seems typical of an early bloom.

In terms of f ratio, the data reveal a general predominance of « new » vs « regenerated» production during the early spring period. Considering the whole data set, the transect average was 0.64. In the diatom bloom associated with the marginal ice zone, the f ratio reached 0.72.

3.2.3 Relation between pigment stocks and nutrient depletions

A first attempt to relate the governing nutrient uptake regime and phytopigment signature was perfomed on the basis on nutrient and phytopigment data obtained during early spring and summer in the Ross Sea. Results are published in Goeyens, Elskens, Catalano, M. Lipizer, Hecq and Goffart (2000). Phytopigment and nutrient data allowed to recognized two distinct groups. The first one was characterized by moderate nutrient (nitrate and silicic acid) depletions in combination with relatively high diatom and *Phaeocystis* abundance. The second group showed very low nutrient depletions and very poor diatom abundance. Average depth specific nitrate depletions were 8.1 and 1.1 μM and average silicic acid depletions were 21.5 and 1.3 μM, respectively. The nutrient consumption patterns did not match the conditions of silicic acid excess or nitrate excess areas, a clear trend being probably obscured by very poor seasonal maturity of several sampling stations

The contrast between both groups is largely explained by small differences in nitrogen uptake regime of the major phytoplankters. During early season the diatoms meet the majority of their nitrogen requirements by nitrate uptake, with few exceptions where ammonium is the most important nitrogenous substrate. On average their nitrate uptake capacity is lower than that of *Phaeocystis* (average

specific nitrate uptake rates were 0.021 and 0.036 d^{-1} for diatoms and *Phaeocystis*, respectively). The latter phytoplankton always shows predominance of nitrate uptake. Both groups are subject to inhibition of nitrate uptake when ammonium availability increases and it is likely that the diatoms are more sensitive to the inhibitory effect of ammonium (Fig. 16).
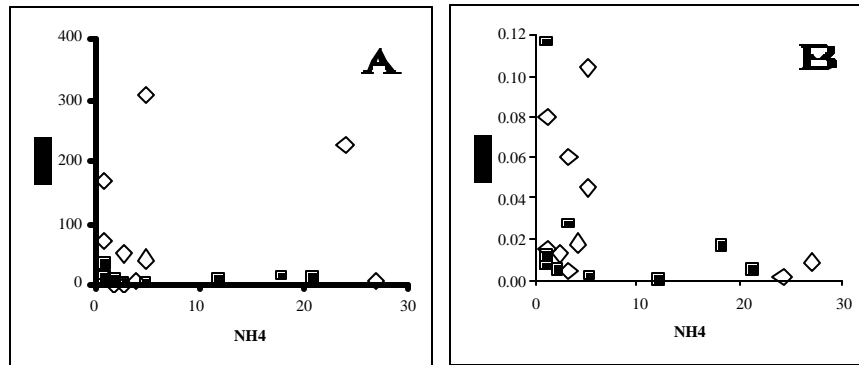

Figure 16: Illustration of the inhibitory effect of increasing ammonium concentrations (mmol m^{-2}) on the absolute nitrate uptake rate (A) and specific nitrate uptake rate (B); open diamonds represent *Phaeocystis* dominated samples and black squares represent diatom dominated samples (from Goeyens et al., 2000).

4. MODELLING STRATEGY

4.1. Conceptualisation of the Ross Sea ecohydrodynamic model (ECOHYDROMVG)

4.1.1. Ecohydrodynamical processes related to the marginal ice zone and to the polynia of the Ross Sea

Formation and retreat of the seasonal ice zone are the major phenomenons which control the plankton ecosystem in the antarctic coastal and shelf waters of the Ross Sea.

In the Ross Sea, the temperature never exceeds values higher than 3 to 4 °C in summer and approaches -2 °C at the ice shelves. The only input of fresh water essential for the vertical stabilization of the upper layers of the water column are due to ice retreat. The principal physical cause of the Ross Sea ecosystem variability is the existence of the Southern Ross Sea polynia generated by the strong winds which advects the ice cover (Zwally et al., 1983) and by sensible heath coming from ocean (Jacobs and Comiso, 1989). During the winter and at the beginning of the spring, the ice-free surface is propagating from the South to the North, as shown by weekly remote sensing pictures (Hecq et al., 1993). As a consequence, in that area, the ice-retreat and melting and the exposure of the water column to the sunlight appear earlier than in other areas. That characteristic extension of the marginal ice-edge around the polynia seems to be responsible for a higher productivity and an increase of the season of production and of the length of the ice-edge. Another smaller polynya is also observed in area of Terra Nova Bay, just north of the Drygalski Ice Tongue and is due to offshore winds which remove ice as fast it is formed (Gordon, 1988). The mode of formation of the polynya imposes a spatial heterogeneity of ice cover and thus the initial time of seasonal plankton cycle varies at the same scale. Moreover the ice-edge retreat is asymmetric and the progress to the north is faster than to the east and the west. The vertical structure of the water column associated to the ice-edge melting is maintained during a longer time along the zonal borders of the polynya (for example Victoria Land) than in the north (central Ross Sea).
Moreover, the progression to the north of the ice-edge of the polynya is not a continuous process in relation to different ice thickness between the South and the North. At the end of winter, the polynia opens slowly in the south by ice melting and

opening of leads. Following successive wind events, the polynia continues its opening by a northward transport of ice floes. Those ice-pieces accumulate around 75°N where the ice pack is thicker and particularly in the western part where they form a barrier between both the Southern Ross Sea and Terra Nova polynyas. That second phase of opening is very fast and does not take the time to ice melting. The third phase occurs later north of 75°S and progresses on a longer time. At the end of the third phase (end of December), the polynya encounters the circumpolar ice-edge and becomes contiguous with the whole Southern Ocean. This discontinuity in the progress of the polynya ice front will develop a strong variability in the light, the stability of the water column, the algae releasing in the water column and influences the pattern of the global ecosystem.

Another source of physical variability is due to local wind conditions. Strong catabatic winds can increase the depth of the mixed layer and impose a decrease of phytoplankton biomass. Two extreme case of variability are observed. In permanent ice-free zone, north to the Antarctic divergence, because of strong winds and low vertical stability, the mixed layer is deep and the plankton productivity is poor. In eastern Ross Sea, below non-melting ice (permanent ice pack), the mixed layer is also deep due to the weak stratification and the high momentum transfer caused by the drift of ice (Niebauer and Smith, 1989).
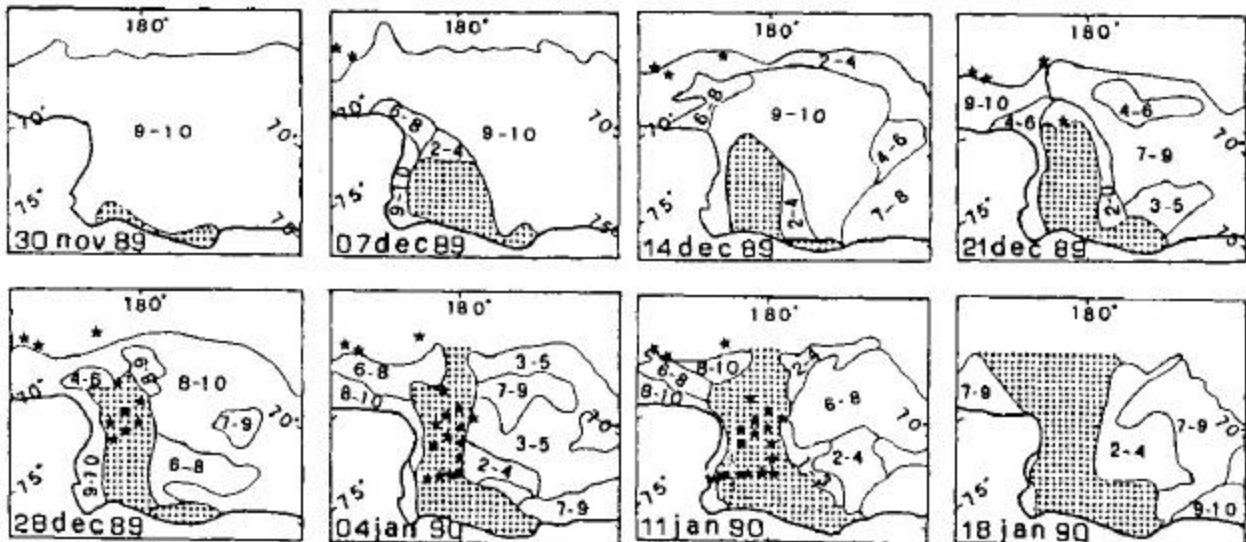

Figure 17. Ice cover temporal evolution in the southern part of the studied area during the cruise period. Numbers (like 7-9) represent the cover ice of the sea-surface in tenths. Data are taken from satellite images published weekly by NAVY-NOAA Jont ICE Center. Stars represent the location of the hydrological stations executed until the date of the image. The dotted area is the ice free area.

4.1.2. The distribution of planktonic communities in relation to the Marginal Ice Zone

The highest phytoplankton concentrations in the world are observed at the edge of the ice floes, at the level of the marginal ice zones.

In December in the Ross Sea, while performing measurements in the marginal ice zone, we observe that the breaking up of the ice flows and the melting of the ice is progressive. The maximum chlorophyll a (phytoplankton) concentrations coincide with the places where the ice cover is approximately 40 – 60% and where there is an active melting. This is also the place where the concentrations in phaeophorbides are at a maximum. These pigments characterise the degradation of chlorophyll a by mesozooplankton grazing.

The chlorophyll a concentrations measured at the surface during a continuous horizontal transect (TR1 fig. 18), show the abundance of phytoplankton in the Marginal Ice Zone, starting at the end of winter. They also show a dominance of *Phaeocystis* at the polynia margin and of diatoms at the Periantarctic margin (fig. 4.3B). Identical measurements performed at the end of December, while the Ross Sea polynia is opening to the ocean, show that the chlorophyll a maxima are situated where the ice cover is approximately 40 – 60 % and where an active melting is taking place. This is also where the phaeophorbides (produced by the degradation of chlorophyll *a* by zooplankton) are the most abundant.
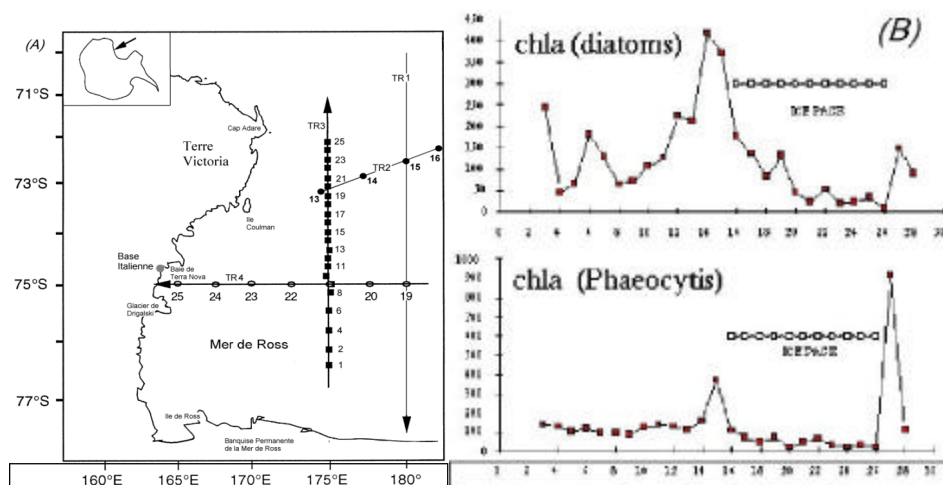

Figure 18. Map showing the sampling transects in the Ross Sea and the position of the stations. B. Distribution of phytoplankton, at the surface, during the TR1 transect in November 1994.

4.1.3. Vertical distribution of the planktonic communities in relation to the Marginal Ice Zone

In order to understand how the vertical distribution of plankton evolves in relation to the marginal ice zone, we performed a series of sampling transects throughout the ice flow (Fig. 19). This type of transect gives us a synoptic image of the spatial distribution of the planktonic variables. As weekly satellite images of the ice front are available, we can deduce, for each sampling station, the time passed since the melting of the ice. This synoptic transect will therefore allow us to deduce the sequence of physical and planktonic events since the tick ice until the open ocean, in relation to the retreat of the ice front.

These transects were done in the Ross Sea during the ITALIANTARTIDE campaigns, where we determined the distribution of phytoplanktonic pigments, zooplankton and nutrients, in relation to the density which has been calculated from temperature and salinity measurements.

The main characteristic of the hydrographic field is the presence of a lens of low salinity and low density located at the Marginal Zone. This low-density lens is due to the release of fresh water from the melting ice. An important vertical stratification is associated to it. In this stratified lens is where the maximum phytoplankton biomass can be found, at the surface of the ice edge and in the stratified part. This is the place where the highest concentrations of krill and whales have been observed. This phytoplanktonic growth in the ice melting zone is due to the release of endogenous algae and the production associated to the stabilisation of the superficial water column. Under the ice flow chlorophyll a concentrations are very low (< 0.5 mg m^{-3}) in the water column, whereas a high level of pigments is observed in the ice itself (300 mg. m^{-3}). At a certain distance from the ice flow, the distribution of the isopycnes shows the mixing of the water column and the reduction of the stability and the phytoplankton biomass.

A sequence of events tributary to the melting of the ice and the stability of the water masses is therefore established.

If we consider the specific composition of the phytopigments (fig 19), it would appear that the phytoplanktonic maximum biomass at the edge of the ice and in the stratified zone, is dominated by fucoxanthine which characterises the large diatom cells. At depth all along the transect, and at the surface in the southern part of the polynia, significant concentrations of 19'hexanoyloxyfucoxanthine indicate the dominance of small non colonial *Phaeocystis* cells.
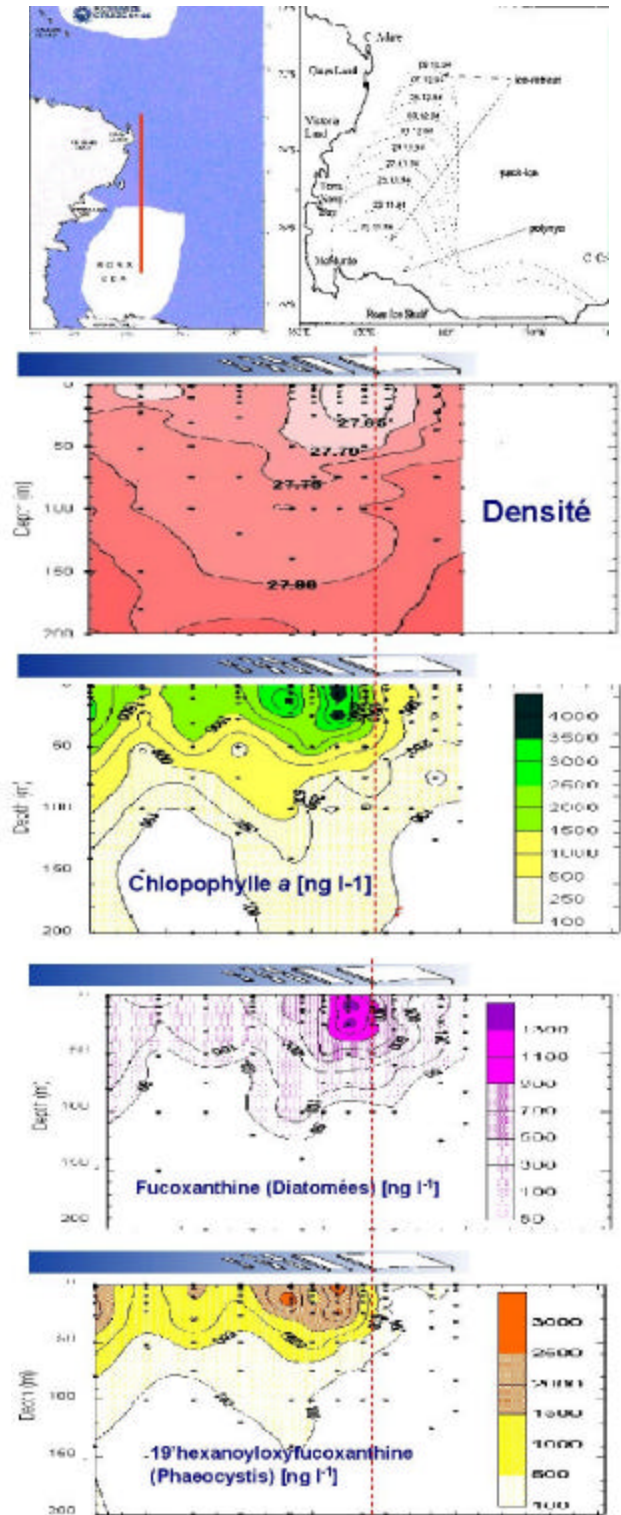
Figure 19

Why are diatoms replaced by phaeocystis in the time-line? It doesn't seem to be due to the macronutrients (NO3, SiO4, NH4) that are never depleted. The water column's stability could be a factor responsible for the selection.

W e have indeed shown in the Ross Sea that the diatom biomass was a function of the stability whereas it's the opposite for the phaeocystis who have an advantage in mixed waters (fig. 15).
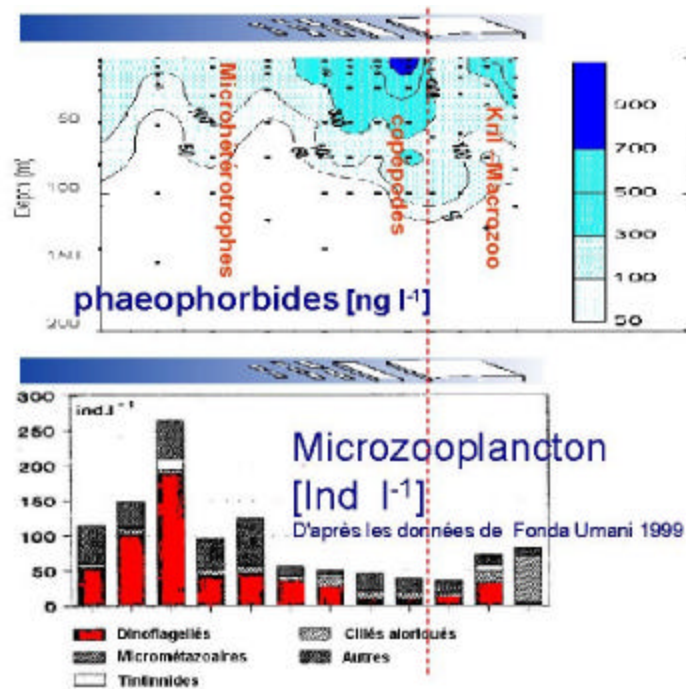

Figure 20.

Another factor is the grazing, as is shown by the high concentrations in phaeophorbides. These are typical of the macro and mesozooplankton grazing who only consume diatoms, which could possibly explain the selection. Under the ice, the grazing is done by krill, and in the open water by copepods.

Zooplankton also participates in the sequence : macroherbivorous krill are dominant at the ice level, copepods and mesozooplankton are dominant in the stratified zone whereas microheterotrophes increase towards the south in the mixed zone.
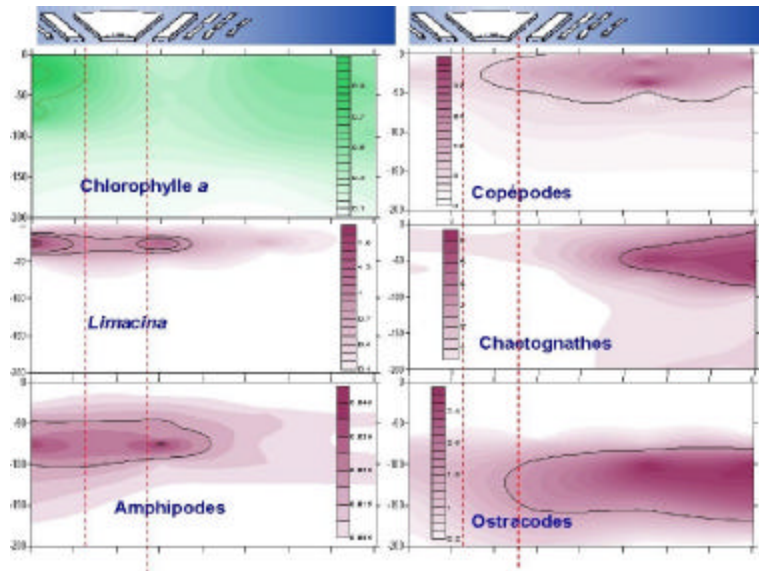
Figure 21

The following transect, done through the ice flow separating the Ross Polynia from that of Terra Nova, illustrates the zooplankton sequence. (Fig. 21)

- At the edge of the coastal ice, the macrozooplanktonic herbivorous mollusc *Limacina helicina*, consumes large quantities of diatoms while the faecal pellets are consumed by a planktonic amphipod with a deeper distribution. There is an important vertical sedimentation flux.
- Further out, in the area that has been ice-free for some time, the biotic assembly is composed of smaller organisms but with identical trophic levels, occupying an equivalent vertical distribution: multivorous copepods dominate at the surface. Beneath them chaetognaths and ostracods constitute the carnivore and detritivore levels.

The zooplankton sequence successive to the ice melt is marked by a size reduction in the organisms and the change from a herbivorous system to a mutlivorous system.

- During this sequence we can also observe an increase in the ammonium levels due to the excretion and a reduction in silicates. The density and salinity profiles remind us that this sequence is in phase with the physical one

The dominant factor in the ecosystem is therefore this sequence of successive planktonic events after the ice melt. When the ice begins to melt, cannals are formed

in the ice mass and the algae are released into the water column where they develop and are consumed and sediment.

Our studies have allowed us to establish this scheme by the sequence of phyto and zooplanktonic events that follow the progression of the ice front and the vertical physical structure of the water column :

- During the release of the algae by the ice, a part of the diatoms is consumed under the ice by macrozooplanktonic organisms attracted to the surface by the light. The rest sediments or develops in the water column and is consumed by the mesozooplankton. Then, depending on the depth of the mixing layer, diatom production stops and gives way to that of Phaeocystis and we go from a herbivorous macrozoolanktonic system to a multivorous microzooplanktonic système.
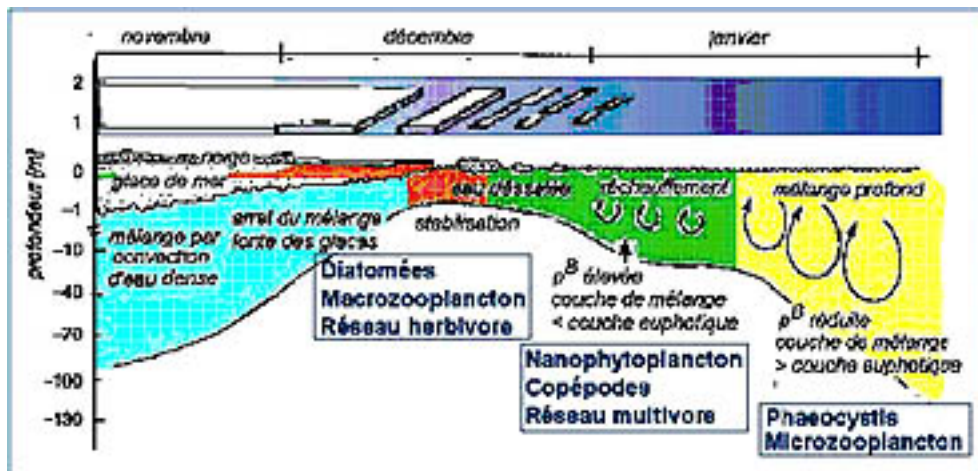

Figure 22. Sequence of planktonic events following the melting of the ice (Hecq, 2001)

4.1.4. Variability of the biotic assemblages of the Ross Sea

The ring shape around polar continent, the isolation by circumpolar fronts, the zonal transport by the strong circumpolar currents coupled with the seasonal changes in the light regime and sea ice cover impose a relative homogeneity in species composition.

This growth and planktonic ecosystem sequence are not simultaneous in all the Seasonal Ice Zones. The results of our campaigns have shown that the phytoplankton growth is progressive and discontinuous in relation to the mode of aperture of the polynia.

A series of CZCS satellite images allows us to note that the growth begins in December, in the Southern Polynia in the Ross Sea, that it slows in January when growth starts in the Terra Nova polynia which isn't open until the month of January.

This spatial variability has repercussions in the distribution of the biotic assemblages that we have identified. Variations in ecosystem patterns characterized by specific biota assemblages were identified on the basis of plankton composition in diverse areas of the Ross Sea:

The « diatom-krill » assemblage occurs in the northern Ross Sea along the periantarctic marginal ice-edge. That assemblage exists where the depth exceeds 500 m in the south and 1000 m in the north. At that location aloric ciliates and cyanobacteria are present in the ice and in the adjacent water.

The « multivorous food web» assemblage is present in the deep Ross Sea, including the northern part of the polynya where reduced ice melting determines a temporary vertical stability favorable to phytoplankton productivity. All groups are present (diatoms - *Phaeocystis*, copepods- krill) including birds and whales.

The « *Phaeocystis* » assemblage dominates the southern Ross Sea along the permanent ice-shelf. *Phaeocystis* dominates the algal community. The zooplankton is scarce and no predation by higher trophic levels occurs.

The «coastal diatom' » assemblage encountered in the Terra Nova Bay polynia where *Limacina helecina* is the dominant herbivorous plankton. In that coastal area a mesozooplankton herbivorous food chain (diatoms, copepods, ostracods) is observed but the plankton ecosystem is mainly dominated by the macrozooplankton food chain (diatoms - molluscs - amphipods). Larvae stages of *Pleurogramma* represent the carnivorous level.

Other assemblages exist such as the oligotrophic subantarctic assemblage but they are poorly documented.

These different biotic assemblages correspond to local particularities and seasonal successions of different phases of the whole Southern Ocean seasonal ice zone ecosystem controlled by specific physical conditions. They are not to be taken as different ecosystems but more realistically as different states of a typical ecosystem

locally controlled by specific constraints or progressing from pack-ice to ice-free waters. The marginal ice zone retreat and melting are not simultaneous in the whole Ross Sea, the central and southern part being open earlier than lateral parts. Some areas (generally shallower than 500 m) seem to be inaccessible to large krill swarms and grazing pressure is modified. The early opening of the polynya and the early spring production period in the polynya could be an attractive factor for krill and hence attract predators like penguins, seals and whales. For unknown reasons, ice algae content (as initial condition for spring bloom) seems to be more important in the western part of the Ross Sea.

This typical ecosystem is summarized as a conceptual model (Fig. 23). The principal variables, processes and forcing functions identified in the Ross Sea seasonal ice shelf are included. The atmospheric forcing, sun energy, cloud cover, air temperature and wind stress will act on the ice melting process and the liberation of low salinity water, on the water turbulence, the mixed layer depth and the stratification and also indirectly on the release of ice algae and the primary productivity. The ice algae growth is explicitly parameterised. Diatoms, *Phaeocystis*, nanophytoplankton (small diatoms and other) and picophytoplankton are the four dominant phytoplankton variables. The zooplankton variables are copepods, krill, *Limacina* and amphipods + ostracods and are explicitly included in the coupled model.

4.2. Development of the coupled physical-biological 1D model (ECOHYDRO-MVG) taking into account the ice formation and melting processes. Application to the Ross Sea variability.

4.2.1. The numerical model of the Ross Sea plankton ecosystem.

On the basis of previous observations, the concept of a Southern Ocean Seasonal Ice Zone Ecosystem has been suggested and can be applied to the Ross Sea. However, limitations and spatial and temporal variability occur in relation to local characteristics of depth, climate, hydrodynamics, wind and ice coverage.
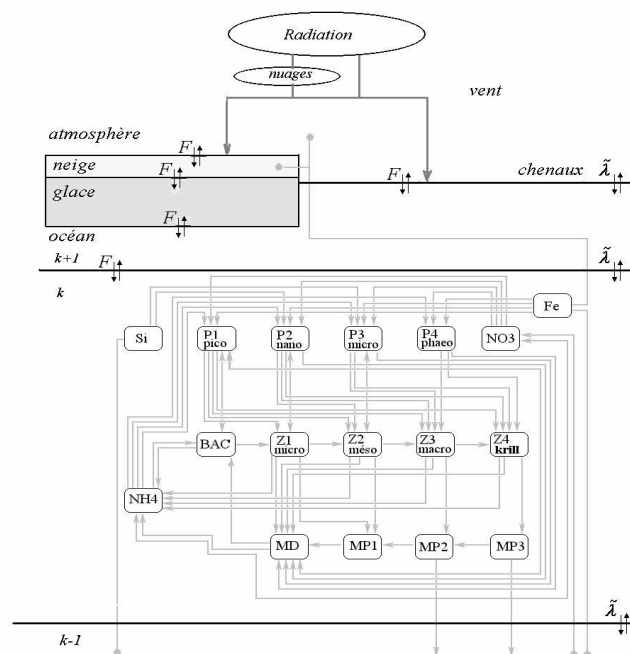

Figure 23. Conceptual scheme of ECOHYDRO-MVG model (Hecq, 2002)

To illustrate the concept of a Ross Sea Seasonal Ice Zone ecosystem and to test the influence of those physical constraints on the variability of the plankton ecosystem, a coupled biological/physical/ ice numerical model of the water column is developed. This model ECOHYDRO-MVG parameterizes explicitly the water column vertical structure and mixing (Hecq et al., 1993) and takes into account the importance of the ice processes, the atmospheric constraints and the presence of ice algae (Goosse and Hecq, 1994, Hecq et al. 1999, Hecq 2002).

The present model (ECOHYDRO-MVG) includes explicitly the effect of vertical profiles of turbulence induced by thermic exchanges and wind stress.

The hydrodynamical model assumes the horizontal homogeneity and the momentum equations are restricted to:

$$\frac{\partial u}{\partial t} = fv + \frac{\partial}{\partial z}\left(\tilde{u} \frac{\partial u}{\partial z} \right) \qquad 1$$

$$\frac{\partial v}{\partial t} = -fu + \frac{\partial}{\partial z}\left(\tilde{u} \frac{\partial v}{\partial z} \right) \qquad 2$$

where u, v are the horizontal components of the velocity, t the time, f the Coriolis parameter, z the coordinate along the vertical axis and $\tilde{u}$ the eddy viscosity.

For temperature T and salinity S in water, equations are:

$$\frac{\partial T}{\partial t} = \frac{\partial}{\partial z}\left(\tilde{I}_T \frac{\partial T}{\partial z} \right) \qquad 3$$

$$\frac{\partial S}{\partial t} = \frac{\partial}{\partial z}\left(\tilde{I}_S \frac{\partial S}{\partial z} \right) \qquad\qquad \tilde{I}_T = \tilde{I}_S = \tilde{I} \qquad 4$$

$\tilde{I}_T$ and $\tilde{I}_S$ are respectively the eddy viscosity for temperature and salinity and are supposed to be equal. The density r is computed by a simplified version of the International Equation of State of Sea Water (1980) (Pond and Pickard, 1983). To compute the eddy diffusivities and viscosities and then close the system, an equation for turbulent kinetic energy, k is added:

$$\frac{\partial k}{\partial t} = \overline{u} M^2 - \tilde{I} N^2 - e + \frac{\partial}{\partial z}\left(\tilde{u} \frac{\partial k}{\partial z} \right) \qquad 5$$

where N and M are the Prandl and Brunt-Väisälä frequency and e is the energy dissipation rate (Nihoul, 1984).

4.2.2. The sea-ice model of the Ross Sea plankton ecosystem Modelling ice formation and melting for ecological purpose.

The sea ice model based on the Semtner model (1976) computes the temperature, the thickness and the concentration of the ice deduced from heat exchanged vertically through the ice-air and ice-ocean interfaces and horizontally through the leads. The sea ice, assumed to be a uniform horizontal slab of ice, develops to balance the heat exchanges between the atmosphere and the ocean.
The details of parametrization of ice and leads dynamics and the determination of boundary conditions have been discussed in Petit and Norro (2000).

4.2.3. The biological equations of the of the Ross Sea plankton model.

The biological equations are similar to those used for physical ones (T, S).

$$\frac{\partial B}{\partial t} = -\frac{\partial}{\partial z}(w.B) + \frac{\partial}{\partial z}\left(\tilde{I}.\frac{\partial B}{\partial z}\right) + f_{biol} \qquad\qquad 11$$

where B is the mass of the biological variable and w a sedimentation or migration speed. Eddy diffusion is supposed to be equal to turbulent diffusion of heat and salt. f_{biol} represents the local modifications due to biological processes.

$$f_{biol} = B.(P^B - R^B - M^B - G^B) \qquad\qquad 12$$

where P^B, R^B, M^B, G^B are the production rate and the metabolic, mortality and predation losses rates of the variable B

Complete equations are developed in Hecq (2002).

4.2.4. Results of the model and discussion.

With the aim to simulate the theoretical standard state of the Ross Sea plankton ecosystem, the ECOHYDRO-MVG model has been tested with initial conditions and physical forcing constraints corresponding to mean values for the whole region (standard run). (Hecq et al. 1999).

As shown on Figure 24, at the end of the winter, before the 20th of December, no ice melting occurs. The mixed layer is deep and the values of the turbulent kinetic energy are high over a large depth. The stabilizing buoyancy flux induced by the melting implies a decrease of the mixed layer thickness. The results of the model indicate that ice melting begins in the second week of December and that the sea is ice-free at the end of the first week of January, which is a reasonable value for the Ross Sea (Jacobs and Comiso, 1989). The ice retreat is nearly linear. But, as the melting and then the flux increase with time, the halocline is more and more strong. When ice disappeared completely, the absence of buoyancy flux allows the wind to deepen the mixed layer. Note that the wind strengthens with time in this season.

The temperature of the upper layer water remains near the melting point when the ice is present and increases with time when ice retreats (Fig. 24). When atmospheric conditions become more rigorous, the temperature decreases until freezing. The computed temperatures are a little too low. This is linked to the delay in the retreat of ice. However, the water temperature exceed rarely 1°C in the Ross Sea (Jacobs and Comiso, 1989).
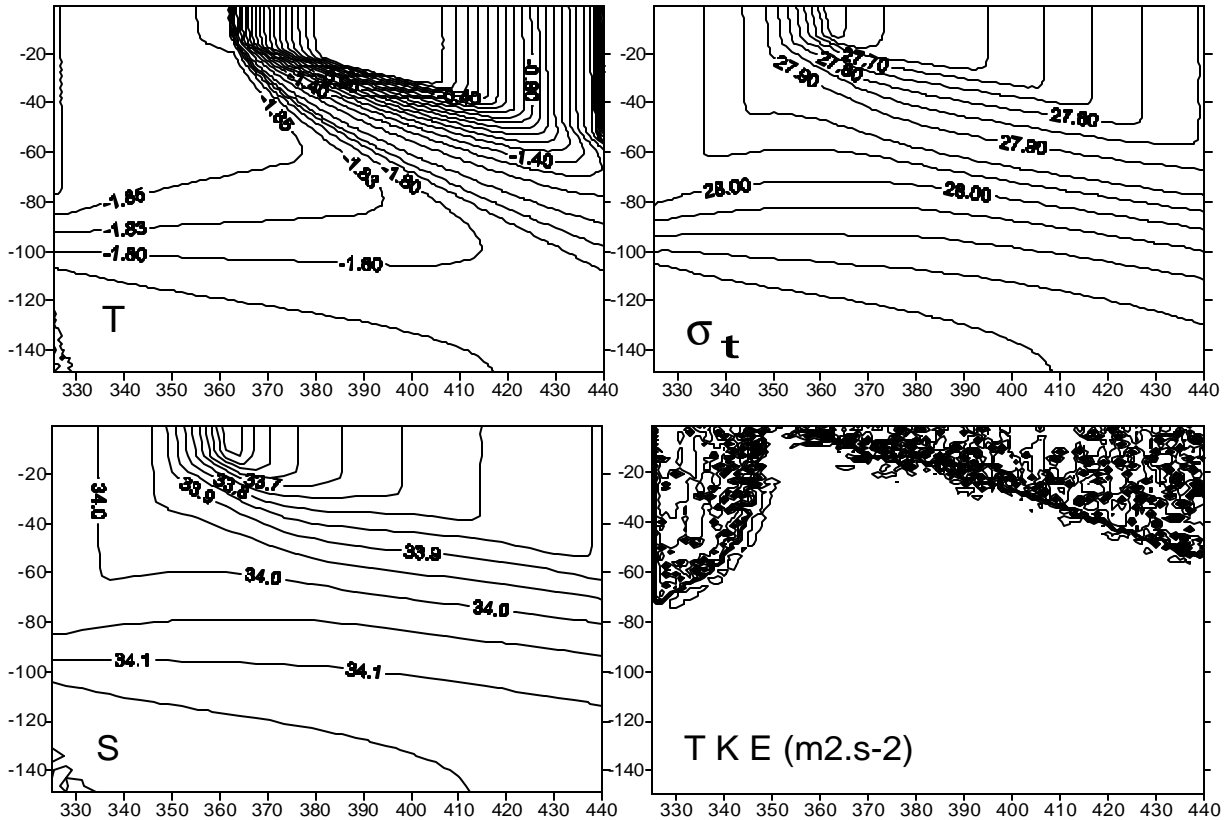
Figure 24: Temporal evolution (Julian days, November to March) of the vertical distribution of the variables in the water column (STANDARD RUN of ECOHYDRO-MVG Model). T: temperature (°C); S: salinity (PSU); σ_t: density and TKE: turbulent kinetic energy ($m^2.s^{-2}$). Oscillations in curves (TKE) are due to wind oscillations.

The phytoplankton results of the standard run (Fig. 25) confirm the prime importance of stratification induced by the melting for the primary productivity. The beginning of ice algae growth corresponds to snow melting. When the ice retreats, the decrease of the mixed layer depth and the increase of the light induce the phytoplankton growth in the water column.

When the ocean is just ice-free, phytoplankton concentration reaches more than 1 mg Chl a m^{-3} (50 mg Chl a m^{-2}) in the surface layer. In the water column, phytoplankton biomass reaches maximum values of 4 mg Chl a m^{-3} (150 to 200 mg Chl a m^{-2}) at the end of December. This estimation corresponds to the observed values for the Ross Sea. The peak of *Phaeocystis* coincides with that of microplanktonic diatoms but is less important and remains later in the season in relation with different production and

grazing processes of these two groups. The maxima of nano- and pico- phytoplankton occur later, respectively in January and February. This last result has to be taken with care because of the limitations of the model at the end of the summer. The zooplankton biomass grows when food is available and decreases when phytoplankton concentrations are too low.
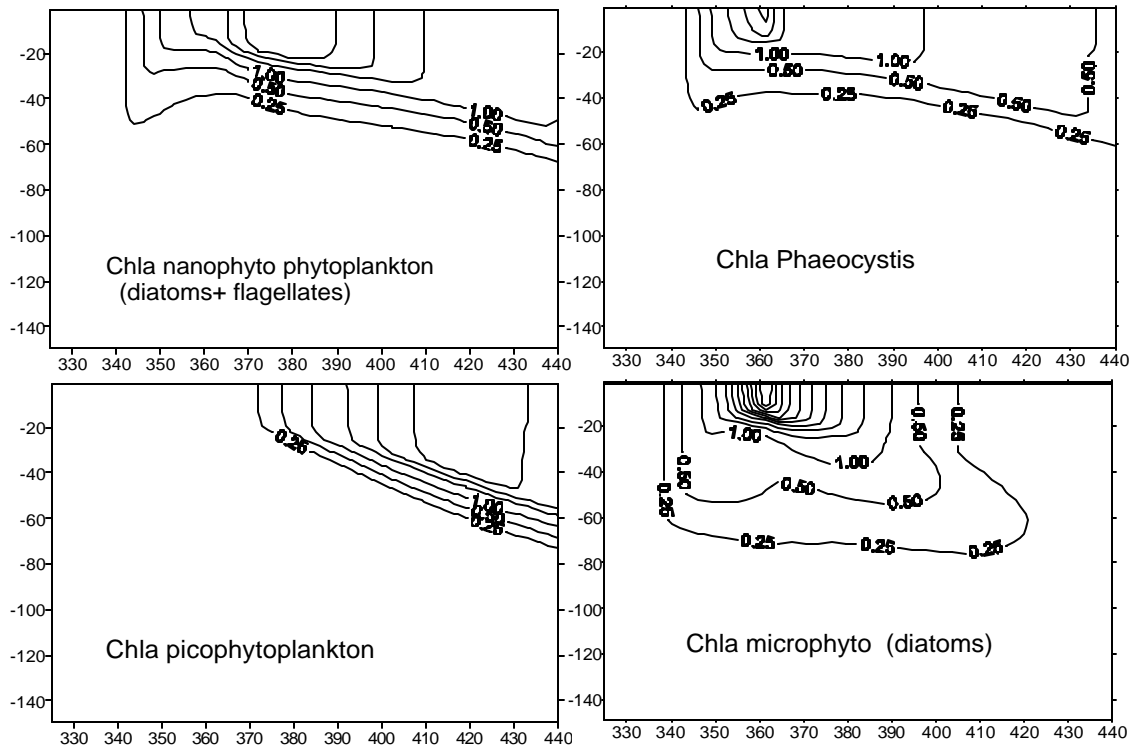

Figure 25: Temporal evolution (November to March) of the vertical distribution of the variables in the water column (STANDARD RUN of ECOHYDRO-MVG Model). Chl *a* of nanophytoplankton, *Phaeocystis*, picophytoplankton and microphytoplankton (mg Chl *a* m^{-3}).

The model was applied to various typical areas or situations in the Ross Sea and simulates explicitly the variability of the marginal ice zone and the phytoplankton growth in function of specific conditions (Table 6, figures 26 and 27).

a.- In the southern part of the Ross Sea polynia (Fig. 26), ice thickness is only 20 cm and snow is neglected. When melting occurs, it implies early water column stabilization and phytoplankton bloom. These two processes occur sooner than in the standard run. However the biomasses are two times lower than in the standard run even if the initial algae concentrations are the same. This result suggests that the presence of ice algae

and their role as seeded organisms is less important than the low phytoplankton growth rate due to low stratification.

Table 6: Initial and forcing values for standard run and local conditions of southern and northern part of the Ross Sea polynia and for hypothetical permanent ice free and ice covered area. *Hginit* and *hninit* are initial values of ice and snow thickness (m.); *cleads* is the lead surface ratio (%) and *cdiv* is the ice divergence ratio (% per month). *Vwind* is the wind velocity (m.sec^{-1}).

	Standard run	South polynia	North polynia	Ice free	Ice permanent
hginit	0.7	0.2	0.2	0	2
hninit	0.2	0.0	0.0	0	0.2
cleads	15	15	15	100	1
cdiv	15	25	25		1
vwind	5.5	5.5	7.5	5.5	5.5

b.- In the northern part of the Ross Sea polynia (Fig. 26), where the wind is stronger, the mixed layer is deeper. *Phaeocystis* and large diatoms dominate the phytoplankton community. An increase of 2 m s^{-1} can be responsible for a decrease of the phytoplankton biomass maximum of 20%. Local storm conditions occurring often in northern part of the Ross Sea polynia can destroy the stratification induced by melting and nearly suppress the favorable conditions for phytoplankton growth whose accumulation is then reduced. These results simulate the situations observed during the Rossmize cruise.

c.- In permanent ice-free areas (Fig. 27), the mixed layer is deep (> 60 m) inducing a small photosynthetic activity. Even in absence of grazing, phytoplankton net production is low. When grazing is included, phytoplankton changes are nearly unobservable.

d.- In permanent ice covered area (Fig. 27), phytoplankton growth is delayed because of the ice, which reduces light availability. However, when melting begins, *Phaeocystis* production increases and its biomass reaches, yet in absence of the total melting, values obtained in the ice-free areas.

Sensitivity of phytoplankton production to some physical parameters was tested. The light available for phytoplankton is modified if the ice melts sooner or if the weather is more cloudy. Sedimentation can also play a role. But these parameters are less influential than biological parameters previously mentioned.
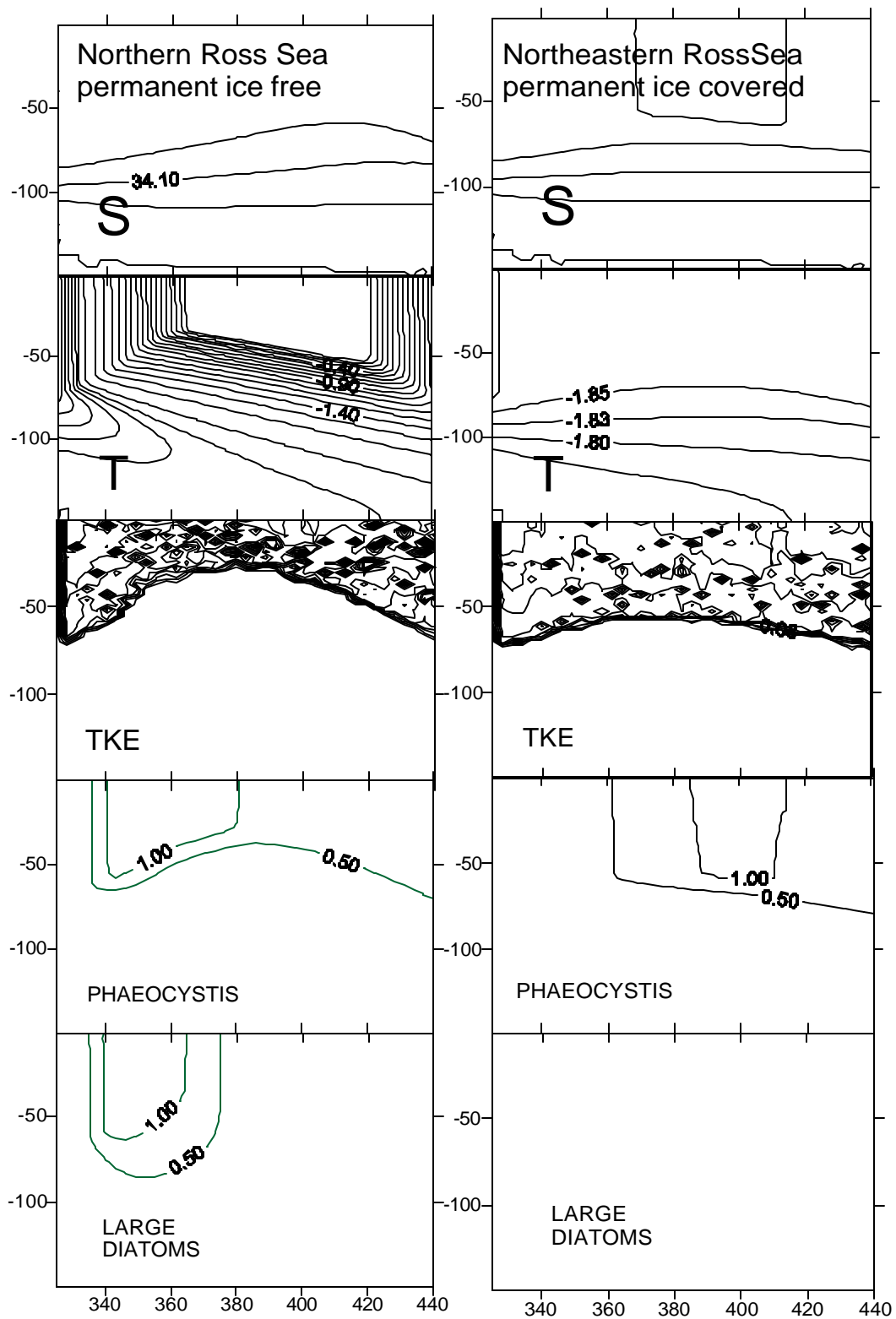
Figure 26: Application of ECOHYDRO-MVG Model to the northern and southern parts of the Ross Sea polynia between November and March. Chl *a* units are mg Chl *a* m^{-3}.
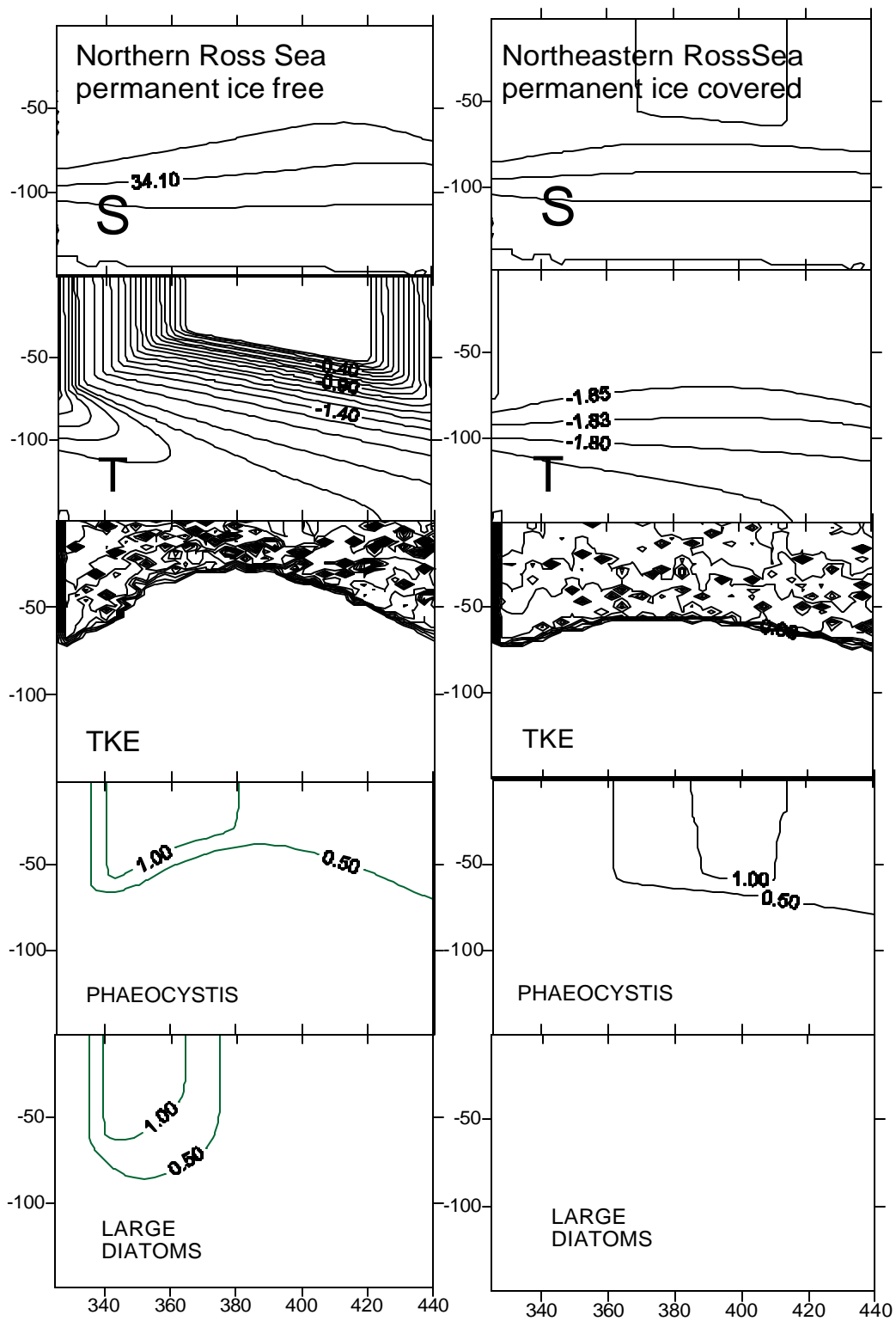
Figure 27: Application of ECOHYDRO-MVG Model to the permanent ice free zone of the Northern Ross Sea and to the northeastern permanent ice covered zone between November and March. Chl *a* units are mg Chl *a* m^{-3}.

Biological results are very sensitive to the values of the parameters included in the formulation of photosynthetic production. Small local or geographical variations of P^B and a can have strong effects on the phytoplankton biomass and might explain some of the variability in Ross Sea (Goosse and Hecq, 1994). As a consequence, even small nutrient limitation, which induces small reduction of photosynthesis could reduce the net growth. Note that a reasonable modification of the light attenuation coefficient has similar consequences as variation of a but is quantitatively less important. It is thus very important in the future to select values of P^B and a corresponding to the population and external conditions occurring in the studied area (Neori and Holm-Hansen, 1982; Tilzer et al., 1986).

5. GENERAL CONCLUSION

The interdisciplinary network has developed a first approach of a coupled physical / biological modelling strategy able in the future to simulate the variability of the Ross Sea, with a particular attention to climate change.

In the last version of the ECOHYDRO-MVG model, parametrization of ice formation and ice biota was developed. Simulations will be presented later. Actually, the simulation in standard conditions reproduces the ice formation at the beginning of March and corresponds to a diminution of the upper layers temperature and a strong mixing of the 100 upper meters of the water column. During the spring, the ice melting (vertical and lateral) corresponds to a decrease of surface waters salinities and the formation of a pycnocline at 40 m. The model simulates the snow layer accumulation during winter and melting during the spring. The snow melting is immediately followed by an increase of light penetration in the ice and the growth of ice algae. At the end of the summer, at the beginning of ice formation which covers 90% of the water surface, the algae of the superficial water are included in ice in formation and the algal concentration in the mixed layer decreases rapidly. At the beginning of spring, ice algae are released progressively in the surface waters during ice melting and growth in the water column immediately after their ice liberation.

As a conclusion, it appears that diverse hydrodynamical and ecological processes control simultaneously the variability of the Ross Sea Seasonal Ice Zone ecosystem. All the trophic levels depend on sea-ice during at least a part of their life. For all these reasons, the ecosystem is essentially sensitive to environmental changes such as climate. An interdisciplinary model approach was developed to understand how the biological and physical processes, interlinked at various scales, govern the ecosystem. The most important interactions between physical and biological processes were simulated by the 1D ECOHYDRO-MVG Model. Simulations of the water column structure and phytoplankton bloom dynamics reproduce realistically the data obtained during oceanographic cruises in the Ross Sea.

The introduction of an explicit ice model is an improvement. The impact of melting on the water column, which is essential to understand the bloom dynamics, is obtained from the model and not as an initial condition or artificial parametrization. Moreover, the evolution of the phytoplankton biomass is studied since the beginning of the bloom (under ice cover) until its decrease and not only after the complete melting. Ice acts mainly as a switch: if ice

melting is present, phytoplankton production is intense and massive blooms are possible even with high losses due to grazing pressure. In absence of ice melting, blooms are nearly impossible even with moderate losses.

In a first step, the biological model was simplified. It includes simple equations for the phytoplankton and zooplankton variables. They are expressed in mg C. m^{-3}. No variable is associated to nutrients because they are rarely limiting, even in massive phytoplankton bloom areas. This model seems to be convenient to understand key interactions between ice, upper ocean and biological populations and their implications for melting, structuration of the water column and productivity. However, we have neglected 3-D phenomena such as ice dynamics or water advection, quantitatively important but less directly concerned in biological/physical vertical coupling. In the present step, complex relations between higher trophic levels were also neglected. The ECOHYDRO-MVG model in its present state is applied only on spring -summer period and is used for the simulation of the microscale physical processes of vertical stabilization of the water column at the level of the marginal ice zone of the Ross Sea. It will need more developments for ice formation and biological processes inside the ice (photo-adaptation, UV, etc.).

Phytoplankton biomass is particularly influenced by modifications of biological parameters. However phytoplankton production is fairly well known, simulation results are very sensitive to parameters for which precise values are essential and need to be measured experimentally. Phytoplankton initial concentration in water and the presence of ice-algae seem to be of lesser importance. Zooplankton is a potential powerful control factor of phytoplankton biomass but its stock and metabolism are scarcely known.

The data for forcing functions, initial values of variables and for validation of the model were issued from oceanographic cruises and from all published information. Publications, workshops with other networks, participation to formatted data bank for Antarctic Global ecosystem applications and organization of a congress on *Hydrodynamical and Ecosystem processes in ice covered seas in southern and northern hemispheres* in 1998 was a valorization objective of the project (Goffart and Hecq Editors, 2000).
The conceptualization, the parametrization and the validation of a coupled numerical modelling system integrating the physical and trophic processes which govern the equilibrium and changes of biodiversity in the Southern Ocean global ecosystem were developed.

Salinity and temperature fields for the Ross Sea and surrounding areas were extracted from the monthly climatology Levitus data for the period particularly relevant for biological activities, from November to February. Available bathymetry data, wind stress data, sea-ice data (concentration and thickness) and Eulerian and Lagrangian data on water masses circulation have been formatted for the calibration and the validation of the model. Hydrological and nutrient data obtained by the authors in the Ross Sea during various oceanographic cruises were treated as an illustration of the water column structure and variability in the Ross Sea. The spatial and temporal distributions of phytoplankton pigments sampled in the western and south central Ross Sea during austral spring 1994 and summer 1990 were investigated. The different plankton assemblages were identified in the Ross Sea and correspond to local particularities and seasonal succession of different phases of the whole Southern Ocean seasonal ice zone ecosystem controlled by specific physical conditions. They are not to be taken as different ecosystems but more realistically as different states of a typical ecosystem locally controlled by specific constraints or progressing from pack-ice to ice-free waters.

In the framework of a more comprehensive study of the picophytoplankton in the Southern Ocean, the genotypic diversity of the different types of organisms present in the size fraction 0.2-2 μm was developed. From the picoplanktonic fraction of two water samples taken at a depth of 20 and 30 m in the Southern Ocean, 16S rDNA sequences from different types of organisms were retrieved: eubacteria, plastids of eukaryotic algae, and cyanobacteria. The cyanobacterial sequences appear almost identical to sequences obtained from the picoplanktonic fraction (*Synechococcus* sp.) of temperate and tropical œceans. Thus, a lineage of taxa defined on the basis of 16S rDNA but with diverse pigment compositions has adapted to different environmental conditions and can be observed from temperate and tropical to Subantarctic regions.

The sea ice model computes the temperature, the thickness and the concentration of the ice deduced from heat exchanged vertically through the ice-air and ice-ocean interfaces and horizontally through the leads.

A numerical model of the upper trophic levels of the Antarctic food chain was developed to simulate the impact of whaling activities in the Southern Ocean. The

model validates the hypothesis of krill limitation by the whale stocks before the whaling period and the control function of whaling on Antarctic birds and seals.

A mechanistic modelling approach (ECOHYDRO-MVG) of the Ross Sea Seasonal Ice Zone ecosystem was used to test the influence of the physical constraints on the variability of the plankton ecosystem. This model parameterizes explicitly the water column vertical structure and mixing and takes into account the importance of the ice melting the atmospheric constraints and the presence of ice algae. A standard run is developed and an application to various local situations is discussed in relation with data acquired during the cruises.

In the aim to compute the role three-dimensional circulation and the turbulence diffusivities on biological variables dynamics, a version of the Princeton Ocean Model (POM) was applied to the Ross Sea. In this model, the classical three-dimensional, time-dependent, non-linear equations describing the conservation of mass, momentum, temperature and salinity are solved on a C-grid and transformed into a σ-coordinates system. The model has a free surface and a split time step. A second moment turbulence closure provides the vertical mixing coefficients.

6 REFERENCES

ALPKEM, 1992b. Silica in seawater. In: Alpkem (Ed.), The Flow Solution Methodology Doc. N° 000671, 5/92 Rev. A. Wilsonville, Oregon, USA, pp 16.

Andreas, E.L., Ackley, S.F., 1982. On the differences in ablation seasons of Arctic and Antarctic sea ice. J. Atmos. Sci., 39, 440-447.

Arrigo, K.R., McClain, C.R., 1994. Spring phytoplankton production in the western Ross Sea. Science, 266, 261-263.

Arrigo, K.R., Weiss, A.M., Smith, W.O.J., 1998. Physical forcing of phytoplankton dynamics in the southwestern Ross Sea. J. Geophys. Res. ,103, 1007-1021.

Arrigo, K.R., Robinson, D.H., Worthen, D.L., Dunbar, R.B., DiTullio, G.R., VanWoert, M., Lizotte, M.P., 1999. Phytoplankton community structure and the drawdown of nutrients and CO_2 in the Southern Ocean. Science, 283, 365-367.

Artegiani, A., Azzolini, R., Paschini, E., Creazzo, S., 1992. Physical oceanographic conditions in the Southern Pacific Ocean and in the Western Ross Sea. In: Anonymous, National Scientific Commission for Antarctica, Oceanographic Campaign 1989-1990. Data Report Part II pp. 5-62.

Azzali, M., Kalinowski, J., 1992. Italian Antarctic Acoustic Survey of Krill In: Gallardo VA, Ferretti O, Moyano HI (eds) Oceanografia in Antartide Oceanografia en Antártica ENEA - Progetto Antartide - Italia Centro Eula - Universidad de Concepcion - Chile pp 321-330

Barlow, R.G., Mantoura, R.F.C., Cummings, D.G., 1998. Phytoplankton pigment distributions and associated fluxes in the Bellingshausen Sea during the austral spring 1992. J. Mar. Syst. ,17, 97-113.

Catalano, G., Benedetti, F., 1990. Distribution of nutrients in the Terra Nova Bay and in the Ross Sea. In: « National Scientific Commission for Antarctica, Oceanographic Campaign 1987-1988. Data Report Part I », Anonymous, pp. 61-83.

Catalano, G., Benedetti, F., Goffart, A., Iorio, M., 1991a. Distribution of Dissolved Oxygen, pH, Total Alkalinity and Nutrients in the Southern Ocean and the Ross Sea (R/V "Cariboo" 1989-1990 cruise). In: National Scientific Commission for Antarctica, Oceanographic Campaign 1989-1990. Data Report Part I, Anonymous, pp. 11-23.

Catalano, G., Benedetti, F., Iorio, M., 1991b. Coastal oceanography from Cape Russel to Campbell Ice Tongue (Terra Nova Bay). In: « National Scientific Commission for Antarctica, Oceanographic Campaign 1989-1990. Data Report Part I », Anonymous, pp. 25-32.

Catalano, G., Povero, P., Fabiano, M., Benedetti, F., Goffart, A., 1997. Nutrient utilisation and particulate organic matter changes during summer in the upper mixed layer (Ross Sea, Antarctica). Deep-Sea Res. 44, 97-112.

Catalano, G., Benedetti, F., Preponzani, S., Goffart, A., Ruffini, S., Rivaro, P. and Falconi, C., 1999. Spatial and temporal patterns of nutrient distributions in the Ross Sea. In Faranda, F., Guglielmo, L. and Ianora, A. Eds., Ross Sea Ecology, Springer, Berlin, Heidelberg, pp. 107-120.

Claustre, H., Kerhervé, P., Marty, J.C., Prieur, L., Videau, C., Hecq, J.H., 1994. Phytoplankton dynamics associated with a geostrophic front: Ecological and biogeochemical implications. J. Mar. Res., 52, 711-742.

Comiso, J.C., McClain, C.R., Sullivan, C.W., Ryan, J.P., Leonard, C.L., 1993. Coastal zone color scanner pigment concentrations in the southern ocean and relationships to geophysical surface Features. J. Geophys. Res., 98, 2419-2451.

Conover, R.J., Huntley, M., 1991. Copepods in ice-covered seas. Distribution, adaptations to seasonally limited food, metabolism, growth patterns and life cycle strategies in polar seas. J. Mar. Syst., 2, 1-41.

Cota, G.F., Legendre, L., Gosselin, M., Ingram, R.G., 1991. Ecology of bottom ice algae: I Environmental controls and variability. J. Mar. Syst., 2, 257-277.

Dugdale, R.C., Goering, J. J., 1967. Uptake of new and regenerated forms of nitrogen in primary productivity. Limnol. Oceanogr. 23, 196 – 206.

Eicken, H., Lange, M.A., Hubberten, H.-W., and Wadhams, P. 1994. Characteristics and distribution patterns of snow and meteoric ice in the Weddell Sea and their contribution to the mass balance of sea ice. Ann. Geophysicae 12, 80-93.

El-Sayed, S.Z., Taguchi, S., 1981. Primary production and standing crop of phytoplankton along the ice-edge in the Weddell Sea. Deep-Sea Res., 28, 1017-1032.

Eppley, R.W., Peterson, B.J., 1979. Particulate matter flux and planktonic new production in the deep ocean. Nature, 282, 677 – 680.

Fichefet, T., Gaspar, P., 1988. A model study of upper ocean-sea ice interactions. Journal of Physical Oceanography, 18, 181-195.

Frangoulis, C., Belkhiria, S., Goffart, A. and Hecq, J.H., 2001. Dynamics of copepod faecal pellets in relation to a *Phaeocystis* dominated bloom: characteristics, production and flux. J. Plankton Res., 23, 75-88.

Garrison, D.L. and Buck, K.R., 1991. Surface-layer sea ice assemblages in Antarctic pack ice during the austral spring: Environmental conditions primary production and community structure. Mar. Ecol. Prog. Ser., 75, 161-172.

Gieskes, W.W.C. and Kraay, G.W., 1986. Analysis of phytoplankton by HPLC before, during and after mass occurrence of the microflagellate *Corymbellus aureus* during the spring bloom in the open northern North Sea in 1983. Mar. Biol. 92, 45-52.

Goeyens, L., Tréguer, P., Baumann, M. E. M., Baeyens, W. and Dehairs, F., 1995. The leading role of ammonium in the nitrogen uptake regime of Southern Ocean marginal ice zones. J. Mar. Syst., 6, 345 - 361.

Goeyens, L., Elskens, M., Catalano, G., Lipizer, M., Hecq, J.H. and Goffart, A., 2000. Nutrient depletions in the Ross Sea and their relation with pigment stocks. J. Mar. Syst., 27, 195-208.

Goffart, A., Catalano, G. and Hecq, J.H., 2000. Factors controlling the distribution of diatoms and *Phaeocystis* in the Ross Sea. J. Mar. Syst., 27, 161-175.

Goosse, H. and Hecq, J.H., 1994. Modelling the ice-ocean-plankton interactions in the Southern Ocean. J. Mar. Syst., 5, 471-484.

Hecq, J.H., 2001. Une Modélisation Conceptuelle et Numérique de l'Ecosystème Planctonique Océanique.. Université de Liège,299 pp

Hecq, J.H., Magazzù, G., Goffart, A., Catalano, G., Vanucci, S. and Guglielmo, L., 1992. Distribution of planktonic components related to vertical structure of water masses in the Ross Sea and the Pacific sector of the Southern Ocean. In: Anonymous, Atti del 9° congresso A.I.O.L., Santa Margherita Ligure, 20-23 Novembre 1990, pp. 665-678.

Hecq J.H., Brasseur, P., Goffart, A., Lacroix, G. and Guglielmo, L., 1993. Modelling Approach of the Planktonic Vertical Structure in Deep Austral Ocean. The Example of the Ross Sea Ecosystem. In: Progress in Belgian Oceanography Research (Brussels, January 21-22 1993). Royal Academy of Belgium, National Committee of Oceanology, pp. 235-250.

Hecq, J.H., Guglielmo, L., Goffart, A., Catalano, G. and Goosse, H., 1999. Modelling approach of the ross sea plankton ecosystem. In: Faranda, F., Guglielmo, L., Ianora, A. (Eds), Ross Sea Ecology. Italian Antarctic Expeditions (1986-1995). Springer, Berlin, Heidelberg, pp. 395-412.

Innamorati, M., Mori, G., Lazzara, L., Nuccio, C., Lici, M., Catalano, G. and Benedetti, F., 1990. Phytoplankton ecology in the Ross Sea. In: Anonymous, National scientific commission for Antarctica. Oceanographic campaign 1987-88. Data Report Part II, 9-63.

Jacobs, S.S. and Comiso, J.C., 1989. Sea ice and oceanic processes on the Ross Sea continental Shelf. J. Geophys. Res., 94, 18195-18211.

Jacques, G., 1983. Some ecophysiological aspects of the Antarctic phytoplankton. Polar Biol., 2, 27-33.

Jeffrey, S.W., 1974. Profiles of photosynthetic pigments in the ocean using thin-layer chromatography. Mar. Biol., 26, 101-110.

Jeffrey, S.W., 1980. Algal pigment systems. In: Falkowski, P. (Ed.), Primary productivity in the sea. Plenum Press, New York, pp. 35-58.

Jeffrey, S.W., Mantoura, R.F.C. and Wright, S.W. (Eds), 1997. Phytoplankton pigments in oceanography. Monographs on oceanographic methodology 10, Unesco Publishing, 661 pp.

Knox, G.A., 1994. The biology of the Southern Ocean. Cambridge University Press, 444 pp.

Kock, K.H. and Shimadzu, Y., 1994. In El-Sayed S.Z. (Ed.) : « Southern Ocean Ecology: The Biomass Perspective », 287-312.

Lancelot, C., Veth, C. and Mathot, S., 1991. J. Mar. Sys., 2, 333-346.

Lipizer, M., Ruffini, S., Predonzani, S., Cozzi, S., Goffart, A. and Catalano, G., 1997. Antarctic spring: the importance of "new" production. In: Picccazzo M., Ed., Atti del 12° Congresso A.I.O.L., Genova, Italia, **1**, 153-164.

Lipizer, M. and Catalano, G., 1999. Nitrogen assimilation and new production in a spring bloom in the Ross Sea. (Cruise of R/V « Italica », 1994). In Faranda, F., Guglielmo, L. and Povero, P. (Eds.): Nat. Prog. Ant. Res. ROSSMIZE 93-95, Data report II.

Mackintosh, N.A., 1973. Distribution of post- larval krill in the Antarctic. Discovery Reports, 36, 95-156.

Mantoura, R.F.C. and Llewellyn, C.A., 1983. The rapid determination of algal chlorophyll and carotenoid pigments and their breakdown products in natural waters by reverse-phase high performance liquid chromatography. Anal. Chem. Acta 151, 297-314.

Marino, D. and Cabrini, M., 1997. Distribution and succession of phytoplankton populations in the Ross Sea (Antarctica) during the austral spring 1994. In: Faranda, F., Guglielmo, L., Povero, P. (Eds.), National Programme for Antarctic Research. Rossmize 1993-1995. Data Report Part I, 307-341.

Martin, J.H. and Fitzwater, S., 1988. Iron deficiency limits phytoplankton growth in the northeast Pacific subarctic. Nature, 331: 341-343.

Martin, J.H., Gordon, R.M. and Fitzwater S.E., 1990. Iron in Antarctic waters. Nature, 345, 156-158.

Mitchell, B.G. and Holm-Hansen, O., 1991. Observation and modelling of the Antarctic phytoplankton crop in relation to mixing depth. Deep-Sea Res., 38, 981-1007.

Nelson, D.M., Ahern, J.A. and Herlihy, L.J., 1991. Cycling of biogenic silica within the upper water column of the Ross Sea. Mar. Chem., 35, 461-476.

Nelson, D.M. and Smith, W.O., 1991. Sverdrup revisited: Critical depths, maximum chlorophyll levels, and the control of Southern Ocean productivity by the irradiance-mixing regime. Limnol. Oceanogr., 36, 1650 - 1661.

Nelson, D.M. and Tréguer, P., 1992. Role of silicon as a limiting nutrient to Antarctic diatoms: evidence from kinetic studies in the Ross Sea ice-edge zone. Mar. Ecol. Progr. Ser., 80, 255-264.

Parkinson, C.L. and Washington, W.M. 1979. A large-scale numerical model of sea ice. J. Geophys. Res., 84, 311-337.

Petit, B. and Norro, A., 2000. Seasonal evolution of sea ice and oceanic heat flux in the Weddell Sea. J. Mar. Syst., 27, 37-52.

Platt, T., Gallegos, C.L. and Harrison, W.G., 1980. Photoinhibition of photosynthesis in natural assemblages of marine phytoplankton. J. Mar. Res., 38, 687-701.

Priddle, J., Croxall, J.P., Everson, I., Heywood, R.B., Murphy, E.J., Prince, P.A., Sear, C.B., 1988. Large-scale fluctuations in distribution and abundance of krill: A discussion of possible causes. In Sahrhage, D. Ed.: « Antarctic Ocean and Resources Variability », Springer-Verlag, Berlin, 169-182.

Russo, A., Gallarato, A., Testa, G., Corbo, C., Pariante, R., 1997. Physical data collected during ROSSMIZE cruise (Ross Sea, November - December 1994). In: Faranda, F., Guglielmo, L., Povero, P. (Eds.), National Programme for Antarctic Research. Rossmize 1993-1995. Data Report Part I, 25-110.

Russo A. 1999. Water mass characteristics during the Rossmize cruise (western sector of the Ross Sea, November - December 1994). In Faranda, F., Guglielmo, L. and Ianora, A. Eds., Ross Sea Ecology, Springer, Berlin, Heidelberg, pp. 83-93.

Saggiomo, V., Goffart, A., Carrada, G.C. and Hecq J.H., 1994. Spatial patterns of phytoplanktonic pigments and primary production in a semi-enclosed periantarctic ecosystem: the Strait of Magellan. Journal of Marine Systems, 5, 119-142.

Sedwick, P.N., DiTullio, G.R., Mackey, D.J., 2000. Iron and manganese in the Ross Sea, Antarctica: Seasonal iron limitation in Antarctic shelf waters. J. Geophys. Res., 105, 11321-11336.

Semtner, A.J. Jr. 1976. A model for the thermodynamics growth of sea ice in numerical investigations of climate. J. Phys. Oceanog., 6: 379-389.

Skliris, N., Goffart, A., Hecq, J.H. and Djenidi S., 2001b. Shelf-slope exchanges associated with a steep submarine canyon off Calvi (Corsica, NW Mediterranean Sea): A modelling approach. J. Geophys. Res., 106, 19883-19901.

Skliris N., K. ElKalay, A. Goffart, C. Frangoulis, J.-H. Hecq. 2001a. One-dimensional modelling of the plankton ecosystem of the north-western Corsican coastal area in relation to meteorological constraints. Journal of Marine Systems, 2001, 27, 337-362.

Tréguer, P., Jacques, G., 1992. Dynamics of nutrients and phytoplankton, and fluxes of carbon, nitrogen and silicon in the Antarctic Ocean. Polar Biol., 12, 149 - 162.

Veeschkens, C., Hecq J.H., 1996. Modelling Approach of the Antarctic ecosystem. In Royal Academy of Belgium (Ed.) : « *Progress in Belgian Oceanographic Research*. Proceedings of the annual workshop on Belgian Oceanographic Research », 75-178.

Veldhuis, M.J.W., Kraay, G.W. and Gieskes, W.W.C., 1993. Growth and fluorescence characteristics of ultraplankton on a north-south transect in the eastern North Atlantic. Deep-Sea Res., 40, 609-626.

Vernet, M., Lorenzen, C.J., 1987. The relative abundance of pheophorbide a and pheophytin a in temperate marine waters. Limnol. Oceanogr. 32, 352-358.

Veth, C., 1991. The evolution of the upper water layer in the marginal ice zone austral spring 1988 Scottia- Weddell Sea. J. Mar. Syst., 2, 451-464.

Veth, C., Lancelot, C., Ober, S., 1992. On processes determining the vertical stability of surface waters in the marginal ice zone of the north western Weddell Sea and their relationship with phytoplankton bloom development. Polar Biol., 12, 237-243.

Wilmotte, A., Demonceau, C., Goffart, A., Hecq, J.H., Demoulin, V. and Crossley, A.C., in press. Molecular and pigment studies of the picophytoplankton in a region of the Southern Ocean (47 to 54° S, 141 to 144 °E) in March 1998. *Deep-Sea Res.*

Zwally, H.T., Parkinson, C.L., Comiso, J.C., 1983. Variability of Antarctic sea ice and changes in carbon dioxide. Science, 220,1005-1012.